



AMD

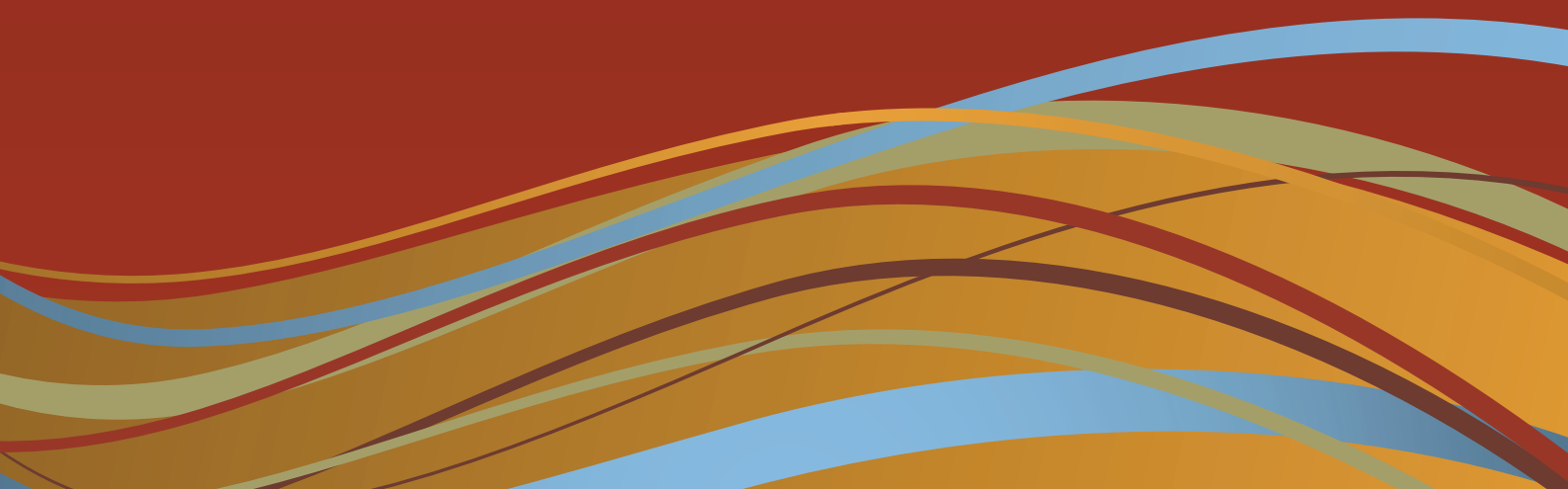
9th TRIENNIAL
WORKSHOP

Proceedings of the
Ninth Australian Workshop on
ACID AND METALLIFEROUS DRAINAGE

Editors: L.C. Bell, M. Edraki and C. Gerbo

20-23 November, 2017

Burnie, Tasmania



Proceedings
of the
Ninth Australian Workshop
on
Acid and Metalliferous Drainage

Editors: L.C. Bell, M. Edraki and C. Gerbo

20 - 23 November 2017

Burnie, Tasmania



**Sustainable Minerals Institute
The University of Queensland**

St Lucia, QLD 4072

Published by Sustainable Minerals Institute, The University of Queensland

© 2017

Material in this publication is protected by copyright but may be used providing both the authors and publisher are acknowledged.

Enquiries and requests for copies should be directed to:

SMI Transformational Learning
Sustainable Minerals Institute
The University of Queensland
St Lucia, QLD 4072

ISBN Number, electronic publication: 978-1-74272-194-1

Citations of this publication should take the form:

Bell, L.C., Edraki, M. and Gerbo C. (Eds) (2017) Proceedings of the Ninth Australian Workshop on Acid and Metalliferous Drainage, Burnie, Tasmania. 20-23 November 2017. (The University of Queensland: Brisbane).

Individual papers should be cited:

Author(s) Name(s) Title of paper. In 'Proceedings of the Ninth Australian Workshop on Acid and Metalliferous Drainage, Burnie, Tasmania. 20-23 November 2017. (Eds. Bell, L.C., Edraki, M. and Gerbo C.) pp. 00-00 (The University of Queensland: Brisbane).

Disclaimer

Material presented in this document is the responsibility of the authors. The opinions expressed do not necessarily represent the views of The University of Queensland.

The University of Queensland accepts no liability (including liability in negligence) and takes no responsibility for any loss or damage which a user or any third party may suffer or incur as a result of reliance on the document.

CONTENTS

Acknowledgements	5
List of Reviewers.....	5
Workshop Sponsors.....	6
Workshop Program	7

ABSTRACTS

Continuous Improvement Through Collaboration

<i>R. Green and R. Marton</i>	13
-------------------------------------	----

Are You Doing All You Could be to Optimise Your Closure Alternatives?

<i>A. Baisely, M. O’Kane and S. Pearce</i>	198
--	-----

Bacteria-Mineral Interactions at Sulphide Mineral Surfaces

<i>G. Southam</i>	325
-------------------------	-----

FULL PAPERS

Instrumented Column Testing of Potentially Contaminating Tailings Under Field Climatic Conditions

<i>D.J. Williams and C. Zhang</i>	14
---	----

Converting Chemistry to Mineralogy for Acid and Metalliferous Drainage Risk Management

<i>J. Taylor, S. Winchester, M. Tyler, K. Ehrig, J. Waters and F. Beavis</i>	26
--	----

Multiple Kinetic Testing Methods to Understand the AMD/NMD Potential of High Sulphur, High ANC Waste Rock

<i>B. Usher, M. Landers and P. Marianelli</i>	35
---	----

Experimental Models of Metal Leaching for Scaling-Up to the Field

<i>Z-S. Liu, C. Huang, L. Ma, E. Dy, Z. Xie, M. O’Kane and S. Pearce</i>	44
--	----

Why Variable Oxidation Rates are Needed for the Prediction of AMD from Dynamic Waste Rock Dumps

<i>J. Pearce, S. Pearce and R. Marton</i>	51
---	----

Classification of Waste Rock for McArthur River Mine, Northern Territory

<i>M. Landers, B. Usher and P. Marianelli</i>	65
---	----

Weathering Sulfidic Waste - Laboratory-Scale Tests for Assessing Water Quality in Backfilled Pits

<i>A. Watson, C. Linklater and R. Marton</i>	74
--	----

Developing of a NAF/PAF Grade Control Programme for Placement of a WRD Cover	
<i>J. Chapman, J. Jones, K. Mandaran, B. Luinstra and A. Hendry</i>	83
The Practicalities and Implementation of a NAF Grade Control Programme for Placement of a WRD Cover	
<i>A. Hendry, B. Luinstra, J. Jones, K. Mandaran and J. Chapman</i>	92
The Formation of Aluminate-Doped Surface Passivating Layers on Pyrite for Effective Acid and Metalliferous Drainage Control	
<i>Y. Zhou, M.D. Short, J. Li, R.C. Schumann, R.St.C. Smart, A.R Gerson and G. Qian</i>	102
The Influence of Sample Numbers and Distribution on the Assessment of AMD Potential	
<i>A.M. Garvie and D. Kentwell</i>	110
A Geoenvironmental Characterisation Tool for the Coreshed During Early Life-of-Mine Assessments	
<i>R. Cornelius, A. Parbhakar-Fox and D.R. Cooke</i>	120
Why Variable Oxidation Rates are Needed for the Prediction of AMD from Dynamic Waste Rock Dumps	
<i>J. Pearce, S. Pearce and R. Marton</i>	132
Observations and Explanations From the Monitoring Data of Equity Silver Mine, Canada	
<i>Z-S. Liu, C. Huang, L. Ma, K.A. Morin, M. Aziz and C. Meints</i>	146
Geochemical Characterisation of Mine Wastes: Does it Matter?	
<i>A.M. Robertson, G.A. Maddocks and M. Landers</i>	156
Designing Tailings and Waste Rock Systems for Chemical and Physical Stability	
<i>G.W. Wilson, B. Wickland and B. Weeks</i>	166
An Integrated Approach to Closure of Landforms Containing Potentially Acid Forming Waste Rock in North-West Queensland	
<i>A. Sexton, A. Butler, J. Chapman and T. Anderson</i>	176
Improved Rehabilitation Outcomes Through Smart Cover Design at Endeavor Mine, NSW	
<i>T. Rohde, K. Hardie and N. Jamson</i>	186
Controlling Acid and Metalliferous Drainage From Decommissioned Underground Mines	
<i>N. Bourgeot, J. Taylor, A. Sampaklis, N. Staheyeff, S. Pape, E. Hardjo and M. Quiatol</i>	199
Rehabilitation Options for Potentially Contaminating Coal Tailings Stored in Pits	
<i>D.J. Williams</i>	209
Forecasting Long Term Water Quality After Closure: Boliden Aitik Au Mine	
<i>M. O’Kane, P. Weber, M. McKeown, D. Christensen, S. Mueller and B. Bird</i>	218

Pit Lake Water Quality Modelling at Century Mine	
<i>C. Linklater, A. Watson, A. Hendy, J. Chapman, J. Crosbie and P. Defferrard</i>	228
Developing Pilbara Pit Lake Analogues to Inform Closure Considerations	
<i>W. Germs, G. Race, R. Green and R. Marton</i>	239
Guidelines for Opencast Coal Pit Void Closure and Relinquishment	
<i>D.A. Salmon</i>	247
Chemical and Economic Feasibility Study of Application of Alkaline CSG Waters in AMD Remediation	
<i>D.R. Cohen, Q. Chen, M.S. Anderson, A.M. Robertson, D. R. Jones and B. Kelley</i>	254
Treatment of Acid and Metalliferous Drainage Including Removal of Contaminants from a Site	
<i>S. Costin</i>	263
Evaluating Applications of Bed and Fly Ash for Controlling Acid and Metalliferous Drainage – Examples from Tasmanian Mine Wastes	
<i>A. Parbhakar-Fox, R. Clifton and N. Fox</i>	274
Portland Cement Application to Control Acid Mine Drainage Generation from Waste Rocks	
<i>M.G. Sephton and J.A. Webb</i>	288
Rehabilitation Planning At the Former Rum Jungle Mine Site in Northern Australia	
<i>Part 1. Geochemical Characteristics of Mine Wastes and Inferred Post Rehabilitation Source Terms</i>	
<i>D. Jones, P. Ferguson and T. Laurencont</i>	295
Rehabilitation Planning at the Former Rum Jungle Mine Site in Northern Australia	
<i>Part 2: Environmental Performance Assessment for the Preferred Rehabilitation Strategy</i>	
<i>P. Ferguson, C. Wels, D. R. Jones and T. Laurencont</i>	304
A Decade of AMD Treatment Initiatives for New Zealand Coal Mines	
<i>P. Weber, W. Olds, K. Malloch and H. Christenson</i>	314
The Link Between Microbial Diversity and At-Source AMD Prevention	
<i>O.T. Ogbughalu, A.R. Gerson, G. Qian, R.St.C. Smart, R.C. Schumann, N. Kawashima, R. Fan, J. Li and M.D Short</i>	326
Extraction of Cobalt from Historic Sulphide Tailings Using Bioleaching	
<i>A. Parbhakar-Fox, J. Glen and D. Kemp</i>	335
Integrated Leaching/Bioleaching and Sulphate Reducing Processes for Metal Recovery and Treatment of Mine Tailings	
<i>D. Villa Gomez, H. Hofmann, A. Kerr, B. Ryan, M. Peces and G. Southam</i>	347

Gas Flux Rates and the Linkage with Predicting AMD Loads in Waste Rock Dumps, and Designing Practical Engineered Solutions – Field Based Case Studies	
<i>S. Pearce, M. Barteaux and J. Pearce</i>	354
Water Quality Predictions Under Highly Variable Moisture and Temperature: A Case Study on the Importance of Thermodynamics	
<i>Y. Tian, R. Strand, G. Wang, J. Tuff and B. Usher</i>	362
Non-Iterative Modelling of Miner Site Hydrogeochemistry	
<i>R. Strand, J. Tuff and B. Usher</i>	373
The Role of AMD in Pilbara Iron Ore: Mobilisation and Fate of Trace Elements During Surface and Groundwater Flow	
<i>P. Ware and R.T. Watkins</i>	384
Geochemical and Mineralogical Characterisation of a Tailings-Rich Sediment Bank, King River, Western Tasmania	
<i>S. Gilmour, A. Parbhakar-Fox, L. Jackson and D.R. Cooke</i>	394
Intrinsic Neutralisation Potential From Automated Drillcore Logging for Improved Geoenvironmental Domaining	
<i>L. Jackson, A. Parbhakar-Fox, N. Fox, D.R. Cooke, A.C. Harris and E. Savinova</i>	405
Characterisation of Arsenic Geochemistry in Mine Tailings from a Mesothermal Au Deposit	
<i>H. Christenson, J. Pope, D. Craw, J. Johns and N. Newman</i>	419
POSTERS	
Investigating the Geochemistry of Selenium in the Residual from Biological Wastewater Treatment at a Coal Mine	
<i>L. Desauvoy and D. Kirste</i>	429
Validation of Sequential Leaching Tests to Predict Potential Impacts of Low Sulfur Iron Ore Waste on Surface and Groundwater Quality	
<i>S. Black, B. Price, N. Rothnie, R. Sharma, R. Marton and D. Allen</i>	430
Determining Bioaccessibility Risks at the Historic Aberfoyle Tailings Site, Northeast Tasmania: Opportunities for Effective Rehabilitation	
<i>R. McLaine, A. Parbhakar-Fox, N. Fox and M. Reid</i>	431
Physicochemical Properties of Iron Oxides Opportunities for Useful AMD Products?	
<i>B. Mooney, B. Paull, T. Lewis and A. Parbhakar-Fox</i>	432
Geoenvironmental Characterisation of the Abandoned Scotia Mine, North East Tasmania: Implications for Management Practices	
<i>A. Parbhakar-Fox, T. Lewis, P. Hamill, A. Wakefield, R. Botrill and J. Parnell</i>	433
Waste Not, Want Not – Using Waste Hay to Improve Pit Lake Water Quality	
<i>R. Green, C. Mather, C. Kleiber, S. Lee, M. Lund and M. Blanchette</i>	434

Acknowledgements

The program for this workshop was developed by an Organising Committee consisting of

Mr Bruce Barrie
Independent Consultant

Ms Tania Laurencont
Department of Mines and Energy,
Northern Territory Government

Emeritus Professor Clive Bell
The University of Queensland

Dr Alan Robertson
Founder and Principal Geochemist,
RGS Environmental

Mr Mike Fawcett
Department of Mines and Energy,
Northern Territory Government

Dr Peter Scott
Independent Consultant

Dr Andrew Garvie
Principal Consultant (Geoenvironmental)
SRK Consulting (Australasia)

Emeritus Professor Roger Smart
School of Natural and Built Environment,
University of South Australia

Dr David Jones
Principal
DR Jones Environmental Excellence

Dr Jeff Taylor
Director - Senior Principal Environmental Geochemist
Earth Systems

Valuable administrative and editorial support to the event has been provided by Carla Gerbo, Kylie Pettitt and Michelle Rowland

List of Reviewers

We would like to thank the following technical referees for their contribution towards enhancing the quality of papers included in these proceedings:

Alan Robertson
Andrew Garvie
Anita Parbhakar-Fox
Barry Noller
Bruce Kelley
Clive Bell
David Jones
David Williams
Gordon Southam

Ian Callow
Ian Swane
Jeff Taylor
John Webb
Mansour Edraki
Michael Short
Neil McIntyre
Paul Brown
Paul Weber

Peter Scott
Roger Smart
Josh Pearce
Ron Watkins
Sue Vink
Tania Laurencont
Thomas Baumgartl
Ward Wilson

Sponsors

We would like to thank and acknowledge the following partners, sponsors, and supporters:

Workshop Major Partner



Sponsors



Trade Exhibitors



Workshop Program

9th Australian Workshop on Acid and Metalliferous Drainage
20 – 24 November 2017 | Burnie, Tasmania

Monday 20 November 2017		
08:00am	Registration and tea/coffee on arrival	
SESSION 1: Opening session Plenary Room: Town Hall		Chair: Mansour Edraki
08:30am	Welcome and introduction	Neville Plint SMI
08:40am	Opening address	Jen Parnell Mineral Resources Tasmania
08:50am	Introduction of program structure	Mansour Edraki SMI
09:05am	Address by major sponsor RGS Environmental Pty Ltd	Alan Robertson RGS Environmental Pty Ltd
09:10am	INAP and Global Alliance update	Gilles Tremblay INAP
09:40am	Keynote presentation: Continuous improvement through collaboration	Ros Green (Rio Tinto Ore), Richard Marton (BHP)
10:10	Morning Tea	
SESSION 2: Forecasting AMD - from laboratory to mine site Plenary Room: Town Hall		Chair: Ward Wilson
10:35am	Keynote presentation: Instrumented column testing of potentially contaminating tailings under field climatic conditions	David Williams (The University of Queensland), C. Zhang
11:05am	Converting chemistry to mineralogy for acid and metalliferous drainage risk management	Fern Beavis (Earth Systems), J. Taylor, S. Winchester, M. Tyler K. Ehrig, J. Waters
11:30am	Multiple kinetic testing methods to understand the AMD/NMD potential of high sulphur, high ANC waste rock of waste rock	Brent Usher (Klohn Crippen Berger), M. Landers, P. Marianelli
11:55am	Experimental models of metal leaching for scaling-up to the field	Zhong-Sheng Liu (National Research Council Canada), C Huang, L. Ma, E. Dy, Z. Xie
12:20pm	Lunch	
SESSION 3: Parallel session		
	Monitoring, assessment and prediction I Room: Braddon Hall	Prevention and control Room: Town Hall
	Chair: Andrew Garvie	Chair: Alan Robertson
01:30pm	Using chromium reducible sulfur to predict acid formation potential Gert du Plessis (MBS Environmental), D. Allen, M. North, S. Black, B. Price, N. Rothnie	Development of a NAF/PAF grade control programme for placement of a WRD cover Alison Hendry (SRK Consulting), J. Chapman, J. Jones, K. Mandaran, B. Luinstra
01:55pm	Classification of waste rock for McArthur River Mine, Northern Territory Matt Landers (RGS Environmental Pty Ltd), J. Taylor, S. Pape, N. Murphy, N. Bourgeot, E. Hardjo	The practicalities and implementation of a NAF grade control programme for placement of a WRD cover Alison Hendry (SRK Consulting), B. Luinstra, J. Jones, K. Mandaran, J. Chapman

02:20pm	Weathered sulfidic waste-laboratory-scale tests for assessing water quality in backfilled pits Alex Watson (SRK Consulting (Australasia) Pty Ltd), C. Linklater, J. Chapman, R. Marton	The formation of aluminate-doped surface passivating layer on pyrite for effective acid and metalliferous drainage control Roger Smart (Blue Minerals Consultancy), Y. Zhou, MD. Short, J. Li, RC. Schumann, R St. C. Smart, AR. Gerson, G, Qian
02:45pm	Afternoon Tea	
SESSION 4: Monitoring, assessment and prediction II Plenary Room: Town Hall		Chair: Mike Fawcett
03:10pm	Keynote Presentation: The influence of sample numbers and distribution on the assessment of AMD potential	Andrew Garvie (SRK Consulting (Australasia) Pty Ltd), D. Kentwell
03:40pm	A geoenvironmental characterisation tools for the coreshed during early life-of-mine assessments	Rebekah Cornelius (University of Tasmania), A. Parbhakar-Fox, D. Cooke
04:05pm	Why variable oxidation rates are needed for the prediction of AMD from dynamic waste rock dumps	Joshua Pearce (O'Kane Consultants), S. Pearce, R. Marton
04:30pm	Observations and explanations from the monitoring data of Equity Silver Mine, Canada	Zhong-Sheng Liu (National Research Council Canada), C. Huang, L. Ma, KA. Morin
04:55pm	End of Workshop Day 1	

Posters
Posters will be available for viewing during break times throughout the workshop in Town Hall Foyer
Investigating the geochemistry of selenium in the residual from biological wastewater treatment at a coal mine L. Desauoy^A and D. Kirste^A (^A Simon Fraser University – Department of Earth Science, Burnaby, British Columbia, Canada)
Validation of sequential leaching tests to predict potential impacts of low sulfur iron ore waste on surface and groundwater quality S. Black^A, B. Price^A, N. Rothnie^A, R. Sharma^A, R. Marton^B and D. Allen^C (^A ChemCentre, Resources and Chemistry Precinct, Bentley, WA, Australia ^B BHP Billiton Minerals Australia, Perth, WA Australia ^C MBS Environment)
Determining bioaccessibility risks at the historic Aberfoyle tailings site, Northeast Tasmania: opportunities for effective rehabilitation R. McLaine^A, A. Parbhakar-Fox^A, N. Fox^B and M. Reid^C (^A ARC Industrial Hub for Transforming the Mining Value Chain (TMVC), University of Tasmania, Australia ^B Co-operative Research Centre for Optimising Resource Extraction (CRC ORE), University of Tasmania, Australia ^C Mineral Resources Tasmania, Australia)
Physicochemical properties of iron oxides: opportunities for useful AMD products? B. Mooney^A, B. Paul^A, T. Lewis^B and A. Parbhakar-Fox^C (^A Australian Centre for Research on Separation Science (ACROSS), University of Tasmania, Australia ^B School of Physical Sciences (Chemistry), University of Tasmania, Australia ^C Industrial Hub for Transforming the Mining Value Chain (TMVC), University of Tasmania, Australia)
Geoenvironmental characterisation of the abandoned Scotia Mine, north east Tasmania: implications for management practices A. Parbhakar-Fox^A, T. Lewis^B P. Hamill^B, A. Wakefield^C, R. Botrill^C and J. Parnell^C (^A ARC Industrial Hub for Transforming the Mining Value Chain (TMVC), University of Tasmania, Australia ^B Discipline of Chemistry, School of Physical Sciences, University of Tasmania, Australia ^C Mineral Resources Tasmania, Australia)
Waste not, want not – using waste hay to improve pit lake water quality R. Green^A, C. Mather^A, C. Kleiber^A, S. Lee^A, M. Lund^B and M. Blanchette^B (^A Rio Tinto Iron Ore, 152-156 St Georges Terrace, Perth, WA 6000, Australia ^B Mine Water and Environment Research Centre (MiWER), Edith Cowan University, 270 Joondalup Drive, Joondalup, WA 6027, Australia)

Tuesday 21 November 2017		
08:00am	Registration and tea/coffee on arrival	
SESSION: Program update		
Plenary Room: Town Hall		
08:30am	Program update	Mansour Edraki SMI
SESSION 1: Influencing closure outcomes		
Plenary Room: Town Hall		
08:40am	Keynote presentation: Geochemical characterisation of mine wastes: Does it matter?	Alan Robertson (RGS Environmental Pty Ltd), G. Maddocks, M. Landers
09:10am	Keynote presentation: Designing tailings and waste rock systems for chemical and physical stability	Ward Wilson (University of Alberta), B. Wickland, B. Weeks
09:40am	An integrated approach to closure of landforms containing potentially acid forming waste rock in north-west Queensland	Alex Sexton (Ernest Henry Mine (Glencore Copper Assets)), A. Butler, J. Chapman, T. Anderson
10:05am	Improved rehabilitation outcomes through smart cover design at Endeavor Mine, NSW	Timothy Rohde (EMM Consulting Pty Ltd), K. Hardie, N. Jamson
10:30	Morning Tea	
SESSION 2: Advancements in closure		
Plenary Room: Town Hall		
11:00am	Keynote presentation: Are you doing all you could be to optimize your closure alternatives?	Mike O’Kane (O’Kane Consultants), A. Baisley, S. Pearce
11:30am	Controlling acid and metalliferous drainage from decommissioned underground mines	Jeff Taylor (Earth Systems), N. Bourgeot, A. Sampaklis, N. Staheyeff, S. Pape, E. Hardjo, M. Quiatol
11:55am	Rehabilitation options for potentially contaminating coal tailings stored in pits	David Williams (The University of Queensland)
12:20pm	Forecasting long term water quality after closure: Boliden Aitik Cu mine	Mike O’Kane (O’Kane Consultants), P. Weber, M. McKeown, D. Christensen, S. Mueller, B. Bird
12:45	Lunch	
SESSION 3: Parallel session		
	Final voids and pit lakes Room: Braddon Hall	Remediation and treatment Room: Town Hall
	Chair: David Jones	Chair: Jeff Taylor
01:45	Pit lake water quality modelling at Century Mine Claire Linklater (SRK Consulting (Australasia) Pty Ltd)), A. Watson, A. Hendry, J. Chapman, J. Crosbie, P. Defferrard	Chemical and economic feasibility study of application of alkaline CSG waters in AMD remediation David Cohen (University of New South Wales), Q. Chen, M. Andersen, A. Robertson, D. Jones, B. Kelly
02:10pm	Developing Pilbara pit lake analogues to inform closure considerations Wijnand Germs (ERM), G. Race, R. Green, R. Marton	Treatment of acid and metalliferous drainage including removal of contaminants from a site Samual Costin (Global Aquatica)

02:35pm	Guidelines for opencast coal pit void closure and relinquishment David Salmon (Amanzi Consulting)	Evaluating applications of bed and fly ash for controlling acid and metalliferous drainage- examples from Tasmanian mine wastes Anita Parbhakar-Fox (University of Tasmania), R. Clifton, N. Fox
03:00pm	Testing a pit lake water quality model against eight years of field data Ursula Salmon (University of Western Australia)	Portland Cement applications to control acid mine drainage generation from waste rocks Michael Sephton (La Trobe University), JA. Webb
03:25	Afternoon Tea	
SESSION 4: Managing past legacies Plenary Room: Town Hall		Chair: David Williams
03:45pm	Rehabilitation planning at the former Rum Jungle mine site in northern Australia Part 1. Geochemical characteristics of mine wastes and inferred post rehabilitation source terms	David Jones (DR Jones Environmental Excellence), P. Ferguson, T. Laurencont
04:10pm	Rehabilitation planning at the former Rum Jungle mine site in northern Australia Part 2. Environmental performance assessment for the preferred rehabilitation scenario	Paul Ferguson (Robertson GeoConsultants Inc), C. Wels, D. Jones, T. Laurencont
04:35pm	A decade of AMD treatment initiatives for New Zealand coal mines	Paul Weber (O’Kane Consultants), J. Pearce, W. Olds, K. Malloch, H. Christenson
05:00pm	Briefing mine site tour - Rosebery	Martin Brownlee (SSHE Superintendent – Australian Operations, MMG Minerals and Metals Group)
05:25pm	End of Workshop Day 2	

Thursday 23 November 2017		
SESSION: Program update Plenary Room: Town Hall		Chair: Mansour Edraki
08:30am	Program update	Mansour Edraki SMI
SESSION 1: Geomicrobiology and AMD Plenary Room: Town Hall		Chair: Roger Smart
08:40am	Keynote presentation: Bacteria-mineral interactions at sulphide mineral surfaces	Gordon Southam (The University of Queensland)
09:10am	The link between microbial diversity and at-source AMD prevention	Omy Ogbughalu (University of South Australia), AR. Gerson, G. Qian, R St. C. Smart, RC. Schumann, N. Kawashima, R. Fan, J. Li, MD. Short
09:35am	Extraction of cobalt from historic sulphide tailings using bioleaching	Anita Parbhakar-Fox (University of Tasmania), J. Glen, D. Kemp
10:00am	Integrated leaching/bioleaching and sulphate reducing processes for metal recovery and treatment of mine tailings	Denys Villa Gomez (The University of Queensland)
10:25	Morning Tea	
SESSION2: Parallel session		
	Monitoring, assessment and prediction III Room: Braddon Hall	Geo-environmental approaches Room: Town Hall
	Chair: Brent Usher	Chair: Peter Scott
10:50am	Gas flux and the linkage with predicting AMD loads in waste rock dumps, and designing practical engineering solutions – field based case studies Steven Pearce (O’Kane Consultants), M. Barteaux, J. Pearce	The role of AMD in Pilbara Iron Ore: mobilisation and fate of trace elements during surface and groundwater flow Amy Ware (The University of Western Australia), RT. Watkins
11:15am	Water quality predictions under highly variable moisture and temperature: A case study on the Importance of thermodynamics Yuan Tian (Klohn Crippen Berger), R. Strand, G. Wang, J. Tuff, B. Usher	Geochemical and mineralogical characterisation of a tailings-rich sediment bank, King River, Western Tasmania Sarah Gilmour (University of Tasmania), A. Parbhakar-Fox, L. Jackson, DR. Cooke
11:40am	Non-iterative modelling of mine site hydrogeochemistry Roald Strand (Klohn Crippen Berger), J. Tuff, B. Usher	Intrinsic neutralisation potential from automated drillcore logging for improved geoenvironmental domaining Laura Jackson (University of Tasmania), A. Parbhakar-Fox, N. Fox, DR. Cooke, AC. Harris, E. Savinova
12:05pm		Characterisation of arsenic geochemistry in tailings from a mesothermal AU deposit Hannah Christenson (CRL Energy Ltd), J. Pope, D. Craw, J. Johns, D. Trumm, N. Newman
12:30pm	Lunch	

SESSION 3		Chair: Bruce Kelley
Plenary Room: Town Hall		
01:30pm	Panel discussion (Chair: Bruce Kelley) Workshop wrap-up Mansour Edraki	
03:15pm	Afternoon Tea	
03:45pm	End of 9th Australian Workshop on Acid and Metalliferous Drainage 2017	

CONTINUOUS IMPROVEMENT THROUGH COLLABORATION

R. Green^A and R. Marton^B

^A Rio Tinto Iron Ore, 152-156 St Georges Terrace, Perth, WA 6000, Australia

^B BHP, Mineral Australia, 125 St Georges Terrace, Perth, WA 6000, Australia

ABSTRACT

Successful innovation involves more than a great idea. Collaboration is an essential component to ensure all aspects of the idea are considered and to achieve buy in. Mining companies are often approached with ideas and proposals however company buy in can be difficult. This can sometimes be due to the proposal not meeting the company's priorities or strategic objectives. Several initiatives have been underway in Australia to better understand common mining company needs in regard to chemically reactive mineral waste.

The International Network for Acid Prevention (INAP) was established by several major mining companies in 1998 with the purpose of reducing liability associated with sulfide mine materials. This is pursued in three ways:

- Knowledge transfer and information-sharing;
- Technology transfer; and
- Gap-driven research.

INAP member meetings were typically held in North America however since 2015 some meetings have been held in Australia. The meetings have involved member companies and companies potentially interested in joining INAP. The later parts of the meetings were expanded to also include AMD experts and this was important to gain a better understanding of AMD issues, expertise, capacity and capabilities across Australia.

Rio Tinto and BHP have further collaborated on three Research and Development projects:

- Upscaling of laboratory tests to waste dump applications in arid regions;
- PAF storage under waste dump slopes; and
- Developing pit lake analogues for the Pilbara region.

All three projects have produced successful initial results and plans are underway to progress the work further.

Collaboration is important within companies too, particularly with the many disciplines at a mine site that work with chemically reactive mineral waste. This paper will discuss successful collaborative approaches.

INSTRUMENTED COLUMN TESTING OF POTENTIALLY CONTAMINATING TAILINGS UNDER FIELD CLIMATIC CONDITIONS

D.J. Williams^A and C. Zhang^A

^AThe University of Queensland, Brisbane QLD 4072, Australia

ABSTRACT

The majority of operating tailings storage facilities continue to employ slurried tailings deposition. On deposition, the tailings undergo beaching, hydraulic sorting down the beach according to their particle size and specific gravity, settling, self-weight consolidation, and desiccation on exposure to sun and wind. To date there has been an absence of a standardised test for assessing the sequential settling, self-weight consolidation and desiccation of tailings for use as a basis for the design and management of tailings deposition. The paper describes a 1.2 m high by 200 mm diameter, purpose-built, instrumented column designed for this purpose. Also described are purpose-built instrumentation including moisture, suction, temperature and salinity sensors spaced down the length of the column. The column test may be conducted in the laboratory with desiccation simulated using a heat lamp and/or a fan. It can also be conducted in the field, subjected to ambient climatic conditions, which are recorded using a weather station. The column data are recorded by a purpose-built data logger, programmed using open-source hardware and software so that they can be observed in real time via a dedicated web page. The results of the instrumented column test can be analysed to describe the physical and chemical behaviour of the tailings as they desiccate and oxidise, and are subjected to cycles of drying and wetting. An important aspect is the calibration of the sensors in the tailings to be tested and under the cycles to which the tailings will be subjected in the field. Calibration data are presented for fine-grained red mud and coarse-grained coal tailings.

1.0 INTRODUCTION

Tailings typically leave the mineral processing plant as an aqueous slurry, which is characterised by its rheological parameters and behaviour. On deposition, the tailings produced from processing hard rock ores settle, consolidate and desiccate (if exposed to sun and wind) to a “soil-like” consistency. In this state, they may be subjected to conventional soil mechanics shear strength and consolidation testing. However, clay mineral-rich tailings, red mud formed from the refining of bauxite to alumina, and laterite nickel tailings, among other tailings, may not settle and consolidate sufficiently to enable conventional soil mechanics testing. To achieve sufficient consistency to enable such testing would take these tailings to a state that they may never achieve in a tailings storage facility (TSF).

The settling and self-weight consolidation of tailings have the most profound effect on the volume that the deposited tailings occupy (Shokouhi and Williams, 2015; Shokouhi *et al.*, 2016). These processes are particularly important where the rate of rise of the tailings in the TSF is rapid and/or deposition is under water. Settling occurs in the upper part of the recently deposited tailings layer, while consolidation occurs simultaneously towards the base of the layer. During the initial rapid settling of tailings slurry, there is limited particle contact and essentially no development of excess pore water pressure. As the tailings form a sediment, particles come into contact, excess pore water pressures develop and, on drainage and consolidation, these transfer to effective stress. The

magnitude of consolidation is far less than the reduction in volume on settling, and consolidation is a far slower process than settling.

Desiccation occurs when the surface of the tailings becomes exposed to the sun and wind and has most effect on the shear strength of the tailings, with limited densification, particularly once the shrinkage limit of the tailings is reached at which pore water is replaced by air. The effect of the sun and the wind drops off exponentially with depth, as does the strengthening effect (Zhang *et al.*, 2016).

The three processes of settling, consolidation and desiccation are conventionally tested separately in the laboratory; settling in a column, consolidation in a consolidometer, and desiccation in a drying tray and/or a Tempe cell or desiccator. The tailings sediment formed in a settling column cannot be transferred to a consolidometer, and neither the tailings sediment nor the consolidated tailings can be transferred to a drying tray or Tempe cell. As a result, there is a disconnect between the three laboratory tests.

A purpose-built, instrumented column has been developed in which tailings slurry may be added in a series of layers at the initial solids concentration representative of field conditions, allowed to settle between layers, allowed to consolidate under its self-weight, and allowed to desiccate and re-wet on drying and wetting cycles.

2.0 INSTRUMENTED COLUMN

The instrumented column was purpose-built in the Geotechnical Engineering Laboratory at The University of Queensland (UQ), following a trial column described in Zhang *et al.* (2016). The intended purpose of the instrumented column is to simulate the settling, self-weight consolidation and desiccation of a given tailings, to assist in optimising the tailings deposition layer thickness and deposition cycle time. The results of the instrumented column test, together with the tailings production rate, enable the tailings footprint to be determined. The instrumented column was designed to be robust and cost-effective to manufacture and instrument, to enable its widespread deployment in laboratories and at mine sites. When deployed in a laboratory, a heat lamp and/or fan are used to simulate solar and wind drying. The instrumented column can also be deployed in the field, in combination with a climate station, to monitor actual climatic conditions and drivers.

The column dimensions are an internal diameter of 200 mm, and a total height of 1.4 m, as shown in Fig. 1. The 200 mm internal diameter was selected to match the largest diameter Perspex or PVC tubing that is readily and cheaply available commercially. The column height comprises two or three sections totalling 1.2 m in height, which are detachable for ease of sample preparation and removal, plus a 200 mm long top section to allow excess tailings slurry to be placed to achieve a settled specimen height of 1.2 m.

The column is instrumented with moisture, matric suction, temperature and salinity sensors, which were specifically and cost-effectively developed in the Geotechnical Engineering Laboratory at UQ. In addition, expensive balances were replaced by in-house developed load cells to measure column mass and water balance. All sensors are connected to a data logger that was also specifically and cost-effectively developed in-house, and is driven by open-source software that enables data collection via the internet. The in-house development of the sensors and data logger enabled costs to be dramatically reduced from those of sensors available commercially, and for the sensors and data logger to be specifically designed for testing tailings from a slurry to the desiccated state. The sensors and data logger developed in-house are described in the following sections.

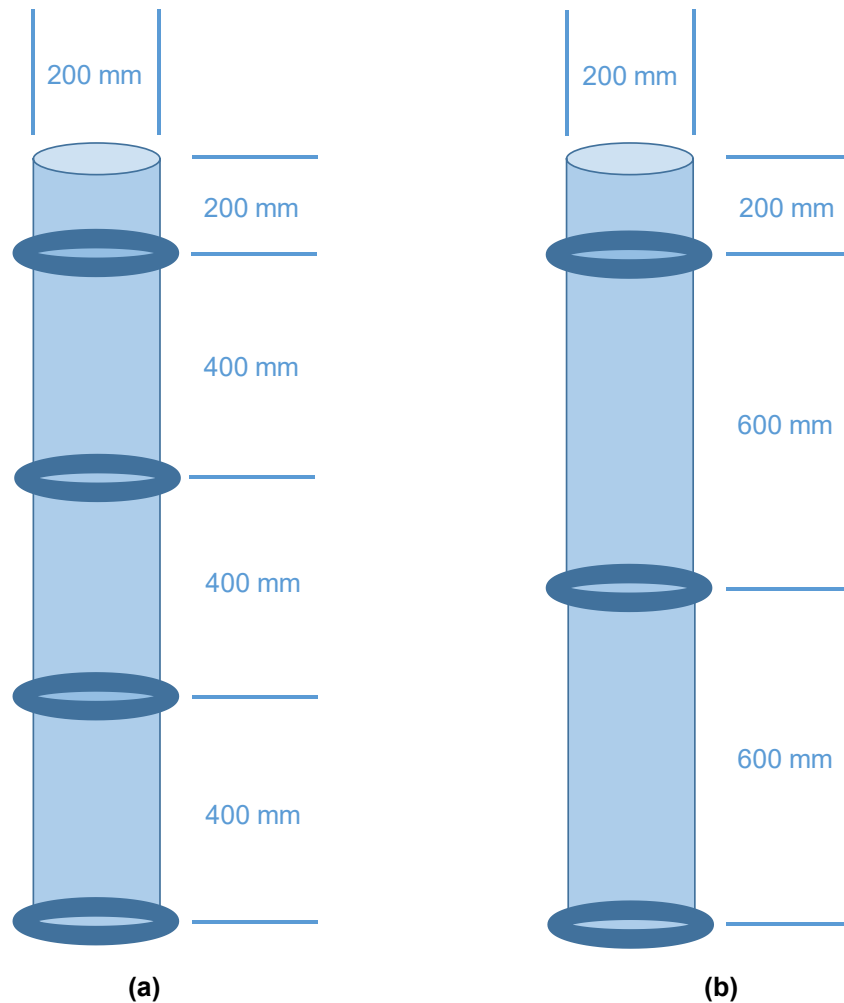


Fig. 1. Alternative column geometries: (a) three by 400 mm sections, and (ii) two by 600 mm long sections, both with a 200 mm extension

2.1 Moisture Sensor

The moisture sensor developed in-house measures the volumetric water content of tailings indirectly from its dielectric permittivity, relying on the much higher dielectric constant of water (80) compared that of dry soil (3 to 5). All of the electrical components of the sensor are carefully sealed, to ensure the longevity of the sensor in hypersaline, acidic or alkaline environments, which are commonly found in mine tailings (see Fig. 2). Commercially available time domain reflectometry-based moisture sensors are affected by changes in both volumetric water content and salinity, as occurs as the tailings desiccate (Hook *et al.*, 2004). The new dielectric permittivity-based moisture sensor were expected to measure volumetric water content irrespective of salinity up to that of seawater (35,000 ppm).

2.2 Matric Suction Sensors

The dielectric matric suction sensor developed in-house is based on the in-house dielectric moisture sensor, and has two porous ceramic plates attached on the two flat surfaces of the sensor (see Fig. 3(a)). At equilibrium, the matric suction in the ceramic plates is the same as that in the surrounding tailings. Since the particle size distribution and the soil water characteristic curve (SWCC) of the ceramic plates are known, the volumetric water content in the ceramic plates measured by the sensor can be converted to matric suction, which is the same suction as that of the surrounding tailings.



Fig. 2. In-house dielectric moisture sensor

The thermal matric suction sensor developed in-house measures the matric suction of the tailings indirectly from the rise in temperature on heating (see Fig. 3(b)), and also provides the ambient temperature. Being able to generate heat as well as measure ambient temperature, the electrical module of the sensor is slotted in a porous ceramic cylinder of which the particle size distribution and the SWCC are known. Heat produced by the electrical element in the centre of the sensor starts to dissipate to the surrounding tailings through the enclosing ceramic cylinder. Thermal equilibrium is achieved in 30 s, when the temperature of the sensor and that of the surrounding tailings equilibrate. As the bulk thermal conductivity of the ceramic cylinder increases monotonically with increasing volumetric water content, low suction (corresponding to a high volumetric water content) would lead to low temperature rise in the tailings on heating. The advantage of these two new matric suction sensors, compared to the commercially available matric suction sensors is that suction measurement range of the sensors can be varied by changing the porous ceramic. Specifically, ceramics with large pores (e.g., silica ceramics) are able to measure a low suction range, and ceramics with small pores are able to measure a high suction range.



Fig. 3. In-house matric suction sensors: (a) dielectric, and (b) thermal, including temperature measurement

2.3 Salinity Sensor

The unique salinity sensor developed in-house (see Fig. 4) measures the relative humidity of the pore air in the surrounding unsaturated tailings, and is capable of measuring salinity over the entire range from fresh to the solubility limit (up to 265,000 ppm). If the pore water is fresh, the sensor can also measure matric suctions up to high values.



Fig. 4. In-house salinity sensor

2.4 Load Cells for Measuring Column Mass and Water Balance

Balances for measuring mass and water balance are expensive and are subject to fluctuation under wind and rain loading. A cost-effective alternative of four load cells between two PVC plates was developed in-house (see Fig. 5). The readings from the four load cells are averaged to give an accuracy of 10 g and a capacity of up to 100 kg.

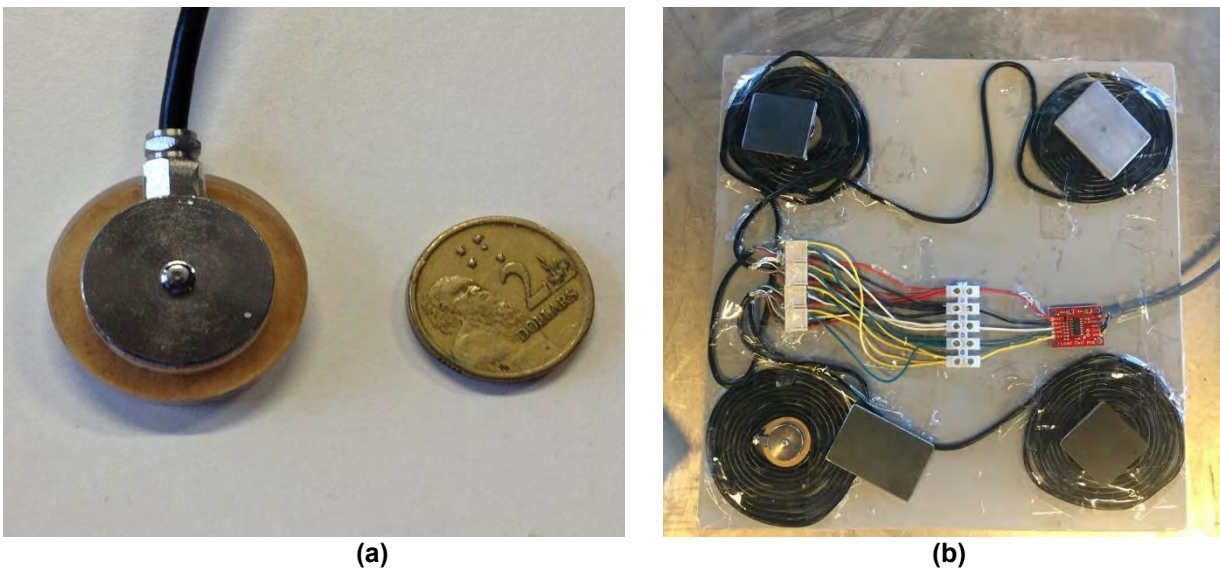


Fig. 5. In-house load cells for column mass and water balance: (a) individual load cell, and (b) four load cells on base plate

2.5 Data Logger

All of the sensors, the balance, and a camera are controlled by a data logger developed in-house, and equipped with 15 analog and 57 digital channels. The new data logger is driven by open-source hardware and software, and is able to acquire data individually and sequentially from each sensor type and each individual sensor at a specified time interval. In addition to data acquisition, each sensor channel provides a relay that powers each individual sensor in turn when data acquisition is due. This results in low power consumption, and little heating of cables and sensors that may cause zero shift and non-linear calibration. In addition, the monitoring frequency can be varied and the data delivered via an internet browser in real-time, enabling access to the system for all interested parties.

Commercially available data loggers are dedicated to a particular sensor type and are driven by propriety software, resulting in multiple, expensive data loggers being required for multiple sensor types, and limited scope for real-time data downloads. They also continuously power all sensors connected to them, leading to heating and excessive power demand.

3.0 SENSOR CALIBRATION AND DURABILITY

The various sensors developed in-house have been subjected to calibration and durability testing in a purpose-built drying/wetting cycle test, as shown in Fig. 6. It is essential to carry out sensor calibration in the tailings in which the sensors will be embedded, rather than rely on the calibration supplied with the sensor, and to subject them to the expected drying and wetting cycles. Sensor durability and reliability is essential for the harsh conditions under which many tailings exist, including high salinity, and highly acidic or highly alkaline pH. For the purposes of calibration, a 4 cm deep layer of settled tailings is allowed to dry, followed by wetting and re-drying. This depth of settled tailings was selected to ensure reasonably uniform conditions with depth, and the sensors being calibrated are embedded in the middle of the layer. Drying is simulated using a fan (a heat lamp could also be used), while wetting is achieved by flooding the desiccated tailings, followed by re-drying using the fan. The sensors performed well and demonstrated high durability and reliability.

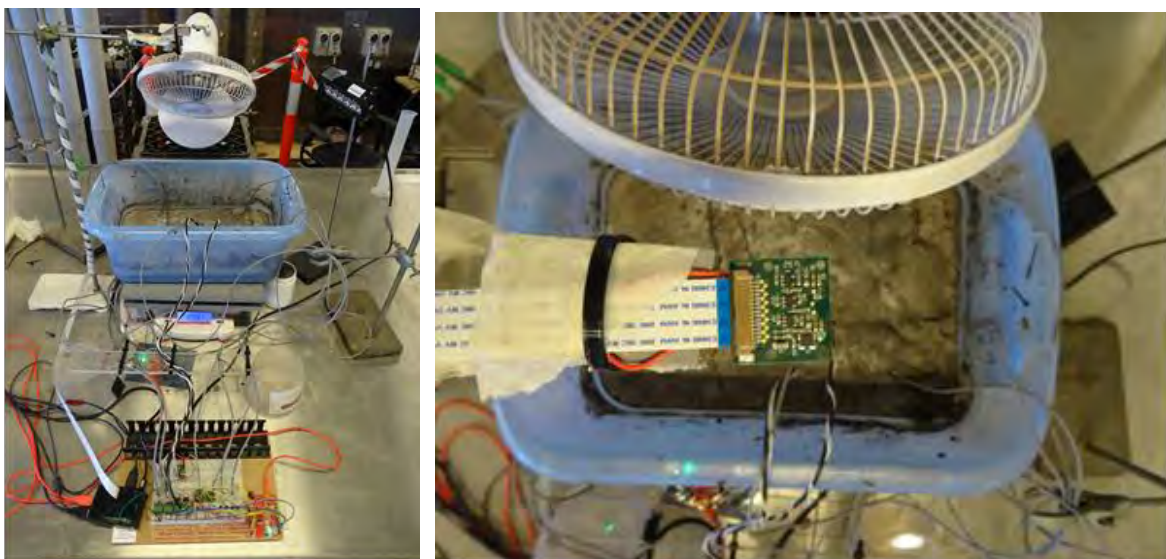


Fig. 6. Calibration and durability testing of in-house sensors

For the calibration experiments reported herein, seven sensors were employed: two dielectric moisture sensors, two dielectric matric suction sensors, and three thermal matric suction sensors. A high-resolution camera was mounted about 400 mm above the tailings surface to capture the desiccation process, including shrinkage and cracking (Konrad and Ayad, 1997) and salt precipitation (Fisseha *et al.* 2010) of the tailings, at four-hourly time intervals. A flash was incorporated to ensure a uniform light source for the photographs, including at night. A dedicated data logger controlled all sensors, the mass and water balance, the camera, and the light source.

3.1 Calibration Testing

Two types of tailings were used to calibrate the sensors: (i) red mud from Queensland Alumina Limited, located in Gladstone, Australia, and (ii) coal tailings from Jeebropilly Coal Mine, located in the Ipswich Coalfields of south-eastern Queensland, Australia. Two desiccation experiments were carried out on each tailings. Both tailings were deposited at an initial solids concentration of 25% by mass, similar to the consistency that they are deposited into their respective TSFs.

The first red mud experiment involved the initial desiccation of the red mud slurry. Due to its fine particle size distribution and low initial dry density, the red mud underwent considerable shrinkage and cracking on initial desiccation. The experiment was continued until there was no further desiccation with time. The second red mud experiment followed re-flooding of the desiccated red mud with 4000 mL of deionised water, amounting to the water lost during initial desiccation. Some of the sensors were located in the previous randomly-located desiccation cracks, while others were within uncracked blocks of red mud. This enabled the different behaviours of the cracked and uncracked red mud to be followed on re-flooding and re-desiccation.

Similarly, the first coal tailings experiment involved the initial desiccation of the coal tailings slurry, while the second desiccation experiment followed re-flooding of the container with 4000 mL of deionised water containing 10 ppt concentration of sodium chloride, designed to investigate the impact of salt on the sensor readings.

In all experiments, the calibration procedure comprised: (i) calculation of the actual volumetric water content and matric suction of the tailings based on their loss of water measured by the balance, and the SWCC obtained using the Fredlund SWCC device (Fredlund, 2002), (ii) measurement of the volumetric water content and matric suction over time using the sensors, (iii) comparison between the actual values of volumetric water content and matric suction with the raw readings from the sensors to obtain calibration factors, and (iv) comparison between the drying SWCCs obtained from the sensors with that obtained from the Fredlund SWCC device.

3.2 Experimental Results

Figure 7 shows the data and photographs of the surface obtained during the initial desiccation of the red mud. As supernatant water was initially abundant on the surface, a relatively high evaporation rate was observed during the first 3 days, with some fluctuations due to the daily changes in temperature and humidity. At the start of the second day, the red mud started to desaturate, as identified by the drop in the volumetric water content and marked by the onset of cracking (see Figs 7E and 7F). The maximum evaporation rate occurred at the start of the third day, when the red mud was unsaturated and cracks were well developed. This was attributed to the newly-formed cracks enlarging the surface area for evaporation, to be greater than that from the top surface alone. This high evaporation rate did not last for long, and the rate declined rapidly as the available moisture diminished. Accompanying the fast decline in volumetric water

content, the suction increased steadily, and salt crystals started to appear on the surface of the red mud. The red mud became completely desiccated, with the evaporation rate and volumetric water content reaching close to zero, and the matric suction remaining at a constant high value.

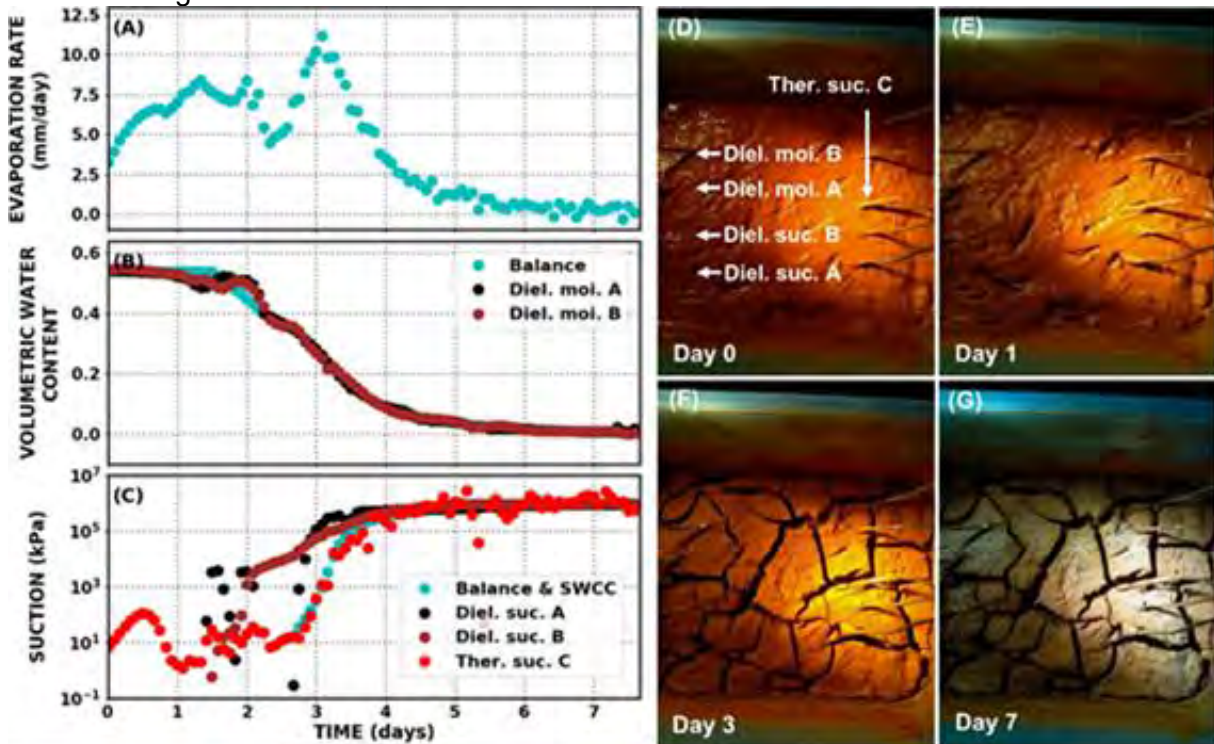


Fig. 7. Initial desiccation of red mud: (A) evaporation rate obtained from balance, (B) volumetric water content obtained from two dielectric moisture sensors and balance, (C) matric suctions calculated from balance and Fredlund SWCC and obtained from matric suction sensors, (D) photograph of surface at beginning of experiment, (E) photograph of surface at onset of cracking, (F) photograph at end of crack formation, and (G) photograph at end of experiment

During the initial desiccation of the red mud, all of the dielectric moisture sensors captured very well the desaturation of the red mud, despite one of the sensors (dielectric moisture sensor B) becoming partially exposed in a crack at the end of the experiment. The readings from the thermal matric suction sensor agreed very well with the matric suctions based on the balance and the Fredlund SWCC. However, the readings from the dielectric matric suction sensors showed a poorer match to those based on the balance and the Fredlund SWCC for suctions lower than 10^5 kPa. This is probably due to the high air-entry suction of 10^3 kPa of the ceramic plate used in these sensors. The thermal suction sensor had a ceramic cylinder with an air-entry suction of only 50 kPa, allowing matric suction measurement from this value and above.

Figure 8 shows the data and photographs of the surface obtained on re-desiccating the red mud following re-flooding. The re-flooding resulted in a reduction in matric suction, but neither broke the blocks nor narrowed the cracks. The added water largely filled the cracks and covered the surface. On re-desiccation, the changes over time of evaporation rate, volumetric water content and matric suction were similar to those obtained on initial desiccation, with some unique features induced by the pre-existing cracks. As deionised water initially covered the entire surface, the evaporation rate in the first 2 days was higher than that on initial desiccation, which involved salty pore water. The moisture sensor partially exposed in the crack (dielectric moisture sensor B) showed desaturation

earlier than the sensor fully embedded in the red mud (dielectric moisture sensor A), reflecting the early loss of water from the crack. Although some matric suction sensors were visible in the cracks (dielectric matric suction sensor B and thermal matric suction sensor C), their readings remained close to that of the sensor completely embedded in the red mud (dielectric matric suction sensor B), although the thermal matric suction sensor recorded lower suctions.

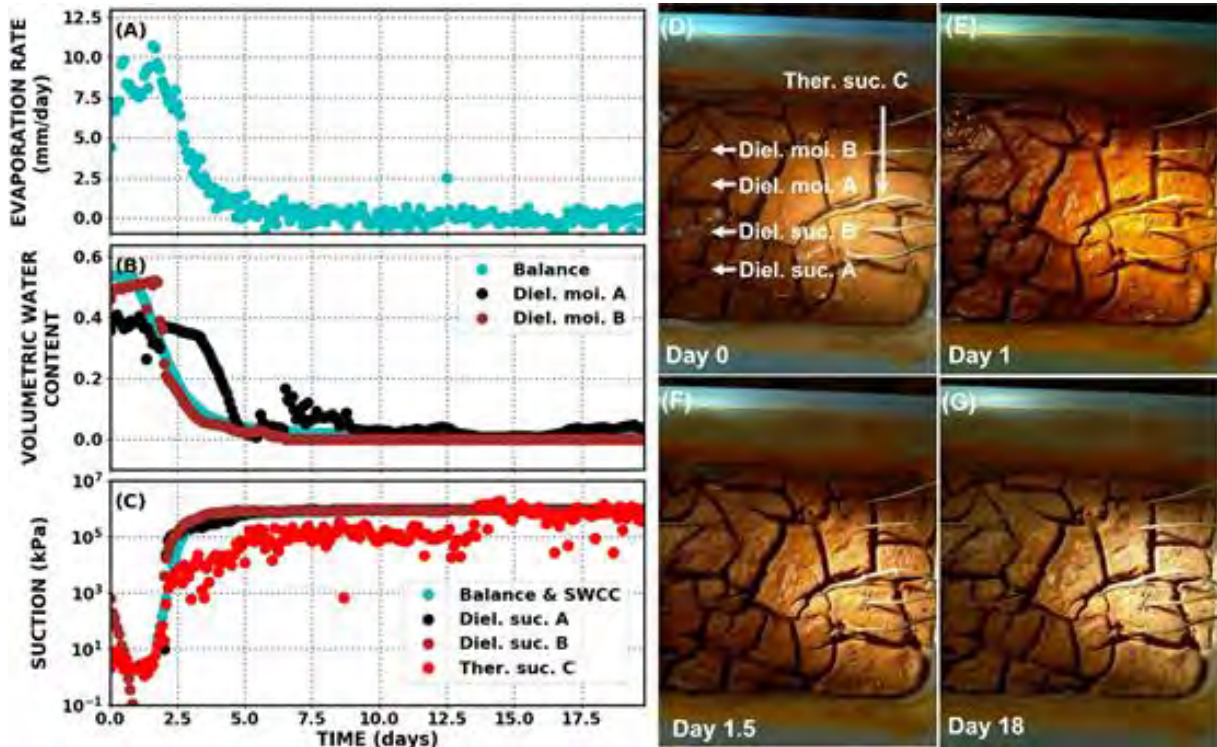


Fig. 8. Re-desiccation of red mud following re-flooding: (A) evaporation rate obtained from balance, (B) volumetric water content obtained from two dielectric moisture sensors and balance, (C) matric suctions calculated from balance and Fredlund SWCC and obtained from matric suction sensors, (D) photograph of surface at beginning of re-desiccation, (E) photograph with water remaining in cracks, (F) photograph when water in cracks had completely evaporated, and (G) photograph at end of experiment

Figure 9 shows the data and photographs of the surface obtained during the initial desiccation of the coal tailings. The evaporation rate was highest at the beginning of the experiment, followed by a sharp decrease in evaporation rate and volumetric water content. Due to their sand-size, the coal tailings did not develop significant cracks on the surface, although dry patches of relatively lighter colour appeared (see Fig. 9E), which subsequently enlarged (see Fig. 9F), indicating an increase in salinity. All of the moisture and matric suction sensors captured relatively well the drying behaviour of the coal tailings, as demonstrated by their consistency with data obtained from the balance and the Fredlund SWCC.

Figure 10 shows the data and photographs of the surface obtained during re-desiccation of the coal tailings following re-flooding with salty water. The effect of the added saline water is seen to be an initial evaporation rate of about half that obtained on initial desiccation with less saline pore water, and evaporation extended for longer. Once the tailings dried, significant salt crystallisation was observed on the tailings surface (see Fig. 10F). The presence of salt also affected the responses of the dielectric moisture sensors (see Fig. 10B), which showed a delayed drop in volumetric water content by 4 to 6 days compared to that shown by the balance. While the thermal matric suction sensors

reproduced well the matric suctions based on the balance and the Fredlund SWCC, the presence of salt led to the dielectric matric suction sensors showing a delayed increase in matric suction (see Fig. 10C).

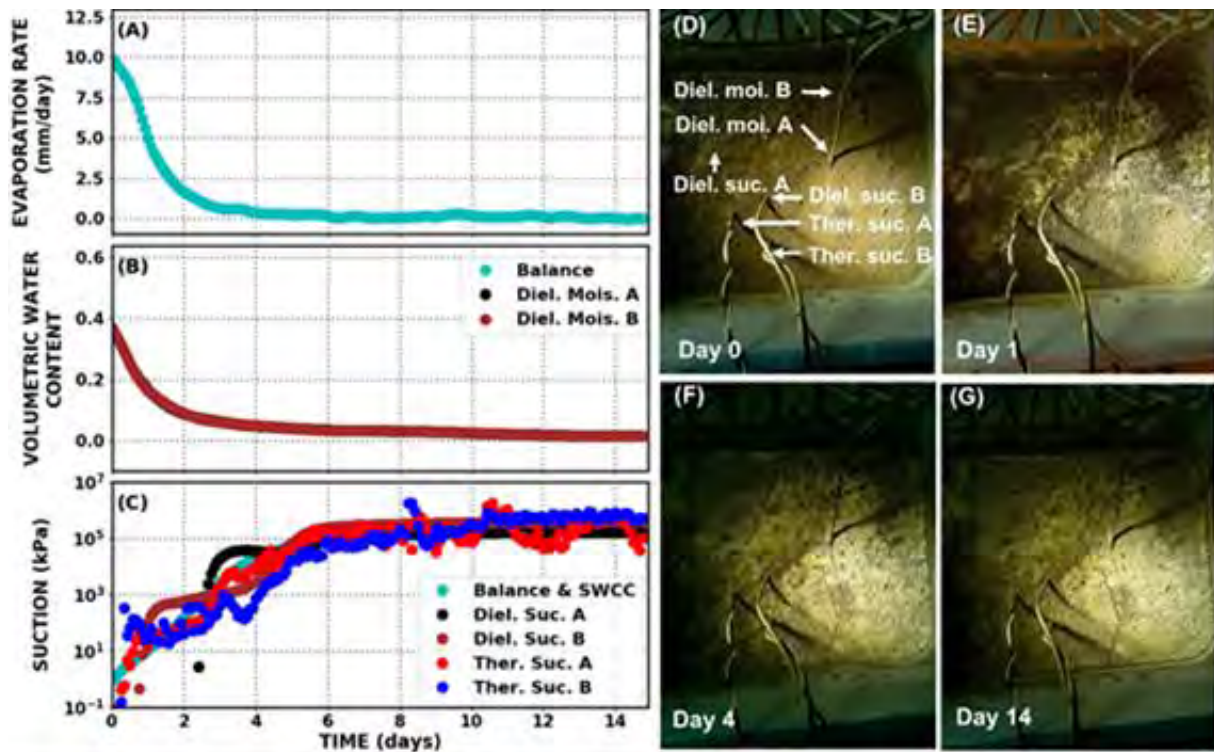


Fig. 9. Initial desiccation of coal tailings: (A) evaporation rate obtained from balance, (B) volumetric water content obtained from two dielectric moisture sensors and balance, (C) matric suctions calculated from balance and Fredlund SWCC and obtained from matric suction sensors, (D) photograph of surface at beginning of experiment, (E) photograph of surface when dry patches started to appear, (F) photograph when salt started to crystallise on surface, and (G) photograph at end of experiment

4.0 CONCLUSIONS

As found in other studies (e.g., Mortl *et al.* 2011; Malicki and Walczak, 1999), the readings from the dielectric moisture sensors were influenced by salinity. Improved accuracy could be achieved if the salinity were independently measured. The readings from the thermal matric suction sensors were confirmed to be independent of tailings salinity. The drying SWCC data obtained from the desiccation apparatus straddled reasonably well the drying SWCC measured using the Fredlund SWCC device, although the data over-estimated the air-entry suction determined using the Fredlund device. The estimation of the air-entry suction could be improved by reducing the air-entry suction of the ceramics applied in the matric suction sensors or by deploying multiple matric suction sensors with different ceramics and measurement ranges.

The further development of the instrumented tailings columns will incorporate the in-house salinity sensor that is able to measure soil salinity over the entire range from fresh water to the solubility limit. The instrumented tailings column has been deployed under controlled conditions in the laboratory, and in the field with a weather station to monitor the climatic drivers of desiccation. It is a robust and cost-effective means of assessing the sequential settling, self-weight consolidation and desiccation of tailings for use as a

basis for the design and management of tailings deposition, to assist in optimising the tailings deposition layer thickness and deposition cycle time.

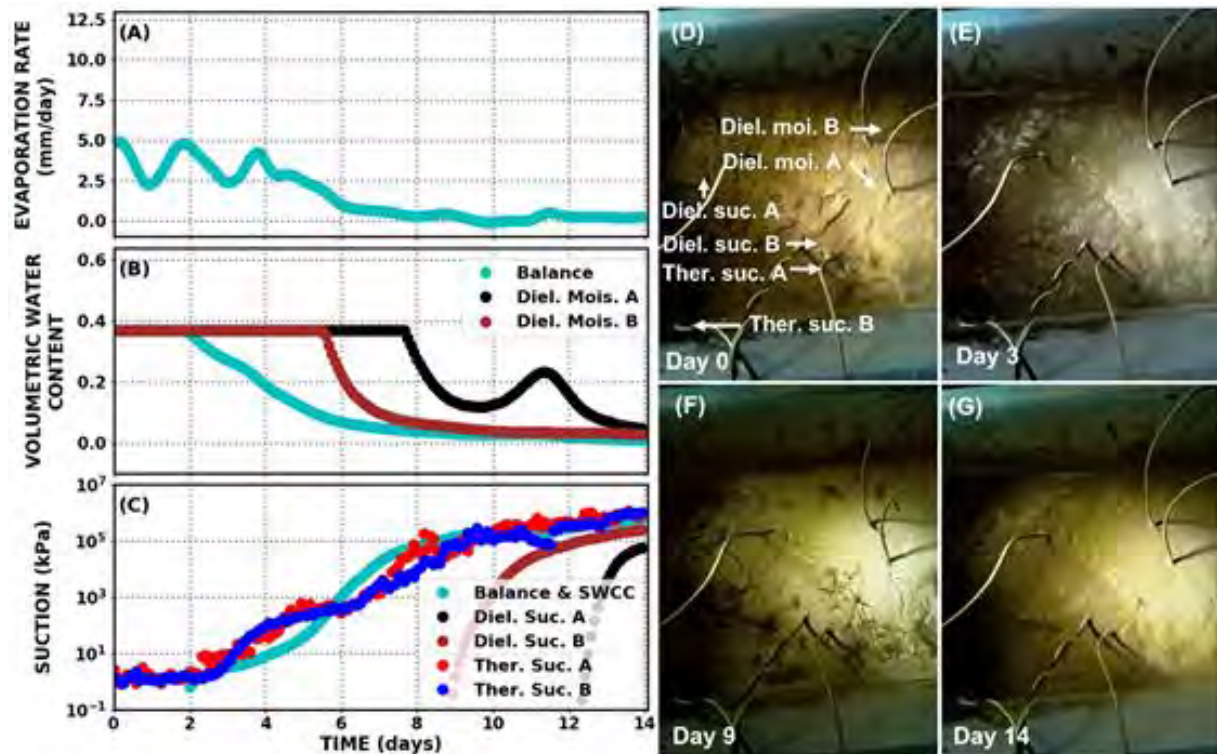


Fig. 10. Re-desiccation of coal tailings following re-flooding: (A) evaporation rate obtained from balance, (B) volumetric water content obtained from two dielectric moisture sensors and balance, (C) matric suctions calculated from balance and Fredlund SWCC and obtained from matric suction sensors, (D) photograph of surface at beginning of re-desiccation, (E) photograph when surface became exposed, (F) photograph when significant salt had crystallised on surface, and (G) photograph at end of experiment

5.0 REFERENCES

Hook, W.R., Ferré, T.P.A. and Livingston, N.J. (2004). The Effects of Salinity on the Accuracy and Uncertainty of Water Content Measurement, *Soil Science Society of America Journal*, **68** (1), 47-56.

Fredlund, D.G. (2002). Use of the soil-water characteristic curve in the implementation of unsaturated soil mechanics. *Proceedings of UNSAT 2002, Recife, Brazil, 10-13 March 2002*, 887-904.

Shokouhi, A. and Williams, D.J. (2015). Settling and consolidation behaviour of coal tailings slurry under continuous loading', *Proceedings of Tailings and Mine Waste 2015, Vancouver, Canada, 25-28 October 2015*, University of British Columbia, Vancouver, Canada, 263-274.

Shokouhi, A., Williams, D.J. and Ridgway, T.H. (2016). Settling and consolidation behaviour of red mud slurry under constant rate and incremental loading. *Proceedings of Tailings and Mine Waste 2016, Keystone, Colorado, USA, 2-5 October 2016*, 85-94.

Zhang, C., Williams, D.J. and Shokouhi, A. (2016). Settling, self-weight consolidation and desiccation of coal mine tailings in a laboratory column. *Proceedings of Tailings and Mine Waste 2016, Keystone, Colorado, USA, 2-5 October 2016*, 95-104.

Fisseha, B., Bryan, R. and Simms, P. (2010). Evaporation, unsaturated flow, and salt accumulation in multilayer deposits of "paste" gold tailings. *Journal of Geotechnical and Geoenvironmental Engineering* 136, 1703-1712.

Konrad, J.M. and Ayad, R. (1997). Desiccation of a sensitive clay: field experimental observations. *Canadian Geotechnical Journal*, **34**, 929-942.

Malicki, M.A. and Walczak, R.T. (1999). Evaluating soil salinity status from bulk electrical conductivity and permittivity. *European Journal of Soil Science*, **50**(3), 505-514.

Mortl, A., Munoz-Carpena, R., Kaplan, D. and Li, Y. (2011). Calibration of a combined dielectric probe for soil moisture and porewater salinity measurement in organic and mineral coastal wetland soils. *Geoderma*, **161**(1-2), 50-62.

CONVERTING CHEMISTRY TO MINERALOGY FOR ACID AND METALLIFEROUS DRAINAGE RISK MANAGEMENT

J. Taylor^A, S. Winchester^B, M. Tyler^C, K. Ehrig^C, J. Waters^A and F. Beavis^A.

^AEarth Systems, 14 Church St., Hawthorn, VIC 3122, Australia

^BGHD, 133 Castlereagh St., Sydney, NSW 2000, Australia

^CBHP, 55 Grenfell St., Adelaide, SA 5000, Australia

ABSTRACT

Static geochemical data provides the foundation for quantifying the risk posed by sulfidic mine materials, including waste rock, tailings, wall rock, ore and low-grade ore stockpiles, heap leach pads and concentrate stockpiles. A new approach to developing a detailed acid and metalliferous drainage (AMD) risk layer for a mine model was recently developed for the Olympic Dam Fe-oxide Cu-U-Au-Ag deposit.

Major and trace element chemistry data from all resource drill holes are routinely collected at Olympic Dam. 65 analytical parameters, including carbon dioxide, were measured for a dataset of 10,000 samples, each representing a 15 m drill hole intersection. A program was developed to allocate the chemical components to 30 ore and gangue minerals known to occur at Olympic Dam, resulting in the production of a highly detailed modal mineralogy for each analysed intersection. The maximum potential acidity (MPA) and acid neutralising capacity (ANC) values were calculated from the key reactive minerals in each intersection. Key acidity generating minerals included pyrite, chalcopyrite, bornite and chalcocite. The dominant acid neutralising minerals included dolomite and ankerite; however, abundant siderite was also present. Net acid producing potential (NAPP) values were calculated from the MPA and ANC from each sample. AMD classification data identifying non-acid forming (NAF) and potentially acid forming (PAF) materials based on calculated NAPP values was produced for part of the deposit. 250 samples of drill hole material were collected and submitted to a NATA accredited laboratory for static geochemical analysis to assess the accuracy of the calculated mineralogy and associated NAPP values. The AMD risk classification for the laboratory data and the calculated mineralogy was shown to be well correlated.

It is concluded that bulk rock chemistry data can be used to accurately calculate mineralogy to develop AMD risk layers for mine block models, potentially dramatically improving AMD management and closure outcomes without the need for additional laboratory-generated geochemical data and at very little relative and absolute cost.

1.0 INTRODUCTION

The Olympic Dam mine is in South Australia, approximately 550 km northwest of Adelaide. The operation mines copper, uranium, gold and silver. While production commenced in 1988, the mine has been owned and operated by BHP Ltd (BHP) since 2005.

The copper mineralisation at Olympic Dam is associated with copper-bearing sulfides, including bornite (Cu_5FeS_4), chalcocite (Cu_2S) and chalcopyrite (CuFeS_2), together with pyrite (FeS_2), hosted in a hematite-rich breccia complex located beneath 350 m of unmineralised sedimentary rocks (BHP 2016). The ore body occurs to a depth of approximately 650 m in Precambrian basement rocks (BHP 2013). The basement rocks are overlain by a generally horizontally bedded overburden sequence comprising three main units. The deepest overburden unit is the Tregolana Shale, which immediately overlies the orebody. The Tregolana Shale is overlain by approximately 200 m of

Arcoona Quartzite, which is overlain by a 40-100 m thick deposit of the Andamooka Limestone (BHP 2013).

Operations at Olympic Dam comprise an underground mine, surface quarry, a mineral processing plant and associated infrastructure located within the Special Mining Lease (SML) area of approximately 180 km² (BHP 2016). The primary extraction method is a variant of sublevel open stoping, in which blocks of mineralised ore are systematically blasted and the ore recovered for crushing below ground. The crushed ore is then raised up one of the shafts to the surface stockpile (BHP 2016). Following extraction, stopes are backfilled with a cemented aggregate of crushed waste rock or crushed dolomite/limestone (BHP 2016). Above ground the metallurgical plant comprises a copper concentrator, a hydrometallurgical plant, uranium calciners, a copper smelter, a sulfuric acid plant, a copper refinery and a gold and silver refinery (BHP 2016).

1.1 Environmental Geochemistry

Previous studies (SRK 2008; AECOM 2010) have suggested that some Olympic Dam materials are potentially acid forming based on limited static geochemical data. These materials include granitic and hematitic major units and a minor laminated hematite-quartz sandstone/siltstone unit within the basement complex.

Future scenarios for Olympic Dam could include the construction of low grade ore (LGO) and waste stockpiles. These will contain elevated copper and sulfur concentrations. Dependent on the nature of these materials and future economic conditions, they may be stockpiled for 40 years or more. Approximately 60 million tonnes (t) of material may ultimately be stockpiled at Olympic Dam. The potential for acid formation in stockpiles and the occurrence of materials that may be used to manage PAF materials is largely unknown but important for the future.

1.2 Available Data

Between 2003 and 2008, BHP completed a routine assay program of approximately 1,000 surface diamond holes (~448,000 m) and approximately 1,600 underground diamond holes (Ehrig et al. 2012). Routine assays were conducted on composited samples over lengths of either 1, 2.5 or 5 metres. This equated to more than 1.3 million samples from the major and minor basement complex units analysed. These samples were analysed for Au, Ag, Al, As, Ba, Ca, Ce, Co, Cu, Fe, K, La, Mg, Mn, Mo, Na, Ni, P, Pb, S, Si, Ti, U₃O₈, Zn, Zr and CO₂. In addition, some 5,236 samples were assayed in overburden. The routine overburden assay included: Ag, Al, As, Ba, Bi, Ca, Cd, Ce, Co, Cr, Cu, Fe, K, La, Mg, Mn, Mo, Na, Ni, P, Pb, S, Sb, Si, Ti, U₃O₈, V, Y, Zn, Zr and CO₂.

Approximately 10,000 samples also underwent extended assaying (Ehrig et al. 2012). The samples were selected from the major and minor basement complex units and were collected on a widely spaced grid across the deposit. The extended assay involved analysing a composited sample over a sample length of between approximately 15 and 20 metres. The assay was for 65 elements including Ag, Al, As, Au, Ba, Be, Bi, Br, Ca, Cd, Ce, Cl, Co, Cr, Cs, Cu, Dy, Er, Eu, F, Fe, Ga, Gd, Hf, Ho, I, In, K, La, Li, Lu, Mg, Mn, Mo, Na, Nb, Nd, Ni, P, Pb, Pr, Rb, S, Sb, Sc, Se, Si, Sm, Sn, Sr, Ta, Tb, Te, Th, Ti, Tl, Tm, U₃O₈, V, W, Y, Yb, Zn, Zr and CO₂.

Mineralogy was also measured on the extended assay database using a Mineral Liberation Analyzer (MLA) (Ehrig et al. 2012). Quantitative XRD (X-ray diffraction) analysis was completed on 6,000 of the 10,000 samples. The MLA and XRD data generated a suite of up to 15 minerals per sample, but as no acid neutralising minerals were identified with these methods, the mineralogy could not be used to conduct acid-base accounting. The major mineralogy of the deposit was defined as quartz, hematite,

sericite, orthoclase, siderite, chlorite, barite, fluorite, chalcopyrite, albite, pyrite, bornite, rutile, ankerite, chalcocite, dolomite, crandallite and apatite (Ehrig et al. 2012). Minor and trace minerals include uraninite, coffinite, brannerite, florencite, bastnasite, cobalt sulphide, millerite, galena, sphalerite, molybdenite, zircon and carrolite (Reeve et al., 1990).

2.0 STUDY SCOPE

BHP engaged GHD Pty Ltd (GHD) and Earth Systems Consulting Pty Ltd (Earth Systems) to undertake a geochemical investigation of the Olympic Dam mineral waste and LGO to assess acid and metalliferous drainage (AMD) risk. Prior to this study, no comprehensive information on the static geochemistry of the ore, LGO and waste rock materials at Olympic Dam had been collected.

To generate an AMD Risk layer in the mine block model, two approaches were considered:

- Analyse thousands of (aged) existing samples for static geochemical parameters; or
- Use available bulk chemical data to calculate the mineralogy of the ore, LGO and waste rock materials, and use this information to calculate the net acid producing potential (NAPP) values of each sample.

The calculation approach was selected as the most appropriate and lowest cost method for obtaining new static geochemical data. This study describes the method for calculating the mineralogy and verifying the accuracy of using bulk chemistry data to classify the AMD risk of geologic materials.

3.0 METHOD

3.1 Calculation of Mineralogy

The method assumes a maximum of 31 minerals are potentially present in the basement rock types. These include primary and hydrothermal phases. Following careful examination of these minerals, a software tool was developed to assign elemental data and CO₂ from the extended assay bulk chemistry database to specific minerals in a sequence that minimised chemical ambiguity. For example, sulfur was initially stoichiometrically assigned to trace metals such as Zn, Pb, Co, Ni and Mo based on their occurrence as sulphide minerals (see below). Remaining sulfur was then stoichiometrically assigned to barite (as the only barium-bearing mineral). Any residual sulfur from this process was then assigned to the three copper sulphide minerals. All sulfur remaining after this process was assumed to be in the form of pyrite. The same method was applied to other silicate, carbonate and oxide phases. Following some experimentation, the optimum explicit order of element assignment was developed and is documented below.

Solid solution compositions for some minerals were varied to ensure that mineral percent totals were as close to 100% as possible. The order of assignment of elemental and CO₂ data to minerals is provided below. Specific solid solution compositions are also provided for each mineral phase.

- Uranium: Pitchblende / uraninite (UO₂), coffinite (U(SiO₄)_{0.9}(OH)_{0.4}), brannerite ((U_{0.5}Ca_{0.3}Ce_{0.2})(Ti_{1.5}Fe_{0.5})O₆);
- Cerium: Florencite (CeAl₃(PO₄)₂(OH)₆), bastnasite (Ce(CO₃)F);
- Zn, Pb, Co, Ni and Mo: Sphalerite (ZnS), galena (PbS), cobalt disulfide (CoS₂), millerite (NiS), molybdenite (MoS₂), carrollite (CuCo₂S₄);

- Barium: Barite (BaSO_4);
- Potassium: K-feldspar (KAlSi_3O_8), muscovite / sericite ($\text{KAl}_3\text{Si}_3\text{O}_{10}(\text{OH})_2$), F-muscovite / F-sericite ($\text{KAl}_3\text{Si}_3\text{O}_{10}(\text{OH})_{1.8}\text{F}_{0.2}$);
- Sodium: Na-feldspar ($\text{NaAlSi}_3\text{O}_8$), paragonite ($\text{NaAl}_3\text{Si}_3\text{O}_{10}(\text{OH})_2$), F-paragonite ($\text{NaAl}_3\text{Si}_3\text{O}_{10}(\text{OH})_{1.8}\text{F}_{0.2}$);
- Calcium: Dolomite ($\text{CaMg}(\text{CO}_3)_2$);
- Residual fluorine: Fluorite (CaF_2);
- Phosphorus: Hydroxyapatite ($\text{Ca}_5(\text{PO}_4)_3\text{OH}$), fluor-apatite ($\text{Ca}_5(\text{PO}_4)_3\text{F}$), apatite ($\text{Ca}_5(\text{PO}_4)_3\text{OH}_{0.33}\text{F}_{0.33}\text{Cl}_{0.33}$);
- CO_2 bearing phases: Siderite (FeCO_3), ankerite ($\text{CaFe}_{0.6}\text{Mg}_{0.3}\text{Mn}_{0.1}(\text{CO}_3)_2$);
- Titanium: Rutile (TiO_2), ilmenite (FeTiO_3);
- Residual Mg and Al: Chlorite ($\text{Fe}_3\text{Mg}_{1.5}\text{AlFe}_{0.5}(\text{AlSi}_3)\text{O}_{10}(\text{OH},\text{O})_8$), kaolinite ($\text{Al}_2\text{Si}_2\text{O}_5(\text{OH})_4$);
- Copper and iron sulfide minerals: Chalcopyrite (CuFeS_2), bornite (Cu_5FeS_4), chalcocite (Cu_2S), pyrite (FeS_2);
- Zirconium: Zircon (ZrSiO_4); and
- Residual Fe and Si: Quartz (SiO_2), hematite (Fe_2O_3).

Algorithms for quantifying the relative proportion of different copper minerals were provided by BHPB staff. The assignment of sulfur to form sulfide minerals with Zn, Pb, Co, Ni and Mo was based on recorded mineralogy from the deposit (Reeve et al., 1990). Solid solution compositions were chosen based on available information for mineral chemistry, as well as by conducting controlled variations to minimise the deviation of mineral totals from 100%.

3.2 Calculation of AMD Risk

Once the modal mineralogy was calculated from the bulk chemistry data, the key acid forming and acid neutralising mineral phases were used to calculate a maximum potential acidity (MPA), an acid neutralising capacity (ANC) and thereby a NAPP value for each sample interval. The main acid generating phases were pyrite, chalcopyrite, bornite and chalcocite, while the key acid consuming phase was dominated by dolomite.

Siderite is both widespread and relatively abundant at Olympic Dam, but it has no net neutralising capacity. While it can initially neutralise acid, the eventual precipitation of ferrihydrite from the iron in siderite generates as much acid as it neutralises.

Earth Systems' AMDact software (Acid and Metalliferous Drainage assessment and classification tool), utilised the calculated MPA, ANC and NAPP values to produce an AMD risk classification for each sample interval. Positive NAPP values were nominated as potentially acid forming (PAF) and negative NAPP values were nominated as non-acid forming (NAF).

3.3 Verification Testing

To validate the accuracy of the AMD risk classification generated from the mineralogical calculations, a laboratory static geochemical testwork program was undertaken on a subset of 250 representative samples from the routine assay database.

Laboratory analysis included acid base accounting (ABA) (ANC and chromium reducible sulfur (S_{Cr})), and single addition net acid generation (NAG) testwork on all 250 samples. Acid buffering characteristics curves (ABCC) and total sulfur analyses were completed on a subset of 25 samples. Results were used to calculate the NAPP values for the 250 samples using S_{Cr} and ANC values. S_{Cr} data rather than total sulfur data was used to calculate NAPP values for the sample intervals due to the widespread occurrence of non-acid forming barite ($BaSO_4$) in the deposit. This approach minimised the inaccuracy of the laboratory data. The laboratory data was then processed using AMDact to quantify the AMD risk classification of each sample.

MPA, ANC, NAPP and AMD risk classifications that were calculated from modelled mineralogical data were compared with the laboratory data to assess the validity of the method.

4.0 RESULTS

The modal mineralogies of four of the 10,000 samples determined by strategic allocation of the extended elemental data and CO_2 to the mineral list provided above are shown in Table 1. Table 2 summarises the AMD risk classifications based on the calculated mineralogy of the extended suite geochemical dataset for all 10,000 samples. The results indicate approximately 61% (n=6,115 of 10,002) of all samples were PAF, 99.6% (n=951 of 955) of ore samples were PAF, and some 92% (n=2,846 of 3,079) of all LGO samples were PAF. Approximately 61% (n=3,643 of 5,959) of waste rock samples were NAF, and 39% (n=2,316 of 5,959) PAF.

To verify the accuracy of the AMD risk classification generated from the mineralogical modelling, the laboratory derived acid-base accounting results were compared with the modelled data in Table 3. There is a relatively good correlation between the mean laboratory determined NAPP values and the mean calculated NAPP values for ore, LGO and waste rock. Median NAPP values were also comparable. The mean ANC also demonstrated a relatively good correlation for ore, LGO and waste rock between the two datasets.

Laboratory $NAG_{7.0}$ values were poorly correlated with laboratory NAPP (S_{Cr}) values, and poorly correlated with calculated NAPP values. The widespread occurrence and relative abundance of siderite suggests that $NAG_{7.0}$ values may be under estimating the acidity generation associated with the oxidation of iron from siderite. This can happen in laboratory testwork if the NAG leachate undergoes titration prior to full oxidation of iron. The full oxidation and precipitation of iron generates acid, but this effect is not seen if the titration is conducted prematurely. This has the effect of erroneously assigning some neutralisation capacity to siderite. The disparity between $NAG_{7.0}$ values and NAPP (S_{Cr}) values suggests that the latter is more appropriate for comparison with calculated NAPP data.

Table 1. Example modal mineralogies for four samples

Mineral	Formula		1	2	3	4
Quartz	SiO_2	wt. %	54.5	36.2	16.9	7.79
K-Feldspar	$KAlSi_3O_8$	wt. %	14.6	1.68	0.28	0.03
Na-Feldspar	$NaAlSi_3O_8$	wt. %	0.00	0.27	0.21	0.15
Hematite	Fe_2O_3	wt. %	4.90	45.0	72.1	85.0
Muscovite / Sericite	$KAl_3Si_3O_{10}(OH)_2$	wt. %	0.00	0.00	0.00	0.00
F-Muscovite / F-Sericite	$KAl_3Si_3O_{10}(OH)_{1.8}F_{0.2}$	wt. %	21.6	3.62	0.61	0.06
Paragonite	$NaAl_3Si_3O_{10}(OH)_{1.8}F_{0.2}$	wt. %	0.00	0.27	0.20	0.00
Siderite	$FeCO_3$	wt. %	2.52	0.00	0.00	0.21

Mineral	Formula		1	2	3	4
Chlorite	$(\text{Fe}_3\text{Mg}_{1.5}\text{AlFe}_{0.5}(\text{AlSi}_3)\text{O}_{10}(\text{OH},\text{O})_8$	wt. %	0.00	1.35	0.87	0.00
Fluorite	CaF_2	wt. %	0.04	2.01	0.12	0.04
Barite	BaSO_4	wt. %	0.45	0.46	0.06	5.04
Ilmenite	FeTiO_3	wt. %	0.00	0.00	0.00	0.00
Kaolinite	$\text{Al}_2\text{Si}_2\text{O}_5(\text{OH})_4$	wt. %	0.00	4.74	2.62	0.00
Dolomite	$\text{CaMg}(\text{CO}_3)_2$	wt. %	0.59	0.00	0.06	1.05
Pyrite	FeS_2	wt. %	0.00	2.16	3.07	0.26
Chalcopyrite	CuFeS_2	wt. %	0.38	0.00	2.63	0.13
Bornite	Cu_5FeS_4	wt. %	0.00	0.51	0.00	0.00
Chalcocite	Cu_2S	wt. %	0.00	1.21	0.00	0.00
Pitchblende / Uraninite	UO_2	wt. %	0.00	0.06	0.03	0.00
Coffinite	$\text{U}(\text{SiO}_4)_{0.9}(\text{OH})_{0.4}$	wt. %	0.00	0.01	0.00	0.00
Brannerite	$(\text{U}_{0.5}\text{Ca}_{0.3}\text{Ce}_{0.2})(\text{Ti}_{1.5}\text{Fe}_{0.5})\text{O}_6$	wt. %	0.00	0.00	0.00	0.00
Florencite	$\text{CeAl}_3(\text{PO}_4)_2(\text{OH})_6$	wt. %	0.03	0.12	0.07	0.06
Bastnasite	$\text{Ce}(\text{CO}_3)\text{F}$	wt. %	0.05	0.12	0.11	0.10
Cobalt Sulfide	CoS_2	wt. %	0.00	0.00	0.00	0.00
Millerite	NiS	wt. %	0.00	0.00	0.00	0.00
Galena	PbS	wt. %	0.00	0.01	0.00	0.00
Sphalerite	ZnS	wt. %	0.01	0.01	0.01	0.01
Molybdenite	MoS_2	wt. %	0.00	0.01	0.00	0.02
Rutile	TiO_2	wt. %	0.32	0.13	0.03	0.05
Zircon	ZrSiO_4	wt. %	0.06	0.02	0.01	0.00
Carrollite	CuCo_2S_4	wt. %	0.00	0.00	0.00	0.00
Total		wt. %	100.0	100.0	100.0	100.0

Table 2. AMD risk classification for 10,000 samples by material type

Material Type	General Classification		Detailed Classification					
	PAF	NAF	PAF			NAF		
			High Potential for Acid Generation (AG)	Moderate/High Potential for AG	Moderate Potential for AG	Low Potential for AG	Unlikely to be AG	Likely to be Acid Consuming
Waste	39%	61%	1%	5%	31%	2%	59%	2%
Ore	100%	0%	17%	55%	27%	1%	0%	0%
LGO	92%	8%	10%	39%	40%	3%	7%	1%

Table 3. Comparison of modelled and laboratory results by material type

Material type	pH (OX)		NAG (pH 4.5)		NAG (pH 7.0)		ANC		MPA (S _{CR})		NAPP (S _{CR})		Sulfur (S _{CR})		
	Laboratory	Unit	Laboratory	kg H ₂ SO ₄ /t	Laboratory	kg H ₂ SO ₄ /t	Laboratory	kg H ₂ SO ₄ /t	Laboratory	kg H ₂ SO ₄ /t	Laboratory	kg H ₂ SO ₄ /t	Laboratory	wt. %	
LGO (n=150 samples)															
Maximum	9.10		25.8		50.4		100		95.5		87.0		97.3		3.12
Minimum	2.80		0.05		0.05		0.80		0.00		-92.7		-238		0.00
Mean	5.66		2.64		13.6		12.5		28.7		16.2		18.7		0.94
Median	5.30		0.05		9.65		8.80		21.6		10.2		13.2		0.71
Range	6.30		25.8		50.4		99.2		95.5		180		335		3.12
Ore (n=25 samples)															
Number samples	25		25		25		25		25		25		25		25
Maximum	8.80		11.4		60.0		112		138		120.5		126		4.51
Minimum	3.30		0.05		0.05		3.10		3.27		-87.7		-55.2		0.11
Mean	6.11		1.46		14.8		18.7		54.3		35.7		37.2		1.78
Median	6.40		0.05		1.60		9.00		49.6		36.0		32.8		1.62
Range	5.50		11.4		60.0		109		135		208		181		4.40
Waste (n=75 samples)															
Maximum	9.50		27.0		44.2		142		74.1		70.7		81.6		2.42
Minimum	2.80		0.05		0.05		1.80		0.18		-122		-107		0.01
Mean	6.79		0.67		3.61		19.1		9.12		-10.0		-2.57		0.30
Median	7.00		0.05		0.05		9.30		3.55		-5.11		-2.35		0.12
Range	6.70		27.0		44.2		140		73.9		193		188.7		2.41

5.0 DISCUSSION

While comparison of the statistics for NAPP (S_{Cr}) values and calculated NAPP values is encouraging, individual values are not always closely correlated. A key problem with this observation is that it is not clear which of the datasets is likely to be more accurate. The laboratory NAPP (S_{Cr}) values are based on the assumption that the key sulfide is pyrite, whereas the calculated NAPP values determine the specific sulfide species (pyrite, chalcopyrite, bornite, chalcocite, sphalerite, galena, cobalt disulfide, millerite, molybdenite and carrollite) and assign a modal mineralogy specific NAPP value. This suggests that the calculated NAPP values could be more accurate than the laboratory data.

Hence, to better assess the correlation between the two NAPP datasets, NAPP values were overlooked in preference to the AMD risk classification of each sample, a less sensitive but still fundamentally important metric. The correlation between NAF and PAF materials for ore, LGO and waste rock, as determined by laboratory testwork and mineralogical calculations, is displayed in Figure 1.

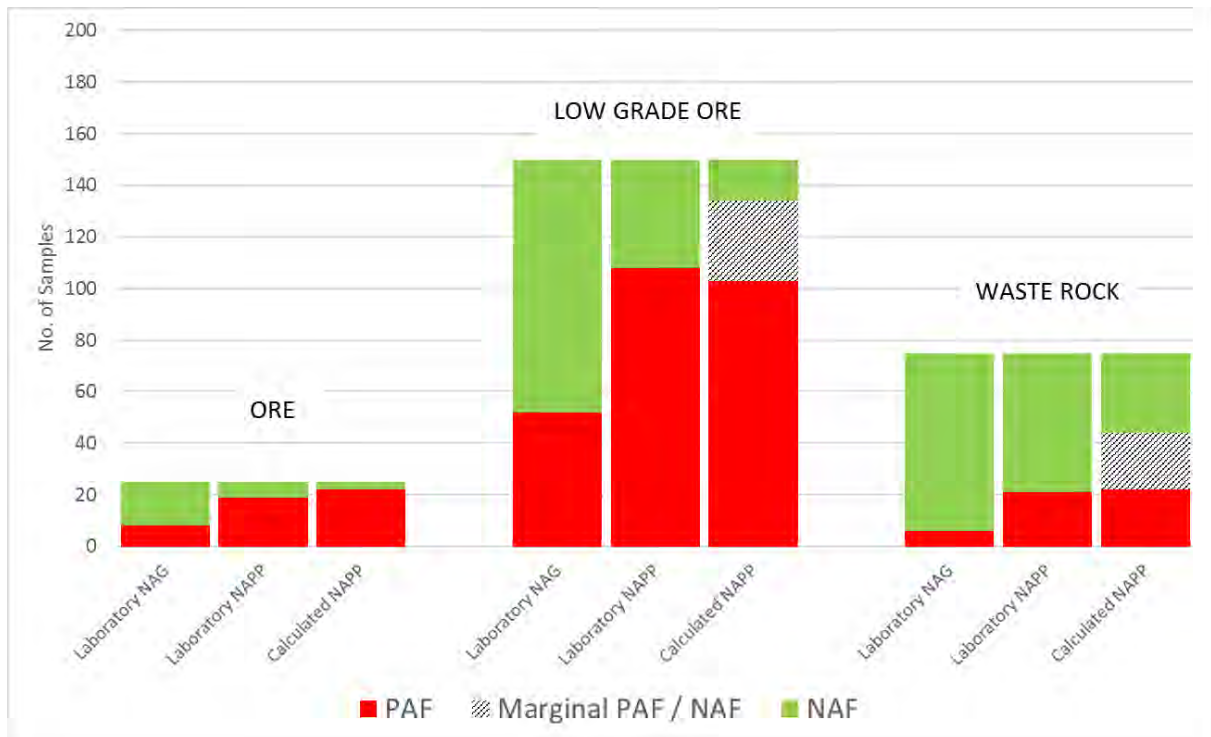


Figure 1. Comparison of AMD Risk classification between laboratory and calculated NAPP data

It is evident from Figure 1 that there is a very good correlation between AMD risk classification as determined for ore, LGO and waste rock materials, between laboratory NAPP (S_{Cr}) values and calculated NAPP values if we regard calculated NAPP values in the range $-5 \text{ kg H}_2\text{SO}_4/\text{tonne}$ to $+5 \text{ kg H}_2\text{SO}_4/\text{tonne}$ as effectively NAF (ie. marginal NAF/PAF). Figure 1 also highlights the poor correlation between laboratory NAG_{7.0} values and either of the NAPP datasets.

6.0 CONCLUSIONS

The study has confirmed that it is possible to generate an AMD risk model for the Olympic Dam deposit using available bulk rock chemistry data to calculate detailed modal

mineralogical data, derive NAPP data and classify AMD risk, rather than conducting widespread and expensive re-analysis of geological samples. The study has also reinforced the importance of calculating the detailed mineralogical composition from major and trace components, rather than just establishing ANC from Ca, Mg and CO₂.

Classifying the AMD risk of the Olympic Dam deposit using the bulk chemistry database is key to understanding the AMD risk for operational and closure management at Olympic Dam. The integration of the AMD risk layer in the mine block model will facilitate short to long-term mine planning, ensuring that the LGO and waste rock is extracted and strategically placed to facilitate optimum metal recovery from LGO or effective AMD management.

It is concluded that bulk rock chemistry data can be used to accurately calculate mineralogy to develop AMD risk layers for mine block models, potentially dramatically improving AMD management and closure outcomes without the need for additional laboratory-generated geochemical data and at a low cost.

7.0 REFERENCES

AECOM (2010) Olympic Dam Kinetic Testing Program, Supplement to Appendix K5 of the Olympic Dam Draft EIS in BHP Billiton 2011, Olympic Dam Expansion Supplementary Environmental Impact Statement, Appendix F6.

BHP (2013) Olympic Dam Mine Closure and Rehabilitation Plan 2013. Document No. 99232 V3. September 2013.

BHP (2016) Olympic Dam Environment Management Manual. Document No. 2617 V20. 9 May 2016.

Ehrig K, McPhie J and Kamenetsky V (2012) Geology and Mineralogical Zonation of the Olympic Dam Iron Oxide Cu-U-Au-Ag Deposit, South Australia. *Society of Economic Geologists, Inc. Special Publication 16: 237-267.*

Reeve, J. S., Cross, K. C., Smith, R. N. and Oreskes, N., 1990. Olympic Dam Copper-Uranium-Gold-Silver Deposit, in Geology of the mineral deposits of Australia and Papua New Guinea (Ed. F. E. Hughes), pp. 1009-1035 (The Australian Institute of Mining and Metallurgy, Melbourne).

SRK (2008) Olympic Dam Expansion Assessment Olympic Dam Mine Rock Geochemistry in BHP Billiton 2009, Olympic Dam Expansion Draft Environmental Impact Statement, Appendix K5.

MULTIPLE KINETIC TESTING METHODS TO UNDERSTAND THE AMD/NMD POTENTIAL OF HIGH SULPHUR, HIGH ANC WASTE ROCK

B. Usher^A, M. Landers^{AB} and P. Marianelli^C

^AKlohn Crippen Berger, Level 5 – 43 Peel Street, South Brisbane, Qld 4101, Australia

^BRGS Environmental Pty Ltd, 123 Wynne St, Sunnybank Hills, Qld 4109, Australia

^CGlencore, McArthur River Mine Pty Ltd, Level 9 – 307 Queen St, Brisbane, Qld 4000, Australia

ABSTRACT

Multiple types of kinetic tests have been used to provide a robust evaluation of geochemical reactivity and water quality at a metalliferous mine, where the waste rock ranges from relatively inert to enriched in sulphides but with high acid neutralisation capacity. More than 20 longer-term kinetic laboratory tests, using standard humidity cells (MEND methodology) and column leach testing (AMIRA), have been supported by oxygen consumption rate (OCR) tests undertaken at a range of moisture contents to assess reactivity as a function of liquid to solid ratios. Laboratory testing is supported by the observations from field water quality monitoring and 15 field barrels containing different mine waste materials.

Kinetic testing has been underway for more than two years for each of these programs, but the elevated sulphide/high ANC nature of much of the waste material means that tests will run for a considerable period before a complete set of data representing various stages of weathering and geochemical evolution is obtained. Results to date indicate that, while the inferred reaction rates are in a similar order, calculated rates from columns are slightly lower, largely related to solubility constraints. Despite this, rates from OCR, humidity cell and column results show good agreement between the data sets and within the ranges of literature values, for given sulphur concentrations. Results obtained from site monitoring, field barrels and laboratory kinetic tests also exhibit consistency in the behaviour of the various geochemical waste rock classes.

Data from the array of kinetic tests so far indicates that the broad waste rock geochemical classification scheme is appropriate. The kinetic testing program provides valuable data to support the proposed design and management of the waste facilities, and has shown the value in undertaking a range of kinetic testing types to provide complementary data.

1.0 INTRODUCTION

1.1 Background

Glencore's McArthur River Mine (MRM) is a major open-cut operation that mines one of the largest known sedimentary stratiform zinc-lead-silver deposits in the world. Underground mining of zinc-lead commenced in 1995, and the mine was converted to an open-cut operation in 2003. The geochemical understanding, prediction and identification of overburden at MRM has evolved significantly over the last decade, driven by advances in geochemical sampling and testing, evolving industry practice, stakeholder expectations and changing regulatory frameworks.

Detailed geochemical characterisation for the site has been completed according to international guidelines including GARD (2009), Price (2009) and Australian interpretation methods such as AMIRA (2002). The key geochemical properties for each class is based on testing of overburden samples including acid base accounting (ABA), sulphur speciation, organic carbon, X-ray diffraction (XRD), whole rock analysis, net acid generation (NAG) testing (including sequential and kinetic NAG tests), shake flask extraction (SFE) and acid buffering characteristic curves (ABCC).

The approach taken for kinetic testing has focused on providing an understanding of the reaction rates, water quality evolution and principle drivers on water quality for the site. To provide increased robustness in the results, multiple types of kinetic testing have been employed so that a robust evaluation of geochemical reactivity and water quality could be obtained and to preclude reliance on a single method. The use of multiple approaches to provide different, but complementary geochemical information, has been followed.

The aims of the kinetic program include:

- Confirmation of the static geochemical characterisation/testing.
- Supporting measured data for the behavior of the different waste classes on site.
- Assessment of the geochemical loading rates for different waste materials/waste classes under a variety of geochemical conditions.
- Measured data to support the conceptual understanding of the drivers on site water quality.
- Providing the conceptual understanding and loading rates for life-of-mine planning, and Closure water quality assessments.

2.0 METHODS

Kinetic laboratory testing includes standard humidity cells (using MEND methodology), column leach testing (using the Australian standard AMIRA methodology) and oxygen consumption rate (OCR) tests undertaken at a range of moisture contents to assess sulphide reactivity as a function of liquid to solid ratios.

The kinetic samples were selected based on detailed static testing of the waste rock, which includes all of the testing specified by the NT regulatory guidance and comprises acid-base accounting, short-term leach tests (using shake flask extraction tests), net acid generation (NAG) tests (including analysis of the resultant supernatant for selected samples) and whole rock elemental analysis. A representative sample set was selected on which static testing included detailed mineralogy through X-ray diffraction (XRD) and quantitative evaluation of mineralogy by scanning electron microscopy (QEMScan), kinetic NAG testing, acid-base characteristic curve determinations (ABCC) and, where needed, assessment of the potential for thiosalts/thiosalt acidification. This was to select samples representing the expected range of variability in geochemical response from the major lithological units/ waste rock classes at MRM.

The ANC (H_2SO_4 kg/t) and sulphide as S (%) contents were important in the selection process, as these define the expected PAF/NAF nature of the samples. A representative distribution of high sulphide, average sulphide and various ANC samples was selected (see Figure 1 and Figure 2).

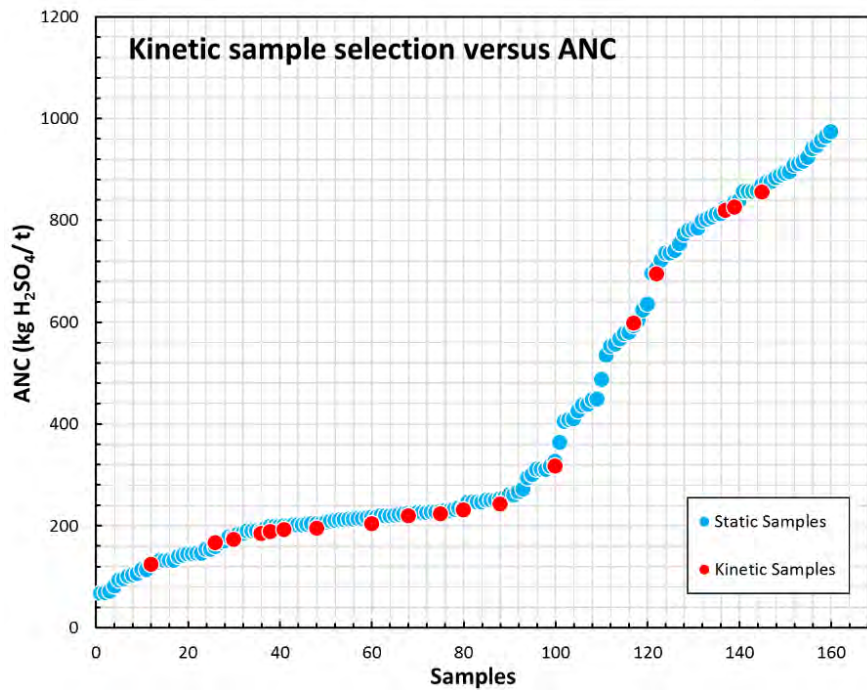


Fig 1. Acid Neutralisation Capacity (ANC) for kinetic and static testing samples.

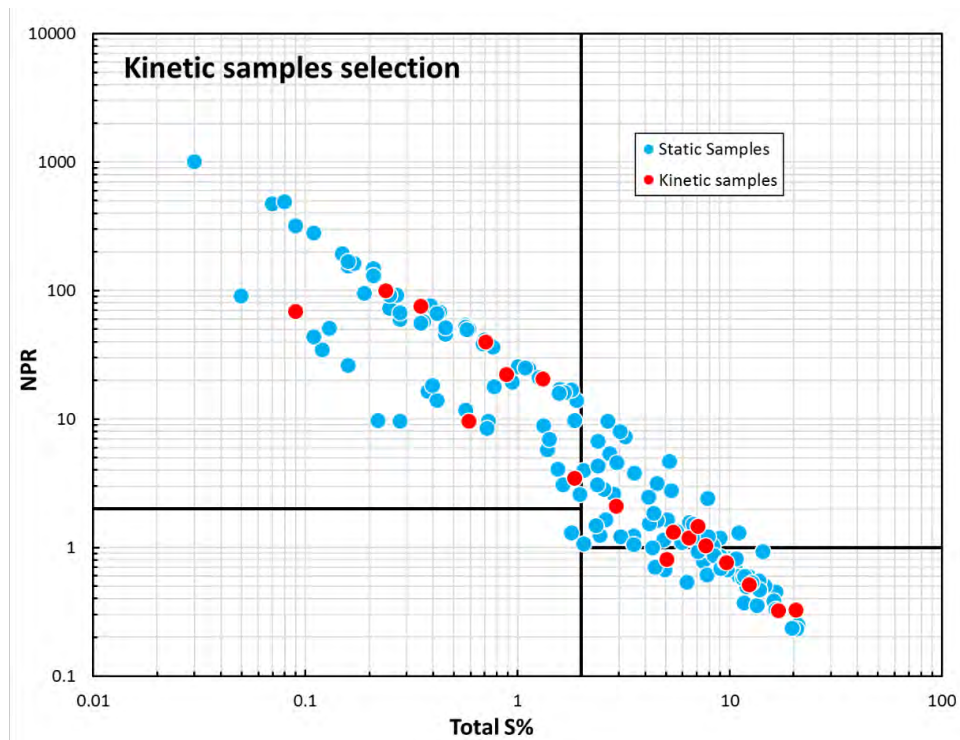


Fig 2. Total Sulphur (%) versus Net Potential Ratio (NPR) for kinetic and static testing samples.

In addition to considering the acid-base nature of the samples, the samples selected for kinetic testing also considered their metal contents.

2.1 Humidity Cells

Humidity cell tests (HTC) are designed to mimic weathering at the laboratory scale in a controlled environment. The tests allow the rate of acid generation to be determined and the variation in leachate water quality to be monitored over time, providing an indication of the behaviour of waste rock subjected to atmospheric exposure and weathering.

The standard HCT is conducted at the bench scale. On a weekly basis, the sample is subjected to cycles of dry and moist air, followed by being soaked with deionised water which percolates through the sample and is collected. Samples were tested using the American Society for Testing and Materials (ASTM) Standard Test Method for Laboratory Weathering of Solid Materials Using a Humidity Cell (2010) procedure. Waste rock samples were processed and screened to result in particle sizes less than 6 mm. Approximately 1-kilogram splits of each processed waste rock sample were loaded into individual humidity cells.

2.2 AMIRA-style Columns

Column leach tests are designed to provide a measure of the relative reactivity of the waste rock under atmospheric oxygen conditions. The free draining column leach tests in this study are based on the standard AMIRA (2002) practices. The design allows the leaching solution to pass through each sample, with air drying between leaching events, providing sufficient oxygen availability, so that this does not limiting sulphide oxidation.

2.3 Oxygen Consumption Testing

Oxygen consumption rate (OCR) testing was undertaken at a variety of moisture contents by Graeme Campbell Associates. OCR testing was undertaken using both small oxygen consumption cells (SOCCs) and large oxygen consumption cells (LOCCs). The test material was subjected to different drying/de-watering scenarios and gravimetric water content (GWC). The moisture contents were generally chosen to represent a range of values that may be encountered at MRM.

2.4 Field Barrels and Field Testing

A large-scale field barrel (FB) leach program has also been conducted on site by MRM (15 barrels currently in the third wet season at MRM). This is designed to complement the laboratory experiments by scaling the testing to conditions that are more appropriate to those on site. Mined waste rock fragments are used rather than the much smaller particles typically present in the crushed samples used in column or humidity cell tests. Each barrel is exposed to on-site climatic conditions and provides a closer approximation of the environment expected in the waste facilities. Each test consists of a 200 litre barrel loaded with ~ 100-250 kg of waste rock material. Holes are drilled into the sides of the barrels to encourage air circulation; the barrels are raised above the ground to allow the collection of leachate (from rainfall) from the bottom of each test. Site personnel sample the 'first flush' leachate at the beginning of each wet season and follows this by monthly sampling for the remainder of the season.

In addition to the kinetic testing, various types of field data are available to understand the reactivity of the waste and the controls on water quality at MRM. Detailed groundwater and surface water monitoring across the site, including drilling and instrument installation programs, provide further data on the reactivity and water quality changes on site.

3.0 RESULTS AND DISCUSSION

The results to date largely confirm the expected geochemical response of the waste rock materials to oxidative leaching, and currently strongly support the waste classification approach proposed for the MRM waste rock.

3.1 Waste Rock Loading Rates from Laboratory Tests

Loading rates calculated from the interim humidity cell, column leach and field barrel tests have been calculated and statistically analysed. Median and 95th percentile values of samples representative of each waste rock type are shown for clarity. As expected, sulphate loading rates are highest for the more reactive potentially acid forming (reactive) [PAF (R)] waste rock and decrease to the least reactive low salinity – non-acid forming (high capacity) [LS-NAF (HC)] waste rock. Calcium and magnesium loading rates are highest in the reactive PAF (R) waste rock leachates and probably reflect the increased sulphate release rate, and the resultant reaction by calcite/dolomite to buffer the resultant acidity. Field barrel loading rates are comparable to those from the humidity cells and column leach tests.

3.2 Comparison with OCR Inferred Reaction Rates

The OCR values for the tested materials ranged from 4.7×10^{-10} – 5.52×10^{-9} kg O₂/kg/s. OCR values in the range of 10^{-11} to 10^{-12} kg O₂/kg/s are typical for a large number of waste rock dumps (Ritchie, 1995), while OCR values $> 10^{-10}$ can be considered extremely high, and values $\sim 10^{-13}$ may be related to marginal acid drainage environmental problems (Fernandes and Franklin, 2001). These values are significantly affected by the moisture content and particle size. Although moisture content is considered in this investigation, particle size is kept relatively consistent. Smaller particle size typically results in larger surface area and increased OCR values. The OCR values can be considered to be conservative, as the maximum particle size for each bulk sample was $\sim 5 - 10$ mm, which is likely to be significantly smaller than average particle sizes encountered within a waste rock dump.

Figure 3 compares the sulphate production rates derived from OCR and from the HC and CLT results, along with a global range of literature values. Sulphate production estimated from the most recent HC and CLT results is reduced compared to the previously estimated values (c. May 2016). This may reflect the reduced reactivity of the samples, as they are exposed to more oxygen and reach a greater level of 'maturity'.

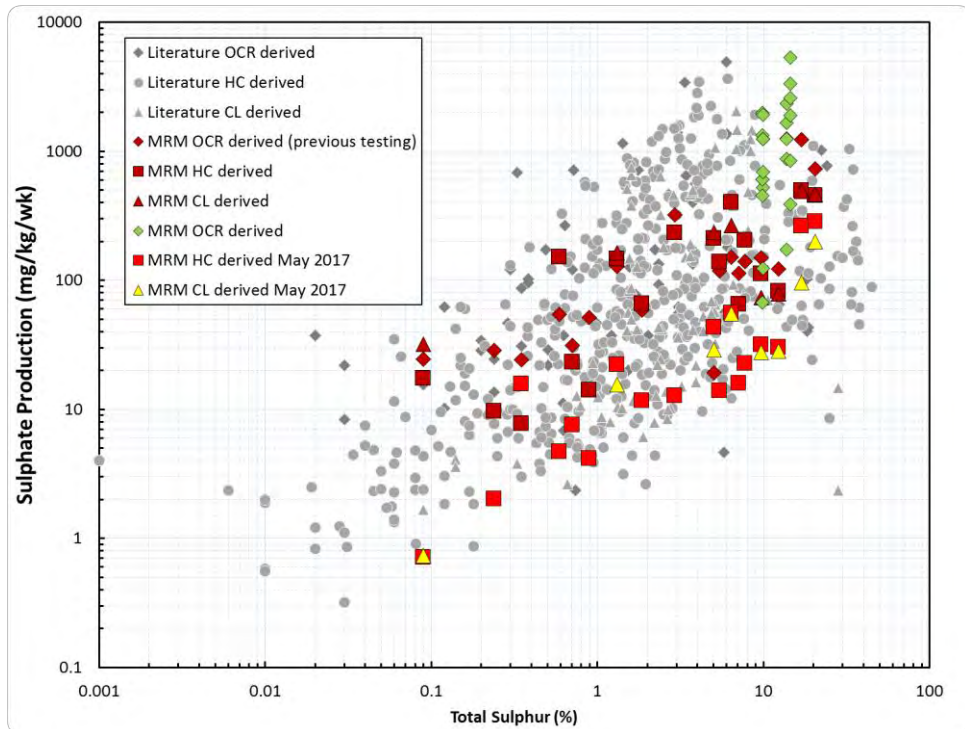


Fig 3. OCR Sulphate Production Rate versus Total Sulphur Content derived from OCR testing, humidity cell testing, column leach testing and literature reference values (MDAG international kinetic database).

3.3 Comparison between OCR and Leaching Test Kinetic Rates

Oxygen Consumption Rate (OCR) testing has been compared to that calculated from the standard leaching laboratory tests. Comparing the results from the OCR testing and the kinetic testing suggests:

- OCR calculated sulphate loading rates are comparable to those derived from laboratory kinetic testing.
- Inferred ANC consumption rates from the kinetic tests is calculated to be slower than those inferred from the OCR tests.
- OCR, humidity cell and column leach test results obtained from this testing are comparable to literature values for mine sites around the world. The International Kinetic Database (IKD©,TM) (Morin et al., 1996) was used as a reference for humidity cell and column leach tests, while the MEND Project 4.6.5b (Nicholson et al., 1997) was used as the source of examples for OCR testing. Comparison of the MRM-derived sulphate production, from OCR, humidity cell and column leach tests, with literature values under similar conditions shows that the MRM rates are within the ranges of the 'global' values, for given sulphur concentrations (see Figure 4).

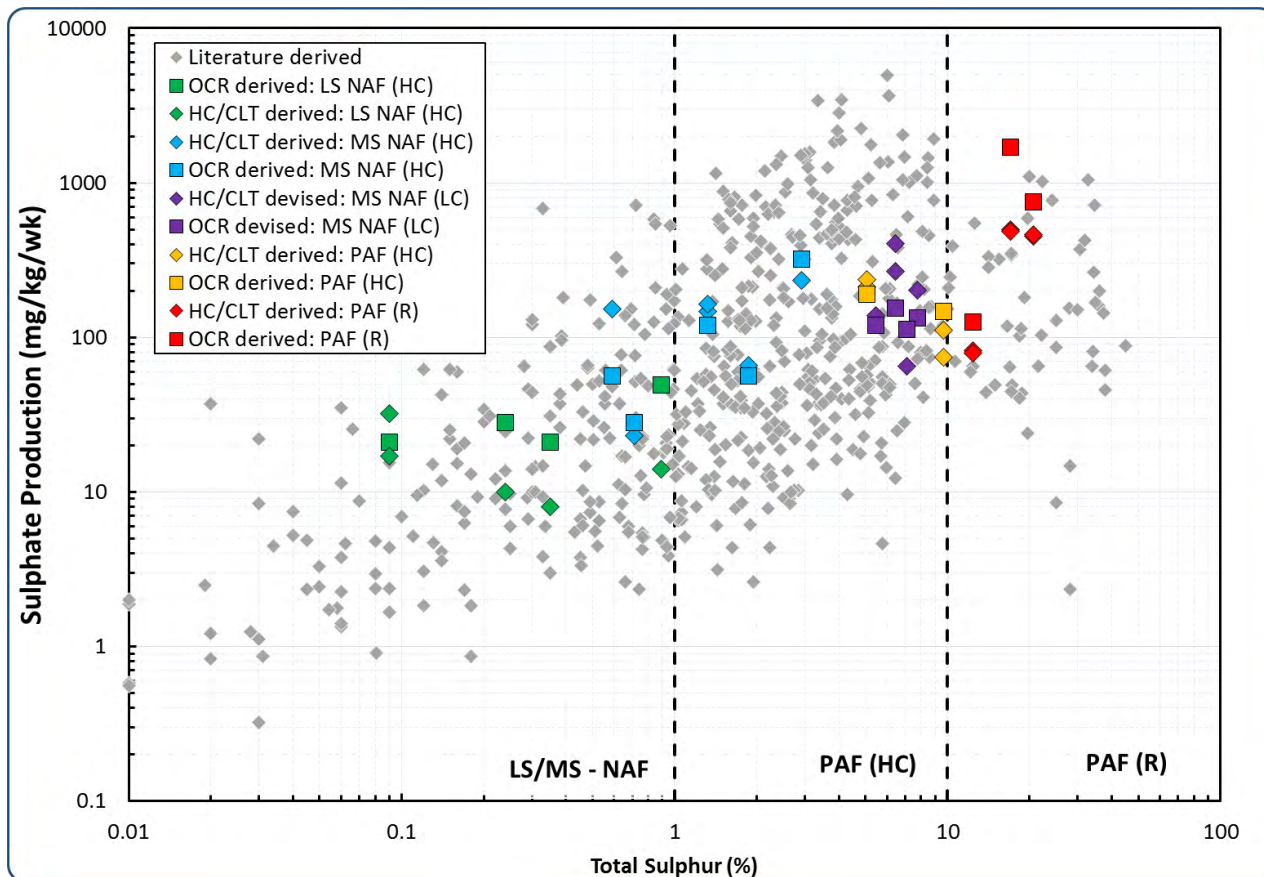


Fig 4. Comparison of MRM sulphate production derived from OCR, humidity cell and column leach tests, with literature values

3.4 Implication from Kinetic Testing Results

The kinetic testing results provide valuable data for planning, design and further hydrogeochemical modelling purposes. The results show that most of the kinetic cells appear to have reached a state of relative stability and are consistent with the waste rock classification (see concurrent paper by Landers et al., 2017).

As anticipated, some PAF (R), potentially acid forming (high capacity) [PAF (HC)], metalliferous saline – non-acid forming (high capacity) [MS-NAF (HC)] and metalliferous saline – non-acid forming (low capacity) [MS-NAF (LC)] have high sulphate loading consistent with their sulphide content. The most reactive samples (PAF (R)) yield leachates showing increasing metal concentrations, especially for the tests which acidified over the course of the testing period. For most of the samples, the inherent carbonate neutralisation is maintaining buffered pH levels. The ongoing testing will provide further understanding of the water quality evolution as these parameters are monitored over the testing period.

Initial high concentrations and subsequent high loading rates seen in leachates are likely to be due to initial flush loading from in-field oxidation providing an initial load of readily solubilised reaction products and elevated dissolved concentrations. There is evidence of available/leachable salts in the overburden, and the waste rock may have experienced some oxidation prior to sampling and laboratory preparation. This has resulted in higher leached concentrations seen in these ‘first flush’ leachates, as expected.

The kinetic testing results reflect the scale of the samples:

- Concentration trends are FB > CLT > HC and follow the rock:water ratios of the tests, which are highest for the field barrels.
- Loading trends, in contrast, are HC > CLT > FB, which reflect the greater reactivity/mobility of the parameters of concern in the laboratory-scale tests, due to the solubility-limited conditions at the field barrel scale.

The systematic variation with testing scale provides a powerful means of assessing the robustness of the laboratory-scale tests. Due to the higher inferred oxidation rates from the OCR compared to the kinetic tests (which are still evolving to reach these rates), the initial estimates of lag times for ANC depletion were obtained using the OCR tests. These tests are still at a relatively early stage of completion, and better estimates of depletion rates will be obtained through extended testing. Continuation of the kinetic tests will provide improved estimates of long-term water quality conditions as well as lag times to ANC consumption. To date, the cells have behaved consistently with expectations and waste rock classification. Importantly for the proposed management of the waste, the testing has shown that, for all the materials, there will be several months of lag-time before the onset of acidification (and for the majority of the materials tested, acidification has not occurred over the period of testing).

In terms of salinity generation, PAF materials have yielded the highest loads, with the MS-NAF (LC) yielding slightly lower salinity, followed by MS-NAF(HC) and far lower for LS-NAF material. The difference between the classes is more marked in terms of metal yields, with the LS-NAF and MS-NAF (HC) yielding low metal loads under the test conditions.

Results to date indicate that as far as reactivity and acidification are concerned:

- All NAF materials have remained neutral to alkaline over the period of testing. This includes the MS-NAF (LC) class (which may be considered uncertain, using conservative NPR criteria).
- All materials, apart from a subset of the most reactive PAF tested, have remained circum-neutral to alkaline over the period of testing (approaching two years).
- The reaction rates obtained to date are consistent with the expected reactivity under optimal aerobic oxidation conditions for the MRM waste rock. The high sulphide content, fine sulphidic grain size and relative high neutralisation capacity of the waste rock would be expected to produce the type of leachate obtained from these tests.
- Results to date indicate the broad waste rock geochemical classification scheme is appropriate. The design and proposed management of the overburden emplacement facilities takes these properties into account.

4.0 CONCLUSIONS

Kinetic testing is an integral part of geochemical characterisation for acid and metalliferous drainage assessments. While there are a variety of testing methods available, the results provided by this case support the use of multiple types of testing, so that a more holistic understanding of the likely geochemical behavior on mining waste under a variety of site conditions can be obtained.

Several researchers, who have specialised in developing kinetic test methods, understanding their application and integrating the findings to case studies, have come to similar conclusions (e.g. Brady et al. 1994; Price, 2009). There is no “best” kinetic test; each of the methods has its own particular advantages and weakness, and some are better suited to providing kinetic rates while others provide more representative indications of likely water quality and/water quality evolution.

While comparable metal loading rates have been derived from the columns and the humidity cells, the columns show lower calculated loading rates, largely related to solubility constraints, due to higher liquid:solid ratios in the humidity cell. The comparative trends are monitored as testing progresses.

For MRM, the tests have provided useful information of the expected reactivity (reaction rates) as well as information of the expected water quality changes that could occur, and the timing for how these could occur under different environmental conditions. The kinetic results have been a valuable addition in developing, refining and confirming the mine waste classification scheme (Landers et al, 2017) as well as supporting the design and operational approach for MRM's mine waste.

5.0 REFERENCES

AMIRA (2002) ARD Test Handbook; Prediction & Kinetic Control of Acid Mine Drainage; AMIRA International.

DITR (2007). *Managing Acid and Metalliferous Drainage*. Manual in the Leading Practice Sustainable Development Program for the Mining Industry series. Department of Industry, Tourism and Resources, (DITR) Canberra. February 2007.

DRAFT Guidelines and Recommended Methods for the Prediction of Metal Leaching and Acid Rock Drainage at Mine sites in British Columbia, Ministry of Employment and Investment, April 1997.

INAP (2009) The International Network for Acid Prevention. Prediction Manual for Drainage Chemistry from Sulphidic Geologic Materials, MEND Report 1.20.1, December 2009. The Global Acid Rock Drainage Guide.

Landers, M, Usher, B and Marianelli, P (2017) Classification of Waste Rock for McArthur River Mine, Northern Territory. 9th Australian Workshop on Acid and Metalliferous Drainage, November 2017, Burnie, Tasmania.

MRM (2017) McArthur River Mine Overburden Management Project, Draft Environmental Impact Statement (2017).

MEND Report 5.10E List of Potential Information Requirements in Metal Leaching/Acid Rock Drainage Assessment and Mitigation, January 2005.

NT EPA Environmental Assessment Guidelines for Acid and Metalliferous Drainage (2013). http://www.ntepa.nt.gov.au/_data/assets/pdf_file/0005/349934/guideline_assessment_acid_metalliferous_drainage.pdf Northern Territory Environmental Protection Authority

Prediction Manual for Drainage Chemistry from Sulphidic Geologic Materials, MEND Report 1.20.1, December 2009. The Global Acid Rock Drainage Guide, http://www.gardguide.com/index.php/Main_Page, International Network for Acid Prevention INAP, 2012.

EXPERIMENTAL MODELS OF METAL LEACHING FOR SCALING-UP TO THE FIELD

Z-S. Liu^A, C. Huang^A, L. Ma^A, E. Dy^A, Z. Xie^A, M. O'Kane^B and S. Pearce^B

^AEnergy, Mining and Environment, National Research Council Canada
4250 Wesbrook Mall, Vancouver, BC, V6T 1W5, Canada

^BO'Kane Consultants Inc., 200 – 1121 Centre Street NW, Calgary, AB T2E 7K6, Canada

ABSTRACT

There has been limited success to date in accurately predicting water quality from waste rock dumps at mine sites. Consequently, it has cost the mining industry hugely to implement mitigating measures for minimizing potential environmental impacts. Since the length scale of waste rock dumps at mine sites is about 3-4 orders greater when compared to lab-based and leach-pad tests, the drainage chemistry of rock samples from these tests is likely to be significantly different from that of the field. Thus a question arises: how to design the experimental models (smaller-scale testing models) so that the test results can be accurately scaled-up to the field? The authors of the paper have recently developed a similitude approach to design experimental metal leaching models and ground the scaling up process on sound scientific foundation. This paper introduces the concept of the similitude approach and presents experimental models of metal leaching for predicting the drainage chemistry of waste rock dumps at mine sites. The experimental setups here are the same as ordinary humidity cell, column-leaching and leach-pad tests, but they are different in that the experimental models meet similitude conditions, which involve water-infiltration rate, rock particle size, rock-sample volume (depth and diameter) and reaction kinetic constants. By doing so, the similitude between the experimental models and the field is kept, and accordingly the drainage chemistry between the two would also be kept.

1.0 INTRODUCTION

When rain/snow-melt water infiltrates into a waste rock dump at a given mine site, it is expected that the water would flow through the waste rock dump, leaching out metals from rock surfaces in the form of dissolved metal ions. Government regulators set limits on metal concentrations for mine effluents in order to ensure they would not pollute surface or ground waters. In a large number of countries with established mining regulations, the situation is such that when the metal concentrations exceed the limits set up by regulations, the owners of the mine site would be required to manage the potential impacts, which may include collecting the effluent water and treating it before releasing it into rivers. Metal leaching and acid rock drainage primarily result from waste rock weathering, and weathering is a gradual and ongoing process that evolves with the mineralogy of the rock near the surface environment. As such, the water quality impacts and mitigating operations pose a significant long tremendous financial risk to the owners of mine sites. In addition, it is crucial for mining companies to build trust with local communities to obtain and maintain a social license to operate.

The key question that is posed by all mine operators is: how to know, within a reasonable degree of certainty, the future concentrations of dissolved metals in mine effluent before the mine waste is placed? The current practice of mine waste drainage quality prediction is mainly through lab-scale testing, which relies on testing the metal concentrations of the water that has flowed through a sample of rock taken from a waste rock dump under laboratory

conditions (Price 2009). However, these lab-scale tests face a significant technical challenge that still needs a comprehensive solution—that is, the lack of theoretical basis for scaling the lab-testing results to real waste rock dumps.

This is one of the major reasons why there has been limited success in accurately predicting long-term metal leaching behaviors from waste rock dumps through lab-scale testing.

Over the past 30 years, a lot of efforts (Amos et al. 2015; Dold 2017; Fretz et al. 2011; Parbhakar-Fox and Lottermoser 2015; Smith et al. 2013) have been made to develop lab-scale testing methods for accurately predicting metal leaching. These include humidity cell, leach-column and leach-pad tests. Being similar in terms of basic concept, they allow a controlled rate at which water flows through a rock sample, and then analyze the water chemistry.

Generally speaking, metal concentrations in the water from lab-scale testing are very different from those flowing from waste rock dumps. So a natural question arises: how to design the lab-scale tests so that the metal concentration in the water from the lab-scale testing will be the same as those flowing from the waste rock dumps?

The similitude concept was proposed by Lord Rayleigh (1915) and further explained by Bridgman (1931). It has been used in aerospace and civil engineering, such as in wind tunnel testing. This paper proposes the application of the similitude approach for designing the lab-scale metal leaching to tackle the scale-up challenge.

2.0 SCALE-UP: PROBLEM STATEMENT

The first task is to establish a theoretical basis for scaling up the lab testing results to the field - that is, to determine how to relate the water chemistry from rock samples in the lab to that from the whole waste rock dump.

The difference between the water chemistry of the lab-scale testing of the “representative” rock sample and the water chemistry of the waste rock dump comes from a few factors: (1) the thickness of the sample rock through which infiltrated water flows in the laboratory is often thinner than the depth of the waste rock dump through which infiltrated water flows; (2) water-infiltration rate in the field is likely very different from the water-infiltration rate in the lab; (3) the grain size of the sample rock is often different from that of the waste rock dump. These three factors are considered here as the most influential factors contributing to the difference between the lab-scale testing and the whole waste rock dump. Of course, the other factors such as temperature, pressure, bacteria and the circulation of gas and water vapor inside the rock and its ambient also affect metal leaching rate. But for simplicity it is assumed here these factors can be neglected without significantly decreasing the scaling up accuracy.

The scaling-up problem can be illustrated by Figure 1. Figure 1(a) shows in black the metal concentration in the effluent water (C) from the waste rock dump as a function (f) of a set of quantities (q); Figure 1(b) shows in red that the metal concentration in the effluent water from the sample rock shares the same function and the same arguments but with different numerical values. The solution to resolve the theory of scaling-up is to answer the question: what are the conditions that these quantities in the lab-scale testing have to meet so that the metal concentration from the lab-scale testing would be the same as the metal concentration in the effluent from the whole waste rock dump?

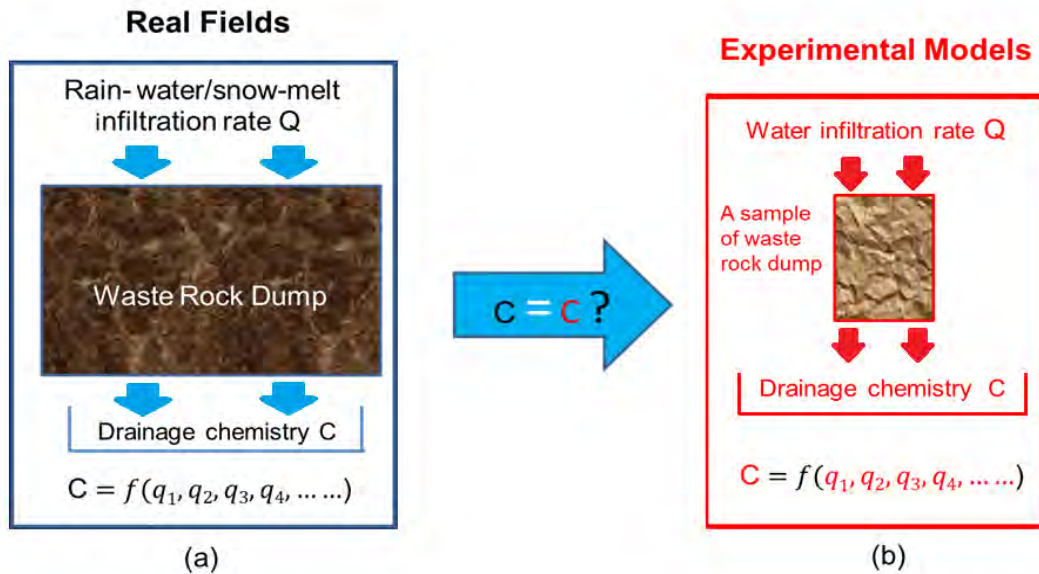


Figure 1. Illustration of metal leaching, (a) metal leaching from the waste rock dump, (b) metal leaching from the lab-scale testing

2.1 The Theory of Scaling-up Using the Similitude Approach

The theory of scaling up with the similitude approach is to use Dimensional Analysis for finding the form of the function $C = f(q_1, q_2, q_3, \dots, q_n)$ as $C = f(\pi_1, \pi_2, \pi_3, \dots, \pi_m)$, where $m < n$. The process is illustrated as follows.

Two steps are involved in the similitude analysis. The first step is to list the relevant quantities. As a principle for selecting the relevant quantities, only those significant quantities should be listed and those unimportant ones should be neglected. In practice, this step requires insights into the hydrological and geochemical processes of metal leaching; otherwise, it would not give any meaningful result. The relevance list (Zlokarnik 1991) for the metal leaching problem, as shown in Table 1, consists of

- 1) the *target quantity*: the metal concentration C ,
- 2) the *geometrical variables*: the total surface area of the rocks that are packed in a unit volume, S , the depth of the rock samples or waste rock dump, β ,
- 3) the *chemical properties*: the kinetic constant, k , the saturation concentration, C_e , and
- 4) the *process-related parameter*: the total volume of infiltration through a unit horizontal area within a unit time, Q .

Table 1. List of quantities and their dimensions.

Quantity	Symbol	Dimension
Metal concentration	C	ML^{-3}
Flush rate: defined by the total volume of water that flows out of a unit length of rock surface boundary within a unit time, with its unit as $L^2 T^{-1}$		
Q: the total volume of water that infiltrates through a unit horizontal area within a unit time, with its unit as LT^{-1}	$\frac{Q}{S}$	$L^2 T^{-1}$
S: the total surface area of the rocks that are packed in a unit volume, with its unit as L^{-1}		
Kinetic constant, k , defined by $dM/dt = Ak(C - C_e)$	k	LT^{-1}
Depth of the rock sample or waste rock dump	β	L
Saturation concentration (equilibrium concentration)	C_e	ML^{-3}

As listed in Table 1, these quantities are the major variables that influence the metal concentration C.

The metal concentration C as a function of the four quantities listed in Table 1 can be written as

$$C = f\left(\frac{Q}{S}, k, \beta, C_e\right) \quad (1)$$

where symbol f denotes a function with the independent arguments listed inside the brackets.

According to the Buckingham π theorem (Bridgman 1931), the function f can be written in the format of the products of the powers of the arguments as,

$$C = \alpha \left(\frac{Q}{S}\right)^x k^y \beta^z C_e^w \quad (2)$$

where x , y , z and w can be determined by dimensional homogeneity, and α is a non-dimensional constant, which cannot be determined by the dimensional analysis, but can be attained by experiments or analytical approaches. The dimensional homogeneity requires that the dimensions in the left side of the equation be the same as the right side of the equation.

Inserting the dimensions of the quantities listed in Table 1 into Eq. (2), and making the dimensions M, T, and L homogeneous:

$$ML^{-3} = \alpha(L^2T^{-1})^x(LT^{-1})^yL^z(ML^{-3})^w \quad (3)$$

This means: in terms of dimension mass M, $w=1$; in terms of dimension length L, $-3=2x+y+z-3w$; in terms of dimension time T, $0=-x-y$. Having four unknowns this set of three linear algebra equations thus gives its solution with one free variable as: $y=-x$, $z=-x$, and $w=1$.

Introducing them into Eq. (2) gives,

$$C = \alpha C_e \left(\frac{Q}{k\beta S} \right)^x \quad (4)$$

Note that here x can be any number, so Eq. (4) should be written as

$$C = \alpha C_e f \left(\frac{Q}{k\beta S} \right) \quad (5)$$

Comparing Eq. (5) with Eq. (1), one can notice the major differences: Eq. (1) has four quantities, and thus is more general than Eq. (5), which has one quantity only. When Eq. (1) is used for scaling up a lab-scale testing to the whole waste rock dump, one has to require that all of the four arguments $\left(\frac{Q}{S}, k, \beta, C_e \right)$ in Eq. (1) stay unchanged from the lab-scale testing to the field, which is impossible to carry out in practice. However, when Eq. (5) is used for scaling up, the requirement becomes that the value of the quantity $\frac{Q}{k\beta S}$ stays unchanged from the lab-scale testing to the whole waste rock dump, which can be carried out in practice. That is to say, the metal concentration C of the water from the lab-scale leaching test is the same as the metal concentration C of the water that flows through the waste rock dump as long as the following condition is met:

$$\frac{Q}{k\beta S_{lab}} = \frac{Q}{k\beta S_{field}} \quad (6)$$

Although Eq. (5) does not tell the exact form of $C = f\left(\frac{Q}{S}, k, \beta, C_e\right)$, it tells the relative role that each and every quantity plays in contribution to the dependent quantity C in the way as $C = \alpha C_e f\left(\frac{Q}{k\beta S}\right)$. It says clearly that the three quantities (kinetic constant k , rock sample depth or waste rock dump depth, and total surface area of the rocks that are packed into a unit volume) play exact equal role in contribution to C . In other words, when the contribution to C due to a 100% increase in k would be exact the same as a 100% increase in S or in β . It also says that the contribution to C due to a 100% increase in water infiltration rate Q can be exactly canceled out by a 100% increase in kinetic constant k , or rock sample depth β , or total surface area S .

In summary, the theory of scaling up using the similitude approach is to find non-dimensional quantities, which comprise all of the important relevant dimensional quantities. When the non-dimensional quantities are kept unchanged between a lab-scale testing to its full-scale testing, the dependent quantity would not change from the lab-scale testing to its full scale testing. In this metal leaching case, there is only one non-dimensional quantity: $\frac{Q}{k\beta S}$. When $\frac{Q}{k\beta S}$ is kept unchanged between the lab-scale testing and the whole waste rock dump, the metal concentration would not change accordingly. In this way, the metal concentration measured from the lab-scale testing would be the same as the metal concentration of the water flowing through the whole waste rock dump.

2.2 The Important Assumptions behind the Theory of Scaling Up

Behind the theory of scaling up with its result expressed by Eq. (5), some assumptions need to be clarified further. There are five important assumptions here:

1) Steady state: here it is assumed that the flow of infiltrated water through the rock sample or rock dump has reached a steady state. The steady state here means that flow speed, water-film thickness and metal concentration at any physical location does not change with time. For example, in a kinetic free draining leaching test, the very beginning when infiltrated water flows through a rock sample would behavior as a transient state, but gradually approaches to a steady state. How long this takes to achieve the steady state varies between columns of different mineralogy.

2) All of the rock surfaces are wet by infiltrated water and thus participate in metal leaching: in Eq. (5) there is a quantity S , the total surface area of rocks that are packed in a unit volume. This quantity S in Eq. (5) tells how large the total surface area of rocks participates in metal leaching. In reality, not all of the rock surfaces are wet by infiltrated water, but only a portion is wet. On the top surface indeed almost all of the rock surfaces are wet, and the percentage of wet surface decreases from top to the lower surface. At the bottom it is common that the portion of wet surfaces is around 30% (Elboushi 1975). How much would the effect be due to any deviation from this assumption? The authors plan to investigate it as the next step of work.

3) Fast diffusion: Metal leaching happening at the interfaces between rock surfaces and water is a chemical reaction. It involves mass transport for transporting reactants to reaction sites and transporting products out of the reaction sites. However, in the relevant quantities in Table 1, diffusion coefficients are not listed there. Here the assumption is: the water film on rock surfaces are relatively thin and the water flow on rough rock surfaces help mixing, so mass transport is not considered as influential factor for chemical reactions.

4) Secondary minerals: Rock surface areas could be partially covered by secondary minerals. This coverage would affect chemical reaction rate. Here we assume the effect of this coverage is counted into kinetic constant k . That is to say, the scaling up would work better when kinetic constant k is counted as an effective kinetic constant.

5) Representative sampling: Rock sample taken randomly from a waste rock dump would not statistically represent the whole waste rock very well. Hence, a number of samples can be tested and the averaged result can be considered as a statistically acceptable. The degree of representation can be improved by increasing the number of the samples and can be quantified by statistical calculations. For simplicity, as part of this study we do not consider the issue of sample representation (this is a separate line of research questioning in its own right), but assume the sample is a perfect representation of the whole rock dump in terms of mineralogy, that is, the properties of metal leaching from the surfaces of the rock sample is the same as that of the waste rock dump.

3.0 CONCLUDING REMARKS

Using the similitude concept, this paper proposes an experimental model of metal leaching from rocks. In the model, the four relevant quantities (infiltration rate Q , rock depth β , total surface area of rocks packed within a unit volume S , kinetic constant k) are picked up as significant quantities affecting metal concentration C . The dimensional analysis reveals that the four quantities affect metal leaching concentration C in a specific format $C = \alpha C_e f\left(\frac{Q}{k\beta S}\right)$.

This format tells how to scale up. When this argument $\frac{Q}{k\beta S}$ does not change, metal concentration C would not change. Thus, the objective here is to design a testing method that can keep $\frac{Q}{k\beta S}$, a non-dimensional quantity, unchanged.

Although the science behind the similitude approach is sound, its application to metal leaching testing involves assumptions and neglecting some factors, such as mineral reactions and transformations, changes in porosity over time, etc. The application needs confirmation and validation or invalidation. The authors hope that this paper would generate interests in further research and development of the method so that the accuracy of predicting metal leaching from mine waste will greatly advance.

4.0 REFERENCES

Amos RT, Blowes DW, Bailey BL, Segó DC, Smith L, and Ritchie AM (2015) Waste-rock hydrogeology and geochemistry, *Applied Geochemistry* **57**, June 2015, 140-156.

Bridgman PW (1931) Dimensional Analysis, Yale University Press.

Dold B (2017) Acid rock drainage prediction: A critical review, *Journal of Geochemical Exploration* **172**, 120–132.

Elboushi IM (1975) Amount of water needed to initiate flow in rubbly rock particles, *Journal of Hydrology* **27**, 275-284.

Fretz N, Momeyer S, Neuner M, Smith L, Blowes D, Segó D, and Amos R (2011) Diavik waste rock project: unsaturated water flow, *Proceedings Tailings and Mine Waste* Nov 30, 2011.

Lord Rayleigh (1915) The Principle of Similitude, *Nature* **95**, 66-68.

Parbhakar-Fox A and Lottermoser BG (2015) A critical review of acid rock drainage prediction methods and practices, *Minerals Engineering* **82**, 107–124.

Price WA (2009) Prediction Manual for Drainage Chemistry from Sulphidic Geologic Materials, MEND Report 1.20.1.

Smith JJD, Moncura MC, Neuner M, Gupton M, Blowes DW, Smith L, and Segó DC (2013) The Diavik Waste Rock Project: Design, construction, and instrumentation of field-scale experimental waste-rock piles, *Applied Geochemistry* **36**, September 2013, 187-199.

Zlokarnik M (1991) Dimensional Analysis and Scale-up in Chemical Engineering, Springer-Verlag.

WHY VARIABLE OXIDATION RATES ARE NEEDED FOR THE PREDICTION OF AMD FROM DYNAMIC WASTE ROCK DUMPS

J. Pearce^A, S. Pearce^B and R. Marton^C

^AO'Kane Consultants, 11 Collingwood Street, Osborne Park WA 6017, Australia

^BO'Kane Consultants, 3A Vale Street Denbigh Wales LL163AD, UK

^CBHP, Level 28, 125 St Georges Terrace, Perth WA 6000, Australia

ABSTRACT

Much effort, time and capital, is expended at mine sites on predicting the potential and quality of acid and metalliferous drainage (AMD) originating from waste rock dumps (WRDs). For many sites, WRDs represent the largest potential source of AMD and subsequently more often than not, reflect the highest risk associated with AMD management and successful mine closure. Compounding this is the dynamic nature of a WRD, which increases the complexity of AMD predictions when incorporating the shifting fluxes of water, gas, and temperature.

Typical AMD predictions for a given WRD will involve combining static and kinetic testing data with net percolation calculations to estimate potential AMD loads, which can also include geochemical modelling of the data. Kinetic data which is traditionally collected from industry standard humidity cell, free draining leach column, or oxygen consumption type tests, are applied to estimated quantities of sulphide-bearing waste rock to predict the quantity of acidity and/or contaminants that are produced with time. However, the oxidation rates applied to these predictions are often fixed, and do not allow fluctuation as water and air availability change within the WRD in response to climatic conditions.

A new kinetic method has been developed that allows dynamic oxidation rates to be measured in parallel with fluctuating moisture, temperature, and airflow. Oxidation rates have been measured for black shale waste rock samples, collected from WRDs within the Pilbara, over a 23 month period in conjunction with replicate industry standard free draining leach columns. Rates were generally significantly faster than their free draining leach column replicates and were found to fluctuate by more than an order of magnitude as the system responds to wetting events, which were applied to achieve liquid to solid ratios similar to those expected within the Pilbara. This paper presents the findings of the completed program.

1.0 INTRODUCTION

Acid and metalliferous drainage (AMD) is recognised internationally and within Australia as one of the most significant and difficult environmental issues facing mining operators and regulators (Egiebor and Oni 2007; Watkins 2007). A key reason for its importance is that AMD has the ability to cause significant ongoing pollution of the surrounding environment that could potentially persist for hundreds of years. As such, AMD has been highlighted in mine closure guidelines by Western Australian regulators as one of the key environmental issues relevant to mine closure (Department of Mines and Petroleum 2015).

For sites requiring disturbance of reactive waste rock, predicting AMD contaminant loads from existing and future waste rock dumps (WRDs) is therefore a key step to understanding a site's

closure liability with respect to AMD. However, predicting contaminant loads from WRDs, as well as tailings storage facilities (TSFs) and pit voids (although not a focus of this paper), is very complex when considering the dynamic forces that play a significant part in the formation, mobilisation, and release of AMD. Contaminant load predictions are then further complicated through the incorporation of parameters determined from standard kinetic testing methods that largely do not give consideration to the dynamic forces within a WRD.

1.1 Dynamic Waste Rock Dumps

There are several factors influencing AMD risk such as waste geochemical and physical properties, WRD geometry and construction method, and climate (Pearce et al. 2016). More often than not, the focus of AMD risk and characterisation assessments focus on the geochemical and climatic factors with very little consideration to the WRD internal structure (Pearce et al. 2016).

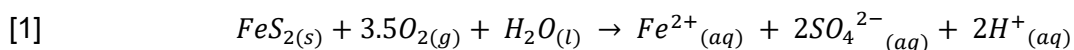
How a WRD is constructed, as well as the physical properties of the waste, will determine how accessible reactive minerals are to water and oxygen for participation in chemical reactions. Depending on climatic conditions (e.g. wet versus dry season), the supply of water and oxygen to these reactive surfaces will vary throughout a given year. Therefore, if reactant supply is variable, the generation of products will also be variable. And like the variable generation of contaminant products, the mobilisation and release of these products will be primarily influenced by the dynamic conditions within the WRD, largely set by the relationship between its internal structure and climatic conditions.

1.2 Typical AMD Prediction Methods

Sulfide (or pyrite) oxidation rates for acid generating waste materials can be used as a proxy for chemical weathering (Sapsford et al. 2009). Oxidation rates can then be used to estimate the rate of acidity/contamination generation resulting from chemical weathering. The rate of acid generation is a key parameter that mining operator's measure to assist the development of effective waste management plans such as WRD construction method, appropriate cover systems design, and contingency water treatment strategies. The two main methods of estimating sulfide oxidation are the sulfate release method and the oxygen consumption method (Elberling 1993; Elberling et al. 1994; Hollings et al. 2001; Kempton et al. 2010):

- Sulfate release method – Utilises the relationship between measured sulfate production and stoichiometric sulfide (usually pyrite) consumption to estimate the oxidation rate (Elberling et al. 1994).
- Oxygen consumption method – Estimates the sulfide oxidation rate by measuring the decrease in oxygen concentration over time (Hollings et al. 2001).

The sulfate release method is the most common method utilised by industry (e.g. humidity cell and free draining leach columns) and utilises analytically determined sulfate concentrations from column leachates (AMIRA 2002 and ASTM 2012). Without mineralogical data specifying what sulfide minerals are present in a sample, pyrite is often assumed to be the dominant sulphide, as it is the most common (Sapsford et al. 2009). The mass of sulfate released over time can then be related to the quantity of pyrite oxidised over time by the stoichiometric relationship in Eqn. [1] (Sapsford et al. 2009).



An important concept to understand when applying the sulfate release rate is the distinction between the release and production rates with the latter (not the former) representing the oxidation of pyrite (Sapsford et al. 2009). If not all generated sulfate is released then the oxidation rate determined from the sulfate release rate will underestimate the actual rate. To ensure production equals release, high flush volumes unrepresentative of field liquid to solid ratios are applied in the laboratory with steady-state release rates being typically used in AMD load predictions (Maest and Nordstrom 2017). This over-flushing (volume and regularity) then negates any possibility for the stored contaminant dominant systems observed in semi-arid regions to be replicated in the laboratory (Price 2009; Maest and Nordstrom 2017). The small size of the columns also discourage leachate concentrating effects resulting from increased pore water residence time.

1.3 Alternative Kinetic Testing Method

A new method using advanced customisable leach columns (ACLs) was developed to address limitations in existing industry standard kinetic testing methods (Pearce and Pearce 2016). Limitations addressed include:

- Flexibility to incorporate variable air supply (WRD gas flux)
- High liquid to solid ratios and short leachate residence times (WRD water flux)
- Low or fluctuating experimental temperatures, and
- Low sample volumes and small particle size.

In addition to typical variables collected from standard kinetic testing, the developed ACLs allow airflow, liquid to solid ratios, and system temperatures to be calibrated to site conditions. Predicted or measured internal airflows within WRDs for various construction methods can be replicated using continuous air supply and flow regulators. Wetting regimes, from a liquid to solid ratio perspective, can be customised to better reflect field net percolation rates. The ACL enclosure is a temperature controlled room with the flexibility to be operated between 6–50°C (Fig. 1). The larger capacity columns (1 m height; 150 mm diameter), which can take up to 25 kg material, accommodate larger particle sizes (up to 100 mm) in comparison to standard kinetic methods, facilitate longer leachate residence times that promotes contaminant concentrating effects observed in the field. Dynamic system parameters temperature, pressure, humidity, airflow, oxygen concentration, and carbon dioxide concentration are continuously logged so that dynamic oxidation rates dependent on both airflow and water availability can be measured.



Fig. 1 ACLC enclosure with 16 operating columns.

2.0 COLUMN CONFIGURATION AND OPERATION

This paper discusses the findings from four replicate ACLCs constructed from one composite sample. The four replicate columns investigated the effects of variable air and water over a period of 12 months. To allow comparison to industry standard, free-draining leach columns, duplicate columns using the AMIRA 2002 method were constructed from the same composite material. However, as the free-draining leach columns do not facilitate variable airflow rates, a duplicate column and a high temperature column were substituted against the ACLC low and high air columns. The four replicates were named as per the following:

- Replicate 1: ACLC – Control Column AMIRA – Control Column
- Replicate 2: ACLC – Low Air Column AMIRA – Control Column Duplicate
- Replicate 3: ACLC – Low Water Column AMIRA – Low Water Column
- Replicate 4: ACLC – High Air Column AMIRA – High Temperature Column

The 100 kg composite sample was prepared from 12 waste rock primary samples collected from a WRD sonic drilling program. The WRD investigation included drilling of more than ten boreholes into four WRDs at an iron ore mine in Western Australia's Pilbara region. The primary samples were majority black shale with the composite sample having the chemical and physical characteristics listed in Table 1.

Table 1. Chemical and physical properties of the composite sample on a weighted average basis.

Parameter	Units	Value
Total Sulfur	wt%	2.89
Sulfate Sulfur	wt%	1.44
ANC	kg H ₂ SO ₄ /t	10.3
Total Carbon	wt%	2.8
^A PSD <2.36 mm	wt%	32.0
^A PSD +2.36 mm	wt%	14.8
^A PSD +4.75 mm	wt%	11.2
^A PSD +6.70 mm	wt%	23.4
^A PSD +13.7 mm	wt%	18.6

^APSD not applicable for free draining leach column duplicate samples as method requires crushing of samples to <4 mm.

2.1 ACLC Air Flow Regime

Air flows were adjusted within the first four months due to initial flow regulators not providing sufficiently low air flow control. Air flows for the ACLC Control, Low Air, and High Air Columns were set using airflows estimated from field oxygen sensor data coupled with particle size data collected from the sonic drilling program. Air flow for the Low Air Flow Column was set at 0.008

L/min and represents lift heights of approximately 10 m. The Control Column was set at 0.06 L/min which reflected lift heights of 20-30 m. The High Airflow Column was set at 0.2 L/min which reflects an unconstrained WRD with respect to oxygen supply. Note that the airflow used for industry standard humidity cell tests is 2.5 times greater than this unconstrained airflow (ASTM, 2012).

2.2 ACLC Wetting Regime

Distilled water was added to each of the columns at the time of column loading. Water was added so that the resulting moisture content was within the range observed in the field (8-12 wt%) with the exception of the low water replicate which was loaded with two thirds the volume of the Control Column. To avoid excessive addition of water to the columns as to achieve liquid to solid ratios as close as practicable to moisture conditions observed in the field, matric potential was monitored in each of the columns. This examination of internal drying rates and comparison with field matric potential resulted in the first application of water after 10 months of operation. A second flushing event was applied to the ACLCs at the completion of the program to determine potential pore water concentration of key contaminants. This wetting regime closely reflected the typical Pilbara pro-longed drying cycle before a large cyclonic wetting event.

2.3 Free Draining Leach Column Wetting Regime

The intention of the weekly wetting applications is to wet the sample with minimal leachate loss during these non-flushing weeks. Initially 0.2 L of distilled water was added during the wetting weeks with no leachate observed. This wetting volume was increased to 0.3 L which generated a very small leachate volume in some columns (0.15 L for the Low Water free draining leach column). The volume applied for the monthly flushing event was 0.8 L for all free-draining leach columns except the Low Water replicate which had 0.4 L applied.

2.4 Temperature Regime

The ACLC enclosure is a temperature controlled room and was operated at 35–36°C at all times. This temperature range is the recorded average annual internal temperature of instrumented WRDs at the site investigated. This regime is significantly different to that applied to the free-draining leach columns. The drying phase for the free- draining leach columns is induced by heat lamps with 150W bulbs automatically operated for eight hours per day for five consecutive days each week. The heat lamps are used to simulate air temperature, during the eight hours of heat lamp operation, of between 30 and 35°C.

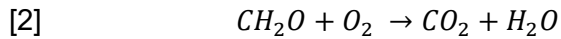
3.0 RESULTS

The following section presents selected results for the four replicate ACLCs over a 12 month period as well as key comparison points to the free draining leach columns.

3.1 Oxidation Rates and Airflow

The intrinsic oxidation rate (IOR) can be considered the overall rate of oxygen consumption reactions within the column. That is, the IOR incorporates oxygen consumed from both pyrite and organic carbon oxidation reactions. Parallel carbon dioxide measurements allowed the conservative calculation of oxygen consumption by organic carbon, that is, all measured carbon dioxide was assumed to be a product of Eq. [2]. Carbon dioxide release into the column air exhaust through the dissolution of carbonate was considered negligible with respect to this specific assessment of replicate columns. For reference, the measured organic carbon oxidation rate (COR) was generally greater than an order of magnitude slower than the pyrite oxidation rate

(POR) when calculating POR from Eq. [3]. Therefore, for the purpose of this assessment, IOR was assumed to be a reasonable proxy for POR.



$$[3] \quad POR = IOR - COR$$

Figure 2 presents the differences observed between IORs when varying water and air supply in comparison to the Control Column. The IORs for the Low Air Flow Column ($7.7E-8$ to $9.3E-7$ kg $O_2/m^3/sec$) are approximately an order of magnitude lower than the control column over the same period ($2.3-4.1E-6$ kg $O_2/m^3/sec$). This indicates that airflow rates are a key limiting factor for oxidation rates and therefore acidity production. Initially, the Low Water Column did not have a meaningful lower IOR relative to the Control Column indicating that controlling moisture content may not likely influence oxidation rates. However, as the Low Water Column approached suction values of 900–1,000 kPa (June–July 2015), the IOR dropped considerably and remained low until the next wetting event. The positive correlation between suction and IOR up to the 900–1,000 kPa range indicates that loss of moisture can accelerate the IOR until the point at which moisture becomes the limiting factor in the oxidation reaction. The High Airflow Column had a significantly faster IOR than the Control Column demonstrating the positive influence of air supply on oxidation rates. The maximum IORs for the High Air Flow Column were approximately $2.0E-5$ kg $O_2/m^3/sec$ which is almost five times the measured IOR for the Control Column.

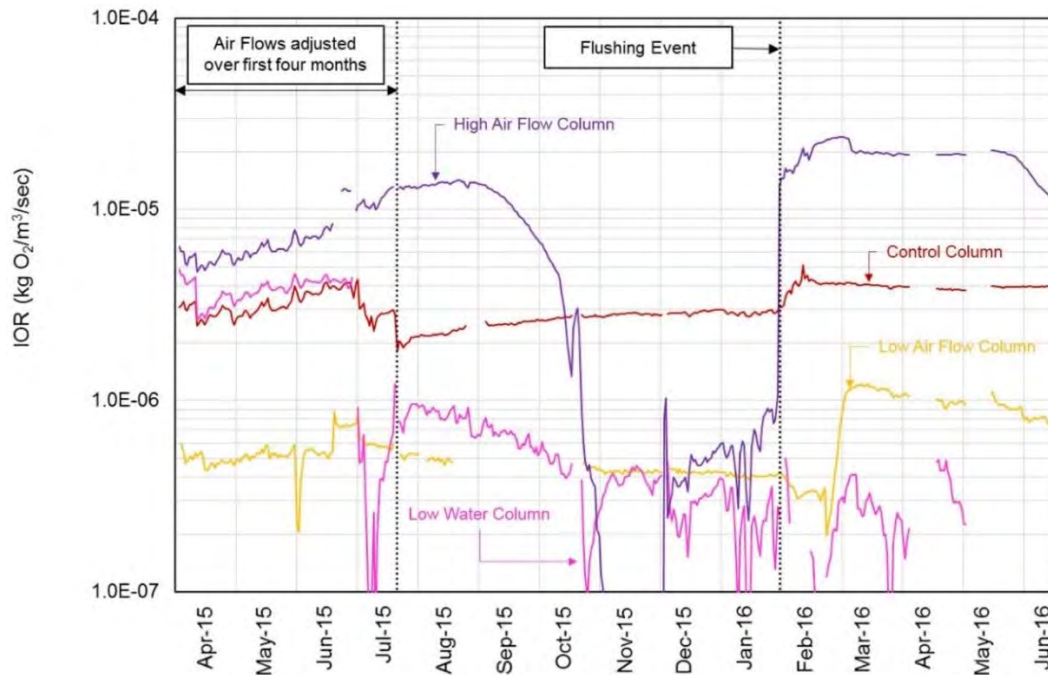


Fig. 2 IORs for each replicate column.

Figure 3 shows the predicted normalised pyrite consumption using the dynamic oxidation rates on a monthly basis for the Control, Low Air, and Low Water Columns plotted against field data collected from WRD installations from iron ore mines within the Pilbara. Using the monthly IORs

measured allows incorporation of dynamic oxidation rates that are changing as the WRD internal conditions respond to climatic conditions (e.g. drying, wetting, change in airflow).

The field data plotted on Fig. 3 represents two construction alternatives (10 m vs 20-30 m lifts) that subsequently result in two different air permeability's. The estimated air permeability's from these two different placement methods were used to set air flows for the ACLC's, specifically the Control and Low Airflow Column. The figure demonstrates one of the most significant findings of the ACLCs in that they were able to closely replicate oxidation rates observed at the field scale when applying the measured dynamic oxidation rates for long-term AMD predictions.

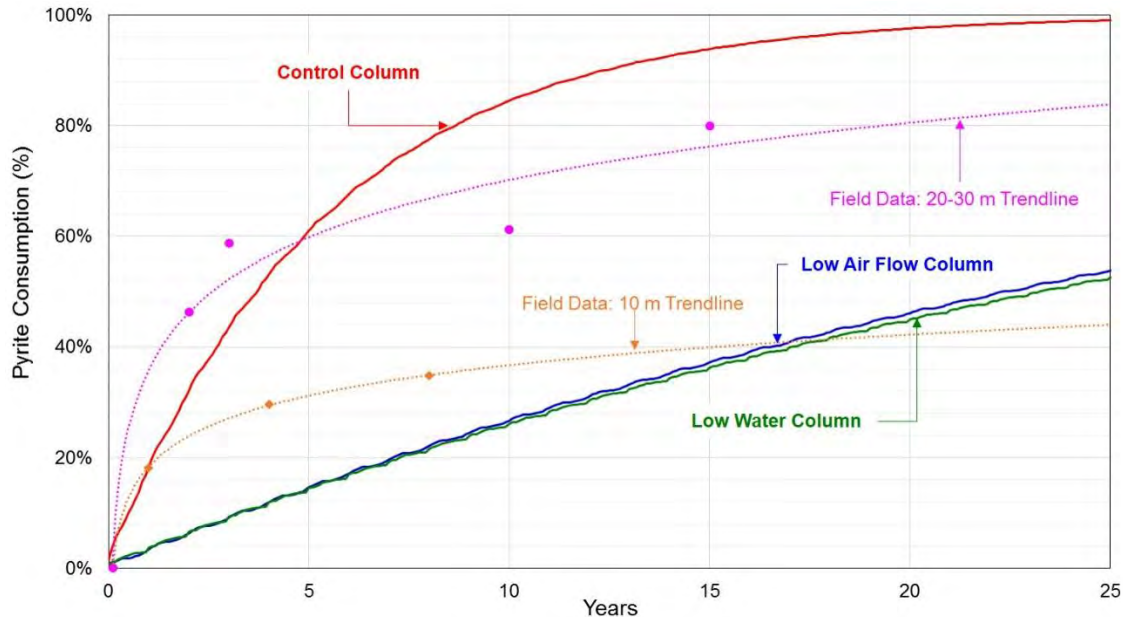


Fig. 3. Predicted pyrite consumption using monthly IORs measured within each of the replicate ACLCs and material geochemical data.

3.2 Oxidation Rates and Drying

Suction data for the replicate columns are presented in Fig. 4. An increase in suction can be inferred to represent drying of the materials in the columns. That is, as moisture is removed from the system suction pressure will increase. Moisture is typically removed from larger pore spaces initially which is indicated by the first inflection change in Fig. 4. (e.g. April to July for the Control Column). Once moisture removal from smaller pore spaces begins, a second inflection in the drying curve can be seen (e.g. September for the High Air Flow Column). Conversely, suction decreases rapidly in all columns after the flushing event. Because all the materials in each column have a unique PSD then the drying curves will be different and as such suction can be expected to occur at both a different rate and to a different final value in each of the columns.

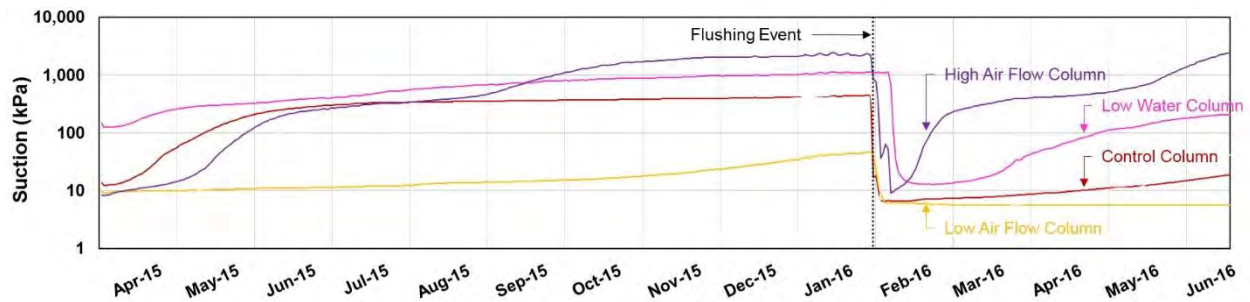


Fig. 4. ACLC suction pressures as measured by installed MPS2 sensors for the four replicate columns. Vertical dotted line represents the 10 month wetting event. Data values (kPa) presented refer to negative pressure.

Figure 5 presents suction and IOR data for the High Air Flow Column and highlights a key finding from the ACLC columns not able to be observed with conventional kinetic testing procedures. The High Air Flow Column produced an initial IOR of $4.8\text{E-}6 \text{ kg O}_2/\text{m}^3/\text{sec}$, this rate increased steadily to a maximum of $1.4\text{E-}5 \text{ kg O}_2/\text{m}^3/\text{sec}$ after four months which was correlated by a simultaneous rise in suction values as the material in the column experienced drying as a result of internal advective drying. Following reaching the maximum IOR and at a suction of 900 kPa, the rate decreased rapidly by almost an order of magnitude to $3.7\text{E-}7 \text{ kg O}_2/\text{m}^3/\text{sec}$, before rebounding sharply to just below $2.0\text{E-}5 \text{ kg O}_2/\text{m}^3/\text{sec}$, where it remained constant for the following four months. When water was added to the column in January 2016, the IOR increased rapidly corresponding with a drop in suction to around 10 kPa. Suction increased progressively as a result of advective drying until approximately 1,000 kPa was reached in late May and again, the rate dropped rapidly. Given that the IOR was seen to record a rapid drop coinciding with suction reaching approximately 900–1,000 kPa, this likely reflects the point at which water becomes the rate limiting factor in the pyrite oxidation reaction.

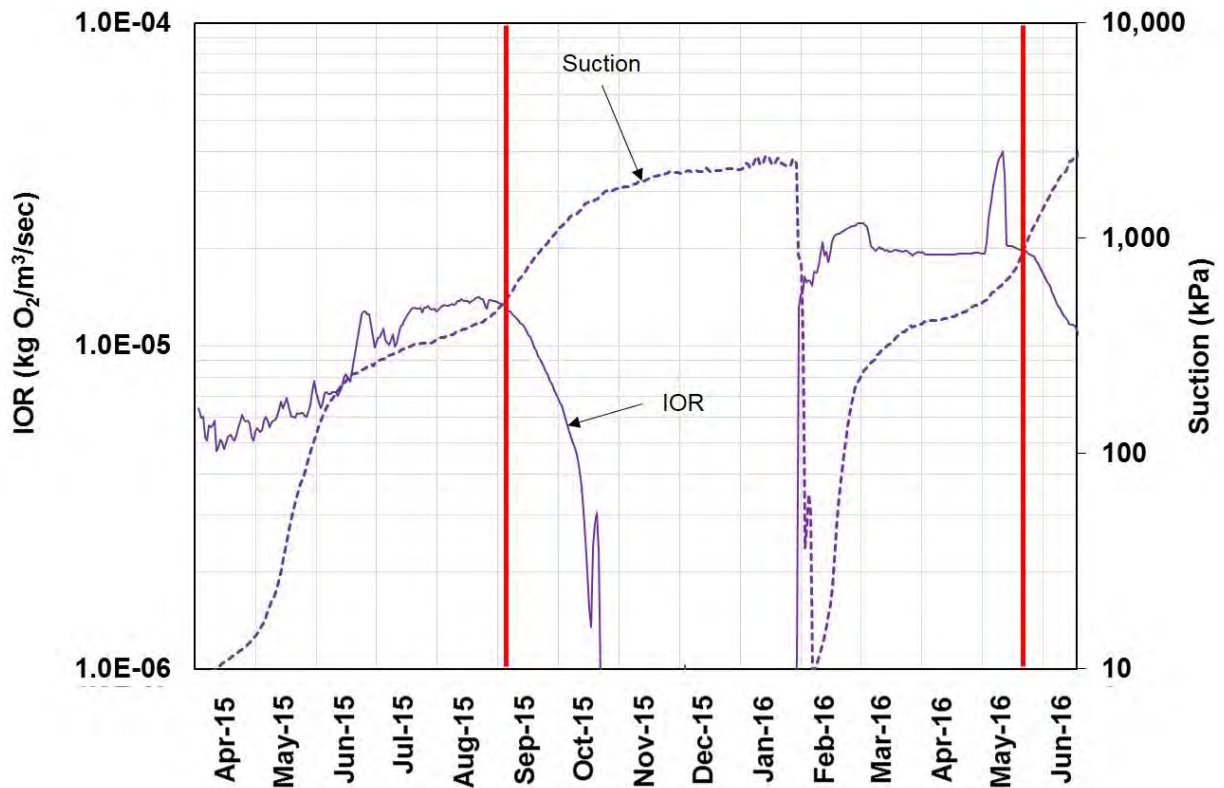


Fig. 5. IOR plotted against suction to illustrate correlation between decreased IOR and second inflection point on suction graph representing point at which pyrite oxidation becomes water limiting.

Once moving beyond the second inflection point on the matric potential figure (approximately 900–1,000 kPa), representing the loss of tightly held water, oxygen consumption ceases. Theoretically, if net percolation can be reduced significantly through sustained (e.g. multiple consecutive) dry seasons, and advective drying continues to the point at which suction can approach this second inflection point in the field, then the IORs within the WRD may be managed in the field. What is evident from Fig. 5 is the ability for the ACLCs to produce a dynamic IOR that is influenced by both air supply and changing moisture content, as would be expected in the field.

The High Air Flow Column demonstrates that a high availability of air, such as that from advective forcing of air, will have significant effects on IOR. During the same testing period, it also highlights the influence that water will have when it becomes limiting in the oxidation reaction as seen after 7–10 months of operation, that is, the IOR reduces sharply but then rebounds fast as water is added such that is experienced in the Pilbara during the wet season.

Figure 6 compares monthly average IORs calculated from oxygen consumption (ACLC) and steady-state sulfate release (free draining leach columns) for the first 12 months of operation for the four replicate columns. Key findings from this comparison is the significantly faster IOR (order of magnitude) of the High Air Flow Column relative to its free draining leach column duplicate, and the significantly lower IORs (up to 5-10 times slower), when airflow and water are controlled (Low Air and Water Columns).

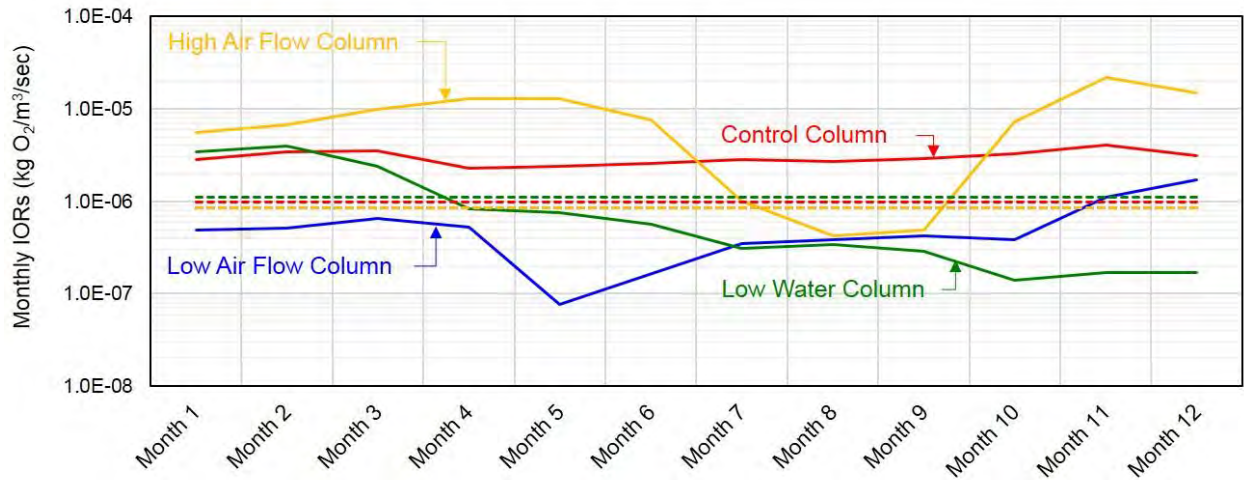


Fig. 6. Comparison of oxygen consumption (ACLC) and sulfate release (AMIRA) calculated monthly average IORs for the first 12 months of operation for the four replicate columns. Free draining leach column duplicates represented by dashed coloured lines of associated ACLC replicate. IORs for free draining leach columns are calculated from the average sulfate values for the final five months representing steady-state conditions as is typically employed for this method (Maest and Nordstrom 2017).

Table 2 presents published IORs for black shale samples, specifically Mt McRae Shale, using the three most common kinetic testing methods for determining oxidation rates. Four of the five IORs are generally lower than the Low Air and Low Water ACLC Columns, and the highest value is consistent with the IORs determined using the free draining leach column method in this study.

Table 2. Measured oxidation rates in kg O₂/m³/sec for several black shale samples associated with Western Australian iron ore deposits utilising industry standard kinetic methods. All total sulfur values are in wt%. Table adapted from Pearce (2015).

Oxidation Rate Measurement Method	Total Sulfur	IOR Range
Free draining leach column (EGi, 2006)	3.0	1.5E-6
Free draining leach column (EGi, 2006)	1.5	4.2E-8
Free draining leach method (Linklater, 2015)	1.8	1.7E-7 ^A
Humidity cell method (Linklater, 2015)	5.1	1.3E-7 ^A
Oxygen consumption method (Earth Systems, 2012)	3.0	6.2E-7 ^B

^AReported results were converted from average sulfate release rates (Linklater, 2015)

^BReported results were converted from normalised PORs (Earth Systems, 2012).

What is evident from Fig. 6 and Table 2 is the ability of the ACLCs and the inability of standard methods to produce a dynamic IOR that is influenced by both air and water availability, as would be expected in the field. The High Air Flow Column data for example shows the effects that a high availability of air, and the suction state of the material will have on an IOR within a WRD that may be influenced by dynamic water and gas flux. The clear influence that water content will have when it becomes the limiting factor in the oxidation reaction is shown in months 7–10. As the figure shows, the IOR reduces sharply but then rebounds fast as water is added in month 10. This variability in suction state is analogous to the semi-arid climate of the Pilbara which experiences cyclonic rainfall events within the wet season.

3.3 Leachate Quality and Liquid to Solid Ratio

Due to the larger sample size and infrequent wetting of the ACLCs to better reflect climatic conditions of the Pilbara, the liquid to solid ratios are far different to those of the free draining leach columns, as presented in Table 3. After the final flushes for each column, the liquid to solid ratios for the ACLCs are over 30 times lower and are far more representative of those observed in the field.

Table 3. Liquid to solid ratios for ACLCs and free draining leach columns following first and final flushes.

Column	ACLC First	Free Draining Leach Final	ACLC Final	Free Draining Leach Final
Control Column	0.15	0.4	0.25	14
Low Air Column	0.15	0.4	0.23	14
Low Water Column	0.10	0.2	0.16	7
High Air Column	0.14	0.4	0.23	14

The restricted application of water and larger column length (increased pore water residence time) allowed the ACLCs to develop a saturated system with respect to secondary oxidation products. Following the final flush, concentrations of key contaminants were generally orders of magnitude greater than those produced by the free draining leach columns during steady-state conditions, despite similar pH values (2.3–2.6). Figure 7 presents sulfate and zinc data for each of the ACLC replicates and their free draining leach column duplicates within first and final flush leachates. First flush concentrations are fairly consistent, with the higher concentrations shown by the free-draining leach columns likely due to the crushing of samples pre-experiment. The key difference is observed in the final flush leachates where zinc is up to two orders of magnitude greater within ACLC leachates and sulfate is generally greater than order of magnitude. Note that, the leachate for the Control Column was collected five months after the replicate columns, as this column was continued (along with its free draining leach column duplicate) as part of a greater study. Therefore, the Control Column (ACLC and free draining leach columns) had an additional five months for the storage of oxidation products which emphasised the importance of allowing the system to saturate, as you would expect within a WRD within the Pilbara. If using steady-state leachate concentrations (release rates) from free draining leach columns to predict pore water chemistry for AMD loading calculations, contaminant concentration within pore water could be underestimated by orders of magnitude.

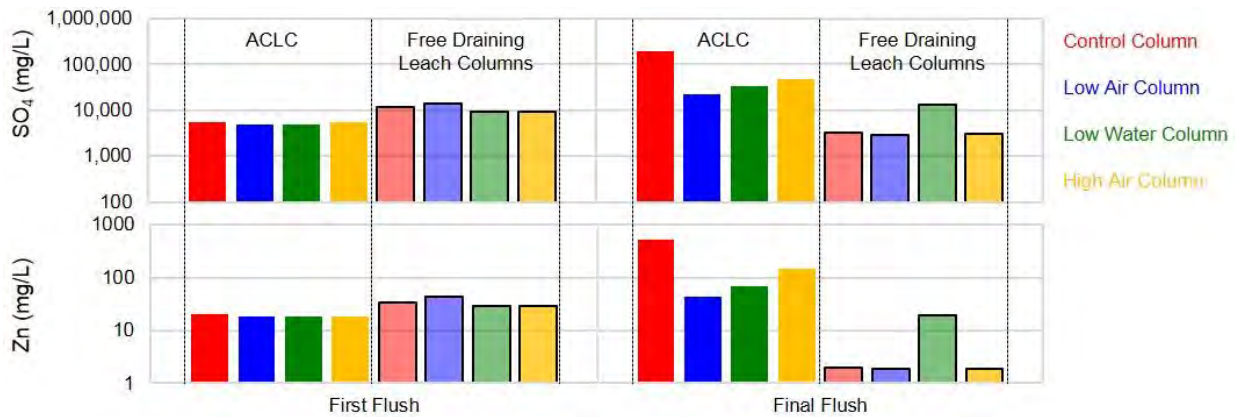


Fig. 7. Comparison of sulfate and Zn concentrations between ACLC and AMIRA first and final flush leachates for the operating period. Free-draining leach column duplicates represented by shaded colour of associated ACLC replicate.

3.4 System Temperatures

Internal temperature was recorded within a free draining leach column to allow comparison with temperatures recorded within the ACLCs containing the same material. The internal temperature fluctuation observed in Fig. 6 for the free draining leach column is a result of the method prescribed drying regime which cycles heat lamps on and off.

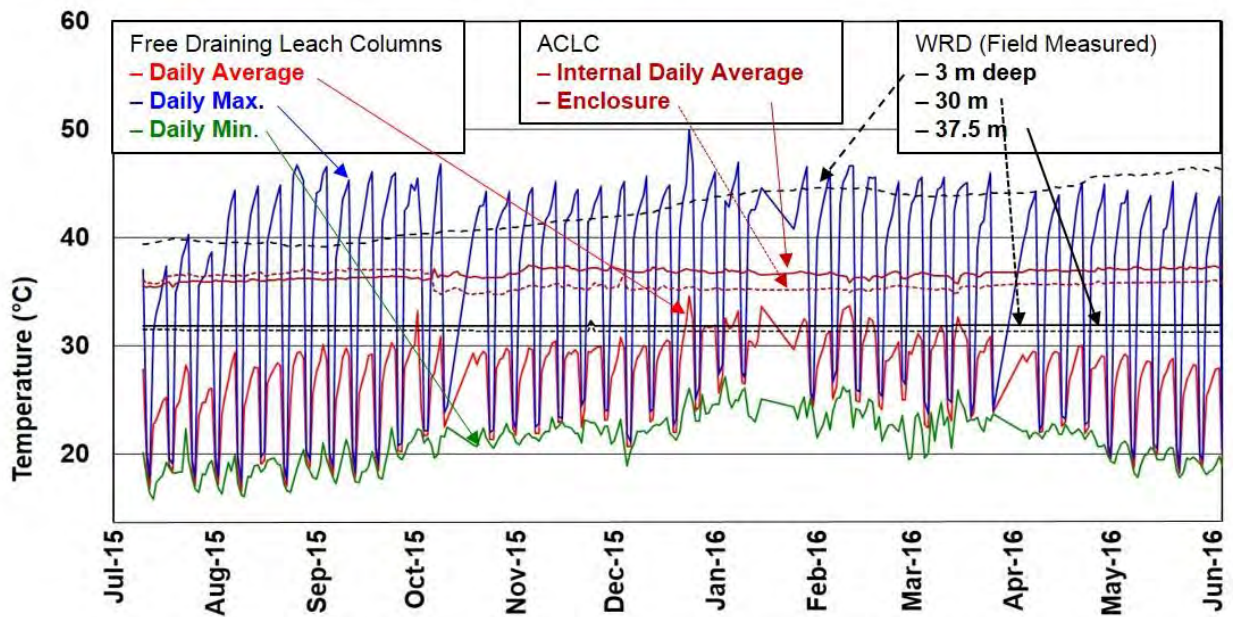


Fig. 8. Daily average, minimum and maximum internal temperatures for a free-draining leach column plotted against measured the internal temperature of an ACLC testing the same material, the ACLC enclosure temperature, and internal WRD temperatures from three instrumented depths.

The internal temperatures for the free-draining leach column were highly variable with minimum and maximum temperatures of 16°C and 50°C respectively. Relevant points regarding the trends noted in the temperature data include:

- The temperature fluctuations in the free-draining leach column appears to be more comparable to those experienced in the outer (<3m) layer of a WRD, where climatic forces have a more pronounced influence, such as a cover system, than the interior of a WRD.
- The internal ACLC and the ACLC enclosure data lie between the temperatures measured in the field at depths of 3-37.5m in one of the boreholes from which the samples were collected.

It should be further noted that temperatures greater than 40°C and 60°C respectively are noted in other WRDs monitored at the same site. When considering that the average daily temperatures of the free-draining leach columns are lower than the average internal ACLC temperatures, it can be concluded that temperature conditions of the free-draining leach columns are not as representative of the internal conditions of the WRDs being monitored. This is an important distinction as temperature is a key factor for oxidation reaction rates.

4.0 CONCLUSIONS

Dynamic oxidation rates were determined through continuous measurement of oxygen and suction using a new kinetic testing method that incorporates the dependency of IORs on air flow and moisture. The method allows variable air flows to be set based on specific WRD construction methods that replicate air supply to reactive minerals. The method also incorporates site calibrated wetting regimes so that liquid to solid ratios observed in the field can be applied and over flushing, typical of standard kinetic testing methods, can be avoided. This allows the build-up of saturated systems (with respect to secondary oxidation products), as is common to the Pilbara, and the production of more realistic leachates reflective of concentrated pore waters. As the method incorporates dynamic WRD variables such as gas and water flux, the combination of the produced dynamic oxidation rates with saturated system leachate data facilitates more site specific AMD contaminant load predictions.

5.0 REFERENCES

AMIRA (2002) ARD Test Handbook - Project P387A Prediction and Kinetic Control of Acid Mine Drainage. May 2002.

ASTM (2012) D5744 - 12 Standard Test Method for Laboratory Weathering of Solid Materials Using a Humidity Cell, 10.1520/D5744-12.

Department of Mines and Petroleum (2015) Guidelines for Preparing Mine Closure Plans. May 2015.

Earth Systems (2012) Comparison of measured pyrite oxidation rates for Mt. McRae Shale. April 2012.

Environmental Geochemistry International (2006) Leach Column Testing of Mt McRae Shale – Final Report. August 2006.

Egiebor NO and Oni B (2007) Acid Rock Drainage Formation and Treatment: A Review. *Asia-Pacific Journal of Chemical Engineering* **2**, 47-62.

Elberling B (1993) Field Evaluation of Sulphide Oxidation Rates. *Nordic Hydrology* **24**, 323-338.

Elberling B, Nicholson RV, Reardon EJ and Tibble P (1994) Evaluation of Sulfide Oxidation Rates - A Laboratory Study Comparing Oxygen Fluxes and Rates of Oxidation-Product Release. *Canadian Geotechnical Journal* **31**, 3, 375-383.

Kempton H, Bloomfield TA, Hanson JL and Limerick P (2010) Policy guidance for identifying and effectively managing perpetual environmental impacts from new hardrock mines. *Environmental Science and Policy* **13**, 6, 558.

Hollings P, Hendry MJ, Nicholson RV and Kirkland RA (2001) Quantification of oxygen consumption and sulphate release rates for waste rock piles using kinetic cells: Cluff lake uranium mine, northern Saskatchewan, Canada. *Applied Geochemistry* **16**, 1215-1230.

Linklater C, Watson A, Chapman J, Green R and Lee S (2015) Weathering and Oxidation Rates in Black Shales – A Comparison of Laboratory Methods. In Proceedings of the 10th International Conference on Acid Rock Drainage. Santiago, Chile. 21-24 April 2015.

Maest AS and Nordstrom K (2017) A geochemical examination of humidity cell tests. *Applied Geochemistry* **81**, 109-131.

Pearce J (2015) Physical and Chemical Weathering of Mount McRae Shale (Thesis). 21 May 2015.

Pearce SR, Dobchuk B, Shurniak R, Song J and Christensen D (2016) Linking waste rock dump construction and design with seepage geochemistry: an integrated approach using quantitative tools. In 'Proceedings of the 2016 International Mine Water Association Conference'. Leipzig, Germany. 11-15 July 2016 (Eds C Drebenstedt and M Paul). (International Mine Water Association).

Pearce SR and Pearce JI (2016) Advanced Customisable Leach Columns (ACLC) – A New Kinetic Testing Method to Predict AMD risks by Simulating Site-specific Conditions. In 'Proceedings of the 2016 International Mine Water Association Conference'. Leipzig, Germany. 11-15 July 2016 (Eds C Drebenstedt and M Paul). (International Mine Water Association).

Price W (2009) Prediction Manual for Drainage Chemistry from Sulphidic Geologic Materials, Mine Environment Neutral Drainage (MEND) Program. December 2009.

Sapsford DJ, Bowell RJ, Dey M and Williams KP (2009) Humidity cell tests for the prediction of acid rock drainage. *Minerals Engineering* **22**, 25-36.

Watkins R (2007) Acid Mine Drainage - The Fundamentals. Treatment Options, (eds), 1-10.

CLASSIFICATION OF WASTE ROCK FOR McARTHUR RIVER MINE, NORTHERN TERRITORY

M. Landers^A, B. Usher^B and P. Marianelli^C

^AARGS Environmental Pty Ltd, 123 Wynne St, Sunnybank Hills, QLD 4109, Australia

^BKlohn Crippen Berger, Level 5 – 43 Peel Street, South Brisbane, QLD 4101, Australia

^CGlencore, McArthur River Mine Pty Ltd, Level 9 – 307 Queen St, Brisbane, QLD 4000, Australia

ABSTRACT

The McArthur River Mine (MRM) is located in the Northern Territory, approximately half way between Darwin and Mount Isa. A comprehensive field and laboratory geochemical investigation was conducted to assess the potential for heavy metal leachate release, saline drainage and acid rock drainage from the overburden materials. The results from the geochemical investigations were used to develop a field and desktop waste rock classification guide. The guide allows mine geologists to classify materials as being potentially acid forming (PAF), non-acid forming (NAF), saline/ metalliferous NAF and reactive PAF (prone to spontaneous combustion), so that they can be appropriately managed and stored.

Discrepancies in waste classification between block model estimations, laboratory results and in-field observations have been resolved through a revised set of waste rock classification criteria. These are based on extensive static and kinetic testing, and incorporate Net Potential Ratio (NPR), total sulfur, zinc, lead, arsenic and cadmium to provide five waste rock classes each with separate management requirements. The field classification criteria are used to validate the classification through in-pit grade control of waste rock involving sampling of materials obtained from blasting charge drill patterns and analysis via a portable X-ray fluorescence (pXRF) spectrometer.

The revision of the waste rock classification has had a significant impact on waste rock management strategy at MRM including a re-design of the Northern Overburden Emplacement Facility (NOEF) which aims to limit the impact from the proposed 600 Mt facility through waste management practices that limit the oxidation of the more reactive materials.

1.0 INTRODUCTION

1.1 Background

Glencore's McArthur River Mine (MRM) is a major open-cut operation that mines one of the largest known sedimentary stratiform zinc-lead-silver deposits in the world. Underground mining of zinc-lead commenced in 1995, and the mine was converted to an open-cut operation in 2003.

The geochemical understanding, prediction and identification of overburden at MRM has evolved significantly over the last decade, driven by advances in geochemical sampling and testing, evolving industry practice, stakeholder expectations and changing regulatory frameworks. The evolution of geochemical understanding at MRM over recent years has resulted in a fundamental revision and update of overburden classification criteria, since the original criteria were established in 2005. MRM allocated significant resources to geochemical studies and overburden characterisation since 2011, in line with commitments to an Environmental Impact Statement (EIS). These include:

- four drilling campaigns focussing on overburden characterisation (2011, 2012, 2014 and 2015);
- numerous detailed overburden geochemistry investigations undertaken between 2012 and 2016; and,
- two drilling campaigns on the Northern Overburden Emplacement Facility (NOEF) with installation of monitoring wells and instrumentation to measure temperature and sample gas (2014 and 2015).

1.2 Historical Waste Classification at McArthur River Mine

The initial overburden classification (2005 classification) used NAG pH and Fe assay data to classify overburden material as either NAF or PAF, with samples showing a discrepancy between the two criteria regarded as unclassified (UC). Mineralogical analysis indicated that iron in the samples is mostly in the form of pyrite (FeS_2), with the exception of some sphalerite ($(\text{Zn, Fe})\text{S}_2$) which has iron-inclusions. The relationship between Fe and S concentration, due to the presence of pyrite, is highlighted in Figure 1. The positive linear relationship for the laboratory data shows how the two elements are discretely related.

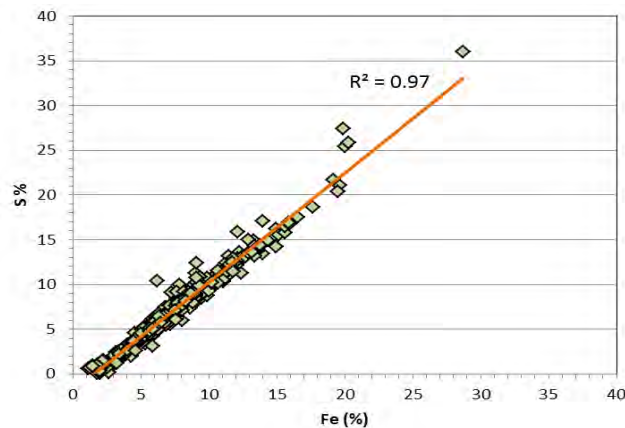


Fig. 1. Iron (%) versus Sulfur (%)

The NAG pH versus Fe concentration graph (Figure 2) provides an indication of the Fe % cut-off for materials that are likely to be PAF based on the NAG pH. The initial site Fe % cut-off was > 7.5 % Fe for PAF (or > 7.5 % S), based on the assumption that NAG pH < 4 is PAF.

Following more recent geochemical analysis of MRM overburden, and improved understanding of its properties, a number of limitations with the 2005 criteria were identified. While conforming to international guidelines such as AMIRA (2002), the classification considered the acid generation risk only, with all NAF material considered to be environmentally benign, and uncertain samples were defaulted to NAF based on their NAG pH value. This led to an underestimation of both PAF material, and of neglected potentially metalliferous and saline materials.

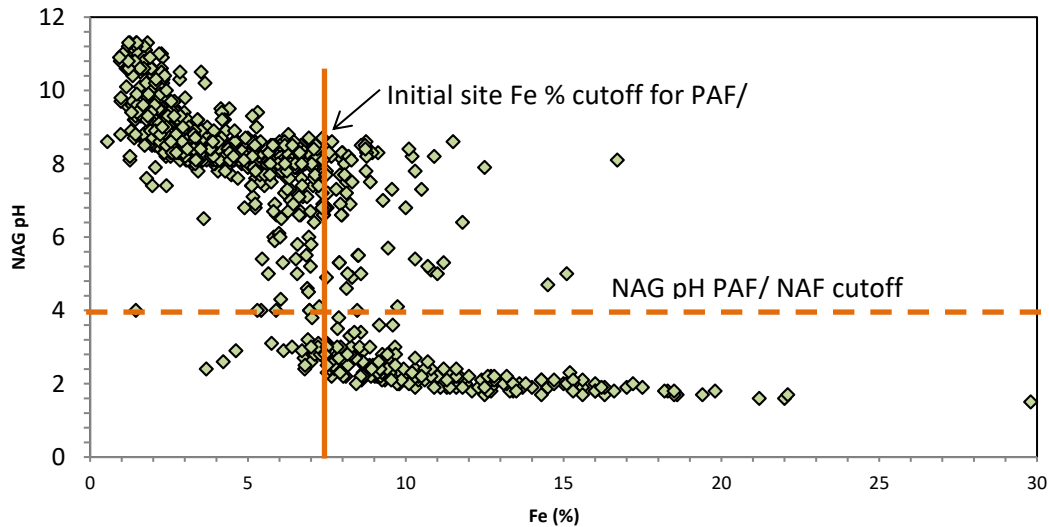


Fig. 2. NAG pH versus Fe % indicating the site Fe % cutoff for PAF (i.e. > 7.5% Fe)

2.0 METHODS

The geochemical characterisation program is based on a combination of field investigations, static laboratory testing and kinetic leach testing. The MRM drill core assay dataset is comprehensive, consisting of over 10,000 assays from over 300 drill holes for overburden lithologies alone. Approximately 4,000 samples have full acid base accounting (ABA) analysis and whole-rock elemental concentration assays. Selected samples have undergone single-addition, sequential and kinetic net acid generation (NAG) tests, chromium reducible sulfur (CRS), acid buffering characteristic curves (ABCC), mineralogy (X-ray diffraction (XRD)) and quantitative evaluation of mineralogy by scanning electron microscopy (QEMScan®), static leach testing and kinetic leach testing (column leach, humidity cell, oxygen consumption rate and field leach barrels; Usher et al., 2017).

3.0 RESULTS AND DISCUSSION

A detailed description of the geochemical testing results is discussed in the McArthur River Mine Overburden Management Project, Draft Environmental Impact Statement (2017). These results, together with all existing geochemical data, were used to establish the more recent revised overburden classification system and to provide ongoing refinements.

3.1 Revised Classification System

The revised classification was initially implemented in January 2014, replacing the original 2005 classification, which had been used by MRM from 2005 to 2013. The objective of the new classification was to establish geochemical criteria for the effective segregation of the various overburden classes by taking into consideration all forms of AMD (acidic drainage (AD), saline drainage (SD) and neutral mine drainage (NMD)), in line with industry leading practice as outlined by both Australian and international guidelines (AMIRA, 2002; DITR, 2007; GARD, 2009). The site-specific potential for spontaneous combustion was also considered.

In 2016, the 2014 classification was updated, following interpretation of kinetic geochemical testing data collected between 2015 and 2016. The changes were relatively minor, but were

needed for the identification of potentially reactive material and the refinement of metal(loid) cut-off values. The waste rock classification criteria are summarised in Table 1.

Table 1. Overburden Classification Criteria

Classification^A	Characteristics	Description and handling
Low salinity – non-acid forming (high capacity) (LS-NAF(HC))	NPR \geq 2 sulfur < 1%, zinc < 0.12 %, lead < 0.04%, arsenic < 40 ppm, cadmium < 10 ppm	Considered at low risk of generating AMD. Generally characterised by a high acid consumption capacity. Suitable for placement in environmentally sensitive areas such as the NOEF outer cover.
Metalliferous saline – non-acid forming (high capacity) MS-NAF(HC)	NPR \geq 2, sulfur \geq 1%, <u>with either</u> zinc \geq 0.12 %, lead \geq 0.04%, arsenic \geq 40 ppm, <u>or</u> cadmium \geq 10 ppm	Considered at low risk of generating AD but higher risk of generating SD and NMD. Generally characterised by a high acid consumption capacity. This material is not considered environmentally benign and requires some form of encapsulation and water management strategy.
Metalliferous saline – non-acid forming (low capacity) MS-NAF(LC)	$1 \leq$ NPR < 2	Considered at low risk of generating AD but higher risk of generating SD or NMD. While non-acid forming, this material is likely to provide limited acid consumption capacity. This material is not considered environmentally benign and requires some form of encapsulation and water management strategy.
Potentially acid forming (high capacity) PAF(HC)	NPR < 1	Considered at risk of generating AD, and is likely to have a significant capacity to do so. Samples classed as undefined according to the DITR 2007 classification are included in the PAF(HC) category. This material is not considered environmentally benign and requires some form of encapsulation and water management strategy.
Potentially acid forming (reactive) PAF(RE)	NPR < 1, sulfur \geq 10%, and BbH (lithology type)	Reactive PAF Material considered at high risk of generating AD, and at high risk of self-heating which may progress into spontaneous combustion. This material is not considered environmentally benign. It requires encapsulation and is likely to require specific additional handling strategies to prevent the onset of spontaneous combustion.

^A The “capacity” of LS-NAF(HC), MS-NAF(HC), and MS-NAF(LC) refers to acid consumption capacity, while for PAF(HC) it refers to acid production capacity.

3.2 2016 Classification Criteria

3.2.1 Net Potential Ratio

Evaluation of the potential acid drainage risk uses the net potential ratio (NPR; acid neutralisation potential (ANC)/ maximum potential acidity (MPA)) in place of the historical NAPP/NAG pH values. This is a robust and more conservative approach given the specific geochemistry of MRM materials.

MRM overburden material contains both high sulfide content and high acid buffering capacity, so the NAG pH may not be a reliable indicator of acidity owing to limitations of the procedure (incomplete oxidation of sulfides, large buffering capacity present). This can lead to an underestimation of the acid generation risk of the material (especially when single addition NAG results are used), and a large proportion of “uncertain” samples classified according to NAPP and NAG pH can result.

MPA, used in the NPR calculation, is calculated using total sulfur and relies on the conservative assumption that all sulfur in the overburden lithologies is present in the form of pyrite. While this assumption is well supported by the geochemical data (Figure 3), CRS results from overburden indicate that approximately 20% of the total sulfur may not be present as oxidisable sulfide sulfur (Figure 3) and therefore may not directly generate acidity. This is likely to result in an overestimation of acid generation potential used in the NPR calculation, providing a conservative classification. Uncertain samples are automatically defaulted to PAF in the current MRM classification. This is a deliberate and conservative approach which is likely to result in an overestimation of PAF quantities, but lowers the risk of PAF not being managed appropriately.

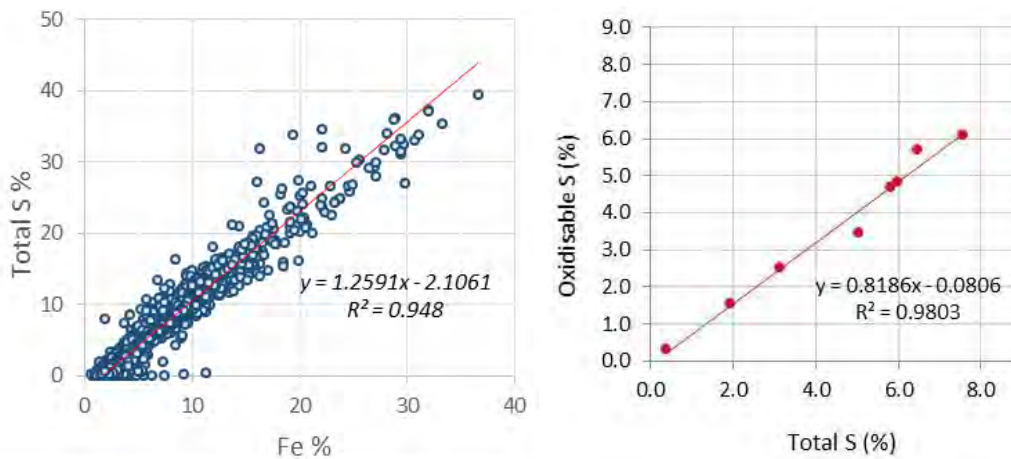


Fig. 3. a) Total sulfur vs. Iron, and b) total sulfur versus chromium reducible sulfur.

3.2.2 Total sulfur

The primary source of saline drainage generation from MRM overburden is associated with the release of soluble sulfate, due to oxidation of sulfide minerals and subsequent neutralisation by carbonates.

The potential risk of saline drainage generation is estimated using total sulfur content. The total sulfur cut-off value used in the new classification is 1% sulfur (S). This is only applied to separate LS-NAF from MS-NAF(HC) waste classes. All other classes are considered to be potentially metalliferous and/or saline.

Whilst 1% S is used as the cut-off value in the classification, in practice, the majority of samples with less than 1% S are significantly below the cut-off, with 76% of all samples having sulfur contents less than or equal to 0.5% S. The median value is low at 0.15% S, and the mean value is 0.23% S. The 1% cut-off value is effective at isolating the very low sulfur fraction of the MRM overburden. Similarly, few samples have sulfur values in the order of 1%, making it an effective cut-off, as it does not artificially split a sample population. Figure 4 presents the frequency distribution of samples with less than 2% sulfur in the MRM drill core data for all lithologies and all overburden classes, and shows the relatively low number of samples between 1% and 1.5% sulfur.

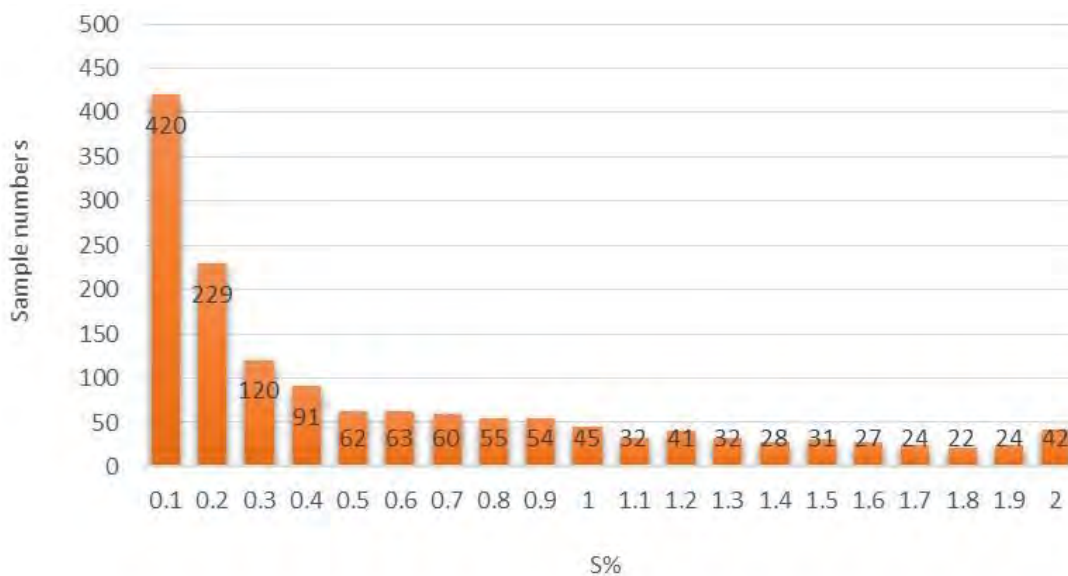


Fig. 4. Frequency distribution of total sulfur < 2%.

3.2.3 Metal(loid)s

Evaluation of the potential NMD effects uses zinc, lead, arsenic and cadmium elemental abundances in overburden material as key indicators of metalliferous enrichment. Zinc, lead, arsenic and cadmium were selected because i) they are well represented in the drill core database, and ii) elevated sulfur, zinc, lead, arsenic and cadmium values correlate well with enrichment of other elements.

The metal cut-off values were initially derived from shake flask extraction and NAG pH liquor analysis results and then updated when comprehensive kinetic test (humidity cells and column leach testing) data became available. The selected cut-off values include:

- zinc, 0.4% (e.g. Figure 5);
- lead, 0.04%;
- arsenic, 40ppm; and,
- cadmium, 10ppm.

While the five elements (sulfur, zinc, lead, arsenic and cadmium) are used as key indicators, 42 elements are routinely monitored for significant enrichment through in-pit grade control (handheld X-ray fluorescence (XRF) verification tests).

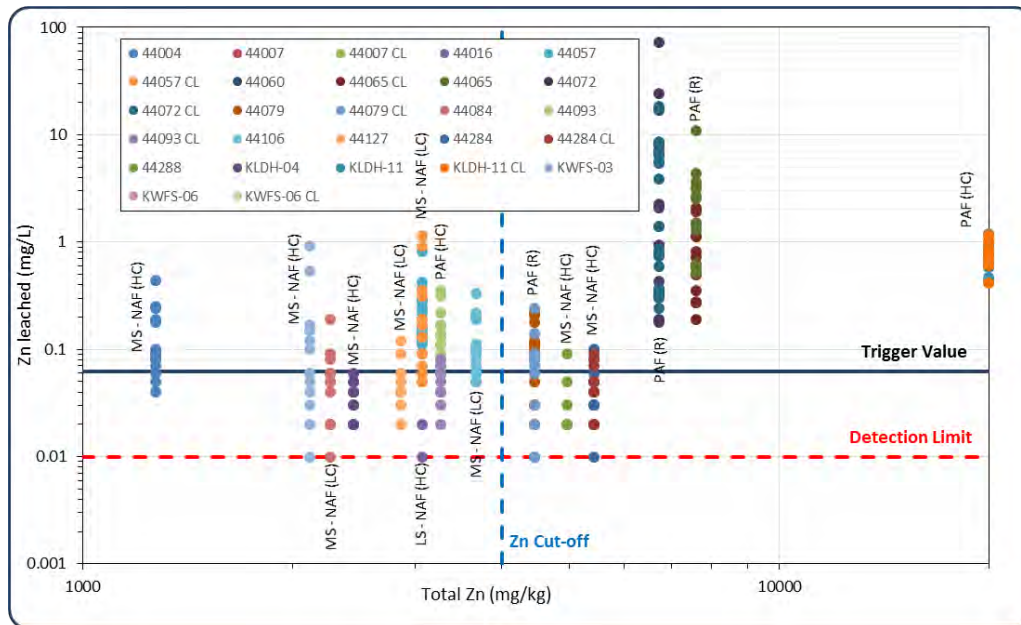


Fig. 5. Leachate zinc concentrations from kinetic testing versus whole rock zinc content for waste rock types.

3.2.4 Reactive PAF

A small quantity of overburden waste rock at MRM is susceptible to spontaneous combustion (classified as PAF(RE)); therefore, correct identification and quantification of these materials in advance of mining activities is needed for the effective management of the material within the NOEF.

Several factors may lead to the onset of self-heating and the development of spontaneous combustion in pyritic overburden. They can be grouped in two broad categories: i) extrinsic factors - those which result from the environment in which the pyritic rocks are placed, such as dumping strategy, storage facility architecture and geometry, and availability of oxygen and water; and ii) intrinsic factors which result from the composition of the rocks themselves, such as presence of organic carbon, fine grained, framboidal pyrite and *in situ* moisture content.

All PAF material has the potential to self-heat and develop spontaneous combustion over time if not mitigated. The aim of the PAF(RE) criteria is therefore to isolate the material which has the intrinsic ability to combust within a short period following exposure, as this material needs to be segregated and requires specific handling and encapsulation.

The new classification criteria based on lithology and sulfur (Black Bituminous Shale and sulfur > 10%) takes into account both the pyrite content and the total organic carbon (TOC) content of the rock. Both parameters have been shown to be important controls on the susceptibility of pyritic rocks to spontaneous combust.

3.3 Evaluation of Classification Criteria

The MRM dataset was reclassified according to the DITR (2007) guidelines to determine the relative performance of the proposed MRM classification against an industry standard guideline (Figure 6 and Figure 7).

Comparison between the MRM and DITR classifications shows that the proportions of NAF and PAF in both classifications are consistent (66.2% vs. 65.7% NAF and 33.8% vs. 34.3% PAF). The proportion of high capacity/acid consuming (AC) NAF is similar in both classifications, the MRM classification being slightly more conservative (39.7% vs. 44.2%). The DITR 2007 NAF class corresponds essentially to the MS-NAF(LC) class in the MRM classification which is again managed conservatively. The primary difference is that the MRM classification considers the potential risk of NMD and SD by incorporating metal cut-offs. The MRM classification is therefore considered to be robust and conservative relative to industry standard classification systems

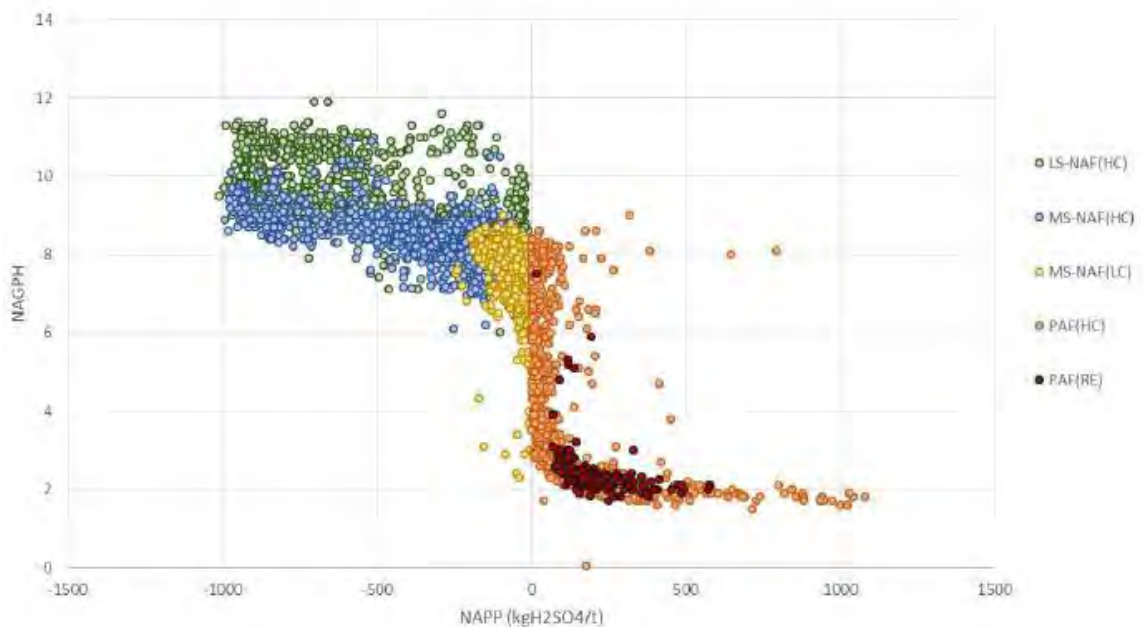


Fig. 6. MRM classification criteria.

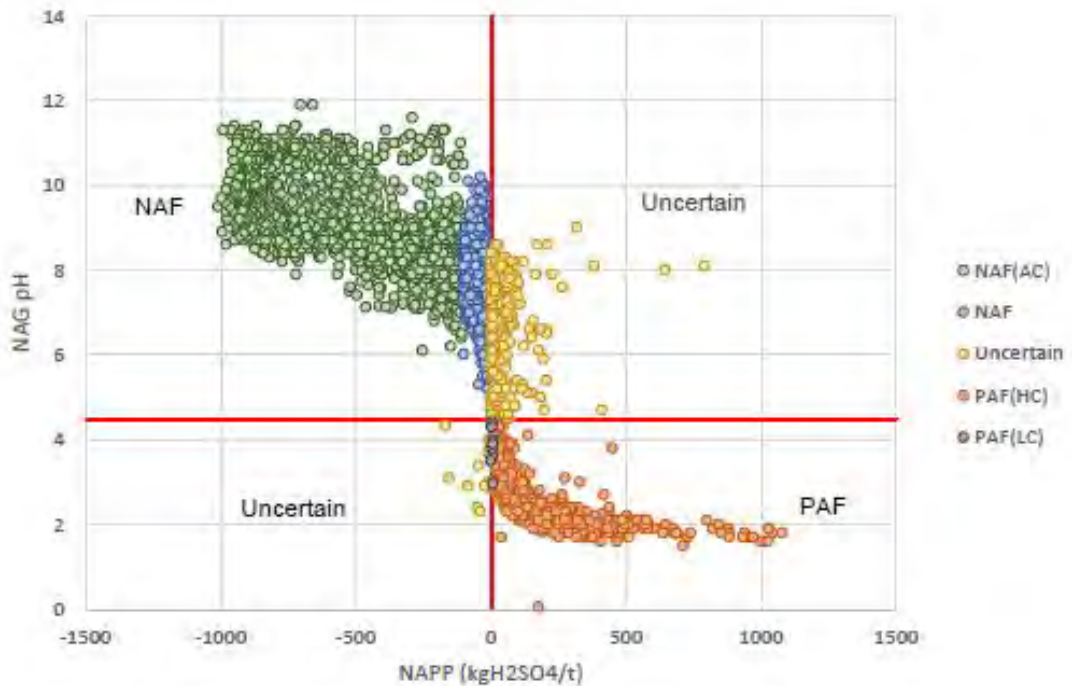


Fig. 7. DITR (2007) classification.

4.0 CONCLUSIONS

A classification guide has been developed for McArthur River Mine that can be applied by mine geologists to classify waste types so that PAF, NMD, SD and particularly reactive PAF materials can be restricted to the appropriate storage facilities. The revised waste classification uses the routine assay suite for the mine. The updated scheme allows for the classification of saline and metalliferous waste types which were not previously included as specific considerations in the waste classification guide. This revised classification guide has been implemented on site, and the initial results are showing promise for large improvements compared to the historical classification guide. Inclusion of aspects other than PAF and NAF has raised awareness of the importance of holistic mine waste management and of the environmental considerations for this material at MRM.

5.0 REFERENCES

AMIRA (2002) ARD Test Handbook; Prediction & Kinetic Control of Acid Mine Drainage; AMIRA International.

DITR (2007). *Managing Acid and Metalliferous Drainage*. Manual in the Leading Practice Sustainable Development Program for the Mining Industry series. Department of Industry, Tourism and Resources, (DITR) Canberra. February 2007.

INAP (2009) The International Network for Acid Prevention. Prediction Manual for Drainage Chemistry from Sulphidic Geologic Materials, MEND Report 1.20.1, December 2009. The Global Acid Rock Drainage Guide.

Usher, B, Landers, M and Marianelli, P (2017) Multiple kinetic testing methods to understand the geochemistry of waste at McArthur River Mine, Northern Territory. 9th Australian Workshop on Acid and Metalliferous Drainage, November 2017, Burnie, Tasmania.

MRM (2017) McArthur River Mine Overburden Management Project, Draft Environmental Impact Statement (2017).

WEATHERED SULFIDIC WASTE – LABORATORY-SCALE TESTS FOR ASSESSING WATER QUALITY IN BACKFILLED PITS

A. Watson^A, C. Linklater^A, J. Chapman^A and R. Marton^B

^ASRK Consulting (Australasia) Pty Ltd, 44 Market St, Sydney, NSW 2000, Australia

^BBHP Pty Ltd, 125 Georges Tce, Perth, WA 6000, Australia

ABSTRACT

Closure options under consideration at some iron ore mine sites in Western Australia include backfilling with mineralised and/or non-mineralised waste rock. Post-closure, following groundwater rebound, flow-through conditions may develop in the backfill located within the saturated zone below the water table and may release solutes accumulated from previous oxidation. The release of solutes may impact on the receiving groundwater quality. It is therefore important to quantify the potential for solute release under these conditions to understand the potential impacts that result.

Geochemical characterisation programmes are the foundation for assessing the potential solute release that may occur to water that has contacted the backfill. Such programmes generally comprise laboratory scale static and kinetic methods designed to obtain data relevant to the closure options under consideration. The tests generally are carried out under ambient atmospheric conditions which may not be representative of the conditions in the porewater of backfill after groundwater rebound. To complement standard testing techniques, SRK employ a saturated column test which is designed to generate site-specific data for solute leaching under the anoxic conditions that may occur within the inundated backfill.

This paper presents the findings of saturated column test work carried out on samples of waste rock from BHP's Eastern Ridge mine located in the Pilbara, Western Australia. The samples were sulfidic, and had been subjected to 'accelerated' weathering and oxidation in free-draining columns prior to saturated column testing.

1.0 INTRODUCTION

BHP are exploring closure options for open pit mines at their Eastern Ridge operations located in the Pilbara region of Western Australia. Options include leaving the pits open or backfilling them on cessation of mining (Figure 1). In areas of net evaporation such as the Pilbara, an open pit will likely become a local groundwater sink (Figure 1A). Where backfill is placed to above the pre-mining water table, evaporative losses will be eliminated, and flow-through conditions are likely to develop following groundwater rebound (Figure 1B). Backfill may include mineralised and non-mineralised waste rock. In a flow-through system, backfill located below the water table may release pre-existing solutes to the downstream groundwater system. Quantification of the potential for solute release under these conditions is important to understand the possible impacts that the backfill could have on post-closure groundwater quality.

Previous testwork examined solute release from low sulfur material (Watson et al, 2016). The current paper extends the dataset to include weathered sulfidic or potentially acid forming (PAF) material.

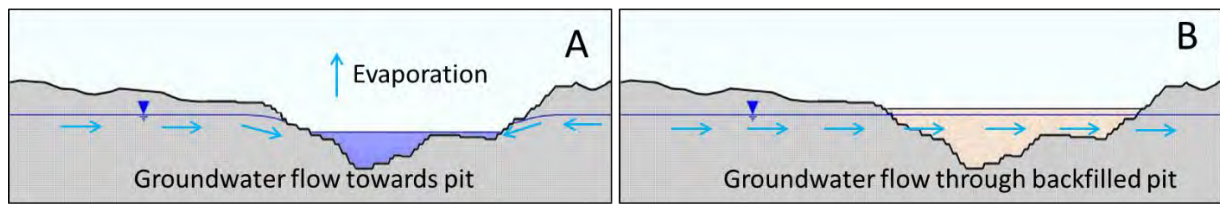


Fig. 1. Effect of pit management on groundwater flow

2.0 METHOD

Two PAF-classed McRae Shale samples were subjected to free draining kinetic column tests to simulate weathering. The tests were carried out over a period of 51 weeks using a modified AMIRA test method (samples were rinsed on a weekly, rather than monthly basis; average weekly rinse volume was 400 mL/kg). On completion of the AMIRA tests, the samples were placed into storage for a period of twelve months (covered, on laboratory bench). The samples were then loaded into columns, with the sample effectively filling the whole column. The columns were equipped with an inlet at the base of the column, and an outlet at the top, and sealed for saturated column test work. Figure 2 illustrates the test setup.

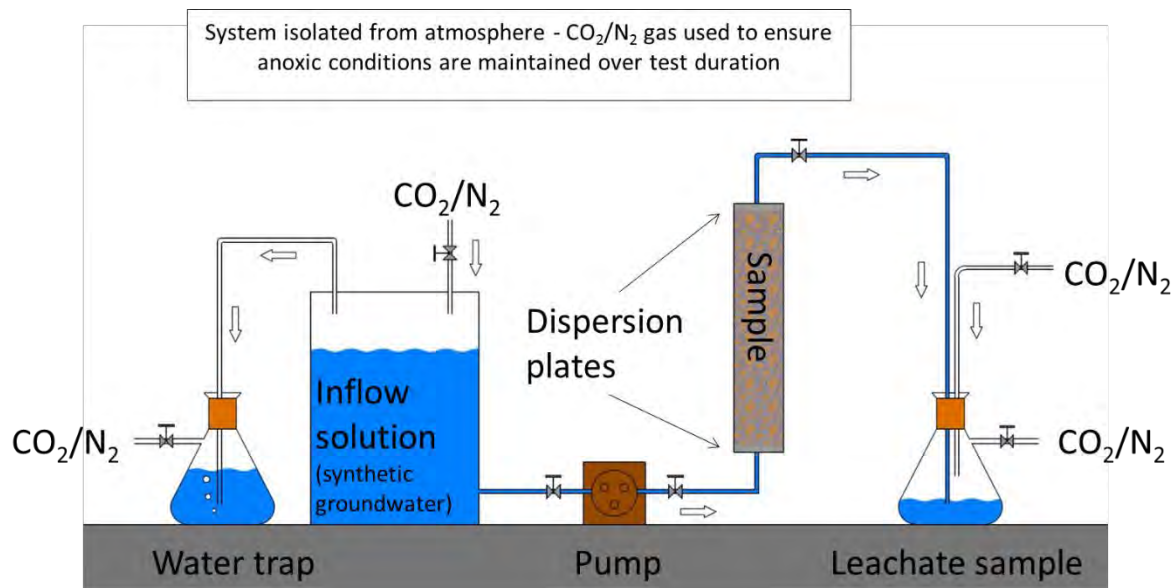


Fig. 2. Saturated column set up

Column inflow for this test was a synthetic groundwater solution. A synthetic solution was prepared by mixing common salts (such as NaHCO_3 , MgSO_4 and NaCl) in deionised water at a ratio to replicate their approximate concentrations in the site groundwater. Anoxic conditions in the synthetic water were achieved by bubbling a mixture of CO_2/N_2 gas through it (comprising 0.5% CO_2 and 99.5% N_2).

Anoxic water was introduced at the base of the column and pore gas displaced to ensure that the samples remained saturated. To maintain de-oxygenated conditions, the head space in

the sample collection vessels and within the initial inflow solution reservoir was filled with the inert CO₂/N₂ gas mixture, as illustrated in Figure 2. The saturated column tests were operated by displacing one pore volume per week.

At the time of preparing this paper, 19 pore volume displacements had been completed. The leachate samples were analysed for a range of parameters including pH, electrical conductivity (EC), oxidation-redox potential (ORP), dissolved oxygen (DO), major cations and anions and a suite of over 20 minor elements. In addition, the water in the inflow water reservoir was sampled and analysed frequently throughout the testing period to verify the inflow composition.

3.0 SAMPLE PROPERTIES

The McRae Shale sample properties prior to kinetic testing are summarised in Table 1. The samples were classified as acid generating; the sulfur contents were 4.8 % and 10.5 % respectively, and were enriched with a range of elements (i.e. elements present at concentrations that were elevated when compared to crustal averages, and gave calculated global abundance indicators, GAIs, of 3 or more).

Table 1. Sample properties

Group	Parameter	Units	Sample ID	
			HEA0320-20-PAF	HEA0320-26-PAF
Saturated Column Loading	Sample mass	kg	0.74	1.5
	Pore volume	mL	236	402
Acid Base Account ^[1]	Total Sulfur	%	4.8	10.5
	ANC	kgH ₂ SO ₄ /t	7.4	3.7
	NAG pH	pH	2.3	2.1
	NAG to pH 4.5	kgH ₂ SO ₄ /t	115	226
	Class	-	PAF	PAF
Minor Element Content (GAI) ^{[1][2]}	As	ppm	197 (6)	169 (6)
	Bi	ppm	3.1 (5)	2.1 (4)
	S	ppm	48,000 (6)	105,000 (7)
	Sb	ppm	5.2 (4)	4.8 (3)
	Se	ppm	4.0 (5)	9.0 (6)
	Te	ppm	0.66 (6)	0.72 (6)
Mineralogy ^[1]	Pyrite	%	3.9	14.9
	Quartz	%	28.5	42.5
	Hematite	%	1.1	1.2
	Rutile	%	0.4	0.5
	Muscovite	%	30.5	21.3
	Kaolinite	%	1.1	2.7
	Amorphous	%	34.4	16.9

Notes: [1] Prior to commencing AMIRA testing; [2] Calculation of GAI values is described in Förstner and Calmano (1993) and the average crustal abundances used are documented in Bowen (1979); ANC – acid neutralising capacity; NAG – net acid generated; PAF – potentially acid forming.

4.0 RESULTS AND DISCUSSION

Solute leachability at laboratory scale is generally controlled by the reactivity of mineral sources under the conditions of the test. Potential solute sources are:

- Dissolution of readily soluble minerals and salts (e.g. gypsum, chlorides) – these could be expected to leach completely in the first few pore volume displacements, especially if they are present in small quantities.

- Sparingly soluble minerals (e.g. hydroxysulfates, oxides) – such minerals may take much longer to leach, even if present in small quantities, and may represent a potential source of contaminants for many leach cycles.
- Interactions involving mineral surfaces, such as ion exchange and sorption/desorption.

4.1. Major Parameters

As noted above, the samples were placed in storage for a period of 12 months following AMIRA testing and before saturated column testing commenced. Plots of pH, SO₄, Ca, Si, K and Fe, illustrating the transition from the weekly flushed AMIRA tests to the once weekly pore volume displacements for the saturated column tests, are shown in Figure 3.

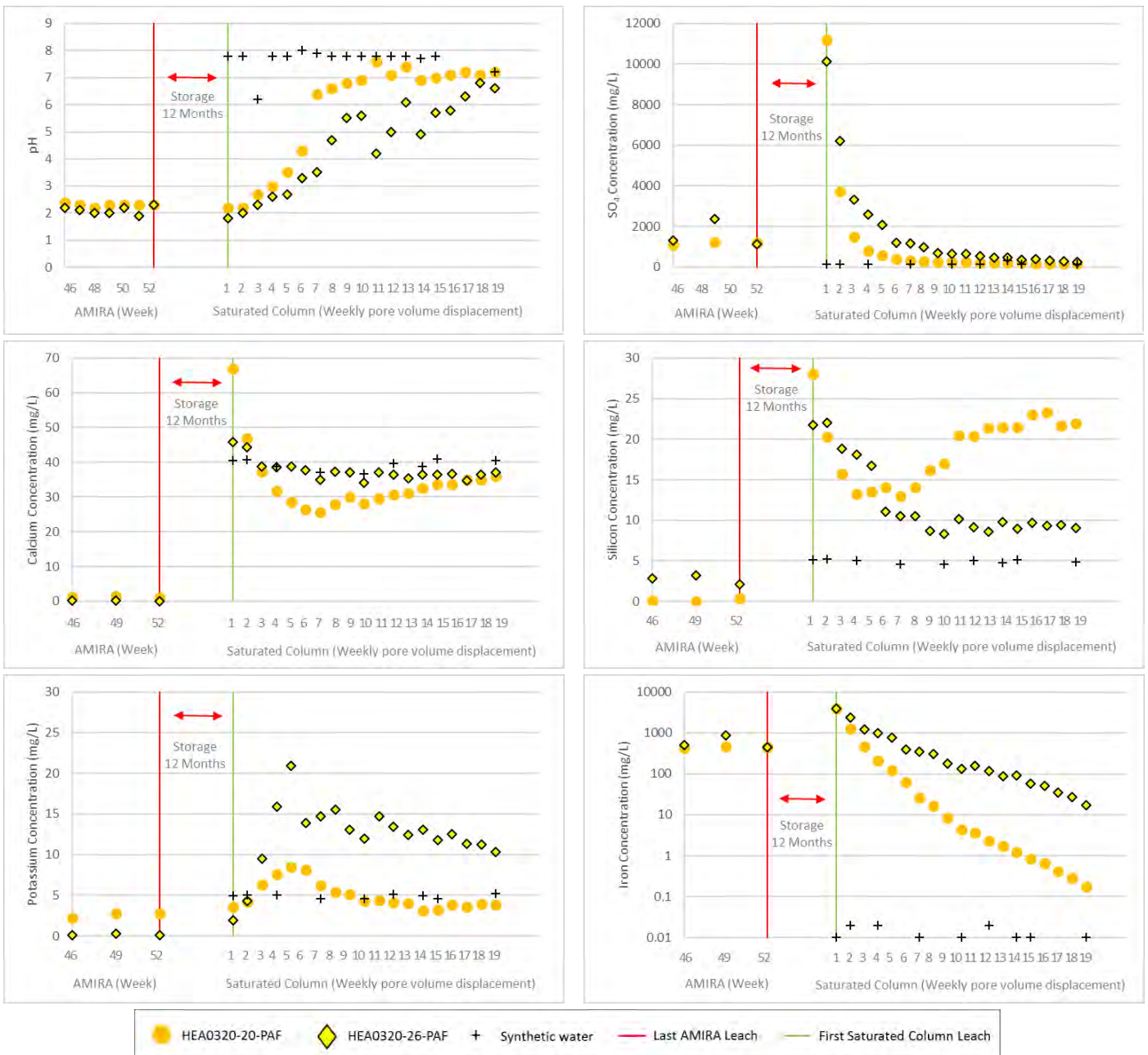


Fig. 3. Column output – pH, SO₄, Ca, Si, K and Fe

The pH of the leachate from AMIRA free draining columns was acidic (around pH 2). Initially, the pH of the outflow from the saturated columns was also acidic, but increased to values close to the inflow solution (i.e. circum neutral) after about seven and 10 pore volume displacements for the lower sulfur sample (HEA320-20-PAF) and 15 pore volume displacements for the higher sulfur sample (HEA320-26-PAF). This represents a flushing of stored oxidation products from the samples.

Under the anoxic conditions of the test, oxygen is no longer available for sulfide oxidation (dissolved oxygen in the saturated columns remained between 0.1 and 2 mg/L). Acid production at the lower oxygen concentration is precluded and the residual acidity is removed by flushing and minor neutralisation by alkalinity present in the inflow solution.

The outflow SO_4 decreases with successive pore volume exchanges, trending towards concentrations equivalent to that of the inflow, confirming that no further oxidation was occurring.

Iron concentrations from the saturated columns followed a trend similar to that of SO_4 (note the log scale used on the y-axis). Fe speciation test work indicated that Fe^{2+} (reduced form of Fe) was the dominant species in solution.

In response to pH increases, mineral solubility controls will come into play; many minerals are less soluble at near-neutral and alkaline pH. Possible solubility control phases were assessed using geochemical modelling techniques (PHREEQC modelling software – v3.3.7.11094, Parkhurst and Appelo, 2013). Measured outflow solute concentrations were used to calculate saturation indices (SI) for key mineral phases. The focus of the calculations was to identify minerals close to equilibrium with the measured outflow water (i.e. SI values close to zero). Such minerals may have dissolved to attain equilibrium with the water (or may be precipitating from solution) and therefore may be used to infer solubility controls or limitations within the tests. PHREEQC modelling indicated that the following minerals were generally near equilibrium at the higher pH values observed in the later stages of the tests:

- Carbonates – Calcite (CaCO_3), dolomite ($\text{CaMg}(\text{CO}_3)_2$) and NiCO_3
- Hydroxysulfates – Jarosite ($\text{KFe}_3(\text{OH})_6(\text{SO}_4)_2$)
- Oxides and Oxyhydroxides – Boehmite and diaspore (both $\text{AlO}(\text{OH})$)
- Halides – Fluorite (CaF_2).

The plot for Ca shows that concentrations were very low in the AMIRA leachate; however, concentrations in the saturated column tests were influenced by the presence of Ca in the inflow (synthetic groundwater). Whilst outflow concentrations from HEA0320-26-PAF were equivalent to the inflow over the test duration, outflow concentrations from HEA0320-20-PAF were lower than the inflow for a portion of the test. A similar result was observed for Mg. The reduction in concentration appears to correspond with an increase in K concentration in the outflow. The change in concentrations may occur as a result of cation exchange, where Ca^{2+} and Mg^{2+} in solution exchanges for K^+ present on mineral surfaces (for example in the clay/ amorphous material).

The dissolved Si concentration trend for HEA0320-26-PAF was similar to that for SO_4 , but stabilised at about 10 mg/L (which was above the inflow concentration of 5 mg/L). However, the Si concentration for the leachate from sample HEA0320-20-PAF initially decreased (similar to that for sample HEA0320-26-PAF) but then increased to about 20 mg/L, which was elevated above the inflow. These results suggest dissolution of a Si-bearing mineral under the conditions of the test.

4.2 Minor Elements

Plots of As, Pb, Sb, Mo and F as a function of time are shown in Figure 4.

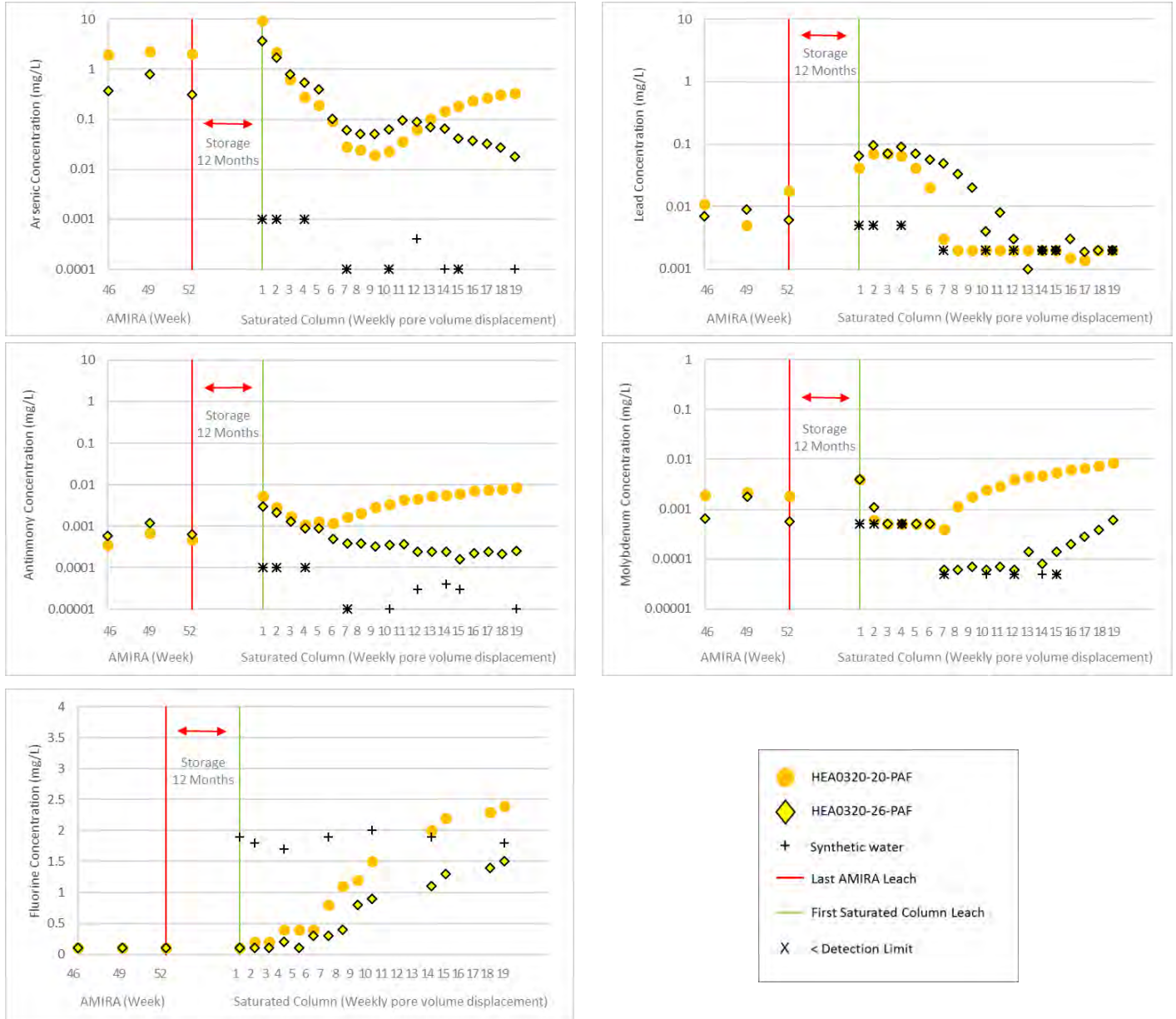


Fig. 4. Column output – As, Pb, Sb, Mo and F

Minor element leaching trends were as follows:

- Ag, Bi, Cd, Cr, Hg, Mn, Se, Sn, Th, Ti, Tl, U and V leached from both saturated columns at concentrations that were low (close to the method detection limit or below it).
- Al, B, Co, Cu, Pb (Figure 4), Sr and Zn showed a similar trend to Fe (Figure 3); however, outflow concentrations were similar to those in the inflow by the end of the test.

- Trends for As (Figure 4), Sb (Figure 4) and U were similar for both samples at the start of saturated column testing. Initial concentrations were higher in the outflow compared to the inflow but showed a decreasing trend. In later stages of the test, outflow concentrations from HEA0320-20-PAF increased.
- Initial inflow and outflow Mo concentrations (Figure 4) were close to the method detection limit for both samples. However, increasing concentrations in the outflow were observed in later stages of the test. The increase in Mo concentration appears to coincide with depletion of Pb (and possibly Al). A trend similar to that observed for Mo was noted for U.
- Concentrations of F were lower in the outflow than the inflow at the start of the test, but steadily increased to values similar to the inflow concentration by the end of the test.

Correlations between minor elements and major parameters may be used to infer sources of minor elements. Pearson coefficients were calculated for a range of minor elements with selected major parameters (i.e. pH, SO₄, Ca, Mg, K and Si). For minor elements, the analysis focused on those with dissolved concentrations that were above detection limits for the majority of the test. Correlations were initially assessed for the whole data set (Weeks 1 to 19); however, due to the variability in outflow concentration for Ca, Mg, K and Si, correlations were re-evaluated based on data generated for pore volume exchanges between Weeks 1 and 6 (where trends are dominated by flushing of accumulated salts) and between Weeks 7 and 19 (where alternative trends are shown). Selected calculated Pearson coefficients for Weeks 7 to 19 are shown in Table 3.

Table 5. Pearson correlations calculated for Weeks 7 to 19

Element	HEA0320-20-PAF				HEA0320-26-PAF			
	pH	SO ₄	Ca	Si	pH	SO ₄	Ca	Si
Al	-0.49	0.43	-0.30	-0.33	-0.38	0.87	0.13	-0.27
As	0.35	-0.85	0.92	0.74	-0.86	0.74	-0.03	0.17
B	-0.59	0.95	-0.92	-0.88	-0.78	0.91	0.13	0.06
Ba	-0.61	0.83	-0.78	-0.74	0.77	-0.67	0.33	-0.19
Co	-0.83	0.94	-0.81	-0.88	-0.56	0.95	0.01	-0.31
Cu	-0.34	-0.16	0.37	0.64	-	-	-	-
Fe	-0.77	0.91	-0.81	-0.91	-0.75	0.99	0.05	-0.13
Mn	-0.10	0.63	-0.79	-0.63	-0.56	0.81	0.10	-0.17
Mo	0.55	-0.96	0.97	0.88	0.77	-0.81	0.21	0.04
Ni	-0.43	0.89	-0.84	-0.79	-0.78	0.88	0.19	0.13
Sb	0.59	-0.96	0.97	0.91	-0.50	0.77	-0.10	-0.04
Se	-0.28	0.54	-0.48	-0.32	-0.42	0.84	-0.01	-0.25
Sn	0.10	-0.47	0.49	0.49	0.32	-0.62	-0.04	0.10
Sr	-0.78	0.89	-0.77	-0.92	-0.77	0.95	0.11	-0.07
Tl	-0.66	0.96	-0.90	-0.93	-0.62	0.93	0.11	-0.15
U	0.57	-0.92	0.92	0.85	-0.31	0.71	0.27	-0.39
Zn	-0.72	0.95	-0.86	-0.95	-0.65	0.94	0.13	-0.12

Note: Green shading – correlations 0.7 or more; grey shading – correlations -0.7 or less.

For Weeks 7 to 19, positive correlations are indicated for several minor elements and SO₄, particularly in leachate from HEA0320-26-PAF. SO₄ was still leaching from the columns in concentrations greater than the inflow in Week 19, with concentrations being greatest from HEA0320-26-PAF. These correlations provide evidence that many of these elements were

present in the matrix of sulfate salts, and that these salts are still being flushed from the HEA0320-26-PAF test.

For HEA0320-20-PAF, positive correlations were indicated between Ca, Mg and Si and the minor elements, As, Mo, Sb and U. This suggests that these minor elements are present within Ca, Mg and Si minerals. Plots for these minor elements (Figure 4) showed an increasing concentration trend in later pore volume exchanges.

It is also expected that F (Figure 4) is being influenced by ion exchange, where F^- is exchanging for Cl^- . Due to the low concentrations of F and significantly higher concentrations of Cl, the increase in Cl in solution was not discernible.

4.3 Comparisons with Results from Low Sulfur Materials

Elements that leached from the low sulfur samples were As, Co, Mn, Mo, Sb, U and Zn. In most cases, the concentrations were relatively constant and low over the duration of the test, and it was concluded that their low rate of release was a result of dissolution of sparingly soluble minerals bearing these elements.

These elements also leached from the weathered sulfidic samples. Compared to the low sulfur samples, the weathered sulfidic samples leached:

- As (both samples) and Sb (HEA0320-20-PAF) at higher concentrations;
- Mo at concentrations that were rising to values similar to the low sulfur samples;
- U at lower concentrations.

5.0 CONCLUSIONS

The results indicated that initial pore water quality from the high sulfur PAF waste will be poor if allowed to oxidise prior to inundation. The presence of stored acidic oxidation products will result in low pH conditions and elevated solute concentrations. Over time and with successive pore volume exchanges, the stored oxidation products will be flushed from the waste rock and the porewater quality will resemble the groundwater quality.

The results further indicated the presence of solubility controlling mineral phases for a number of solutes, and consequently the number of pore volume displacements, before stored oxidation products will be flushed from the waste rock, will depend on the initial quantity of stored oxidation products present. For the test conditions and quantities of stored oxidation products present in the samples tested, the number of pore volumes required may range from six to more than 19 displacements.

6.0 REFERENCES

AMIRA International Limited, ARD Test Handbook: Project P387A Prediction and Kinetic Control of Acid Mine Drainage, May 2002.

Bowen HJM, 1979. Environmental Chemistry of the Elements, Academic Press, London.

Förstner U, Ahlf W and Calmano W. Sediment quality objectives and criteria development in Germany. Water Science & Technology 28:307-316, (1993).

Parkhurst, D.L., and Appelo, C.A.J., 2013, Description of input and examples for PHREEQC version 3—A computer program for speciation, batch-reaction, one-dimensional transport, and

inverse geochemical calculations: U.S. Geological Survey Techniques and Methods, book 6, chap. A43, 497 p., available only at <http://pubs.usgs.gov/tm/06/a43/>.

Watson, A., Linklater, C. and Chapman, J., Backfilled Pits – Laboratory-scale Tests for Assessing Impacts on Groundwater Quality, in proceedings of Life of Mine 2016, Brisbane, 28 to 30 September 2016.

DEVELOPMENT OF A NAF/PAF GRADE CONTROL PROGRAMME FOR PLACEMENT OF A WRD COVER

J. Chapman^A, J. Jones^B, K. Mandaran^B, B. Luinstra^A and A. Hendry^A

^ASRK Consulting (Australasia) Ltd Pty, Level 5 – 200 Mary Street, Brisbane, QLD 4000, Australia

^BMount Isa Mines, Mount Isa, QLD 4825, Australia

ABSTRACT

Mount Isa Mines (MIM) has commenced rehabilitation of the Handlebar Hill Open Cut (HHOC) Waste Rock Dump (WRD). This includes reshaping of the WRD and placement of an interim cover over any exposed potentially acid forming (PAF) and neutral mine drainage (NMD) waste rock exposed following the reshape. The interim cover comprises inert oxide non-acid forming (NAF) material recovered from the adjacent Magazine WRD. A key requirement of the interim cover was that only NAF non-NMD material was used for the cover placement to limit solute release from the WRD, until a final closure cover is designed and agreed with the Department of Environment and Heritage Protection (EHP) (informed by a comprehensive WRD rehabilitation trial). Since the Magazine WRD contained some PAF and NMD materials, it was necessary to characterise materials during mining (from the Magazine WRD) and selectively utilise only NAF non-NMD material for cover construction.

The basis for the development of a sampling and control program to identify suitable material from the Magazine WRD for cover placement is described. This includes the basis for the recommended sampling frequency and specific testing requirements based on first assessing the maximum tolerance for misclassification (i.e. maximum allowable exposure of NMD and/or PAF materials in the NAF cover), and relating these to the mining method.

1.0 INTRODUCTION

Mount Isa Mines (MIM) intend to reshape and then cover the potentially acid forming (PAF) and neutral mine drainage (NMD) waste rock exposed on the Handle Bar Hill Open Cut (HHOC) Waste Rock Dump (WRD), to place the WRD in care and maintenance until final closure and reclamation can be undertaken. As such, the primary objective of the cover is to isolate any PAF material that that may be exposed on the WRD following the reshape and thus limit solute release from the WRD, noting that i) runoff and toe seepage is controlled on site in downstream sediment dams, and ii) release off-site is managed to less than 1% annual exceedance probability (AEP).

Field and laboratory investigations were carried in support of developing the care and maintenance plan for the HHOC WRD. These included: i) assessment of the extent of PAF and NMD materials on the HHOC WRD surface and the adjacent Magazine WRD that may be exposed following the reshape, and ii) identification and characterisation of suitable borrow sources for cover construction. The extent of PAF and NMD materials estimated to be exposed following the reshape was used to define the extent of the area to be covered and supported the engineering design and materials balances. The supporting investigations indicated that a large proportion of the Magazine WRD comprised NAF non-NMD materials that were considered suitable for construction of the care and maintenance cover. The benefits for utilising the material sourced from the Magazine WRD included: i) reduced need for new borrow pits and associated disturbance and rehabilitation requirements, ii) the Magazine WRD

is in close proximity to the HHOC WRD (short haul distance), iii) the material can be recovered by truck and shovel operation (i.e. is 'free dig'); and, iv) the WRD footprint is reduced and associated closure costs would be reduced.

Since a key requirement for cover construction was that only NAF non-NMD material be used, and since the Magazine WRD did contain some sulphidic materials, a control program was required to ensure that only suitable materials would be used for the cover construction. The basis for developing the control program is described in the next section, and the program that was adopted is described in the subsequent section.

2.0 BASIS OF CONTROL PROGRAM

The general approach that was adopted for developing the control program comprised the following:

- i) material variability within the Magazine WRD and specific distribution
- ii) material mining and handling (at source and at placement)
- iii) sources of error and misclassification
- iv) material properties and implication on runoff water quality (from the as-placed cover)

Key factors are identified and discussed briefly in the following sections.

2.1 Magazine Waste Rock Properties and Distribution

Field investigations showed that a proportion of the Magazine WRD contains sulphidic materials that may be acid forming. The NAF non-NMD material in the Magazine WRD has been shown to typically contain less than 0.6% total sulphur. This material is characterised by a low sulphide sulphur content (typically less than 0.15%) and a low soluble solute content, and hence is considered suitable as cover placement on the HHOC WRD.

The field sampling (test pits limited to 5-8 m depth from surface) and geochemical investigation identified at two major zones of material placement within the Magazine WRD as follows:

- A zone of encapsulated PAF material that extends radially from the access road to about 150 to 200 m from the access road entry point to the east; and
- An outer zone of NAF material.

These observations are illustrated in Figure 1 and are consistent with the series of available aerial photographs that span the period 2005 to 2015 as shown in Figure 2.

The main objective of the material selection control program will be to identify and ensure that only NAF material is recovered for the cover construction at the HHOC WRD.

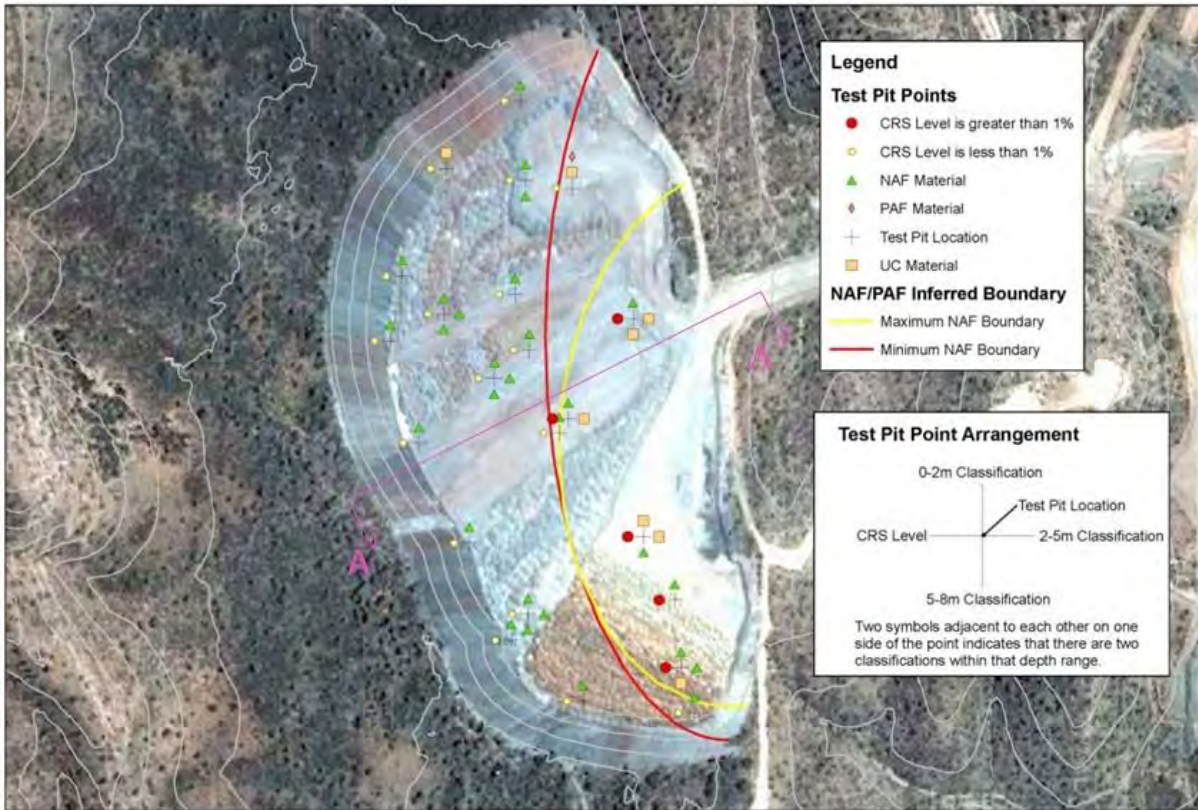


Figure 1: Magazine WRD material characterisation and inferred NAF/PAF contact



Figure 2: Aerial photographs showing the development of the Magazine WRD

2.2 Materials Mining and Handling

The proposed mining method was to commence mining with a front-end loader in 5m cuts from west to east until the NAF/PAF interface is encountered. The mining face would be progressed north to south, removing each cut sequentially from top to bottom. The proposed sequence of mining is illustrated in Figure 3. As shown, approximately five cuts would be required.

The indicated mining production rate was $970 \text{ m}^3 \cdot \text{hr}^{-1}$, with the machinery working 10 hours per shift to achieve a production rate of about $9,700 \text{ m}^3$ per shift.

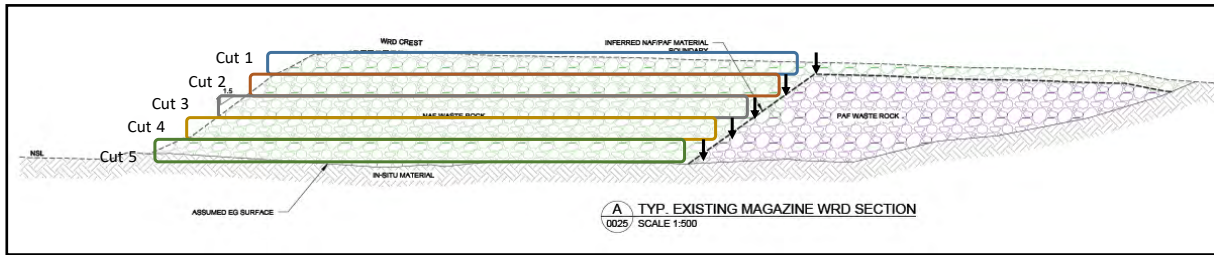


Figure 3: Original mining plan for materials from the Magazine WRD

2.3 Basis for Sampling and Testing Frequency

2.3.1 Target classification accuracy

The primary objectives of the cover are to:

- isolate the PAF materials that that may be exposed on the surface of the WRDs following the reshape; and,
- limit solute release from the WRDs.

In the event that material is misclassified or improperly identified as NAF, when in fact it is PAF or NMD, and utilised as cover placement material, then the surface area of that portion of the WRD would generate NMD or even acidic runoff. When mixed with the remainder of WRD runoff, the solutes from that portion of the WRD would be diluted and therefore some misclassification can be tolerated, provided the combined runoff does not exceed the proposed water quality objectives. For the purposes of the evaluation, livestock drinking water quality guidelines for cattle were adopted.

In the long-term, all runoff and seepage from the WRDs will be directed to the adjacent HHOC open pit, which is predicted to act as a long-term groundwater sink. Therefore, potential impact pathways to receptors will be limited to surface runoff and toe seepage collected in toe drains and directed to the open pit. Receptors are therefore likely to be limited to animals which may drink drainage water immediately following rainfall events, prior to that water draining to the open pit or evaporating. Such impacts are anticipated to be negligible; however cattle were identified as potential receptors for conservative evaluation. In the short-term to medium-term (i.e. during the care and maintenance period), cattle are excluded, where practicable, from water storages on site where water quality exceeds the stock exclusion limits defined in the site's Environmental Authority.

As run-off would occur only intermittently, and animals are likely to consume water for short periods only, an upper sulphate concentration guideline level of $2,000 \text{ mg} \cdot \text{L}^{-1}$ was adopted (concentrations of sulphate above $2,000 \text{ mg} \cdot \text{L}^{-1}$ may result in chronic or acute health problems; ANZECC, 2000). To estimate the impacts on runoff, the surface area of the WRD needed to be considered. Following reshaping activities, the exposed PAF area on the HHOC which will be covered by the NAF non-NMD material is in the order of 55 ha; the entire footprint of the HHOC WRD is in the order of 120 ha. Conservatively assuming that: i) the concentration in runoff from the final cover (comprising misclassified as well as correctly classified cover materials) of the entire WRD does not exceed $2,000 \text{ mg} \cdot \text{L}^{-1}$ sulphate, ii) the sulphate concentration in the misclassified materials corresponds to a maximum of $12,000 \text{ mg} \cdot \text{L}^{-1}$ (i.e. the sulphate concentration associated with samples that would not meet the NAF classification

requirements, obtained from leach extraction tests), and, iii) the average concentration of the correctly classified material is 1,200 mg.L⁻¹ (90th percentile of all NAF non-NMD samples tested), then it can be shown that up to 5 ha of the cover could be represented by misclassified material without resulting in an exceedance of sulphate concentration guideline level in the runoff. (Simply put, 5 ha of cover would yield runoff with 12,000 mg.L⁻¹ with the runoff from the remaining 115 ha at 1,200 mg.L⁻¹, then the combined runoff from the covered area and the rest of the dump as a whole would be 2,000 mg.L⁻¹ or less.)

Based on an as-placed cover thickness of 1.5 m, the 5 ha area of misclassified material would equate to a total volume of about: 50,000m² x 1.5m = 75,000 m³, which equates to about 9% of the total volume of material that would be placed over the 55 ha area. Therefore, overall the sampling frequency and testing at source (mining face) would need to be accurate to 9% or better (i.e. misclassification should be less than 9%) to ensure that the area that is exposed is equal to or less than 5 ha.

2.3.2 Testing and classification accuracy

An assessment of the available results for the Magazine WRD indicated that the rinse pH and EC values may be used to some degree to classify the materials. Samples with a pH of greater than 6 and an EC of less than 1.7 mS.cm indicated an accuracy of about 86% (i.e. 14% of the samples would actually have a sulphur content in excess of 0.6%) for identifying as non-NMD NAF. This approach would also lead to a large number of false positives; about 36% of the samples classified as unsuitable (due to high EC values) would actually have a sufficiently low sulphur content (i.e. less than 0.6%) to meet the NAF cover placement requirement. Recognizing this error, the rinse pH and EC may be used as an early field screening tool, but by itself would not meet the accuracy required for classification.

In the initial assessment, all the material with a total sulphur content of 0.6% or less was shown to be NAF. Therefore, using the total sulphur cut-off of 0.6% would provide a 100% accuracy for identifying NAF material. Although 3 of the 33 samples with a sulphur content of 0.6% or less (or about 9% of the samples) resulted in extractable sulphate concentrations above 1,700 mg.L⁻¹ (based on the leach extraction tests), none of these had a sulphate concentration above 2,000 mg.L⁻¹ (i.e. all samples were below the maximum concentration guideline level adopted herein). On that basis, total sulphur analysis was considered to meet the requirements for a control program for the selection of non-NMD NAF materials suitable for cover placement.

2.3.3 Sampling requirements

Key to achieving effective material classification and placement control will be to complete sampling and testing ahead of mining, in order to ensure that the material is classified before it is relocated.

As determined previously, the maximum allowable misclassification of material to preclude NMD runoff is estimated to be 9% of the total mass to be relocated. The use of the sulphur content will result in a 100% accuracy in identifying NAF material, but may potentially result in up to 9% of NMD material being placed within the cover. However, local variability may be present which may increase the error above the acceptable level – i.e. if the sampling frequency is too widespread, there is a risk that PAF materials may be present between sampling locations that have been ‘missed’. For example, if the mining face is sampled at 10 m intervals, and the short range variability is 5 m, it is possible that 2.5 to 5 m of material could be misclassified (or between 25 and 50%). However, when the Magazine WRD was constructed in the first instance, mining from the pit would have occurred from specific zones

within the pit for extended periods, so that largely similar materials would have been mined and placed together in the WRD.

The test pits excavated during the initial investigation broadly targeted identification of zones of material types within the Magazine WRD and were not intended to assess short range variability. Nevertheless, even at the widely-spaced test pits, within the PAF and within the NAF zones, in general indicated similar material properties which suggested that the variability in the waste rock dump is likely to be in the tens of metres. Apart from variability, the key constraints on the sampling requirements are as follows:

- The highest risk of misclassification is likely to be at the NAF/PAF interface or transition.
- The length of the NAF/PAF contact zone is about 500 m to 600 m.
- Up to 75,000 m³ (or 9%) of material to be relocated could be misclassified without adversely impacting the outcome.

Assuming that the active mining face width is about 15 m (with mining progressing in strips from west to east), approximately 40 strips would be mined that would intersect the PAF/NAF boundary. The contact between the NAF and PAF material is illustrated in Figure 4 and represents the sample locations adjacent to the contact zone. Assuming furthermore that the:

- first sample originates from the very edge of the NAF zone;
- next sample is within the PAF zone; and,
- interpreted boundary for PAF / NAF contact will be set at half distance between the two samples.

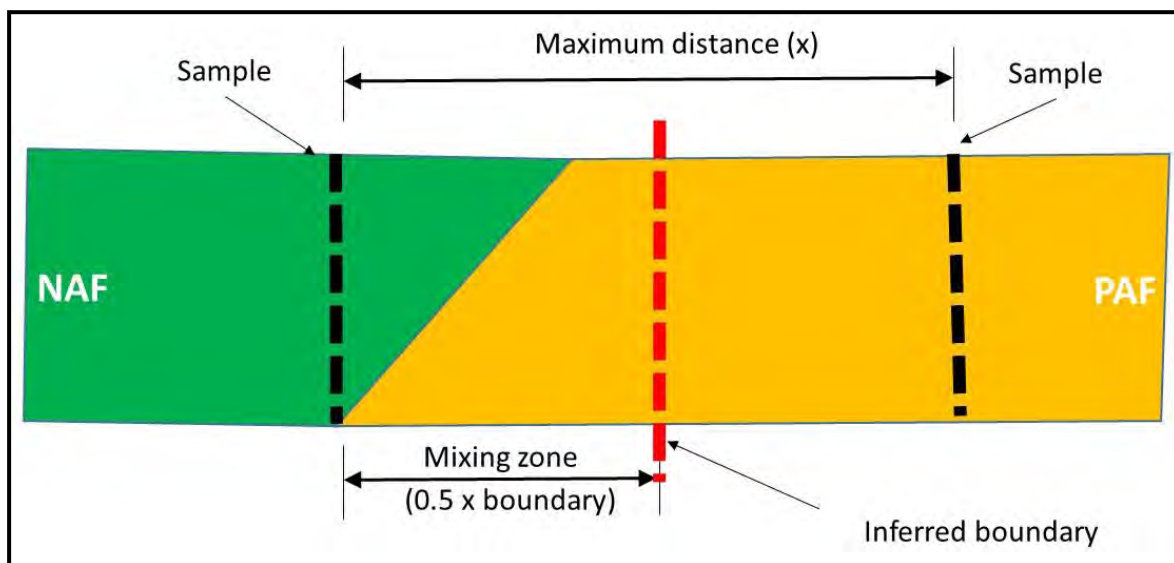


Figure 4: Contact and Mixing Zones between NAF and PAF (section of 5 m cut)

The maximum distance between sample locations, that should result in an amount of PAF material that is mined that does not exceed the total amount of material that may be placed in the cover (i.e. 75,000m³), can then be calculated based on the maximum proportion of PAF that could be captured erroneously in each cut. Using an angle of repose slope of 1:1.3 (V:H) for the contact face, the maximum distance between samples (distance x) can be calculated as follows:

$$75,000 \text{ m}^3 / (40 \text{ strips} * 5 \text{ cuts}) = (0.5 (x) \text{ m} * 15 \text{ m} * 5 \text{ m} - 0.5*(6.5 \text{ m} * 5 \text{ m} * 15\text{m}))$$

Solving x yields a maximum distance of 16.5 m. This effectively requires a sampling grid of 16.5 m x 15 m (east to west and north to south). For simplicity, a regular grid of 15 m x 15 m was adopted.

At this distance, the maximum amount of PAF material that could be mixed into the NAF would not be exceeded. Whilst this only addresses the contact zone, monitoring of the mining face would further ensure that pockets of PAF that may exist elsewhere are not inadvertently mixed into the NAF materials.

3.0 PROPOSED CONTROL PROGRAM

The recommended control program for the identification and relocation of non-NMD NAF material would rely on observations and testing of materials in advance of mining. A two-pronged sampling and testing approach was adopted as follows:

1. Test pitting, sampling, testing and classification in advance of mining on a 15 m x 15 m grid; and,
2. Control sampling, mapping and verification during mining.

3.1 Test Pitting and Sampling

In advance of mining the first lift (upper layer), a 15m x 15 m grid is to be laid out, commencing from the initiation point of mining, across the NAF/PAF boundary to enable clear identification of the NAF/PAF boundary prior to mining. The grid is to extend across to the crest of the WRD on the west. The test pitting is completed on the upper cut (first layer) in advance of mining; test pitting of the next layer can commence behind the mining face, whilst ensuring safe working conditions. At the intersection of each gridline, a test pit is to be excavated to a depth of 5 m (i.e. depth of the mining cut or layer). The test pit is to be logged, photographed and sampled. An integrated composite sample of about 2 kg of the less than 10 mm material for the entire depth of the test pit is to be obtained. Where there is a clear layering of PAF material, and the PAF layer is more than 10% of the wall height of the test pit, then the layers are to be sampled separately.

Each sample is to be submitted for pH and EC determination, and for total sulphur analysis. A representative split is to be retained for future verification and analysis as required.

Sample classification will then be undertaken as follows:

- i) If Total S < 0.6 % and paste EC < 1,700 uS/cm and paste pH > 6, then the sample is classified as NAF-nonNMD.
- ii) If Total S < 0.6 % and 1,700 uS/cm < paste EC < 4,000 uS/cm and paste pH > 6, the ANC is to be determined, and if the ANC/MPA > 2, then the sample is classified as NAF (with an acceptable short-term risk of NMD).
- iii) If total S > 0.6 %, then the sample is classified as PAF.

The sample classification is to be transposed onto the surface map of the Magazine WRD and colour coded. Where multiple samples are taken from a single test pit, then the test results will be weighted based on the stratification of the material each sample represents. For example, if three samples each representing 2 m, 2 m and 1 m layers respectively of material in a 5 m test pit return assays of 0.3, 0.2, and 0.7 % sulphur, then the weighted average will be determined as:

$$S(\text{avg}) = (2 \times 0.3 + 2 \times 0.2 + 0.7 \times 1) / 5 = 0.35\%$$

and the test pit will be classified accordingly – i.e. NAF in this instance.

The mapping will be used to delineate the contact between NAF and PAF material. Where adjacent holes are classified as NAF and PAF respectively, the contact between NAF and PAF will be assumed to fall at half distance between the test pits. The surface map will be developed as test results become available. Since test pitting is expected to precede mining by several days, a daily updated map will be developed and supplied to mining operations.

As mining of the upper bench progresses, test pit excavation and sampling of the next lower bench will be undertaken as and when safe to do so. The same sample classification approach as noted above will be adopted to demarcate the bench to distinguish between NAF and PAF materials.

3.3 Mining Face Mapping and Monitoring

During mining, the mining face will be mapped visually to identify colour transitions and/or material boundaries. Where a clear boundary is encountered, mining is to be directed elsewhere until the properties of the new face can be verified. The mining face is to be photographed and mapped visually at the beginning of each day shift (active as well as inactive face), and as and when safe to do so during the mining to verify the transition between NAF/PAF material and to ensure that PAF material is not inadvertently being placed as NAF. This will include logging and photographing of the mining face and the upper surface of the lower bench based on colour (transition from reddish oxidized material to fresher greyish material), sulphur content and lithology to identify boundaries and to guide mining. Mapping of the active face will be verified against the surface grab sampling to verify classification in advance of mining and may be used to either increase or decrease the grid size based on the observed material variability in the face.

The face mapping will essentially be used to verify the initial material classification. Where obvious NAF material is exposed that is not indicated by the initial sampling and testing, then it may be necessary to either temporarily stockpile the material until their properties can be verified, or the material is to be placed as PAF in a suitable location.

Mining of materials not suitable for cover construction are to be avoided where possible. Where an entire face is classified as not suitable for construction, then the materials are to be:

- i) left in place if located near the inferred contact between NAF and PAF, or,
- ii) stockpiled temporarily on the Magazine WRD (for later dozing down the face and then covered), or,
- iii) placed on the HHOC in an existing PAF area as fill where required, provided it does not impact on the surface drainage design. Alternatively, it can be stored on the Magazine WRD for later relocation (to the face) and covering. This is to be an operational decision at the time of relocation.

4.0 CONCLUSIONS

A basis for determining sampling frequency and testing requirements were developed based on the outcomes of an initial geochemical investigation completed on materials to be used for cover construction. The sampling and testing requirements were incorporated into a control program to ensure that only suitable materials will be placed as cover materials on the HHOC WRD to isolate PAF materials. The control program has since been implemented, and

operational constraints and actual performance of the control strategy are described in a companion paper.

5.0 REFERENCE

ANZECC 2000, *Australian Guidelines for Water Quality Monitoring and Reporting* Australian and New Zealand Environment and Conservation Council, Agriculture and Resource Management Council of Australia and New Zealand, 2000.

THE PRACTICALITIES AND IMPLEMENTATION OF A NAF GRADE CONTROL PROGRAMME FOR PLACEMENT OF A WRD COVER

A. Hendry^A, B. Luinstra^A, J. Jones^B, K. Mandaran^B and J. Chapman^A

^ASRK Consulting (Australasia) Ltd Pty, 10 Richardson St, West Perth, WA 6005, Australia

^BMount Isa Mines, Mount Isa, QLD 4825, Australia

ABSTRACT

Mount Isa Mines (MIM) has commenced rehabilitation of the Handlebar Hill Open Cut (HHOC) Waste Rock Dump (WRD). This includes reshaping of the WRD and placement of an interim inert cover over potentially acid forming (PAF) and neutral mine drainage (NMD) waste rock exposed following the reshape. The interim cover material was recovered from the adjacent Magazine WRD. To ensure that only non-acid forming (NAF) non-NMD material was used, a grade control programme was implemented which ran simultaneously with the active mining of the Magazine WRD (November 2016 – April 2017).

To ensure that only NAF non-NMD material was used for construction, a sampling and grade control programme was implemented to delineate NAF non-NMD materials contained in the Magazine WRD. Material was sampled from test-pits, excavated to a depth equal to the mining flitch, on a variable grid in advance of mining. Samples were then analysed to support material classification. Several logistical, scheduling and safety challenges were faced, including:

- *Classification sufficiently in advance of active mining.*
- *Safe working procedures without causing delays or interference to mining.*
- *Strategies to reduce mining time and costs associated with unsuitable materials.*

Waste rock classification was found to agree well with the NAF/PAF boundary identified from a preliminary site geochemical field investigation. Whilst “NAF” and “PAF” materials could mostly be identified based on geological characteristics, in the southern end of the Magazine WRD “NAF” lithologies contained higher sulphur and had been impacted by seepage from overlying PAF materials.

Post-placement verification indicated that the resolution of the sampling and testing was sufficient to meet the requirements of the cover specification.

1.0 INTRODUCTION

Mount Isa Mines (MIM) intend to cover the potentially acid forming (PAF) and neutral mine drainage (NMD) waste rock exposed in the Handle Bar Hill Open Cut (HHOC) waste rock dump (WRD) to place the WRD in care and maintenance until final closure and reclamation can be undertaken. As such, the primary objective of the cover is to isolate any PAF material that is exposed on the WRD and limit contaminant release in runoff from the WRD, noting that runoff is controlled on site in downstream sediment dams and release off-site is managed to less than 1% annual exceedance probability (AEP).

As described in Chapman et al. (2017), field and laboratory investigations undertaken in support of the development of the care and maintenance plan for HHOC WRD indicated that a large proportion of the adjacent Magazine WRD comprised NAF non-NMD materials that

were considered suitable for construction of the care and maintenance cover.

Material balances also indicated that sufficient NAF material was present in the Magazine WRD to complete most of the cover construction, and represented a cost-favourable source for cover materials due to the short-haul distance to HHOC WRD and the mining methods that could be employed (truck and shovel operation).

As the Magazine WRD contained some sulphidic PAF material, MIM required that a comprehensive grade control programme be developed to ensure that materials recovered from the Magazine WRD were NAF non-NMD. The development of the control programme is described in Chapman et al. (2017). Key to achieving effective material classification and placement control was to complete sampling and testing ahead of mining, in order to ensure that the material was classified before it is relocated.

The geochemical classification criteria developed for the control programme sampling were:

- i) If Total S < 0.6 % and paste electrical conductivity (EC) < 1700 $\mu\text{S}/\text{cm}$ and paste pH > 6, then the sample is classified as NAF (non-NMD).
- ii) If Total S < 0.6 % and 1700 $\mu\text{S}/\text{cm}$ < paste EC < 4000 $\mu\text{S}/\text{cm}$ and paste pH > 6, the acid neutralisation capacity (ANC) and maximum potentially acidity (MPA) are to be determined, and if the ANC/MPA > 2, then the sample is classified as NAF (with an acceptable short-term risk of NMD).
- iii) If total S > 0.6 % then the sample is classified as PAF.

The following sections give an overview of the implementation of the design of the grade control programme, provide a summary of the test-pit characterisation results, and describe some of the practical challenges overcome during the programme which was run simultaneously with the active mining of the WRD.

2.0 IMPLEMENTATION OF THE GRADE CONTROL PROGRAMME

The original control programme design was based on a mining plan that included five 5 m flitches. However, the mining plan was revised due to the constraints of the mining fleet equipment size. That is, the depth of the flitches was constrained by the depth that the excavator bucket could reach to dig test pits. Whilst it would have been possible to slightly reduce the density of the test pit and sampling grid, the original strategy was retained as it would result in a slightly more conservative outcome. The Magazine WRD materials were therefore characterised by test pitting on a 15x15 m grid to the proposed mining flitch depth (4 m), on seven successive levels (Figure 1).

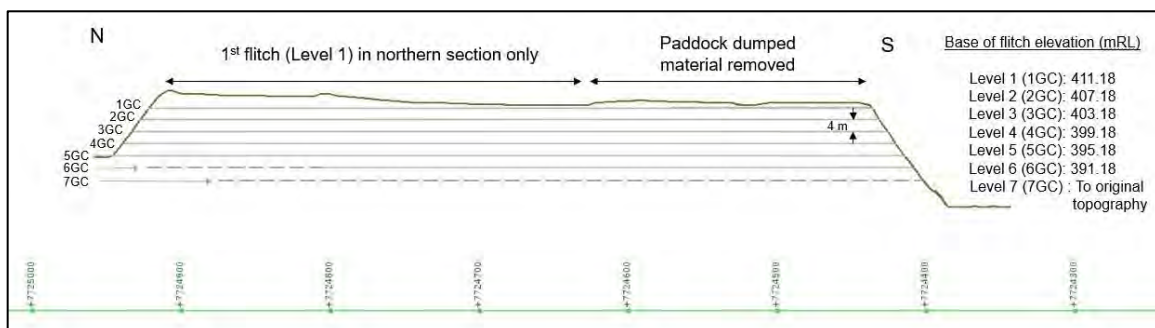


Fig. 1. Magazine WRD mining level and elevations

Note: Due to the topography of the WRD following removal of the paddock dumped material, the first mining lift (Level 1) was restricted to the northern section of the dump to achieve a consistent elevation across the dump (~411 mRL). Subsequent levels of 4 m depth were mined in cuts orientated from E-W, progressing from south to the north of the WRD.

The test pit grid was constrained towards the eastern side of the WRD, using the minimum and maximum inferred PAF/NAF interface boundaries developed using the findings of the previous geochemical site investigation (Figure 2).

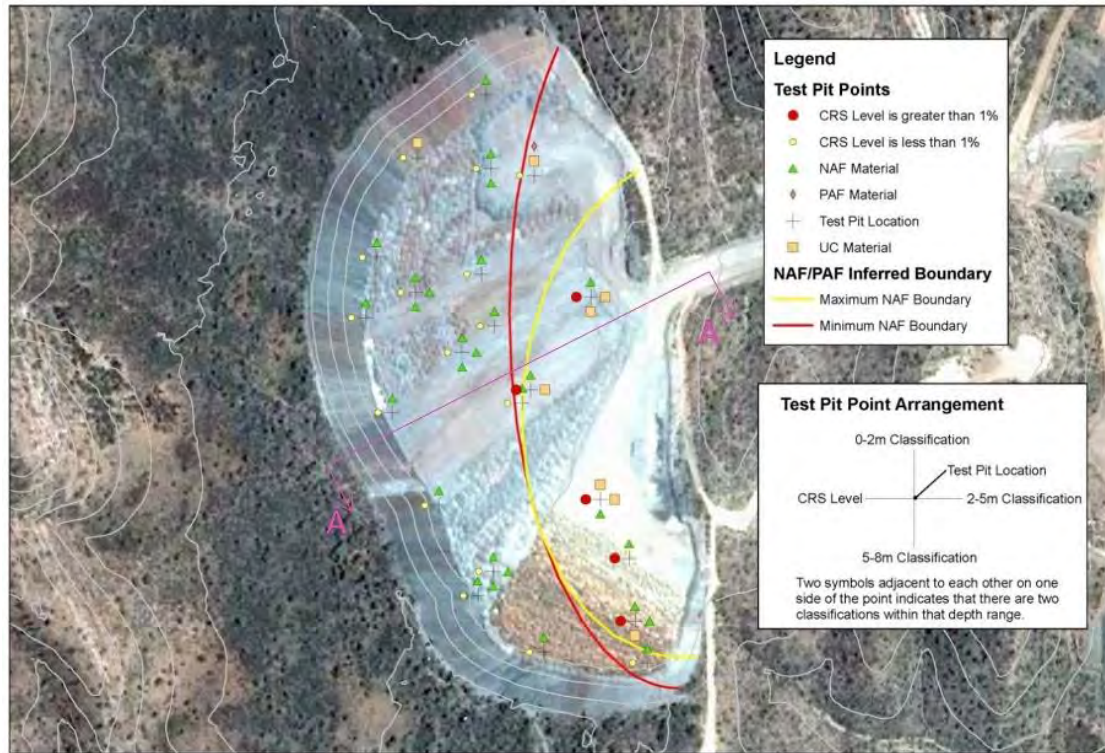


Fig. 2: Magazine WRD material characterisation and inferred NAF/PAF contact

Following the removal of paddock-dumped materials from the top of the Magazine WRD, test-pitting for material characterisation was completed on the uppermost level of the WRD between August-November 2016, in advance of the commencement of mining operations (12th November 2016).

Characterisation of the subsequent lower levels was undertaken simultaneously with mining of the WRD, requiring the test pitting to be performed in areas bunded off from the mining vehicle traffic (Figure 3) for safety reasons.

Test pit samples were collected as composite samples over 4 m depth (to be representative of the flitch depth) unless distinct PAF and NAF lithology layers were identified, in which case layers were sampled separately generally, and test results were weighted based on the stratification of the material represented by each sample. For each sample, approximately 2 kg of material (sieved to < 10 mm) was collected and homogenised. A sub-sample was taken and sieved to below 2 mm for paste parameter¹ measurement (pH and EC). The 2 kg sample bags were delivered to the on-site laboratory where a sub-sample was taken by laboratory staff for XRF analysis².

¹ Paste tests were performed using a 1:2 solid to liquid (v/v) ratio.

² XRF parameters Al₂O₃, As, Ba, CaO, Cd, Co, Cu, Fe, MgO, Pb, S, SiO₂, Zn.



Fig. 3. Test pit logging and sampling (a) prior and (b) during active mining

In order to avoid impact on the mining and placement schedule, the materials were required to be classified and the NAF/PAF interface (the “No Dig Line”) delineated sufficiently in advance of the mining front. Typically, during the test pitting of the uppermost surface, approximately 10-15 test pits were completed each day, increasing to 20-30 test pits as the field geologists became more familiar with the waste rock lithologies.

Daily mined volumes varied approximately between 9,000-24,000 m³, which were largely dictated by the number and size of trucks operating and the driving conditions. Two excavators were sometimes available to mine the face simultaneously (Figure 4); however this did not always significantly increase the daily volume mined, as the operations were limited by the available truck fleet.

Mining delays normally were a result of machinery breakdowns or inclement weather (heavy rain or lightning risk stoppage). Heavy rainfall sometimes resulted in the Magazine WRD ramp conditions becoming too dangerous for trafficking (due to slippage risk). This resulted in stoppage time and reduced mining rates but improved test pitting rates due to easier access to test pit locations.

The characterisation of materials were achieved well in advance of the mining front; however, this required short laboratory data turnaround times (2-3 days) and efficient data processing and geochemical interpretation. A spreadsheet tool was developed to aid the storage and interpretation of the geological logging, assay and paste test results and plotting the spatial distribution of test pit classifications (to aid the delineation of the NAF/PAF boundary). The NAF/PAF boundary was delineated as soon as the assay results were issued, and a mining control “No Dig Line” was issued to the mining supervisors on a level-by-level basis, several days in advance of the mining front advancing to the next level down.

This allowed time for mine planning, such as determining ramp access, traffic routing, and so on.



Fig. 4. Two excavators mining the face

3.0 WASTE ROCK LITHOLOGIES ENCOUNTERED

Generally, the waste rock encountered could easily be distinguished as either NAF or PAF by lithology (Figure 5). Typical NAF material comprised laminated siltstone of (variable colour) with sulphur contents below 0.6 %. Obvious PAF material occurred as dark grey siltstone with some quartz veining, often mineralised, with sulphur content of 1-13 wt%, with calcite present (strong fizz test) (Figure 5). An ochre/mustard weathered top to the PAF material was often present. Most waste rock was found to comprise gravel to boulders in a silty matrix. PAF lithology clasts were often present in reworked “waste rock conglomerates”, particularly in the upper weathered zone. The interface between the NAF and PAF material was typically encountered at a 45 degree angle away from the early WRD extent (circa 2005 (Chapman et al. 2017)), due to the tipping method by which the dump was constructed.

4.0 GRADE CONTROL MATERIAL CLASSIFICATION RESULTS

The test pit locations, located on the intersects of the 15 x 15 m grid, were classified based on the grade control geochemical criteria and plotted spatially to delineate the NAF/PAF boundary. The test pit classifications for Level 1 are shown on Figure 6a. The data were reviewed and a “No Dig Line” was developed as a boundary of PAF material that should be left in-situ (to the east of the line), and material to the west of the line to be mined. PAF lithologies were found to be restricted to the eastern side of the WRD. Test pits, that were classified as either PAF or NMD NAF to the west of the line, on the most part comprised the “NAF” laminated siltstone lithology with intermediate sulphur content (0.6-1 wt % S) or EC 1700 $\mu\text{S}/\text{cm}$ < paste EC < 2500 $\mu\text{S}/\text{cm}$ (Figure 6b).



Fig. 5. Typical NAF and PAF lithologies encountered

As the test pit classification was required to be determined mostly within 2-5 days of the sample collection, it was not practical to schedule the samples for ANC testing (using a modified Sobek method (1978)) at an external laboratory. Instead, when required, it was necessary to make judgement calls on the suitability of a marginal NMD NAF or PAF classified test pits. To make such a call, factors such as inferred ANC (based on available XRF assay data, i.e. CaO), geological field observations (e.g. presence/absence of visible pyrite within the waste rock), and the characteristics of the surrounding waste rock (i.e. potential mixing/dilution effects if utilised as cover on HHOC WRD) were considered. If a test pit was classed unsuitable as cover, it was categorised as “reject” material, to be mined and stockpiled on the top of the Magazine WRD, or at other suitable locations on HHOC WRD that were to be subsequently covered, with dig boundaries defined as half distance to the adjacent test pit (if that test pit was deemed acceptable).

Waste rock to the south of the uppermost level of the Magazine WRD was found to have higher sulphur contents (up to 1.3 wt% S) and EC values (up to 2700 $\mu\text{S}/\text{cm}$) than typical NAF lithology material west of the “No Dig Line”. This “contaminated NAF” material is thought to have been impacted by mixing and seepage from overlying waste rock. The contaminated NAF material was mined and placed in a stockpile on top of the dump so as not to sterilize volumes of underlying material that may not have been impacted. Some samples of the material were selected for additional geochemical analysis, to determine sulphur speciation, ANC and leach test metals contents. Based on those results, the material was subsequently verified to be unsuitable for use as cover material (using the classification criteria), and provided confidence in the control programme and material characterisation strategy.

The test pit sampling plan and classifications for Level 5 are shown on Figure 7. The test pit grid spacing was increased to 30 m x 30 m on the western side of the WRD, when NAF material had been encountered consistently in test pits excavated on the eastern sector of the level. The average sulphur content of waste rock accepted for cover was 0.28 wt% (as total S), and electric conductivity values were lower than encountered on the uppermost level (< 1000 $\mu\text{S}/\text{cm}$), and thus no material was classified as NMD NAF.

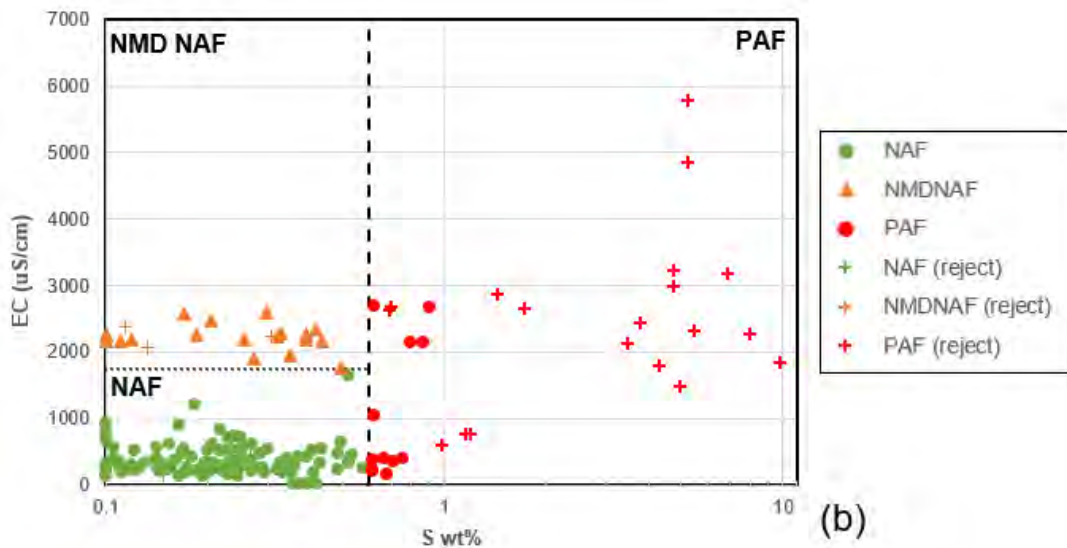
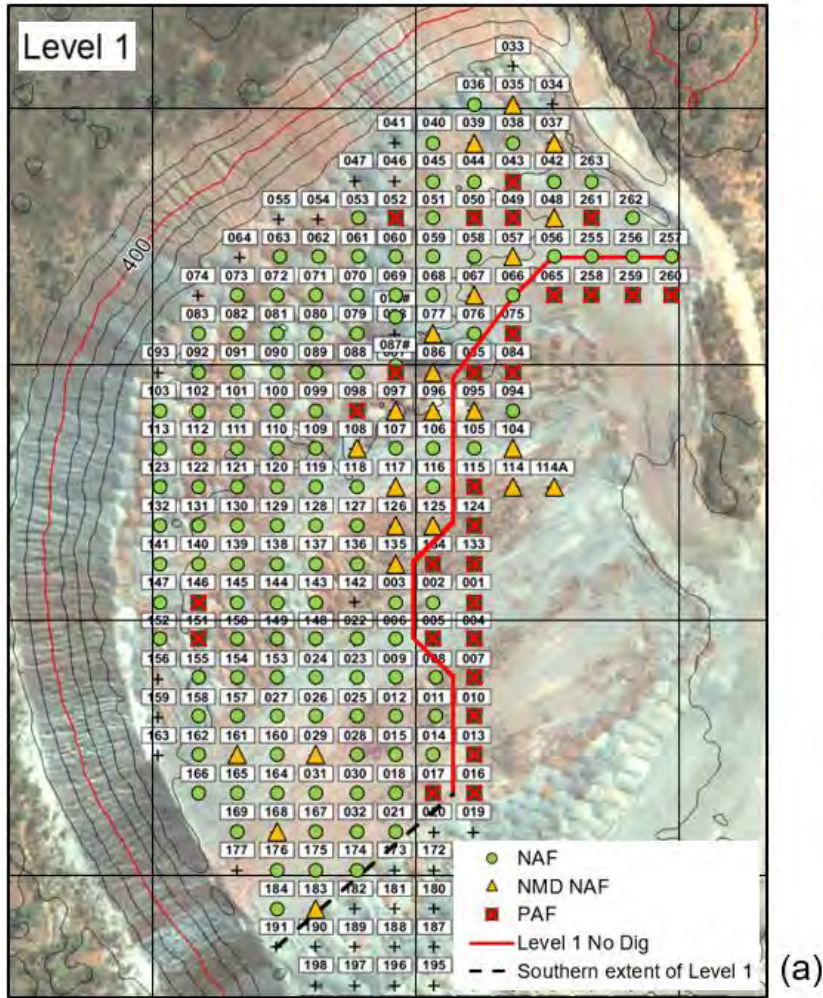
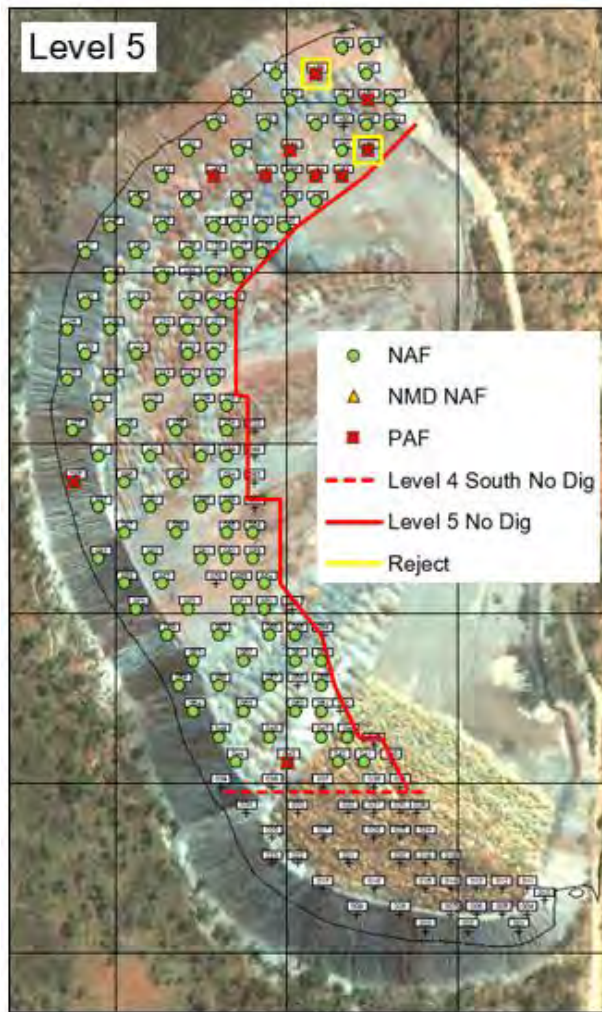
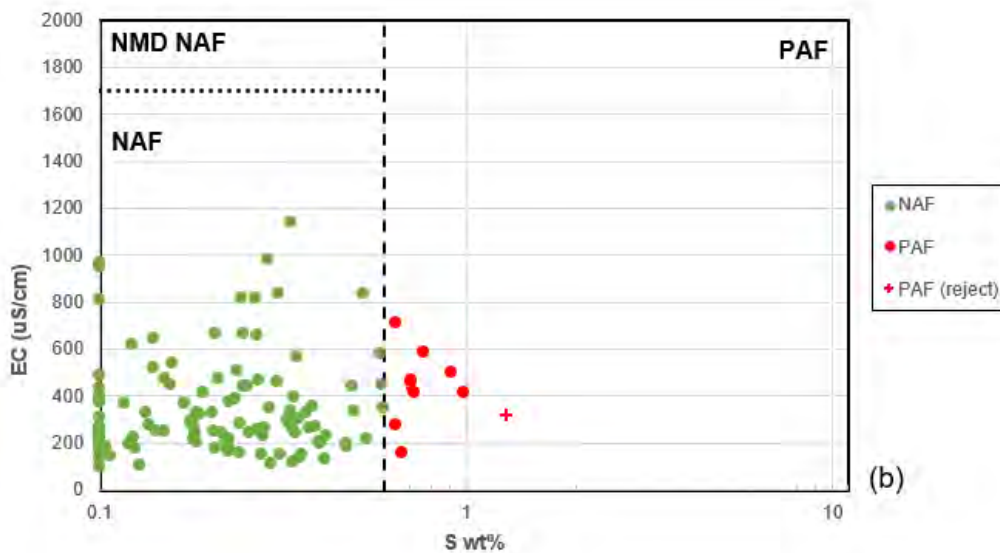


Fig. 6. Level 1 test pit classifications (a) in plan and plotting (b) S against EC

Notes: The classifications of test pits that were rejected as cover material include material to the east of the “No Dig Line” are shown as crosses (+). Data shown are reported composite sample results or weighted average results where two or more samples were collected from test pits.



(a)



(b)

Fig. 7. Level 5 test pit classifications (a) in plan and plotting (b) S against EC

Notes: The classifications of test pits that were rejected as cover material include material to the east of the “No Dig Line” are shown as crosses (+).

Initial verification sampling of the as-placed cover on HHOC WRD (i.e. of materials sourced from the Magazine WRD) has been undertaken by test pitting to depth of 1.5 m (equal to the required cover thickness). The results have uniformly been returned as NAF, indicating that the resolution of sampling and testing was sufficient to meet the requirements of cover specifications.

5.0 PRACTICALITIES AND DEVIATIONS FROM DESIGN

Rationalisation of the grade control programme sampling design was required to minimise delays to mining, reduce health and safety risks and make the site geologist's daily tasks achievable. First, the proposed pit face sampling was not undertaken, as accessing the active mining face every two hours would have temporarily halted mining, impacting mining rates and also increasing health and safety risks to the sampler. Instead, the site geologist inspected the mined face during crib time each day. Negligible PAF material to the west of the "No Dig Line" was encountered and was limited to the immediate vicinity of the NAF/PAF contact. Excavator operators became sufficiently experienced to flag material suspected as being PAF to the on-site geologist (i.e. called up on the radio). Second, based on the general homogeneity of the materials encountered to the west of the NAF/PAF contact, it was possible to reduce the test pit grid spacing in the lower mining levels (i.e. Levels 3 to 7).

From a practical perspective, the excavators did not have GPS equipment to inform them electronically of the location of "No Dig Lines", or the flitch elevations to be mined. Therefore, "No Dig Lines" were required to be marked out by the on-site geologist to guide the excavator operators. Dozer machines, that were used to tidy up the floor of the mined face, were equipped with GPS, and were able to instruct the excavator operator as to achieving the required flitch mining elevation. Graders were used to level out the mine floor behind the advancing mine face, working around trucks as required.

Reject materials within the mining zone were required to be marked out for the mining team using pegs and tape, which could be easily damaged by mining vehicles (i.e. the excavators) or impacted by wind, and were hard to see during night-shift mining. In such instances, a GPS control would have facilitated operations significantly.

Off-site geochemical verification testing was undertaken (including the contaminated NAF material at the south of the dump). However, due the freight times and laboratory turn-around times, this test work had a long lag time and if relied on, would have held up mining. Consequently, materials sampled and scheduled for off-site verification testing were either mined and stockpiled (e.g. contaminated NAF) or left in-situ until laboratory results were issued and the suitability of the material could be more accurately determined. This resulted in a balance between potential delays to mining or increasing the complexity of the mining process versus robustly maximising the volume of potential cover material.

6.0 CONCLUSIONS

A NAF/PAF grade control programme was developed and successfully implemented to determine the geochemical suitability of waste rock materials to be used in the construction of a care and maintenance WRD cover. The strategy relied on both field and on-site laboratory analyses to ensure a quick turnaround to prevent impacts on mining activities.

The waste rock classification and delineation of the NAF/PAF boundary was in good agreement with the previous geochemical site investigation and historic aerial photographs

of the WRD. The programme did, however, successfully identify a zone of material to the west of the contact boundary that was classified as unsuitable for cover construction, which allowed the material to be stockpiled for later rehabilitation. The homogeneity of the waste rock materials to the west of the NAF/PAF boundary allowed the sampling grid to be relaxed to 30m x30 m when sufficiently far removed from the contact boundary (i.e. 30 m or more), with the constraint that infill test pitting (to a 15 m x 15 m grid) would be undertaken should unsuitable materials be encountered.

Initial verification sampling results of the as-placed cover have uniformly been returned as NAF, indicating that the resolution of sampling and testing was sufficient to meet the requirements of cover specifications.

7.0 REFERENCES

Chapman J, Jones JJ, Mandaran K, Luinstra B and Hendry A (2017). Development of a NAF/PAF Grade Control Programme For Placement of a WRD Cover. 9th Australian Workshop on Acid and Metalliferous Drainage, Burnie, Tasmania (November 2017).

Sobek, A.A., Schuller, W.A., Freeman, J.R., and Smith, R.M. (1978). Field and Laboratory Methods Applicable to Overburdens and Minesoils., EPA-600/2-78-054, p.p. 47-50.

THE FORMATION OF ALUMINATE-DOPED SURFACE PASSIVATING LAYERS ON PYRITE FOR EFFECTIVE ACID AND METALLIFEROUS DRAINAGE CONTROL

Y. Zhou^A, M.D. Short^{A,B}, J. Li^A, R.C. Schumann^C, R.St.C. Smart^{A,D}, A.R. Gerson^D
and Gujie Qian^{A,B*}

^ANatural and Built Environments Research Centre, School of Natural and Built Environments, University of South Australia, Mawson Lakes, SA 5095, Australia

^BFuture Industries Institute, University of South Australia, Mawson Lakes, SA 5095, Australia

^CLevey & Co. Environmental Services, Edinburgh, SA 5111, Australia

^DBlue Minerals Consultancy, Wattle Grove, TAS 7109, Australia

ABSTRACT

Acid mine drainage associated with elevated concentrations of dissolved toxic metals/metalloids (AMD) results primarily from the oxidation of pyrite, and is considered to be the most serious environmental issue facing the mining industry. The development of cost-effective and sustainable management solutions for AMD prevention and remediation is of importance to both the mining industry and government. In this work, we carried out a series of pyrite dissolution experiments at various pH values (2, 4 and circum-neutral) to test the performance of a novel but practical method for AMD control through the formation of aluminate-doped surface passivating layers on pyrite. At pH 2 and 4, no obvious inhibition of the pyrite oxidation rate was observed by addition of $AlCl_3$ (10 to 20 mg Al L⁻¹). In comparison, the pyrite oxidation rate at circum-neutral pH (7.0–7.8) decreased (>98% over 282 days) with increasing concentration of added $AlCl_3$, which mainly exists in the form of aluminate precipitates at this pH. Electron microscopy analysis showed that compact crystalline surface layers (confirmed to be goethite by electron diffraction) were formed on pyrite when leached in the presence of added $AlCl_3$ at circum-neutral pH, in contrast to porous crystalline goethite surface layers on pyrite leached without added Al^{3+} under otherwise identical conditions. This work demonstrates the potential for novel Al-based pyrite passivation which could be of relevance to the mining industry, where suitable Al-rich waste materials are available for AMD control interventions.

Keywords: Acid and metalliferous drainage; Aluminate-doped passivating layer; Pyrite oxidation; Surface layer structure

1.0 INTRODUCTION

Acid rock drainage and associated metalliferous release (AMD), occurring when sulfides (principally pyrite)-containing rock from mining activities and from some natural environments is exposed to the elements, is acknowledged as a major environmental problem. AMD management is often focused on treating acid on release rather than preventing it at source. More recently, the role of silicates in the passivation of pyrite oxidation and reduction of acid generation rate has been recognised. We have described a viable, practical mechanism for reduced AMD through the formation of silicate-stabilised iron hydroxide surface layers on pyrite limiting oxygen access to the pyrite surface (Fan et al. 2017; Zeng et al. 2013; Schumann et al. 2009). Without silicate, oxidised pyrite particles form an over-layer of crystalline goethite or lepidocrocite with porous structure. With silicate addition, a smooth, continuous, coherent and

apparently amorphous iron hydroxide surface layer is observed, with consequent pyrite dissolution rates reduced by more than 90% at neutral pH. Silicate is structurally incorporated within this layer and inhibits the phase transformation from amorphous iron (oxy)hydroxide to goethite, resulting in pyrite surface passivation. This mechanism and its controlling factors are described in the recent *Environmental Science and Technology* paper (Fan et al., 2017). As a consequence of the greatly reduced acid generation rate, neutralisation rates from reactive (alumino)silicate minerals may be used to maintain neutral pH and the integrity of these layers for effective ARD management. This combination offers cost-reduction in ARD management but has yet to be fully implemented in site trials or operation.

The dissolved silicate can be generated by dissolution of more reactive silicates and aluminosilicates (e.g. olivines, anorthite, chlorite) in the mineral assemblage of the ARD waste (Gerson et al. 2014). A similar role for dissolved aluminate from these sources or as additives has also been proposed but has yet to be investigated in detail. The effect of dissolved aluminate on pyrite oxidation and acid generation rate has also not been defined.

Schwertmann et al. (2000), who examined the effect of pH (4–7) and co-precipitated versus mechanical mixtures of added Fe and Al ions, reported that Al^{3+} addition resulted in the incorporation of Al^{3+} into ferrihydrite, inhibiting the transformation to goethite and hematite. Cismasu et al. (2012) supported this conclusion based on characterisation of two synthetic Al-bearing ferrihydrites formed at different precipitation rates in the presence of 5–40 mol% Al^{3+} . Furthermore, they found that the crystallinity of Al-ferrihydrite precipitates was affected by precipitation rates and an increase in the concentration of Al^{3+} doping, and that the maximum amount of Al^{3+} incorporated into ferrihydrite was independent of the synthesis method.

Pinney and Morgan (2013) recently employed *ab initio* quantum simulations to study Al-containing Fe oxide and (oxy)hydroxide structures, and found that the thermodynamic driving force for transformation of iron (oxy)hydroxides to hematite was reduced when doped with Al^{3+} . They also suggested that surface segregation of Al^{3+} dopants occurred preferentially at low concentrations of Al^{3+} based on the simulation of Al-substitution on the goethite (101) surface.

These studies suggest that inclusion of Al^{3+} into iron (oxy)hydroxides on the surface of pyrite could reduce both the rate and driving force for transformation to non-passivating crystalline iron oxides, thus stabilising the passivation layer. Nevertheless, the role of aluminate in stabilising iron (oxy)hydroxides surface layers on pyrite and its potential for enhanced pyrite passivation and acid generation reduction has not yet been investigated. This additional passivation of pyrite at source has the potential to provide further ARD management options and cost reduction.

In this study, we have investigated the dissolution kinetics of pyrite in the presence and absence of aqueous Al^{3+} and a mechanistic understanding of the role of aluminate ions in pyrite surface passivation. The study confirms that aluminate incorporation into surface layers on pyrite reduces the acid generation rate by magnitudes similar to silicate incorporation. The surface layer structure, however, is considerably different.

This interim report has been prepared as part of a journal publication to follow.

2.0 METHODOLOGY

2.1 Materials and Batch Leaching Preparation

Pyrite (Geo Discoveries, NSW, Australia) was ground and wet-sieved to obtain a 38–75 μm fraction prior to sonication for removal of fines. Pyrite was washed with 3 M HCl followed by ethanol and dried in a vacuum oven at room temperature overnight. The BET surface area of the pulverized pyrite sample was measured to be $0.85 \pm 0.01 \text{ m}^2 \text{ g}^{-1}$ by a 5-point, N_2 BET analysis using a Micromeritics Gemini 2375 instrument. All rates were normalised to this surface area.

2.2 Experimental Set-up

2 g of pyrite was added to 1 L of solution for each batch leaching test. The tests were kept in quiescent conditions to simulate ARD in rock or tailings storage for 290 days at room temperature. 0.01 M KCl solution was used for all batch leaching experiments to maintain similar ionic strength for all pH conditions (Khare et al. 2004). For batch leaching experiments containing Al^{3+} , a 0.01 M KCl solution containing 20 mg L^{-1} Al^{3+} (as $\text{AlCl}_3 \cdot 6\text{H}_2\text{O}$) was used. For pH adjustment, dilute HCl and NaOH solutions were used to maintain pH at 2.0 and 4.0, whereas pH 7.0–7.8 experiments were buffered using 1 g calcite (100–200 μm ; wrapped in nylon mesh). 15 batch tests in total were set up at pH 2.0, 4.0 and 7.0–7.8 with/without Al^{3+} . pH and Eh were periodically monitored over 290 days, and acid or base were added to maintain pH as necessary. Periodic solution samples (10 ml) were taken for elemental analysis (ICP-MS) after membrane filtration (0.45 μm).

Scanning electron microscopy (SEM) (Quanta 450 Environmental SEM, FEI, Hillsboro, OR, USA) equipped with energy dispersive spectrometry (EDS) was used for examination of freshly collected pyrite samples leached for 282 days at pH 7.0–7.8 with and without Al^{3+} addition to obtain images and semi-quantitative analysis of surface layers.

3.0 RESULTS AND DISCUSSION

3.1 Dissolution Rates

The kinetic data for pyrite dissolution with no Al^{3+} addition are generally consistent with the rate law (Eq. 1) developed by Williamson and Rimstidt (1994), showing that pyrite oxidation rate (controlled by dissolved O_2) increases with increasing pH.

$$r = 10^{-8.19(\pm 0.10)} \frac{m_{\text{DO}}^{0.5(\pm 0.04)}}{m_{\text{H}^+}^{0.11(\pm 0.01)}} \quad (1)$$

The amount of pyrite dissolved calculated from the dissolved S in the absence of Al^{3+} at pH 2.0, 4.0 and 7.0–7.8 is plotted as a function of time (Fig. 1). The results show that the long-term pyrite dissolution rates (Table 1) in the calcite-buffered solution (pH 7.0–7.8) without Al^{3+} addition ($7.08 \times 10^{-11} \text{ mol m}^{-2} \text{ s}^{-1}$) is greater than at pH 4 ($4.81 \times 10^{-11} \text{ mol m}^{-2} \text{ s}^{-1}$) and pH 2 ($2.94 \times 10^{-11} \text{ mol m}^{-2} \text{ s}^{-1}$), consistent with pyrite oxidation by dissolved O_2 (Williamson and Rimstidt, 1994). This is in contrast to the relative rates of pyrite dissolution in the presence of Al^{3+} where pyrite dissolution at pH 7 was slowest (Fig. 2).

The measured pyrite dissolution rates in the absence of added Al^{3+} are about an order of magnitude smaller those calculated using Eq.1. This difference is due to the unstirred,

quiescent experimental conditions in this work applied to more closely simulate field conditions. The Williamson and Rimstidt rate law was derived from measurements in stirred conditions. This difference suggests that pyrite dissolution rate may be partially bulk diffusion-controlled under quiescent conditions.

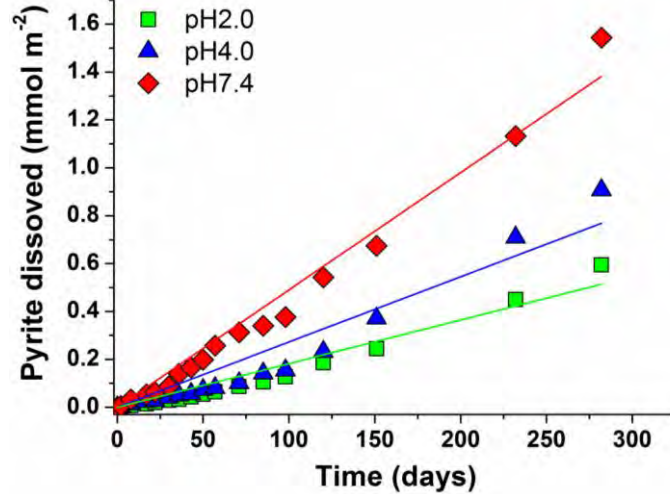


Figure 1. Pyrite dissolution kinetics without Al³⁺ addition at pH 2.0, 4.0 and 7.0–7.8.

The concentration of S released from pyrite batch dissolution with/without Al³⁺ addition under different pH conditions is shown in Fig. 2. It is clear that pyrite dissolution is reduced by Al³⁺ addition at pH 7.0–7.8, but no obvious inhibition was observed at pH 2.0 or 4.0. This result is similar to the behaviour of silicate additions at these pH values.

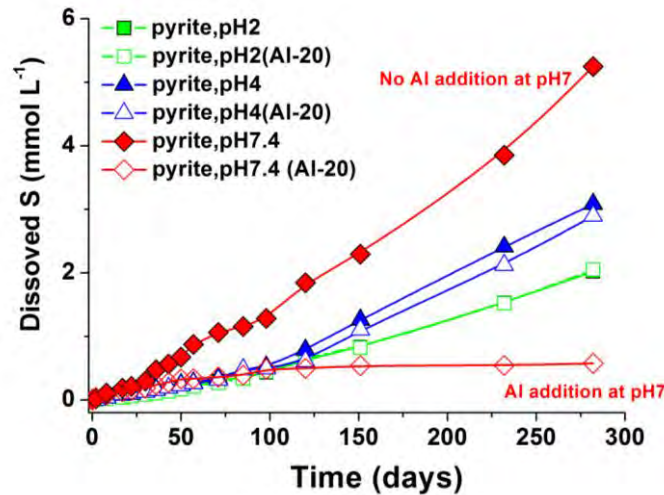


Figure 2. Solution concentration of S as a function of time for pyrite dissolution tests with/without 20 mg L⁻¹ Al³⁺ addition at pH 2.0, 4.0 and 7.0–7.8.

This dramatic reduction in pyrite dissolution at pH 7.0–7.8 is further illustrated in Fig. 3 where the amount of pyrite dissolved without Al³⁺ at each pH is subtracted from that dissolved with Al³⁺. Fig. 4 shows that the pyrite oxidation rate decreases with increasing initial Al³⁺ concentration (10 to 20 mg L⁻¹) at pH 7.4.

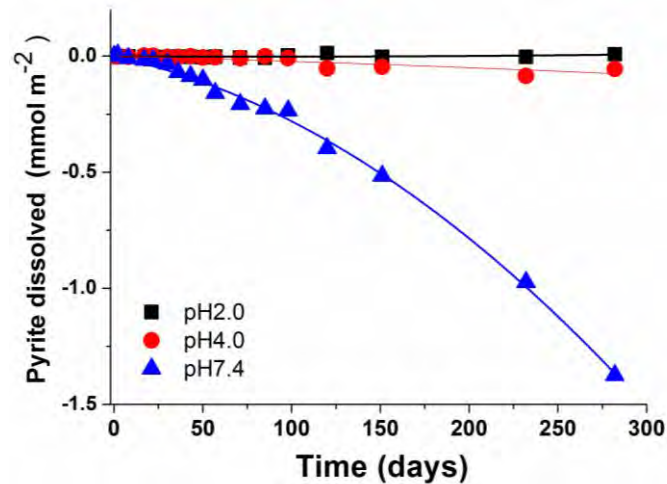


Figure 3. Pyrite dissolution with added Al^{3+} (20 mg L^{-1}) minus pyrite dissolution without Al^{3+} at pH 2.0, 4.0 and 7.0–7.8.

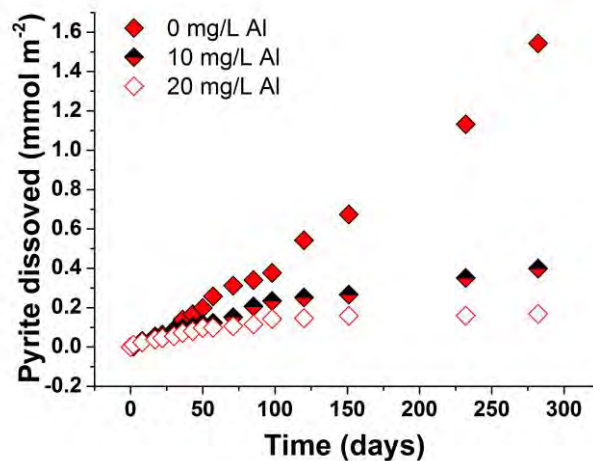


Figure 4. Pyrite dissolution as a function of time for different added Al concentrations at pH 7.0–7.8.

Results for all data have been analysed by fitting linear equations to initial (<50 days) and long-term (>120 days) pyrite dissolution data for each treatment and are presented in Table 1. They confirm a reduction of the long-term pyrite dissolution rate by close to 85 % with Al^{3+} addition of 10 mg L^{-1} and close to 98 % with 20 mg L^{-1} Al^{3+} addition. These concentrations are often found in dissolution of reactive aluminosilicates at neutral pH as discussed in (Gerson et al., 2014).

Table 1. Initial and long-term pyrite dissolution rates (mol per unit surface area; ± 1 SE) with and without Al^{3+} addition (10 and/or 20 mg L^{-1}) at pH 2.0, 4.0 and 7.0–7.8, derived from linear regression of the corresponding Figure 1 data.

Treatment	Initial (<50 days) pyrite dissolution rate (mol m^{-2} s^{-1})	Long-term (>120 days) pyrite dissolution rate (mol m^{-2} s^{-1})
pH 2.0	$1.15(\pm 0.03) \times 10^{-11}$	$2.94(\pm 0.12) \times 10^{-11}$
pH 2.0 +Al-20	$1.05(\pm 0.04) \times 10^{-11}$	$2.92(\pm 0.21) \times 10^{-11}$
pH 4.0	$1.59(\pm 0.03) \times 10^{-11}$	$4.81(\pm 0.07) \times 10^{-11}$
pH 4.0 +Al-20	$1.52(\pm 0.03) \times 10^{-11}$	$4.70(\pm 0.15) \times 10^{-11}$
pH 7.4	$4.27(\pm 0.17) \times 10^{-11}$	$7.08(\pm 0.54) \times 10^{-11}$
pH 7.4 +Al-10	$2.84(\pm 0.06) \times 10^{-11}$	$1.09(\pm 0.07) \times 10^{-11}$
pH 7.4 +Al-20	$2.26(\pm 0.06) \times 10^{-11}$	$1.31(\pm 0.46) \times 10^{-12}$

3.2 Surface Analysis

Scanning electron microscopy (Fig. 5) clearly shows significant differences in the morphology of the iron (oxy)hydroxide coating formed on the pyrite surface during dissolution with/without Al^{3+} at circum-neutral pH. A coating with needle-like morphology in the absence of added Al^{3+} is clearly visible, suggestive of a crystalline phase similar to the goethite or lepidocrocite found in the previous work without silicate additions (Fan et al., 2017). However, in the presence of Al^{3+} , the surface coating is distinctly different, with a more uniform structure. Much smaller (20–100 nm), more rounded projections are seen in the pyrite surface layer. ED's spectra (Fig. 6) indicated that both surface layers contained Fe, S and O, with substantially more O in the surface layer where Al^{3+} is absent. This suggests that in the presence of Al^{3+} the oxidised surface layer is thinner than in its absence, consistent with previous findings in the presence of silicate, which in turn supports a reduced oxidation rate. Al^{3+} was found within the surface layers formed on pyrite dissolution with Al^{3+} addition (Fig. 6), suggesting that it is responsible for the different morphology of this layer.

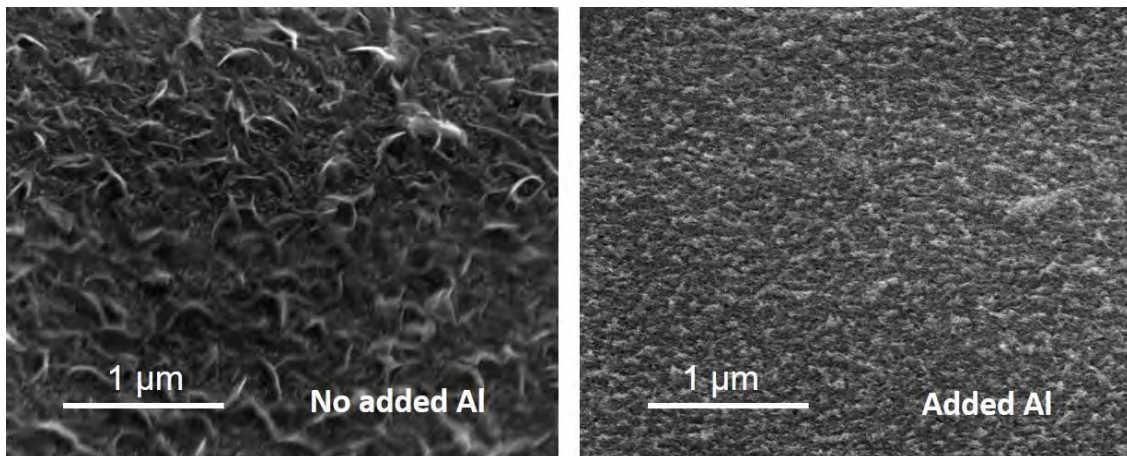


Figure 5. SEM images of pyrite surfaces leached in pH 7.0–7.8 (calcite-saturated) solution for 230 days, without added Al^{3+} (left) and with 20 mg L^{-1} added Al^{3+} (right).

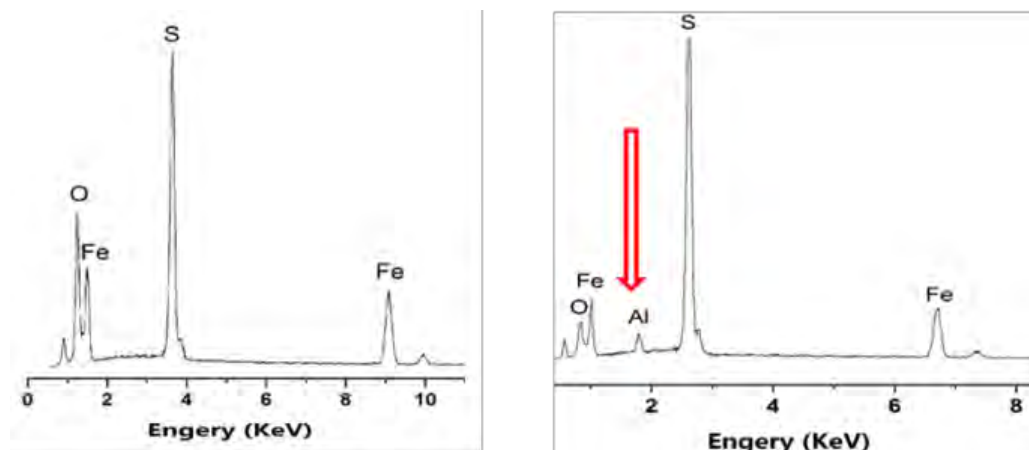


Figure 6. EDS spectra of pyrite surface coatings (from Fig. 5) after dissolution in pH 7.0–7.8 (calcite-saturated) solution for 230 days, without added Al^{3+} (left) and with 20 mg L^{-1} added Al^{3+} (right).

4.0 CONCLUSIONS

The role of soluble silicate in the stabilisation of passivating layers on pyrite, inhibiting the transformation of amorphous iron (oxy)hydroxide surface layers into porous crystalline goethite and reducing the acid generation rate by close to 90%, is now well defined. A similar role for soluble aluminate has been shown to also produce passivating layers on pyrite giving rise to a reduction of pyrite oxidation up to 98 % at neutral pH. In summary:

1. At pH 2.0 and 4.0, there is no obvious inhibition in pyrite oxidation rate in the presence of aqueous Al^{3+} (20 mg L^{-1}).
2. At pH 7.0–7.8, the pyrite oxidation rate decreases with increasing concentration of added aqueous Al^{3+} (by 85 % with 10 mg L^{-1} and by 98 % with 20 mg L^{-1}).
3. The pyrite surface layer resulting from dissolution in the presence of Al^{3+} at pH 7.0–7.8 appears to be less porous compared to that in the absence of Al^{3+} likely inhibiting oxygen access to the pyrite surface as found in the silicate-stabilised iron (oxy)hydroxide surface layers.

Further definition of the surface layers using FIB/TEM analysis and synchrotron XAS is currently underway to study the structure of the layers seen in the SEM imaging. This is intended to define the mechanism of the formation of the layers and the factors controlling their stability.

5.0 ACKNOWLEDGEMENTS

The work was supported by two Linkage Grants from the Australian Research Council and the AMIRA P933B project. The sponsors of the AMIRA P933B project, BHPBilliton Iron Ore, (Dr Rick Marton) and Teck Metals (Dr Stephane Brienne) are gratefully acknowledged.

6.0 REFERENCES

- Cismasu, A.C., Michel, F.M., Stebbins, J.F., Levard C., Brown G.E. 2012. Properties of impurity-bearing ferrihydrite I. Effects of Al content and precipitation rate on the structure of 2-line ferrihydrite. *Geochimica et Cosmochimica Acta* 92: 275-291.
- Fan, R. Short, M.D., Zeng, S.J., Qian, G., Li, J., Schumann, R.C., Kawashima, N., Smart, R.St.C, Gerson, A.R. 2017. Effect of pH and dissolved silicate on the formation of surface passivation layers for reducing pyrite oxidation. *Environmental Science & Technology*, <http://dx.doi.org/10.1021/acs.est.7b03232>.
- Gerson, A.R., Smart, R.St.C., Li, J., Kawashima, N., Fan R., Zeng, S., Schumann, R., Levay, G., Dielemans, P., Mc Latchie, P., Huys, B., Hughes, A., Kent, S., Hutchison, B. 2014. Mineralogy Of Mine Site Neutralising Materials: A Missing Link In AMD Control Planning, *Proc. Eighth Australian Workshop on Acid and Metalliferous Drainage* (Eds. H. Miller and L.Preuss), ISBN: 978-0-9924856-0-3, Publ. JKTech Pty Ltd, Indooroopilly, Qld, Australia, 313-324.
- Khare, N., Hesterberg, D., Beauchemin S., Wang S-L. 2004. XANES determination of adsorbed phosphate distribution between ferrihydrite and boehmite in mixtures. *Soil Science Society of America Journal* 68(2): 460-469.
- Pinney, N., Morgan, D. 2013. Thermodynamics of Al-substitution in Fe-oxyhydroxides. *Geochimica et Cosmochimica Acta* 120: 514-530.
- Schumann, R., Kawashima, N., Li, J., Miller, S., Smart, R., Stewart, W.S. 2009. Passivating surface layer formation on pyrite in neutral rock drainage. In *Proc. 8th Int. Conf. Acid Rock Drainage* (8 ICARD), Skellefteå, Sweden. website <http://www.proceedings-stfandicard-2009.com>. 1–12.
- Schwertmann, U., Friedl, J., Stanjek H., Schulze D.G. 2000. The effect of Al on Fe oxides. XIX. Formation of Al-substituted hematite from ferrihydrite at 25 C and pH 4 to 7. *Clays and Clay Minerals* 48(2): 159-172.
- Williamson M.A., Rimstidt J.D. 1994. The kinetics and electrochemical rate-determining step of aqueous pyrite oxidation. *Geochimica et Cosmochimica Acta* 58(24): 5443-5454.
- Zeng, S., Li, J., Schumann, R., Smart, R. 2013. Effect of pH and dissolved silicate on the formation of surface passivating layers for reducing pyrite oxidation. *Computation Water, Energy Environ. Eng.* 2: 50–55.

THE INFLUENCE OF SAMPLE NUMBERS AND DISTRIBUTION ON THE ASSESSMENT OF AMD POTENTIAL

A.M. Garvie^A and D. Kentwell^B

^ASRK Consulting (Australasia) Pty Ltd, Level 17, 44 Market St, Sydney, NSW 2000, Australia

^BSRK Consulting (Australasia) Pty Ltd, Level 20, 31 Queen Street, Melbourne, VIC 3000, Australia

ABSTRACT

The number and distribution of waste rock samples geochemically characterised before and during mine operation impacts the ability to accurately represent the waste characteristics and to predict the potential for acid and metalliferous drainage (AMD). Numerous regulatory and industry bodies recommend the number of samples that are to be characterised. Commonly, the practitioner is advised to take account of the complexity of the geology and the scale of the mine. However, in many instances, the scientific and statistical basis for the recommended numbers is either not provided or is not clear. Consequently, there is ambiguity as to how the recommendations should be applied to a particular mine at a particular stage of development and no quantitative method of gauging the accuracy of conclusions drawn, based on the approach taken to sampling is recommended.

This paper demonstrates how conclusions regarding the potential for AMD production at a mine can depend on the number of samples characterised and the specific samples selected for characterisation. Data from three mines are used to illustrate the impact of various sample numbers on preliminary conclusions related to the potential for AMD.

1.0 INTRODUCTION

Various Australian and international regulatory bodies require an initial assessment of the geochemistry of waste rock at the early stages of mine development. This often includes estimates of the locations and masses of potentially acid forming (PAF) materials and requires sampling of the waste rock zones and submitting the samples for a series of tests.

Government and industry guideline documents (BCAMDTF, 1989; INAP GARD Guide 2017; US EPA, 1994; Aus. Gov. 2016, WA Gov. 2016, MEND 2009) provide guidance on sampling approaches to be taken so that the volumes and variability of parameters of interest (such as sulfur content and acid-neutralizing capacity (ANC)) can be quantified with some level of confidence. Perhaps the most comprehensive discussion is provided by MEND (2009), which states that it is important to provide good spatial, geological and geochemical representation, because contaminant discharge may be produced by only a portion of the geological material. Further, it states that sufficient numbers of samples should be taken to accurately characterize the variability and central tendency of the different waste materials, project components and geological units.

All the above guidelines indicate that the number of samples tested will depend on the stage of mine development and will be site specific. However, it is not necessarily clear when enough samples have been tested. As an indication of the number of samples required, Aus. Gov. (2016) recommends testing up to several hundred samples at the pre-feasibility stage of mine development, whilst WA Gov. (2016) recommends that, as a starting point, 8 to 26 samples are used for disturbed waste units of mass between 100,000 and 1,000,000 tonnes, with the number of samples varying with the mass of waste. For a comprehensive presentation of the

recommendations, the original documents should be consulted.

This paper presents assessments of the average values and variability of total sulfur content for nine geological units across three mines of different commodities in different geological settings to illustrate how these can vary with the number of samples. The units cover low, moderate and high sulfur scenarios.

2.0 BACKGROUND

Many exploration and resource evaluation drill hole datasets include assays of total sulfur content. In preliminary assessments for the potential for acid and/or metalliferous drainage (AMD), it is common practice to use the distribution of sulfur as an indicator of potentially acid forming (PAF) material, because the total sulfur content is an indication of the maximum potential acidity. Often, a sulfur cut-off threshold is used to classify materials, whereby materials with sulfur contents below the threshold are considered to represent a low risk of acid generation. In this paper, we use a total S cut-off of 0.1%; however, identification of defendable sulfur cut-off requires site-specific assessment of the availability of acid neutralising capacity (ANC). Final AMD assessments are therefore supported by more rigorous geochemical characterisation that includes an examination of ANC and sulfur speciation within the mined materials.

Statistical methods were applied to large exploration drill hole data sets from nine units across three ore deposits (Table 1) to illustrate the relationship between sample numbers, sample locations, and levels of confidence on AMD assessment outcomes based on sulfur content.

Table 1. Types of ore deposits assessed

Ore Deposit	Type
Ore deposit A	Iron ore
Ore deposit B	Gold-copper
Ore deposit C	Copper gold porphyry

3.0 STATISTICAL ANALYSIS

The drill hole data sets were reviewed, and samples were grouped into units based on their lithology, alteration, and degree of oxidation. The number of drills holes per unit available for random sampling varied between 40 to more than 1000. Nine of these groups were selected to examine changes in the average sulfur content with increasing numbers of samples.

A sub sampling procedure utilising a random number generator was used to select samples randomly from the full data set (population) for each unit. Initially, four hundred samples were randomly selected, and sets of different sizes were selected from the 400 samples (Figure 1). The first set consisted of the first ten samples, the second set consisted of the first 20 samples and other sets were constructed in a similar manner for totals of 50, 100 and 200 samples. Note that the sets are therefore dependent sets in that the larger sets contain all the samples from the smaller sets. The average total S content was calculated for each set, the set of 400 samples and the population. This selection and calculation process, which generated a representation of the sulfur distribution, was performed four more times. Each representation was designated as Rx, where x had the values 1 to 5. The five representations are only a small fraction of the many thousands that are possible.

The construction of the larger sample sets performed by adding samples to smaller sample sets was expected to be representative of the manner that larger sample sets would be produced by practitioners. This approach can be contrasted with collecting a small sample set and independently collecting a larger sample set, which was not expected to be the approach taken by practitioners.

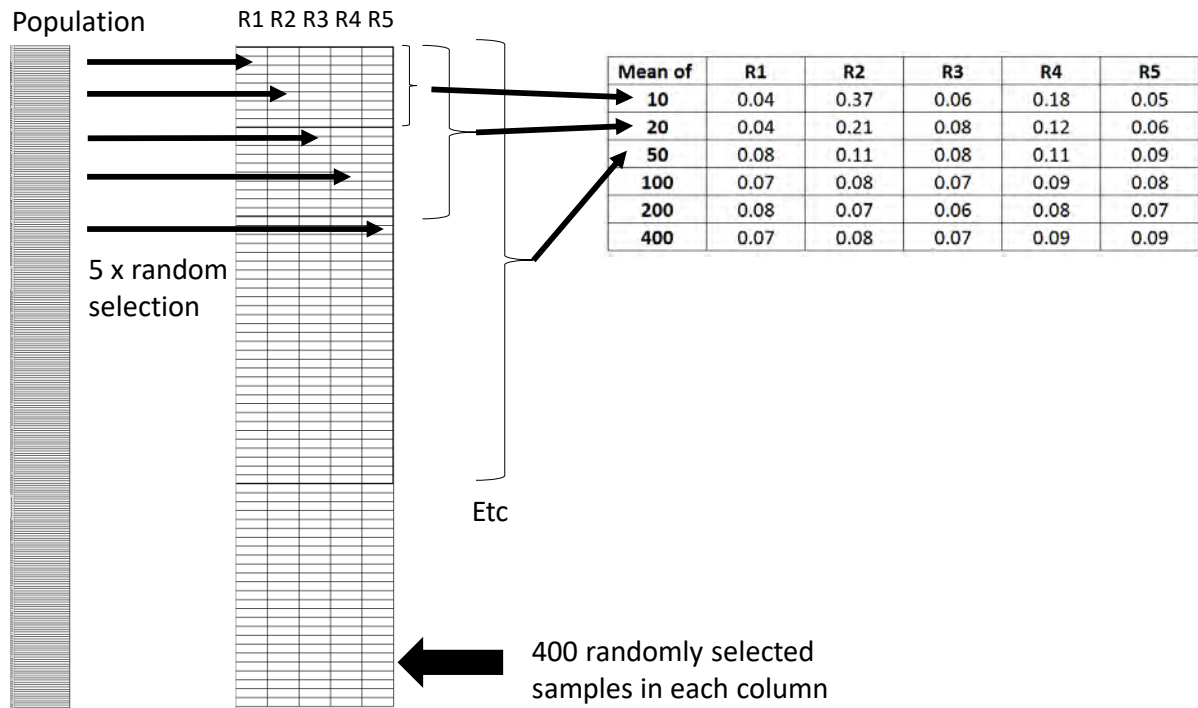


Fig. 1. Procedure for generation of realisations and calculation of means

Figure 2 presents results of five representations for one rock type for each of two ore deposits for sample numbers 10, 20, 50, 100, 200 and 400.

Figure 2a shows that, for Realisation R3, 50 samples are required to indicate that the rock type is NAF. It also shows that it is possible at higher sample numbers (R3) to conclude that the waste may be PAF, when the average total S value for the population (0.08) indicates that on average the rock type is NAF. Figure 2b indicates that, by characterizing only 10 samples, it may be concluded, based on realization R5, that the rock type is NAF, whereas the full average total S for the population indicates that the rock type may be PAF.

These examples illustrate the possibility that a rock type, based on an assessment of a small number of samples, may be inappropriately classified. This outcome may detrimentally influence early planning for waste management, for example, the volume of waste that needs to be managed as PAF may be over or underestimated.

Figure 2b also shows that the assessment of 20 samples produced upper and lower limits of the average total S content of 0.16 and 0.68% across the five realisations, a variation of a factor of more than four. Although these values are above the threshold, the lower value is less than one-third of the average total S content for the population (0.52). This may be significant, for example, when making water quality predictions, as the maximum potential acidity used in calculations would be less than a third of that of the population. In comparison, at more than 50 samples, the difference from the population average for all realizations is

20% or less, potentially leading to more reliable predictions.

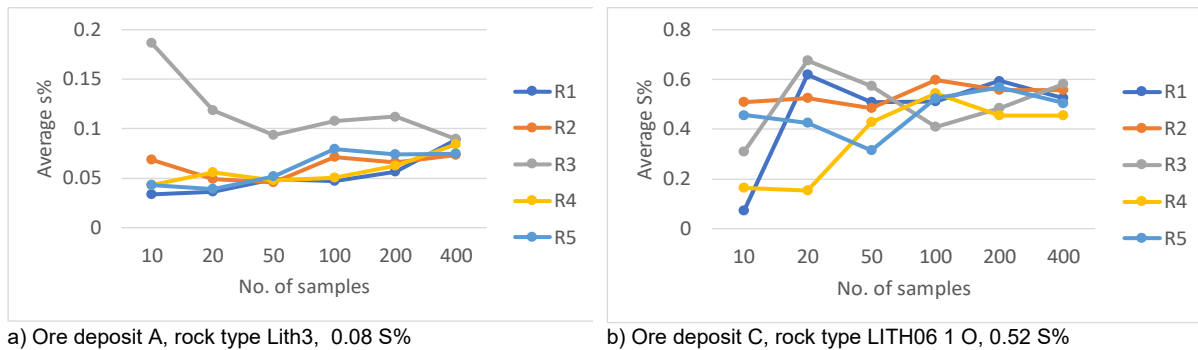


Fig. 2. Five representations for one rock type from ore deposits A and C

Note: The sub caption indicates the average total S content for the population.

Figure 3 to 5 present statistics for five realisations of each of seven sample sizes for nine units. Eight of the nine plots indicate that, as the number of samples increases, the average values, minima and maxima tend towards the average total S content of the population, which is shown as a red dashed line. This is the expected trend; however, it is not exhibited in Figure 3c), and the causes are discussed below.

Figure 3a shows that, for one realization at 10 and 20 samples, the material is possibly PAF on average, whereas the average total S content for the population indicates that on average the rock type is NAF. This is also the case for at least one realization of 10, 20, 100 and 200 samples of Figure 3b. (Note that Figure 3b is an alternative display of data presented in Figure 2a.) In contrast, most realisations of Figure 3c for 1, 20 and 50 samples, and for three realizations at 100 samples, indicate the rock type 131 1 is NAF, when it is possibly PAF.

Figure 3d to Figure 3f present the total S distributions of the population for the rock types presented in Figure 3a to Figure 3c. The average total S content is provided in the captions. The total S distribution on the logarithm plot in Figure 3d is symmetric, centred approximately on the average value of the distribution and has limited low and high tails. For this case, the average total S contents of the realizations converge smoothly to the average S content of the population. The sulfur distribution of Figure 3f is markedly different. It has a high frequency of samples of total S content of about 0.005% and a long high total S content tail. These two factors would have contributed to the disparate and widening spreads in average total S content with increasing sample numbers of Figure 3c.

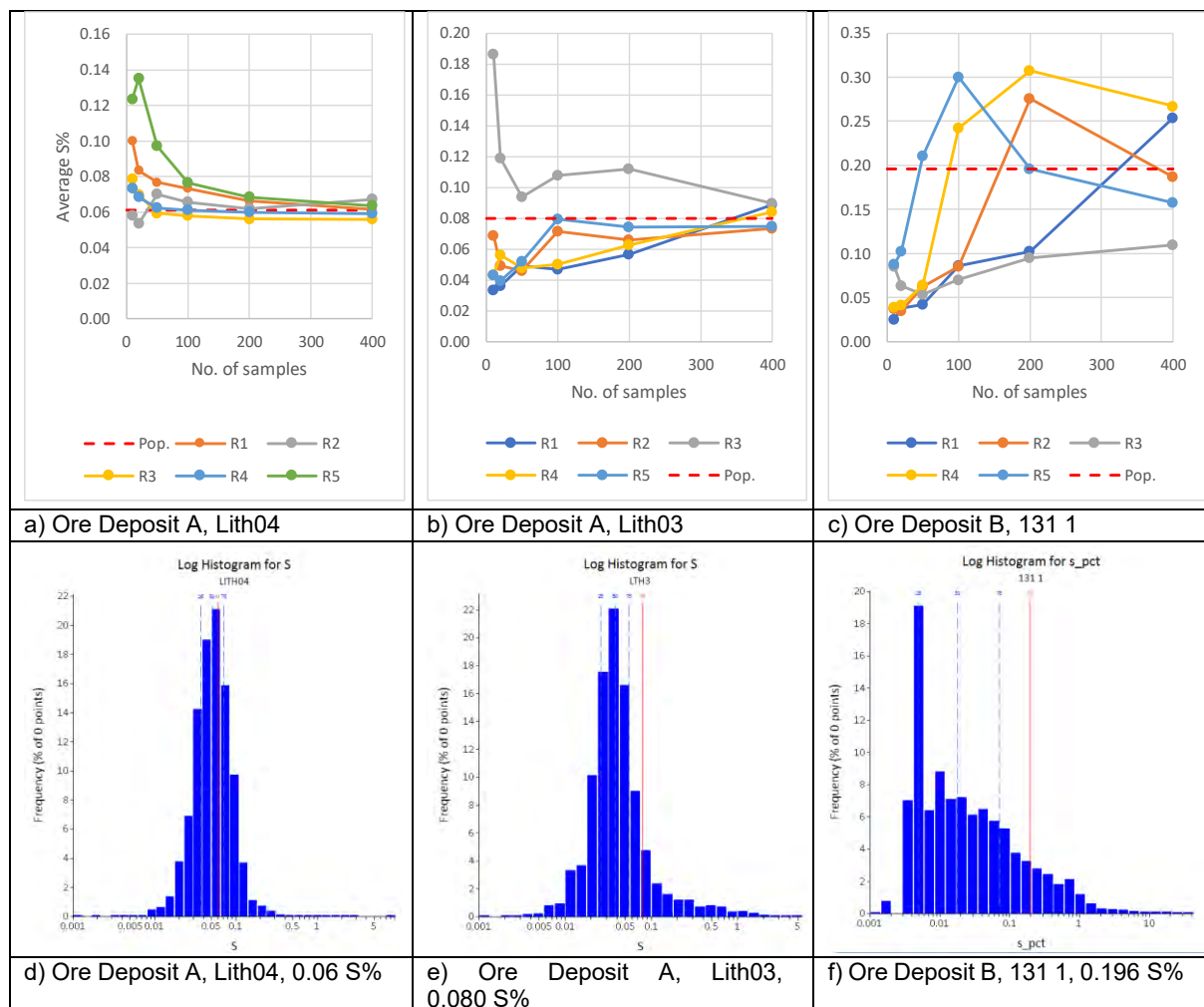


Fig. 3. Summary of realization statistics for low S rock types and total S distribution plots

A review of the spatial distribution of the total S contents of Figure 3f using the 3D geological modelling software Leapfrog Geo provided insight to the origins of the total S distribution. The high number of 0.005 S% values is real and for samples from a rock type of large extent, whilst the high S content values generally occurred in a specific part of the unit controlled by a series of interacting folds and faults that also host the high Au / Cu values.

The potential for inappropriate conclusions regarding the acid generating capacity of this rock type was investigated further by generating 60 realisations as opposed to the 5 initially examined. Table 2 shows that for 50 samples, 35% of the realisations produced average total S contents less than threshold and that indicate that the rock type is NAF, whereas the population average indicates the rock type may be PAF.

Table 2. Ore Deposit B, 131 1 - results from 60 realisations

No. samples	10	20	50	100	200	400
No. realisations with avge S% <0.1	19	25	21	12	5	2
% realisations with avge S% <0.1	32	42	35	20	8	3

Thorough interpretation of sulfur data for this rock type would involve the production of sub domains and independent analysis of these to provide insight as to how differences in likelihoods of AMD production might be managed. Kentwell et al., 2016, upon investigating anomalies in total sulfur content realisations of a waste lithology at an iron ore deposit, showed that high total S samples originated in a spatially localized region. Having identified the presence and location of the high S samples meant that high S content waste could be selectively mined and managed separately. Similar considerations might be justified for unit 313 1.

Figure 4 presents the summaries of realization statistics and total S distributions for units with medium level sulfur contents with average values for the populations above the 0.1 S% threshold. Figure 4a shows that, even at 100 samples, there is a realization with an average total S content less than the threshold. Figure 4b and 4c show that, although the units have a population average total S content more than five times the threshold, there can be realizations with small sample numbers that are below the threshold. Such realisations are likely to lead to the conclusion that the unit is NAF when it is potentially PAF.

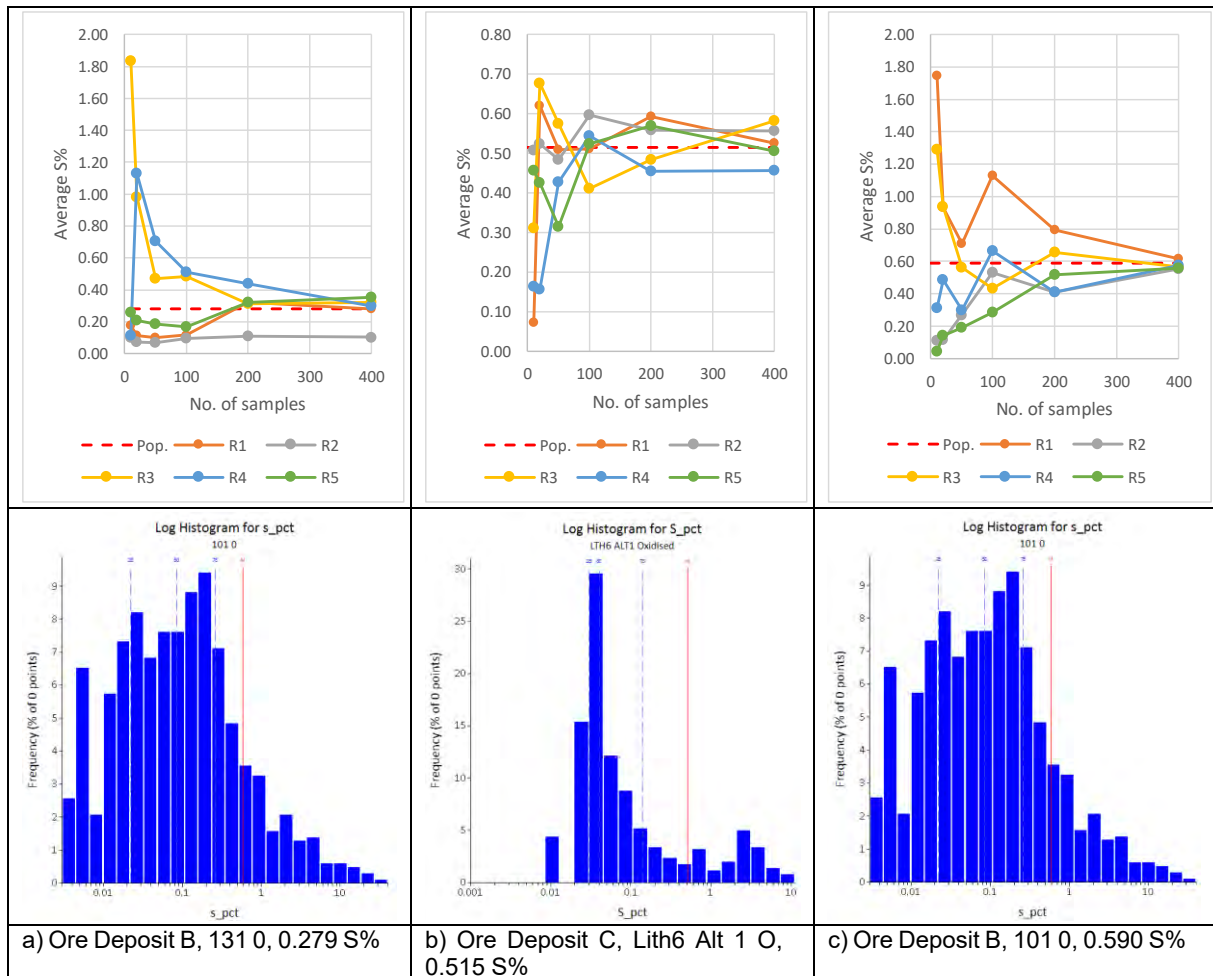


Fig. 4. Medium S content units - summary of realization statistics and total S distributions

Realisation results are presented for high sulfur content units with three differently shaped distributions in Figure 5. The range of realisations at low sample numbers indicate that accuracy with which the maximum potential acidity can be estimated may be unacceptable,

and 50 samples or more may be required depending on the accuracy required of AMD characterisation. The spread of the five realisations of Ore Deposit C, Lith3 Alt 2 Oxidised in Figure 5b is relatively narrow, even though the sulfur distribution is bi-modal. The results of further investigation of this unit using a total of 60 realisations are presented in Figure 6 and Table 1. The results indicate that the potential spread of average total S contents is larger than indicated in Figure 5b. For example, for 50 samples, the average total S content of 22% of the realizations differed from the mean value by more than 15%.

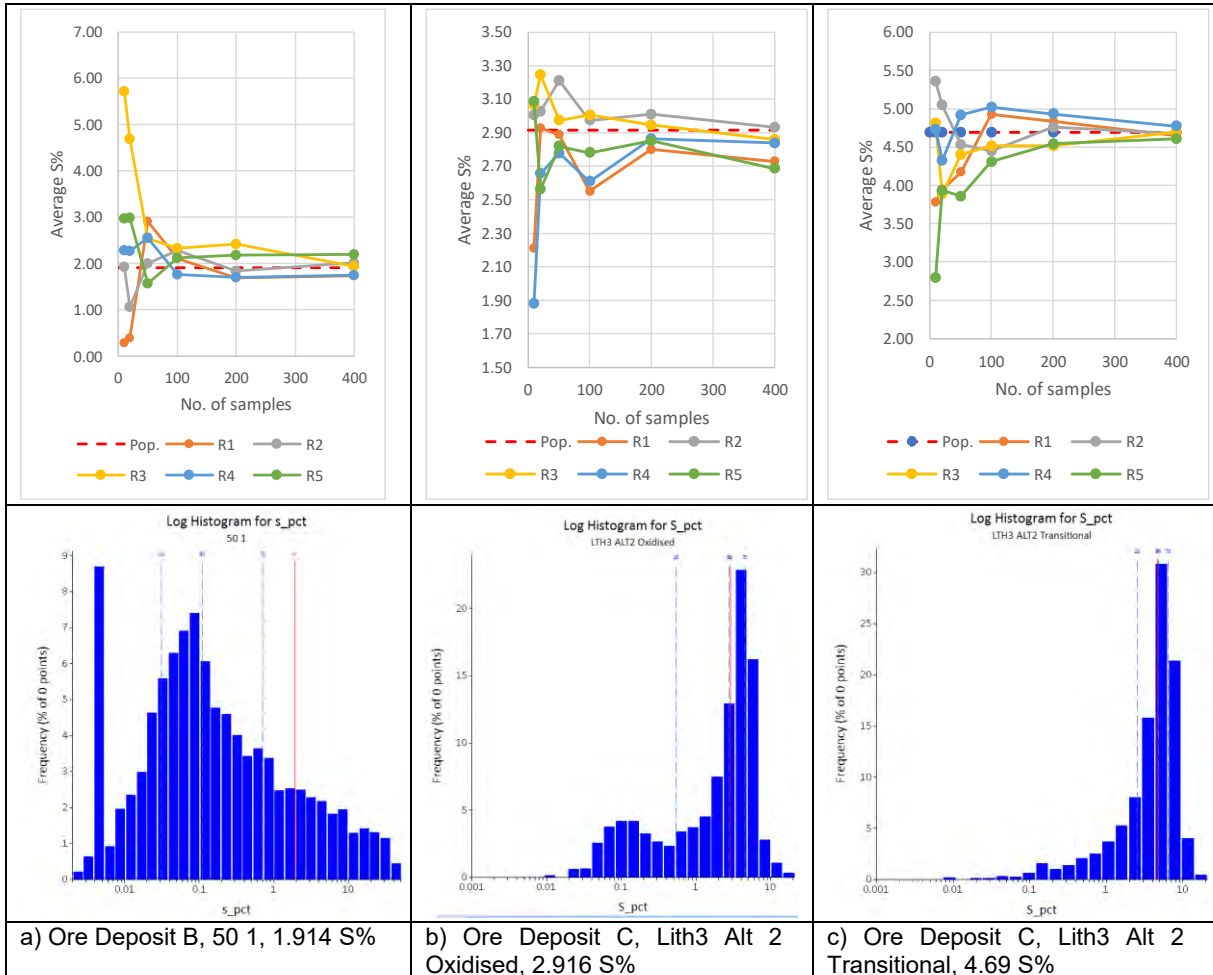


Fig. 5. High S content units - summary of realization statistics and total S distributions

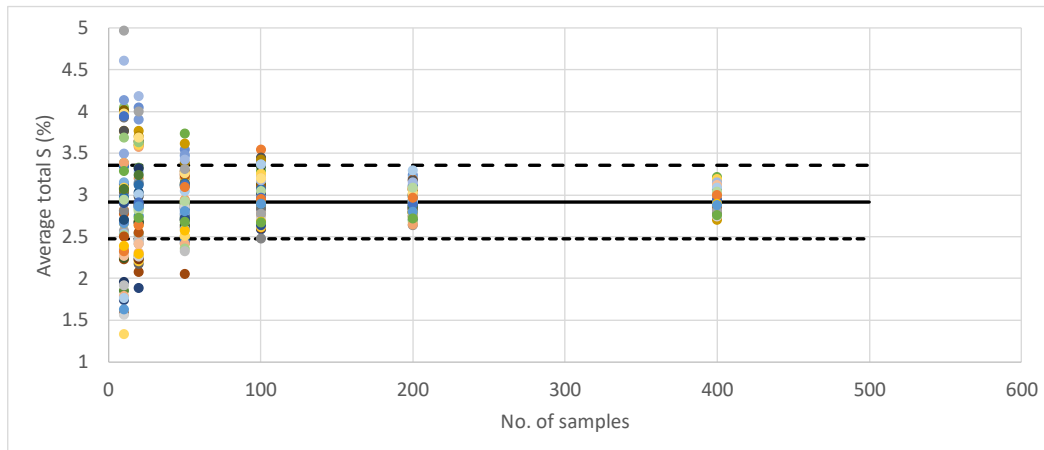


Fig. 6. Average total S content for 60 realisations for Ore Deposit C, Lith3 Alt 2 Oxidised

Note: The solid and dashed lines indicate average total S content of the population and +/-15%.

Table 3. Ore Deposit C, Lith3 Alt 2 Oxidised - Average total S spread

No. samples	10	20	50	100	200	400
Minimum	1.3	1.9	2.0	2.5	2.6	2.7
Maximum	5.0	4.2	3.7	3.5	3.3	3.2
No. of average total S contents within +/-15%	29	32	47	52	60	60
Percentage of average total S contents within +/-15%	48	53	78	87	100	100

Note: Results are for a total of 60 realisations, average total S content of population is 2.916%.

4.0 CONCLUSIONS

- Decisions based on a small number of samples are more likely to be inappropriate. For example, misclassifications are more likely for units with an average total S content near a threshold value used to distinguish a unit as NAF or PAF. This type of wrong decision may initiate the development of plans that could lead to mismanagement of the waste.
- Based on the nine units assessed in this paper, 400 samples or more may be required to estimate the average total sulfur content of a unit to within +/- 10%. From the nine units and five realisations, 45 individual tests were completed. The success rate (+/- 10% of population average) by number of samples for these 45 tests was as shown in the Table 4. Over a range of different geological conditions, even with 400 samples, +/- 10 % of the true average value was only achieved 71% of the time. It should be noted that this is still a very limited overall data set and that the conclusions drawn are representative of this data only. However, it shows that the minimum required samples for characterization of sulfur data averages from drillhole sized samples may be in the order of hundreds rather than tens.

Table 4. Success rate for given sample numbers

Number of samples	Success rate (%)
10	20
20	13
50	29
100	38
200	42
400	71

Note: Success means percentage of realizations with average total S within +/-10% of population value.

- The nature of the sulfur populations examined is such that their experimental average values and variability are dependent not only on the number of samples taken but on the locations of those samples.
- The exercise has shown that, below a certain number of samples, the same number of samples chosen at five different sets of random locations, can give an unacceptably wide range of averages and standard deviations and that the sample averages can be markedly different to the population average. The number of samples at which the sample statistics converge on the population statistics to an acceptable level varies depending on the geological characteristics of each particular unit and on how well the unit has been defined.
- In high sulfur cases, where all samples are above the selected PAF threshold and a PAF outcome is not in doubt, there remains the assessment of the quantity of potential acid production which also requires a level of confidence in the average and variability of a unit.
- As the number of samples increases, the average total S content tends towards the average total S content of the population; however, the trend may not be smooth and consistent for some units and sample sets.
- Generally, the number of samples required to estimate the average sulfur content of a unit depends on the specific samples selected, the sulfur distribution within the waste, and the required accuracy of the estimate.
- Provision of a detailed guideline for determining the number of samples to be used for a geochemical assessment in specific geological settings is beyond the scope of this paper. However, it is recommended that practitioners identify the accuracy required in any assessment, develop an understanding of the total S distribution (possibly via the resource database) and estimate the likely level of accuracy that could be expected when interpreting data from the generally relatively small number of samples submitted for geochemical characterisation. Comparison of the likely and required accuracies could then guide the need to modify the number of samples to be geochemically characterised.

5.0 REFERENCES

- Aus. Gov. (2016) Preventing Acid and Metalliferous Drainage, Leading Practice Sustainable Development Program for the Mining Industry, September 2016, Commonwealth of Australia.
- BCAMDTF (1989) Draft Acid Rock Drainage Technical Guide, Vol. 1, Prepared for the British Columbian Acid Drainage Task Force by Steffen Robertson and Kirsten (BC) Inc.

INAP GARD Guide, http://www.gardguide.com/index.php?title=Main_Page, accessed 25/08/2017.

Kentwell D, Garvie A and Linklater C. (2016) Geostatistics and Sample Numbers from an Acid and Metalliferous Drainage Perspective, Proceeding of the Life of Mine Conference, 28-30 September. Brisbane, AusIMM SMI/CLMR.

MEND (2009) Price, W.A., Prediction Manual for Drainage Chemistry from Sulphidic Geologic Materials, MEND Report 1.20.1, Prepared by CANMET – Mining and Mineral Sciences Laboratories, Smithers, British Columbia.

US EPA (1994) Acid Mine Drainage Prediction, US Environmental Protection Agency (EPA) Report number EPA-530R-94-036.

WA Gov. (2016) Government of Western Australia, Draft Guidance: Materials Characterisation Baseline Data Requirements for Mining Proposals, March 2016, Western Australian Government, Department of Mines and Energy.

A GEOENVIRONMENTAL CHARACTERISATION TOOL FOR THE CORESHED DURING EARLY LIFE-OF-MINE ASSESSMENTS

R. Cornelius^A, A. Parbhakar-Fox^A and D.R. Cooke^{A,B}

^AARC Industrial Hub for Transforming the Mining Value Chain (TMVC), University of Tasmania, Private Bag 79, Sandy Bay, TAS 7001, Australia

^B ARC Centre of Excellence in Ore Deposits (CODES), University of Tasmania, Private Bag 79, Sandy Bay, TAS 7001, Australia

ABSTRACT

Defining the acid forming potential during the exploration stages of a mining project is critical for financial modelling and waste management planning. However, at such early stages, there are limited resources for evaluating the geoenvironmental characteristics of future waste materials. Considering this, a geoenvironmental logging code was developed and trialled using drill cores from a low-grade porphyry copper prospect in Northern Europe. Four drill holes were targeted with a focus on zones which were marginal or below economic grade. The logging code developed required that, for each metre interval, a visual estimate of each sulfide present was recorded. As a conservative approach was adopted, the area (8.5 cm by 5.5 cm i.e., grain size card dimensions) recognised to contain the most sulfides was assessed using the acid rock drainage index (ARDI). A geoenvironmental risk factor was calculated based on ARDI values scaled to the sulphide mineral abundance over the interval. To enhance the classification, results were plotted against sulphur assay values. As corresponding drill core pulps (< 75 µm) were available in this project, they were analysed using the ASTM D492-01(2007) paste pH method. Collectively, these cost-effective low-technology methods enabled the identification of high and low-risk waste zones and will allow the mine planners to start developing robust waste management strategies rightly guided by the deposit's mineralogy and texture.

1.0 INTRODUCTION

The formation of acid and metalliferous drainage (AMD) can be credited to the oxidation of sulfide minerals at the Earth's surface due to interactions with oxygen (O₂), water (H₂O) and microorganisms (e.g., *Acidithiobacillus ferrooxidans*; Parbhakar-Fox and Lottermoser, 2017). It is considered a primary cause for environmental degradation on and around mine sites due to the polluting nature of the derived effluents. AMD is typified by a low pH (acidic), and high sulfate, hydroxide and heavy metal concentrations Ag, As, Bi, Cd, Co, Hg, Mo, Ni, Pb, Pd, Pt, Ru, Sb, Se, Te, Tl and Zn (e.g., Lottermoser, 2010). The principal mineral responsible for AMD generation is pyrite (FeS₂). It is the most abundant sulfide mineral in the crust and is heavily associated with economic minerals which are mined and processed to extract base, precious and critical metals. The exposure of acid forming minerals through mining activities and associated earth moving operations significantly increases the risk of acidic effluent generation. If managed correctly, the acid forming nature of these minerals can be monitored and strategies can be adopted to prevent and mitigate against AMD formation. However, current standard operating procedures tend to focus environmental management efforts towards the end of the mining cycle, whereby remediation and rehabilitation are the primary strategies for pre- and post-mine closure (the exception to this is the waste rock pile and tailings dam construction methods for O₂ and H₂O mitigation used during operational phases). This management technique is costly both economically and environmentally, as sulfidic waste

rocks and tailings are prone to oxidation in surficial environments throughout mining operations, facilitating AMD formation.

A shift in the management of mine waste from the end to the beginning of the mining cycle offers a solution to excessive AMD generation. Predictive tools and techniques may be used to assess the acid forming (and neutralising) potential of waste products during the exploration and pre-feasibility/feasibility stages of mining to inform environmental management plans, and mine planning and design. Currently, the AMIRA P387A Handbook (Smart et al., 2002) and the GARD Guide (2014) exist to provide guidelines regarding appropriate mineralogical and geochemical testing for prediction in the mining industry. The recently developed modified geochemistry-mineralogy-texture-geometallurgy approach (GMTG) by Parbhakar-Fox (2017) offers a procedural framework for AMD prediction that can be applied at any stage during the LOM cycle. Developed in the preceding GMT (geochemistry-mineralogy-texture) approach (Parbhakar-Fox et al., 2011) and used in the GMTG approach, the acid rock drainage index (ARDI) affords textural assessment of sulfide minerals by means of environmental logging, which is lacking in methods recommended in the aforementioned AMIRA P387A Handbook (Smart et al., 2002) and GARD guide (2014). This ARDI uses a series of parameters to assess the content, distribution and textural relationship of pyrite present in intact drill core for meso- and micro-scale evaluations. In this paper we present revisions and improvements to the ARDI, as well as an example of its applicability and effectiveness for predictive geoenvironmental field work on polysulfidic drill core materials from a low-grade copper porphyry prospect in Northern Europe.

2.0 MATERIALS AND METHODS

2.1 The Geochemistry-Mineralogy-Texture- Geometallurgy (GMTG) Approach

The GMT approach was developed by Parbhakar-Fox et al. (2011) to address the lack of textural assessment in predictive schemes for geoenvironmental characterisation. This approach employs parallel geochemical, mineralogical and textural analyses, implemented across three stages. Advancements from one stage to the next stipulates an increase in analytical complexity, and a decrease in the number of samples. In a later version of the GMTG, the initial stage utilises simple and low-cost pre-screening tools for a first-pass assessment of waste material. Basic geochemical tests, such as paste pH and carbon-sulfur analysis are performed alongside hyperspectral analyses (using automated hyperspectral instruments such as the Hylogger™) and ARDI geoenvironmental logging. Waste materials are domainned into one of five classifications (ANC- acid neutralising capacity, NAF- non-acid forming, PAF- potentially acid forming, AF- acid forming, or EAF- extremely acid forming) based on the results of these pre-screening assessments. Those which classify as ANC or NAF do not require further testing; however those classified as PAF, AF or EAF are advanced to stage two for more detailed analysis. For examples of plots used for during this stage, the reader is referred to Parbhakar-Fox (2017).

Stage two involves sample screening using advanced geochemical testing. A minimum of 50% of samples nominated at the end of stage one should be analysed during this stage. Multi-addition NAG testing is recommended over single-addition and sequential NAG due to more efficient and complete sulfide oxidation. Leachate from NAG testing is recommended for analysis using solution ICP-MS methods to determine heavy metal concentrations, thereby indicating likely contaminants from sulfide oxidation. Field leaching tests (FLT; e.g. the USGS

field leach test) are also recommended at this stage, for measurement of leachable metals. Samples dominated as acid forming (i.e. PAF, AF or EAF) are progressed to the next stage. Those nominated as NAF do not require further testing.

The final stage (three) utilises high precision and accuracy analytical tools for characterisation of constraints on sulfide oxidation, and thus acid generation. Best representative PAF (and above) samples are chosen for analysis using LA-ICP-MS, SEM, EMPA and MLA. SEM and MLA analyses provide information regarding mineralogy, and LA-ICP-MS and EMPA on the spatial distribution and contents of trace elements, respectively.

2.2 Environmental Logging

2.2.1 Interval assessment

Prior to ARDI parameter assessment, visual estimation of sulfide mineral abundance across the interval was performed (given as a percentage across the interval). Total sulfur (S) values were used on occasion to guide estimations in events of uncertainty. Following this, three primary sulfide phases were identified (chalcopyrite, pyrrhotite, and pyrite) and assigned a value from 0 to 1 reflecting respective ratios across the interval. An example of this assessment stage is shown in Figure 1.

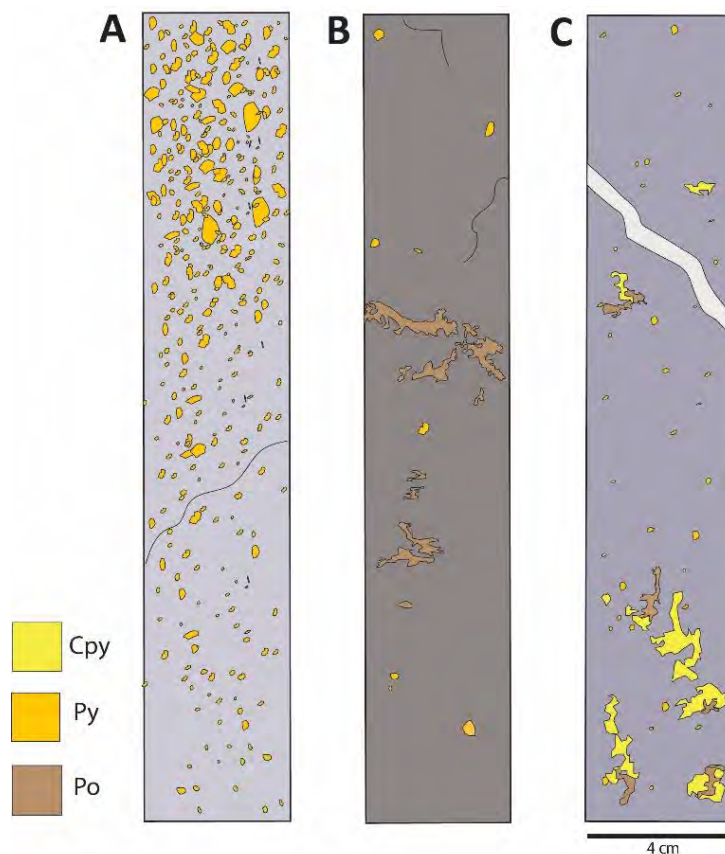


Figure 1. Cartoon examples of interval sulfide assessment. (A) interval contains Py only- Py=1, Cpy=0, Po=0; (B) Both Po and Py are present, however Po is more abundant affording a higher overall value to be given- Py=0.2, Cpy=0, Po=0.8; (C) All three primary sulfide phases are present within the interval such that Cpy>Po>Py- Py=0.2, Cpy=0.5, Po=0.3. Abbreviations: Py, Pyrite; Cpy, Chalcopyrite; Po, Pyrrhotite.

2.2.2 Modified ARDI

Five parameters, A to E, are evaluated by the ARDI through visual assessment, using criteria specified within the parameter. Parameters A through C are scored from 0 to 10, and parameters D and E from -5 to 10. Each parameter represents a factor with direct influence on sulfide oxidation; therefore all parameters must be assessed for the ARDI to be representative. When performing meso-scale assessment, end member representations of each parameter are defined using site-specific examples. This is followed by area selection (an 8.5 cm x 5.5 cm area is recommended) within each interval for ARDI assessment. For a comprehensive overview of each parameter, the reader is referred to Parbhakar-Fox et al. (2011).

Parameter A acts as a proxy for maximum potential acidity through modal estimation of iron sulfides (sulfide content) over the selected area. Parameter B uses an adaptation of the sulfide alteration index (SAI) developed by Blowes and Jambor (1990) to assess the extent of weathering/freshness of pyritic sulfides. Sulfide morphology is assessed in Parameter C, with textures associated with increased acid generation scored highest. The presence of neutralising phases is considered in Parameter D. Areas containing >80% primary neutralisers are given the lowest possible score, and areas containing acid-forming phases only are scored the highest. The final parameter, E, assesses mineral associations between the sulfides and surrounding mineralogy. Sulfide-sulfide boundaries afford high values, whereas contact with primary neutralising phases yields negative values.

Although the ARDI has been proven effective for AMD domaining, its application has been restricted to use on pyritic mine wastes only. Most sulfidic waste materials, however, consist of multiple sulfide phases such as pyrrhotite and chalcopyrite, which, although are less acid forming than pyrite, are environmentally significant. Therefore, a modified ARDI was developed using marginal/below economic grade materials from four polysulfidic exploration drill cores, sampled from a low-grade copper porphyry prospect in Northern Sweden.

Morphologies displaying high surface areas typically display heightened acid generation to those with smaller surface areas. This is due to greater reactivity and faster rates of oxidation, as more material is available to participate in oxidative reactions (Weber et al., 2004; Liu et al., 2008; Weisener and Weber, 2010). Sulfide morphology is therefore an important factor to consider during predictive geoenvironmental assessment, as it will, in part, influence the acid generation potential of waste materials. In this modified ARDI, sulfide morphology is addressed by parameter C.

Sulfides found in exploration drill core displayed a texture dissimilar to those described in Parbhakar-Fox et al. (2011). The two end member morphologies, disseminated and massive, were present; however the intermediate (large) hexagonal was lacking. Instead, a clotted morphology was observed. This was primarily associated with pyrrhotite and chalcopyrite phases, but was occasionally displayed by pyrite. To address the differences in the ARDI to those observed on-site, parameter C was modified such that clotted morphologies replaced hexagonal as the intermediate morphology, as illustrated in Figure 2.

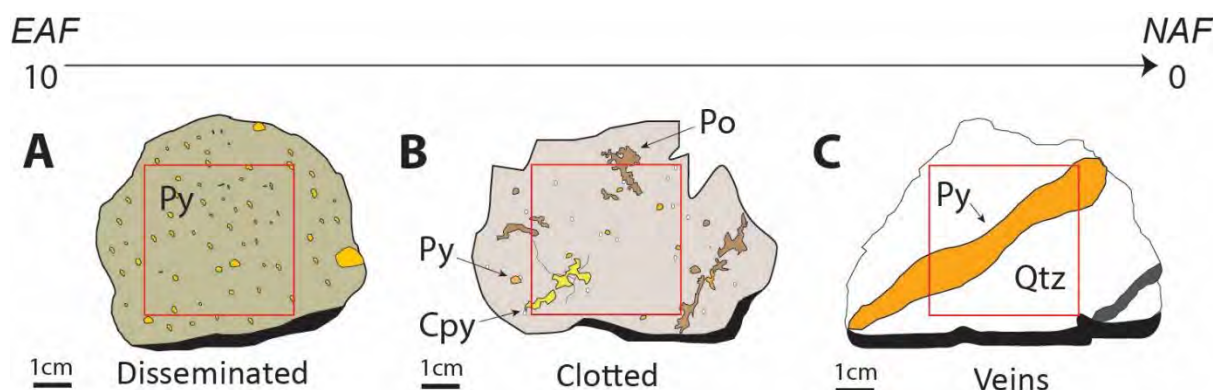


Figure 2. Cartoon example of sulfide morphologies assessed in Parameter C: (A) Disseminated sulfide texture across <80 % of the selected area- ranked 8/10; (B) Clotted sulfide texture identified in pyrrhotite (Po) and chalcopyrite (Cpy) <50 %- ranked 5/10; (C) Sulfide vein- ranked 1/10. Abbreviations: Py, pyrite; Qtz, quartz; EAF, extremely acid forming; NAF, non-acid forming.

2.2.3 Interval Classification

Once whole-interval estimations were completed, ARDI parameter assessment (A-E) was performed on each primary sulfide phase according to criteria specified in Parbhakar-Fox et al. (2011), with the exception of parameter C. Total ARDI scores for each phase were then multiplied by whole-interval estimations to determine geoenvironmental risk. If one or more of the primary phases were not present across the interval, ARDI assessment was not performed and the phase removed from the final ARDI calculation.

3.0 RESULTS

ARDI values are plotted down-hole to show changes in acid-forming nature with depth. For comparison, plots containing total sulfur (%; collected during routine assaying) and paste pH (ASTM, 2007) data with classification domains are given, alongside lithology logs to provide geological context and identify characteristics, respectively.

3.1 464

In general the ARDI values were in agreement with S_{total} and paste pH, suggesting sulfide assessment using this modified technique was relatively successful in identifying potentially acid-forming lithologies within the drill-hole. Using the ARDI, 8 samples were classified as NAF, compared to 2 based on S_{total} , and 14 from paste pH analysis. Discrepancies in classification between the two techniques are found primarily in samples with S_{total} values slightly above or below (± 0.1) the 0.3 % cut-off (Parbhakar-Fox et al., 2011).

As S_{total} considers only a single factor with direct influence on sulfide oxidation, the additional factors assessed by the ARDI likely afforded recognition of characteristics typical of NAF waste, resulting in observed domain differences. Interval 76.1-79.2 (m) exemplifies this (Figure 3), as S_{total} was 1.12 %; however it scored 16.35 using the ARDI. This was due to the presence of carbonate in the sample (Figure 6), resulting in negative scores given for parameters D and E, and subsequent NAF classification.

Variability between ARDI and paste pH may be explained by the presence of abundant secondary neutralising phases such as micas, feldspars and silicates (i.e., chlorite), which, at

this grain size, buffer the paste pH solution during analysis to yield a higher pH than suggested by ARDI and S_{total} . The combination of un-oxidised samples, test simplicity and reactivity, and assessment of immediate acid-forming potential only are suggested to be responsible for observed differences.

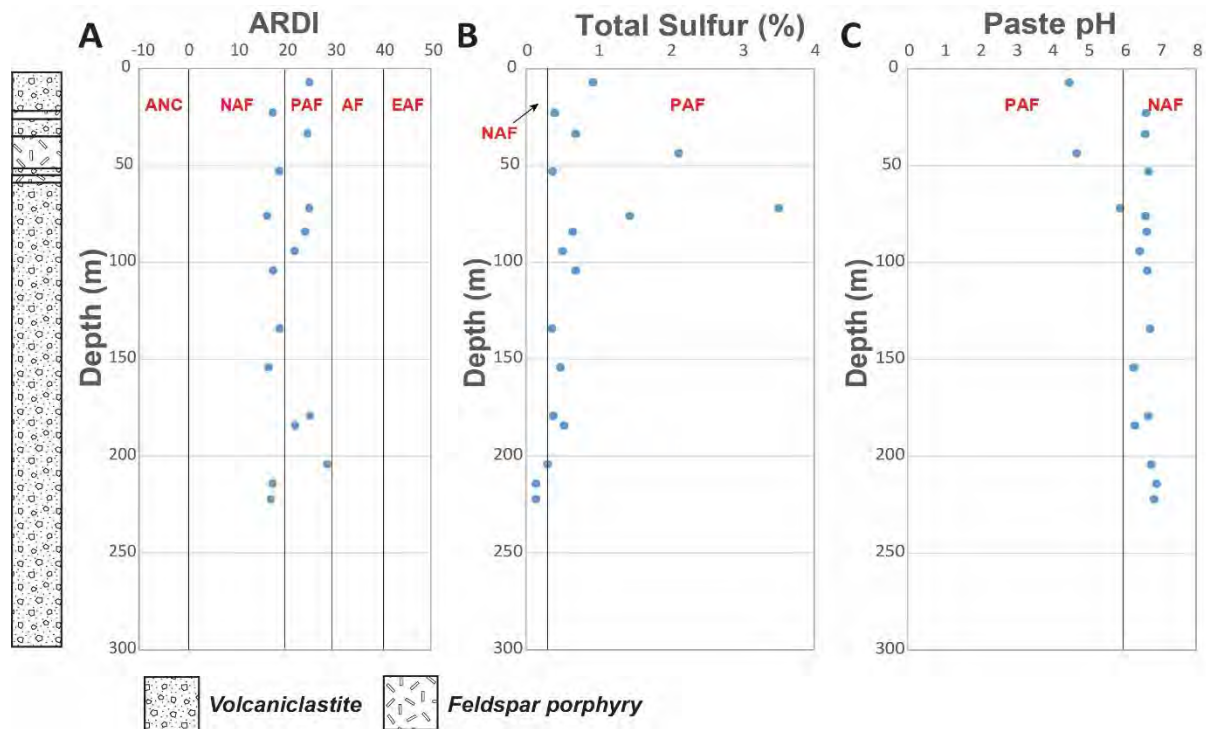


Figure 3. Geochemical and environmental logging data from drill hole 466 shown alongside a cartoon down-hole lithology log. (A) ARDI scores shown against depth; (B) Total sulfur (S_{total}) values obtained from assay data against depth; (C) Paste pH data ranging from ~4-7 shown with depth. Classification cut-offs are shown on all plots. Abbreviations: ANC, acid neutralising capacity; NAF, non-acid forming; PAF, potentially acid-forming; AF, acid forming; EAF, extremely acid-forming.

3.2 466

According to results from both S_{total} and paste pH data, the *overall* classification of this hole is NAF. The ARDI data is contradictory to this, however, suggesting a majority PAF classification. Acid-forming potential increases down-hole, as shown by the shift from NAF to PAF at ~178 m in S_{total} and ~250 m in paste pH (Figure 4). Although there are discrepancies between overall classification of this hole, the ARDI successfully identified samples with high sulfur and low pH values as PAF, with the exception of one classified as AF. There is no obvious association between classification trends and lithology; however 3 of the 4 samples identified as PAF in paste pH analysis have been logged as 'volcaniclastite'.

The presence of garnet throughout this drill hole (observed in core and identified using x-ray diffractometry) alongside primary and secondary neutralising phases may explain pH values greater than 8.5, as garnet exhibits significant neutralising potential under paste pH conditions. An example of garnet with carbonate is shown in Figure 6.

The disseminated nature of sulfides and high occurrence of sulfide-sulfide mineral association within this hole are responsible for PAF classification using ARDI, despite low S_{total} values. This is demonstrated in interval 81.7-84.9 m (Figure 4 and 6), where pyrite was scored 25 based primarily on lack of weathering and disseminated textures (parameters B and C).

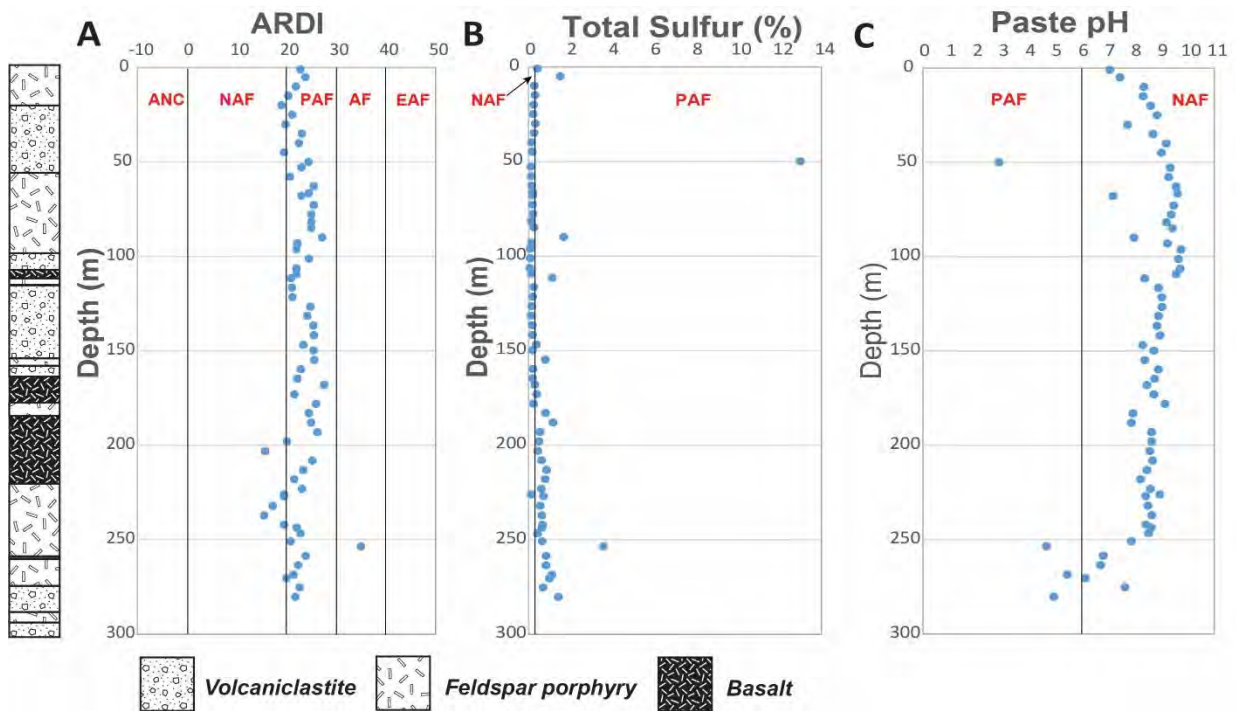


Figure 4. Environmental logging results shown alongside geochemical data and a cartoon example of the down-hole lithology for drill-hole 466. (A) ARDI scores shown against depth; (B) Total sulfur (S_{total}) values obtained from assay data against depth; (C) Paste pH data ranging from ~2.5-10 shown with depth. All plots are shown with respective cut-offs for classifications. Abbreviations: ANC, acid neutralising capacity; NAF, non-acid forming; PAF, potentially acid-forming; AF, acid forming; EAF, extremely acid-forming.

3.3 473

ARDI has identified the bulk of samples as NAF, which conflicts with the majority PAF classification using S_{total} . In context, paste pH and ARDI are generally in agreement, with the exception of two samples towards the bottom of the hole (Figure 5). Lithology in this hole is significantly more heterogeneous than observed in 464, 466 and 474; however all samples classified as PAF from paste pH data are found within the volcaniclastite unit. Similarly to that seen in 464, the variation between classification using ARDI and S_{total} can be explained by the presence of carbonates, found within minor vein arrays. Negative values were therefore assigned to parameters D and E, resulting in a NAF classification, despite PAF S_{total} values. This demonstrates the power of the ARDI over S_{total} data in samples containing minor to abundant carbonate phases, such as observed in the waste rocks of the low-grade copper prospect in Northern Europe.

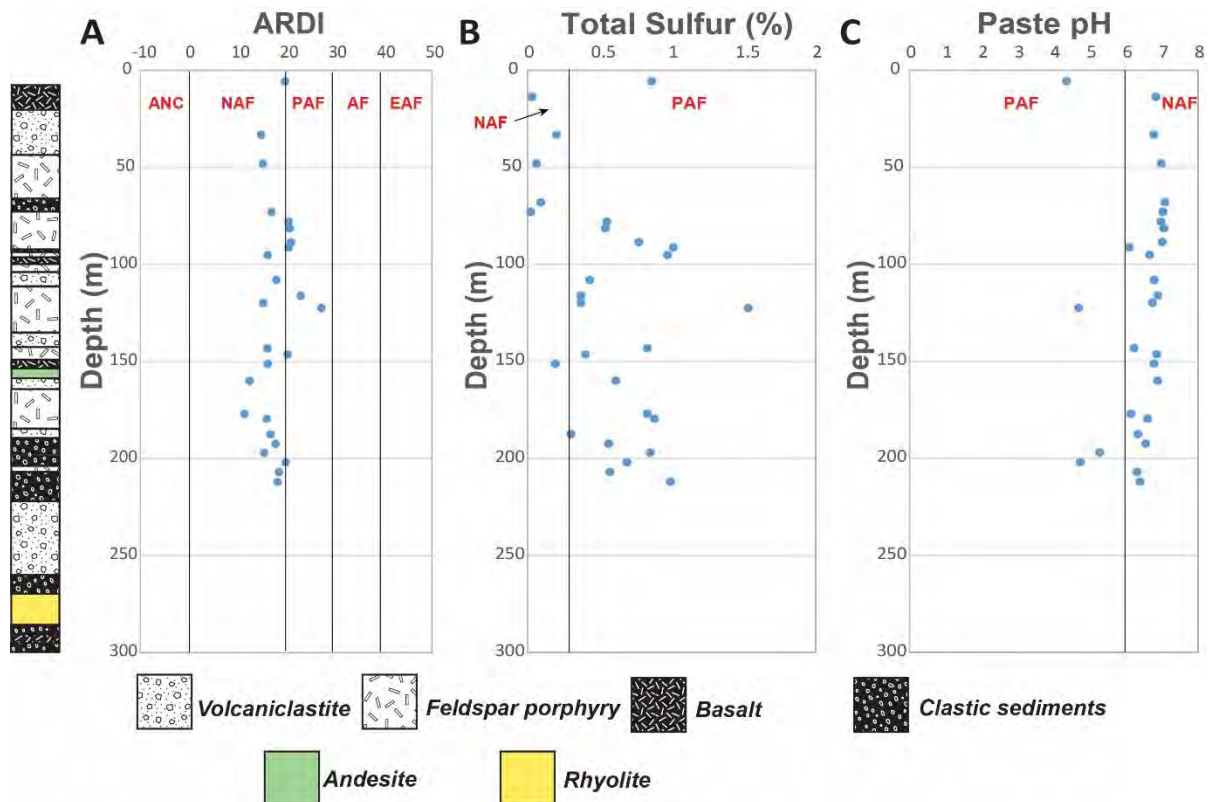


Figure 5. Results from geochemical and environmental logging with a down-hole lithology log, illustrating the heterogeneity of drill-hole 473. (A) ARDI scores plotted against depth; (B) Total sulfur (S_{total}) values obtained from assay data against depth; (C) Paste pH data ranging from ~4-7 shown with depth. All plots are shown with respective cut-offs for classifications. Abbreviations: ANC, acid neutralising capacity; NAF, non-acid forming; PAF, potentially acid-forming; AF, acid forming; EAF, extremely acid-forming.

The abundance of high sulfur values in this hole may be explained by the presence of additional sulfide phases such as galena, arsenopyrite and sphalerite (Figure 6). These were identified on-site in the drill-core and through XRD analysis, and may be responsible for elevated S_{total} and subsequent PAF classification. The combination of additional sulfide phases and the presence of carbonate minerals is therefore suggested to be the cause of discrepancies observed between ARDI and S_{total} classifications. Paste pH values are thus likely to reflect the participation of both sulfides (oxidised) and carbonates in the reaction, with low pH values indicative of either additional sulfide phases (oxidised) or lack of carbonate. The former is suggested to be the cause for low pH values at 197.05 m and 202 m despite the presence of carbonate in hand specimen.

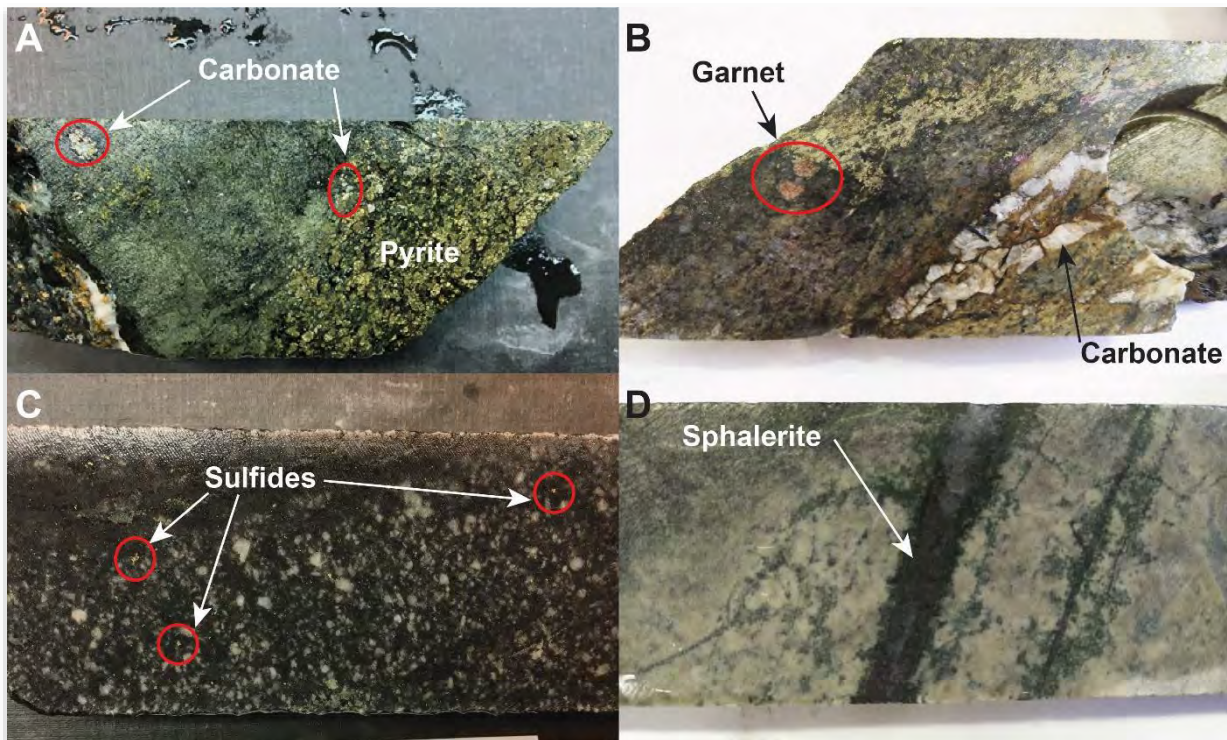


Figure 6. Examples of mineralogy and textures controlling results. (A) 464- Patchy carbonate in isolation and direct association with pyrite, resulting in a low ARDI score despite abundant sulfides; (B) 466- Example of garnet and carbonate existing in close proximity to one another and sulfides. The presence of garnet is used to explain the exceptionally high pH values for certain intervals within this hole; (C) 466- disseminated sulfides (pyrite and chalcopyrite), yielding a high ARDI score despite low S_{total} ; (D) 473- Quartz vein containing abundant inward growths of sphalerite giving the interval a high S_{total} despite low ARDI and high paste pH.

3.4 474

Overall, ARDI, S_{total} , and paste pH are in agreement. The two samples classified as PAF in paste pH data were also identified as such using S_{total} and, more importantly, the ARDI. An increase in sulfur from ~155 m to ~200 m is loosely reflected in the ARDI trend down-hole (Figure 6). The lithology of this hole is dominated by carbonaceous 'clastic sediments', which hosts the majority of PAF samples, with the exception of two S_{total} samples within the 'feldspar porphyry' and 'basalt' units, respectively.

Differences observed between the ARDI and S_{total} from ~40-80 m is, again, due to the presence of carbonates. This is reflected by the exceptionally high paste pH values, and validates the NAF classification given during ARDI assessment. This hole offers the best example of the effectiveness of the ARDI in successfully domaining waste material based purely on visual estimation of parameters A-E.

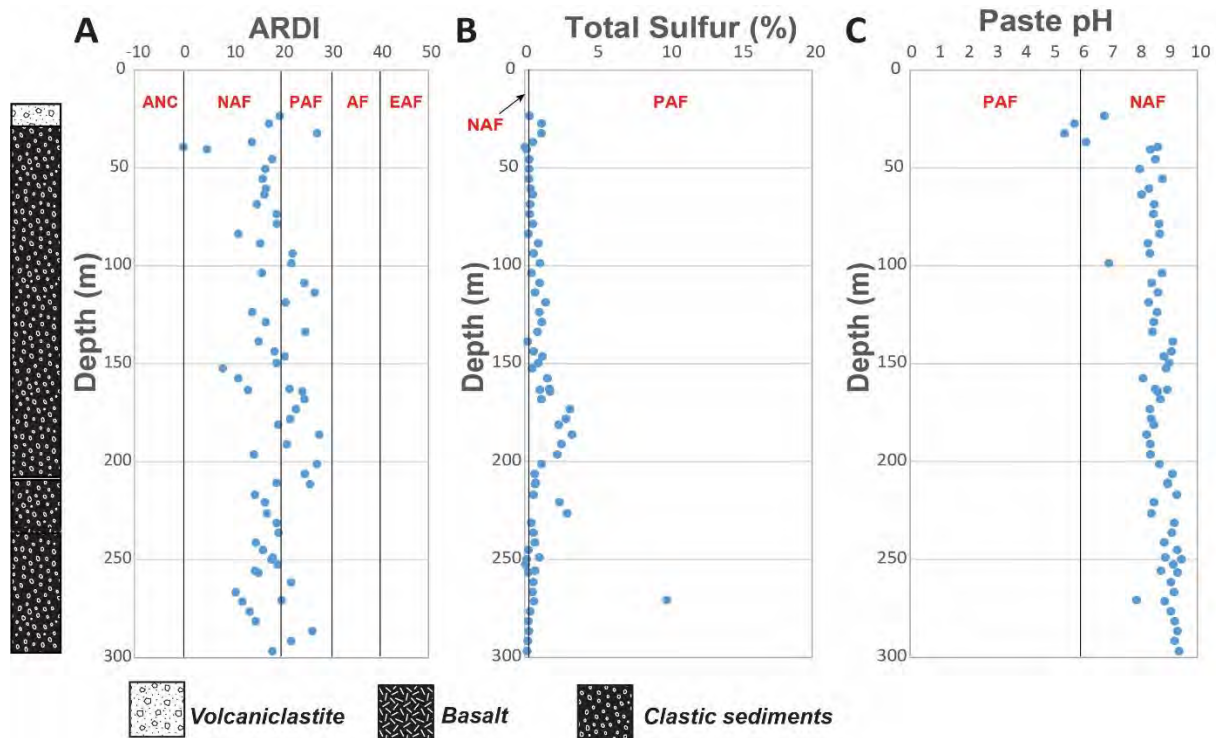


Figure 7. Geochemical and environmental logging results with a down-hole lithology log. (A) ARDI scores shown against depth; (B) Total sulfur (S_{total}) values obtained from assay data against depth; (C) Paste pH data ranging from ~5-9.5 shown with depth. Respective cut-off values for classification are shown on all plots. Abbreviations: ANC, acid neutralising capacity; NAF, non-acid forming; PAF, potentially acid-forming; AF, acid forming; EAF, extremely acid-forming.

4.0 DISCUSSION

The use of simple geochemical data for predictive purposes underpins most geoenvironmental procedures during early life-of-mine stages, e.g. exploration and pre-feasibility. Existing data such as the total sulfur from assaying, alongside paste pH, are typically used during the initial stage of the GMT approach as a means of sample screening for stage two analyses. S_{total} is used in the calculation of MPA (maximum potential acidity) on the premise that sulfur values reflect the total (or near total) sulfide fraction of the waste material. It can therefore be used as a proxy for sulfide abundance and used for domaining and screening, as shown in Figures 3, 4, 5 and 6.

Various paste pH methods exist to assess the immediate acid forming potential of waste material for short-term prediction of acid generation. Unlike more advanced geochemical tests, such as NAG pH, paste pH testing involves weak reactions with samples, as either water or electrolyte rich solutions are used during analysis. It is therefore common for samples which have undergone some degree of weathering/oxidation to exhibit lower pH values than un-oxidised samples due to pre-existing dissolution (in the absence of readily available neutralising material). Paste pH may still be used as an effective screening tool, and is powerful when used in combination with S_{total} (S_{total} vs paste pH plots).

Using the GMT(G) approach, plots of ARDI vs S_{total} , and ARDI vs paste pH are used alongside S_{total} vs paste pH plots to assess acid-forming potential and screen samples analysed in stage one for advancement to stage two. With the development of the modified ARDI more accurate

and representative estimations of acid forming potential can be made, due to consideration of non-pyritic sulfide phases with substantial acid generating capabilities (e.g. pyrrhotite and chalcopyrite). Screening is therefore more efficient and effective at identifying acid-forming samples and ensuring appropriate mineralogical and geochemical testing is performed.

It is important to consider that areas containing worst-case examples of sulfides in the waste material are selected for ARDI. Values obtained for each parameter, and therefore the final ARDI score, represent the worst possible outcome of that waste material. This is one possible explanation for the apparent over-estimation of acid-forming potential in samples with particularly undesirable morphologies and sulfide freshness, such as observed in 466. A potential improvement for the ARDI may therefore be the incorporation of values derived from the total modal estimation of sulfides during interval-wide evaluation. This may resolve some of the classification issues between ARDI, S_{total} and paste pH, as ARDI scores can be scaled up or down depending on estimation of total sulfide contents. Sulfur data may aid estimations (if available) by preventing under or overestimation of sulfide abundance. It should be used, however, with caution if sulfate minerals are present.

Although the ARDI may contain pitfalls with regards to overestimation of acid-forming potential, it is a significant improvement on the current lack of environmental logging specified within the GARD Guide (2014). Visual estimations of sulfide (and carbonate) content, mineralogy, grain size and 'mode of occurrence' are mentioned as recommended geological and logging observations (Chapter 5, Table 5-2); however it does not specify how this should be done. The ARDI therefore offers a relatively accurate, easy and cost-effective way to undertake AMD prediction in the coreshed across all stages of mining.

Variance in data may also be attributed to the subjectivity of the assessment procedure, as ARDI logging was performed by multiple personnel. Ultimately, the removal of subjectivity from the ARDI process will yield more accurate and consistent results. The identification of end-member examples for each parameter prior to environmental logging is essential in minimising variability; however it cannot remove subjectivity completely. The desired outcome is the development of ARDI software that can be incorporated into routine analyses performed by automated logging technologies such as Hylogger and Corescan.

5.0 CONCLUSION

The modified ARDI technique was developed and trialled using waste material from four exploration drill-holes at a low-grade copper porphyry deposit in Northern Europe. Assessment of additional sulfide minerals (i.e., pyrite, as well as chalcopyrite and pyrrhotite) on an interval scale was performed to better predict the acid-forming characteristics of the polysulfidic waste material. ARDI parameter C was also modified to suit morphologies observed in primary sulfide phases present in exploration drill-core. Refinement of this environmental logging technique affords more accurate and efficient means for predicting acid-forming potential in sulfidic waste rocks, thus allowing better waste and environmental management plans to be developed.

6.0 ACKNOWLEDGEMENTS

The staff at the company sponsor site in Northern Europe are thanked for provision of research funds and hosting UTAS staff and students at the site to develop this methodology. The ARC TMVC Hub partners are also thanked for the provision of additional funds.

7.0 REFERENCES

Blowes DW and Jambor JL (1990) The pore-water geochemistry and the mineralogy of the vadose zone of sulphide tailings, Waite Amulet, Quebec, Canada. *Applied Geochemistry* **5**, 327–346.

The International Network for Acid Prevention (INAP) (2014) Global Acid Rock Drainage Guide (GARD Guide). <http://www.gardguide.com/>

Lottermoser BG (2010) (Ed) Mine wastes: characterization, treatment and environmental impacts. (Springer, Berlin)

Liu R, Wolfe AL, Dzombak DA, Stewart BW and Capo RC (2008) Comparison of dissolution under oxic acid drainage conditions for eight sedimentary and hydrothermal pyrite samples. *Environmental Geology* **56**, 171-182.

Parbhakar-Fox A, Edraki M, Walters S and Bradshaw D (2011) Development of a textural index for the prediction of acid rock drainage. *Minerals Engineering*, **24** (12), 1277-1287

Parbhakar-Fox A (2017) Predicting Waste Properties Using the Geochemistry-Mineralogy-Texture-Geometallurgy Approach. In 'Environmental Indicators in Metal Mining' (Ed Lottermoser) pp. 73-92. (Springer International Publishing Switzerland).

Parbhakar-Fox A and Lottermoser BG (2017) Prediction of Sulfidic Waste Characteristics. In 'Environmental Indicators in Metal Mining' (Ed Lottermoser) pp. 35-50. (Springer International Publishing Switzerland).

Smart R, St C, Weber P, Thomas JE and Skinner WM (2004) Improvements in acid rock drainage testing for short and long-term neutralisation kinetics. In 'Waste Processing and Recycling in Mineral and Metallurgical Industries V, Proceedings of the 5th International Symposium on Waste Processing and Recycling in Mineral and Metallurgical Industries.' (Eds Rao SR., Harrison FW, Konzinski JA, Amaratunga LM, Cheng TC and Richards GG). pp. 525–540 (Canadian Institute of Mining, Metallurgy and Petroleum)

Weber PA, Stewart WA, Skinner WM, Weisener CG, Thomas J and Smart RSC (2004) Geochemical effects of oxidation products and framboidal pyrite oxidation in acid mine drainage prediction techniques. *Applied Geochemistry* **19**, 1953-1974.

Weisener CG and Weber P (2010) Preferential oxidation of pyrite as a function of morphology and relict texture. *New Zealand Journal of Geology and Geophysics* **53**, 167-176.

WHY VARIABLE OXIDATION RATES ARE NEEDED FOR THE PREDICTION OF AMD FROM DYNAMIC WASTE ROCK DUMPS

J. Pearce^A, S. Pearce^B and R. Marton^C

^AO'Kane Consultants, 11 Collingwood Street, Osborne Park WA 6017, Australia

^BO'Kane Consultants, 3A Vale Street Denbigh Wales LL163AD, UK

^CBHP, Level 28, 125 St Georges Terrace, Perth WA 6000, Australia

ABSTRACT

Much effort, time and capital, is expended at mine sites on predicting the potential and quality of acid and metalliferous drainage (AMD) originating from waste rock dumps (WRDs). For many sites, WRDs represent the largest potential source of AMD and subsequently more often than not, reflect the highest risk associated with AMD management and successful mine closure. Compounding this is the dynamic nature of a WRD, which increases the complexity of AMD predictions when incorporating the shifting fluxes of water, gas, and temperature.

Typical AMD predictions for a given WRD will involve combining static and kinetic testing data with net percolation calculations to estimate potential AMD loads, which can also include geochemical modelling of the data. Kinetic data which is traditionally collected from industry standard humidity cell, free draining leach column, or oxygen consumption type tests, are applied to estimated quantities of sulphide-bearing waste rock to predict the quantity of acidity and/or contaminants that are produced with time. However, the oxidation rates applied to these predictions are often fixed, and do not allow fluctuation as water and air availability change within the WRD in response to climatic conditions.

A new kinetic method has been developed that allows dynamic oxidation rates to be measured in parallel with fluctuating moisture, temperature, and airflow. Oxidation rates have been measured for black shale waste rock samples, collected from WRDs within the Pilbara, over a 23 month period in conjunction with replicate industry standard free draining leach columns. Rates were generally significantly faster than their free draining leach column replicates and were found to fluctuate by more than an order of magnitude as the system responds to wetting events, which were applied to achieve liquid to solid ratios similar to those expected within the Pilbara. This paper presents the findings of the completed program.

1.0 INTRODUCTION

Acid and metalliferous drainage (AMD) is recognised internationally and within Australia as one of the most significant and difficult environmental issues facing mining operators and regulators (Egiebor and Oni 2007; Watkins 2007). A key reason for its importance is that AMD has the ability to cause significant ongoing pollution of the surrounding environment that could potentially persist for hundreds of years. As such, AMD has been highlighted in mine closure guidelines by Western Australian regulators as one of the key environmental issues relevant to mine closure (Department of Mines and Petroleum 2015).

For sites requiring disturbance of reactive waste rock, predicting AMD contaminant loads from existing and future waste rock dumps (WRDs) is therefore a key step to understanding a site's

closure liability with respect to AMD. However, predicting contaminant loads from WRDs, as well as tailings storage facilities (TSFs) and pit voids (although not a focus of this paper), is very complex when considering the dynamic forces that play a significant part in the formation, mobilisation, and release of AMD. Contaminant load predictions are then further complicated through the incorporation of parameters determined from standard kinetic testing methods that largely do not give consideration to the dynamic forces within a WRD.

1.1 Dynamic Waste Rock Dumps

There are several factors influencing AMD risk such as waste geochemical and physical properties, WRD geometry and construction method, and climate (Pearce et al. 2016). More often than not, the focus of AMD risk and characterisation assessments focus on the geochemical and climatic factors with very little consideration to the WRD internal structure (Pearce et al. 2016).

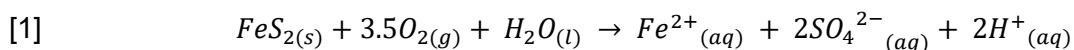
How a WRD is constructed, as well as the physical properties of the waste, will determine how accessible reactive minerals are to water and oxygen for participation in chemical reactions. Depending on climatic conditions (e.g. wet versus dry season), the supply of water and oxygen to these reactive surfaces will vary throughout a given year. Therefore, if reactant supply is variable, the generation of products will also be variable. And like the variable generation of contaminant products, the mobilisation and release of these products will be primarily influenced by the dynamic conditions within the WRD, largely set by the relationship between its internal structure and climatic conditions.

1.2 Typical AMD Prediction Methods

Sulfide (or pyrite) oxidation rates for acid generating waste materials can be used as a proxy for chemical weathering (Sapsford et al. 2009). Oxidation rates can then be used to estimate the rate of acidity/contamination generation resulting from chemical weathering. The rate of acid generation is a key parameter that mining operator's measure to assist the development of effective waste management plans such as WRD construction method, appropriate cover systems design, and contingency water treatment strategies. The two main methods of estimating sulfide oxidation are the sulfate release method and the oxygen consumption method (Elberling 1993; Elberling et al. 1994; Hollings et al. 2001; Kempton et al. 2010):

- Sulfate release method – Utilises the relationship between measured sulfate production and stoichiometric sulfide (usually pyrite) consumption to estimate the oxidation rate (Elberling et al. 1994).
- Oxygen consumption method – Estimates the sulfide oxidation rate by measuring the decrease in oxygen concentration over time (Hollings et al. 2001).

The sulfate release method is the most common method utilised by industry (e.g. humidity cell and free draining leach columns) and utilises analytically determined sulfate concentrations from column leachates (AMIRA 2002 and ASTM 2012). Without mineralogical data specifying what sulfide minerals are present in a sample, pyrite is often assumed to be the dominant sulphide, as it is the most common (Sapsford et al. 2009). The mass of sulfate released over time can then be related to the quantity of pyrite oxidised over time by the stoichiometric relationship in Eqn. [1] (Sapsford et al. 2009).



An important concept to understand when applying the sulfate release rate is the distinction between the release and production rates with the latter (not the former) representing the oxidation of pyrite (Sapsford et al. 2009). If not all generated sulfate is released then the oxidation rate determined from the sulfate release rate will underestimate the actual rate. To ensure production equals release, high flush volumes unrepresentative of field liquid to solid ratios are applied in the laboratory with steady-state release rates being typically used in AMD load predictions (Maest and Nordstrom 2017). This over-flushing (volume and regularity) then negates any possibility for the stored contaminant dominant systems observed in semi-arid regions to be replicated in the laboratory (Price 2009; Maest and Nordstrom 2017). The small size of the columns also discourage leachate concentrating effects resulting from increased pore water residence time.

1.3 Alternative Kinetic Testing Method

A new method using advanced customisable leach columns (ACLs) was developed to address limitations in existing industry standard kinetic testing methods (Pearce and Pearce 2016). Limitations addressed include:

- Flexibility to incorporate variable air supply (WRD gas flux)
- High liquid to solid ratios and short leachate residence times (WRD water flux)
- Low or fluctuating experimental temperatures, and
- Low sample volumes and small particle size.

In addition to typical variables collected from standard kinetic testing, the developed ACLs allow airflow, liquid to solid ratios, and system temperatures to be calibrated to site conditions. Predicted or measured internal airflows within WRDs for various construction methods can be replicated using continuous air supply and flow regulators. Wetting regimes, from a liquid to solid ratio perspective, can be customised to better reflect field net percolation rates. The ACL enclosure is a temperature controlled room with the flexibility to be operated between 6–50°C (Fig. 1). The larger capacity columns (1 m height; 150 mm diameter), which can take up to 25 kg material, accommodate larger particle sizes (up to 100 mm) in comparison to standard kinetic methods, facilitate longer leachate residence times that promotes contaminant concentrating effects observed in the field. Dynamic system parameters temperature, pressure, humidity, airflow, oxygen concentration, and carbon dioxide concentration are continuously logged so that dynamic oxidation rates dependent on both airflow and water availability can be measured.



Fig. 1 ACLC enclosure with 16 operating columns.

2.0 COLUMN CONFIGURATION AND OPERATION

This paper discusses the findings from four replicate ACLCs constructed from one composite sample. The four replicate columns investigated the effects of variable air and water over a period of 12 months. To allow comparison to industry standard, free-draining leach columns, duplicate columns using the AMIRA 2002 method were constructed from the same composite material. However, as the free-draining leach columns do not facilitate variable airflow rates, a duplicate column and a high temperature column were substituted against the ACLC low and high air columns. The four replicates were named as per the following:

- Replicate 1: ACLC – Control Column AMIRA – Control Column
- Replicate 2: ACLC – Low Air Column AMIRA – Control Column Duplicate
- Replicate 3: ACLC – Low Water Column AMIRA – Low Water Column
- Replicate 4: ACLC – High Air Column AMIRA – High Temperature Column

The 100 kg composite sample was prepared from 12 waste rock primary samples collected from a WRD sonic drilling program. The WRD investigation included drilling of more than ten boreholes into four WRDs at an iron ore mine in Western Australia's Pilbara region. The primary samples were majority black shale with the composite sample having the chemical and physical characteristics listed in Table 1.

Table 1. Chemical and physical properties of the composite sample on a weighted average basis.

Parameter	Units	Value
Total Sulfur	wt%	2.89
Sulfate Sulfur	wt%	1.44
ANC	kg H ₂ SO ₄ /t	10.3
Total Carbon	wt%	2.8
^A PSD <2.36 mm	wt%	32.0
^A PSD +2.36 mm	wt%	14.8
^A PSD +4.75 mm	wt%	11.2
^A PSD +6.70 mm	wt%	23.4
^A PSD +13.7 mm	wt%	18.6

^APSD not applicable for free draining leach column duplicate samples as method requires crushing of samples to <4 mm.

2.1 ACLC Air Flow Regime

Air flows were adjusted within the first four months due to initial flow regulators not providing sufficiently low air flow control. Air flows for the ACLC Control, Low Air, and High Air Columns were set using airflows estimated from field oxygen sensor data coupled with particle size data collected from the sonic drilling program. Air flow for the Low Air Flow Column was set at 0.008

L/min and represents lift heights of approximately 10 m. The Control Column was set at 0.06 L/min which reflected lift heights of 20-30 m. The High Airflow Column was set at 0.2 L/min which reflects an unconstrained WRD with respect to oxygen supply. Note that the airflow used for industry standard humidity cell tests is 2.5 times greater than this unconstrained airflow (ASTM, 2012).

2.2 ACLC Wetting Regime

Distilled water was added to each of the columns at the time of column loading. Water was added so that the resulting moisture content was within the range observed in the field (8-12 wt%) with the exception of the low water replicate which was loaded with two thirds the volume of the Control Column. To avoid excessive addition of water to the columns as to achieve liquid to solid ratios as close as practicable to moisture conditions observed in the field, matric potential was monitored in each of the columns. This examination of internal drying rates and comparison with field matric potential resulted in the first application of water after 10 months of operation. A second flushing event was applied to the ACLCs at the completion of the program to determine potential pore water concentration of key contaminants. This wetting regime closely reflected the typical Pilbara pro-longed drying cycle before a large cyclonic wetting event.

2.3 Free Draining Leach Column Wetting Regime

The intention of the weekly wetting applications is to wet the sample with minimal leachate loss during these non-flushing weeks. Initially 0.2 L of distilled water was added during the wetting weeks with no leachate observed. This wetting volume was increased to 0.3 L which generated a very small leachate volume in some columns (0.15 L for the Low Water free draining leach column). The volume applied for the monthly flushing event was 0.8 L for all free-draining leach columns except the Low Water replicate which had 0.4 L applied.

2.4 Temperature Regime

The ACLC enclosure is a temperature controlled room and was operated at 35–36°C at all times. This temperature range is the recorded average annual internal temperature of instrumented WRDs at the site investigated. This regime is significantly different to that applied to the free-draining leach columns. The drying phase for the free- draining leach columns is induced by heat lamps with 150W bulbs automatically operated for eight hours per day for five consecutive days each week. The heat lamps are used to simulate air temperature, during the eight hours of heat lamp operation, of between 30 and 35°C.

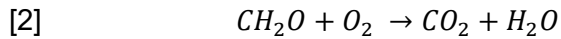
3.0 RESULTS

The following section presents selected results for the four replicate ACLCs over a 12 month period as well as key comparison points to the free draining leach columns.

3.1 Oxidation Rates and Airflow

The intrinsic oxidation rate (IOR) can be considered the overall rate of oxygen consumption reactions within the column. That is, the IOR incorporates oxygen consumed from both pyrite and organic carbon oxidation reactions. Parallel carbon dioxide measurements allowed the conservative calculation of oxygen consumption by organic carbon, that is, all measured carbon dioxide was assumed to be a product of Eq. [2]. Carbon dioxide release into the column air exhaust through the dissolution of carbonate was considered negligible with respect to this specific assessment of replicate columns. For reference, the measured organic carbon oxidation rate (COR) was generally greater than an order of magnitude slower than the pyrite oxidation rate

(POR) when calculating POR from Eq. [3]. Therefore, for the purpose of this assessment, IOR was assumed to be a reasonable proxy for POR.



$$[3] \quad POR = IOR - COR$$

Figure 2 presents the differences observed between IORs when varying water and air supply in comparison to the Control Column. The IORs for the Low Air Flow Column ($7.7E-8$ to $9.3E-7$ kg $O_2/m^3/sec$) are approximately an order of magnitude lower than the control column over the same period ($2.3-4.1E-6$ kg $O_2/m^3/sec$). This indicates that airflow rates are a key limiting factor for oxidation rates and therefore acidity production. Initially, the Low Water Column did not have a meaningful lower IOR relative to the Control Column indicating that controlling moisture content may not likely influence oxidation rates. However, as the Low Water Column approached suction values of 900–1,000 kPa (June–July 2015), the IOR dropped considerably and remained low until the next wetting event. The positive correlation between suction and IOR up to the 900–1,000 kPa range indicates that loss of moisture can accelerate the IOR until the point at which moisture becomes the limiting factor in the oxidation reaction. The High Airflow Column had a significantly faster IOR than the Control Column demonstrating the positive influence of air supply on oxidation rates. The maximum IORs for the High Air Flow Column were approximately $2.0E-5$ kg $O_2/m^3/sec$ which is almost five times the measured IOR for the Control Column.

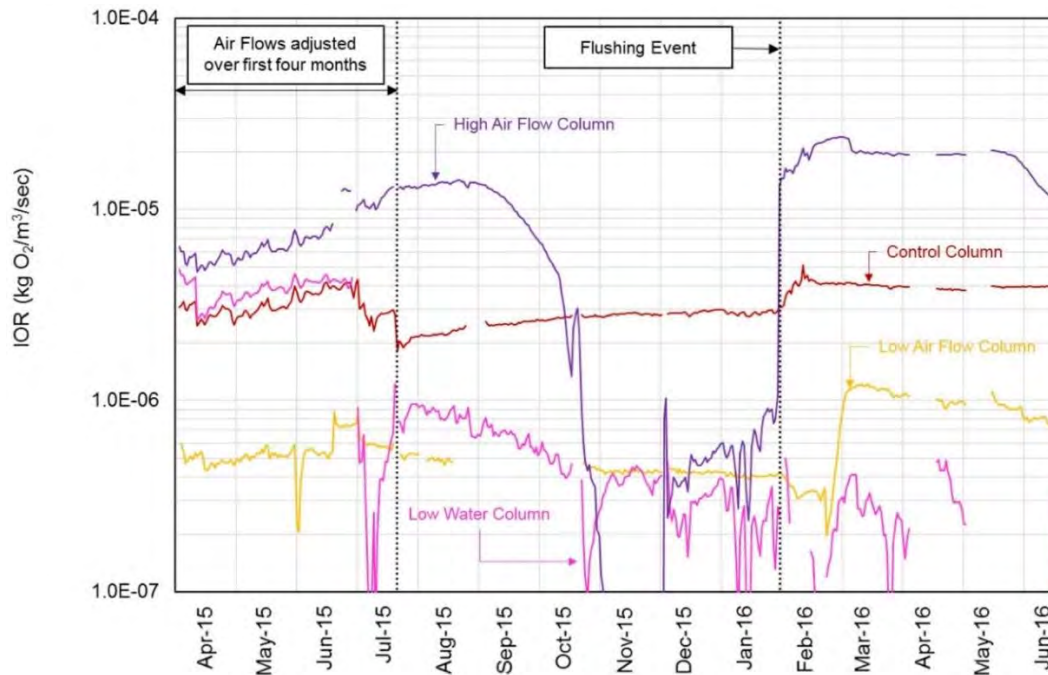


Fig. 2 IORs for each replicate column.

Figure 3 shows the predicted normalised pyrite consumption using the dynamic oxidation rates on a monthly basis for the Control, Low Air, and Low Water Columns plotted against field data collected from WRD installations from iron ore mines within the Pilbara. Using the monthly IORs

measured allows incorporation of dynamic oxidation rates that are changing as the WRD internal conditions respond to climatic conditions (e.g. drying, wetting, change in airflow).

The field data plotted on Fig. 3 represents two construction alternatives (10 m vs 20-30 m lifts) that subsequently result in two different air permeability's. The estimated air permeability's from these two different placement methods were used to set air flows for the ACLC's, specifically the Control and Low Airflow Column. The figure demonstrates one of the most significant findings of the ACLCs in that they were able to closely replicate oxidation rates observed at the field scale when applying the measured dynamic oxidation rates for long-term AMD predictions.

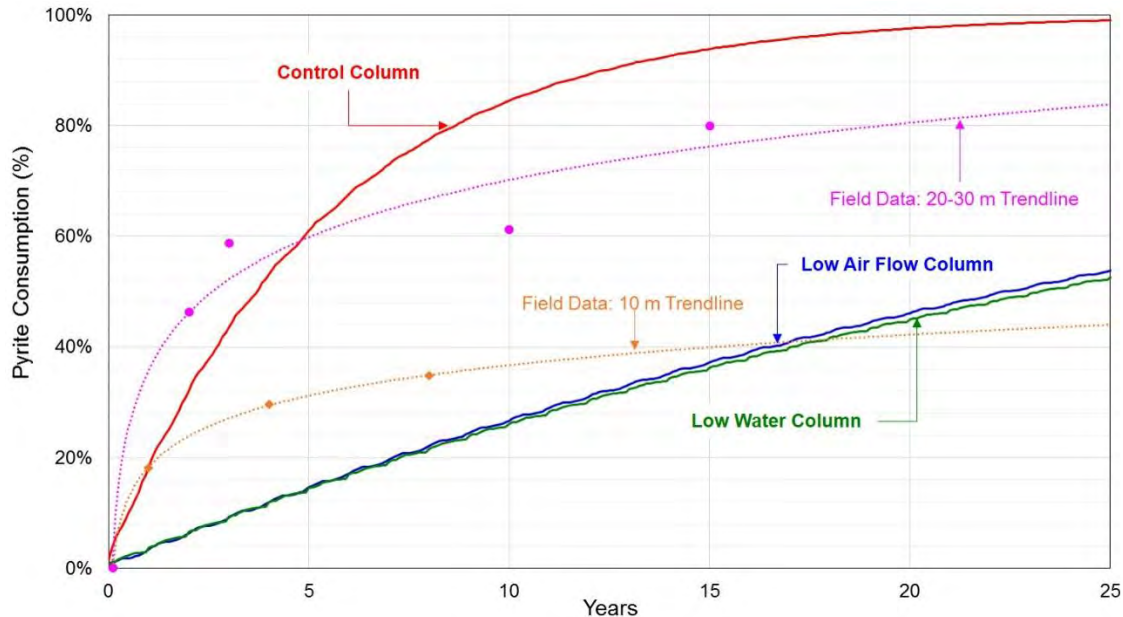


Fig. 3. Predicted pyrite consumption using monthly IORs measured within each of the replicate ACLCs and material geochemical data.

3.2 Oxidation Rates and Drying

Suction data for the replicate columns are presented in Fig. 4. An increase in suction can be inferred to represent drying of the materials in the columns. That is, as moisture is removed from the system suction pressure will increase. Moisture is typically removed from larger pore spaces initially which is indicated by the first inflection change in Fig. 4. (e.g. April to July for the Control Column). Once moisture removal from smaller pore spaces begins, a second inflection in the drying curve can be seen (e.g. September for the High Air Flow Column). Conversely, suction decreases rapidly in all columns after the flushing event. Because all the materials in each column have a unique PSD then the drying curves will be different and as such suction can be expected to occur at both a different rate and to a different final value in each of the columns.

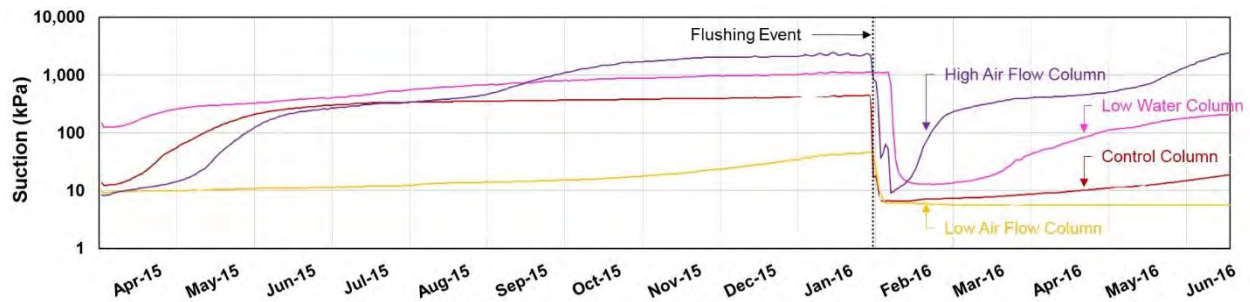


Fig. 4. ACLC suction pressures as measured by installed MPS2 sensors for the four replicate columns. Vertical dotted line represents the 10 month wetting event. Data values (kPa) presented refer to negative pressure.

Figure 5 presents suction and IOR data for the High Air Flow Column and highlights a key finding from the ACLC columns not able to be observed with conventional kinetic testing procedures. The High Air Flow Column produced an initial IOR of $4.8\text{E-}6 \text{ kg O}_2/\text{m}^3/\text{sec}$, this rate increased steadily to a maximum of $1.4\text{E-}5 \text{ kg O}_2/\text{m}^3/\text{sec}$ after four months which was correlated by a simultaneous rise in suction values as the material in the column experienced drying as a result of internal advective drying. Following reaching the maximum IOR and at a suction of 900 kPa, the rate decreased rapidly by almost an order of magnitude to $3.7\text{E-}7 \text{ kg O}_2/\text{m}^3/\text{sec}$, before rebounding sharply to just below $2.0\text{E-}5 \text{ kg O}_2/\text{m}^3/\text{sec}$, where it remained constant for the following four months. When water was added to the column in January 2016, the IOR increased rapidly corresponding with a drop in suction to around 10 kPa. Suction increased progressively as a result of advective drying until approximately 1,000 kPa was reached in late May and again, the rate dropped rapidly. Given that the IOR was seen to record a rapid drop coinciding with suction reaching approximately 900–1,000 kPa, this likely reflects the point at which water becomes the rate limiting factor in the pyrite oxidation reaction.

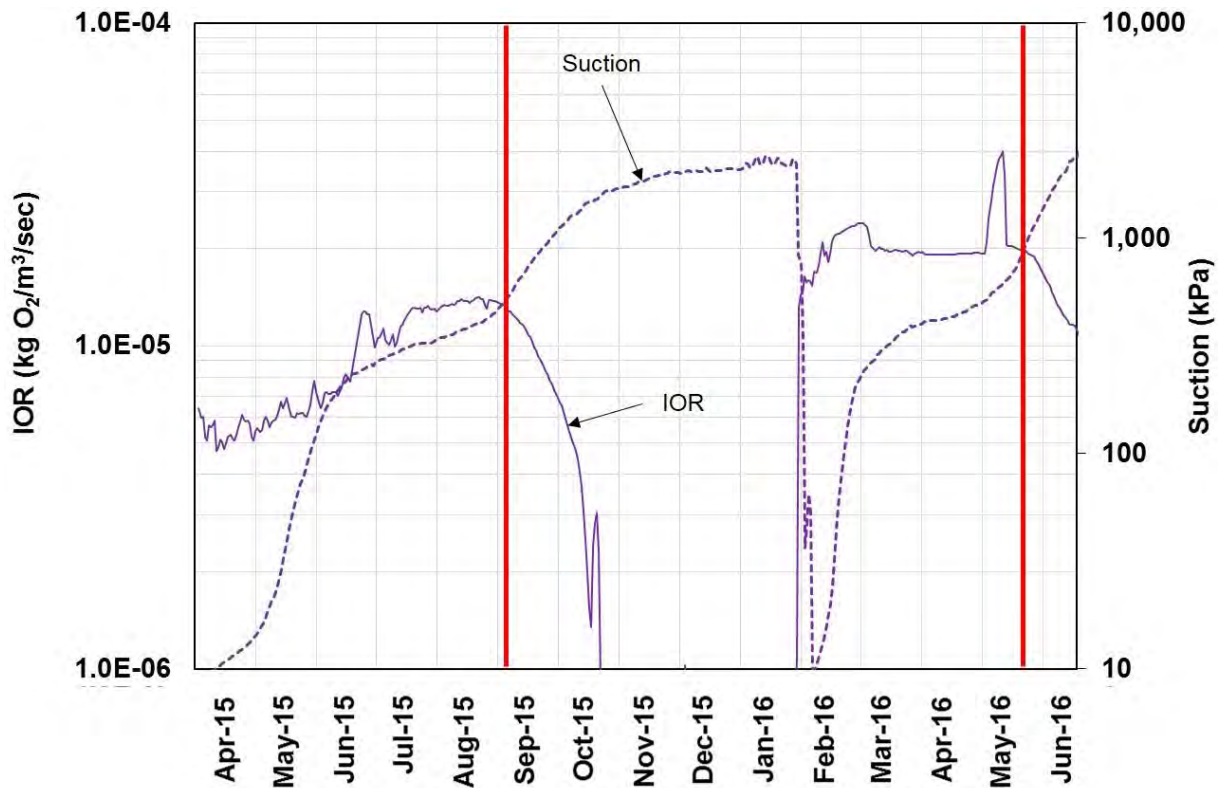


Fig. 5. IOR plotted against suction to illustrate correlation between decreased IOR and second inflection point on suction graph representing point at which pyrite oxidation becomes water limiting.

Once moving beyond the second inflection point on the matric potential figure (approximately 900–1,000 kPa), representing the loss of tightly held water, oxygen consumption ceases. Theoretically, if net percolation can be reduced significantly through sustained (e.g. multiple consecutive) dry seasons, and advective drying continues to the point at which suction can approach this second inflection point in the field, then the IORs within the WRD may be managed in the field. What is evident from Fig. 5 is the ability for the ACLCs to produce a dynamic IOR that is influenced by both air supply and changing moisture content, as would be expected in the field.

The High Air Flow Column demonstrates that a high availability of air, such as that from advective forcing of air, will have significant effects on IOR. During the same testing period, it also highlights the influence that water will have when it becomes limiting in the oxidation reaction as seen after 7–10 months of operation, that is, the IOR reduces sharply but then rebounds fast as water is added such that is experienced in the Pilbara during the wet season.

Figure 6 compares monthly average IORs calculated from oxygen consumption (ACLC) and steady-state sulfate release (free draining leach columns) for the first 12 months of operation for the four replicate columns. Key findings from this comparison is the significantly faster IOR (order of magnitude) of the High Air Flow Column relative to its free draining leach column duplicate, and the significantly lower IORs (up to 5-10 times slower), when airflow and water are controlled (Low Air and Water Columns).

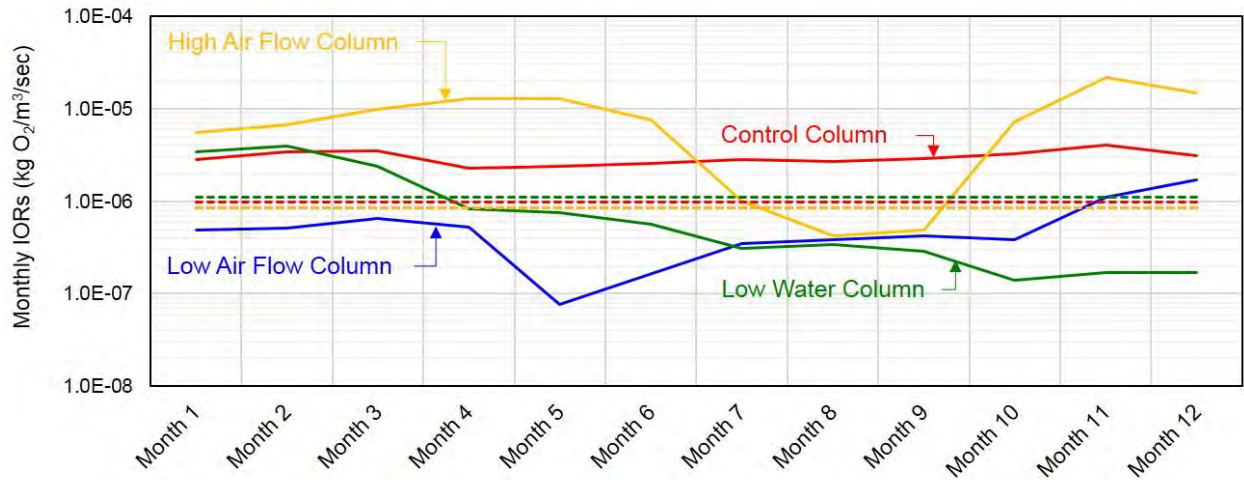


Fig. 6. Comparison of oxygen consumption (ACLC) and sulfate release (AMIRA) calculated monthly average IORs for the first 12 months of operation for the four replicate columns. Free draining leach column duplicates represented by dashed coloured lines of associated ACLC replicate. IORs for free draining leach columns are calculated from the average sulfate values for the final five months representing steady-state conditions as is typically employed for this method (Maest and Nordstrom 2017).

Table 2 presents published IORs for black shale samples, specifically Mt McRae Shale, using the three most common kinetic testing methods for determining oxidation rates. Four of the five IORs are generally lower than the Low Air and Low Water ACLC Columns, and the highest value is consistent with the IORs determined using the free draining leach column method in this study.

Table 2. Measured oxidation rates in kg O₂/m³/sec for several black shale samples associated with Western Australian iron ore deposits utilising industry standard kinetic methods. All total sulfur values are in wt%. Table adapted from Pearce (2015).

Oxidation Rate Measurement Method	Total Sulfur	IOR Range
Free draining leach column (EGi, 2006)	3.0	1.5E-6
Free draining leach column (EGi, 2006)	1.5	4.2E-8
Free draining leach method (Linklater, 2015)	1.8	1.7E-7 ^A
Humidity cell method (Linklater, 2015)	5.1	1.3E-7 ^A
Oxygen consumption method (Earth Systems, 2012)	3.0	6.2E-7 ^B

^AReported results were converted from average sulfate release rates (Linklater, 2015)

^BReported results were converted from normalised PORs (Earth Systems, 2012).

What is evident from Fig. 6 and Table 2 is the ability of the ACLCs and the inability of standard methods to produce a dynamic IOR that is influenced by both air and water availability, as would be expected in the field. The High Air Flow Column data for example shows the effects that a high availability of air, and the suction state of the material will have on an IOR within a WRD that may be influenced by dynamic water and gas flux. The clear influence that water content will have when it becomes the limiting factor in the oxidation reaction is shown in months 7–10. As the figure shows, the IOR reduces sharply but then rebounds fast as water is added in month 10. This variability in suction state is analogous to the semi-arid climate of the Pilbara which experiences cyclonic rainfall events within the wet season.

3.3 Leachate Quality and Liquid to Solid Ratio

Due to the larger sample size and infrequent wetting of the ACLCs to better reflect climatic conditions of the Pilbara, the liquid to solid ratios are far different to those of the free draining leach columns, as presented in Table 3. After the final flushes for each column, the liquid to solid ratios for the ACLCs are over 30 times lower and are far more representative of those observed in the field.

Table 3. Liquid to solid ratios for ACLCs and free draining leach columns following first and final flushes.

Column	ACLC First	Free Draining Leach Final	ACLC Final	Free Draining Leach Final
Control Column	0.15	0.4	0.25	14
Low Air Column	0.15	0.4	0.23	14
Low Water Column	0.10	0.2	0.16	7
High Air Column	0.14	0.4	0.23	14

The restricted application of water and larger column length (increased pore water residence time) allowed the ACLCs to develop a saturated system with respect to secondary oxidation products. Following the final flush, concentrations of key contaminants were generally orders of magnitude greater than those produced by the free draining leach columns during steady-state conditions, despite similar pH values (2.3–2.6). Figure 7 presents sulfate and zinc data for each of the ACLC replicates and their free draining leach column duplicates within first and final flush leachates. First flush concentrations are fairly consistent, with the higher concentrations shown by the free-draining leach columns likely due to the crushing of samples pre-experiment. The key difference is observed in the final flush leachates where zinc is up to two orders of magnitude greater within ACLC leachates and sulfate is generally greater than order of magnitude. Note that, the leachate for the Control Column was collected five months after the replicate columns, as this column was continued (along with its free draining leach column duplicate) as part of a greater study. Therefore, the Control Column (ACLC and free draining leach columns) had an additional five months for the storage of oxidation products which emphasised the importance of allowing the system to saturate, as you would expect within a WRD within the Pilbara. If using steady-state leachate concentrations (release rates) from free draining leach columns to predict pore water chemistry for AMD loading calculations, contaminant concentration within pore water could be underestimated by orders of magnitude.

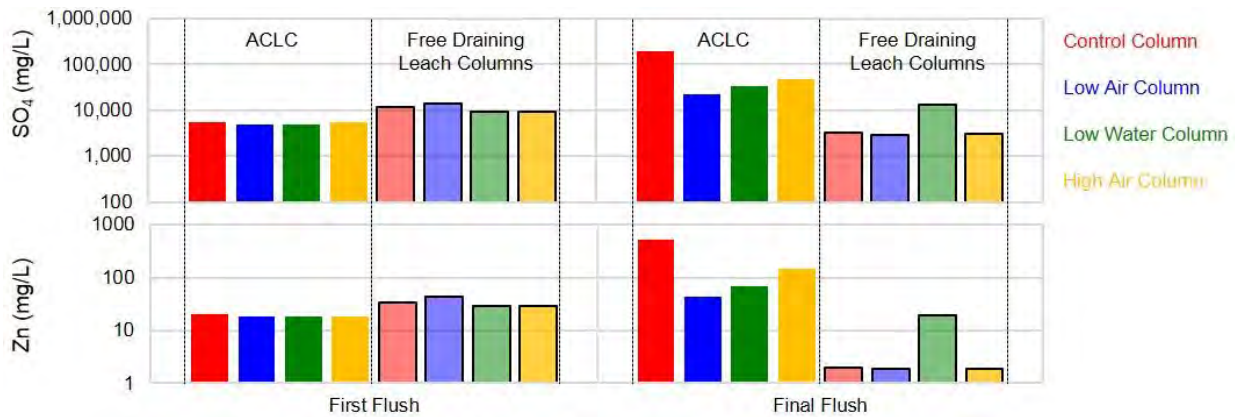


Fig. 7. Comparison of sulfate and Zn concentrations between ACLC and AMIRA first and final flush leachates for the operating period. Free-draining leach column duplicates represented by shaded colour of associated ACLC replicate.

3.4 System Temperatures

Internal temperature was recorded within a free draining leach column to allow comparison with temperatures recorded within the ACLCs containing the same material. The internal temperature fluctuation observed in Fig. 6 for the free draining leach column is a result of the method prescribed drying regime which cycles heat lamps on and off.

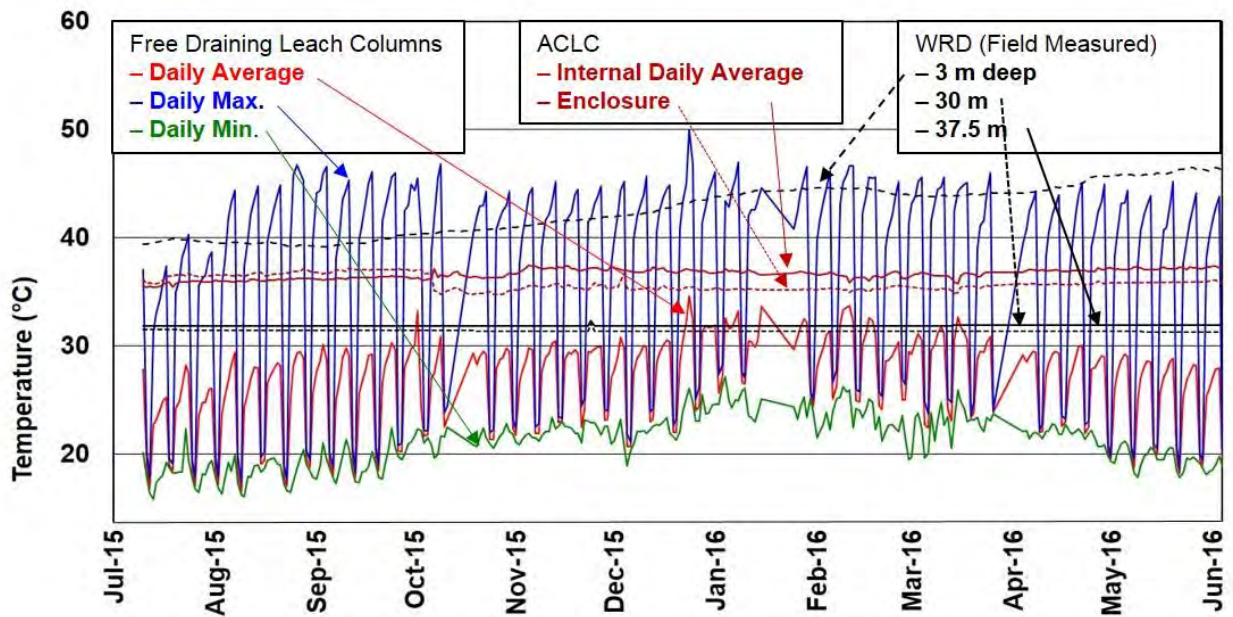


Fig. 8. Daily average, minimum and maximum internal temperatures for a free-draining leach column plotted against measured the internal temperature of an ACLC testing the same material, the ACLC enclosure temperature, and internal WRD temperatures from three instrumented depths.

The internal temperatures for the free-draining leach column were highly variable with minimum and maximum temperatures of 16°C and 50°C respectively. Relevant points regarding the trends noted in the temperature data include:

- The temperature fluctuations in the free-draining leach column appears to be more comparable to those experienced in the outer (<3m) layer of a WRD, where climatic forces have a more pronounced influence, such as a cover system, than the interior of a WRD.
- The internal ACLC and the ACLC enclosure data lie between the temperatures measured in the field at depths of 3-37.5m in one of the boreholes from which the samples were collected.

It should be further noted that temperatures greater than 40°C and 60°C respectively are noted in other WRDs monitored at the same site. When considering that the average daily temperatures of the free-draining leach columns are lower than the average internal ACLC temperatures, it can be concluded that temperature conditions of the free-draining leach columns are not as representative of the internal conditions of the WRDs being monitored. This is an important distinction as temperature is a key factor for oxidation reaction rates.

4.0 CONCLUSIONS

Dynamic oxidation rates were determined through continuous measurement of oxygen and suction using a new kinetic testing method that incorporates the dependency of IORs on air flow and moisture. The method allows variable air flows to be set based on specific WRD construction methods that replicate air supply to reactive minerals. The method also incorporates site calibrated wetting regimes so that liquid to solid ratios observed in the field can be applied and over flushing, typical of standard kinetic testing methods, can be avoided. This allows the build-up of saturated systems (with respect to secondary oxidation products), as is common to the Pilbara, and the production of more realistic leachates reflective of concentrated pore waters. As the method incorporates dynamic WRD variables such as gas and water flux, the combination of the produced dynamic oxidation rates with saturated system leachate data facilitates more site specific AMD contaminant load predictions.

5.0 REFERENCES

AMIRA (2002) ARD Test Handbook - Project P387A Prediction and Kinetic Control of Acid Mine Drainage. May 2002.

ASTM (2012) D5744 - 12 Standard Test Method for Laboratory Weathering of Solid Materials Using a Humidity Cell, 10.1520/D5744-12.

Department of Mines and Petroleum (2015) Guidelines for Preparing Mine Closure Plans. May 2015.

Earth Systems (2012) Comparison of measured pyrite oxidation rates for Mt. McRae Shale. April 2012.

Environmental Geochemistry International (2006) Leach Column Testing of Mt McRae Shale – Final Report. August 2006.

Egiebor NO and Oni B (2007) Acid Rock Drainage Formation and Treatment: A Review. *Asia-Pacific Journal of Chemical Engineering* **2**, 47-62.

Elberling B (1993) Field Evaluation of Sulphide Oxidation Rates. *Nordic Hydrology* **24**, 323-338.

Elberling B, Nicholson RV, Reardon EJ and Tibble P (1994) Evaluation of Sulfide Oxidation Rates - A Laboratory Study Comparing Oxygen Fluxes and Rates of Oxidation-Product Release. *Canadian Geotechnical Journal* **31**, 3, 375-383.

Kempton H, Bloomfield TA, Hanson JL and Limerick P (2010) Policy guidance for identifying and effectively managing perpetual environmental impacts from new hardrock mines. *Environmental Science and Policy* **13**, 6, 558.

Hollings P, Hendry MJ, Nicholson RV and Kirkland RA (2001) Quantification of oxygen consumption and sulphate release rates for waste rock piles using kinetic cells: Cluff lake uranium mine, northern Saskatchewan, Canada. *Applied Geochemistry* **16**, 1215-1230.

Linklater C, Watson A, Chapman J, Green R and Lee S (2015) Weathering and Oxidation Rates in Black Shales – A Comparison of Laboratory Methods. In Proceedings of the 10th International Conference on Acid Rock Drainage. Santiago, Chile. 21-24 April 2015.

Maest AS and Nordstrom K (2017) A geochemical examination of humidity cell tests. *Applied Geochemistry* **81**, 109-131.

Pearce J (2015) Physical and Chemical Weathering of Mount McRae Shale (Thesis). 21 May 2015.

Pearce SR, Dobchuk B, Shurniak R, Song J and Christensen D (2016) Linking waste rock dump construction and design with seepage geochemistry: an integrated approach using quantitative tools. In 'Proceedings of the 2016 International Mine Water Association Conference'. Leipzig, Germany. 11-15 July 2016 (Eds C Drebenstedt and M Paul). (International Mine Water Association).

Pearce SR and Pearce JI (2016) Advanced Customisable Leach Columns (ACLC) – A New Kinetic Testing Method to Predict AMD risks by Simulating Site-specific Conditions. In 'Proceedings of the 2016 International Mine Water Association Conference'. Leipzig, Germany. 11-15 July 2016 (Eds C Drebenstedt and M Paul). (International Mine Water Association).

Price W (2009) Prediction Manual for Drainage Chemistry from Sulphidic Geologic Materials, Mine Environment Neutral Drainage (MEND) Program. December 2009.

Sapsford DJ, Bowell RJ, Dey M and Williams KP (2009) Humidity cell tests for the prediction of acid rock drainage. *Minerals Engineering* **22**, 25-36.

Watkins R (2007) Acid Mine Drainage - The Fundamentals. Treatment Options, (eds), 1-10.

OBSERVATIONS AND EXPLANATIONS FROM THE MONITORING DATA OF EQUITY SILVER MINE, CANADA

Z-S. Liu^A, C. Huang^A, L. Ma^A, K.A. Morin^B, M. Aziz^C and C. Meints^C

^AEnergy, Mining and Environment National Research Council Canada, 4250 Wesbrook Mall, Vancouver, BC, V6T 1W5, Canada

^BMinesite Drainage Assessment Group, Surrey, BC, Canada

^CEquity Silver Mine, Reclamation Operations, Goldcorp Inc, PO Box 1450, Houston BC, V0J 1Z0 Canada

ABSTRACT

The waste rock dump of Equity Silver Mine produces acid rock drainage with high concentrations of metal ions. Over the past 25 years temperature and concentrations of CO₂ and O₂ at different lateral locations and different depths of the waste rock dump have been measured, which turns out to be very valuable for understanding the acid-generating and metal leaching processes. Our observations from the monitoring data include (1) strong positive correlations among O₂ concentrations at different locations, strong positive correlations among CO₂ concentrations at different locations, and strong negative correlations between CO₂ and O₂; (2) seasonal variations of O₂ concentrations and CO₂ concentrations with O₂ concentrations decreasing from March to June/July and increasing from August to February; (3) substantial temperature variations, about 20 degree C, throughout the waste rock dump. The authors provide their explanations of the above observations. These explanations are useful for identifying the conditions that could reduce the problem of acid rock drainage and metal leaching (ARD-ML).

1.0 INTRODUCTION

Collaborating with consultants, universities, Natural Resources Canada and mine owners, the National Research Council Canada is putting efforts to develop core-knowledge and technologies for tackling the problem of acid rock drainage and metal leaching (ARD-ML) through the research program "Environmental Advances in Mining". The current focus is on fundamental understanding of the ARD-ML processes and on the development of the methods of ARD-ML testing for scaling up. This paper reflects a part of our current effort.

Since 1990 the Equity Silver Mine in BC Canada has been monitoring the ARD-ML processes inside the main waste rock dump through the on-going measurement of temperature, O₂ concentration, CO₂ concentration, infiltrated water and ground water level. They have been regularly measured using thermistors, O₂ sensors, CO₂ sensors, lysimeters and piezometers, respectively. This set of data has allowed us to develop a fundamental understanding of ARD-ML processes. This understanding assists the mining industry in mitigating the ARD-ML problem.

The ARD-ML problem begins with the extraction of minerals from the ground. The acidity is produced by the action of air and water upon sulfur compounds, for example, iron sulfide, in the rocks. The result is acid drainage with high concentrations of metals. This problem was recognized as early as in 1920's, but its threat to the environment was then relatively little because of relatively low tonnage of ores processed then. Today the problem has escalated in

scale due to the accumulation of mine waste over the past 100 years of mining activities plus the 2-3 orders of increase in tonnage of ores and waste rock processed today. One current practice to manage ARD-ML is to collect and treat the drainage and then release it back to the environment. Collecting and treating the drainage is very costly and requires the proper handling of the treatment sludge. It is not uncommon that the operating cost for treating the drainage at one mine site can reach \$1M to \$2M per year (GoldCop Inc., 2013, Morin and Hutt, 2006). Note that the ARD-ML problem is a type of rock weathering, and as a consequence it could continue for a few decades to a few centuries, at least.

In order to address the prevention or control of the ARD-ML problem, one needs to understand a few things that include (1) how are oxygen O_2 and water H_2O transported to sulfide minerals? (2) the mechanisms of the ARD-ML processes, and (3) the factors that influence the rate of ARD-ML.

In this paper, we focus on the question (1) and (3). Through analyzing the set of monitoring data, this paper reveals some insights into the behaviors of the waste rock dump in terms of producing ARD-ML.

Equity Silver Mine

- Houston, BC
- Au, Ag, Cu mine
- 1980-1994 mining operation
- Closed in 1994
- Sulfide mine waste 80 million tons
- Effluent pH 2-3
- About \$1.5M/year for effluent treatment
- \$5M for the cover in 1994



Figure 1. The Equity Silver mine site

2.0 THE EQUITY SILVER MINE

2.1 Site Description

The Equity Silver Mine site is described in detail in O’Kane (1998) and Price (2003). The site is located in the central interior of British Columbia, Canada, approximately 575 km north-northwest of Vancouver BC. An old view of the mine property during its operation is illustrated in Figure 1. There is approximately 80 Mt of waste rock, covering an area of approximately 1.4 km square. A soil cover system was installed on the waste rock dump starting in 1991 with average thickness of 0.5 m compacted till and 0.3 m uncompacted till for reducing the amount of infiltrated water and oxygen.

The mine is situated on a plateau in a humid alpine environment. Historical site records indicate the average annual precipitation is about 600 mm with approximately 60% of the precipitation occurring as snow. It snows from November to April. Snow starts to melt in April. The rainy season starts from late April and ends by the end of June.

The waste rock in the waste rock dump is relatively coarse. The D_{80} ranges from 127 to 28 mm and the D_{10} ranges from 3.5 to 4.0 mm, indicating a lack of silt- and clay-sized particles (O’Kane et al. 1998). Note that pore sizes inside the waste rock dump are generally proportional to the sizes of waste rock. As a result, the gas permeability inside the waste rock dump is a few orders larger than that of the cover system. In the next section, we will discuss what role the large gas permeability plays in producing ARD-ML.

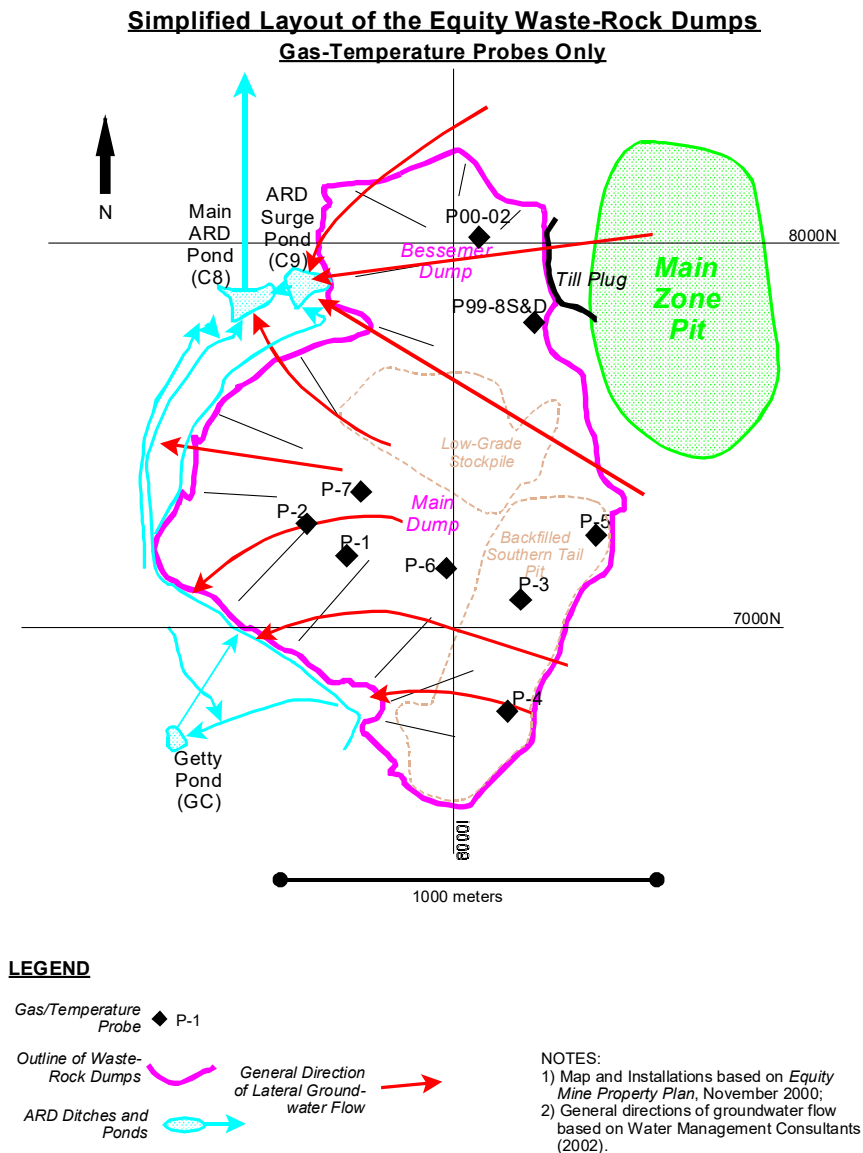


Figure 2. Locations at which O₂ and CO₂ stations and thermistors are installed

2.2 The Instrumentation and the Monitoring Data

O'Kane et al. (1998) described in detail the instrumentation for measuring temperature, gaseous oxygen concentrations, gaseous carbon dioxide concentrations within the main waste rock dump and the backfilled southern tail waste rock dump. In addition, field lysimeters were installed at the base of the soil cover system for measuring infiltrated water. At each of the nine locations shown in Figure 2, temperature, O₂ concentration and CO₂ concentration were measured at different depths ranging from one meter to twenty meters. The sensors are situated in each of the areas of the waste rock dump.

The data we used for this study include the readings from fifty four O₂ stations, fifty four CO₂ stations and nine thermistors. The time period within which the data was used for this analysis is from 1992 to 2009. The time interval between two adjacent measurements is approximately one month. Within the 17 years from 1992 to 2009, approximately 160 readings from each station were recorded and used for this analysis.

3.0 OBSERVATIONS FROM THE MONITORING DATA

3.1 Correlations among O₂ Concentrations and CO₂ Concentrations

Treating the readings of gas concentration at each station as a time-series, we calculated the correlation coefficients of the fifty four O₂ concentration readings and the fifty four CO₂ concentration readings. The time period covers 1992-2009. They give 1431 correlation coefficients $[(1+53) \times 53 / 2 = 1431]$, as shown in Figure 3. Here we treat those correlation coefficients larger than + 0.6 as positively correlated and mark them by pink color. We treat those correlation coefficients smaller than - 0.6 as negatively correlated and mark them by green color. It can be seen from Figure 3 that approximate 70% of the area in Figure 3 is covered by pink color and green color. That is to say, majority of the O₂ concentrations and the CO₂ concentrations are correlated statistically. More importantly, Figure 3 indicates that (1) all of the pink color data, the positively correlated data, are associated with a correlation coefficient between O₂ concentration at one station and O₂ concentration at another station, or associated with a correlation coefficient between CO₂ concentration at one station and CO₂ concentration at another station; (2) all of the green color data, the negatively correlated, are associated with correlation coefficients between O₂ concentration at a station and CO₂ concentration at a station. That is to say: all of the O₂ sensors' readings increase together or decrease together in a statistical sense, even though they are situated laterally at different locations; all of the CO₂ sensors' readings increase together or decrease together in a statistical sense even though they are situated at different lateral locations; when a O₂ sensor's reading increases, a CO₂ sensor's reading would decrease in a statistical sense.

correlation coefficients are indicated by white color. (a) the pattern of the correlation coefficients; (b) the zoomed-in pattern

3.2 Seasonal Variations of O₂ Concentrations

Figure 4(a) shows the seasonal variations of oxygen concentrations at different depths (5 m, 6 m, 10 m, and 17 m) at P-7 location near the central location of the main waste rock dump from 1997 to 2004. One of the pronounced features of the O₂ variation with time is its periodic pattern with one year as its time period. Figure 4(b), zoomed in, shows that the highest O₂ concentration appears around March; and the lowest O₂ concentration occurs around July. The highest O₂ concentration is about 12% and the lowest O₂ concentration is about 2%.

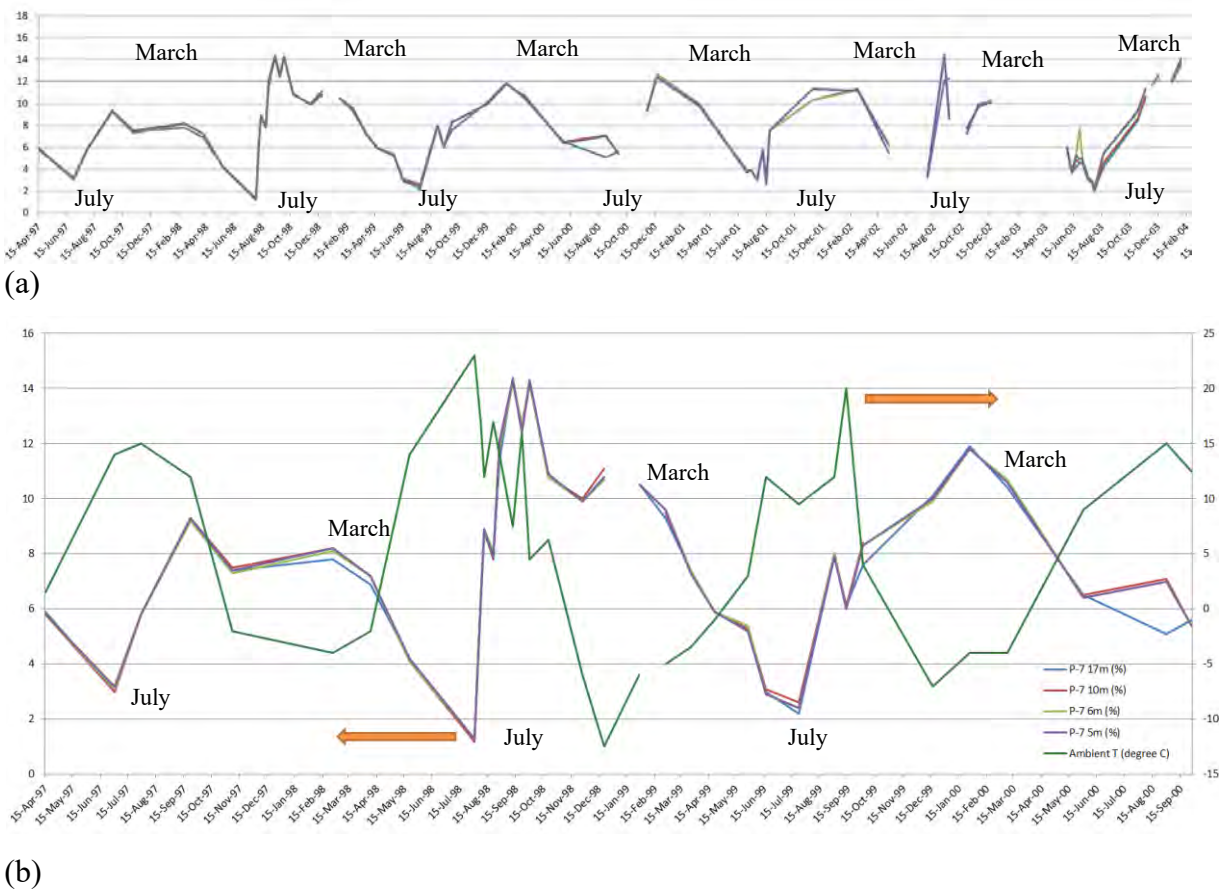


Figure 4. The seasonal variations of O₂ concentrations at P-7 location, depth 5m,6m, and 17 m; (a) O₂ concentrations from April 1997 to 2004; (b) O₂ concentrations and ambient temperature (dark green color) from April 1997 to April 2000

3.3 Uneven Temperature Distribution across the Waste Rock Dump

The temperature measurements across the waste rock dump indicate that temperature varies with depth and with lateral location. The temperature variation with depth is not difficult to understand: the temperature at shallow depths varies with ambient temperature, seasonal temperature changes. The temperature below a certain depth is not affected much

by the change of ambient temperature. However, an interesting phenomenon is: the temperature below a certain depth, though not affected by ambient temperature, varies substantially across the extent of the waste rock dump. For example, the temperature at 17 m depth at P-6 location was about 4 degree C. In comparison, the temperature at 17 m depth at P-7 location was about 54 degree C, which is a huge difference.

3.4 Decreasing Temperature with Time

From Figure 5 it can be seen that temperature inside the waste rock dump has been decreasing at a relatively steady rate. In 1993 it was about 54 degree C at 17 m depth at P-7 location, but it dropped to about 30 degree C in 2009. In other locations, temperature has also dropped.

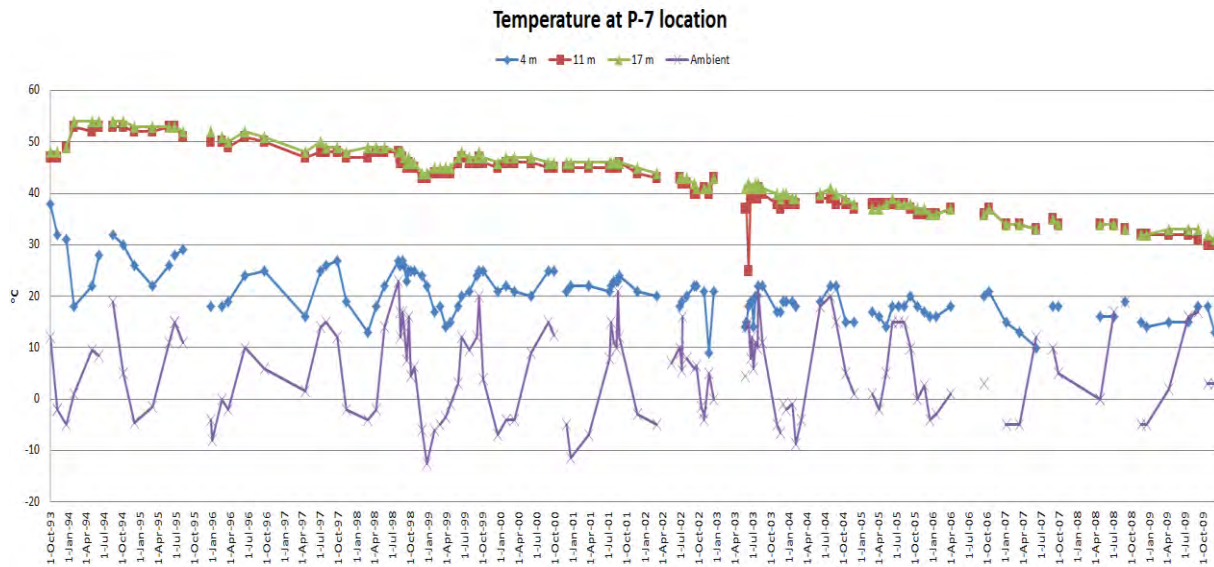


Figure 5. Temperature at depth 17 m (green color), 11 m (red color), 4 m (blue color) and ambient (purple color) at P-7 location from 1993 to 2009

4.0 OUR EXPLANATIONS

4.1 The Correlations among O₂ and CO₂ Concentrations

The negative correlations between the O₂ concentrations and the CO₂ concentrations basically tell that the CO₂ concentrations increase when the O₂ concentrations decrease in a statistical sense. Why? The CO₂ is primarily produced by the neutralizing reactions between metal carbonates and the produced acidity. The ARD reactions consume O₂. As a result, when more O₂ is consumed, more CO₂ would be produced. This explanation is in agreement with the negative correlations between the O₂ concentrations and the CO₂ concentrations. However, it seems that additional factors contribute to CO₂ variability, because CO₂ levels can be significantly higher than, and lower than, that expected from simple stoichiometry (Morin, et al., 2010 and 2012).

The positive correlations among the O₂ concentrations and the positive correlations among the CO₂ concentrations basically tell that when the O₂ concentration at one location goes up, the O₂ concentrations at the other locations would go up as well in a statistical sense;

when the CO₂ concentration at one location goes up, the CO₂ concentrations at the other locations would go up as well in a statistical sense. The two factors that definitely contribute to these positive correlations are as follows. First, the sizes of rocks inside the waste rock dump are quite large (the D80 ranges from 127 to 28 mm and the D10 ranges from 3.5 to 4.0 mm). This makes the waste rock dump inter-connected in terms of gas flow. An interconnected gas-flow system tends to make its O₂ concentrations at different locations follow a common trend. Second, the temporal variations of O₂ concentrations at different locations are driven by the common driving force: the temperature difference between the ambient air temperature and the temperature inside the waste rock dump. This temperature difference drives the flow of gas between the ambient air and the inside of the waste rock dump, thus transferring heat between the ambient air and the inside of the waste rock dump.

4.2 Seasonal Variations of O₂ Concentrations

There are seasonal variations of the O₂ concentrations inside the waste rock dump. O₂ starts to decrease starting from March and keeps decreasing until July, and then it starts to increase from August and keeps increasing until the following March. Why? The O₂ concentrations are affected by two dominant factors. First, convective gas flow between the ambient air and inside the waste rock dump is seasonal. From March to August, the gas convective flow rate is gradually reduced with time, because the temperature difference between the ambient air and inside the waste rock dump decreases with time from March to August. That is to say, the amount of O₂ entering into the waste rock dump decreases with time from March to August. This factor tends to make the O₂ concentrations inside the waste rock dump decrease from March to August. Second, infiltrated water that flushes waste rocks is much more available from March to July than from the rest of the year. This would lead to relatively higher O₂ consumption rate from the ARD reactions due to more fresh water available (Chandra and Gerson, 2010). Note that there is relatively larger amount of water infiltration into the waste rock dump from March to July than from August to the following February. In addition, in spring season, water from melting snow may increase the degree of saturation of the cover and decrease the gas permeability and the oxygen diffusion coefficient. As a result, the O₂ concentrations decrease from March to July. From November to the end of February, it snows there, and in those months water infiltration into the waste rock dump is low. As a consequence, rock surfaces are not frequently flushed from August to the end of February as in the time period of March to July.

4.3 Uneven Temperature Distribution across the Waste Rock Dump

The temperatures among locations vary substantially. We thought that this would be due to uneven ARD reactions only inside the waste rock dump. It is a fact that some locations are associated with the rocks that do not produce or produce little ARD reactions due to relatively low and naturally variable sulphide levels, and other locations are associated with the rocks that contain high percentage of metal sulfides. But we have found an additional factor that also contributes to the unevenness of temperature distribution. Our numerically simulated results of the gas-flow and heat transfer inside the waste rock dump show that the temperature distribution inside the waste rock dump is in agreement with the monitoring data of temperature, when a uniform chemical reaction rate is assumed across the waste rock dump. This indicates that a very uneven temperature distribution across the waste rock dump does not have to be caused by an uneven ARD chemical reaction rate only. This seems to imply that there is an inherent pattern of gas flow and heat transfer inside the waste rock dump, which constitutes partially the pronounced temperature pattern inside this waste rock dump.

Figure 6 shows the temperature distribution inside the waste rock dump, obtained from our numerical modeling. Here we assume a uniform ARD reaction rate across the waste rock dump and thus uniform heat generation rate. The modeling counted the air diffusion, convection, heat transfer by conduction through the rocks and in the convecting air. The modeling domain only included the dump and assuming no heat exchange between the dump and the bedrock. The detailed modeling results of the waste rock dump will be published in our next paper. It can be seen that the temperature distribution is not uniform at all. The location with the highest temperature is P-7 location, in agreement with the temperature monitoring data. This match makes us not doubt the modeling result and makes us believe that the temperature pattern inside the waste rock dump is partially the result of an inherent property of the waste rock dump in terms of gas flow and heat transfer.

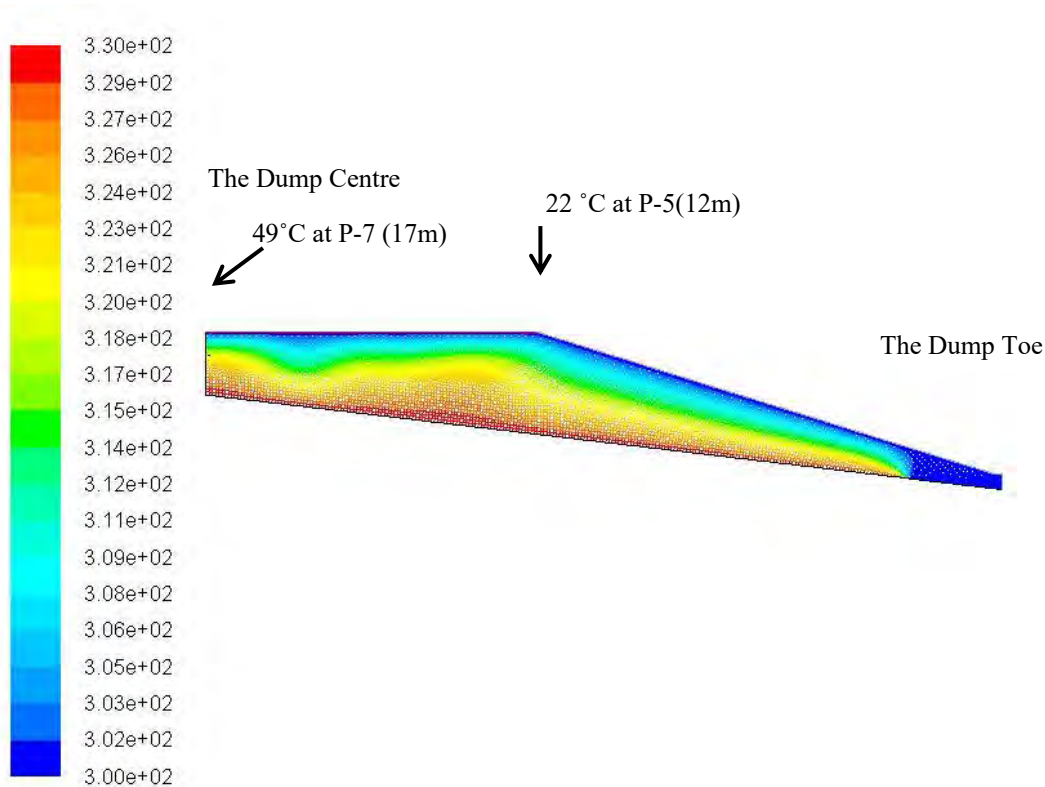


Figure 6. Temperature distribution inside the waste rock dump simulated with a uniform ARD reaction rate (temperature unit: degree K)

5.0 CONCLUDING REMARKS

This paper is a preliminary work of our on-going research on the fundamental understanding of the ARD-ML processes inside a waste rock dump. The explanations provided here should not be considered as proven conclusions at this time. But we hope our explanations generate in-depth discussions so that the understanding of the ARD-ML processes can be advanced.

6.0 ACKNOWLEDGMENT

Liu, Huang and Ma thank Dr. Bill Price, Mr. Mike O’Kane, and Dr. R. V. (Ron) Nicolson for the technical discussions on the ARD-ML processes.

7.0 REFERENCES

Chandra AP and Gerson AR, 2010, The mechanisms of pyrite oxidation and leaching: A fundamental perspective, *Surface Science Reports* **65**, 293–315.

GoldCorp Inc., 2013, 2012 Sustainability Report for Closed Sites. csr.goldcorp.com/2013

Morin KA, and Hutt NM, 2006, Case studies of costs and longevities of alkali-based water-treatment plants for ARD and minesite-drainage chemistry, and their implications on net-present-value estimates, Proceedings of the 7th International Conference on Acid Rock Drainage, St. Louis, MO, USA, March 26-30.

Morin KA, Hutt NM, and Aziz ML, 2010, Twenty-Three Years of Monitoring Minesite-Drainage Chemistry, During Operation and After Closure: The Equity Silver Minesite, British Columbia, Canada. MDAG Internet Case Study #35, www.mdag.com/case_studies/cs35.html

Morin KA, Hutt NM, and Aziz ML, 2012, Case Studies of Thousands of Water Analysis through Decades of Monitoring: Selected Observations from Three Minesites in British Columbia, Canada. IN: Proceedings of the 2012 International Conference on Acid Rock Drainage, Ottawa, Canada, May 22-24.

O’Kane M., Wilson GW, and Barbour SL, 1998, Instrumentation and Monitoring of an Engineered Soil Cover System for Mine Waste Rock, *Canadian Geotechnical Journal* **35**, 828-846.

Price WA, 2003, The Mitigation of Acid Drainage: Four Case Studies from British Columbia, Proc, Sudbury 2003, CD-ROM, P. 1121.

GEOCHEMICAL CHARACTERISATION OF MINE WASTES: DOES IT MATTER?

A.M. Robertson^A, G.A. Maddocks^A and M. Landers^A

^AARGS Environmental Pty Ltd, PO Box 3091, Sunnybank South, QLD 4109, Australia

ABSTRACT

This paper presents information on the geochemical nature of mine waste materials at a coal mine located in the Bowen Basin of Queensland. The mine was operated from 1983 using large scale open pit mining methods, which did not allow the adequate segregation of Non-Acid Forming (NAF) and Potentially Acid Forming (PAF) material types. This mining method led to a build-up of a number of significant legacy issues associated with Acid and Metalliferous Drainage (AMD) including a deficit of NAF cover material and a 20GL AMD water balance proposed to be reduced through expensive active water treatment.

In 2014 an intensive geochemical sampling and testing program was completed for mine waste materials to be generated from future mining areas as part of a review of the AMD Management Strategy used at the site. The aim was to evaluate the AMD potential of the samples and determine if changes to the material characterisation and classification process could lead to improved site mine waste and water management practices and contribute to a reduction in long-term financial and environmental liability.

On the basis of the geochemical results, a simple “traffic light” system was developed for managing mine waste materials at the site based on a number of simple parameters commonly used in Acid Base Accounting (ABA) at mining operations. The mine operator then implemented a recommendation to alter the mining process to allow identified high risk PAF waste materials, to be mined and handled by truck and shovel and placed back in the open pit void, prior to covering with less reactive NAF waste materials within a short period of time. Overall, it was expected that this process would eliminate the cover deficit and significantly reduce the AMD load emitted by high risk PAF materials in spoil storage areas.

1.0 INTRODUCTION

1.1 Geochemical Characterisation

For several decades, geochemical characterisation of mine waste materials has been established as an integral component of mine planning and a prerequisite to obtaining regulatory approval to mine in Australia. The characterisation work is normally carried out to understand the geochemical nature of mine wastes and assist with managing these materials throughout the life of mine and following closure to minimise the potential for AMD (Parker and Robertson, 1998; INAP, 2009; and COA, 2016). In more recent times, the potential for Neutral Metalliferous Drainage (NMD) and Saline Drainage (SD) has also been recognised as a significant issue at some mining operations.

Whilst it is generally possible and indeed mandatory (DME, 1995; DEHP, 2013) to develop an appropriate plan for managing mine wastes to minimise the potential for environmental harm at new mining operations in Queensland, it is more challenging at existing operations, where mining may have been completed over several decades and/or through several mining phases by different operators. There has also been a lack of recognition that historical mining practices at such operations can limit the range of potential management options available and significantly add to closure costs. Similarly, mine operators tend to assume that because a particular mine waste has been classified as NAF, it also has suitable physical properties to

be used for all of the multi-faceted tasks required for site rehabilitation (e.g. as part of multi-layered cover systems, drainage lines), when this is patently not the case at most mining operations.

1.2 AMD Potential in the Bowen Basin

Queensland's Bowen Basin contains the largest coal reserves in Australia and one of the world's largest deposits of bituminous coal. The Basin contains much of the known Permian coal resources in Queensland including virtually all of the known mineable prime coking coal. In the 2012 calendar year, Queensland produced 194.5 million tonnes of saleable coal, of which 80% was produced from 47 operating coal mines in the Bowen Basin. Whilst most of this Bowen Basin coal production is generated by large companies such as BMA, Anglo American, Peabody and Glencore, there are also a number of smaller mining companies and many exploration companies with interests in the area.

Over the past 10 years, RGS Environmental Pty Ltd (RGS) has completed mine waste geochemistry studies at over 30 planned and operating coal mines in the Bowen Basin as well as over 150 mining projects worldwide. Based upon this experience, it is clear that only certain parts of the Bowen Basin have issues related to AMD management, and most of these are well known with information existing in the public domain. For example, the presence of some materials with the potential to cause AMD has been documented at Collinsville, Kestrel, German Creek, Gregory Crinum, Middlemount and South Blackwater coal mines over the past 20 years (Robertson et al. 2015).

The geology of the Bowen Basin and the particular coal measures mined at a proposed or existing mining operation can provide an early insight into the potential for PAF materials to occur and require management. For example, Figure 1 provides a map and cross section illustrating the location of BMA (and BMC) coal mines relative to particular coal measures in the Bowen Basin (BMA, 2013). It is commonly known that coal and mine waste materials generated from particular coal measures within certain geological formations (e.g. German Creek) carry a higher risk of producing PAF materials and potentially AMD. However, it should be stressed that, in most areas in the Bowen Basin, spoil materials tend to be low sulfur with excess alkalinity (i.e. NAF), or in some cases, acid consuming.

Whilst overburden and interburden materials generated at coal mines in the Bowen Basin can occasionally present a risk of AMD at spoil storage areas, this is unusual and typically localised. Most of the geochemical action in terms of presence of sulfur (as a reactive sulfide such as pyrite or marcasite) is either within or close to particular coal seams and is therefore more closely associated with some coal and coal reject materials. In simplistic terms, a coal seam (including highly carbonaceous non-coal or uneconomic coal units) can be thought of as a 'geochemical sponge' with some potential for elevated sulfur content and possibly AMD.

Sulfur in coal is derived from two sources that include the plant materials and ambient fluids in the coal forming environment. Abundance of sulfur in coal is controlled by the depositional environment and the diagenesis of the coal seams and overlying strata. Typical low sulfur coal seams were deposited in an alluvial environment, and the peat was not influenced by seawater. The sulfur in these low-sulfur coals is derived mostly from its parent plant materials. In contrast, high sulfur coal seams are generally associated with marine strata, where sulfate in the seawater diffuses into the peat and is reduced by micro-organisms to hydrogen sulfide, elemental sulfur and polysulfides. During early diagenesis in a reducing environment, ferric iron is reduced to ferrous iron, which reacts with hydrogen sulfide to form iron monosulfide (e.g. mackinawite). Iron monosulfide is later transformed by reaction with elemental sulfur into sulfide minerals such as pyrite or marcasite.

Organic sulfur is formed by reaction of reduced sulfur species with the preacetal humic substances in the peat. Organic sulfur species formed in coals are mainly thiols, sulfides, disulfides and thiophene and its derivatives. The thiophenic fraction of organic sulfur increases with the carbon content of coals. Organic sulfur compounds formed in peat are mostly thiols and sulfides, which gradually convert to thiophenes with increasing coal maturation and essentially evolve during the history of coal formation.

The potential for AMD at a mine site in the Bowen Basin will therefore depend upon the specific coal measures being mined and the genesis and history of the coal seams. Where pyrite or marcasite minerals are present, these tend to be in a framboidal crystal structure, which reacts rapidly upon exposure to oxidising/weathering conditions to generate acid and can contribute to the risk of spontaneous combustion. Compounding this fact is that mining wastes derived from processing coal seams, such as coal rejects and tailings materials, generally have very little, if any, ANC and can generate low pH values very quickly. In general, overburden and interburden materials, which report as spoil at coal mines in the Bowen Basin, have very little potential for AMD (as a bulk material), and in fact some of these materials have acid neutralising characteristics. At some mining operations, the risk from PAF coal reject and tailings materials is managed by liming, compacting and co-disposing of these materials in cells within acid neutralising spoil materials. The volume of PAF materials is quite small compared to the spoil material and the risk of AMD is therefore reduced.

Overall the risk of AMD from coal mining operations in the Bowen Basin is limited to specific materials from those mines located in geological formations with some potential for sulfides to occur in elevated concentrations, mainly associated with specific coal seams. Occasionally, carbonaceous materials from minor uneconomic seams that report to spoil storage areas can be a potential source of AMD; however these generally do not require selective handling as they represent small volumes of materials compared to large volumes of spoil materials, which often have excess neutralising capacity. This is also true of coal reject materials, which can typically represent less than 5 % of the total mine waste materials generated at a particular mining operation.

In the Bowen Basin, PAF coal reject and tailing materials typically report to above ground storage facilities until such time as some capacity becomes available in mined out final void areas to dispose of such materials. Tailing material disposed into an above-ground Tailing Storage Facility (TSF) is rarely relocated into a mined-out pit, although this has happened at one BMA operation, and usually remains within the above-ground TSF in perpetuity. Again there are competing interests at mining operations, and the potential for sterilisation of remnant coal resources can be a key factor in determining when final void areas actually become available to accommodate PAF materials. For example, mine planners may want to maintain a potential future access route to underground resources from a final void, should the market price for coal increase and coal extraction from a particular seam become a more attractive economic proposition. It is also a regulatory requirement to avoid or minimise coal resource sterilisation.

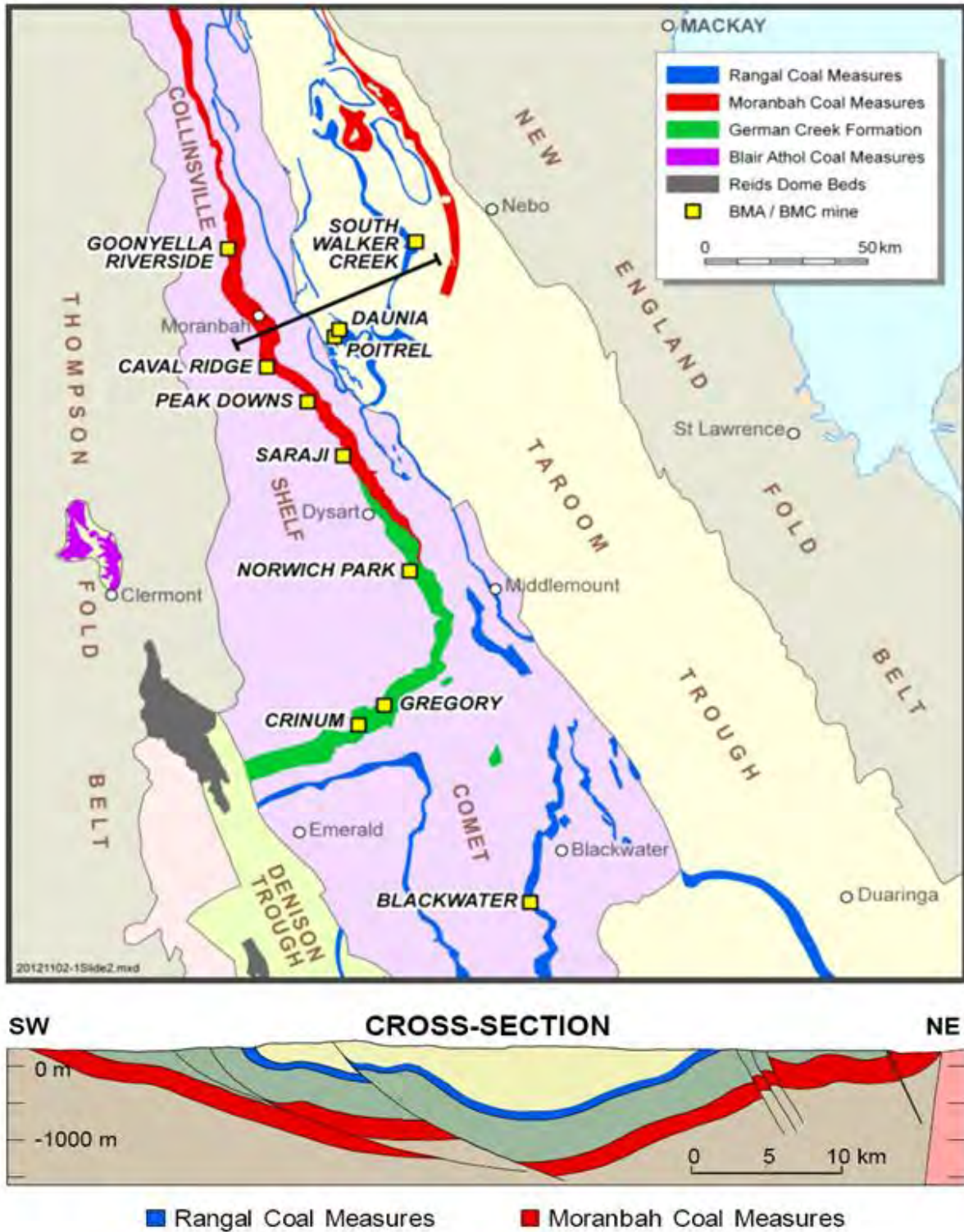


Fig 1. Location of BMA [and BMC] mining operations in the Bowen Basin.

Source: BMA (2013)

2.0 CASE STUDY

2.1 Overview

This paper presents a case study for a coal mining operation located in the Northern Bowen Basin of Queensland, which has been operated by various owners from 1983, initially using underground mining methods, and then large scale open pit mining methods. The mine is currently operational and is likely to remain in operation for several decades, depending on the market price of coal. Historically, the large scale open pit mining methods at the site have not incorporated adequate characterisation of mine waste materials or adequate segregation of materials classified as NAF and PAF. This has led to a build-up of a number of significant legacy issues associated with AMD, including a deficit of NAF cover material and a 20GL AMD pit water balance proposed by the mine owners to be reduced through expensive active water treatment.

2.2 Geochemical Characterisation Program

In 2014 an intensive geochemical sampling and testing program was completed for mine waste materials to be generated from future mining areas as part of a review of the AMD Management Strategy used at the case study site. The aim was to evaluate the AMD potential of the samples and determine if changes to the material characterisation and classification process could lead to improved site mine waste and water management practices and contribute to a reduction in long-term financial and environmental liability.

The geochemical assessment included geochemical characterisation of 1,493 samples of overburden, interburden and basement samples from within pit shells that were expected to be developed as part of an extended life of mine plan. The aim was to evaluate the AMD potential of the samples, and determine if changes could be made to the AMD characterisation and classification process that could lead to opportunities for improvement to mine waste and water management practices and contribute to a reduction in long-term financial and environmental liability at the site.

2.3 Summary of Findings

The geochemical assessment program demonstrated that most of the high risk (high capacity) PAF overburden and interburden materials were located relatively close to particular coal seams in the stratigraphic profile. In addition, much of the material with relatively low sulfur content and a low risk of acid generation had previously been incorrectly classified as PAF (due to limitations of the standard NAG test for classifying coal mine wastes (ACARP, 2008; Stewart, 2009), or should have been classified as PAF (low risk). Extensive static and kinetic geochemical testing showed that most of the low risk material could either be reclassified as NAF or could be remediated using a relatively small amount of agricultural limestone. The outcome of using this approach was to essentially convert a deficit of NAF cover material into a positive material balance.

On the basis of the geochemical results, a simple “traffic light” system (Red, Amber and Green) was developed for managing mine waste materials at the site based on a number of simple parameters commonly used in Acid Base Accounting (ABA) at mining operations. Whilst the ABA method proved to be the most reliable approach to classify spoil materials at the site, it relied upon off-site laboratory analysis which added costs and time delays. For fresh drill core/drill chip material, it was found that a total sulfur value could be used as a screening tool to classify waste materials. The total sulfur screening (cut-off) concentrations were carefully selected and calibrated through a detailed review of the geochemical dataset described in Section 2.2.

In late 2015, the site successfully trialed a rapid and inexpensive material classification system using a hand-held X-ray fluorescence (XRF) field instrument to determine the total sulfur content of a large number of samples in a short period of time. The trials demonstrated that the field XRF instrument was suitable for this task and could be used to rapidly differentiate between material types.

2.4 Material Management

The mine operator has now implemented a recommendation to alter the mining process to allow identified high risk PAF waste materials, to be mined and handled by truck and shovel and placed back in the open pit void, prior to covering with less reactive waste materials within a relatively short period of time. The new mining process is a significant improvement on the existing mining and mine waste placement method, which involved drag lines and very little segregation and selective handling of spoil materials.

Adoption of the improved material characterisation and segregation process has eliminated the cover deficit and has the potential to significantly reduce the AMD load emitted by high risk PAF materials in spoil storage areas. An additional benefit of the changed material management process has been to reduce the risk and occurrence of spontaneous combustion in spoil storage areas, which had previously been an ongoing issue at the mine.

3.0 CONCLUSIONS

A case study has been presented illustrating the importance of appropriate geochemical characterisation and management of mine waste materials throughout the life of mine. The case study also highlights some of the issues that can arise if this process does not occur. The selected mine has been operating since 1983, at which time the potential for AMD was recognised, but the importance of recommendations regarding potential material management options were not recognised and implemented by various mine operators. This has resulted in a legacy of insufficient cover material for PAF wastes and a 20GL AMD water balance, which is proposed to be reduced through expensive active water treatment.

In more recent times, adoption of a more appropriate geochemical characterisation program and a significant change to the mining and waste material management process has resulted in a surplus of NAF cover material, potentially reduced the AMD load from PAF materials, and reduced the risk and occurrence of spontaneous combustion in spoil storage areas.

4.0 REFERENCES

ACARP (2008). *Development of ARD Assessment for Coal Process Wastes*. ACARP Project C15034. Report prepared by Environmental Geochemistry International and Levay and Co. Environmental Services, ACeSSS University of South Australia, July 2008.

BMA (2013). BHP Billiton Coal Briefing and Queensland Coal Site Tour, May 2013. Presentation from Stephen Dumble, Asset President, BMA. 30 May 2013. Date accessed: 6 February 2014. Source: http://www.bhpbilliton.com/home/investors/reports/Documents/2013/130530_Coal_BriefingDay2Presentation.pdf.

COA (2016) Leading practice sustainable development program for the mining industry. Preventing Acid and Metalliferous Drainage. Published by the Commonwealth of Australia (COA). September.

DEHP (2013). *Application Requirements for Activities with Impacts to Land Guideline*. Queensland Department of Environment and Heritage Protection.

DME (1995). Draft Technical Guidelines for the Environmental Management of Exploration and Mining in Queensland, Technical Guideline – Assessment and Management of Acid Drainage. Queensland Department of Minerals and Energy (DME). January.

INAP (2009) Global Acid Rock Drainage Guide. Document prepared by Golder Associates on behalf of the International Network on Acid Prevention (INAP) (<http://www.inap.com.au/>).

Parker, G. and Robertson, A.M. Acid Drainage. Occasional paper published by the Australian Minerals and Energy Environment Foundation (AMEEF), November, 1999, Melbourne, Victoria, Australia.

Robertson A.M., Maddocks G.A. and Swane I. (2015). Understanding mine waste geochemistry in the Bowen Basin: from exploration to mine closure. In proceedings of the Bowen Basin Symposium 2015 – Bowen Basin and Beyond. Geological Society of Australia Inc. Coal Geology Group and the Bowen Basin Geologists Group, Ed. Beeston J.W. Brisbane, Qld 6-9 October, pp 473-480.

Stewart W., Schumann R., Miller S. and Smart R. (2009). *Development of Prediction Methods for ARD Assessment of Coal Process Wastes*. In Proceedings of Securing the Future and 8th International Conference on Acid Rock Drainage (ICARD), June 22-26, Skelleftea, Sweden.

DESIGNING TAILINGS AND WASTE ROCK SYSTEMS FOR CHEMICAL AND PHYSICAL STABILITY

G.W. Wilson^A, B. Wickland^B and B. Weeks^B

^ADepartment of Civil & Environmental Engineering, University of Alberta, Edmonton, Canada

^BGolder Associates, #200 - 2920 Virtual Way, Vancouver V5M 0C4, Canada

ABSTRACT

The breach in the perimeter embankment at the Mount Polley Tailings Storage Facility, British Columbia, has had substantial impact on the Canadian mining industry. The incident has given rise to comprehensive recommendations for best available tailings technologies (BAT) based on principles such as the elimination of surface water from impoundments with the promotion of unsaturated conditions in the tailings through drainage provisions. The implementation of such best available technologies for the physical stability (BAT-PS) of tailings impoundments competes directly with the best available technologies for the chemical stability (BAT-CS) of reactive tailings that may produce acid and metalliferous drainage. Recent developments in mine waste management directed at achieving both BAT-CS and BAT-PS are discussed in the present paper.

1.0 INTRODUCTION

On August 4, 2014, a breach occurred within the perimeter embankment of the Mount Polley Tailings Storage Facility in British Columbia. The loss of containment was sudden and occurred without warning. The British Columbia Ministry of Energy and Mines established an Independent Expert Engineering Investigation and Review Panel (IEEIRP) to investigate the breach. The panel released its report on January 30, 2015.

As a result of its investigation at Mount Polley, the IEEIRP recommended the implementation of best available tailings technologies (BAT). In terms of risk-based dam safety practice, “the panel does not accept the concept of a tolerable failure rate for tailings dams” and advocated the implementation of the best available tailings technology based on the BAT principles outlined as follows:

- 1) eliminate surface water from the impoundment,
- 2) promote unsaturated conditions in the tailings with drainage provisions,
- 3) achieve dilatant conditions throughout the tailings deposit by compaction.

The implementation of such best available technologies for the physical stability (BAT-PS) of tailings impoundments competes directly with the best available technologies for the chemical stability (BAT-CS) of reactive tailings that may produce acid and metalliferous drainage. While a water cover over potentially acid generating waste is considered best practice to prevent or limit acid generation, ponds and water covers introduce a risk related to the potential for release. Loss of the pond can lead to damage and destruction downstream of the mine waste facility and is often associated with loss of tailings.

Recent developments in mine waste management directed at achieving both BAT-CS and BAT-PS are discussed in the present paper. Technologies examined include tailings dewatering for surface deposition of thickened and paste tailings, and an emerging technology for the co-disposal of tailings and waste rock. Examples at sites where the deposition of paste

and thickened tailings have demonstrated benefits in achieving both BAT-CS and BAT-PS are reviewed. Finally, a relatively new co-disposal technique where tailings and waste rock are blended to form a material known as paste rock is described.

2.0 PHYSICAL AND CHEMICAL STABILITY OF TAILINGS

The implementation of the BAT principles creates challenges current best practice. In general, BAT principles for physical stability (BAT-PS) directly conflict with BAT for chemical stability (BAT-CS). The implementation of the BAT-PS principles in reactive tailings is to dry and drain, and may result in increased potential for acid rock drainage and metal leaching (ARD/ML). In contrast, a key strategy and design principle for the prevention of ARD for tailings is to maintain full saturation within the tailings profile. Figure 1 illustrates the preferred solution of water covers for the prevention and control of ARD. Water covers are routinely employed as a preferred strategy for the long-term closure of reactive tailings worldwide as outlined by the global acid rock drainage (GARD) guide (INAP, 2014).

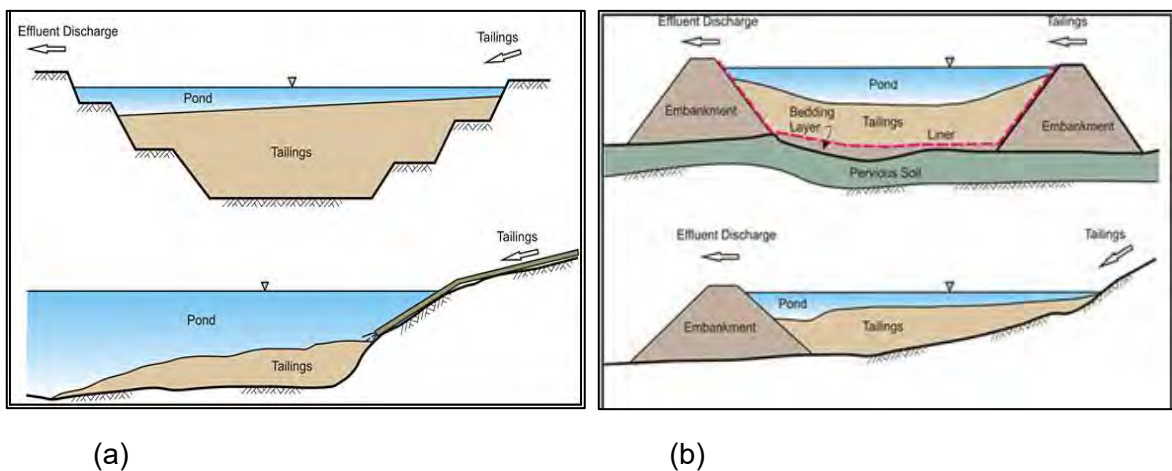


Fig. 1. Sub-aqueous disposal for chemical stability (modified from INAP, 2014)

The examples shown in Figure 1a are ideal closure configurations for sub-aqueous disposal since the tailings and water cover do not require above ground containment structures and both chemical and physical stability (i.e. BAT-CS and BAT-PS) are completely satisfied. On the contrary, the examples shown in Figure 1b, while satisfying chemical stability (BAT-CS), the condition for long-term physical stability (BAT-PS) can be questioned. The required confinement of a water cover above the surrounding topography is a permanent geo-hazard that must be maintained into perpetuity. Tailings dams that require regular inspections and maintenance eliminate the possibility of walk away at closure. In fact, strict application of a risk-based approach dictates the probability of failure over longer time scales approaching is arguably 100%.

3.0 DE-WATERED TAILINGS

The IEEIRP stated that the use of filtered tailings could be used to satisfy the implementation of the BAT principles for the surface storage of tailings. The panel points out that when properly designed and constructed, filtered tailings can satisfy each of the BAT components listed above. Greens Creek mine in Alaska, shown in Figure 2a, is used an example where “dry stack tailings” has been successfully constructed in a wet climate that is similar to numerous sites in the province of British Columbia.



(a)



(b)



(c)



(d)

Fig. 2. Examples of de-watered tailing (a) filtered tailings, (b) and (c) paste tailings, (c) thickened tailings

The use of filtered tailings at Green Creek clearly eliminates the surface water pond from the waste facility, promotes unsaturated conditions in the tailings with drainage provisions, and achieves dilatant conditions throughout the tailings deposit by the use of mechanical compaction. However, the de-watering of tailings to produce an acceptable filtered product can be expensive, especially in the case of pressure filtration. Furthermore, the implementation of filtering tailings at sites with high tonnages is also very challenging. Some of the BAT principles for physical stability can be achieved with much less de-watering effort for paste and thickened tailings deposits. Figures 2b, c and d show examples of paste and thickened tailings deposits. The greatest benefit of paste and thickened tailings is the elimination of the threat and impact of catastrophic dam failure associated with the loss of the water pond normally found on conventional tailings impoundments.

The primary concern with all de-watered tailings impoundments is that they are positive topographic structures that rise above the surrounding terrain and water tables. Consequently, they become unsaturated mined earth structures as a result of drainage to the foundation and water losses to the atmosphere due to evaporative drying, particularly in arid climates. Figure 3 shows the surface of a thickened tailings deposit with a layer of unoxidized tailings overlying oxidized tailings. The thickened tailings profile is clearly unsaturated, and the lower layer of reactive tailings has oxidized with the ingress of atmospheric oxygen. The upper unoxidized layer of fresh thickened tailings can be expected to oxidize with time in the same way as the previous lower lift of acid-forming tailings. In summary, the BAT-PS principles for the elimination of surface water from the impoundment and the promotion of unsaturated conditions in the tailings can be seen to directly contradict the general principles laid out in the GARD guide (INAP 2014) for the prevention of ARD and metalliferous drainage or BAT-CS. Clearly, mine waste professionals are left with a serious and competing conflict in their design criteria.



Fig. 3. Thickened tailings with unoxidized layer overlying oxidized tailings

A key component for the design of de-watered tailings deposits is the degree of water saturation within the tailings profile. Tailings profiles with water saturation levels greater than 85% are considered resistant to oxygen diffusion and subsequent ARD. Figure 4 shows the effective diffusion coefficient of oxygen (D_e) as a function of the degree of saturation (S). The figure shows that D_e decreases by several orders of magnitude as the degree of saturation increases from zero to 100%. Furthermore, the decrease in D_e becomes most significant in the range of 85% saturation, thus maintaining S at 85% or greater has become a target or criteria in design of mitigative measures designed to control or prevent ARD in potentially acid forming (PAF) mine waste materials.

Satisfying the condition for physical stability (BAT-PS) in tailings is controlled in part by the degree of saturation. Saturated tailings are the most susceptible to liquefaction, while dry tailings are non-liquefiable. While saturated tailings are most resistant to oxygen diffusion that drives ARD (BAT-CS), saturated tailings are the worst in terms of physical stability (BAT-PS). However, it is generally accepted that tailings profiles with water saturation levels less than 85% are considered resistant to liquefaction. A degree of water saturation equal to 85% marks a key design target or metric for both BAT-CS and BAT-PS, albeit in an inverted or overturned

fashion. In summary, successful implementation of the BAT principles for both PS and CS demands insight and knowledge to the field of unsaturated soil mechanics.

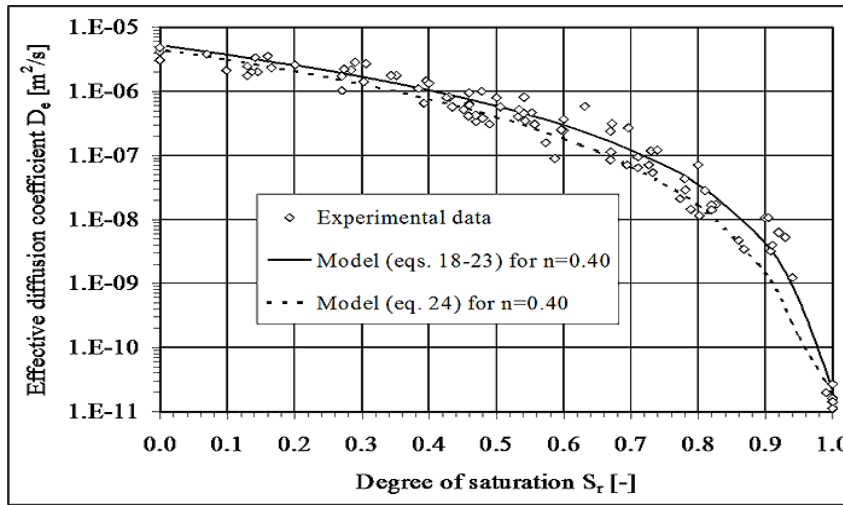


Fig. 4. Oxygen diffusion coefficient versus degree of saturation (source: Aubertin, 2005)

The degree of water saturation equal to 85% appears to be a key target or “Sweet Spot” so to speak for achieving both chemical and physical stability in reactive tailings. Figure 5 shows a typical soil-water characteristic curve (SWCC) for tailings. The SWCC controls water saturation as a function of matric suction. A value of $S = 85\%$ generally corresponds to a very important point on the SWCC known as the air entry value (AEV). The AEV corresponds to the value of matric suction at which the largest pores drain and air enters to matrix of the tailings (i.e. bubbles). It is important to note that while air bubbles exist in the matrix, the air phase is not continuous. This explains why the diffusion coefficient for oxygen D_e decreases dramatically at $S = 85\%$, corresponding to the AEV. In a similar way, the development of air bubbles at the AEV reduces the potential for liquefaction since excess porewater pressures can be dissipated with the flow of water to the air-filled voids in the largest pores of the tailings matrix. In summary, the AEV corresponds to an optimum point on the SWCC for the simultaneous minimization of both oxygen diffusion in reactive tailings and porewater pressure generation in liquefiable tailings.

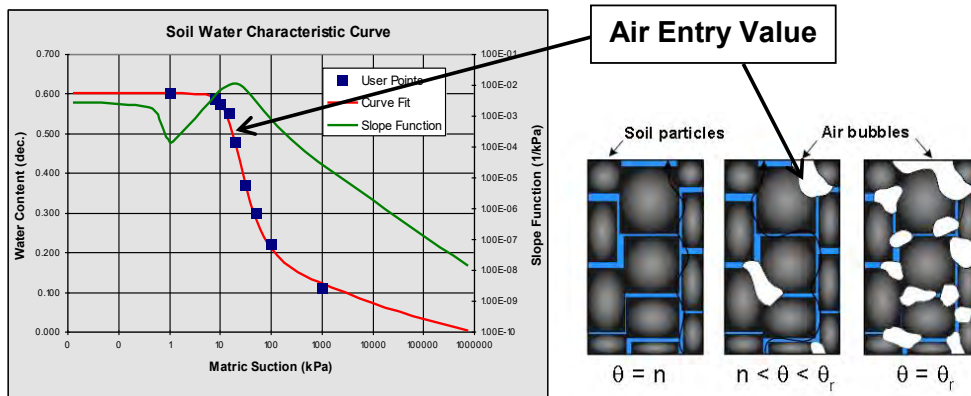


Fig. 5. Typical soil-water characteristic curve for tailings

Controlling the saturation profile demands coupling of the net infiltration rate with hydraulic properties of the tailings that are controlled by the SWCC, AEV and unsaturated permeability function of the tailings. In general, under downward drainage with a hydraulic gradient of unity, the long-term steady state net percolation rate shown in Figure 6 entering the surface of the tailings profile must be equal to the unsaturated hydraulic conductivity of the tailings as defined by the SWCC and AEV. Furthermore, the control of infiltration rates is based on coupling hydraulic properties of the surface of the tailings with the microclimatic conditions and cover system design for closure to provide infiltrative fluxes that optimize unsaturated flow conditions in the tailings.

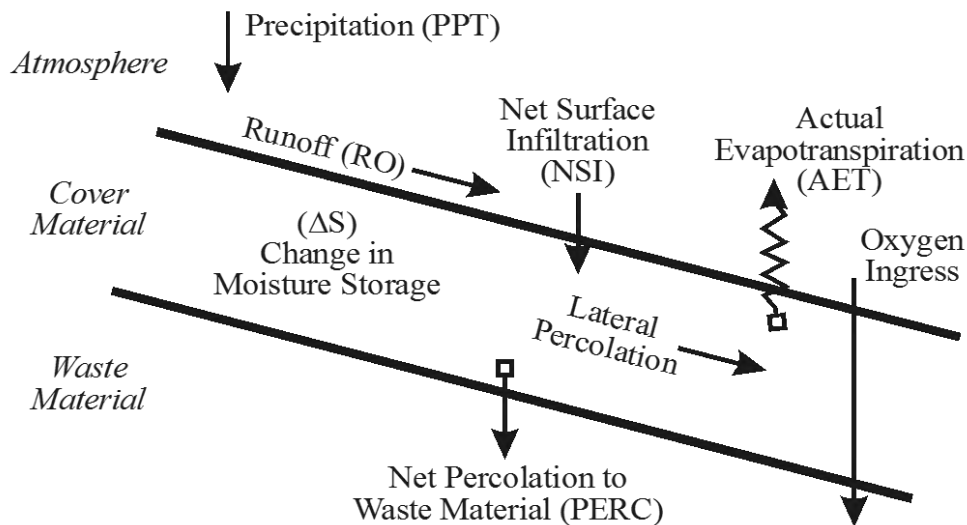


Fig. 6. Components of the surface water budget and net percolation for tailings (Source: MEND)

4.0 EXAMPLE APPLICATIONS FOR DEWATERED TAILINGS

Two example applications for de-watered tailings are described here. The first case is for paste tailings at Neves Corvo mine in Portugal and the second example is for thickened tailings at Musselwhite mine in eastern Canada.

4.1 Paste Tailings at Neves Corvo

Verburg et al. (2009) and Junqueira et al. (2009) describe the application of paste tailings for surface disposal at Neves Corvo mine in detail. Neves Corvo has produced pyritic tailings that have a high acid generation potential since 1988. Sub-aqueous disposal of the tailings was initially adopted with a water cover to prevent acid generation. The site is located in the Mediterranean climate of southern Portugal. Potential evaporation in this semi-arid climate is about three times greater than the annual precipitation, and the use of a permanent water cover for long-term closure is not a sustainable option. More importantly, there was a local loss of social acceptance to permanent water covers due to the tailings dam failure at the nearby Los Frailes mine.

In response to the requirement for a new closure design, the surface water cover was eliminated with the conversion from sub-aqueous slurry tailings discharge to sub-aerial paste

deposition. In addition, the paste tailings will be closed with a dry cover. While elimination of the water cover satisfies the requirement for physical stability (BAT-PS), the cover must prevent the paste from desaturating and limit oxygen diffusion to the reactive tailings profile for chemical stability (BAT-CS). The installation of a dry cover to evaluate the proposed cover system is shown in Figure 7.



Fig. 7. Dry cover construction on paste tailings at Neves Corvo

Performance of various dry cover systems was modelled by Junqueira et al. (2009). Desaturation to values of 'S' less than 85% within the paste profile could occur in the arid climate (i.e. evapotranspiration > precipitation) if long-term recharge for vertical seepage to the foundation of the tailings is not sufficient. Junqueira et al. (2009) showed that the long-term saturation profile of the paste was strongly controlled by the net infiltration at the surface of the paste tailings (i.e. net percolation from the cover). Figures 8a and b show the saturation profiles in paste over a period of 100 years given infiltration rates of 25 mm/yr and 64 mm/yr, respectively corresponding to two different cover designs. The results demonstrate that an infiltration rate of 25 mm/yr is not adequate to maintain a degree of saturation greater than 85%, while an infiltration rate of 64 mm/yr exceeds the requirement.

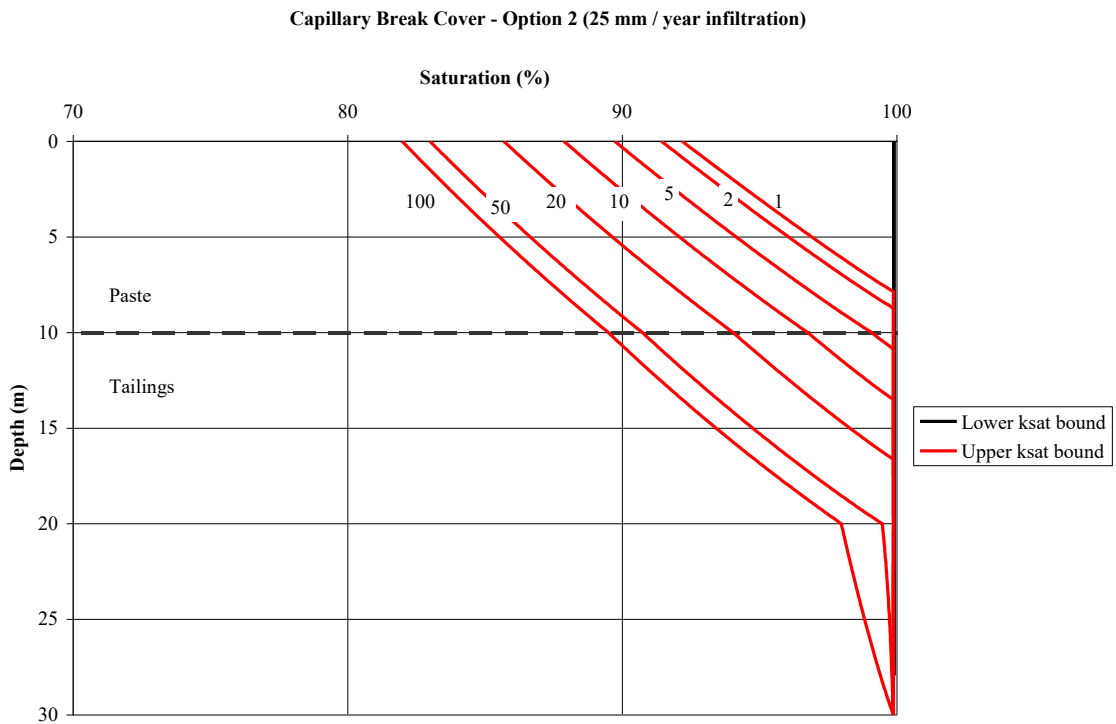


Fig. 8a. Degree of saturation versus depth in the paste tailings at Neves Corvo with net percolation equal to 25 mm/yr (Source: Junqueira et al, 2009)

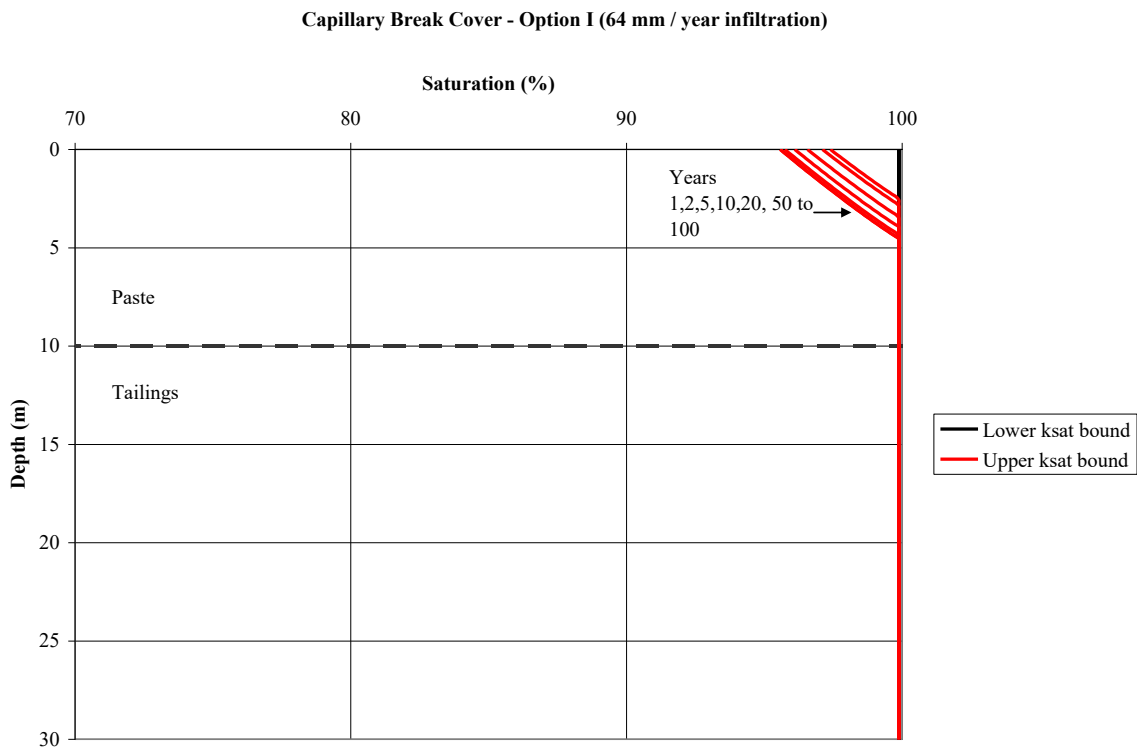


Fig. 8b. Degree of saturation versus depth in the paste tailings at Neves Corvo with net percolation equal to 64 mm/yr (Source: Junqueira et al., 2009)

In conclusion, converting to paste tailings at the Neves Corvo mine achieved vastly improved physical stability (BAT-PS) with the elimination of the water cover. In addition, the water-retaining characteristics and high AEV of the non-segregated paste tailings provides high saturation to prevent oxygen ingress to the tailings with a low flux soil cover, thus satisfying chemical stability (BAT-CS). Removing the need for a permanent water cover provides a sustainable long-term closure solution for the highly reactive tailings.

4.2 Thickened Tailings at Musselwhite

The disposal of thickened tailings at the Musselwhite mine in northern Ontario, Canada, has been described in detail by Kam et al., (2011). Elimination of the surface pond has been achieved with the conversion from slurry discharge to thickened tailings disposal in 2010. The alternative to convert to thickened tailings primarily selected to increase the capacity of the existing tailings management facility (TMF). While conversion to thickened tailings was found to be the most cost-effective option for maximizing storage capacity within the existing footprint TMF, the use of thickened tailings eliminated the pond associated with slurry discharge and thus reduced the risk associate with potential failure of the dam.

Figure 9a shows the discharge of non-segregating thickened tailings. Figure 9b shows upstream lifts with berms constructed using waste rock. The existing pond was pushed off the tailings impoundment with the advancing lifts of rapidly de-watering thickened tailings. Thin lift deposition provides the release of water through evaporation and drainage to produce an increase in the density of the deposit. An important additional benefit for closure achieved with the conversion to thickened tailings at Musselwhite mine was eradicating the requirement for a water cover to prevent to ARD. The non-segregating nature of the thickened tailings results in a uniform texture and hydraulic properties throughout the impoundment. Thickened tailings have a low hydraulic conductivity and high AEV (high water retention) compared to the segregated beaches formed in conventional slurry deposits. The non-segregating characteristics of thickened tailings leads to a higher degree of water saturation in the tailings profile and a reduction in oxygen diffusion and associated acid generation, results that previously would have required a water cover. Should it be found that the degree of water saturation is less than 85% in the upper zones of the final lifts of the thickened tailings stack, the tailings can be desulphurised. Cash et al (2012) demonstrate the successful application of desulphurised tailings as a cover material.



Fig. 9a. Thickened tailings deposition at Musselwhite Mine, Ontario



Fig. 9b. Thickened tailings deposition at Musselwhite Mine, Ontario

In summary, the conversion from conventional slurry tailings to thickened tailings at Musselwhite mine dramatically improved physical stability (BAT-PS) as well as chemical stability (BAT-CS). Elimination of a water cover following closure removes a permanent geo-hazard, reduces the potential for catastrophic dam failure, and minimizes the needs for long-term monitoring.

5.0 A NEW CO-DISPOSAL TECHNIQUE – PASTE ROCK

The co-disposal of de-watered tailings and waste rock to form an engineered mixture provides the opportunity to design mine waste repositories that achieve both physical (BAT-PS) and chemical stability (BAT-CS). Wickland et al. (2006) describe the design and evaluation of mixtures of waste rock and tailings. The method of co-disposal described here is called 'paste rock', which is a mixture of waste rock and tailings blended to produce an engineered material with superior physical and hydraulic properties for the construction of mine waste repositories without a water pond. This new material has a high density, high shear strength, low compressibility, low hydraulic conductivity, and high AEV. These properties can be used to minimize oxygen fluxes, water seepage rates and the desaturation of mine waste deposits in order to prevent the oxidation and metal leaching of sulphide bearing materials. The higher density of paste rock compared to either tailings or waste rock reduces the total volume of waste and thus reduces surface area requirements for repositories.

Wickland (2006) describes the hydraulic, compressibility and consolidation properties of mixtures of waste rock and tailings that were produced and tested at Porgera mine. Figure 10 shows an example of the paste rock material produced at Porgera mine. Wickland (2006) constructed a meso-scale column experiment using four 1 m diameter by 6 m high columns. The first column contained pure waste rock as a control, and the remaining columns were filled with paste rock with mixture ratios of 5:1, 6:1 and 7:1 (rock to tailings by dry mass). The tailings were thickened to a solids content of 42% for blending with the waste rock. Vibrating wire and pneumatic piezometers were installed during placement of the paste rock in the columns to measure porewater pressures along with tensiometers to measure matric suction. Magnetic sensors were also installed to measure settlement. A constant head drain was established at the base of each column to monitor drainage rates.



Fig. 10. Example of paste rock at Porgera Mine

The experimental results obtained from the meso-scale columns exhibited the paste rock to have excellent properties with respect to chemical (BAT-CS) and physical stability (BAT-PS). The paste rock had a high density and low compressibility similar to waste rock, and a low water permeability, high AEV and high water saturation characteristics similar to tailings.

Wilson et al. (2008) describes the design and construction of field scale lysimeters at Copper Cliff mine in Ontario, Canada, used to evaluate the performance of cover systems for the closure of PAF (potentially acid forming) tailings. The study investigated the potential of blending tailings with waste rock and slag to produce a suitable material for a barrier cover system. Blending ratios of waste rock, slag and tailings were designated with numbers such as 1:1:2 to indicate 1 unit of waste rock, 1 unit of slag and 2 units of tailings based on dry weight. Blend 1:1:2 was found to produce a well graded material with a particle size distribution similar to Equity till as described by Wilson et al. (1997), which was the natural glacial moraine used for constructing the cover on the waste rock dump to control ARD at Equity Silver mine in British Columbia.

Five 15 m x 15 m field lysimeters were constructed to test the use of the paste rock for the construction of barrier-type cover systems. The field lysimeters measured net infiltration and drainage rates for each tailings cover using various paste rock blends and layer thickness. The capacity of each paste rock cover to maintain high saturation for the minimisation of oxygen diffusion was also measured. Each lysimeter was constructed with a total depth of 2.5

m and lined with high density polyethylene graded to a collection sump for the measurement of vertical seepage due to infiltration. Approximately 1 m of coarse sand tailings were placed in each lysimeter followed by the placement of the paste rock cover systems and final vegetated surfaces.

The paste rock covers were observed to be highly resistant to cracking, which was attributed to the high density (typically in the range of 2,000 to 2,200 kg/m³) and low compressibility established by the rock-dominated matrix of the material. Drainage rates measured from the lysimeters demonstrated that the paste rock covers dramatically reduced infiltration. In summary, the uncovered tailings profiles produced 55% of the total annual precipitation as net infiltration (500 mm) compared to the paste rock covers that produced between 1 % and 16% of the total annual precipitation as net infiltration. Furthermore, in situ sampling and tensiometer measurements also showed the paste rock covers maintained high saturation at all times and will minimize oxygen diffusion rates and ARD. In summary, paste rock material appears to be a new material that will satisfy the requirements for both chemical stability (BAT-CS) and physical stability (BAT-PS).

6.0 SUMMARY AND CONCLUSIONS

The incident at Mount Polley has had significant impact on the Canadian mining industry. The IEEIRP report for Mount Polley recommends the use of BAT principles to improve the physical stability (BAT-PS) of tailings. The criteria for physical stability (BAT-PS) compete with the principles for chemical stability (BAT-CS). The use of de-watered thickened tailings and paste tailings to satisfy both BAT-PS and BAT-CS was discussed. Two case studies were reviewed for the de-watering of tailings to produce thickened tailings at Musselwhite mine and the use of paste tailings at Neves Corvo mine. Both examples illustrated the potential for de-watered tailings to eliminate conventional tailings ponds and/or the need for water covers. Removal of a permanent post-closure pond is a clear benefit for long-term physical stability, reducing the risk of catastrophic dam failure, with resulting reductions in the need for risk control activities such as post-closure monitoring. De-watering may be used to improve physical stability (BAT-PS), while still maintaining chemical stability (BAT-CS) for the control of acid generation.

Field trials completed for paste rock at the Porgera and Copper Cliff mines demonstrated that the blending of tailings with waste rock may be the optimum approach in terms of designing mine waste systems that achieve both physical BAT-PS and chemical BAT-CS stability.

7.0 REFERENCES

Journal article

Wickland, B.E., Wilson, G.W., Wijewickreme, D., and Klein B. 2006. Design and Evaluation of Mixtures of Mine Waste Rock and Tailings. Canadian Geotechnical Journal. Vol 43(9) pp. 928-945.

Book

Wickland, B. 2006. Volume Change and Permeability of Mixtures of Waste Rock and Fine Tailings. Ph.D. Thesis. University of British Columbia.

Published Proceedings

Cash, A.E., Urrutia, P., Wilson, G.W., Robertson, J. and Turgeon, M.H. 2012. A 2011 Update for the Single-Layer Desulphurised Tailings Cover Completed in 1999 at Detour Gold.

Proceedings Mine Closure 2012. Australian Centre for Geomechanics, Perth, ISBN 978-0-9870937-0-7.

Junqueira, F.F., Wilson, G.W., and Oliveira, M. 2009. Surface Paste Disposal of High-Sulfide Tailings at the Neves Corvo Mine in Portugal. Part 1: Estimation of Tailings Desaturation and Implications on ARD Generation. Proceedings of the Eighth International Conference on Acid Rock Drainage, June 22-26, 2009, Skellefteå, Sweden.

Kam, S., Girard, J., Hmidi, N., Mao, Y., and Longo S. 2011. Thickened Tailings Disposal at Musselwhite Mine. Proceedings 14th International Seminar on Paste and Thickened Tailings. Australian Centre for Geomechanics, Perth, 5-7 April, ISBN 978-0-9806154-3-2, pp 225 -236.

Verburg, R., Ross, C. and Oliveira, M. 2009. Surface Paste Disposal of High-Sulfide Tailings at the Neves Corvo Mine in Portugal. Part 2: Field Trials, Cover Performance Monitoring and Impact Assessment. Proceedings of the Eighth International Conference on Acid Rock Drainage, June 22-26, 2009, Skellefteå, Sweden.

Wilson, G.W., Wickland. B., Miskolczi, J. 2008. Design and Performance of Paste Rock Systems for Mine Waste Management. Proceedings of Rock Dumps Stockpiles and Heap Leach Pads, Australian Center of Geomechanics, Perth, Australia, March 5 - 7.

Wilson, G.W., Newman, L.L., Barbour, S.L., O'Kane, M.A., and Swanson, D.A., 1997. Show Case Paper, The Cover Research Program at Equity Silver Mine Ltd., Proceedings of the Fourth International Conference on Acid Rock Drainage, Vancouver, Canada - June 6.

Report/Bulletin

Aubertin, M. 2005. Coefficient of diffusion versus degree of saturation for saturated porous media. Figure from unpublished presentation, reproduced in *Global Acid Rock Drainage Guide*. Chapter 6. (INAP [International Network for Acid Prevention] 2014. http://www.gardguide.com/index.php?title=Chapter_6).

INAP (International Network for Acid Prevention) 2014. Global Acid Rock Drainage Guide Rev 1. www.gardguide.com.

AN INTEGRATED APPROACH TO CLOSURE OF LANDFORMS CONTAINING POTENTIALLY ACID FORMING WASTE ROCK IN NORTH-WEST QUEENSLAND

A. Sexton^A, A. Butler^B, J. Chapman^C and T. Anderson^B

^AErnest Henry Mine (Glencore Copper Assets), Cloncurry, QLD, Australia

^BNRA Environmental Consultants, Cairns, QLD, Australia

^CSRK Consulting, Brisbane, QLD, Australia

ABSTRACT

Mount Margaret Mine (MMM) is located near Cloncurry in NW Queensland. Copper/gold/magnetite ore was mined from several open pits and processed at Ernest Henry Mine (EHM). With no tailings dam, the main residual risk at MMM is the potential for off-site migration of acid mine drainage (AMD) or neutral mine drainage (NMD) from potentially acid forming (PAF) rock placed in waste rock dumps (WRDs).

The potential long-term performance of cover designs was a critical consideration for closure. Any cover, however well designed and engineered, may allow percolation of rainfall and the generation of poor quality seepage that has the potential to impact the receiving environment. The approach described in this paper integrated the geochemical, hydrogeological, hydrological, engineering, and revegetation aspects of closure into WRD design for E1 lease areas at MMM.

1.0 PROJECT DESCRIPTION

Mount Margaret Mine (MMM) is a large-scale copper project located in the Mount Isa mineral district in north-west Queensland. It is owned and operated by Mount Margaret Mining Pty Ltd (a Glencore Company) (MMMPL). The MMM project is located north-east of Cloncurry. Copper/gold/magnetite ore was mined from several small pits at the E1 and Monakoff mining leases, and then transported to the adjacent Ernest Henry Mine (EHM) for processing via a crush-grind-float-dewater processing plant. The MMM project commenced construction and mining in 2012, and was placed into care and maintenance in 2014. This paper describes closure planning at the E1 lease areas.

Waste rock from the E1 North (E1N) open-pit was deposited in a single dedicated waste rock dump (WRD) located immediately north of the E1N pit (the northern WRD or NWRD). To the east, the E1 East (E1E) pit was excavated through overburden material only when mining ceased.

The region has a wet-dry monsoonal climate with most rainfall occurring in the summer months, as shown in Figure 1. The mean annual precipitation (MAP) for the MMM area is 452 mm, and the maximum is 1,330 mm. MMM is located in an area locally dominated by 'black soil plains' and unimproved native Mitchell Grassland. The underlying land tenure of the project is pastoral lease and the region has maintained a long association with grazing.

2.0 STUDY RATIONALE

When mining ceased, the E1N pit had been mined to completion, whereas the E1E pit was only partially mined. Overall, geochemical characterisation at MMM indicated some waste rock to be potentially acid forming (PAF). It was accepted that complete control of acid generation

and prevention of poor quality leachate could not be achieved in the long-term without cost-prohibitive options being adopted. WRD covers were however considered as one mitigation strategy that could, with appropriate planning and design, achieve site wide closure objectives.

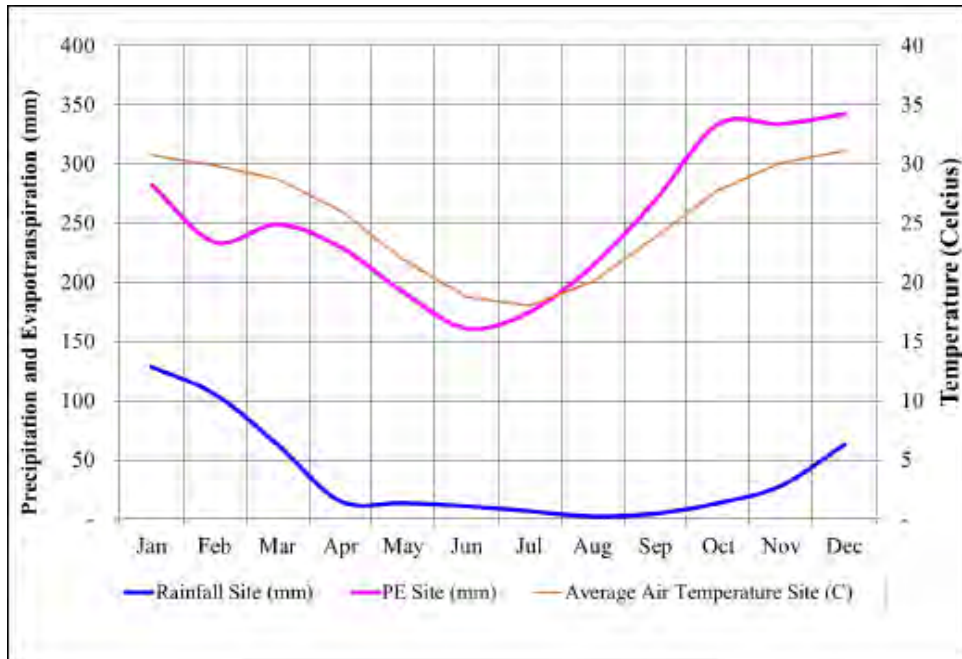


Figure 1: Average Monthly Rainfall, Evaporation and Temperature

The final E1 NWRD concept design entailed the encapsulation of PAF waste rock with non-acid forming (NAF) waste rock (low sulphur content) to limit exposure to atmospheric conditions and reduce acid generation. Further, the concept included a suitable cover system to limit infiltration and net percolation (NP) to achieve post-mine rehabilitation goals inclusive of receiving water quality objectives (Table1).

Table1. MMM NWRD rehabilitation goals and objectives

Rehabilitation Goal	Objectives*
Non-polluting	Stormwater and seepage managed to prevent environmental values identified in the receiving environment (surface water and groundwater) from being diminished
Stable	Minimise accelerated erosion by providing soil surface conditions that promote the establishment and maintenance of adequate groundcover on waste landforms
Self-sustaining	Establish a vegetation community that is self-sustaining (ecologically functional) and minimises the potential for degradation of grasslands on the surrounding pastoral leases
Safe	Make safe for humans and wildlife by maximising stability based on agreed designs

* Detailed performance targets were developed to validate achievement of these objectives but are not presented in the interests of brevity.

3.0 APPROACH TO CLOSURE OF LANDFORMS CONTAINING PAF WASTE ROCK

For closure planning purposes MMM required:

- An assessment of the requirements to complete encapsulation of the PAF material;
- Conceptual landform designs to manage water onsite;
- Conceptual cover designs for the waste rock dumps; and
- Conceptual landform designs to achieve post mining land use objectives and achieve the rehabilitation goals for the site (i.e. safe, stable, non-polluting and self-sustaining).

The adopted approach utilised the mine pits to capture and retain seepage and percolate from the WRDs, preventing off-site release of contaminants. This approach was consistent with the rehabilitation objectives and approval conditions in MMMPLs Environmental Authority (EA). Since evaporation exceeds rainfall, the pits are expected to remain as water sinks in the long-term. With seepage and percolate from the WRD routed to the pits, the design objectives for the cover system are primarily to:

- Limit the amount of seepage to the extent that it would not exceed evaporative capacity of the pits (maintaining their function as long-term sinks); and
- Provide a sustainable landform meeting the final land use requirements and rehabilitation objectives.

The approach that was adopted for the development of the conceptual cover design was therefore to assess the potential cover functions and configurations that would meet these requirements. This was done based on the decision tree shown in Figure 2 and considered:

- Cover construction materials properties and quantities available at site;
- Water management strategy; and
- Net water balance for the site.

Evidence-based outcomes from rehabilitation undertaken progressively since 2002 at the adjacent EHM (with similar available cover materials) (Butler et al. 2015) were utilised to provide guidance and technical support for selection of proposed rehabilitation strategies at MMM.

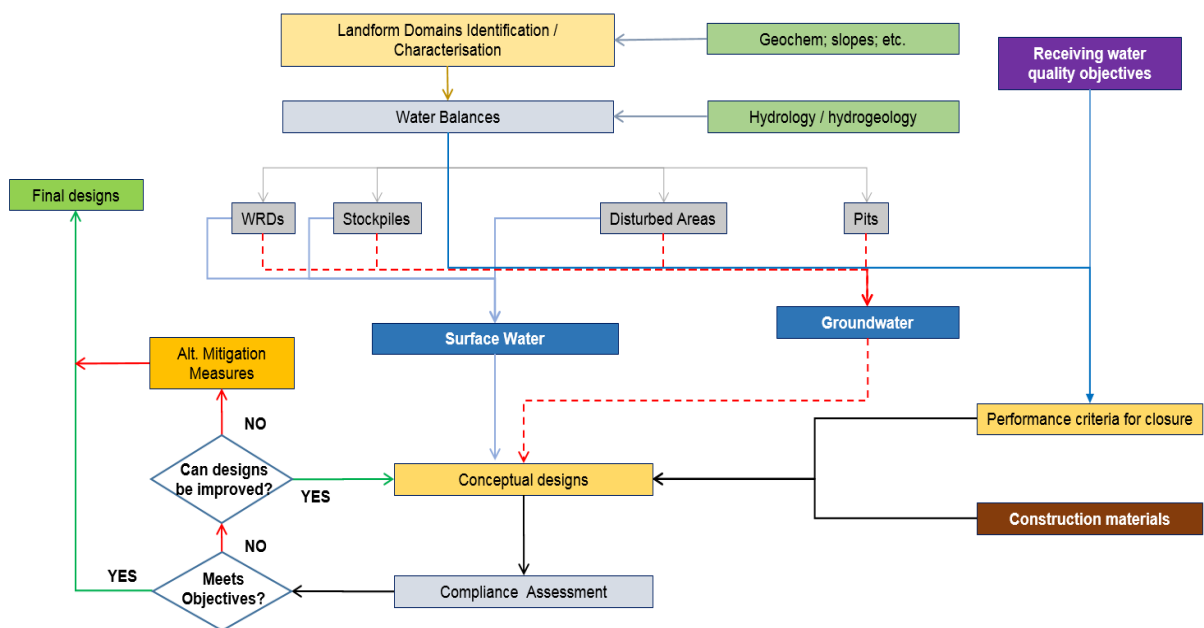


Figure 2. MMM Conceptual Landform Closure Approach

4.0 WATER MANAGEMENT STRATEGY AND WATER BALANCE

A water balance was developed to assess whether the pit would remain a net groundwater sink for a given cover performance and water management strategy. The water balance therefore considered:

- Direct rainfall on the pit lake;
- Groundwater inflows;
- Runoff from natural upstream terrain that couldn't be diverted away;
- Runoff from the WRD landforms;
- Seepage and percolate from infiltration to the WRD landforms; and
- Evaporative losses from the pit lakes.

The water balance was set up on a monthly time step, utilising long-term average monthly rainfall estimates. Although the water balance was set up for long-term mean rainfall, a mechanism was included to assess the effects of periodic higher rainfall at regular intervals. The water balance resulting from different scenarios of water management and NP through the WRDs was used to develop performance criteria for the cover system to aid design.

4.1 Hydrogeological Setting

The E1 copper/gold deposits occur in fault bound, brecciated felsic volcanic rocks, which are of Proterozoic age. The deposits are unconformably overlain by Mesozoic sediments of the Carpentaria Basin (the Wallumbilla Formation being important at MMM). The E1 deposits are at the south-western margin of the Carpentaria Basin, with Proterozoic basement outcropping approximately 20 km to the west and south-west.

The pre-mining water table at the E1 site was estimated to be between 120 to 124 mAHD (26 to 30 m bgl). Analysis of groundwater levels indicated a drawdown within the Wallumbilla Formation and the Proterozoic, with hydraulic gradients indicating groundwater flows toward the open pit. The analytical method of Marinelli and Niccoli (2000) was used, following calibration from observed data, to predict future groundwater recharge. The pit lake water balance included recharge as a function of water elevation and estimation of the potential range of drawdown around the pit (important for the capture of seepage beneath the WRD), as illustrated in Figure 3.



Figure 3. Observed Groundwater Levels (solid contours) and Inferred Drawdown Zone (dotted circles)

4.2 Conceptual Water Management

The conceptual water management strategy for the E1N open pit, the E1E open pit and the NWRD (a catchment area of 193 ha) is illustrated in Figure 4. The strategy incorporates as much existing infrastructure as possible. It isolates the high-risk landforms with a clean water diversion bund and utilises existing in-situ drainage interception (Figure 4). This restricts inflow of clean run-on water and directs contaminated run-off and seepage to the pits.

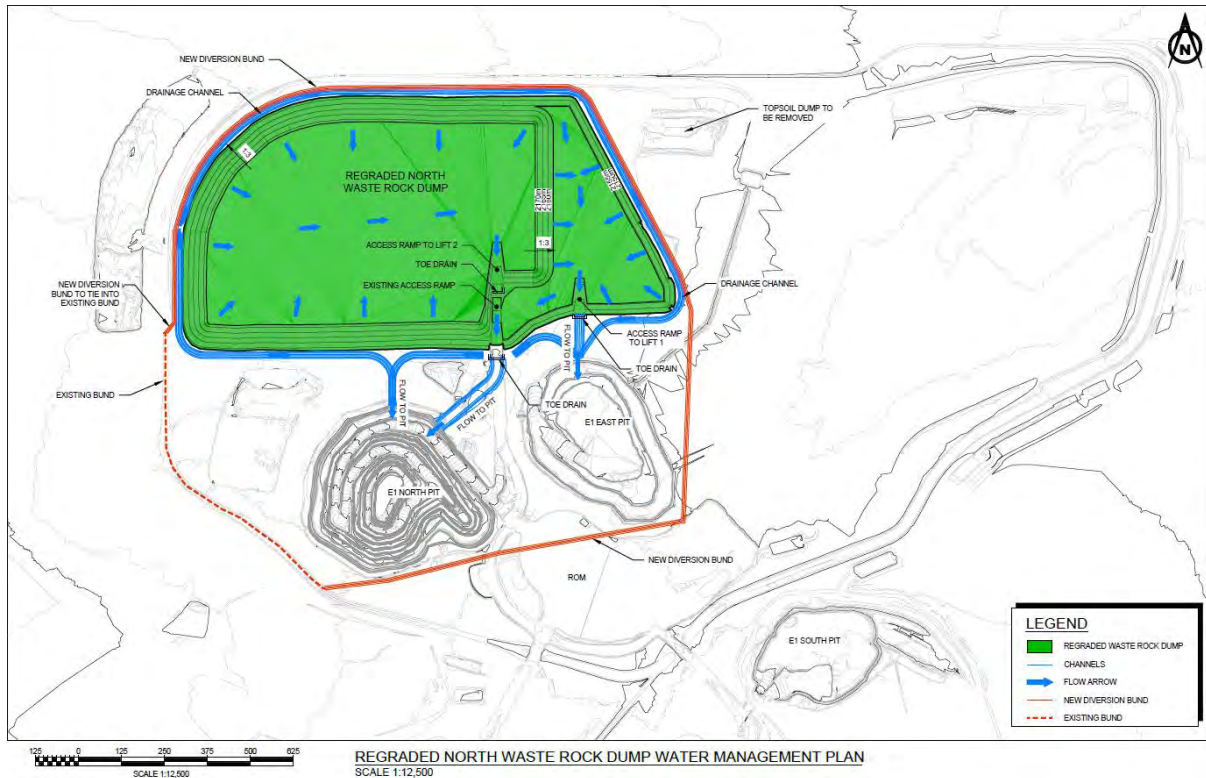


Figure 4. E1 Site and Conceptual Water Management Strategy

4.3 Water Balance Assessment

The base case water management scenario allowed for all runoff from the NWRD to be diverted to the E1N open pit and assumed average NP through the NWRD would be about 5% of mean annual precipitation (MAP). Monitoring of two cover configurations at the adjacent EHM site indicated long-term average NP rates of 8% (for a 1 m cover comprising 0.5 m rock overlain by 0.5 m soil) and 2% (for a 1.8 m cover comprising 0.6 m rock, overlain by 0.85 m clay, overlain by 0.45 m soil) of MAP could be achieved. Therefore, adopting a 5% NP rate of MAP as a base case, and upper range of 15% was considered reasonable in the context of the area and available materials.

4.4 Sensitivity Analysis

While numerical models can be very effective for comparing the relative performance of different management options, they need to be used cautiously when predicting outcomes. Therefore, sensitivity analyses, to simulate the potential range of outcomes subject to the variation of key input variables, are essential. Rainfall variations were assessed as the key input variable to the water balance.

For the base case, a steady state water level would be reached in the E1 North Pit in about 150 years at about 103 mAHD (or 17 m below the pre-mining water table) (Figure 5). The pit is forecast to remain a permanent groundwater sink and the drawdown would extend beyond the NWRD footprint. Therefore, all percolate from the NWRD would be captured and flow toward the pit lake. When the NP through the NWRD is increased from 5% of MAP to 10 % of MAP, the steady state water level is predicted to rise by about 5 m to 108 mAHD. At 15 %NP, the pit lake level would rise to about 112 m AHD (or 8 m below the pre-mining water table), and the zone of influence would contract. However, the pit would still act as a net groundwater sink and would remain effective as a means of attenuating solutes indefinitely.

Sensitivity analyses revealed that the pit lake elevation would not exceed the pre-mining water table for the extreme rainfall case (i.e. 95th percentile and maximum rainfall wet season). The sensitivity analysis also indicated that NP of up to 15% of MAP would not compromise long-term closure objectives.

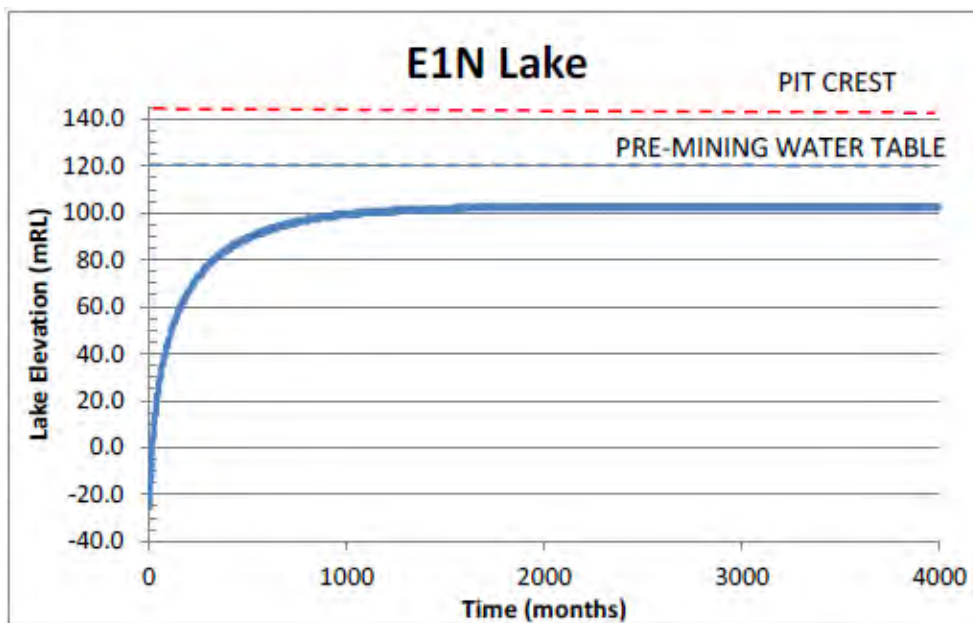


Figure 5. Predicted Water Level in the E1N Pit for base case conditions (NWRD NP at 5% of MAP)

An alternate case utilising the E1E Pit as a supplemental evaporation basin was also developed as part of the assessment. In the alternate case, a portion of runoff from the NWRD, together with seepage from within the E1E pit catchment, would be directed to the E1E pit, thus reducing the volume that would report to the E1N pit. The effects of average, 95th percentile and maximum recorded wet season rainfall were assessed for the alternate case. By utilising the E1E pit as a complementary evaporation basin, the net water balance for the E1N pit would be improved significantly under all scenarios (Figure 6).

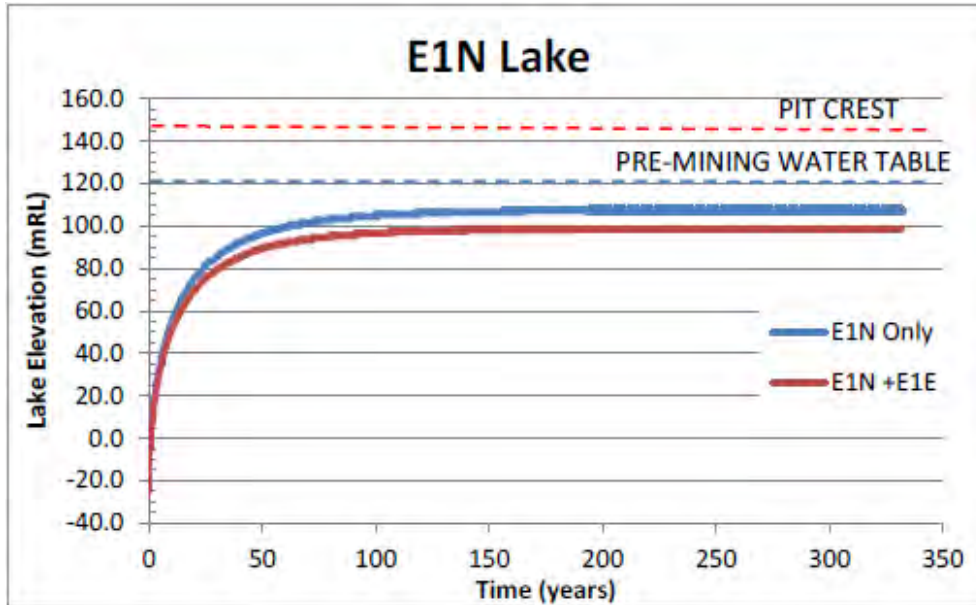


Figure 6: Comparison of water elevation in E1N Pit with and without utilising E1E as an evaporation basin

5.0 COVER DESIGN ASSESSMENT

Generally, material properties that determine the suitability of materials for covers include:

- Saturated hydraulic conductivity (for barrier covers intended to reduce infiltration);
- Particle size gradation (i.e. moisture holding capacity, or storage capacity, calculated as the difference between the field capacity and wilting point); and
- Surface erosion resistance.

Based on the properties for the materials identified at the MMM sites, the soils generally are not suitable for construction of low infiltration (barrier) covers, without further intervention or amelioration (i.e. bentonite or synthetic liner). The materials, however, are suitable for the construction of a store-and-release type of cover system.

The oxidation rate of sulphides within the waste rock will be dictated by the rate of oxygen ingress into the WRD. Materials that perform best to limit oxygen entry are fine grained materials such as clay, which has a low gaseous permeability at saturation. In a drier climate, clays tend to de-saturate and desiccate which allows air and water ingress. Therefore, whilst oxygen entry could be reduced, this will not be a primary function of the cover.

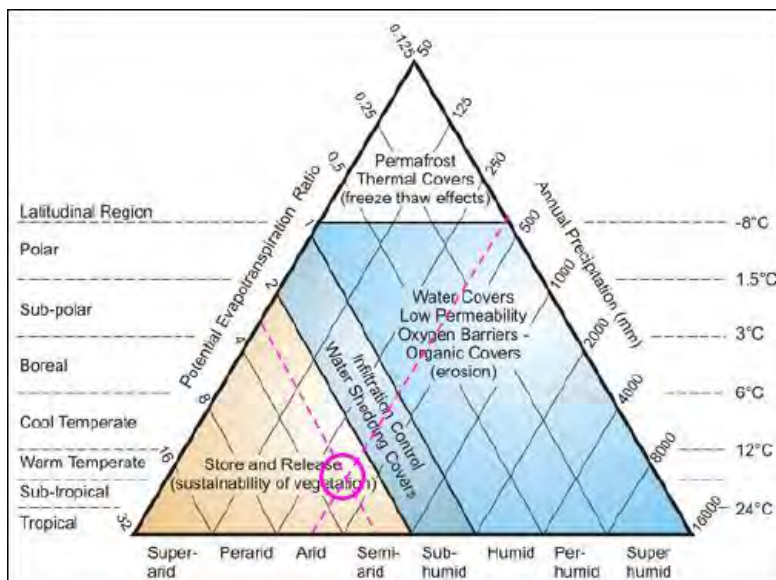
The climatic water balance and climate classification are good indicators for the selection of the most appropriate cover type at a given site. Figure 7 relates climatic conditions to cover type (adapted from the Global Acid Rock Drainage (GARD) Guide (INAP 2009)) to indicate site conditions at MMM.

Based on the site annual precipitation (452 mm) and potential evapo-transpiration (1500 to 1700 mm), and available material types and properties, a store-and-release type cover system is shown to be the preferred option. The primary function of the cover system would not be to prevent NP altogether but to reduce it nominally to about 5 % of MAP (which has been shown to be adequate to meet closure objectives).

A set of proposed design criteria is provided in Table 2, and in general are aimed at meeting the site rehabilitation goals and objectives.

Table 2. Proposed Design Criteria for the Conceptual Cover System

Component	Criteria
Design life	100 years (while it is recognised that the cover will remain for longer period, design performance will be measured against this criterion)
Oxygen reduction	Not required
Infiltration reduction	E1 NWRD - NP nominally 5% of mean annual precipitation.
Waste settlement	No criteria due to granular and dry nature of waste rock material
Trafficability	No criteria due to granular and dry nature of waste rock material
Physical exposure	As far as practicable keep PAF mine waste covered
Slope stability	Stable
Wind erosion	None selected
Overland surface runoff	<p>Top of Waste Rock Dump:</p> <ul style="list-style-type: none"> Designed to have minimal erosion (through velocity control and lining) under 100 year AEP event Designed not to overtop external batters at any time during Probable Maximum Precipitation (PMP) event <p>Drop structure and stilling basin from top to bottom of dump: Designed to withstand Probable Maximum Precipitation (PMP) event.</p> <p>Perimeter channel/cut-off bunds: designed for 100 year AEP event.</p>
Evapoconcentration	Limited salt wicking into cover layer.
Vegetation	Self-sustaining vegetation cover endemic to the region as soon as practicable after cover construction, mainly to preserve topsoil.
Land use	Native grassland

**Figure 7. Preliminary Cover Selection based on Climate MMM from INAP (2009)**

The estimated hydraulic and material properties of the available cover soils at MMM were used together with empirical methods (Chen 1999) to estimate the likely range of store-and-release cover thicknesses that would be required to reduce the average annual NP to 5% of MAP. The Chen (1999) method utilises an upper bound design approach which is based on the maximum site precipitation for wettest year on record.

The criteria for the cover system were based on the following parameters:

- Total precipitation for wettest year on record (P_{TW}) = 1331 mm
- Nominal NP reduction = 95% of MAP.

Store-and-release cover thicknesses were determined for three cover materials and the results are summarised in Table 3.

Table 3. Minimum Store and Release Layer Dimensions for Alternate Cover Materials

Material	Sub Soil	Oxide	Low Sulphur Waste
Field Capacity (VWC)	0.271	0.244	0.217
Wilting Point (VWC)	0.160	0.140	0.120
Storage Layer Thickness (m)	1.33	1.47	1.66

The 95th percentile annual rainfall of 950 mm was also used to assess the minimum cover thickness, which indicated a minimum storage layer of 1.22 m (i.e. providing sufficient storage to store the annual rainfall 95% of the time). Results from the test covers at EHM for a combined 1 m cover (comprising 0.5 topsoil and 0.5 m waste rock) is achieving a 75% to 80% reduction 95% of the time; therefore, increasing the layer as per the 95th percentile assessment, would be expected to support the 92 to 96 % NP reduction. The storage layer would be covered with a minimum of 0.3 m topsoil which would further enhance the performance of the cover system. Therefore, a cover storage layer thickness of between 1.22 and 1.66 m is expected to be suitable, and the upper value was adopted.

Consideration was also given to the potential for salt wicking. Salt wicking could occur if the underlying reactive waste rock wets up and is subject to evapo-transpiration. To prevent salt wicking, the capillary barrier should have a residual suction lower than the air entry value of the overlying fine soil to prevent capillarity. A capillary break normally would comprise a layer of about 0.3 to 0.5 m of graded competent material that would prevent water migration upwards into the NAF layer. An alternate strategy is to place a layer of compacted material with a lower permeability than the underlying reactive material. The lower permeability layer would ensure that the storage layer functions optimally and would effectively regulate the flow into the underlying material to prevent it from wetting up completely thus minimising the risk of salt wicking. It is therefore proposed that a lower permeability layer be placed directly over the coarser reactive material. The proposed conceptual cover design is illustrated in Figure 8.

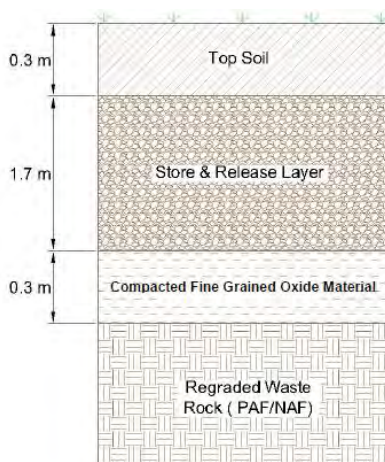


Figure 8. Proposed Cover Design (Not to Scale) for the NWRD

6.0 CONCLUSION

Based on the overall water balance, the model predictions suggest that the E1N pit would remain a net groundwater sink and would be an effective means of containing contaminated surface and groundwater on site. In general, the pit would have the capacity to capture all of the runoff and percolate from the NWRD dump, and maintain a sufficient capture zone, for NP rates of between 5 % and 10 % of MAP.

The underlying assumption is that the cover effectiveness is constant - the reality is that the cover efficiency, especially if the design relies on a store-and-release principle, will be variable depending on pre- and antecedent precipitation events. Therefore, even though the modelling indicates that a long-term average NP rate of up to 10 % should not adversely affect the performance of the strategy, a nominal NP rate of 5 % of MAP was adopted as a target for the conceptual cover design, to allow for changing conditions without compromising the rehabilitation and closure objectives relating to water quality in the receiving environment.

7.0 ACKNOWLEDGEMENTS

The authors wish to acknowledge Australasian Groundwater and Environmental Consultants (AGE) for their contribution to the groundwater assessment and O'Kane Consultants for their contribution to the cover trial assessments at EHM.

8.0 REFERENCES

- Butler, AR, Anderson, TR and Sexton, A (2015) Optimisation – a rationalised approach to developing mine closure objectives. In 'Proceedings of the Tenth International Conference on Mine Closure' (Eds: AB Fourie, M Tibbett, L Sawatsky and D van Zyl), pp 517-530 (InfoMine: Canada).
- Chen, C. (1999) Meteorological Conditions for Design of Monolithic Alternative Earthen Covers (AEFCs). MS Thesis, University of Wisconsin, Madison, Wisconsin, USA.
- The International Network for Acid Prevention (INAP) (2009) Global Acid Rock Drainage Guide (GARD Guide). <http://www.gardguide.com/> .
- Marinelli, F and Niccoli, WL (2000) Simple analytical equations for estimating groundwater inflow to a mine pit. *Groundwater* **38**, 311-314.

IMPROVED REHABILITATION OUTCOMES THROUGH SMART COVER DESIGN AT ENDEAVOR MINE, NSW

T. Rohde^A, K. Hardie^B and N. Jamson^A

^AEMM Consulting Pty Limited, PO Box 10424, Brisbane, QLD 4000, Australia

^BEndeavor Operations Pty Ltd, Louth Road Cobar, NSW 2835, Australia

ABSTRACT

The Endeavor Mine (the mine) is an underground zinc (Zn), lead (Pb) and silver (Ag) operation in central New South Wales (NSW), 47 kilometres (km) north-west of Cobar and 700 km from Sydney. The mine currently has five years of operation before it transitions through closure and rehabilitation to a future land use after 2023. Broadly speaking the mine has two domains that require rehabilitation, the mine industrial area (MIA) and the tailings storage facility (TSF). The MIA has been used for the handling and processing of ore and contains elevated sulfate, sulfide and metals (the constituents) (Pb, Zn). The TSF receives the by-products of processing that is, potentially acid forming (PAF) tailings which also contain elevated sulfate, and constituents.

Typically the rehabilitation of a TSF involves two controls. Firstly controlling the potential for PAF tailings to form acid mine drainage (AMD) by limiting interaction with oxygen. Secondly, once the tailings are unsaturated, limiting interaction with water (usually as rainfall) to reduce the potential for AMD to be transported to the receiving environment. These two controls are often employed in the form of a cover.

In semi-arid environments there are many Australian examples of covers that have been built to limit interactions of tailings with oxygen and water. Typically the covers contain two or more layers and are built from soil and rock which may include run of mine waste rock. The mine however has limited supplies of stockpiled soil; and waste rock is not generated in large volumes because it is used as backfill underground.

A cover design strategy was developed to cater for these rehabilitation parameters. The strategy identified soil, ore and rock accretion (the accretion) below the MIA could be a potential source of borrow material for the TSF cover. This strategy creates three opportunities for the mine. Firstly, it improves the volume of soil and rock available for rehabilitation of the TSF. Secondly, any potential contamination will be removed from the MIA effectively rehabilitating the domain. Finally, the mine will improve upon the previous thin (0.3 m) cover design for the TSF.

The purpose of this paper is three-fold and describes the SMART (Specific, Measurable, Achievable, Realistic, and Timely) cover design process employed by the mine. That is, the paper describes the desktop cover design process that the mine used to develop a thick cover for the TSF that created an opportunity to improve the rehabilitation outcomes for the MIA and the TSF. Secondly the paper describes the method and results of large (2 m tall) column trials that were used as a cost-effective way to trial three cover options. Finally the paper describes the water balance that was developed from the column trial results.

1.0 INTRODUCTION

The mine is located in central New South Wales (NSW), 47 kilometres (km) north-west of Cobar and 700 km from Sydney. The mine operates within western land lease (WLL) 13839 over five mining leases (ML): ML168, ML169, ML170, ML171 and ML930.

Operations commenced at the mine in 1983 under the ownership of Pasminco as the Elura Mine. In 2003 the mine was acquired by CBH Resources Pty Ltd (CBH Resources) and renamed to the Endeavor Mine under the ownership of Endeavor Operations Pty Ltd.

The mine currently has five years of operation until closure after 2023. Rehabilitation of the mine, broadly speaking, is concerned with two domains: the MIA and the TSF. Rehabilitation efforts require careful planning and must be site specific so that the mine can limit the potential for both domains to contaminate the receiving environment with AMD in the future.

A gap analysis and risk assessment of rehabilitation planning at the mine identified that a cover was required to limit the potential for rainfall percolation into the tailings. Limiting percolation will limit the potential for seepage and limit the potential for an impact on the receiving environment. Further the gap analysis also identified shortages of soil and rock to build the cover which is further exasperated by the fact that the thin cover, currently built on a section of the TSF, was unlikely to limit future potential for AMD.

1.1 Previous Rehabilitation of the TSF

In 1998 the mine rehabilitated 11ha of the TSF using a thin cover of soil above a plastic liner. The purpose of the soil layer was to allow grasses to establish and the purpose of the plastic liner was to limit percolation and capillary rise. In 2003 the cover was assessed by URS (now Aecom). They found that the cover contained both grasses and trees up to 3 m tall. Test pits were excavated at the base of three trees ranging from 0.5 m to 3 m in height. It was found in each of the cases that the tree roots had not penetrated the plastic liner (Figure 1). However, since that time a number of large trees have blown over on the cover requiring repair to the liner and back filling of the hole in the soil layer.



Fig.1. Tree root penetration in the thin cover

Landform function analysis completed by DnA Environmental in 2012 and 2013 (DnA 2012 and DnA 2013) found that the rehabilitated section of the TSF had an elevated electrical

conductivity (EC) (0.8 dSm^{-1}) likely the result of elevated sulfate and to a lesser extent calcium, magnesium and potassium. Further the 2012 and 2013 studies also found elevated constituent concentrations for Zn, Pb and iron (Fe), likely present in the soil layer due to puncturing of the plastic liner during installation.

The gap analysis and risk assessment therefore identified that the mine would require a thicker cover ($>0.5 \text{ m}$) that incorporated a more substantiated reduced permeability layer (RPL) to reduce the potential risk of reduced cover performance.

1.2 Future Rehabilitation

It was identified during the gap analysis and risk assessment that accretion below the MIA could be a potential source of borrow material for the future cover. The advantage of this strategy is that any potential contamination will be removed from the MIA.

The capability of the future cover to result in a more robust environmental outcome will in part be determined by the level of contamination in the accretion and whether potential contamination will result in capillary rise and/or plant intolerance.

The requirement for remediation of contaminated land is documented in *NSW Contaminated Land Management Act 1997* (CLM Act) as follows:

The CLM Act defines contaminated land as:

Contamination of land, for the purposes of this Act, means the presence in, on or under the land of a substance at a concentration above the concentration at which the substance is normally present in, on or under (respectively) land in the same locality, being a presence that presents a risk of harm to human health or any other aspect of the environment.

The potential risk is typically determined by exceeding the appropriate health investigation limit (HIL) reported in the *National Environment Protection (Assessment of Site Contamination) Measure 1999* (NEPM).

Analysis of accretion was completed by EMM Consulting in 2016 (Table 1) and compared to the geochemical abundance index (GAI) and NEPM HIL C (public open space and recreational areas).

Table 1. Accretion constituent analysis

Constituent	Constituent concentration (mg/kg)	NEPM HIL C (mg/kg)	GAI ^A	Comment
Arsenic (As)	approximately (~)70-1,260	300	2.9-7	Potentially above NEPM HIL C and enriched
Pb	~740-3,130	600	3.8-5.9	Potentially above NEPM HIL C and enriched
Copper (Cu)	~90-900	17,000	1-4.3	Below NEPM HIL C and enriched
Zn	~4,500-28,900	30,000	0.8-3.5	Below NEPM HIL C and enriched

^A GAI = $\log_2 [C/(1.5 \times S)]$ where C is the concentration of the constituent in the sample and S is the median abundance in the earth crust (Bowen 1979)

Table 1 shows that accretion is enriched with As, Pb, Cu and Zn, but the constituent concentrations remained below the HIL C guidelines, with the exception of As and Pb, suggesting that accretion may be appropriate for use in the future cover.

1.3 Regional Cover Design

Among other factors, climate is an important element in determining the type of cover that is most suited to the mine (International Network for Acid Prevention (INAP) Global Acid Rock Drainage (GARD) Guide 2009). The climate at the mine is semi-arid with low humidity, low rainfall and high evaporation. Annual average rainfall is ~400 millimetres (mm) and is typically evenly distributed throughout the year. Rainfall is exceeded by evaporation and averages ~2,000 mm/year. The combined effect of evaporation and transpiration (evapotranspiration) at the mine is about five times greater than rainfall. The GARD Guide (INAP 2009) suggests that a store and release cover (the cover) might be an effective tool, in combination with other safe guards (i.e. a capillary break or RPL to reduce the potential for environmental harm from the TSF at the mine after closure (Figure 2).

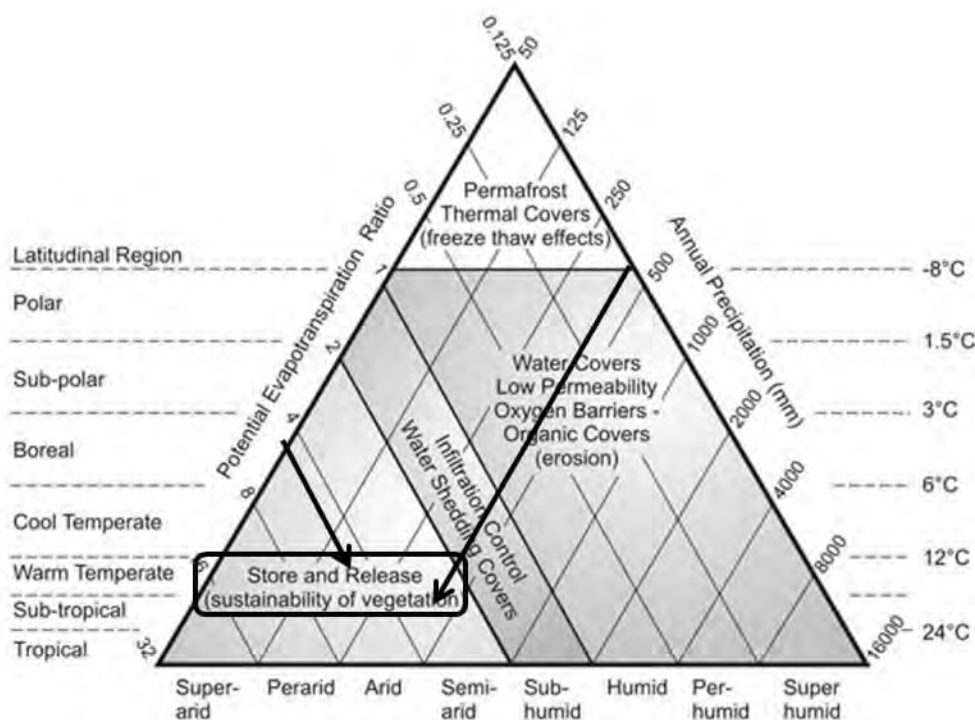


Fig. 2. Covers and climate types (from GARD 2009)

Regionally there is little published data that can inform cover design for the mine. Two studies have been published for CSA Mine and Peak Gold Mine (PGM).

TSF cover trials at CSA Mine reported in the Annual *Environmental Management Report* (AEMR) (CSA Mine 2015) reports that a 0.4 m cover will hold sufficient water and nutrients to support vegetation growth, noting that the CSA Mine trials do not appear to have addressed capillarity or the ongoing AMD potential. It is also important to note that CSA Mine intend to use the near surface tailings as part of the infiltration storage layer for the cover.

PGM have been running field scale cover trials since 2002, which were first set-up by O’Kane Consulting and later reported by Schneider (2012) and the University of Queensland Centre for Mined Land Rehabilitation which has been reproduced in Figure 3.

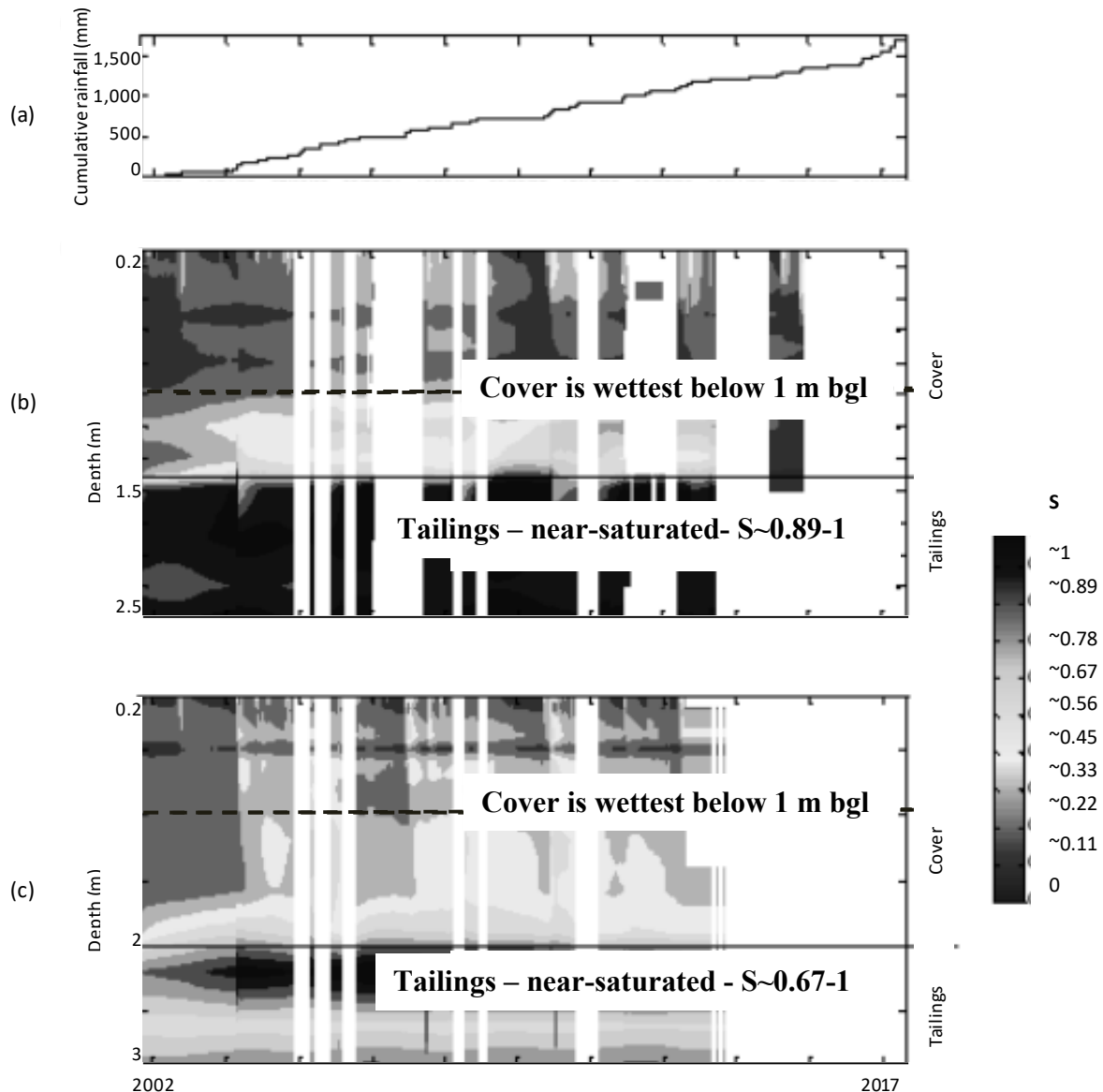


Fig. 3. PGM cover trials: (a) cumulative rainfall (b) and volumetric water content for 1.5 m cover trial (c) and 2 m cover trial

The presented PGM cover trial data spans a period of five years from 2002 to 2007 over which time approximately 1,600 mm rainfall fell. The following overarching trends are noticeable:

- The tailings remain near-saturated throughout the monitoring period for both the 1.5 m and the 2 m cover trials with a degree of saturation (S) range of $\sim 0.67-1$. It should be noted that other cover trials in Australia have shown that a S greater than ~ 0.6 is sufficient to result in desaturation of the layer by percolation; or in the case of the tailings seepage to the receiving environment (Rohde 2011);
- The infiltration storage layer below 1 m below ground level (bgl) is typically wetter than the infiltration storage layer above 1 m bgl with a S ranging between $\sim 0.5-0.6$. It is likely that

the S is sufficient to result in percolation to the underlying tailings resulting in the high S in the tailings; and

- Evapotranspiration from vegetation is effective to a depth of 1 m bgl, i.e. the top 1 m of the cover oscillates between partially wet ($S \sim 0.33$) and dry ($S \leq 0.11$). That is infiltration that percolates below 1 m bgl cannot be effectively removed by evapotranspiration and has resulted in an increase in S with depth in the cover and a high S in the underlying tailings.

Unlike the CSA Mine cover described previously, it is not the intention of the cover at PGM to use the surface of the tailings as part of the rooting zone. Therefore the near saturated conditions at the surface of the tailings indicate an increased potential for seepage.

The results indicate that a thick cover may result in reduced cover performance, because not all infiltration can be effectively removed by evapotranspiration. The review of CSA Mine and PGM suggests that the optimum cover thickness for the region is likely between 0.4-1 m with covers thicker than 1 m potentially increasing the risk of seepage. Noting that a seepage risk also exists for a thin cover option (<1 m) if a RPL is not included within the cover design.

2.0 METHOD

The following method statement describes the SMART approach used by the mine to develop the future cover for the TSF.

The purpose of the SMART approach was to provide enough in situ data for volumetric water content, matric suction, seepage and weather to develop a maximum probable water balance that could be used in desktop model such as Vadose/w (at a later time) to decide on a final future cover thickness. It is not the sole purpose of the SMART approach to validate any particular trialed configuration; albeit, that it is accepted that this may also be an outcome of the approach.

2.1 Specific

On the basis of the gap analysis, risk assessment and desktop review, it was decided that the mine would establish three cover trials to determine the future cover for the TSF. Based on the risk assessment, it was decided that the future cover would require a RPL to limit the potential for percolation into the tailings resulting in seepage. The following covers were trialed:

- 0.45 m cover made up of a 0.3 m RPL of accretion overlain by a 0.15 m infiltration storage layer of soil.
- 0.6 m cover made up of a 0.3 m RPL of accretion overlain by 0.3 m infiltration storage layer of soil.
- 0.8 m cover made up of 0.3 m RPL of accretion overlain by 0.5 m infiltration storage layer of soil and accretion.

2.2 Achievable, Realistic and Timely

The low rainfall environment was seen as limiting factor to achieving a timely response from the field trials. Since regional experience would indicate that several years of data would be required to capture a representative window of how the cover responds to seasonal changes. For example the PGM cover trials had five years of data.

In order to achieve interim data of cover performance, it was decided that the cover trials would be constructed as large column trials (Figure 4). Each column trial is 2 metres (m) tall, has a

surface area of 0.25 m and is perforated in the base to allow percolation to pass out of the column.

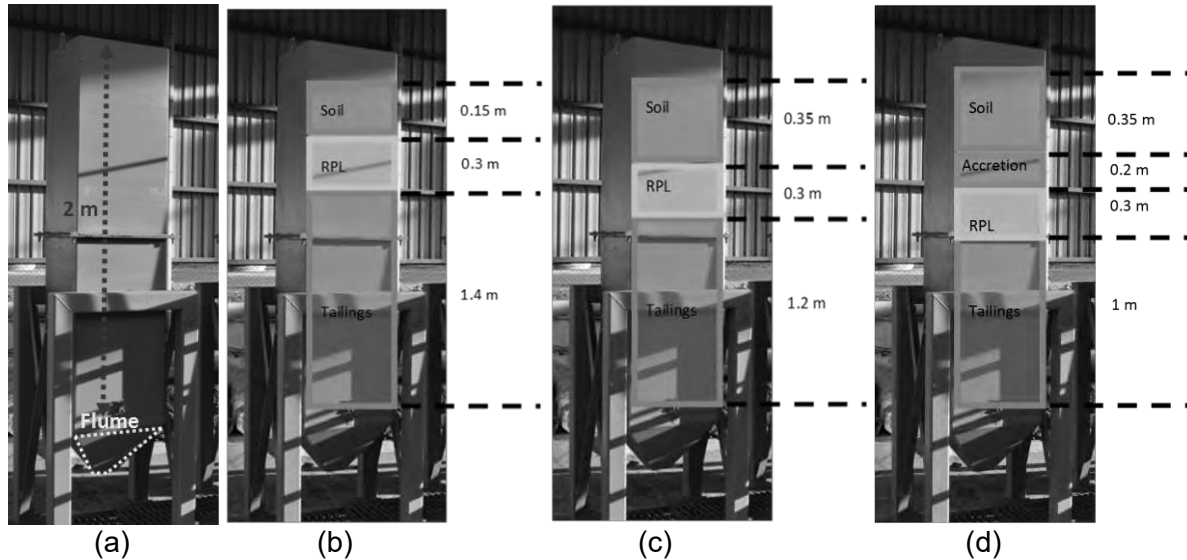


Fig. 4. Column trials: (a) Column components (b) 0.45 m cover (c) 0.6 m cover (d) 0.8 m cover

2.3 Measurable

The column trials were instrumented with volumetric water content sensors (also capable of measuring EC) and matric suction sensors to measure how rainfall infiltration and dissolved ions move and are stored within the cover. The sensors were buried so that they were positioned at the upper and lower boundary of the soil infiltration layer and at the upper, middle and bottom of the RPL.

Seepage was recorded using rain gauge tipping buckets placed under the flume (Figure 4), and the remaining element of the water balance, evaporation was calculated using Eqn.[1].

$$\text{Evaporation} = \text{Artificial rainfall} - \text{stored infiltration} - \text{seepage} \quad [1]$$

3.0 RESULTS AND DISCUSSION

3.1 Artificial Rainfall

The column trials were subjected to 14 artificial rainfall events over approximately 9 months (Figure 5):

- seven fortnightly 100 mm artificial rainfall events starting on 19 April and concluding on 4 June 2016; and
- seven artificial rainfall events of varying intensity, roughly at fortnightly intervals commencing 1 October 2016 and concluding on 27 December 2016.

From 4 June 2014 to 1 October 2016 (four months), the column trials were allowed to dry-out with no artificial rainfall added (Figure 5).

In total 1,450 mm of artificial rainfall was added to the columns, equivalent to approximately three times the annual rainfall of 400 mm (Figure 5).

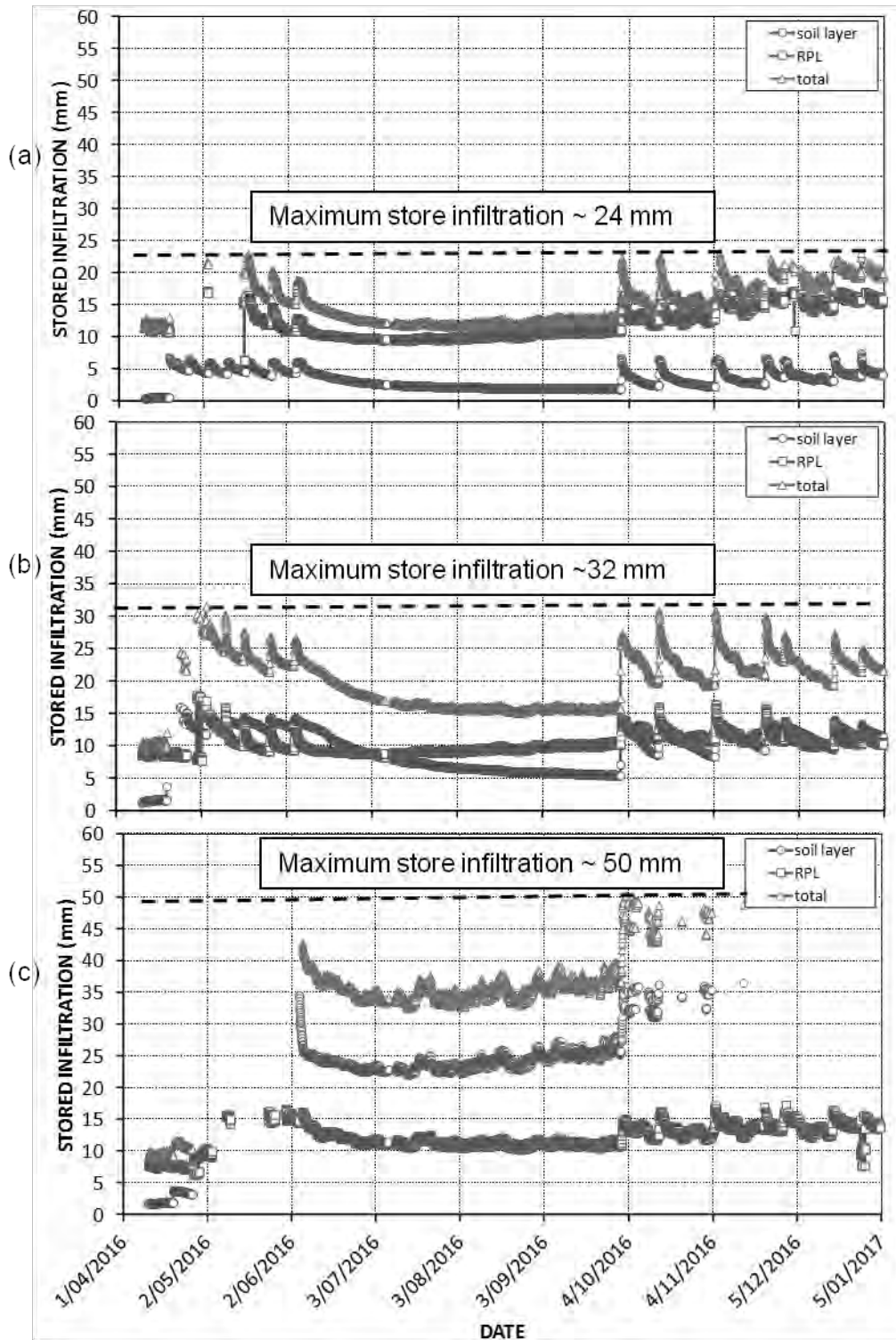


Fig. 6. Stored infiltration: (a) 0.45 m cover (b) 0.6 m cover (c) 0.8 m cover

3.3 Seepage

Figure 7 presents the measured seepage (from the rain gauge tipping buckets) for the covers and shows:

- the maximum seepage from the 0.45 m cover was 139 mm;

- the maximum seepage from the 0.6 m cover was the lowest recorded, 125 mm; and
- the maximum seepage from the 0.8 m cover was the highest, 169 mm.

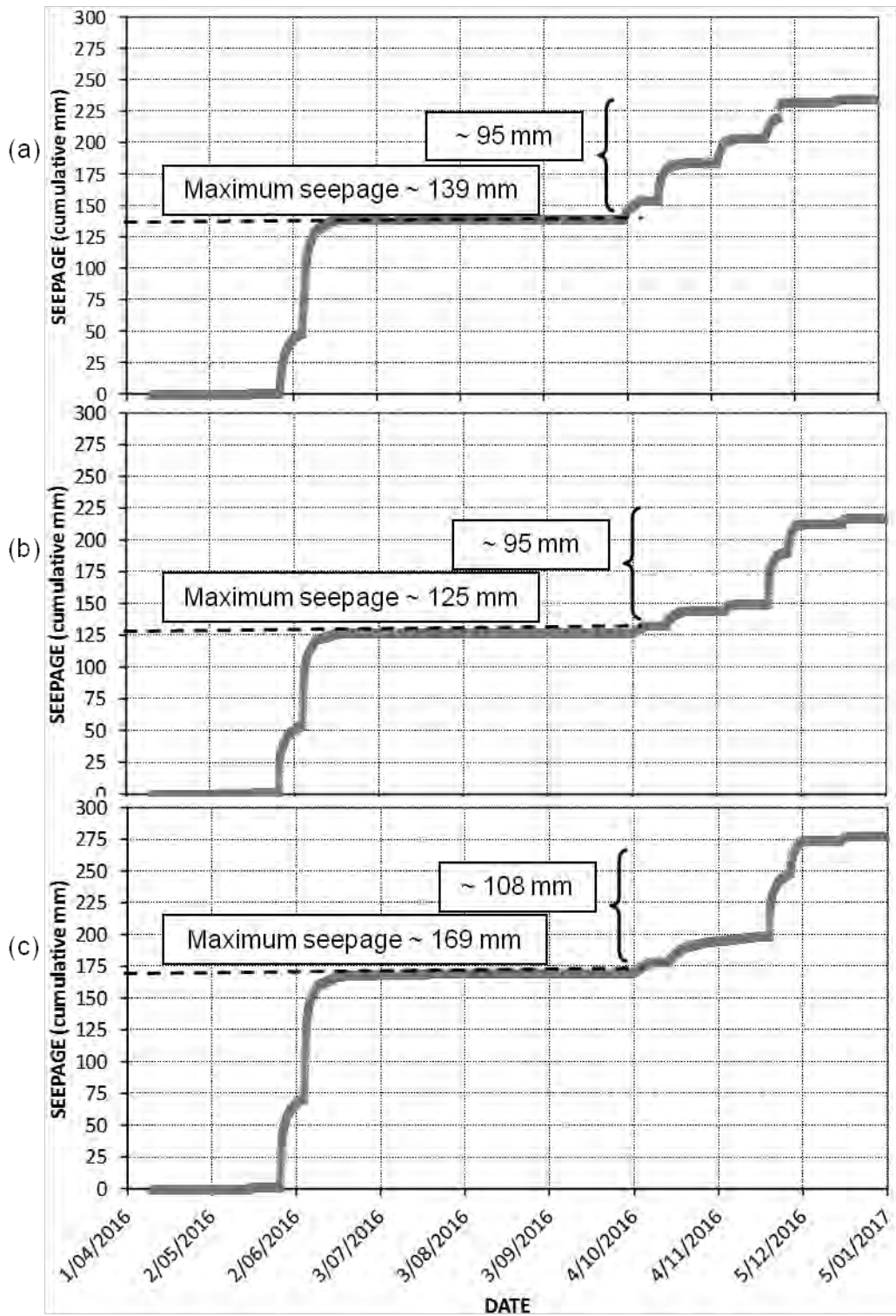


Fig. 7. Seepage: (a) 0.45 m cover (b) 0.6 m cover (c) 0.8 m cover

3.4 Water Balance

Incorporating artificial rainfall, stored infiltration results and seepage allows for the calculation of a water balance (Table 2) for each column trial by solving for evaporation using Eqn. [1].

Table 2. Water balance for each column trials (based on maximum stored infiltration)

Cover thickness	Water balance element	Flux (mm)	Flux (% of cumulative artificial rainfall)
0.4 m	Stored infiltration	24	3
	Seepage	139	19
	Evaporation	562	78
0.6 m	Stored infiltration	32	4
	Seepage	125	17
	Evaporation	568	78
0.8 m	Stored infiltration	50	7
	Seepage	169	23
	Evaporation	506	70

Therefore the column trials have shown (Table 2):

- That although infiltration storage increases with cover thickness, the effect of evaporation decreases. The result is that as the cover thickness increases so too does the potential for seepage.
- Conversely if the cover thickness is too thin then there is insufficient infiltration storage capacity, resulting in more rapid development of near saturated conditions correlating to an increase in the seepage potential.
- The preferred cover is the 0.6 m cover, since it provides the best balance between infiltration storage and evaporation effect resulting in the lowest recorded seepage.

Finally it is important to note that the results presented represent a worst case scenario, and it is expected that the preferred cover (0.6 m) will perform better at a field scale, since the cover will be vegetated and the mine is located in a semi- arid environment, resulting in a highly unsaturated cover for most of the year.

4.0 CONCLUSIONS

The mine has five years of mining until closure and is currently in the process of developing a rehabilitation plan for the TSF that will allow the domain to transition to a future land use. The mine has identified during rehabilitation planning that it can improve the rehabilitation outcomes for the TSF and MIA resulting in a thicker cover for the TSF by utilising accretion from the MIA as part of the cover.

Regional experience at CSA Mine and PGM indicates that an appropriate cover thickness is likely between 0.4 m to 1 m.

Column trials for three cover thicknesses (0.4 m, 0.6 m and 0.8 m) have been run and have resulted in a maximum probable water balance for each cover. The results indicate that the 0.6 m cover is the preferred cover option. The results presented represent a worst case scenario, and it is expected that the preferred cover will perform better at a field scale, since

the cover will be vegetated and the mine is located in a semi- arid environment, resulting in a highly unsaturated cover for most of the year.

The preferred cover has been scaled up to a field scale cover trial, and there are plans to assess the cover performance for a number of seasons followed by modeling using Vadose/w calibrated using both the column trial and field scale trial performance data.

5.0 REFERENCES

Bowen HJM (1979) 'Environmental Chemistry of Elements'. (Academic Press: New York)

CSA Mine (2015) 'CSA Mine Annual Environmental Management Report'. Available at http://www.csamine.com.au/uploads/51687/ufiles/AEMR_2015_-_Final_Version.pdf

DnA Environmental (2012) '2012 Rehabilitation Monitoring Report' Report prepared for CBH Resources Ltd

DnA Environmental (2013) '2013 Rehabilitation Monitoring Report' Report prepared for CBH Resources Ltd

International Network for Acid Prevention (INAP) (2009). 'The Global Acid Rock Drainage Guide'. Available at <http://www.gardguide.com>.

Rohde T, Williams, DJ and Burton, J (2011) 'Store and release cover performance at Cadia Hill Gold Mine, Australia', in Proceedings Sixth International Conference on Mine Closure, 18-21 September 2011, (Eds A Fourie and M Tibbett), pp. 333-343. (Perth: Australian Centre for Geomechanics).

Schneider AC (2012) 'Plant-soil relationships in constructed covers of mine waste material'. PhD thesis

CONTROLLING ACID AND METALLIFEROUS DRAINAGE FROM DECOMMISSIONED UNDERGROUND MINES

**N. Bourgeot^A, J. Taylor^A, A. Sampaklis^B, N. Staheyeff^B, S. Pape^A, E. Hardjo^A and
M. Quiatol^A**

^AEarth Systems, 14 Church St., Hawthorn, VIC 3122, Australia

^BNSW Department of Planning and Environment, 516 High St., Maitland, NSW 2320,
Australia

ABSTRACT

Operating and decommissioned underground mines can contribute a substantial amount of acid and metalliferous pollution to waterways worldwide. The key sources of pollution include unsaturated sulfidic materials in void wallrock and backfilled waste rock. Potential management measures are limited to passive or active treatment in perpetuity, or the installation of pressure bulkheads. Bulkheads are designed to facilitate flooding of the sulfidic materials to halt acidity generation, but are prone to chronic and catastrophic failure.

An alternative strategy has been developed and is currently being implemented at two decommissioned, polluting mine sites in New South Wales (NSW), supported by the Derelict Mines Program of the NSW Department of Planning and Environment. The sites are the Nevada Au mine and the Sunny Corner Ag-Pb-Zn mine, both located in the Daylight Creek catchment near the township of Sunny Corner. The strategy involves a two-stage process to remove oxygen from mine void atmospheres and replace it with an inert gas phase. In the absence of oxygen, sulfide oxidation and acidity generation cannot proceed.

Stage 1 involves the identification and isolation of all significant air entry points into the mine void. This usually includes features such as shafts, adits, declines, stopes, glory holes, subsidence zones and drill holes. Air entry control works need to retard oxygen addition to the mine voids, but not prevent water discharge. Once air entry points have been managed with appropriate earthworks and materials, the oxidation of sulfides within the mine can passively decrease internal oxygen concentrations. If the rate of internal oxygen consumption exceeds the rate of oxygen resupply, then net reductions in acidity generation can occur. Acidity (pollution) reductions of around 60-70% are considered possible following Stage 1 air entry control works. Barometric pumping or the breathing of the mine due to changing weather fronts is the prime control on oxygen resupply to isolated mine voids. Hence, if required, Stage 2 works include the active injection of small quantities of an inert gas (e.g. nitrogen or carbon dioxide) into the mine void to overcome barometric pressure gradients that act to intermittently resupply the void with air (i.e. 20.9 vol.% O₂), during high pressure climatic events.

Early results from the Nevada mine already demonstrate a 60% reduction in the acidity (acid and metals) generated from the site within 6 months of completing Stage 1 works. Key water quality data including pH, EC, acidity and metal concentrations are presented and discussed. Stage 1 works have also been completed at the Sunny Corner mine, and a 50% reduction in acidity load has also been achieved to date. These results clearly demonstrate the major water quality benefits of the Inert Atmosphere Technology for lowering pollution discharges from decommissioned underground mines at low cost.

1.0 INTRODUCTION

Tens of thousands of operating and decommissioned underground mines worldwide are ongoing sources of acid and metalliferous drainage or acid rock drainage (AMD/ARD) pollution. The key sources of pollution in recent and historic underground mines include unsaturated sulfidic materials in void wallrock and waste materials such as sulfidic waste rock and tailings that are often backfilled in the mine voids to facilitate mining or waste disposal. Sulfidic waste rock, rather than wallrock, is most commonly the primary source of AMD in underground mines (DIIS, 2016).

Many decommissioned underground mine sites are in remote areas and are left to pollute receiving waters with AMD due to the lack of cost effective solutions. The two key management measures are the installation of pressure bulkheads to flood reactive sulfidic materials and the active treatment of the AMD in perpetuity. These measures tend to be adopted only at a limited number of sites, where pollution generation is affecting sensitive receiving environments.

Pressure bulkheads are being used increasingly in coal mines, where the hydraulic heads are relatively low. The catastrophic failure of pressure bulkheads is limiting their uptake and increasing the requirement for improved engineering designs, improved construction methods and ongoing monitoring (Harteis et al., 2005; Mutton and Remennikov, 2011). In general, pressure bulkheads are regarded as moderate cost, relatively high risk and only moderate success structures. In comparison with pressure bulkheads, water treatment in perpetuity is normally regarded as a relatively high cost, low risk and high success management strategy.

2.0 INERT ATMOSPHERE TECHNOLOGY

A new low-cost, low risk and high success approach to lowering or preventing AMD from underground mines has been devised by Earth Systems to address the short-comings of the limited management options outlined above. This new approach is based on leading practice "atmosphere control technology" that aims to remove oxygen from mine void atmospheres and replace it with an inert gas phase. This technology was first introduced as a reducing atmosphere technology by Taylor and Waring (2001). In the absence of oxygen, sulfide oxidation and acidity generation cannot proceed. The mine void gas composition is controlled via a two-stage process:

- Stage 1: Identification and treatment of all significant air entry points into the mine void, including features such as shafts, adits, declines, stopes, glory holes, subsidence zones and drill holes. This Stage aims to passively lower oxygen concentrations within the mine due to oxygen consumption from internal pyrite oxidation. Air entry control works need to retard air re-supply to the mine void, but not prevent water discharge.
- Stage 2: Active injection of small volumes of an inert gas (e.g. nitrogen or carbon dioxide) into the mine void to overcome leakage or barometric pressure gradients that act to intermittently resupply the void with air (i.e. 20.9 vol.% O₂), during high pressure weather events.

Following the air entry control works, the initial control on void oxygen concentrations is provided by the sulfidic materials within the void. As long as the rate of oxygen consumption by sulfidic waste exceeds the rate of oxygen re-supply through the mine air entry control structures and fractured rock carapace surrounding the mine, then net reductions in acidity

generation can occur passively. The extent to which this can happen is expected to be a function of:

- The mass of unsaturated sulfidic material in the void, including wallrock and backfilled material.
- The pyrite concentration (wt.% FeS₂) and pyrite oxidation rate (POR, wt.% FeS₂ / year) of unsaturated sulfidic material backfilled in the void.
- The depth of air entry into unsaturated, in situ sulfidic wallrock material in the void, and hence the volume of void wallrock exposed to oxidising conditions.
- The relationship between POR and variables such as oxygen concentration, moisture content and void temperature, for both backfilled waste materials and in situ wallrock.
- Local geological and hydrogeological properties of materials surrounding the void, and the effectiveness of the air entry control works (Stage 1 program).
- Local rainfall and infiltration characteristics of the site, and/or the extent to which the mine void has been flooded.
- The extent of internal methane and/or carbon dioxide production from the anaerobic decomposition of structural timbers or coal seam gas, or the production of carbon dioxide via limestone neutralisation.
- Local pressure gradients and the associated extent of barometric pumping, or the “breathing” of the mine, due to changing weather fronts. This is considered to be the prime control on oxygen resupply to sealed mine systems.

The extent of barometric pumping, and other site-specific factors listed above, determines the requirement, if any, to proceed with Stage 2 works.

The inert atmosphere technology outlined above is currently being implemented at two decommissioned, polluting mine sites in New South Wales (NSW), supported by the Derelict Mines Program of the NSW Department of Planning and Environment. The sites are the Nevada gold mine (Earth Systems, 2017a) and Sunny Corner silver-lead-zinc mine (Earth Systems, 2017b) and are presented as case studies below, with early results illustrating the benefits of inert atmosphere installations and their potential application to numerous other polluting underground mines throughout the world.

3.0 CASE STUDY – NEVADA MINE SITE

The Nevada site is a legacy gold mine located in Central West NSW, approximately half way between Lithgow and Bathurst, near the town of Sunny Corner. The site is located on NSW State Forestry land, within the steep valley of Daylight Creek. Vehicle access to the site is generally limited to 4WD light vehicles, due to track condition, and there is no power, mobile phone reception or other services available on site. The site features a main adit and several remnant surface features from the historic operation. These include smelter pads, small waste rock and slag piles and old shafts and stopes.

Water discharge from the site occurs solely from the main adit (Plate 1) at a rate of 1-5 litres per minute. AMD is clearly visible in drainage from the main adit, having discoloured the

riverbank immediately downstream. Prior to 2017, the drainage pH ranged from 3.0-4.0, with an electrical conductivity (EC) that peaked at ~2,400 $\mu\text{S}/\text{cm}$.



Plate 1. AMD from the main adit at the Nevada mine site, prior to remediation works.

Key components of the inert atmosphere system installation program at the Nevada mine site included:

- Site survey and earthworks to enable detailed investigation of the main adit.
- Air-entry and drainage system control works at the main adit.
- More extensive air-entry control works at other locations at the site, including a shaft and several subsidence fractures at the ground surface.
- Installation of monitoring equipment in the mine void to quantify void gas composition and internal pressure and temperature.

The earthworks fleet consisted of a 9-tonne excavator, 4 tonne front tipping dump truck and a 20-tonne dump truck. Most natural geological materials were sourced from a State Forestry quarry located on Bob's Creek Rd, approximately 7 km from the work area. Air entry control earthworks were conducted at six areas in total, three of which could be accessed via existing tracks, with temporary tracks established for the remaining three areas.

Earthworks at the main adit area revealed an opening approximately 1.5 metres high and 1 metre wide. The walls and roof of the drive were partially collapsed with no direct visibility into the workings beyond approximately 5 metres.

During excavation, some existing mine water was discharged from the adit and treated in-situ using hydrated lime. A trench was dug across the road and a water discharge control pipe was installed 10 metres into the void, with an outlet to the Daylight Creek river bank directly opposite the adit. The discharge pipe incorporated a U-bend to prevent air entry back into the adit via the pipe, and two access points for pipe maintenance if ferrihydrite precipitation becomes a flow restriction issue. Imported clay materials were blended with commercial bentonite to seat the adit discharge pipe and form the basis for the adit seal. Adit sealing works were capped with gravel armour to protect the adit entry earthworks from erosion.

Air entry control works were completed over shafts, stopes and subsidence cracks using a combination of local and imported materials. Prior to all engineering works, all loose surface material was removed to expose the opening, or bare rock surrounding the adit opening.

A 100mm diameter PVC pipe was installed into one of the larger subsidence cracks, approximately 8 metres upgradient of the main adit, prior to completing earthworks in this area. Monitoring instruments were installed in this pipe to measure and record the mine void gas composition (oxygen and carbon dioxide), temperature and pressure.

All sensors were mounted into a custom fabricated 75 mm PVC housing that permitted lowering of the sensor assembly into the 100 mm PVC pipe. The sensor assembly was connected via cable to an external data logger. All cable connections were made via hermetically sealed terminals to prevent gas leakage. All monitoring sensors and the dataloggers are powered by 12V DC batteries and enclosed within a steel, tamper-proof enclosures fitted onto a concrete pad (e.g. Plate 2).

A weather station installed at the Sunny Corner Mine site was used to provide local ambient climate data (i.e. rainfall, pressure, temperature, wind speed and wind direction) for the Nevada (and Sunny Corner) site. This instrument was connected to a data logger with cellular telemetry capability, with surge protection equipment installed to prevent damage from high voltage surges such as lightning strikes.

Baseline monitoring of the adit drainage water chemistry was conducted in January 2017, with follow-up monitoring conducted from April 2017 onwards (pH, EC, ORP and acidity monthly and major ions and metals every 2 months). Continuous monitoring of void gas composition and internal pressure and temperature data commenced in mid-2017. Monitoring will continue for 24 months to evaluate the performance of the air entry control works and to inform the need for Stage 2 inert gas injection works.

Figure 1 provides key pH, EC and acidity concentration data for the main adit drainage, before and after completing Stage 1 of the inert atmosphere system installation. Data collected in January 2017 represent baseline chemistry for the site. The key results include:

- A step-wise improvement in discharge water chemistry is evident following the air entry control activities. Since these works the acidity of adit discharge decreased by close to 70% from 1,240 mg/L CaCO₃ (17/1/17) to 360 mg/L CaCO₃ (25/9/17). The EC decreased by approximately 50%, from 3.0 mS/cm to 1.5 mS/cm, over the same period.
- There is a strong correlation between EC and acidity data. The relationship between pH and acidity is more complex, and often large changes in acidity are required to produce even small changes in pH.

Consistent with the results presented in Figure 1, most metals present in the water exhibited decreasing trends since January 2017. The largest decreases have been observed in iron (from 111 mg/L on 17/1/17 to 13.6 mg/L on 28/8/17) and zinc (from 475 mg/L on 17/1/17 to 174 mg/L on 28/8/17).



Plate 2: Gas monitoring instrumentation and enclosure typical of that at the Nevada and Sunny Corner mine sites.

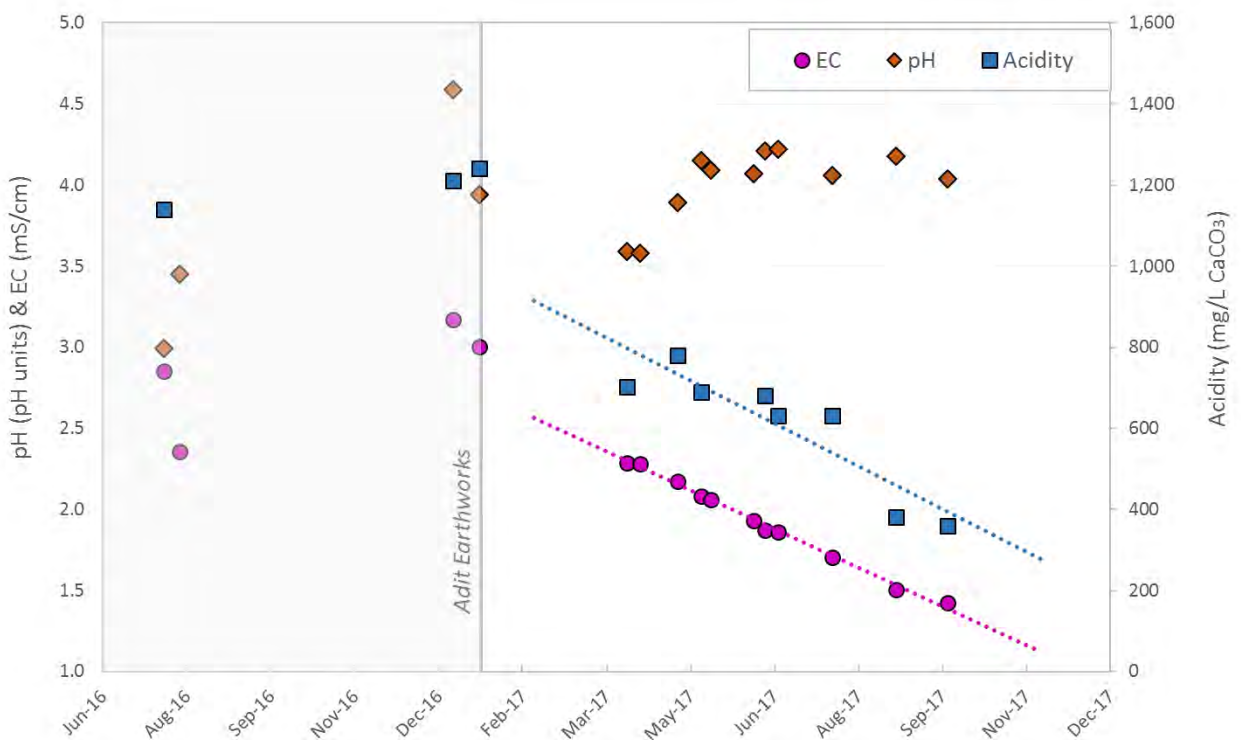


Figure 1: pH, EC and acidity data for the Nevada Mine site.

Key results from the void gas monitoring data reviewed to date indicate that:

- The mine void exhibits low oxygen concentrations and the rate of oxygen supply to the void is being substantially limited as a result of the earthworks program.
- Trends in oxygen concentrations appear to be associated with barometric pumping of air in and out of the workings. That is, when a low-pressure (climatic) system moves over the area, air is drawn out of the mine to equilibrate with the atmospheric pressure. Conversely, when the atmospheric pressure increases, air is forced into the mine void to equilibrate with atmospheric conditions.

The following conclusions can be drawn from the Nevada mine site case study to date:

- Following Stage 1 earthworks, the adit discharge water chemistry data is showing major decreases in pollution release the site. Clear decreasing trends in mine water discharge acidity and salinity are evident. Current acidity concentrations are close to 70% lower than baseline concentrations, and salinity concentrations have dropped approximately 50% over the same period. As expected, most metal concentrations have also decreased, particularly iron and zinc.
- The air entry and discharge control activities have resulted in the lower void oxygen concentrations that are responsible for rapid and sustained decreases in pollution from the site.
- Pollution concentrations are expected to decrease further; however some residual AMD is likely to persist from the site due to minor unavoidable air ingress via barometric pumping. An active inert gas generation system (Stage 2) would overcome this effect and prevent the residual AMD.

The results obtained to date provide clear validation that the inert atmosphere technology can substantially lower pollution from decommissioned underground mine sites.

4.0 CASE STUDY – SUNNY CORNER MINE SITE

A larger scale and more complex inert atmosphere installation is currently underway at the Sunny Corner mine site in NSW. Stage 1 works were completed in May 2017. This site also drains to Daylight Creek, approximately 2 kilometres upstream of the Nevada mine drainage confluence. Early monitoring results from the Sunny Corner mine site are very encouraging, indicating that:

- Oxygen concentration within the northern parts of the workings (near the main adit discharge point – Level 4 Adit) are significantly lower than atmospheric oxygen concentrations (3-10 vol.%). Some limitations on air re-supply to the southern parts of the workings are also evident in the water quality monitoring data.
- Flow rates from the Level 4 Adit (as measured via a v-notch weir) have decreased from ~1.5 L/s (November 2016) to ~0.7 L/s (June 2017), largely due to air entry control works (refer to Figure 2).
- Since completion of earthworks in May 2017, the adit drainage pH has been slowly increasing, and the salinity has been slowly decreasing over time, despite decreasing

flow rates. EC correlates well with acidity concentrations, reflecting small decreases in acidity over time. In the future, remotely-monitored continuous EC data (combined with pH and flow rates) could be used as the primary measure of rehabilitation success.

- A progressive long-term decrease in redox potential (Eh) of the mine drainage (700 mV in November 2016 to 510 mV in 25/9/17) appears to be consistent with observed decreases in oxygen concentrations within the void.
- The acidity load discharged from the Level 4 Adit has decreased significantly from approximately 60 tonnes H_2SO_4 -eq per year (November 2016) to approximately 24 tonnes H_2SO_4 -eq per year (August 2017) (refer to Figure 2). This decrease is considered largely attributed to the decrease in mine water discharge resulting from the air entry earthworks that are likely to have significantly altered the mine hydrology.
- A more delayed improvement in drainage water quality is expected at the Sunny Corner site, relative to the Nevada site, due to the substantially higher volume of stored AMD water that will need to be progressively flushed from the Sunny Corner mine void.

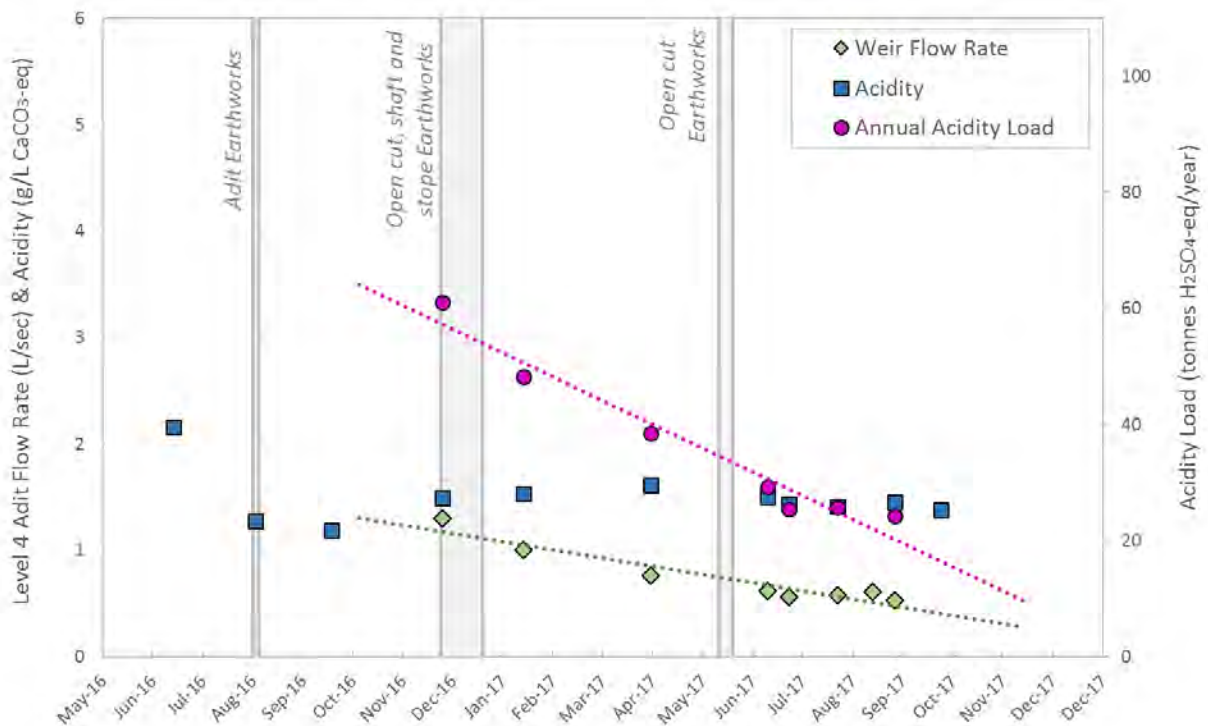


Figure 2: Level 4 Adit flow rate, acidity concentration and calculated annual acidity load equivalent from the Sunny Corner Mine site.

5.0 CONCLUSIONS

Substantial improvements in underground mine drainage water chemistry can be achieved in less than 3 months, with further improvements over time following the initial stage of an inert atmosphere installation, as highlighted by data from the Nevada mine site in NSW. Early results from the larger scale and more complex inert atmosphere installation at Sunny Corner

are also very encouraging, but water chemistry improvements are slower. This is because there are significant volumes of stored AMD in the mine voids at Sunny Corner, retarding rapid improvements in the water chemistry and masking the apparent effectiveness of the air entry control works in the short term. However, at both sites the observed adit drainage quality improvements in such a short timeframe have exceeded expectations.

Monitoring results to date have already provided an improved understanding of key controls on the behaviour of mine void aqueous geochemistry and gas compositions at both sites. Additional monitoring data collected over the next 24-months will enable a more comprehensive evaluation of the performance of both Stage 1 inert atmosphere installations.

While further improvements in adit drainage water chemistry can be expected throughout this period, it is predicted that inert gas injection will be required to completely prevent AMD generation at both sites.

The broader implications of early results from the Nevada and Sunny Corner mine site case studies are that:

- Substantial reductions in pollution loads can be achieved from historic and temporarily decommissioned underground mines worldwide, by implementing strategic air entry and drainage control (Stage 1) works.
- AMD generation from underground mines can likely be fully prevented with inert gas injection installations, following the Stage 1 works.
- The cost of an inert gas injection system powered by renewable energy sources (e.g. wind or solar) is expected to dramatically lower the cost of managing AMD from underground mines relative to treatment in perpetuity.
- Inert atmosphere system installations offer a promising alternative to current treatment in perpetuity approaches for underground mine drainage. This approach will be substantially lower cost by avoiding the need for reagent manufacture and transport, full time personnel requirements and sludge management.

6.0 REFERENCES

DIIS (2016). *Preventing Acid and Metalliferous Drainage – Leading Practice Sustainable Development for the Mining Industry*. Australian Federal Government, Department of Industry and Science, Canberra, Australian Capital Territory.

Earth Systems (2017a). *Nevada Inert Atmosphere System Installation: Report on Stage 1A Activities*. Prepared for the NSW Department of Planning and Environment – Derelict Mines Program. September 2017.

Earth Systems (2017b). *Sunny Corner Inert Atmosphere System Installation: Report on Stage 1A Activities*. Prepared for the NSW Department of Planning and Environment – Derelict Mines Program. September 2017.

Harteis, S P, Dolinar, D R and Taylor, T M, (2005). *Guidelines for Permitting, Construction and Monitoring of Retention Bulkheads in Underground Coal Mines*, IC 9506, NIOSH, Department of Health and Human Services, CDC.

Mutton, V. S. and Remennikov, A. M., (2011). Design of Water Holding Bulkheads for Coal Mines, 11th Underground Coal Operators' Conference, University of Wollongong & the Australasian Institute of Mining and Metallurgy, pages 257-268.

Taylor, J. and Waring, C., 2001, The Passive Prevention of ARD in Underground Mines by Displacement of Air with a Reducing Gas Mixture: GaRDS. Mine Water and the Environment, Technical Communication, Vol. 20, pages 2-7.

REHABILITATION OPTIONS FOR POTENTIALLY CONTAMINATING COAL TAILINGS STORED IN PITS

^AD.J. Williams

^AThe University of Queensland, Brisbane, QLD 4072, Australia

ABSTRACT

Over the last decade, as surface tailings storage facilities (TSFs) have become more difficult to permit, and with the availability of completed pits, New South Wales and Queensland coal mine operators have turned to the use of completed pits to store coal tailings. However, pits have a very different geometry to surface TSFs in the flat Australian topography, typically having a large footprint area and relatively shallow depth. Pits have a substantial depth and a relatively small areal footprint. As a result, the rate of rise of slurried coal tailings is typically magnified by about an order of magnitude in a pit compared with that in a surface TSF, particularly at the start of deposition due to the reduced footprint at the base of the pit. The high rate of rise of slurried coal tailings in a pit will likely lead to underwater deposition, and not allow full consolidation of the tailings, which will limit the dry density and shear strength achieved. Further, in-pit tailings are likely to remain largely covered by supernatant water, due to the difficulty of recovering water and reduced evaporation. Hence, exposure of the tailings surface to evaporation and desiccation will be limited. Lastly, evaporation of the supernatant water will concentrate salinity, and any acid and metalliferous drainage generated from sulfidic tailings. The paper describes the nature of slurried coal tailings deposited in-pit and outlines the unintentionally limited options for closure and rehabilitation.

1.0 INTRODUCTION

The disposal of slurried coal tailings in surface TSFs was, until the last decade, the most common practice in the coal mines of New South Wales and Queensland. Coal tailings have conventionally been disposed in surface TSFs as a slurry at about 25% solids by mass.

The conventional disposal of slurried tailings in surface TSFs is coming under increasing resistance. Among the reasons for this are ongoing TSF failures. Azam and Li (2010), in reviewing 218 tailings dam failures worldwide over the last 100 years, identified the following vulnerabilities to failure:

- dam construction using mine wastes;
- sequential dam raises together with an increase in tailings production;
- lack of regulations on design criteria, particularly in developing countries; and
- high maintenance cost post-closure.

Azam and Li (2010) found that the average tailings dam failure rate over the last 100 years is 1.2% or 2.2/year, which is more than two orders of magnitude higher than that reported for water retention dams of 0.1%.

Surface TSFs also cover ever-larger footprints as tailings volumes increase exponentially, and tailings become increasingly more fine-grained. There is escalating community concern about mining in general, and tailings dams in particular, despite attempts to label them as TSFs. This has led to regulatory resistance to approving conventional surface slurried tailings disposal for

coal mine expansions and new coal mining projects, particularly in the New South Wales coalfields. Further, there is concern about the depletion of scarce water resources.

Since existing tailings thickeners were set up to produce tailings slurry at about 25% solids by mass, the enforced move to tailings disposal into completed pits occurred at the same tailings consistency. However, the high rate of rise of tailings in-pit limits consolidation, and disposal underwater and reduced evaporation (perhaps half that occurring in surface TSFs due to shading and reduced wind) prevents desiccation. In some cases, an attempt is made to thicken the coal tailings, to decrease their rate of rise on in-pit deposition. However, the effectiveness of thickening is largely a function of the type and proportion of clay minerals present, with smectite being the most problematic. A typical in-pit coal tailings storage is shown in Fig. 1.



Fig. 1. Typical in-pit coal tailings storage

The supernatant water overlying in-pit coal tailings will be exposed to evaporation, albeit at a reduced rate compared with evaporation from water on the surface. However, this tends to concentrate salinity, and to concentrate any acid and metalliferous drainage that is generated from sulfidic tailings. The source of sulfides could be of organic or natural origin, including pyrite where the coal was formed under marine deposition. Provided that the water level in the pit remains below the groundwater table during tailings deposition, the pit will remain a “sink” for contaminated water.

On the cessation of tailings deposition, and provided that excess surface runoff is not directed to the pit, ongoing evaporation should sustain the pit as a sink. However, the soft, water-covered in-pit tailings deposit will be difficult to close and cap for rehabilitation and future land use purposes. Retaining a pit lake, representing a sink for poor quality water, could be the only viable post-deposition option. Closed surface and in-pit coal tailings storages are both required to be safe, stable and non-contaminating, and to meet the agreed post-mining land use. This challenge faces mine operators and regulators, and must address the concerns of a cynical community. Failure to address these concerns threatens the coal mining industry’s financial and social licence to operate and to initiate coal mine expansions and new projects.

2.0 POSSIBLE MEANS OF CAPPING UNCONSOLIDATED IN-PIT TAILINGS

It is generally the expectation of the community and regulators that both surface and in-pit coal tailings storages be capped to cover the tailings and to facilitate some post-mining land use and/or ecological function. The purpose of the cover is to isolate the underlying coal tailings from the receiving environment, particularly if they are saline or potentially acid forming. This would require a cover that either prevents evaporation-driven salt migration from the tailings to the root zone of the future revegetation, and/or excludes oxygen ingress and/or rainfall infiltration into the tailings. Such a cover would be difficult to achieve even on a firm foundation, and is even more difficult on unconsolidated, in-pit coal tailings.

The physical impediments to capping in-pit coal tailings are discussed in the following section, followed by a discussion of possible methods of placing a cover over unconsolidated, in-pit coal tailings. These include hydraulically-placing or pushing cover material over soft, wet coal tailings, dozing cover material over desiccated coal tailings, and the use of geotextile and geogrid layers. Examples of these possible capping methods are described.

2.1 Physical Impediments to Capping In-Pit Coal Tailings

Coal tailings deposited in a flooded pit and maintained below water can at best settle and consolidate under their self-weight, which is also limited by the low specific gravity of coal tailings (typically less than 2.0). If the rate of rise is high, the tailings may not fully consolidate. Tailings that consolidate below water under their self-weight alone develop effective stress and shear strength profiles from zero at the tailings surface, increasing linearly with depth at a rate dependent on the specific gravity of the tailings solids and the degree of consolidation (Williams, 2015). Close to the surface, coal tailings would be expected to consolidate under their self-weight to a dry density of about 0.6 t/m³ at most (up to about 47% solids by mass, and down to about 75% water by volume). The near-surface state is most relevant to the capacity of the tailings to support a capping layer. For this dry density, the fully-consolidated rate of increase with depth of effective stress would be about 4 kPa/m depth. For normally consolidated conditions (underwater), the corresponding increase in the peak shear strength developed with depth is about 0.25 times the effective stresses, or about 1.0 kPa/m depth.

Figure 2 shows the expected profiles of shear strength with depth for the following cases:

- self-weight consolidation with the water table always at or above the coal tailings surface, which would be expected with in-pit deposition;
- desiccation due to surface drying by solar and wind effects, accompanied by an assumed drop in the water level to 2 m below the coal tailings surface, which could occur on removal of the supernatant water at the cessation of in-pit deposition but is effective to only shallow depth with its effectiveness dropping off exponentially with increasing depth; and
- increased shear strength due to subsequent loading of the desiccated coal tailings surface by 2 m of cover material, assuming that it can safely be placed and that excess pore water pressures generated in the tailings by the loading imposed by the fill have fully dissipated, noting that capping over a large area is effective to the full depth of the tailings.

2.2 Hydraulically-Placed Cover

Coarse-grained cover material could be placed hydraulically, even over soft coal tailings. However, the tailings beach would need to be shallow and free of supernatant water so that the cover material would “daylight”. Further, durable, coarse-grained cover material such as sandstone spoil or coarse reject would be required, to facilitate drainage of the loaded tailings, and this material would be difficult and expensive to pump. With hydraulic placement, the coarse-grained material essentially “floats” on the tailings. The coarse-grained material forms a steep beach at about 1 in 10, and the pipe discharge would need to be moved out as sufficient thickness of coarse-grained material is achieved. The layer of coarse-grained material loads, consolidates and strengthens the underlying tailings, enabling further material to be placed. The required cover thickness of 2 m would increase the shear strength of the tailings by about 10 kPa. However, the coarse-grained cover would not be compacted and hence it would not be a very effective sealing layer over the coal tailings.

Fine-grained and/or degradable cover material would not facilitate drainage of the loaded tailings, and clay minerals may be prone to dispersion, potentially leading to break down and softening of the cover material on hydraulic placement. Again, the cover would not be compacted, and hence it would not be a very effective sealing layer over the coal tailings.

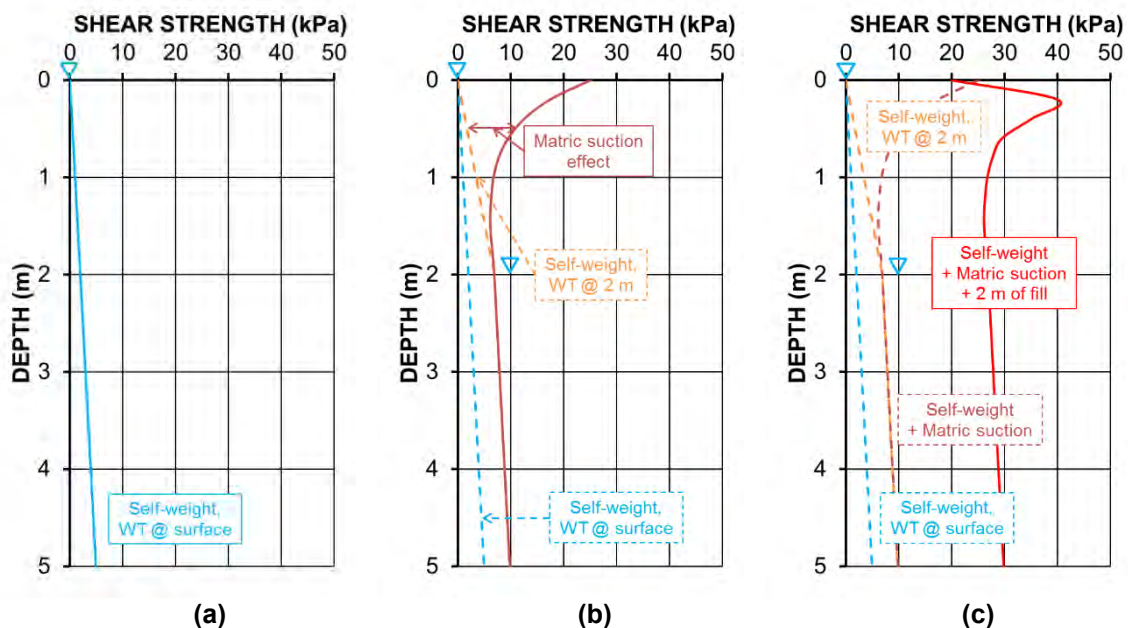


Fig. 3. Expected profiles of peak shear strength with depth for: (a) underwater, self-weight consolidation, (b) desiccation, and (c) increased shear strength due to subsequent loading

2.3 Pushed Cover

Coarse-grained cover material could be pushed from a stable base into soft tailings, including soft tailings underwater (see Fig. 3; Williams and King, 2016). However, the tailings beach would need to be shallow, and the water depth should normally be limited. In addition, durable, coarse-grained spoil or coarse reject would be required to facilitate drainage of the loaded tailings and to form a stable cover. End-dumped, coarse-grained cover material would displace water from the tailings to the surface, and the coarse particles would find their own level forming a stable mixture of coarse and tailings to a depth of perhaps 3 to 5 m below the original surface of the coal tailings. This advancing mixed layer of coarse-grained cover material and

tailings would likely support a D9 Dozer and additional fill, and would consolidate and strengthen the underlying tailings. The mixture would provide a reasonable sealing layer over the coal tailings.

2.4 Dozed Cover over Desiccated Coal Tailings

Substantial desiccation would be required to achieve adequate tailings shear strength to support a dozer and a nominal height of cover material. Ideally, progressive desiccation of the tailings should be allowed, as each layer of tailings is deposited. Tailings deposited and maintained underwater would need to be sequentially drained of supernatant water and allowed to desiccate. Placing a cover by dozing material over desiccated tailings is normally applied to a relatively flat (nominally 1%) tailings beach. Fine-grained and/or clay mineral-rich coal tailings have a low hydraulic conductivity that would inhibit desiccation and crusting. Desiccation crusting of the final surface of the tailings deposit only may take a considerable time and may not occur to sufficient depth to support even a D6 Swamp Dozer and a nominal thickness of fill. If a cover can be successfully placed, it could provide a reasonable sealing layer over the coal tailings.

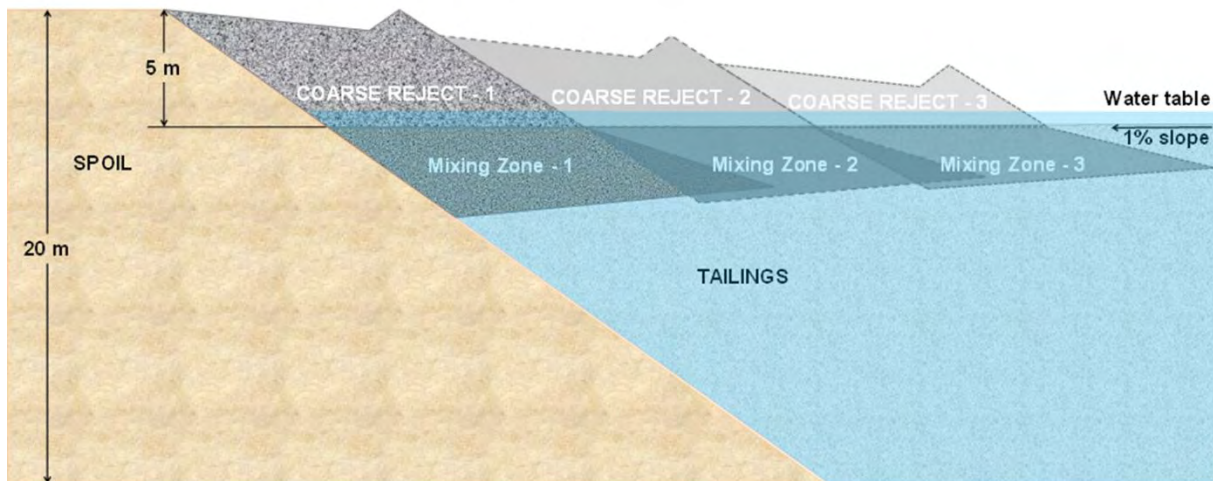


Fig. 3. Schematic of capping soft, underwater in-pit coal tailings

The fill height H that may safely be placed on adequately desiccated coal tailings by pushing using a D6 Swamp Dozer, without causing remoulding and “bow-waving”, is given by (adapted from Williams, 2005):

$$H = (N_c s_v / F \gamma) - H_e \quad [1]$$

= $0.190 s_v - 1$, where s_v represents the average shear strength of the coal tailings overall;
and

= $0.226 s_{v2} - 1$, where s_{v2} represents the average shear strength of the lower, softer layer in two-layer idealisation.

where N_c is a bearing capacity factor (= 5.14, assuming that a strip of fill is pushed over a broad front, and the shear strength of the coal tailings may be taken as uniform, or 6.1 applied to the shear strength of the layer below the desiccated crust for a two-layer idealisation); s_v is the representative shear strength of the coal tailings overall or the shear strength of the layer below the desiccated crust for a two-layer idealisation; F is the adopted factor of safety (a

minimum of say 1.5); γ is the unit weight of the fill (say 18 kN/m³); and H_e is the equivalent height of fill corresponding to the average bearing capacity of the D6 Swamp Dozer (say 1 m).

If the surface desiccation crust is too thin, the tailings beneath the crust (where a perched water table would be expected) will be soft and prone to remoulding, leading to a drop in shear strength of 2 to 3-fold or more, and the rapid and uncontrolled formation of a bow-wave failure on fill placement. If the D6 Swamp Dozer operator feels the initiation of a bow-wave, the dozer should immediately be turned off to stop engine vibrations, and the dozer operator should get off the machine. The excess pore water pressures generated by fill placement will dissipate relatively rapidly (over 1 to 4 weeks, depending on the hydraulic conductivity of the coal tailings, affected by their particle size distribution and clay mineral content), after which the dozer should be safe to move, and fill placement can recommence.

The peak shear strength of loaded coal tailings will increase as they drain, according to Williams (2005):

$$\Delta\tau = \Delta\sigma' \tan \phi' \quad [2]$$

= 10 H on full drainage after about 1 to 4 weeks, depending on the hydraulic conductivity of the coal tailings.

where $\Delta\tau$ is the increase in shear strength of the loaded coal tailings; $\Delta\sigma'$ is the increase in vertical effective stress on dissipation of the equivalent excess pore water pressure; and ϕ' is the drained friction angle of the coal tailings.

2.5 Use of Geotextiles and Geogrids

Under-desiccated tailings could possibly be covered by geotextile and geogrid layers, with the overlapping layers cable tied to avoid gaps developing, providing support for filling in thin layers placed by very small equipment. However, placement of the geotextile and geogrid layers requires that the tailings surface be safely trafficable for this purpose. The placement of fill would largely displace water, with little change in the elevation of the tailings surface and rapid and uncontrolled bow-waving ahead of the fill. If a cover can be successfully placed on geotextile and geogrid layers, it could provide a reasonable sealing layer for the coal tailings.

3.0 EXAMPLES OF CAPPING UNCONSOLIDATED IN-PIT COAL TAILINGS

There is no known example of a soil cover being placed hydraulically on soft coal tailings in a flooded pit.

At New Acland Coal Mine in South-East Queensland, durable and free-draining coarse reject was successfully pushed from the highwall into soft tailings in a flooded pit to facilitate a cover (see Fig. 4; Williams and King, 2016). It proved more successful than dozing coarse reject over desiccated tailings, which tended to bow-wave.

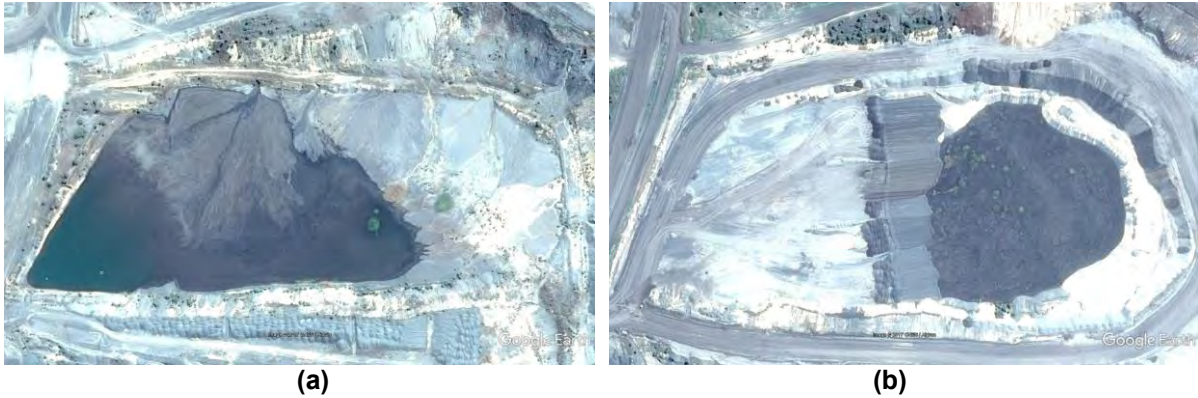


Fig. 4. Capping water-covered, soft in-pit coal tailings by end-dumping coarse reject at New Acland: (a) March 2014 before capping, and (b) progress of capping in September 2016 (Google Earth)

Figure 5 shows the placement of the initial 1 m thick cap of coarse reject on the surface TSF at New Acland (Williams and King, 2016). Preceding placement, the peak and remoulded shear strength profiles of the coal tailings ahead of the placement were determined using a shear vane to confirm that the 1 m fill height and D6 Swamp Dozer (with a track bearing pressure of about 36 kPa, equivalent to about 1 m height of fill) could safely be supported. Care was taken to avoid hydraulic fracturing and bow-waving. Once the first 1 m cap had been placed, it was followed up by a further 2 to 3 m of clayey spoil placed by D9 Dozer. The final cover layers were further clayey spoil to achieve a final landform, and topsoil that will be grassed for a grazing post-mining land use, as required by the Environmental Authority. Figure 6 shows aerial views before and after capping.



Fig. 5. Capping New Acland surface TSF: (a) pushing coarse reject by D6 Swamp Dozer, and (b) rising water table and drainage on capping



Fig. 6. Capping New Acland surface TSF: (a) August 2009 before capping, and (b) almost completed capping in February 2016 (Google Earth)

Wambo Coal Mine in New South Wales attempted to cap smectite-rich coal tailings deposited into a completed pit (Fig. 7). The tailings were still slurry-like (under-consolidated and undesiccated), and geotextile and geogrid layers were first rolled out across the width of the pit and anchored at each side. A further layer of geogrid was then placed lengthwise along the pit. The overlapping layers were cable tied at 15 cm centres. The cost of supplying the geotextile and geogrid for the 24 ha area was about \$3.5 million (about \$150,000/ha), not counting the laying cost. Placing and cable tying the geotextile and geogrid layers raised safety issues.

Fill was then pushed in a 300 mm thick layer using a D2 Dozer. The use of a very small dozer was necessitated by the very low bearing capacity of the very soft tailings, even with the geotextile and geogrid layers. The fill largely displaced water, with little change in surface elevation, and rapid and uncontrolled bow-waving ahead of the fill. Eventually, the capping project was abandoned. The projected cost of this capping method, if it had been successful, was about \$1 million/ha.

4.0 CONCLUSIONS

The paper describes the nature of slurried coal tailings deposited in-pit and outlines the unintentionally limited options for closure and rehabilitation that result from this enforced approach. The physical impediments to capping in-pit coal tailings are discussed, together with a discussion of possible methods of placing a cover over unconsolidated, in-pit coal tailings. These include hydraulically-placing or pushing cover material over soft, wet coal tailings, dozing cover material over desiccated coal tailings, and the use of geotextile and geogrid layers. Examples of these possible capping methods are described.

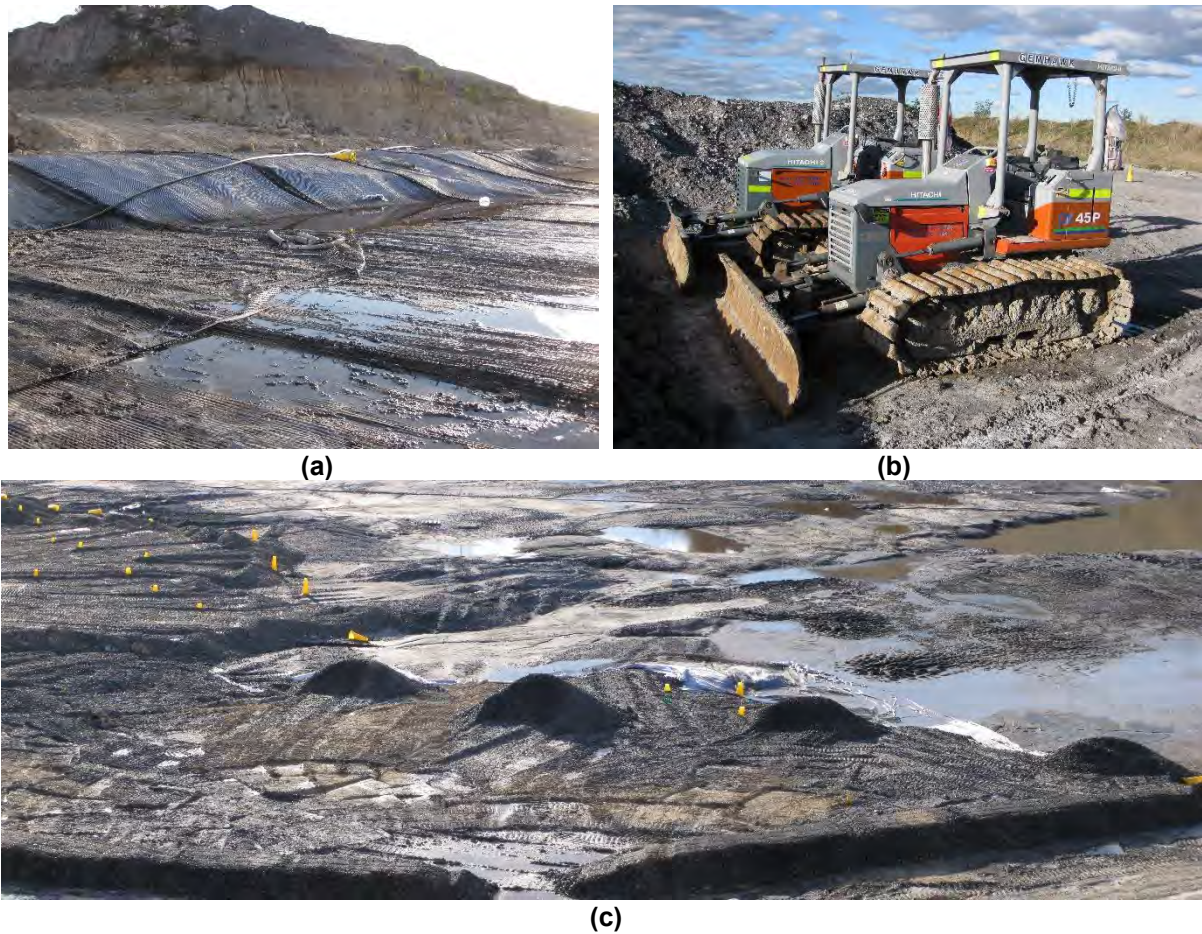


Fig. 7. Attempted capping of Wambo smectite-rich coal tailings deposited in a completed pit: (a) anchored geotextile and geogrid, (b) D2 Dozer, and (c) initial attempt at cover placement

5.0 REFERENCES

Azam, S. and Li, Q. (2010) Tailings dam failures: A review of the last one hundred years. *Geotechnical News*, December 2010, 50-53.

Williams, D.J. (2005). Chapter 17: Placing covers on soft tailings. In: *Ground Improvement-Case Histories*, 491-512, Eds B. Indraratna and Chu Jian, Elsevier, Oxford, England.

Williams, D.J. (2015). Keynote Lecture IV: Towards the elimination of conventional surface slurried tailings storage facilities. *Proceedings of First Conference on Tailings and Mine Waste Management for the 21st Century, Sydney, Australia, 27-28 July 2015*, 11-23. AusIMM.

Williams, D.J. and King, G. (2016). Capping of a surface slurried coal tailings storage facility. *Proceedings of Mine Closure 2016, Perth, Australia, 15-17 March 2016*, 263-275, Australian Centre for Geomechanics.

FORECASTING LONG TERM WATER QUALITY AFTER CLOSURE: BOLIDEN AITIK CU MINE

M. O’Kane^A, P. Weber^B, M. McKeown^C, D. Christensen^C, S. Mueller^D and B. Bird^E

^AO’Kane Consultants Inc., Calgary, Canada

^BO’Kane Consultants (NZ) Ltd., Canterbury, New Zealand

^CO’Kane Consultants Inc., Saskatoon, Saskatchewan, Canada

^DBoliden Mineral AB. SE 936 81, Boliden, Sweden

^ENew South Wales Minerals Council, PO Box H367, Australia Square, NSW 1215, Australia

ABSTRACT

The Boliden Aitik Mine is located near Gällivare, northern Sweden. Since mining started in 1968, more than 500 Mt of waste rock have been deposited in waste rock storage facilities (WRSFs). Determination of long term water quantity and quality for the WRSFs, emanating as basal and toe seepage, was a key input for evaluating risk in terms of managing impacts to the aquatic receiving environment for the site at closure.

This paper describes the approach to utilizing current hydrogeological and geochemical conditions for assessing current contaminant load emanating from the WRSFs. On the basis of this assessment, coupled with implementing different closure management tools, and using various numerical and analytical modelling techniques, long-term estimates for WRSF loading were developed. Numerical modelling was used to estimate long-term oxygen ingress and net percolation rates for closure conditions based on inputs obtained from seven years of in situ cover system monitoring and field testing.

The overarching findings of the study were that water quality from the Potentially Acid Forming (PAF) WRSFs will improve over time as the closure cover system limits oxygen to the underlying waste rock; soluble stored acidity and metal load is flushed and sparingly soluble load is neutralized by available alkalinity associated with neutralizing minerals in the waste rock. As stored acidity is flushed, the model predicts that pH will increase and acidity loads will decrease, resulting in circum-neutral basal and toe seepage with associated low dissolved metals concentration within ~50 years.

The approach described herein may be adopted for a wide variety of mine waste facilities. Fundamental to the evaluation is development of a conceptual model for both current and closure conditions. The conceptual model is then enhanced through the risk assessment process, which is used as an engineering design tool and serves to identify and prioritize additional studies and work.

1.0 INTRODUCTION

The Boliden Aitik Mine (Aitik) is a Cu-Au-Ag deposit situated in the Baltic shield near Gällivare, northern Sweden. Host rocks consist primarily of muscovite schists, biotite gneisses, and amphibole-biotite gneisses of volcanoclastic origin (Boliden, 2015). The mine area includes two open pits (Aitik and Salmijärvi), service buildings, a tailings management facility (TMF), and WRSFs. (Eriksson, 2012). Since mining started in 1968, more than 500 Mt of waste rock have been deposited in WRSFs.

Waste rock is classified into PAF waste rock or Non Acid Forming (NAF) environmental waste rock. Environmental waste rock is described as waste rock that meets criteria rendering it suitable for construction and rehabilitation activities; environmental waste rock is not

considered capable of producing acid or metalliferous leachate, having very low Cu content. Waste rock that does not meet the environmental waste rock definition is considered PAF, although some PAF rock would be considered NAF based on industry standard acid base accounting techniques.

The primary objective of this study was to understand long-term water quality of PAF WRSF basal seepage for the purpose of determining environmental risk to aquatic receptors downstream of the mine site at closure. Evaluating risk, in terms of impacts on the aquatic receiving environment, required determination of both current and long-term water quality and quantity from the WRSFs. This paper focusses on determination of long-term water quantity and quality emanating as basal and toe seepage from the WRSFs.

2.0 METHODS

2.1 Geochemical Characterisation

The initial basis for the geochemical conceptual model was a literature review of waste rock mineralogy, which has been discussed in various papers including Strömberg (1997), Strömberg and Banwart (1994, 1999) and Lindvall (2005). Additional field investigations were completed in 2014 to provide further geochemical characterisation of the waste rock. Field investigations included a WRSF test pit sampling program, and a seepage sampling program. Data from additional seepage sampling in the following spring supports the 2014 seepage data.

Waste rock samples were collected from 27 test pits excavated in WRSFs, and three water samples were collected from seepage points emanating from PAF WRSFs. Industry standard acid base accounting (ABA) geochemical testing was undertaken to understand sources of acidity and alkalinity within the PAF WRSF, including potential sulfide acidity, stored acidic oxidation products, and acid neutralisation potential. Field rinse pH data from samples collected demonstrated a range of pH values representing acid forming and non-acid forming waste rock, with older samples generally having lower pH values. Key mineralogy is presented in Table 1. Key sulfide minerals with the PAF WRSFs were identified as pyrite, chalcopyrite, and sphalerite. Melanterite- and jarosite- type minerals represent soluble- and sparingly soluble- stored acidity respectively; acidity contained in these minerals would be released as a function of pore-water flushing. Calcite and anorthite are the key acid neutralizing minerals.

At closure, it was estimated that potential acidity associated with unoxidised pyrite within the PAF WRSF was 4.5 Mt CaCO_3 eq. Stored soluble acidity associated with melanterite type minerals is ~0.06 Mt CaCO_3 eq. Stored sparingly soluble existing acidity associated with jarosite type minerals is ~0.5 Mt CaCO_3 eq. Potential acid neutralisation capacity for the PAF WRSF was estimated to be ~1. Mt CaCO_3 eq, based on measured calcite content. With such substantial potential acidity, control of oxygen ingress and hence sulfide mineral oxidation is the key management tool required to control long-term acid generation and seepage water quality from the PAF WRSF.

Table 1. Mineral composition of unoxidized waste rock (percentage by volume and weight).

Mineral	Strömberg and Banwart (1994) Volume % (mean \pm 1 SD)	Strömberg and Banwart (1999) Volume %	2014 WRSF sampling program (weight %) (OKC, 2015)
Anorthite	6 \pm 4	3 - 9	
Calcite	0.1 \pm 0.5	0.5	
Pyrite	0.57 (0.08 – 1.7)		
Chalcopyrite	0.09 (0.02 – 0.3)		
Jarosite			0.41
Melanterite			0.02

2.2 Conceptual Flow Model

In the context of this project, the term “conceptual model”, or CM, is used in the sense of the CM being the communication tool to describe current conditions, and mitigation strategies that arise from addressing risk. Hence, the CM could simply be a description based on very little information and based on an expert’s opinion. And then, as additional information is developed while addressing risk, the CM is enhanced. However, it remains as the communication tool, regardless as to the level of detail.

Characterisation of each component of the conceptual flow model in terms of water quality and flow rate was necessary to determine current and long- term water quality from the PAF WRSF. Physical characterisation of current conditions included development of a conceptual model for flow mechanisms, and controls on those mechanisms, at site. Pre-mine contours were used to analyze surface topography, infer flow direction and delineate underlying catchment areas. The majority of surface and shallow groundwater flow at site reports to water monitoring location 558, along the main WRSF collection channel (Fig. 1). Each flow component contributing to water monitoring location 558 was characterized to allow for development of a conceptual model as to how flow quantity and quality would evolve in the long term. Flow components include infiltration through WRSFs (PAF and environmental), flow emanating from the TMF, and near surface ground flow.

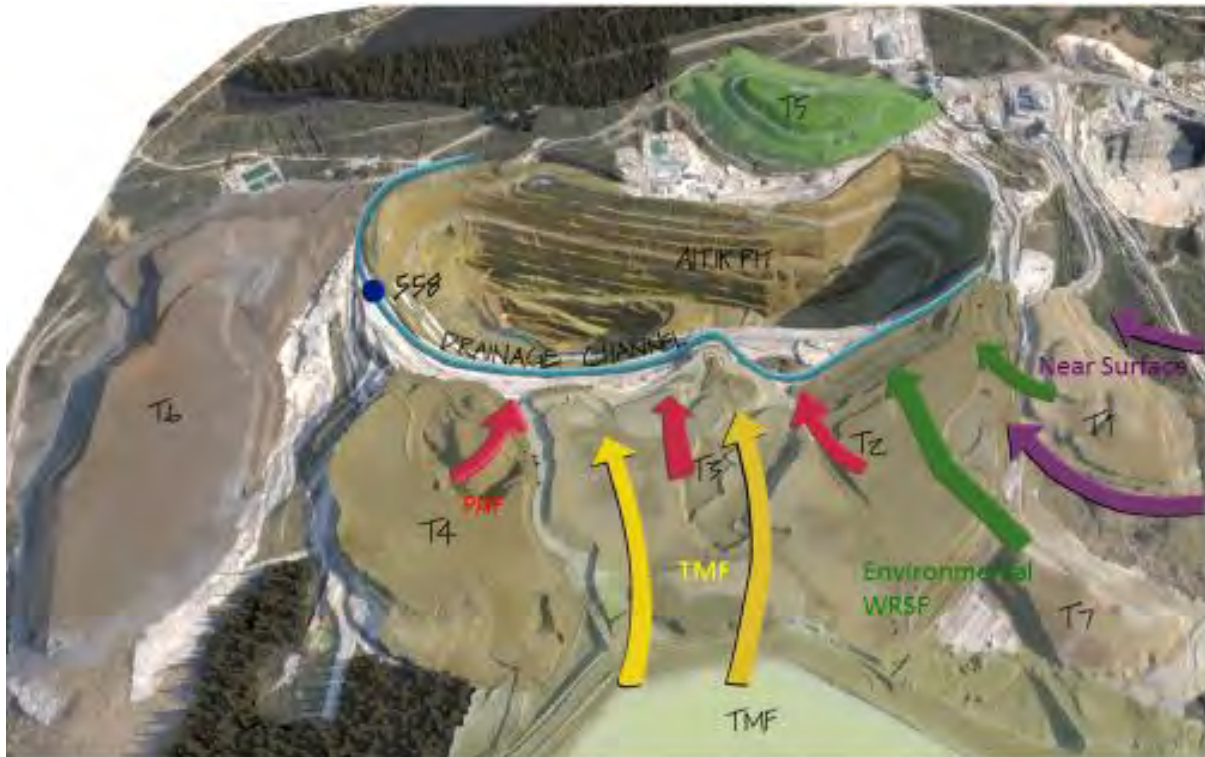


Figure 1. Conceptual flow model contributing to drainage collection channel, Aitik Cu Mine

Flow rates of each component were estimated based on footprint areas. For WRSFs, a net percolation rate (55 - 60% of annual precipitation) was applied to the bare waste rock surface based on numerical modelling for current conditions. Applying annual precipitation of 600 mm, total seepage from the PAF and environmental WRSFs was estimated to be 40 L/s and 10 L/s, respectively. A comparison between flow volume measured in the WRSF collection channel and estimated flow emanating from WRSF catchments and adjacent natural ground catchments indicated that a large flow component was being contributed by the TMF area, which is consistent with the flow model for the site (e.g., Eriksson and Destouni 1997). A seepage flow rate of 160 L/s was assumed based on a literature review of previous work at site, flow rates recorded in the collection channel, and dimensions of the TMF area and structure adjacent to the WRSF catchments. Finally, near surface groundwater flow was calculated as the difference between the flow measured in the channel and remaining characterized flow components, which was 20 L/s.

2.3 Derivation of PAF Source Term

Water quality for PAF WRSF drainage is not directly available at the site, as collection channels at toes also collect water from other sources, as noted above. Hence, this characteristic was determined by empirical inverse geochemical modelling. Water quality and flow rates are available for the water monitoring location 558 in the WRSF collection channel (refer to Figure 1). As such, contaminant loads from other flow components were deducted from the load measured at water monitoring location 558, and the remaining load was assigned to net percolation through PAF WRSFs to generate the source term for PAF drainage water chemistry; this is illustrated in Figure 2 (data is also shown in Table 2). Characterisation of other flow components is described below.

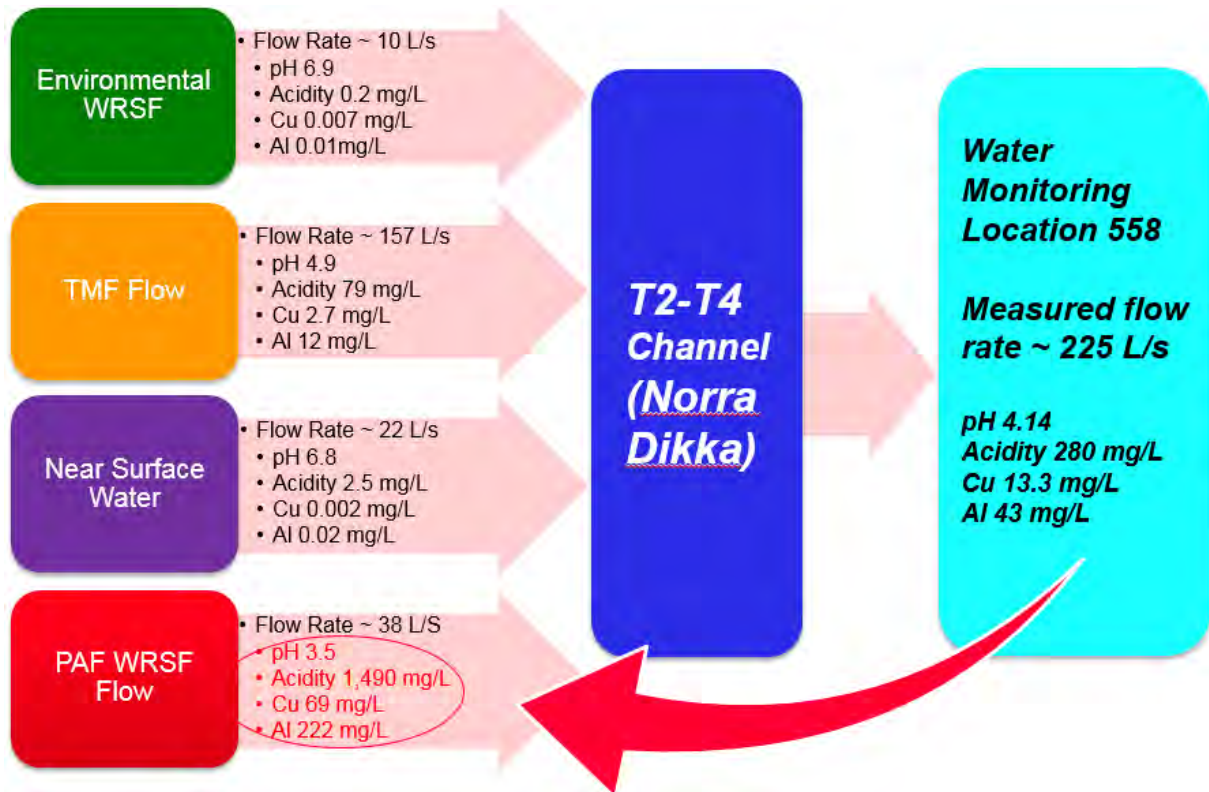


Figure 2. Empirical geochemical model for determining PAF WRSF seepage water quality

Contaminant load for each flow component is a product of concentration and flow rate. Flow rates for each component were estimated as described above. Water quality of the TMF seepage was derived from two seepage samples collected from the TMF dams in 2014 and 2015. Environmental WRSF drainage water quality was derived based on four seepage samples (three in summer, one in winter), from which a weighted mean value was calculated to address seasonal variation. Near surface water quality was derived based on median results for Aitik water quality monitoring location 522, which is located on Myllyjoki Creek. Water quality for water monitoring location 558 were derived based on a mean of monthly samples collected at the site.

The source terms (key terms defined in Table 2) were modelled using the computer program REACT, which is part of Geochemists Workbench (GWb) suite (Bethke, 2005, 2008). The modelling program essentially determined PAF WRSF water quality by utilizing the difference in measured contaminant load at water monitoring location 558 and the loads from other flow components reporting to water monitoring location monitoring 558. The remaining load (mg/s) was allocated to the flow rate (40 L/s) through the PAF WRSFs to derive a concentration (mg/L). The derived concentration for PAF WRSF seepage was then modelled using GWb to determine final estimated water quality and solubility constraints. Based on this assessment, the dominant source of acidity and contaminants at water monitoring location 558 was PAF WRSF drainage, which contributes ~2,000 tonnes per year, while the TMF contributes ~390 tonnes per year. The source term derived for PAF WRSF drainage was used as the initial pore water quality in forward reaction path modelling.

Table 2. Key water quality inputs for flow components.

Flow Component	PAF WRSF	Environmental WRSF	TMF	Near surface	Monitoring location 558
pH	3.5	6.9	4.9	6.8	4.1
Acidity (mg/L)	1,490	0.2	79	2.5	280
Cu (mg/L)	69	0.007	2.7	0.002	13
Al (mg/L)	222	0.01	12	0.02	43
Flow rate (L/s)	40	10	160	20	230

2.4 Closure Cover System Design

An engineered cover system will be implemented on the PAF WRSF as part of the mine closure process with the primary objective of improving long term quality of seepage waters and surface water from the reclaimed WRSFs by substantially reducing ingress of oxygen and meteoric waters into the facility. The PAF WRSF cover system design is based on field studies and numerical modelling processes as described by McKeown et al. (2015) and includes a 0.3 m highly compacted till layer with an overlying 1.5 m of moderately compacted till and 0.3 m till and organic mix layer acting as a growth medium.

One dimensional soil-plant-atmosphere modelling was completed to simulate performance of the cover system over the long term and under selected sensitivity scenarios. Inputs to the modelling program included material properties obtained from field investigations, data obtained from cover system monitoring at site, and RCP4.5 climate change scenario generated by the Swedish Meteorological and Hydrological Institute.

The key indicator of performance for the simulation was total oxygen ingress by diffusion, which previous performance monitoring had indicated was the dominant transport mechanism for the PAF WRSFs. Results indicated that the cover system reduced oxygen ingress by diffusion from $>2,000$ g/m²/yr (bare waste rock) to an average of 32 g/m²/yr. Net percolation rates decreased from between 55 - 60% of annual precipitation (bare waste rock) to between 27 - 32% of annual precipitation in the long term after cover system installation (noting that annual precipitation increases from ~600 mm/yr currently to 820 mm/yr by 2100 under the RCP4.5 climate change scenario).

In the long term, acidity and metal loading from the PAF WRSFs will be a function of oxygen ingress associated with oxygen diffusion through the cover system, and dissolved oxygen in net percolation. Numerical modelling determined that oxidation occurs predominantly in the upper 5 m of the PAF WRSF surface, indicating that the remaining WRSF profile remains in an anoxic condition as a result of the presence of the cover system. For GWb modelling, it was assumed that all oxygen is consumed by pyrite oxidation within this zone. Long- term closure annual acidity loading was derived based on area of the PAF WRSFs at closure (540 ha), the amount of oxygen ingress over this area, and the assumption that all this oxygen reacted with pyrite to produce 4 moles of H⁺ ion per mole of pyrite oxidized. In current (bare) WRSF, the entire depth was assumed to be potentially oxidizing as oxygen moves freely within it as a result of advection and diffusion. Calculations for the WRSF after cover system construction (5 m oxidizing; 75 m anoxic) indicate that the system was net non-acid forming from a conventional acid-base accounting perspective.

2.5 Basal Seepage Analysis

PAF WRSF draindown is important for forecasting long-term water quality after closure, as it controls the rate at which current water quality is replaced by a lower-acidity water type created by minimizing oxygen ingress to the WRSF. To determine draindown, one-dimensional seepage modelling was completed to simulate current conditions and long-term basal seepage from the WRSFs using SEEP/W, a software package designed to analyze groundwater seepage and pore-water pressure dissipation within porous materials. The seepage analysis was completed using a transient analysis of several 1D representative columns for both plateau and sloped areas of the WRSFs.

Results for current (bare waste rock) conditions indicate that the WRSFs are ‘wetted up’; meaning, as additional surface infiltration occurs, a pore-pressure response occurs at the base of the WRSF resulting in basal seepage (in addition to any drainage due to gravity flow). The response of the system is dampened due to the height of the WRSFs and the time required to percolate to the WRSF base, but water infiltrating into the top of the WRSF displaces seepage from the base of the facility. In the long term, construction of the cover system will reduce net percolation and ultimately basal seepage compared to the bare waste rock condition, but the volume of basal seepage does not decrease dramatically, because long-term annual precipitation is predicted to increase by 15 to 20% in the RCP4.5 climate change scenario.

2.6 Derivation of PAF Long Term Water Quality after Closure

Evolution of WRSF drainage water quality (prior to mixing with other flow components in the collection channel) was considered as three water quality phases, including current water quality, transition water quality, and long term water quality. Geochemical modelling performed with REACT estimated long term water quality and thus risks associated with water quality after closure, and after installation of the cover system. Model inputs for forward path geochemical modelling were initial pore-water quality, mineralogy (based on field and laboratory data, company records), influent precipitation water quality, oxygen flux, and net percolation rates. Oxygen flux and percolation rates were determined by cover system modelling. Peer reviewed estimates were obtained for kinetic rate constants for dissolution of key initial waste rock components (pyrite, calcite, jarosite, anorthite) and precipitation of plausible secondary phases that might form from long term weathering. A numerical model was established to predict water quality during the transition period between current and long term water quality.

2.7 Modelling Approach

Current water quality is represented by the water-type derived from the inverse geochemical modelling process (e.g., PAF source term derived above). Duration of the current water quality phase was a function of the draindown phase, which was estimated to be 20 years based on seepage modelling. That is, it will take an estimated 20 years for the current pore-water near the top of the WRSF to percolate to the base and be replaced by the new lower acidity water-type. It was assumed that the acidity load reporting to the base of the WRSF is derived from the available stored soluble melanterite-type acidity load that is present within the WRSF, as oxygen is excluded due to the presence of the cover system. Sparingly soluble jarosite-type acidity was not considered in the numerical modelling of the transition phase, as it was confirmed (in GWb geochemical modelling of the longer term water quality) that the calcite and anorthite present would also neutralize acidity from this source.

Long-term water quality was a function of sulfide oxidation (pyrite), jarosite dissolution, and neutralisation of this acidity by minor calcite and abundant anorthite. Water quality was predicted using GWb. It was assumed that long-term water quality could not develop until all

available reactive soluble melanterite-type acidity present in the WRSF was flushed out by net percolation.

It was assumed that not all the soluble melanterite-type acidity would be flushed from the WRSF during the transition period; one third of acidity (and contaminants) would remain in stagnant areas of the WRSF, being generally immobile (as noted by Eriksson and Destouni, 1997). Thus two thirds of the soluble melanterite-type acidity reports to the base of WRSF prior to transition to long term water quality.

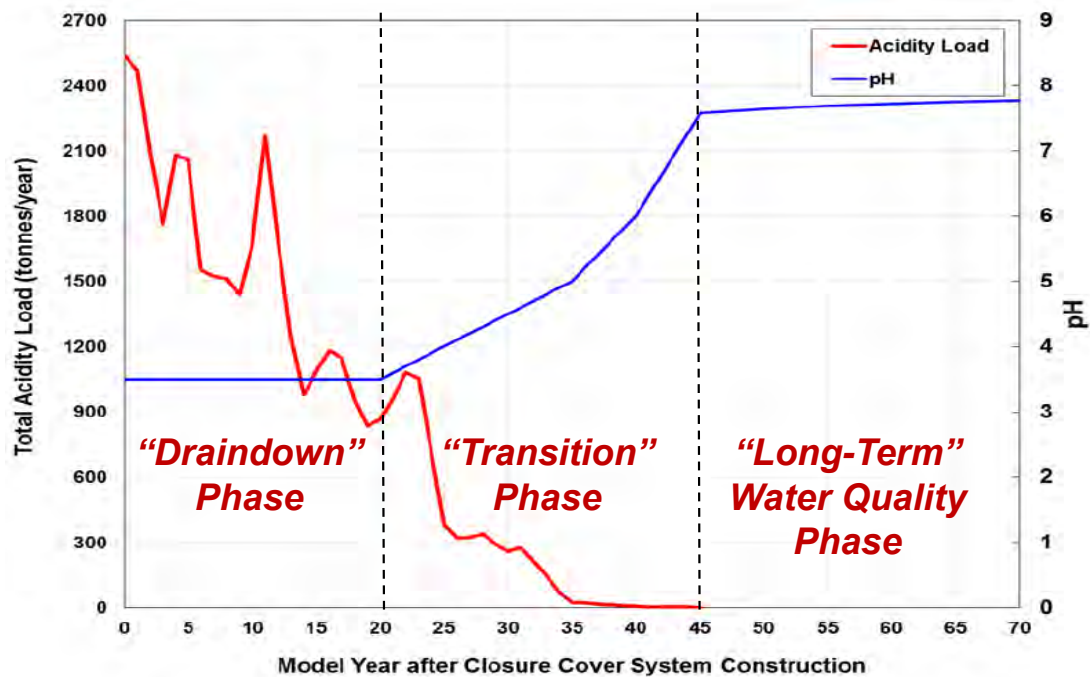
2.8 Evaluation of Risk

In the context of this project, evaluation of risk represents an engineering tool for developing informed closure planning decisions. Risk can be managed through mitigation, which allows for enhancement of the CM for closure. These aspects were developed through a top-down, expert-based risk process that assigned a set of probabilities for site specific conditions; namely, the Failure Modes and Effects Analysis, or process (FMEA).

A FMEA was completed to evaluate the closure design for Aitik site (Boliden, 2015), providing a comprehensive review of the closure strategy. Each potential failure mode was evaluated based on the assessed water quality risk for adverse impacts to aquatic receptors downstream of the mine site, where water quality is evaluated primarily in terms of spatial extent, magnitude, and frequency. The majority of potential failure modes and effects ranked a 'low' risk score, meaning that the long-term risk of occurrence and severity of effects is within the broadly acceptable range. Failure modes and effects ranking a risk score of 'moderate' or higher highlighted the requirement for carefully considered risk controls. The need for additional studies has been identified to supplement available data and compare against the conceptual model for performance. In identifying mitigation measures, it was noted that regular maintenance in the initial stages of closure are vital for managing risk at the site (e.g. sediment in channels, etc.).

3.0 CONCLUSIONS

The WRSF evaluation involved desktop review and interrogation of previous studies completed at Aitik, a field based geochemical assessment, and development of conceptual and numerically-driven models to characterize the hydrological components in regards to flow and quality. It was concluded that post-closure water quality from the PAF WRSF area will improve over time as the closure cover system begins to limit oxygen ingress within the WRSF profile. Oxidation reactions will continue to occur, but at a much lower rate due to decreased oxygen availability following cover system construction (Figure 3). As stored acidity is flushed out and neutralisation reactions occur within the WRSF profile, pH will increase, and acidity loads will decrease with time. In approximately 50 years, circum-neutral pH drainage and associated low dissolved metals are predicted to emerge from the PAF WRSF. Within the 50 year period, WRSF seepage water is managed in conjunction of the development of the pit lake (Eriksson et al, 2017).



O'Kane
Consultants
Site Management and Closure Services
Acid Mine Drainage and Unsaturated Zone Hydrology

4.0 ACKNOWLEDGEMENTS

The authors thank the Boliden Mineral AB for permission to publish this information. The authors also thank Boliden Mineral's Closure Planning Group, including Nils Eriksson (Boliden), Alan Martin and Colin Fraser (Lorax Environmental Services), and Ted Eary (Hatch USA) for input during the analysis.

5.0 REFERENCES

- Bethke, C., 2005. Reaction Modelling Guide, The Geochemist's Workbench Release 6, User's Guide to React and Gtplot. University of Illinois Hydrogeology Program 74 p.
- Bethke, C., 2008. Geochemical and Biogeochemical Reaction Modelling (2nd Edition). Cambridge, Cambridge University Press. 543 pp.
- Boliden Mineral AB, 2015. Aitik mine closure plan base case description. August.
- Brown MC, Wigley TC, Ford, DC (1969) Water budget studies in karst aquifers. J Hydrology 9:113—116, doi:10.1016/0022-1694(69)90018-3
- Caruccio FT, Geidel G (1984) Induced alkaline recharge zones to mitigate acidic seeps. In: Groves DH, DeVere RW (Eds), 1984 Symp of Surface Mining, Hydrology, Sedimentology and Reclamation, Univ of Kentucky, p 27—36
- Eriksson, N. and Destouni, G. (1997). Combined effects of dissolution kinetics, secondary mineral precipitation, and preferential flow on copper leaching from mining waste rock. Water Resources Research **33** (3), 471-483.
- Eriksson, N, Mueller, S., Forsgren, A., Sjöblom, A., Martin, A., O'Kane, M., Eary, L.E., and Aronsson, A. (2017) Developing closure plans using performance based closure objectives: Aitik Mine (Northern Sweden), IMWA 2017.
- Gammons CH, Mulholland TP, Frandsen AK (2000) A comparison of filtered vs. unfiltered metal concentrations in treatment wetlands. Mine Water Environ 19(2):111—123, doi:10.1007/BF02687259

Jennings JN (1971) Karst – An Introduction to Systematic Geomorphology – Vol 7. The MIT Press, Cambridge, Massachusetts, 252 pp

Lindvall, M., 2005. Strategies for remediation of very large deposits of mine waste; the Aitik mine, Northern Sweden. Licentiate Thesis, Luleå University of Technology, Department of Chemical Engineering and Geosciences, Division of Applied Geology.

McKeown, M., Christensen, D., Taylor, T., and Mueller, S. 2015. Evaluation of cover system field trials with compacted till layers for waste rock dumps at the Boliden Aitik copper mine, Sweden.

10th International Conference on Acid Rock Drainage & IMWA annual conference. Santiago, Chile.

O’Kane Consultants Inc. (OKC). 2015. Boliden Aitik Project – Aitik mine closure project waste rock storage facility: cover system design, prediction of geochemistry and discharge water quality. Submitted to Boliden Mineral AB. September. Report no. 771/9-01.

Strömberg B. 1997. Weathering kinetics of sulphidic mining waste. Ph.D. thesis. Department of Chemistry, Royal Institute of Technology, Stockholm, Sweden. TRITA-OKK-1043.

Strömberg B and Banwart S., 1994. Kinetic modelling of geochemical processes in the Aitik mining waste rock site in northern Sweden. Applied Geochemistry, Vol. 9, pp.583-595.

Strömberg B. and Banwart S., 1999. Experimental study of acid-consuming processes in mining waste rock: Some influences of mineralogy and particle size. Appl. Geochem. 14(1999)1-6.

PIT LAKE WATER QUALITY MODELLING AT CENTURY MINE

C. Linklater^A, A. Watson^A, A. Hendry^A, J. Chapman^A, J. Crosbie^B
and P. Defferrard^C

^ASRK Consulting (Australasia) Pty Ltd, 44 Market St, Sydney, NSW 2000, Australia

^BMMG Limited, Level 23/28 Freshwater Place, Southbank, Melbourne, VIC 3006, Australia

^CNew Century Resources, Level 9, 350 Collins Street, Melbourne, VIC 3000, Australia

ABSTRACT

The Century open cut zinc mine at Lawn Hill recently changed ownership from MMG Limited (MMG) to New Century Resources (NCR). Closure planning for the site was initiated by Zinifex, developed further by MMG, and is continuing under the new ownership. The waste rock dumps will be covered with a store and release cover system to meet closure objectives. However, the open pit, which is partially backfilled with waste rock, is expected to fill with water post closure to form a pit lake. As part of developing the site closure strategy, the final pit lake level (i.e. risk of discharge), and water quality that may develop within the lake post closure, were identified as potential risks to meeting downgradient water quality objectives. To evaluate this risk, a pit lake model has been developed that integrates outputs from geochemical characterisation programmes, water balance studies and hydrogeological modelling. The model quantifies solute production from pit walls and mineralised wastes located within the pit, and accounts for potential influence from out-of-pit waste dumps. Pit lake water quality is calculated over time, allowing assessment of potential impacts to surface and groundwater, and third party receptors. Using the predictions from the model, it has been possible to compare potential environmental outcomes for different closure strategies and assumptions, thus allowing prioritisation of forward works and informed selection of optimal closure measures.

1.0 INTRODUCTION

Figure 1 shows the layout of Century mine site, and the mine setting with respect to local surface watercourses. Page Creek, the most proximal creek to the pit, has undergone a number of phases of diversion and realignment (1997-2014) to re-route streamflow around the western margin of the pit.

The Century pit is approximately 330m deep, with a circumference of 6,800 m. The pit wall rock comprises predominantly siltstone and shales near the base (including mineralised zones). The intermediate portion of the walls are sandstone, and the topmost portions are Thornton limestone.

Three external waste rock dumps are located around the edge of the pit, and a fourth dump is located within the confines of the pit (the in-pit dump). The in-pit dump occupies a significant volume, and contains highly reactive sulfide minerals as evidenced by elevated temperatures (up to 300°C) and periodic gaseous emissions (SO₂, steam and smoke) from the dump surface.

A tailings storage facility (TSF) and an evaporation dam are located to the south east of the pit. Due to mounding of the local groundwater table beneath these facilities during operations, the TSF and evaporation pond have been linked to surface expressions of localised seepage and minor ephemeral impacts within the surface water regime. Closure options for the TSF include (i) leaving the existing facility in place and emplacing a cover, or

(ii) deposition of the tailings in the pit, either with or without re-processing to recover metals. The evaporation dam would be dewatered and the embankment removed.

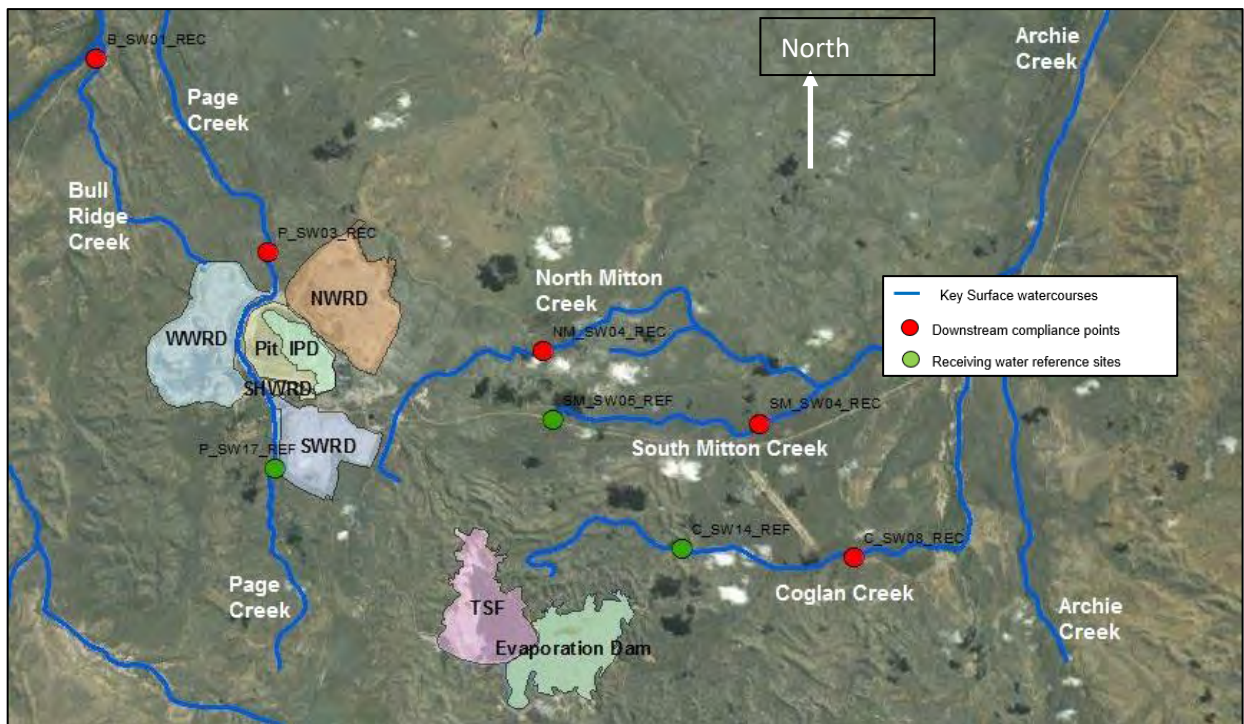


Fig. 1. Schematic of Century Mine and surrounds

Post-closure, a lake will develop within the pit. This paper describes modelling of pit lake water chemistry, accounting for the influence of solute production from exposed pit walls, external and internal waste rock dumps, and the tailings. Three primary closure scenarios were assessed for the tailings as summarised in Table 1.

Table 1. Summary of assessment scenarios

Scenario	Description
1	No tailings in pit
2	Tailings deposited in-pit (not re-processed) based on the two hydraulic mining rates: 650 tonnes per hour (tph) and 2,000 tph.
3	Tailings deposited in-pit (re-processed for metal recovery) based on the two hydraulic mining rates: 650 tph and 2,000 tph.

2.0 LONG-TERM PIT HYDROGEOLOGY AND WATER BALANCE

The most recent hydrogeological model for the Century site was developed on behalf of MMG by others, and implemented using a FEFLOW modelling platform. This included modelling to support the current assessment. Based on the groundwater inflow modelling, a pit water balance model was also developed on behalf of MMG (using GoldSim). The Goldsim model was modified to calculate pit water balances for the transfer of tailings from

the existing TSF and the modified model was made available to SRK for the current assessment.

If current creek and catchment diversions remain in place, surface catchment inflows are minimized and pit lake elevations are expected to remain low. The pit would become a long-term groundwater sink (Figure 2). For this outcome:

- Water rebound times were of order 130 to 170 years.
- Water elevations in pit would remain approximately 30 to 40 m below the pit crest, and would remain below the pre-mining groundwater table.
- A groundwater drawdown cone could extend many kilometres from the pit, particularly to the north where the main aquifer host is the more permeable Thornton Limestone.
- External waste rock dumps footprints would fall within the drawdown zone for the pit.

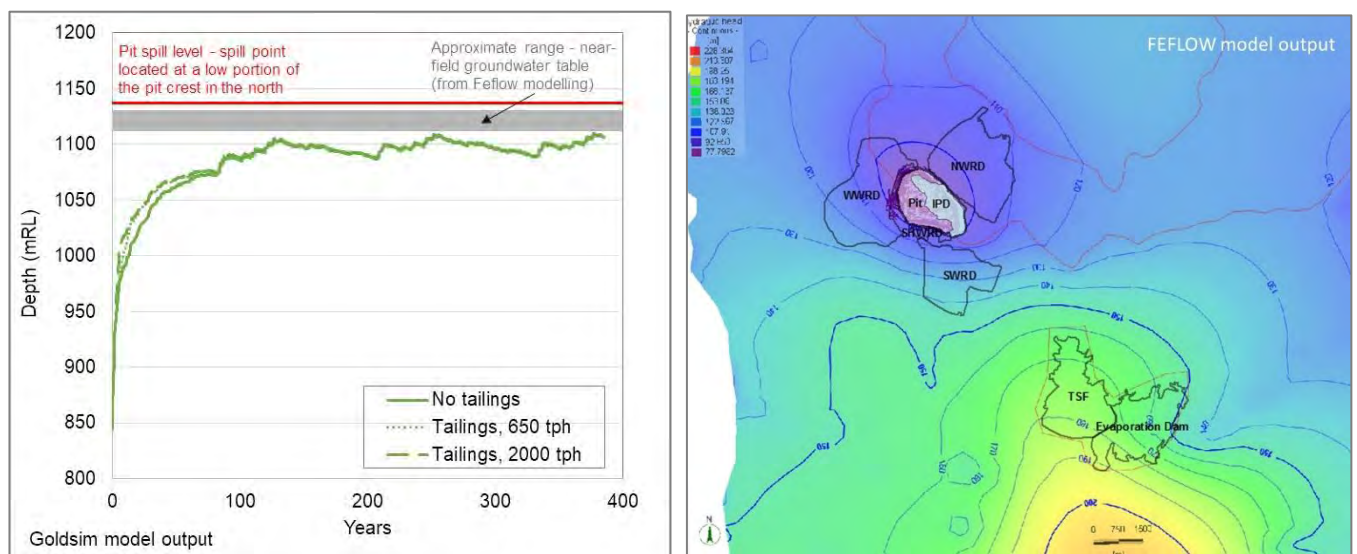


Fig. 2. Lake elevations and groundwater contours around the pit, for a permanent sink case

Should diversions fail (e.g. breaching of diversions close to the pit crest due to pit wall failure or flows greater than the design flood), then the water balance would change and lake levels would rise. For such a case, intermittent pit discharges are predicted to occur in the long term (Figure 3). These could comprise both groundwater (through-flow) and surface water discharges.

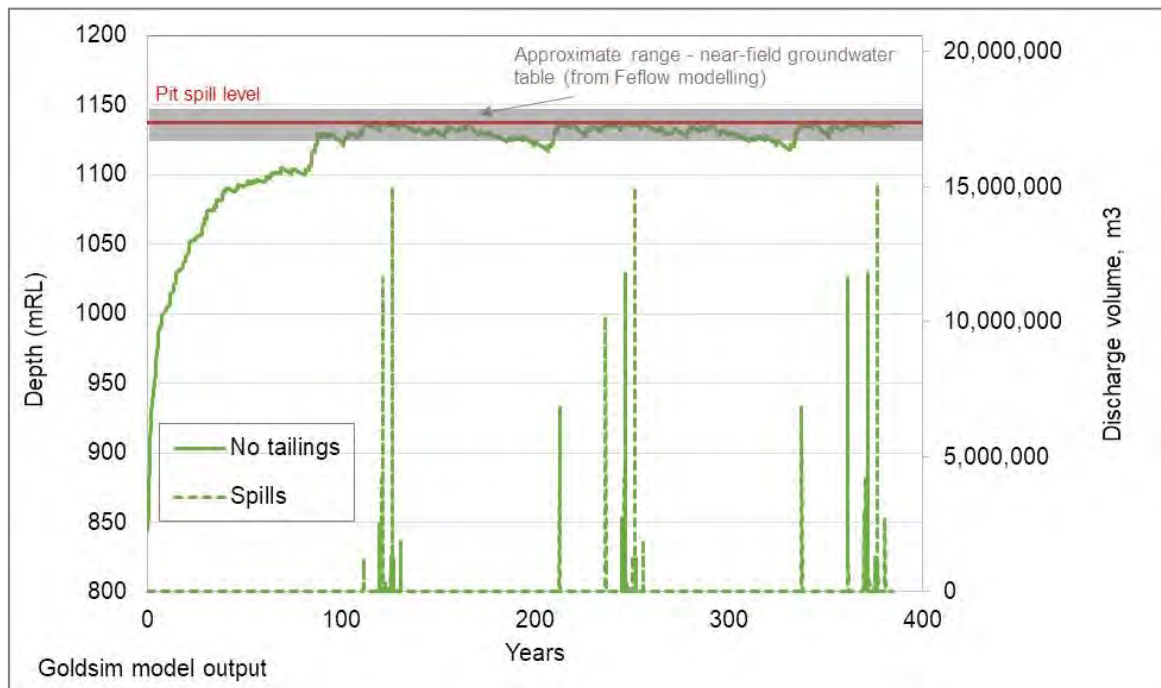


Fig. 3. Pit lake elevation as a function of time (intermittent pit discharge)

3.0 SOLUTE SOURCES

Figure 4 shows a schematic representation of pit lake solute sources, which include:

- Inflowing groundwater (groundwater in the area can be saline; total dissolved solid content up to 1000 mg/L);
- Pit wall run-off (e.g. soluble salts that form on exposed walls, or within rubble (talus) that has accumulated along benches);
- Percolate and runoff from mineralised wastes placed within the pit (i.e. the in-pit dump, and possibly tailings); and
- Percolate and runoff from external waste rock dumps located within the pit catchment and groundwater drawdown zone.

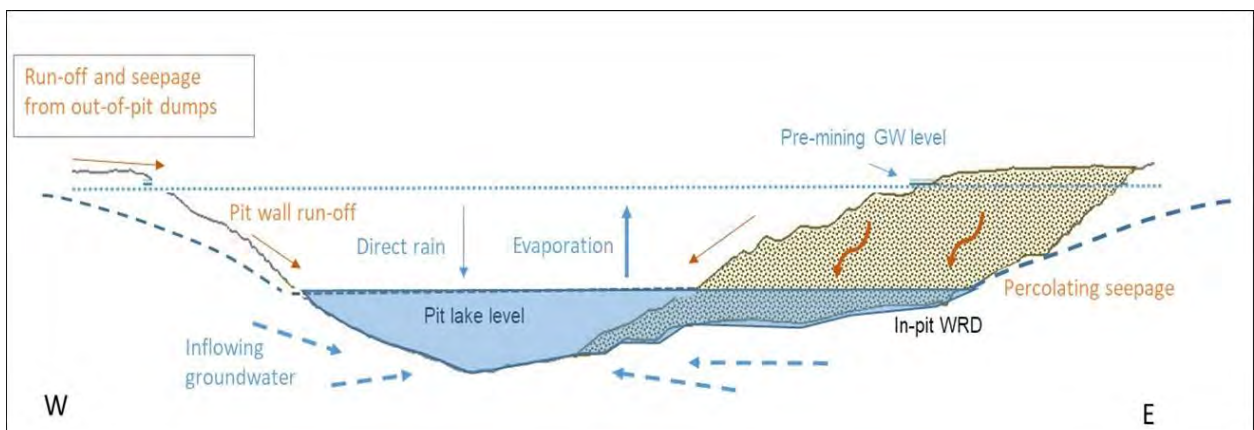


Fig. 4. Schematic showing potential pit lake solute sources

Geochemical characterisation of Century materials included kinetic (column) testing of waste rock and tailings. Results from these tests were used to develop an understanding of key

controls on solute production from pit walls and internal/external waste rock dumps, and indicated:

- Sulfate release rates did not correlate well with total sulfur content – probably reflecting complex sulfide mineralogy within the samples. Abundant sulfides included pyrite, galena and sphalerite. Oxidation rates determined from sulfate generation rates were influenced by sulfate storage in the columns (e.g. galena-rich samples likely were influenced by lead sulfate formation).
- Non acid forming (NAF) classed samples generated near neutral pH leachates with molar ratios of Ca (or Mg) to SO₄ that were consistent with neutralisation by Ca- or Mg-carbonates.
- Acidic leachates contained relatively high concentrations of elements such as Al, Co, Fe, Mn, Ni and Zn.
- The highest sulfate and metal release rates were observed for samples believed to have been affected by high temperature alteration (considered evidence of high oxidation rates). Such samples are expected to contain high quantities of soluble oxidation products.

From the kinetic test results, 'average' solute release rates were calculated for NAF and PAF-classed materials (Table 2). These laboratory-derived release rates were scaled to the field conditions to account for particle size distributions, water-rock contact, temperature, and the availability of oxygen. Whilst not expected to be limiting under laboratory operating conditions, oxygen availability would constrain reaction rates in the field. Elevated temperatures – such as those observed within the in-pit dump – would be expected to result in increases to solute production rates. The scaling factors adopted were modified according to the regime: intact pit walls, talus on benches, in-pit dump material or out-of-pit dumps.

Table 2. Laboratory-derived solute production rates and scaling factors^[1]

Parameter	Average release rate, mg/kg/week		Scaling factors ^[2]	Regime			
	Acid conditions	Neutral conditions		Talus on benches	Intact wall rock	In-pit dump	Ex-pit dump
SO ₄	500	76	Surface area correction	0.2	0.01	0.2	0.2
Ca	15	7.8					
Mg	57	13					
K	30	0.62	Fraction flushed by contact water	0.3	0.3	0.3	0.3
As	0.0025	0.000074					
Cd	0.06	0.00095					
Co	0.39	0.0024					
Cu	0.1	0.00013					
Fe	1.8	0.003	Temperature correction	1	1	10	2
Mn	43	0.28					
Ni	0.58	0.0012					
Pb	0.0036	0.066	Oxygen availability	1	1	1	0.1
Se	0.0028	0.00088					
Zn	31	0.5					

Note:

[1] Laboratory rates are multiplied by the scaling factors to derive release rates applicable to field conditions

[2] Scaling factor values are assigned based on theoretical considerations (e.g. surface area as a function of particle size, Arrhenius equation for the temperature dependence of reaction rates) and professional experience.

The tailings, if placed in the pit, would be placed as a slurry; the liquid component of the slurry will be saline and result in an increase in solute loading to the pit. Geochemical properties of the tailings solids, before and after reprocessing to recover metals, are

presented in Table 3. The total sulfur, sulfide and associated metal contents of reprocessed tailings would be reduced, compared to the current tailings. A consequent reduction in net acid production potential and metal leachability is indicated for reprocessed tailings.

Once the tailings have been placed in the pit and inundated, little difference to environmental outcomes would result whether the tails are reprocessed or not, since future sulfide oxidation will be precluded (rates of sulfide oxidation are limited by the low solubility of oxygen in water).

Table 3. Geochemistry of tailings, before and after re-processing

Parameter	Current tailings (n=10, unless indicated otherwise)	Re-processed tailings (n=2)
Total sulfur, %	3.4 – 7.3	1.8 – 2.2
Sulfide sulfur, %	2.5 – 5.4 (n=4)	1.6 – 1.7
Acid neutralising capacity, kg H ₂ SO ₄ /t	16 – 40	5 – 17
Net acid production potential, kg H ₂ SO ₄ /t	72 – 206	38 – 61
AMIRA classification	Potentially acid forming (PAF)	Uncertain (PAF)
Fe, %	7.3 – 9.4	9.0 - 9.6
Pb, ppm	2,900 – 8,100	3,500 – 3,700
Zn, ppm	25,200 – 56,300	14,800 – 17,800

4.0 ESTIMATED PIT WATER QUALITY

The pit lake water is expected to become more saline over time due to solute accumulation combined with evapo-concentrating effects. Figure 5 shows calculated sulfate concentrations as a function of time for two scenarios – permanent sink and intermittent through-flow/over-topping. Similar profiles are calculated for other solutes. Small-scale variability in concentration reflects fluctuation in pit lake volume due to seasonal rainfall and evaporation patterns.

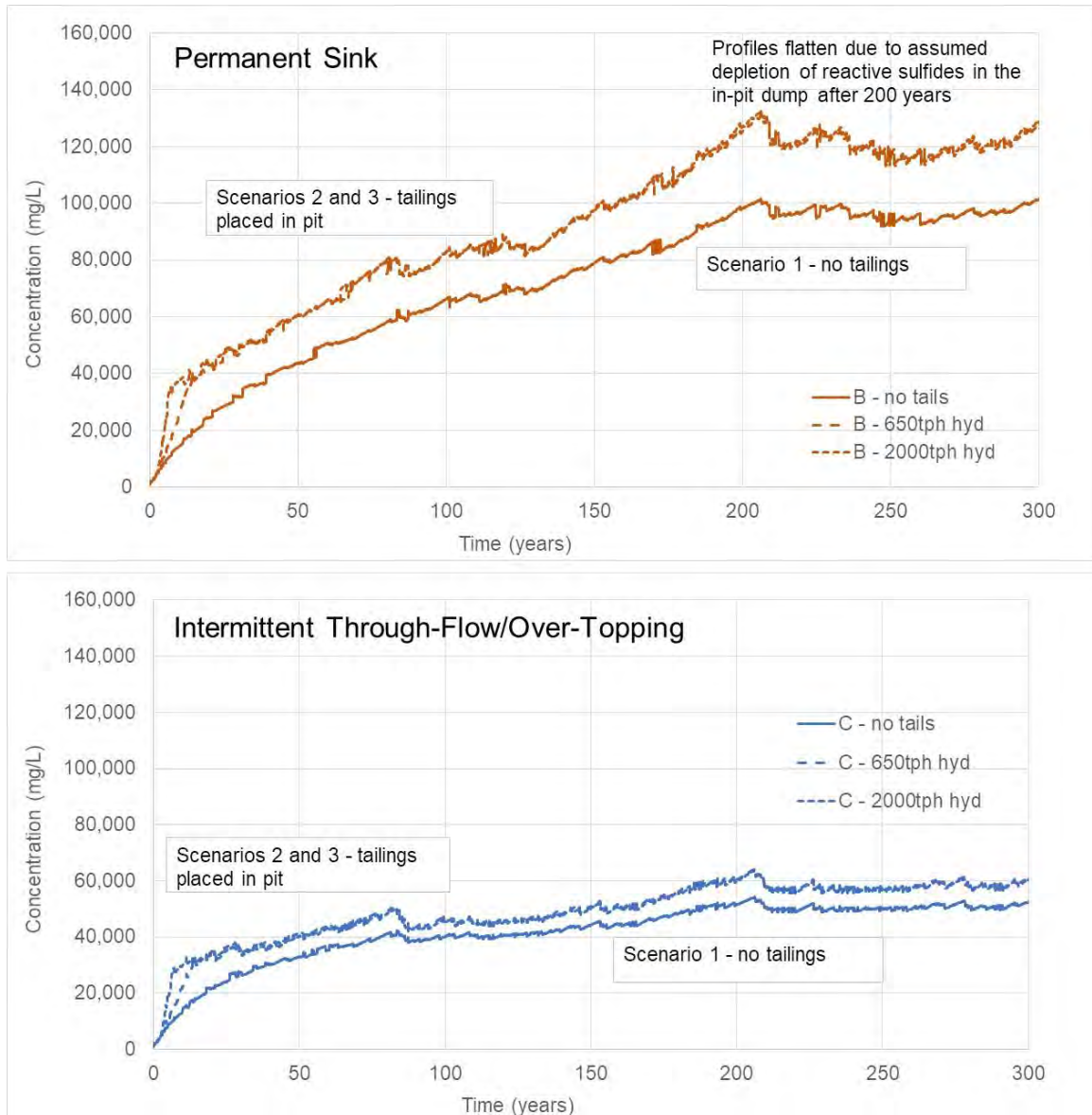


Fig. 5. Sulfate concentration as a function of time – base case input parameters

For the permanent sink case, concentrations are consistently higher than those calculated for the intermittent through-flow/over-topping case due primarily to: i) greater exposure of reactive sulfide on pit walls and unsaturated in-pit dump materials leading to higher net solute loadings; ii) no solutes are removed from the system (i.e. no discharge); and iii) the effects of ongoing evaporation (i.e. evapo-concentration and the pit remaining a net water sink).

In the event that tailings are deposited in the pit, solute loadings are higher due to high solute content in the process water component of the tailings slurry. Calculations were completed based on two tailings deposition rates (650 and 2,000 tph). Comparison of the sulfate profiles for the two cases shows that tailings placement rates influences the rate of change in sulfate concentration in the short-term; however, it has little influence on the long-term outcomes.

Since certain model inputs were based on assumed values, sensitivity analyses were carried out to determine the degree of influence certain key inputs and assumption had on model outcomes. Selected outcomes from these calculations are illustrated in Figure 6. Uncertainty in parameterization of solute production from the in-pit dump was found to have the greatest influence on model outcomes.

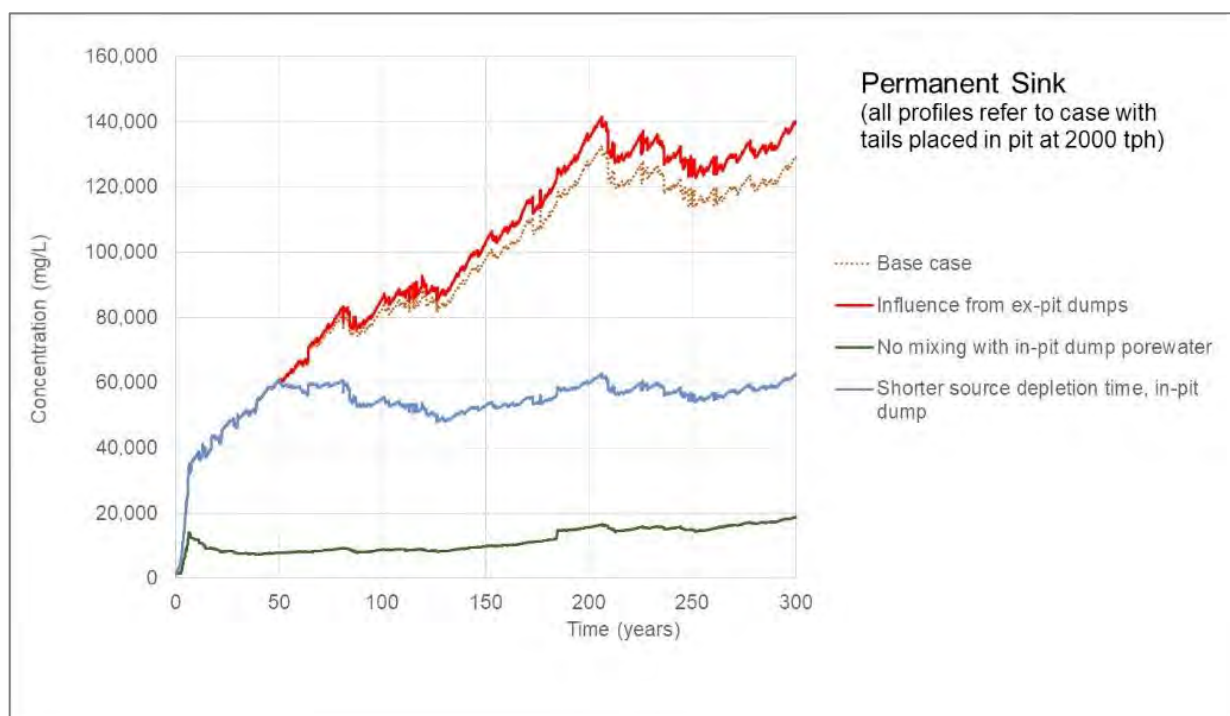


Fig. 6. Sulfate concentration as a function of time – selected outputs from sensitivity calculations

The profiles shown in Figure 5 and Figure 6 do not account for mineral solubility controls. A range of minerals could be expected to form as the pit lake water becomes more concentrated. Precipitation of sulfates, hydroxysulfates and oxides/hydroxides would commonly place upper bounds on the dissolved concentrations of sulfate and many metals. Many of these mineral controls are pH dependent; however, the overall acid-base balance in the lake remains uncertain. Monitoring has demonstrated that conditions in the pit remained pH neutral during operations, and early data for the developing pit lake shows that pH is decreasing (pH ranges from 6 down to a minimum of 4.5, see later). Current predictions indicate that dissolved metal concentrations increase over time, representing a trend of increasing acidity load. Although alkalinity is introduced to the pit via groundwater inflows, for most of the simulations the alkalinity loads are not sufficient to balance accumulated acidity loadings within the pit, suggesting that acidic conditions will develop.

Portions of the pit walls would also provide neutralisation capacity. Limestone – the lithology with the highest neutralization capacity – is exposed at pit wall elevations above 985mRL. If pit lake elevations remain low (e.g. permanent sink conditions), the water may not come into direct contact with the limestone and acidic conditions will develop in the pit lake over time. For the intermittent through-flow/over topping case, contact with the limestone walls will occur, which may offer some degree of neutralization. Conservatively, neutralization by pit walls has not been addressed in the calculations presented in this paper.

The calculated pit lake water quality was assessed using PHREEQC to account for relevant mineral solubility limits. Table 3 includes equilibrated solute concentrations based on precipitation of over-saturated minerals.

Table 3. Calculated pit lake chemistries (long-term, post-closure – permanent sink)

Parameter	No solubility control (mg/L except pH)		Precipitation of Over-Saturated Phases (mg/L except pH)	
	No tails	Tails, 2,000 tph	No tails	Tails, 2,000 tph
pH	0.95	0.85	0.92	0.82
SO ₄	100000	140000	94000	120000
Ca	4400	5900	280	250
Mg	13000	17000	13000	17000
As	0.47	0.6	0.47	0.6
Cd	11	15	11	15
Co	72	93	72	93
Cu	19	24	19	24
Fe	360	460	360	470
Mn	8000	10000	8000	10000
Ni	110	140	110	140
Pb	10	13	2.5	2.3
Se	0.65	0.83	0.65	0.84
Zn	5800	7500	5800	7500
Solubility controls	None		gypsum (CaSO ₄ ·2H ₂ O), alunite (KAl ₃ (SO ₄) ₂ (OH) ₆), K-jarosite (KFe ₃ (SO ₄) ₂ (OH) ₆), [2000 tph only], PbSO ₄	

Notes:

- The pit lake was assumed to be well-mixed; no chemical stratification has been represented.
- Redox conditions were assumed to be relatively oxic, and pe was fixed at +10 (~Eh – 590 mV).
- The calculations were performed assuming that the system is open to exchange with CO₂ in the atmosphere, and assuming that the pit water was slightly over-saturated with respect to dissolved CO₂(g) – a common observation in pit waters (Cole et al., 1994). The solutions were equilibrated so that saturation index for CO₂ was -3.

5.0 COMPARISONS WITH OBSERVED WATER QUALITY

Only limited comparisons can be made between the predicted pit lake water chemistry and available water quality data. The majority of the monitoring data represents pit water quality during operations, while dewatering was active. Dewatering activities ceased during February 2015, and therefore only a few of the more recent measurements correspond to early times during the pit water rebound phase, i.e. the time period represented by the modelling calculations.

Monitoring has included sampling of water within the main pit lake (Stage 8) and a perched water body collecting drainage/seepage within the Stage 10 portion of the pit (known as the Stage 10 Sump). The Stage 10 water is believed to represent a combination of pit wall rock runoff and in-pit dump surface runoff and toe seepage. This water is very acidic (pH <3) and saline (electrical conductivity, >5 mS/cm). Water sampled within the main pit area remained

near-neutral (pH 6-7) during operations, but recent results indicate that pH is decreasing (i.e. acidity loadings are exceeding alkalinity loadings from groundwater); the pH measurements between November 2016 and June 2017 have ranged from 4.5 to 5.5.

Table 4 compares measured concentrations with values calculated for the period between 1 and 2 years of simulation. The calculated values lie within the range of the measured values. However, monitoring data for a longer period is required to verify the predictive capabilities of the model.

Table 4. Comparison of measured data and calculated pit lake chemistries

Parameter	Measured data – summary statistics (mg/L, except pH)						Range of values calculated between 1 and 2 years of simulation – base case input assumptions	
	Stage 10 (Acid Sump)			Stage 8 (Main Pit)				
	n	Min	Max	n	Min	Max		
pH	7	2.7	3.2	6	4.5	6.0	2.5	2.4
SO ₄	7	4589	18078	6	2740	4521	2500	3700
Ca	7	388	538	6	345	426	130	170
Mg	7	472	1993	6	385	666	320	480
As	5	0.001	0.12	4	0.0005	0.004	0.011	0.017
Cd	7	0.0084	0.94	6	0.0012	0.12	0.3	0.4
Cu	5	0.0017	0.26	4	0.0005	0.017	0.4	0.7
Fe	5	12	354	4	0.083	2.0	10	14
Mn	5	0.001	1111	4	1.2	115	180	280
Ni	5	0.023	9.3	4	0.0066	0.61	2.5	3.8
Pb	7	0.003	0.41	6	0.001	0.13	0.2	0.4
Se	3	0.0005	0.0005	3	0.0005	0.013	0.01	0.02
Zn	7	765	2973	6	103	221	140	210

6.0 CONCLUSIONS

The size of the catchment reporting to the pit lake will determine whether it remains a permanent sink or transitions to an intermittent flow-through condition. To ensure the pit lake remains a permanent groundwater sink, Page Creek diversions will need to remain in place. Should the diversion be breached, then the creek would flow into the pit, and a flow-through condition would arise.

The water quality in the permanent sink case is expected to become progressively worse due to compounding effects of evapo-concentration and ongoing solute loadings reporting to the pit lake; the pit lake is expected to become acidic, and solute concentrations would increase to very high values.

For the flow-through case, water quality would also become progressively worse prior to discharge, and may or may not be suitable for release when overtopping occurs. However, in the long term, the water quality would not be as acidic or metalliferous as the permanent sink case due to: (i) dilution from increased pit inflows, (ii) potential neutralising capacity that may be contributed by limestone in the pit walls at higher elevations (encountered at

elevations above 985 mRL), and, (iii) solute loss from the pit lake in intermittent pit discharges (see Figure 5 which shows time series calculations for sulfate).

Overall, relocating the tailings to the pit would remove the likelihood of ongoing post-closure environmental impacts from the TSF. Post-closure, should the TSF remain in place, the local groundwater mounding would recede and surface expressions of seepage are less likely. However, due to desaturation of the tailings, oxidation and solute production rates would increase leading to long-term impacts on groundwater quality within the footprint of the TSF.

Relocated tailings (re-processed or not), once submerged in the pit lake, would no longer represent an ongoing contaminant source. High solute concentrations in the tailings water would result in an initial increase to the overall solute load in the pit. However, the higher initial loads would not have a material effect on predicted longer-term water quality.

7.0 ACKNOWLEDGMENTS

Scott Weeks (Golder Associates) performed FEFLOW modelling used to support the current assessment. Tony Marszalek (Gilbert and Associates, now HEC) are acknowledged for making the current Goldsim model available for use in the current study. The paper has also benefited from comments by an anonymous reviewer.

8.0 REFERENCES

Cole, J.J., Caraco, N.F., Kling, G.W. and Kratz, T.K., 1994. Carbon dioxide supersaturation in the surface waters of lakes, *Science*, **265**, 1568-1570.

DEVELOPING PILBARA PIT LAKE ANALOGUES TO INFORM CLOSURE CONSIDERATIONS

W. Germs^A, G. Race^B, R. Green^C and R. Marton^D

^AERM, Level 15, Lumley House, 309 Kent Street, Sydney, NSW 2000, Australia

^BERM, Level 6, 99 King Street, Melbourne, VIC 3000, Australia

^CRio Tinto, Central Park, 152 – 158 St. Georges Terrace, Perth, WA 6000, Australia

^DBHP, 125 St Georges Terrace, Perth, WA 6000, Australia

ABSTRACT

The long-term water quality of pit lakes that form following the cessation of mining activities plays a significant role in mine closure considerations. Potential deleterious impacts to water quality that require consideration include acidity impact, metalliferous impact and saline impact with controlling factors including the local geology, hydrogeological and climatic conditions.

While predictive work is based on geochemical testing and modelling, there is a lack of existing and publically available pit lake data for the Pilbara that would increase confidence in the predictive modelling process. Given the scale of open-cut mining below pre-mining groundwater levels in the Pilbara, having pit lake analogues available against which predictive modelling results could be compared would be of considerable value in mine closure planning. To this end Rio Tinto and BHP have initiated a study for the potential development of Pilbara pit lake analogues.

This paper presents the methodology and results of the initial phase of works, entailing a desktop-based survey of existing pit lake features in the Pilbara. The survey included the review of publically available information, the use of geographic information systems and specialised image analysis software to undertake spectral analysis to identify and map pit lakes features. Validation included the use of high resolution imagery to distinguish between pit lakes and other water holding facilities such as tailings storage facilities and purpose built water storage ponds located within mine tenements.

A total of 109 pit lakes were identified of which 63 are categorised as being inactive, 21 in care and maintenance and 25 as operating according to the available MINEDEX database (DMP, 2016a). Note that as mine pits at active mine sites have been classified as “Shut” in the MINEDEX database, the term “Inactive” is considered more appropriate for the purposes of this study and these pit lakes have been categorised accordingly. The highest numbers of identified pit lakes are associated with iron ore mines, followed by construction materials quarries, and gold and manganese mines.

Based on the results of the survey a shortlist of pit lakes have been put forward for potential further study. Analogue development related data collection should include direct characterisation of water quality and information that will help elucidate controlling processes and functional dynamics of pit lakes. A broad assessment of water quality indicators is recommended during the early stages of monitoring to enable the comprehensive identification of risk drivers.

1.0 INTRODUCTION

The long-term evolution of water quality within pit lakes that form following the cessation of open-cut mining activities plays a significant role in mine closure considerations. Potential impacts to water quality that require consideration include acidity impact, metalliferous impact and saline impact, while the potential for pit lake stratification also plays an important role. Factors that control the long-term evolution of water quality include local geology, hydrogeological and climatic conditions.

Water quality evolution predictive work is based on geochemical testing and modelling. There is however a lack of existing and publically available pit lake data for the Pilbara that would increase confidence in the predictive modelling process. Rio Tinto and BHP have initiated a study for the potential development of Pilbara pit lake analogues, with the initial phase entailing a survey for the identification and mapping of existing pit lake features in the Pilbara. This paper presents the methodology and results of the desktop-based survey. Based on the results of the survey, specific pit lakes can be identified for the development of potential analogues through further study including the characterisation of water quality evolution in these pit lakes.

2.0 METHODOLOGY

The survey methodology used to identify and map pit lake features was based on the use of freely available geographic information system (GIS) datasets and imagery combined with spatial image analysis.

As a first step, relevant GIS datasets and imagery were collated into a project GIS. Once the project GIS had been collated, image analysis was used to identify surface water features within the study area. The nature of identified surface water features was then assessed using high resolution imagery to distinguish between pit lakes and other water holding facilities such as tailings storage facilities and purpose-built water storage ponds located within mine tenements. Identified pit lakes were attributed with ancillary data (such as the mine owner, current status, geology etc.), following which additional validation was undertaken to further characterise the nature of the pit lake features identified.

The methodology utilised is described further in *Section 2.1* through to *Section 2.4*.

2.1 Collating GIS Dataset and Imagery

GIS datasets and imagery were collated for the creation of an overarching project GIS. The GIS datasets included:

- Mining tenements from the Department of Mines and Petroleum (DMP) (DMP, 2016a);
- The MINEDEX database which provides project-based location coordinates of notice of intent to mine and mineral resources as well as the location of mine pits (DMP, 2016b);
- Surface geology mapping (Geoscience Australia, 2012);
- Interpreted Bedrock Geology Mapping of Western Australia at 1:500 000 scale (DMP, 2008);

- Hydrology and water body/wetlands mapping layers from the Land Information System - Shared Location Information Platform (Landgate, 2016);
- Digital elevation models (DEM) and 1:250,000 topographic data sourced from Geoscience Australia (Geoscience Australia, 2011 & 2006 respectively);
- The National Groundwater Geodatabase from the Bureau of Meteorology (BoM) including water table aquifer mapping sourced from aquifer mapping data as available from state agencies including the Department of Water (DoW) (BoM, 2014); and
- Satellite imagery including the October/November 2016 Landsat Thematic Mapper (TM) imagery downloaded from the United States Geological Survey (USGS) / National Aeronautics and Space Administration (NASA) portal (USGS, 2016).

2.2 Image Analysis and Mapping of Pit Lakes

Image analysis and mapping of pit lakes included:

- Selecting the best coverage of the study area from the Landsat TM archive taking into considering the most recent cloud free images, while minimising date differences between images for different areas. Following evaluation of the aforementioned, Landsat imagery captured during October and November 2016 were utilised;
- Using specialised image analysis software to undertake spectral analysis of imagery to identify and map water bodies. The image analysis entailed the use of ER Mapper to mosaic Landsat images (collected between 21 October 2016 and 15 November 2016) and to calculate the Normalised Differential Water Index (NDWI) to highlight areas of surface water. The index is calculated as:

$$\text{NDWI} = \frac{\text{Landsat Band 3} - \text{Landsat Band 5}}{\text{Landsat Band 3} + \text{Landsat Band 5}}$$

- Landsat Band 3 is the surface reflectance measured for wavelengths in the 0.525 – 0.600 μm range in the green region of the electromagnetic spectrum; and
- Landsat Band 5 is the surface reflectance measured for wavelengths in the 0.845 – 0.885 μm range in the near-infrared region of the electromagnetic spectrum.

The NDWI successfully highlighted water in the landscape with pit lakes being especially prominent. The Landsat imagery is however relatively coarse (with a pixel resolution of 30m X 30m), and the remote sensing GIS layer was reviewed against higher resolution imagery as available in ArcGIS (ESRI, 2016) and Google Earth Pro (Google, 2015) to verify the identification of pit lakes. This verification task also facilitated identification of features such as tailings storage facilities (TSF) and constructed water storage ponds that had been identified through the NDWI. The manual verification provided the means to distinguish these features from pit lakes within mine tenements.

2.3 Attribution of Mine Pit Lakes with Ancillary Data

The attribution of mine pit lakes with ancillary data entailed the overlay of mapped pit lakes with mine tenements information (DMP 2016a) and the environmental GIS datasets listed in Section 2.1 to develop a set of attributes to characterise the setting of the identified pit lakes. This attribution captured information relating to the commodity type mined, the mine name and owner, status of the feature, a description of the geology (note that the description provided is based on the mapped surface geology at the centre point of the pit) and a summary of climate variables. The climate variables included annual rainfall (1961 – 1990), mean annual evaporation (1985 – 2005) and average annual aerial potential evapotranspiration (1961 - 2000). In this manner an attributed GIS dataset of mine pit lakes was developed.

2.4 Validation of Pit Lake Classification at Rio Tinto and BHP Operations

As described in Section 2.2, the GIS layer created through the use of spectral analysis and the NDWI was reviewed against higher resolution imagery as available in ArcGIS (ESRI, 2016) and Google Earth Pro (Google, 2015) to verify the identification of pit lakes. This process provided the means to distinguish between features such as TSFs and purpose-built water storage ponds from pit lakes within mine tenements and in essence provide the first stage of pit lake classification and validation.

Additional validation included:

- Identifying instances where more than one expression of surface water (i.e. more than one surface water feature) was identified in a single mine pit;
- Identifying minor depressions that were water filled at the time of the Landsat imagery being captured (October/November 2016), but which were located outside the footprint of mine pits, and therefore were likely to represent shallow and possibly ephemeral water;
- Identifying mine pits used for in-pit tailings disposal; and
- With Rio Tinto and BHP's assistance, identifying mine pits where backfilling had commenced since capture of the Landsat imagery.

Where more than one surface pond was identified in a single mine pit, only one of the water ponds was counted for the purposes of creating a tally of pit lakes within the study area. Minor depressions located outside the footprint of mine pits were considered likely to represent shallow and possibly ephemeral water; these were not included in the validated list of mine pits. Further features that were not included in the validated mine pit list included mine pits used for in-pit tailings disposal and those where backfilling had commenced since capture of the Landsat imagery. Rio Tinto and BHP further provided information on pit lakes identified within mine tenements under their control, where those mine pits have been earmarked for backfilling, dewatering and further mining, tailings storage purposes in future or where the pit lake features are used for mine water management purposes. Pit lakes falling into these categories were included in the list of identified pit lakes, since the above modifying actions were planned for the future and had not yet commenced.

3.0 RESULTS

3.1 Identified Pit Lakes

A total of 109 pit lakes were identified, and *Table 1* below provides a summary of the categories into which the pit lakes fall as per the MINEDEX categorisation (DMP, 2016b). Given that mine pits at active mine sites have been classified as “Shut” in the MINEDEX database, the term “Inactive” is considered more appropriate for the purposes of this study, and these pit lakes have been categorised accordingly.

Table 1. Pit Lakes Status Categories

Category ¹	Number of pit lakes	% of total
Total	109	100%
Inactive ²	63	58%
Care & Maintenance	21	19%
Operating	25	23%

¹ Based on MINEDEX categorisation (DMP, 2016b) with the exception of “Inactive” category

² Classified as “shut” in the MINEDEX database

As would be expected, the largest number of identified pit lakes fall within mine pits categorised as being inactive (classified as “shut” in the MINEDEX database), as it is likely that groundwater levels at these mine pits would have had the longest time to recover following cessation of mining. Pit lakes identified within pits categorised as operational may present water-filled sumps within pits, and these features should be considered transient in nature (they do however indicate mining below the regional water table). The pit lakes located within inactive mine pits are likely to form long-term pit lakes in the Pilbara, whilst the pit lakes falling into the other categories may not depending on pit modification (such as backfilling) that could occur at some of these mine sites depending on site specific closure planning.

A summary of the commodity types for the identified pit lakes is provided in *Table 2*.

Table 2. Pit Lakes Commodity Types and Status Categories

Commodity Type ¹	Total	Inactive	Category C&M ²	Operating
Iron ore	48	28	0	19
Construction materials	18	9	4	5
Gold	16	10	6	0
Manganese	11	8	2	1
Copper – lead - zinc	5	4	1	0
Chromite	4	1	3	0
Tin – tantalum - lithium	5	1	4	0
Dimension stone	1	0	1	0
Limestone	1	1	0	0
Nickel	1	1	0	0

1. Commodity type as per MINEDEX database (DMP, 2016a)

2. C & M = Care and Maintenance

The majority of pit lakes in the Pilbara are associated with iron ore mines. Features associated with construction materials as a commodity type are likely to include some quarries of relatively shallow depth with the expression of water in those quarries disproportionately influenced by rainfall when compared to deeper features that would have a larger component of groundwater inflow. The presence of water in shallow quarries may also be more ephemeral in nature. As

such, when the total number of identified pit lakes was considered, we recommend that features associated with construction materials (as well as dimension stone and limestone) be considered as a distinct group. Gold and manganese were the next most prevalent commodity types when considering the number of pit lakes identified.

3.2 Evaluation Of Pit Development for Pit Lake Subset

For a subset of pit lakes that have been identified as potential analogues, the timeframes of first appearance of a pit lake (as per the review of historic Landsat TM images from 1985 in five yearly time steps) are summarised in *Table 3* below.

Table 3. Evaluation of Pit Lake Age for Selected Pit Lakes

Pit Lake #	Commodity	First Pit Lake Appearance ¹
1	Iron Ore	Pre 1985
66	Iron Ore	2010 - 2016
106	Iron Ore	2010 - 2016
6	Gold	1990 - 1995
70	Gold	2005 - 2010
80	Gold	1995 - 2000
2	Manganese	2005 - 2010
46	Manganese	2000 - 2005
88	Manganese	2010 - 2016

1. Based on historical Landsat TM images evaluated in five yearly time steps from 1985

As can be seen in *Table 3*, Pit Lake #1 (that formed at an inactive iron ore mine) shows the earliest date of pit lake formation followed by Pit Lakes #6 and #80 that formed at gold mines. Of the nine shortlisted pit lakes, all formed prior to 2010 with the exception of Pit Lake #88 associated with a manganese mine and Pit Lakes #66 and #106 associated with iron ore mines.

3.3 Proposed Shortlist for Further Study

The subset of pit lakes summarised in *Table 3* provides a draft shortlist of pit lakes that can be considered for further study. The list includes three of the four commodity types with the most prevalent occurrence of pit lakes in the Pilbara (refer to *Table 2*), with the exclusion of the construction material commodity type. While the subset of pit lakes listed in *Table 3* provides nine current pit lakes that may be developed as analogues for three different commodity types, additional focus on different geological settings for iron ore mines may be warranted given the scale of iron ore mining below pre-mining groundwater levels in the Pilbara. The shortlisted iron ore-related pit lakes are situated in mine tenements controlled by Rio Tinto and BHP. These pit lakes have been identified as potential candidates for analogue development following the validation of the pit lakes features within these mine tenements by Rio Tinto and BHP discussed in *Section 3.1*. Other pit lakes associated with iron ore commodities have also been identified as part of this assessment, and following broader stakeholder engagement, additional candidates for the development of iron ore related pit lake analogues may be identified. The final selection of analogues should consider accessibility of the pit lakes, existing data and access to those data, and existing monitoring infrastructure or the potential to add infrastructure following the aforementioned stakeholder engagement.

4.0 CONCLUSIONS AND RECOMMENDATIONS

Using a combination of geographic information systems, specialised image spectral analysis software and mineral resource databases, it has been possible to identify pit lake features within the Pilbara region of Western Australia. The techniques used in this study could be applicable at other locations to identify pit lake features.

There are estimated to be 109 pit lakes currently in the Pilbara region. Approximately 77% of these lakes are within inactive mining areas or under care and maintenance. Iron ore mines contain the most pit lakes in this region followed by construction materials, gold and manganese mines.

For the development of pit lake analogues, data collection should include direct characterisation of water quality and information that will help elucidate controlling processes and functional dynamics of pit lakes (such as specific water inputs to pit lakes, verification of pit geology and documentation of the presence of reactive wall rock with specific reference to sulfide containing material). Potential impacts to water quality that need consideration include acidity impact (as indicated by pH and latent acidity), metalliferous impact, and saline impact. In addition, further information on the influence of lake stratification and nutrient dynamics on water quality would be valuable.

To facilitate the comprehensive identification of risk drivers, a broad assessment of water quality indicators is recommended during the early stages of monitoring. This will help to identify and inform the parameters/elements that are likely to be the key risk drivers requiring further monitoring at each analogue site.

5.0 REFERENCES

Bureau of Meteorology (BoM), (2014) Geofabric Groundwater Cartography Geodatabase. Version 2.1.1. Government of Western Australia.

Bureau of Meteorology (BoM), (2015) Climate Data Online. [<http://www.bom.gov.au/climate/data/index.shtml>] Accessed December 2016. Government of Western Australia.

Department of Mines and Petroleum (DMP), (2008) 1:500 000 Interpreted bedrock geology of Western Australia, 2008 update (DMP-013) (Accessed August 2016). Government of Western Australia.

Department of Mines and Petroleum (DMP), (2016a) Mining Tenements (DMP-003) (Accessed August 2016). Government of Western Australia.

Department of Mines and Petroleum (DMP), (2016b) MINEDEX (DMP-001) (Accessed August 2016). Government of Western Australia.

ESRI, (2016) ESRI World Imagery Service. Accessed via ArcGIS December 2016.

- Geoscience Australia, (2006) Geodata Topo 1:250,000 Scale Series 3. Topographic Data.
- Geoscience Australia, (2010) Landsat Mosaic Data (1972 – 2010).
- Geoscience Australia, (2011) One Second Shuttle Radar Topography Mission (SRTM) Derived Products (1 Arc Second DEM) Version 1.0.4.
- Geoscience Australia, (2012) Surface Geology of Australia, 1:1 000 000 scale, 2012 Edition.
- Google, (2015) Google Earth Pro Version 7.1.5.115. Accessed December 2016.
- Landgate, (2016) Western Australia Land Information System - Shared Location Information Platform (WA LIS SLIP [<https://www2.landgate.wa.gov.au/ows/wmpublic>]) Accessed December 2016.
- National Environment Protection Council (NEPC), (2013) National Environment Protection (Assessment of Site Contamination) Measure 1999, NEPC, Canberra.
- Oldham, C. E., (2014) Environmental sampling and modelling for the prediction of long-term water quality of mine pit lakes. Crawley Western Australia UWA Publishing.
- United States Geological Survey (USGS), (2016) Landsat 8 OLI/TIRS Archive [<https://earthexplorer.usgs.gov/>]. Accessed December 2016.
- United States Geological Survey (USGS), (2017) Landsat 4 – 5 TM Archive [<https://earthexplorer.usgs.gov/>]. Accessed April 2017.

GUIDELINES FOR OPENCAST COAL PIT VOID CLOSURE AND RELINQUISHMENT

D.A. Salmon

Amanzi Consulting Pty Ltd, 44 Lakeside Drive, Peregian Springs, QLD 4573, Australia

ABSTRACT

The Australian Coal Association Research Program (ACARP) project C25030 report was developed to provide guidance material to address the uncertainty that exists when planning closure and relinquishment of opencast coal mine final pit voids.

Existing mine void guidelines are often too general to address the site-specific characteristics of opencast coal mines. These characteristics define the practice required to meet the closure goals of developing safe, stable, sustainable and non-polluting landforms. Site characteristics change over time so these goals will change accordingly, making the application of closure criteria and estimation of residual risk difficult to assess. These difficulties are reflected in the fact that no coal mine pit voids have been relinquished in the Queensland coalfields of Australia.

The guideline provides a knowledge base of existing coal mine pit void closure management practice. These practices provided the basis to the development of a pit void closure and relinquishment decision making process. Generic principles for managing the process and the specific practices are documented. The purpose of the guidance is to enable mine operators to better assess pit void closure management options, thereby minimising the uncertainty in applying a specific measure. It also provides a reference for regulators and stakeholders and some assurance that residual risks can be addressed.

1.0 INTRODUCTION

Increased focus on closure planning by Australian coal mines has occurred as these mines mature and as some mines face early closure. Relinquishment of the mining lease to the State is a common closure strategy that mines adopt when planning closure. Closure of the opencast coal mine void domain provides significant challenges such that relinquishment of mine sites, in the Queensland (QLD) coalfields of Australia, has not been achieved.

Uncertainty exists when assessing and planning rehabilitation and closure options, implementing rehabilitation designs, and implementing rehabilitation and closure methods with the aim of ensuring land uses are safe, stable, sustainable, and non-polluting.

An Australian Coal Association Research Program (ACARP) project C25030 report (Salmon, 2017) was developed to provide guidance material to address the uncertainty that exists when planning closure and relinquishment of opencast coal mine final pit voids. The project was supported by six mining houses for ACARP funding; Anglo American, BHPBilliton, New Coal, Peabody Energy, Premier Coal and Qcoal. The project ran for fourteen months.

This paper presents a very brief overview of this work.

1.1 Project Objectives

The project had eight key objectives; to document examples of practices applied to coal pit voids; to provide a reference list of examples of practice; to identify and confirm challenges to pit closure; to provide a list of findings; to identify gaps in knowledge that could increase residual environmental risk post-closure; to identify stakeholder perceptions of risks associated with void closure; to record regulator understanding and requirements for void closure including scientific and engineering studies and methodologies needed for relinquishment application; and to develop a guideline and a process for opencast coal pit void closure.

The overarching goal was provision of guidance to support decisions made by coal mine staff planning and implementing closure activities, which enables residual risk reduction, lists the aspects needing assessment by mines preparing relinquishment applications, and provides assurance to regulators and other stakeholders that residual risk is minimised or removed.

1.2 Scope of the Guideline

The report is applicable to hard bituminous thermal and coking coal pits, brown coal and lignite mines, and coal pit voids that are dry or contain water. Some approaches may be applicable to other types of opencast mining and commodities, but this is not the focus of the report.

1.3 Some Challenges in Closing and Relinquishing Coal Mine Final Voids

Existing guidance is often too generalised and frequently based more on experience in hard rock mines and quarries. Such guidance can be inappropriately applied when planning closure options for coal mines that have their own unique characteristics. There is no single strategy, package of practices or set of methodologies and techniques that can be applied across all mine sites since each mine has unique issues reflecting site-specific characteristics. General guidance may lead to misunderstanding by regulators and other stakeholders of what can be practicably and appropriately applied to a particular coal mine site. Hence, uncertainty occurs in planning and implementing coal mine closure activities. The application of inappropriate management options financially impacts mining companies wanting to expend effort and resources on workable and acceptable actions leading to relinquishment.

2.0 METHODOLOGY

Global literature searches were used to identify appropriate information and examples. Meetings were held with ACARP member companies supporting the project, and site visits to thirteen mine sites were completed, to gather information on measures and techniques being practiced. Coal mine sites located in the north, central and southern parts of the Bowen Basin coalfield and in the West Moreton coalfield of QLD, and sites in the Hunter Valley coalfield and the Newcastle coalfield of New South Wales (NSW) were visited.

Thirteen criteria were used to assess the suitability of sites visited including; mine site geographic location, geological location, coal type, climatic, mining methods employed, surface water regimes, groundwater regimes, rehabilitation methods used or planned, backfilling, final void type, landform design, planned final land use, stakeholder and community engagement and the closure criteria in place.

The guideline development was based on practices used at sites as well as those found in the literature. This information also formed the basis to develop decision making processes.

3.0 FINDINGS

3.1 Generic Findings

Twelve findings common to all coal mines were determined. These included; uncertainty in acceptable practice occurs throughout the industry; void terminology has not been adequately defined leading to confusion amongst practitioners and stakeholders; variability in geology and mining methods creates differing pit void geometries; a variety of rehabilitation management measures are employed; a variety of different planned final land uses occur; planning and implementing rehabilitation measures for the final pit cannot be considered in isolation from the rest of the void because they are intimately interlinked; stakeholder engagement gives a better outcome; mines have been overly optimistic in stating final land use; external stakeholders have elevated and often uninformed expectations of post-closure land use; closure costing is an uncertain economic science; safety and health are important aspects of closure and relinquishment; and final void management plans are being requested more frequently by regulators.

3.2 Gaps in Knowledge

Two notable knowledge gaps were found that impact assessment of post- closure residual environmental and safety risks. Firstly, in the understanding of the hydrogeology of backfill in the void and secondly, the understanding of the geotechnical stability of open pit void walls.

Other gaps in information needed for void closure management planning found included; lack of or inadequate monitoring data, geochemical characterisation of mine materials, and characterisation and classification of voids, and inadequate or no development of void water balances and mine waste material balances. A further twenty-six additional constraints and issues that could affect void closure and relinquishment are listed.

4.0 GENERAL GUIDANCE

The guideline provides general guiding principles for planning void closure measures. Some of these principles include the need to:

- Define the total void area, including the backfilled areas as well as any final pit void.
- Determine the final land use of the total void area and the final void with special reference to type and extent of the backfill used and the surface landform.
- Define the geology in detail with geochemical assessment and geotechnical testing of all materials mined and placed in the void.
- Develop a void water balance.
- Develop a mine waste material balance.
- Investigate thoroughly the applicability of measures used by other mining types and other geographic jurisdictions before applying them to a mine site. Do not plan to apply directly hard rock mine rehabilitation measures and land use to a coal mine void without detailed investigation. Be cautious and investigate application of rehabilitation measures between coal mines especially those with different geographical locations.
- Develop the geometries of the coal mine pits. The guideline documents a series of different geometries, in cross section profiles and by photographic evidence, for various coal mine void scenarios. The basic cross section for a coal mine pit void is given in Figure 1.

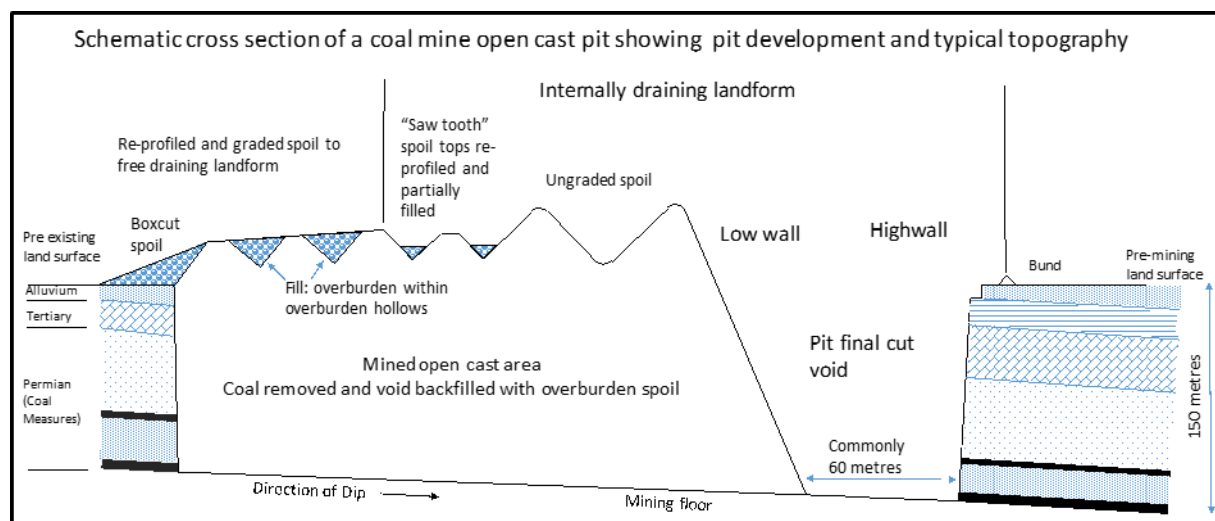


Fig. 1. Schematic cross section of a conventional opencast coal mine showing pit development and typical back filled void topography

5.0 BODY OF KNOWLEDGE

The guideline contains examples of existing practice. Some of these include:

- Investigation of the impacts of mining methods and development of void geometry.
- The development of void water balances and modelling.
- The development of mine waste material balances.
- Pit void backfilling methods and backfill material types both solid and liquid waste such as overburden, coal processing coarse discards and wet and dewatered tailings, reactive waste materials, water storage and water treatment waste.
- Descriptions of high wall and low wall treatments for stability and development of final landforms slopes, including the methodology and practice of leaving highwalls and side walls in place, reprofiling highwalls and sidewalls to shallower slopes and blending these into the adjacent void backfilled landforms.
- Final land uses.
- Final void water uses.
- Description of options analysis methods.
- Description of risk assessment methodology based on source, pathway and receptor analysis.
- Environmental risks associated with the landforms implemented.
- Land rehabilitation and closure strategies, specifically actions to achieve safe, stable and sustainable and non-polluting landforms.
- Development of final void management plans.

6.0 A PROCESS FOR CLOSURE AND RELINQUISHMENT

A number of decision making processes are provided in the guideline. The process considers discussion of benefits and challenges of relinquishment, an analysis of alternative options and a risk assessment for pit voids.

An overarching process from closure of coal mining operations to the relinquishment application is described. This fourteen-step process is summarised in Figure 2. Consideration is also given to the implementation of a post-relinquishment ownership plan.

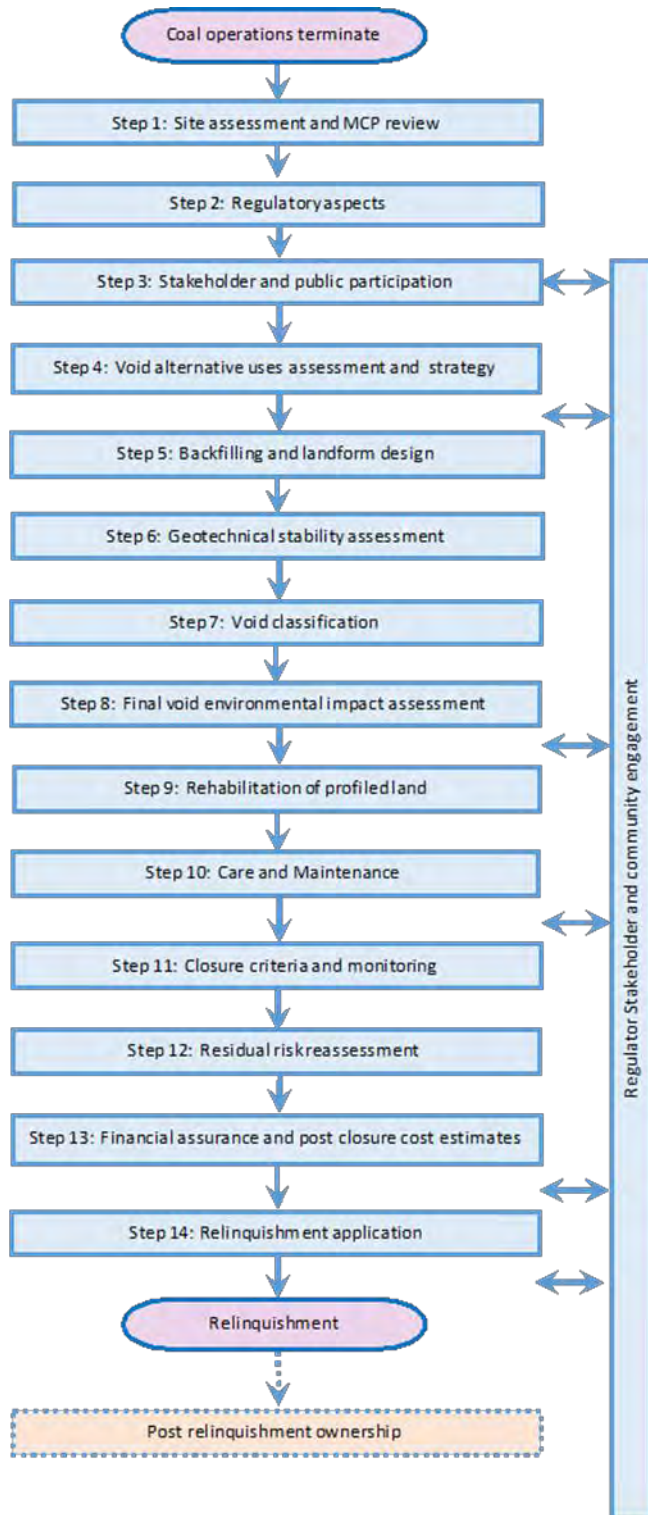


Fig. 2. A process flowchart of actions for closure and relinquishment of coal mine voids

Within these process steps there are other process flowcharts depicting actions. An example of one of these is the flowchart of actions to characterise void type. Voids are divided into three distinct types; dry voids, seasonal pit lakes and permanent pit lakes. The pit lakes are further classified, according to their water balance, into terminal sinks, through flow recharge or overflow systems. This is shown in Figure 3.

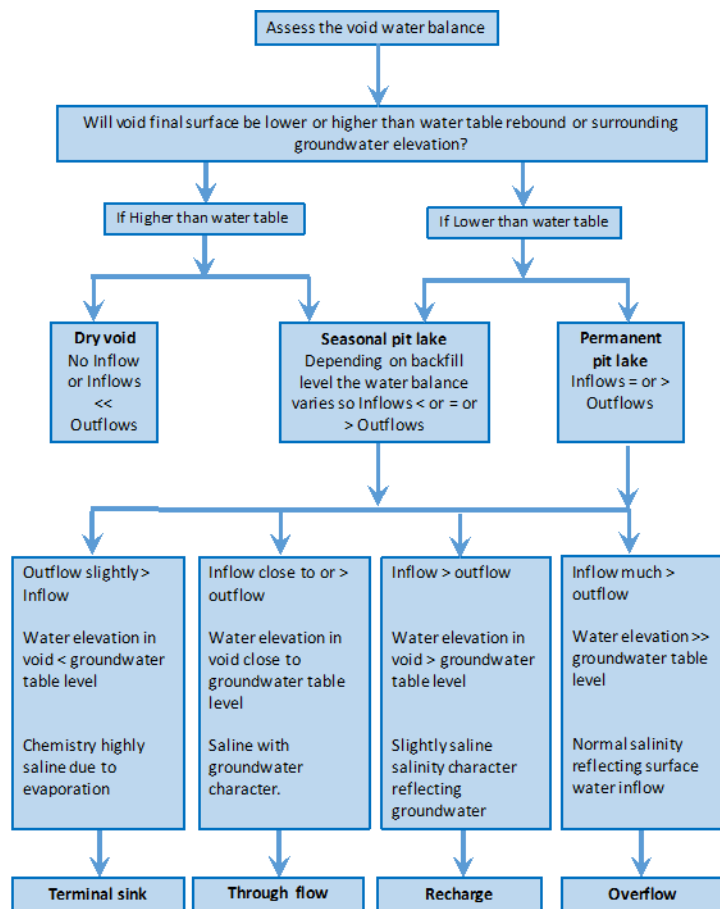


Fig. 3. Decision making process flowchart for pit void characterisation

7.0 CONCLUSION

Coal is a finite resource so coal mines will inevitably close as resources are depleted or depressed economic conditions reduce demand and coal prices drop to uneconomic levels. Open pit strip mining will, for most pits, end in a permanent void which, if mined below the water table, will fill as groundwater rebounds and surface runoff inflows to form a pit lake.

Each coal mine void has unique characteristics that are site specific, requiring specific approaches to rehabilitation and final land and water uses. Therefore, void closure and relinquishment needs to be dealt with on a site by site basis. Any application of generic rehabilitation and closure measures must ensure practical relevance to a mine site. Closure and rehabilitation practices, used in other jurisdictions, that are ill-suited to a mine site due to its particular characteristics, are being highlighted as remedies in the media. Uninformed stakeholders, and the media, tend to use such examples to berate both mining companies and government regulatory authorities for lack of innovation. In doing this, community expectations are elevated, and unsustainable, impractical demands are made to rehabilitate to unsuitable final uses. There is a strong need for education on what appropriate methodologies are available.

Mining rehabilitation has tended to follow the practice of highest achievement, leading to mine company statements of returning land to equal or better than pre-mining uses. Such statements raised stakeholder expectations and now create distrust of mines by regulators

and communities as these levels of rehabilitation cannot be reached. This situation has been amplified by regulators applying and demanding their highest level of rehabilitation standard without careful assessment of site conditions. Scientifically based practice is required.

Final void post- closure uses are highly dependent on the geographic location of the mine; its proximity to urban areas, transport routes or its location in remote areas. There are numerous examples of final land use, but the most appropriate and successfully implemented ones are those that match the surrounding landscape and have received endorsement by local communities and regulators.

Planning and implementing rehabilitation measures for the final pit cannot be considered in isolation from the rest of the void because they are intimately interlinked.

Knowledge on aspects of backfill spoil hydrogeology and pit void wall geotechnical stability is inadequate to provide confidence about post- closure residual risks to the environment and safety. These aspects require further investigation.

Uncertainty continues to exist on what is required to be done to achieve relinquishment due to the generic nature of existing guidelines and lack of regulatory process. Additional information on existing practice, as provided in the ACARP report, and opening up communication between mines to share their knowledge should provide confidence to operators that they are planning or implementing the right practice to achieve the best possible outcomes. Guidance material can help mines, regulators and stakeholders to make better and informed decisions.

8.0 REFERENCES

Salmon, DA (2017) Guidelines for coal mine open pit final void closure and relinquishment. ACARP Project C25030 Report 169pp June 2017.

CHEMICAL AND ECONOMIC FEASIBILITY STUDY OF APPLICATION OF ALKALINE CSG WATERS IN AMD REMEDIATION

D.R. Cohen^A, Q. Chen^A, M.S. Andersen^B, A.M. Robertson^C, D.R. Jones^D and B. Kelly^E

^ASchool of Biological, Earth and Environmental Sciences, University of New South Wales, Sydney, NSW 2052, Australia. Email: qian.chen@unsw.edu.au

^BSchool of Civil and Environmental Engineering and the Connected Waters Initiative Research Centre, University of New South Wales, Sydney, NSW 2052, Australia.

^CRGSG Environmental Pty Ltd, PO Box 3091, Sunnybank South, Qld 4109, Australia.

^DDR Jones Environmental Excellence, 7 Edith St, Atherton, Qld 4883, Australia.

^ESantos, Lvl 22, 32 Turbot Street, Brisbane, Qld 4000, Australia

ABSTRACT

Coal seam gas (CSG) extraction may generate significant volumes of co-produced water. Some deposits contain groundwaters with high concentrations of NaHCO₃. After reclaiming most of the water following reverse osmosis, the residual may be further converted to a high concentration brine or even crystallised to reduce disposal costs. This study investigates the use of such salts or brines to neutralise acidity and precipitate metals from acid and metalliferous drainage (AMD) at the former Sunny Corner Ag-Pb-Zn mine, and compares the performance against the conventional neutralants Ca(OH)₂, NaOH and CaCO₃. A sensitivity analysis of costs associated with the use of the Na₂CO₃/NaHCO₃ as a neutralant indicates overall cost is mainly controlled by transportation costs and to a lesser extent the production costs of the various forms of the neutralant. Similar application to AMD sites closer to the CSG source would alter relative cost contributions. Beneficial use of the neutralant is economically preferable to disposal in landfills.

1.0 INTRODUCTION

1.1 Prospects for Treatment of AMD at Sunny Corner

AMD is a major environmental issue for many operating and legacy extractive industries (INAP 2009). There are over 500 derelict mine sites in NSW of which 27 are undergoing some form of rehabilitation (Audit Office of NSW, 2012). The former Sunny Corner Ag-Pb-Zn mine is one such legacy site, where ~10 L/min of water drains from the main adit at pH of 2.6–3.1 and containing elevated concentrations of various chalcophile elements and sulfate (Chapman et al., 1983; Seccombe et al., 1984).

Various approaches to active and passive AMD neutralisation, involving different combinations of neutralants, reductants (chemical and biological) and sedimentation systems, have been tested at various locations around the world (Skousen et al., 2000; Hammarstrom et al., 2003; Johnson and Hallberg, 2005; Akcil and Koldas, 2006; McCullough, 2008; Caraballo et al., 2011; Kefeni et al., 2017). Many passive systems fail in the longer-term due to processes such as mineral surface passivation, the inability of reductants to replenish or simply the infill of zones used to precipitate the Fe-rich AMD precipitates (Kalin et al., 2006). Whereas passive AMD treatments have lower operating costs, they may not achieve the necessary water quality targets set for intended end-uses by environmental regulations or engineering requirements.

Advanced active treatment techniques such as the *Savmin* process and reverse osmosis (RO) have been applied in the last two decades (Brown et al., 2002; Zhong et al., 2007; Al-Zoubi et al., 2010), but the use of alkaline reagents such as CaCO_3 , Ca(OH)_2 and NaOH to neutralise large volumes of acidic waters and precipitate metals remains the most widely used primary process for treatment of AMD and other waste mine waters (Fu and Wang, 2011).

1.2 AMD Neutralant from Coal Seam Gas Produced Water

Production of unconventional gas resources such as coal seam gas (CSG) and shale gas has grown exponentially in the last two decades (Day, 2009). CSG operations typically extract large volumes of saline co-produced water. Such waters require further treatment for subsequent disposal or beneficial uses, with RO the most common method. The composition of reject brine from RO systems varies with the geological characteristics of the host units and hydrochemistry of the formation groundwater. In the case of the CSG resource near Narrabri, the reject brine is uniquely dominated by Na^+ and $\text{CO}_3^{2-}/\text{HCO}_3^-$ with a minor amount of Cl^- and only traces of other metals. In event that the Narrabri project is approved, the default position is that the brine produced by RO treatment will be further concentrated and/or crystallised and disposed of in regulated landfill sites. The question posed here is whether such materials could be used for remediation of AMD, or other applications requiring a neutralant, rather than being disposed of in this way. Whereas such beneficial use is consistent with modern principles of sustainable development, the practicality of such use depends on the cost of this material relative to the conventional alkaline neutralants described above.

1.3 Economics of AMD Remediation

Whereas there have been many studies on AMD characterisation and remediation, few studies have attempted to quantify the overall economics of such processes and account for:

- i. the composition, quantity and variability in the AMD being generated at a given site;
- ii. the composition, form and cost of production (both capital and operations) of a neutralant, and potential pricing to an end-user;
- iii. the minimum amount of neutralant required to produce treated AMD waters to a composition dictated by the end-use;
- iv. the cost of transportation of the neutralant (for beneficial use or just disposal); and
- v. the cost of the neutralant delivery system and possible cost of removal and disposal of AMD precipitates.

The technical choice of neutralants in active systems depends primarily on their specific capacity to alter pH, the practicality of mixing them with the stream to be neutralised and the cost of supply. An indicative comparison between common inorganic neutralants is set out in Table 1.

Table 1. Unit cost comparison of alkalis used for AMD treatment (after Skousen et al., 2000).

Chemical Name	Formula	Relative neutralising cost
Calcium carbonate	CaCO_3	0.10
Calcium hydroxide	Ca(OH)_2	0.20
Calcium oxide	CaO	0.27
Sodium bicarbonate	NaHCO_3	0.79
Sodium carbonate	Na_2CO_3	1.00
Sodium hydroxide	NaOH	2.05

This current work is focused specifically on evaluating the main factors affecting the cost sensitivity of the supply of Narrabri RO brine, brine concentrate or derived salts on remediation of AMD waters at the Sunny Corner site. It is not a comparison of the relative costs of using other neutralants for this purpose, though the relative costs of the neutralants in Table 1 could be used to inform such a comparison. In this study, the brine products are assumed to be delivered to the end user as a tradeoff against the cost (including transport) that would otherwise be incurred for disposal of the material at a registered landfill site.

2.0 COST MODEL FOR USE OF NARRABRI CSG CO-PRODUCED WATERS

There are four major components to the model:

1. The quantity of neutralant needed to adjust the AMD to the required pH. This is based on characterising the AMD and the end-use which is based on pH and concentration of various dissolved species.
2. The cost, including capex and opex, of producing the required amount of neutralant in four different optional forms – raw co-produced water, RO brine, brine concentrate and crystallised salts.
3. The cost of transporting the neutralant to the AMD site.
4. The (alternative) cost of disposal of the neutralant as a waste.
5. (Optionally) The cost of removal of the AMD precipitate and disposal

2.1 Quantity of Neutralant

Co-produced waters from the Narrabri CSG operations and AMD waters exiting the main adit of the abandoned Sunny Corner Ag-Pb-Zn mine have typical compositions set out in Table 2. Evaporation of the Narrabri waters to dryness at 150°C results in a salt containing 89% natrite (Na_2CO_3), 11% halite (NaCl) and minimal nahcolite (NaHCO_3) (Chen *et al.* 2017).

Table 2. Composition of mine water from Sunny Corner and Narrabri co-production water (as received). Concentrations in mg L^{-1} , EC in mS cm^{-1} .

	pH	Alka- linity ¹	EC	Al	Ca	Cu	Fe	K	Mg	Mn	Na	Zn	SO_4	Cl
Sunny Corner	2.6		2.84	57.4	21.6	3.7	173	0.6	47.8	4.2	4.8	298	1750	3.6
Narrabri co- produced water	8.3	9580	18.1	0.04	11.5	<0.1	0.24	46.9	7.2	<0.1	5660	<0.1	5.1	1210

¹Total alkalinity

Neutralisation experiments were conducted on the Sunny Corner mine water using the Narrabri brine salt as well as three common neutralising agents – NaOH , $\text{Ca}(\text{OH})_2$ and CaCO_3 . The relationship between neutralant added and resulting pH of the Sunny Corner AMD samples are shown in Figure 1 follows similar trends to other reported neutralisation tests on AMD waters (e.g. Ouakibi *et al.* 2013). Subsamples collected at various pH values during the neutralisation process were centrifuged and the supernatant solutions analysed for a range of elements by ICP-OES/MS. The Narrabri salt brine was found to be as effective to treat AMD as the other neutralants, with some advantages compared with CaCO_3 in terms of solubility. However, it was unable to significantly reduce the sulfate content of the water compared with the Ca-based reagents.

The general pH dependence of removal of metals was similar for all neutralants (within a comparable pH range). The removal of selected metals and metalloids following addition of Narrabri brine salts is plotted as a function of pH in Fig. 2. Both MINTEQA modelling of the data and comparison between the experimental results and those from similar published studies indicates that removal of the metals from the AMD waters is dominated by adsorption to the precipitating Fe/Al-oxyhydroxides rather than simple precipitation of metal hydroxides or carbonates (Chen *et al.*, 2017).

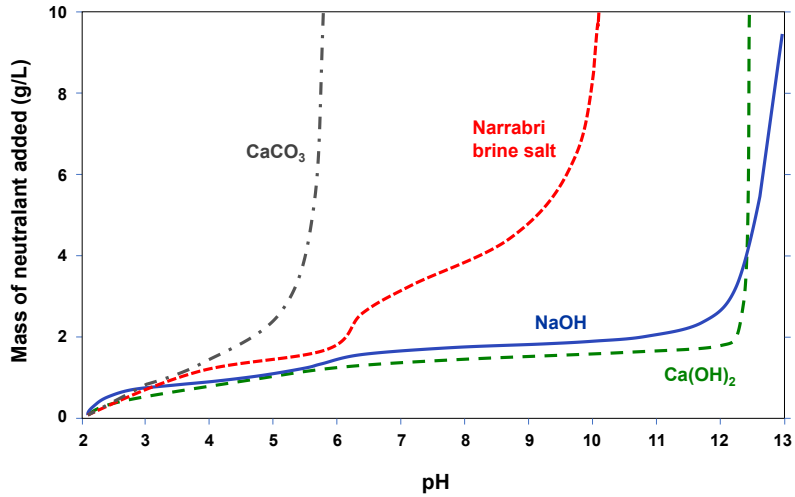


Fig 1. Relationship between mass of neutralants added and resultant pH of Sunny Corner AMD water.

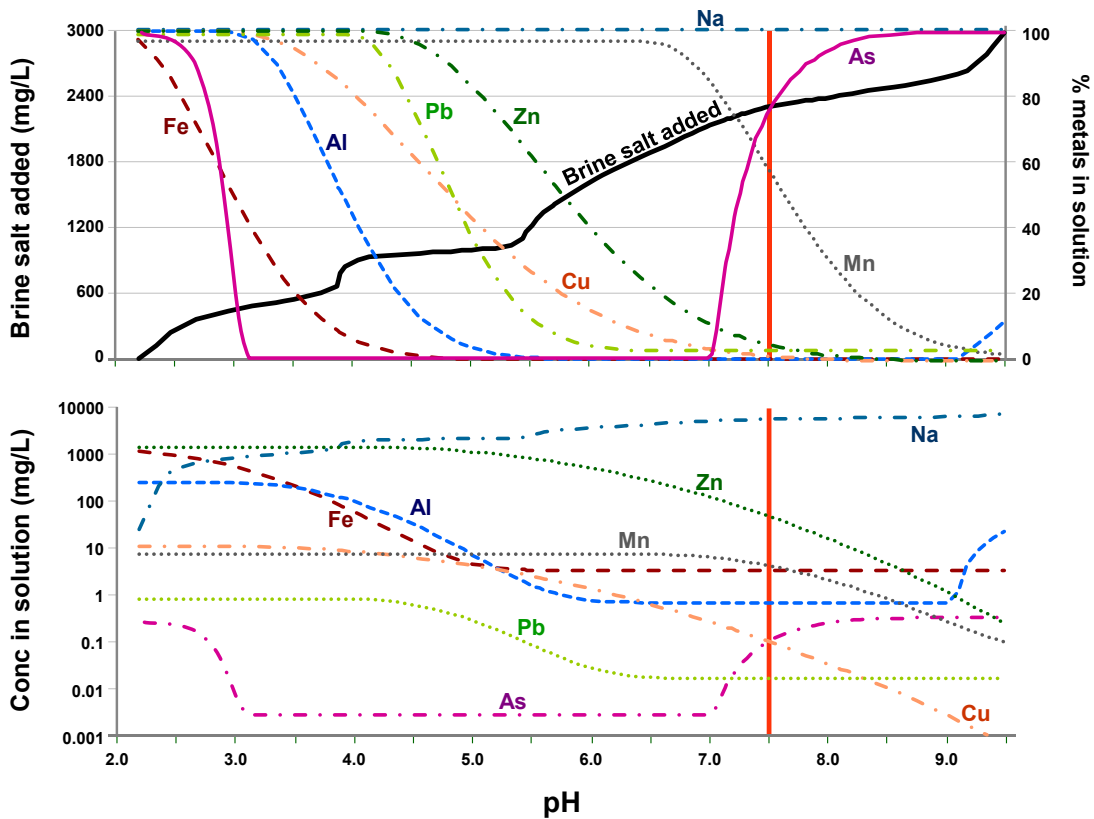


Fig. 2. pH-dependent removal of selected metals using Narrabri brine salts.

2.2 Cost Parameters

The costing parameters in the model are broadly divided into neutralant production and transportation, for which some parameters are permitted to vary using a gaussian distribution for pre-defined mean and standard deviations (Table 3). Most parameters are independent of each other, including: AMD pH and flow rate; the neutralisation plant capital costs, life expectancy, specific power consumption and efficiencies of the reverse osmosis system, brine concentrator and crystalliser; transportation costs including upload/download and kilometrage rates. Transport movements between the neutralant supply site and the AMD site are integers, but average monthly movements can be used. Costs are indicative.

2.3 Calculations

Calculations follow a three-step process. The first is to determine the required target pH in the remediated AMD waters. This is largely based on the end-use for the treated water and the associated regulatory discharge limits for pH, metal and other chemical species. In the case of the Sunny Corner AMD, a minimum pH of 7.5 was required to remove sufficient Zn to meet the selected environmental target (livestock drinking water).

The second step is to determine the quantity of neutralant (based on neutralant type) required to adjust the pH of the AMD to the target pH. This is determined using experimental data and aqueous speciation modelling. The third step is to calculate the number of truck movements required to transport the neutralant to site, which is dependent on the form of the neutralant and vehicle capacity. The model permits all key physical and cost parameters to be set, and optionally allows one or more parameters to vary as required (Table 2). A 1000-iteration Monte Carlo type simulation of final costings was used in the ensuing analysis.

Table 3. Parameters used in the example costing of the use of neutralant from Narrabri brine to remediate Sunny Corner AMD.

Sector	Variable	Value	St.dev	Units	
AMD	AMD pH at adit outflow	2.8	0.1	pH units	
	Flow rate	10	2	L/min	
	Target pH	7.5	0.2	pH units	
	Environmental water regulatory limits	Dependent on element ¹			
Neutralant plant	Power costs	0.2	fixed	\$/kW	
	Capital costs	<i>RO brine</i>	3.08	fixed	\$M
		<i>Brine concentrate</i>	1.00	fixed	\$M
		<i>Crystallised salt</i>	1.87	fixed	\$M
	Expected lifetime	<i>RO brine</i>	15	fixed	years
		<i>Brine concentrate</i>	20	fixed	years
		<i>Crystallised salt</i>	20	fixed	years
	Specific power consumption	<i>RO brine</i>	7.5	0.5	kWh/t
		<i>Brine concentrate</i>	25	3	kWh/t
		<i>Crystallised salt</i>	65	4	kWh/t
	Efficiency	<i>RO brine</i>	80	5	%
		<i>Brine concentrate</i>	65	4	%
<i>Crystallised salt</i>		75	4	%	
Transport	Loading fees	200	fixed	\$/trip	
	Maximum cost per km	2.00	fixed	\$/km	
	Transport distance factor	0.14	0.02		
	Distance from Narrabri operations to Sunny Corner	400	fixed	km	
	Distance from Narrabri operations to nearest regulated landfill site	620	fixed	km	
	Transport distance factor	0.14	0.02		
Other	Cost of disposal of salt to landfill	80	fixed	\$/t	
	Sale price for neutralant to clients	?			

¹ ANZECC (2000)

3.0 RESULTS

With all permitted parameters allowed to vary, the simulation indicates a significant reduction in both monthly cost and the variability in cost when progressing from reverse osmosis to brine concentrate and finally crystallised salt (Figure 3). The ~51% increase in power costs required to go from RO brine to crystallised salt is exceeded by the ~78% reduction in transportation costs resulting from the smaller volume of material for the salt compared with the much larger volume of the brine. The difference in costs between use of the brine concentrate and the salts is marginal, and would become negligible if the distance between the sites was under 200 km.

Assuming there would be a drop in the kilometrage rate for transportation as distance increased, the model parameters indicate only a marginal increase in costs beyond 400 km trucking distances. The capacity to significantly reduce transportation costs, possibly via purchase of vehicles by the neutralant supplier, would be the critical factor in reducing overall costs.

The characteristics of the final cost distributions reflect the effects of incorporating a series of normally-distributed parameter estimates of varying influence on the sum value (in this case the total monthly cost). This has resulted in positively skewed distributions for which an overall

χ^2 distribution has been fitted (Johnson *et al.*, 1994). Using the RO brine as a neutralant, the median cost estimate is \$988 per month but the upper 8% tail of the distribution sits above \$2000 per month.

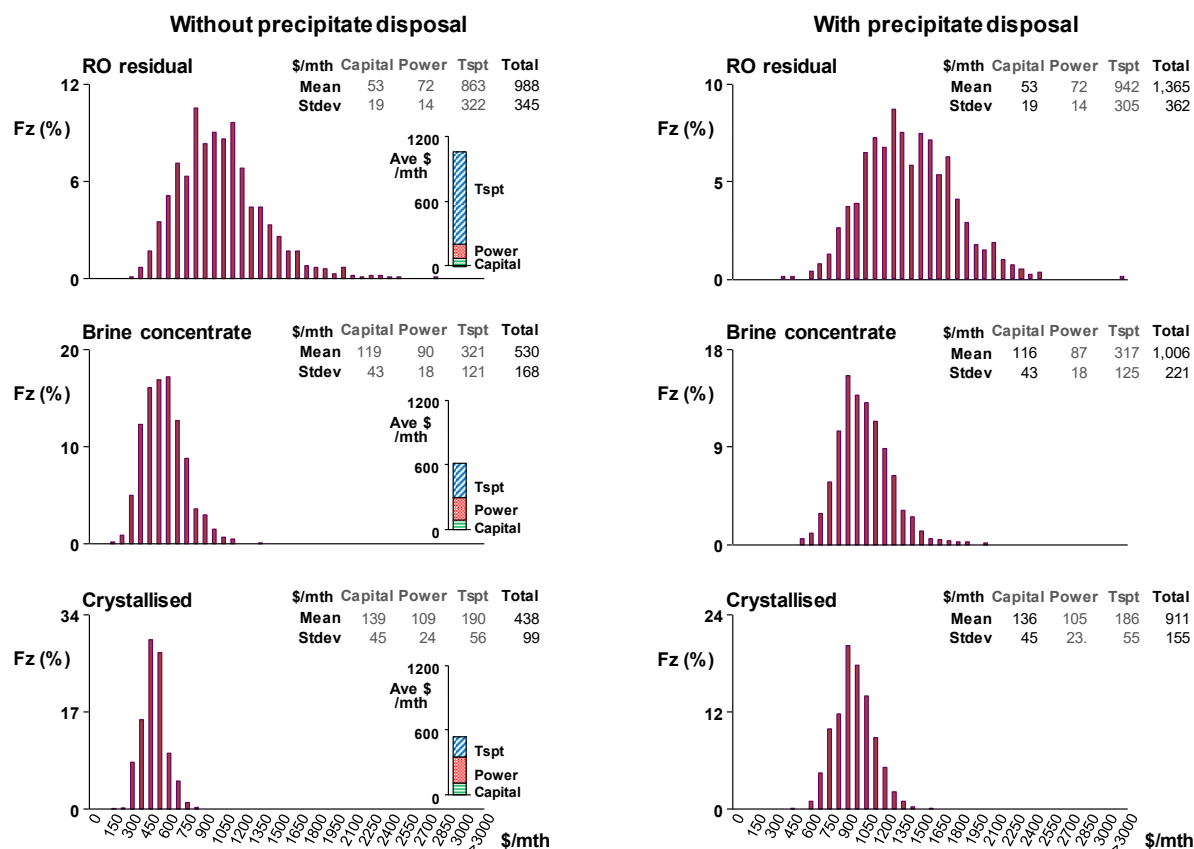


Fig. 3. Comparison between the final monthly cost estimate distributions for neutralisation of the Sunny Corner AMD using reverse osmosis brines, brine concentrates and crystallised salts. Models presented without and with the cost of disposal of the neutralised AMD precipitates.

For the model parameters selected, comparing the costs of transporting the Narrabri brine salt to Sunny Corner (400 km distance) with disposal of the salt at a specialist landfill near Brisbane (620 km distance and a charge of \$80 per t), there is distinct economic advantage of around \$70/t in using the salt to neutralise the AMD. This advantage increases even more if used on AMD sites closer to Narrabri and/or a price is paid by a client using the neutralant.

4.0 CONCLUSIONS

CSG operations such as that at Narrabri may potentially provide a neutralant that is very effective at both increasing pH and removing a high proportion of metals and metalloids from AMD. The beneficial use of the brine for neutralisation of AMD would be preferable, from an environmental sustainability perspective, to the alternative of disposal and containment at a regulated disposal facility.

Transportation costs would typically be the major contributor to overall costs. Despite the higher cost of production, the use of crystallised salts would generally be the preferred form of the neutralant due to the higher intrinsic neutralisation capacity of Na_2CO_3 compared with the NaHCO_3 -dominated brines, and the much smaller volume needed to be transported. The

economic and environmental benefits of the use of the brines is further enhanced when compared with the costs of simply disposing of the materials in landfill.

5.0 REFERENCES

- Akcil A and Koldas S (2006) Acid mine drainage (AMD): Causes, treatment and case studies. *Journal of Cleaner Production* 14, 1139–1145.
- Al-Zoubi H, Rieger A, Steinberger P, Pelz W, Haseneder R and Härtel G (2010) Optimization study for treatment of acid mine drainage using membrane technology. *Separation Science and Technology* 45, 2004–2016.
- ANZECC (2000). *Guidelines for Fresh and Marine Water Quality, Vol 1*. Australian and New Zealand Environment Conservation Council.
- Audit office of New South Wales (2012) Department of Trade and Investment, Regional Infrastructure and Services.
- Brown M, Barley B and Wood H (2007) Minewater treatment: Technology, application and policy. *Water Intelligence Online*.
- Caraballo MA, Macías F, Rötting TS, Nieto JM and Ayora C (2011) Long term remediation of highly polluted acid mine drainage: A sustainable approach to restore the environmental quality of the Odiel River Basin. *Environmental Pollution* 159, 3613-3619.
- Chapman BM, Jones DR and Jung R (1983) Processes controlling metal ion attenuation in acid mine drainage streams. *Geochimica et Cosmochimica Acta* 47, 1957–1973.
- Chen Q, Cohen DR, Andersen MS, Robertson AM, Jones DR and Kelly B (2017) Application of alkaline coal seam gas waters to remediate AMD from historical sulfide ore mining operation. In “Proceedings of 13th International Mine Water Association Congress”. Lappeenranta, Finland, 25-30 June 2017.
- Commonwealth of Australia (2016) Leading practice sustainable development program for the mining industry. Preventing Acid and Metalliferous Drainage.
- Day RW (2009) Coal seam gas booms in eastern Australia. *Australia Resource Investment* 3, 42-47.
- Fu F and Wang Q (2011) Removal of heavy metal ions from wastewaters: a review. *Journal of Environmental Management* 92, 407–418.
- Hammarstrom JM, Sibrell PL and Belkin HE (2003) Characterization of limestone reacted with acid-mine drainage in a pulsed limestone bed treatment system at the Friendship Hill National Historical Site, Pennsylvania, USA. *Applied Geochemistry* 18, 1705–1721.
- INAP (2009) *Global Acid Rock Drainage Guide*. Document prepared by Golder Associates on behalf of the International Network on Acid Prevention (INAP) (<http://www.inap.com.au/>).
- Johnson DB and Hallberg KB (2005) Acid mine drainage remediation options: A review. *Science of the Total Environment* 338, 3–14.
- Johnson NL, Kotz S and Balakrishnan N (1994) *Chi-Squared Distributions including Chi and Rayleigh. Continuous Univariate Distributions*. John Willey and Sons. 415–493.
- Kalin M, Fyson A and Wheeler WN (2006) The chemistry of conventional and alternative treatment systems for the neutralization of acid mine drainage. *Science of the Total Environment* 366, 395-408.
- Kefeni KK, Msagati TAM and Mamba BB (2017) Acid mine drainage: Prevention, treatment options, and resource recovery: A review. *Journal of Cleaner Production* 151, 475-493.
- McCullough CD (2008) Approaches to remediation of acid mine drainage water in pit lakes. *International Journal of Mining, Reclamation and Environment* 22, 105-119.

Morgan B and Lahav O (2007) The effect of pH on the kinetics of spontaneous Fe (II) oxidation by O₂ in aqueous solution—basic principles and a simple heuristic description. *Chemosphere* 68, 2080-2084.

Ouakibi O, Loqman S, Hakkou, R and Benzaazoua, M (2016) The potential use of phosphatic limestone wastes in the passive treatment of AMD: A laboratory study. *Mine Water and the Environment* 32, 266–277.

Secombe PK, Lau JL, Lea JF and Offler R (1984) Geology and ore genesis of silver-lead-zinc-copper sulphide deposits, Sunny Corner, NSW. *Proceedings of the Australasian Institute for Mining and Metallurgy* 289, 51–57.

Skousen JG, Sexstone A and Ziemkiewicz PF (2000) Acid mine drainage control and treatment. Ch 6. *Reclamation of Drastically Disturbed Lands*. American Society for Agronomy and American Society for Surface Mining and Reclamation. Agronomy No. 41.

Zhong CM, Xu ZL, Fang XH and Cheng L (2007) Treatment of acid mine drainage (AMD) by ultra-low-pressure reverse osmosis and nanofiltration. *Environmental Engineering Science* 24, 1297–1306.

TREATMENT OF ACID AND METALLIFEROUS DRAINAGE INCLUDING REMOVAL OF CONTAMINANTS FROM A SITE

^AS. Costin

^AGlobal Aquatica Pty Ltd 9 Claxton Street Adelaide, SA, Australia

ABSTRACT

A new patent pending process for the treatment of acid and metalliferous drainage (AMD) was developed. A 31,200 litre/day demonstration plant was built and operated at the abandoned Brukunga mine in South Australia. The AMD contains approximately pH 2.8, 19.5 g L⁻¹ of metals, and 6.5 g L⁻¹ of sulphate.

The multistage process commences with a first stage where cavitation produces molecular cleaving removing the acid and metals. The water is split into hydroxyl radicals and hydrogen. The hydroxyl radicals oxidise the metals forming insoluble metal hydroxides and the hydrogen is oxidised to water removing the acid. In a second stage, the sulphates are reduced to sulphide and the cations formed into carbonates. In a third stage, oxidising bacteria split the sulphides to elemental sulphur and hydrogen, the hydrogen being oxidised into water and the sulphur formed into elemental sulphur. In a fourth stage, the calcium is precipitated as carbonate and the magnesium as hydroxide.

A specific carbohydrate is produced from rubbish tip green waste forming a nutrient which is fully utilised by the bacteria. Other than the fully utilised nutrient for the bacteria, there are normally no imported chemicals required for this multistage process.

The South Australian government department, SA Water took samples from a working plant and analysed them, maintaining full chain of custody. They reported that the treated water contained pH 7.4, 176 mg/L sulphate and 1.5 mg/L of total metals. This meets the parameters stated in the Australian Drinking Water Guidelines ².

The contaminants are converted into recyclable products such as mixed metal oxides, sulphur, calcium carbonate and magnesium hydroxide. These recyclable products are sold, funding plant operation and normally resulting in no stored wastes.

Mining companies typically have a low wastewater management skill level. Therefore all aspects of the AMD treatment and removal or recycling of the water and the contaminants are provided by Global Aquatica.

1.0 INTRODUCTION

The BioAqua technology described in this paper is the subject of several patent applications by Global Aquatica Pty Ltd (Global Aquatica). AMD (acid and metalliferous drainage) water typically consists of elevated levels of dissolved metals, acidity and sulphates. The Global Acid Rock Drainage Guide¹ by INAP describes the chemistry and formation of AMD. As an alternative to current methods of treating AMD, the BioAqua process can convert sulphates-rich AMD into water that meets the water quality parameters of the Australian Drinking water guidelines ².

All existing processes for treating this type of wastewater extract the contaminants from the water and retain them on the site in an environmentally hazardous form. For example,

hydrated lime dosing produces a difficult-to-dewater, gypsum and metal hydroxide bearing sludges. This product cannot be routinely recycled. Hydrated lime may be dosed into AMD in flooded mine pits to reduce contamination to a level sufficient for release. However, the contaminants are usually replaced back into the pit.

Sulphate reducing bacteria in anaerobic wetlands has been successful at largely removing metals in AMD, but have significant acidity load and pH limitations. Australian mine sites produce large volumes of low pH and high acidity AMD that typically exceeds the treatment capacity of passive systems.

The BioAqua process employs physics and biotechnology to improve the chemistry of the AMD and recyclable products without the addition of chemicals. This aspect alone is expected to dramatically lower the cost of AMD treatment in Australia.

The AMD and treated water was sampled and reported by SA Water (see Appendix 1) from an operating plant at Brukunga in South Australia. The output products were measured and analysed by Australian Laboratory Services. This analysis indicated that, in the first cavitation stage, 19.5 g L^{-1} dry mass of mixed metals hydroxides are being removed, and approximately 6.3 g L^{-1} of sulphates are being removed from the water by the second stage that utilises sulphate reducing bacteria. Analysis of the products of the (fourth) stage downstream of the sulphate reduction indicated that the cations have been converted from sulphates to carbonates. This is based on the analysis of calcium that entered the bioreactors as sulphate and were precipitated from the water as carbonates.



Figure 1. BioAqua at the Brukunga site.

The mixed metal oxides, sulphur, calcium carbonate and magnesium hydroxide can be dried and sold as recycled products. These products can be sold by Global Aquatica which may discount the plant operating cost. These constitute all products removed from the water at Brukunga. The SA Water report indicates the AMD at Brukunga was treated to the water quality parameters described in the Australian Drinking Water Guidelines.

2.0 PROCESS DESCRIPTION

The BioAqua process consists of four parts; a metal and acid removal stage without importing chemicals; a sulphate removal stage; a sulphur removal stage; and a cation conversion to carbonate stage. The metal and acid removal is the pre-treatment required for the principal treatment process which is bacterial in nature.

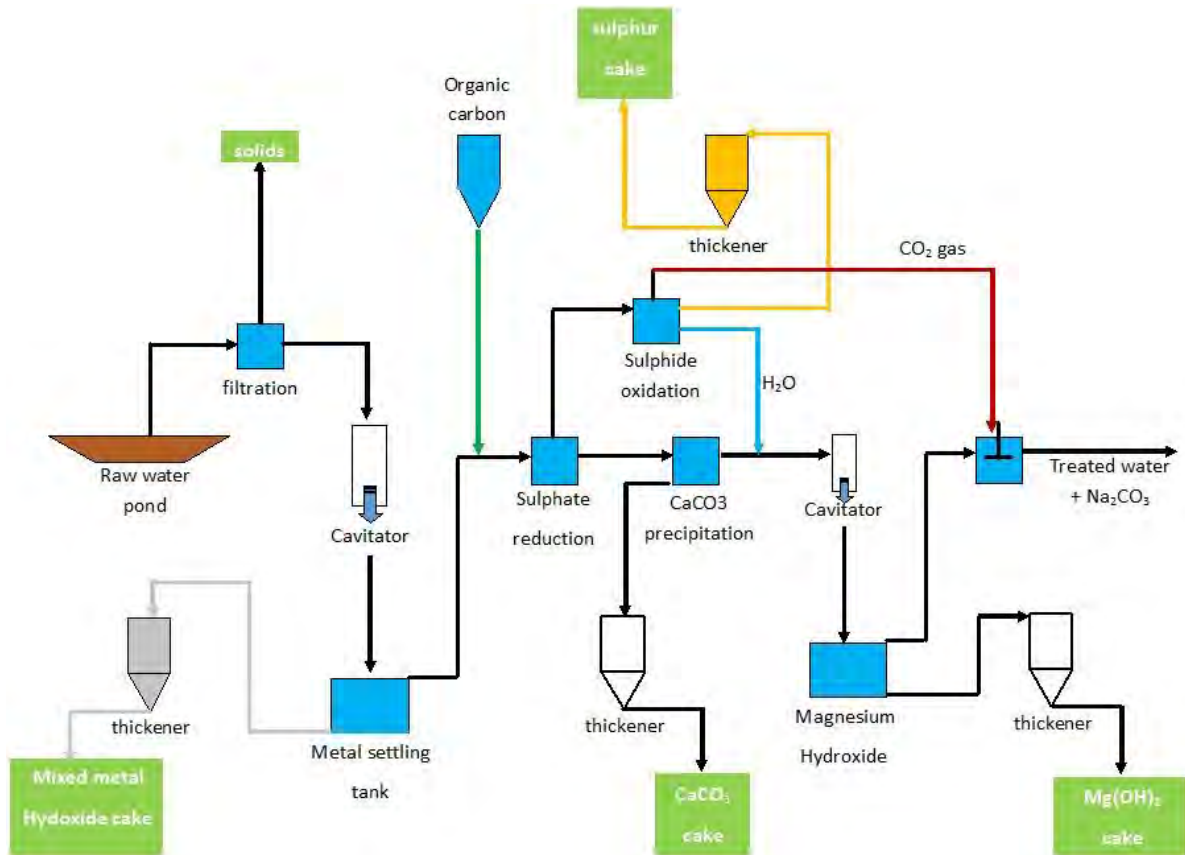


Figure 2. Process flow diagram

2.1 Stage 1. Acid and Metal Removal

To ensure the biotechnical processes, it is essential the bacterially preferential metals are removed before the bacterial treatment. However, all conventional processes produce an environmentally toxic product from this process. For example, lime dosing combines the metal hydroxides with gypsum to create a waste product that cannot be feasibly recycled. Reverse osmosis produces a mixed metal brine which is also toxic and usually cannot be recycled.

Metals in AMD can exceed 20 g L⁻¹. Chemical separation involves the importation of chemicals that add to the volume of stored toxic products. Therefore, Global Aquatica has developed a process using physics, where the raw water is molecularly cleaved using cavitation. Hydrodynamic cavitation is generated by throttling the AMD fluid flow through a series of constrictions. These constrictions produce large shear forces and increase the desired rate of bubble collapse. This is exploited in the cavitation activity within the constriction. The collapse of the cavities results in the generation of high temperatures and pressures locally which induces the cleavage of water molecules to yield OH⁻ radicals. These

OH radicals are responsible for the oxidation of the metals resulting in the formation of metal hydroxides.

In this state, the water is dissociated into hydrogen and hydroxyl radicals that are extremely oxidising. The hydroxyl radicals oxidise the metals out of solution, and the contaminants are also dissociated forming a sludge with a settling rate of approx 1.2m hr^{-1} . The water forms a water vapour gas and the mixture of gases, together with the dissociated contaminants, are then saturated with oxygen. There is no mechanical equipment or moving parts in the molecular cleaving device. The cavitation process does not erode the cavitators and they are very quiet, producing considerably less noise than a centrifugal pump for example. No additional energy components are required for this process other than the pump.



Figure 3. Cavitators and settling tanks.

The metals in the water form hydroxides and precipitate out of solution in a tank and any unused hydroxyl radicals reform into water. The process is typically tuned to cause the cations such as calcium, magnesium, sodium and potassium to mostly reform as sulphates.

The cavitation process is de-oxygenating, producing an anoxic water for the anaerobic bacteria. Any oxygen remaining in the water after settling in the tank is consumed by the added organic carbon (nutrient). Also, the 'free' hydrogen resulting from the molecular cleaving is oxidised to water removing the acidity, typically increasing the pH of wastewater to approximately 7.0.

As a result, the effect of the process, including bacterial treatment, is to increase pH to circum neutral, and substantially remove the following metals: aluminium, dysprosium, arsenic, bismuth, erbium, boron, europium, gadolinium, titanium, beryllium, gallium, cadmium, cobalt, chromium, indium, copper, lanthanum, rubidium, lithium, thorium, cerium, neodymium, molybdenum, praseodymium, nickel, samarium, lead, terbium, ytterbium, tin, yttrium, thallium, zirconium, zinc and iron.

The treated water from the cavitators is characterised by negligible metals, no acidity, and containing sulphate salts. This product is highly efficient when used as a dust suppressant on mine site roads, as the salts bind the dust particles as the water evaporates.

A flocculant is added to the settled solids and pumped from the oxide tanks into a 1.5 hour retention thickener. The underflow typically has a solids fraction of 16.2% weight solids per weight of water. Dried density of solids at Brukunga was 4167 kg m⁻³. The underflow from the thickener consists of a mixed metal hydroxide cake which is self standing. This mixture can be solar dried to powder in 2 hours during summer.

The mixed metal oxide powder may then be sold by Global Aquatica to assist in funding the BioAqua operation. A thickener is required for each output product followed by solar drying to powder form. The product is packaged into sealed 1 tonne bulker bags for truck or rail transport from site.

2.2 Stage 2. Biological Treatment Process

The bacterial process utilises sulphate reducing bacteria (SRB) to convert the contaminant chemistry from environmentally toxic to environmentally safe for recycling. These bacteria have been successfully used for the passive treatment of AMD in relatively low volumes over the past 40 years, where they convert the metal sulphates into insoluble and soluble metal sulphide species. However, these metal sulphides produce a toxic environment to the bacteria, eventually resulting in their death. Also the process is rate limited by the availability of nutrient to the bacteria.

Prior to BioAqua, there were no low-cost, fully utilised nutrient sources available for the bacteria. As a result, previous processes have utilised very large volumes of low-cost plant matter, where the bacteria typically utilise only a small portion of the mass. This produces large volumes of waste nutrient product on site. The rate at which these sources can be utilised by the bacteria also retards the treatment potential of the process. Also, competing micro-organisms consume the nutrient intended for the SRB or outcompete the SRB. Eventually, the food source is depleted or metal sulphide toxicity kills the bacteria or the competing bacteria change the water chemistry.

A three stage bacterial sulphate reduction, sealed bioreactor process is used providing 3 hours of retention time to fully remove sulphates from the water and convert the remaining cations to carbonates. The underlying approximate biochemical reaction occurring in the described processes is as follows:



This reaction describes the conversion of sulphate into sulfide, and the organic carbon into carbonate, carbon dioxide and water. CH₂O represents organic carbon.



Figure 4. Three bioreactors on the front pod (1300 L hr⁻¹)

2.3 Stage 3. Hydrosulphide Removal

The sulphate reducing bacteria reduce the sulphates into sulphides. Due to the redesigned kinetics of the bacteria, these sulphides bond with hydrogen producing a hydrosulphide product instead of metal sulphide. The bacteria also oxidise the nutrient through several stages resulting in carbon dioxide which is released with the hydrosulphide as a biogas.

The hydrosulphide and carbon dioxide gases are removed together, dissolved in water. Sulphide oxidising bacteria are used which prefer to return the hydrosulphide to sulphate. However, this is not permitted by denying the bacteria the oxygen they requires to complete the biochemical processes. Hence, the bacteria partially oxidise the hydrosulphide to form high purity bacterial elemental sulphur which is recycled by Global Aquatica to fund plant operation.

The chemical equation describing the process is as follows:



The hydrogen in the gas is typically oxidised into water in the aqueous environment of the bioreactor. After the HS⁻ is removed, the remaining carbon dioxide is recycled back into the process applications as required by the BioAqua process.

A dry high purity synthetic elemental sulphur cake is produced as a sludge, from which the solids are separated using a thickener. Alternatively, a hydrogen sulphate (sulphuric acid) or sodium sulphide floatation product can be produced for mineral processing by minesites. This method can also be used to recycle the sodium sulphide and sulphuric acid from treatment plant effluent for such applications as copper refining.

A 5 hour retention time in sealed tanks is required to convert all the sulphide into elemental sulphur.



Figure 5. Sulphide oxidation tanks (1300 L hr⁻¹)

2.4 Stage 4. Carbonate Precipitation

Due to the chemistry of the nutrient, reduction of sulphates by the bacteria creates a solution high in carbonates (alkalinity). The bacteria have been designed to bond the cations with the carbonate forming carbonate and hydroxide compounds. These products are separated from the water and recycled by Global Aquatica to fund plant operations.

Downstream of the sulphate reducing bioreactor, calcium carbonate and manganese carbonate precipitates from solution and is then permitted to settle in a tank and the treated water skimmed from the top. A dry high purity synthetic calcium carbonate cake and manganese carbonate cake is produced as a sludge, from which the solids are separated using thickeners.

The remaining water principally consists of magnesium, sodium and potassium as carbonates. The water is then treated with hydroxyl radicals and the carbonates consumed to form hydroxides. A high purity magnesium hydroxide precipitates from solution in a settling tank, leaving a treated water that contains only sodium hydroxide and trace concentrations of other compounds. It has been observed by Global Aquatica that AMD typically has comparatively low concentrations of potassium. This sodium hydroxide product may be partially reused to assist other BioAqua processes. The magnesium hydroxide sludge is converted into a high purity synthetic magnesium oxide solid cake using a thickener.

After removal of the magnesium, the carbon dioxide from the previously described processes, and that scavenged from the above reaction, can be added to the treated water, converting the hydroxides back into carbonates resulting in a treated water whose main compound is sodium carbonate. This product is produced by BioAqua to protect aquatic

ecosystems from the errant acidity that often escapes acid producing mine sites. This water neutralises any acidity in the river that may escape the site, prevents scaling of pipes and prevents corrosion when used for mining activities. Otherwise it may remain as hydroxide if required by the stakeholders.

3.0 TREATMENT KINETICS

3.1 Carbonate Production Kinetics

The natural processes of the sulphate reducing bacteria that utilise metals are not preferred for the eradication of sulphates from an AMD site. In the BioAqua process, all metals are usually removed, typically to 99.97% prior to the bacteria stages with the exception of sodium, magnesium, manganese, potassium and calcium. Global Aquatica has redesigned the kinetics of the bacteria, permitting them to operate without the galvanic charge differential normally provided by the metals. A fully utilisable low cost nutrient was also essential in assisting that process, including converting the remaining cations to carbonates and hydroxides. It is also essential in causing their rapid precipitation for removal and sale by Global Aquatica.

With the removal of the metals, a galvanic charge differential no longer exists for the bacteria to utilise, so we designed a significantly more efficient bio-electro-chemical process. To achieve this, we have developed a specific carbohydrate substrate for the bacteria and altered the biochemical structure of the bacteria to increase their electro-chemical potential. This effectively increases the capacity of the bacteria to convert the contaminants without metals.

3.2 Electrochemical Substrate

We have designed a process that fully transforms greenwaste from rubbish tips into the very specific carbohydrate required to perform the above biochemical processes. These conversion processes typically occur off site, preferably at the ligno-cellulose (greenwaste) source. The resulting carbohydrate has a similar appearance to table sugar. This product is trucked to the BioAqua located at the contamination source and the carbohydrate loaded into silos. The BioAqua process then automatically feeds the carbohydrate into the process as it is required. The bacteria utilise 100% of the carbohydrate resulting in BioAqua not producing any stored wastes.

The net result is that conventional bacterial methods typically convert sulphates into toxic sulphides at a maximum rate of $3\text{g SO}_4 \text{ d}^{-1} \text{ L}^{-1}$ of bioreactor volume. BioAqua bacteria typically convert the sulphates into environmentally safe carbonates at approximately $85\text{g SO}_4 \text{ d}^{-1} \text{ L}^{-1}$. This faster conversion rate permits the biochemical processes to be contained within sealed tanks instead of the open ponds common to passive treatment. This permits Global Aquatica to precisely control the bacteria environment creating the steady state condition vital for maximising the efficiency of the bacteria.

3.3 Fats, Oils and Greases (FOG)

The bacteria typically consume approximately 78% of the FOG. This is useful on mine sites where effluent from vehicle workshops is frequently stored in AMD wastewater ponds.

4.0 PROCESS FLEXIBILITY

The BioAqua process was designed in conjunction with site superintendent level personnel from international mining companies operating in Australia. As a result the process is attendant to the variables and conditions typical of mine sites. For example, the BioAqua process is a multistage process. The first stage of that process removes the toxic metals and acidity but retains the salts in the water, forming an excellent road dust suppressant.

The pH and most chemical properties of the water can be adjusted to suit the stakeholder requirements. For example, a mine site may be producing too much water in the form of acidic wastewater. Whereas an adjacent mine site may not have sufficient water or the water quality is alkaline. Global Aquatica can adjust the BioAqua operation to produce acidity of the required concentration to neutralise the alkaline water.

Alternatively, the metals, acidity or salts may be extracted from mineral process plants and the water returned for reuse by the plant at the optimum chemistry complete with the necessary reagent concentration such as sulphuric acid or floatation agents. This would considerably reduce the consumption of those reagents and significantly reduce overall water consumption by the mine site by recycling of the process water.

5.0 WASTEWATER MANAGEMENT

Global Aquatica provides total waste water management in stages.

1. **Investigate.** The wastewater chemistry is compared with the required treated water chemistry and a determination made regarding the likely ability of BioAqua to treat the water.
2. **Confirm.** A pilot plant is operated on site to confirm the engineering calculations and develop design parameters. Also, actual treated water can be produced at the site providing additional security to regulators and providing planning information for stakeholders such as an operating mine site.
3. **Design.** A one ML d⁻¹ plant is designed, based on the parameters produced from the pilot plant.
4. **Construct.** Global Aquatica will build the components and construct a one megalitre/day BioAqua on the contaminated site. A nutrient facility will also be constructed.
5. **Manage.** The plant will be commissioned and the optimum operational parameters maintained during operation.
6. **Value add.** The high purity products from the BioAqua production will be recycled by Global Aquatica. The revenue will be used to operate the plant and upgrade its flow rate capacity as required.

6.0 DISCUSSION OF PROCESS PARAMETERS

A one ML day⁻¹ BioAqua plant is expected to have a footprint of approximately 60m x 35m.

RETENTION TIME

PROCESS	HOURS
Cavitation	instantaneous
Settling tanks below cavitator	1.7
Thickener	1.5
Sulphate reduction, including carbonate conversion	3

Sulphide oxidation, and sulphur settling	5
Calcium Carbonate settling	1.5
Magnesium hydroxide precipitation	2
TOTAL PROCESS RETENTION TIME	8.2 hours

OUTPUTS

All contaminants in the water are converted to recyclable products except sodium and chloride. These elements can be removed by post treatment if required without the use of reverse osmosis.

Mixed metal oxide powder. The cavitators can be 'tuned' to selectively remove elements and form desired compounds depending on the AMD chemistry. For example, at Brukunga, the cavitators are 'tuned' to remove all metals at once, except magnesium and manganese where 50% of the manganese is removed at the cavitator as a hydroxide and the other 50% as an insoluble carbonate with the calcium carbonate. The manganese is later separated from the calcium. Thirty to fifty percent of the magnesium is removed as hydroxide by the cavitators and the rest as magnesium hydroxide after the calcium is removed.

The form of products produced are:

Mixed metal oxides.

High purity elemental sulphur.

High purity calcium carbonate. All calcium is removed as carbonate.

High purity manganese carbonate.

High purity magnesium oxide.

All products are solar dried to a fine powder, bagged and sold. There are no stored wastes left on the site after treatment by BioAqua.

INPUTS

The only input is carbohydrate, which may be recycled and is fully utilised by the bacteria. Hence, there are no carbon wastes from BioAqua. The amount of carbohydrate added varies with water chemistry and biological demand. Comparison of carbohydrate consumption with acidity removal may be misleading, as there are negligible metals in the bioreactors. On average, the Brukunga plant consumes 0.83 kg carbohydrate for every kg of acidity removed. The plant consumes 1.6 KW of power for every kilogramme of acidity removed.

Usually there are no imported chemicals.

7.0 ACKNOWLEDGEMENT

Global Aquatica thank the South Australian government for the use of the Brukunga site and SA Water for their full custody sampling and analysis of the treated water from the operating plant at the Brukunga site.

8.0 REFERENCES

1. Global Acid Rock Drainage Guide. International Network for Acid Prevention. (INAP)
2. Australian Drinking Water guidelines 6. (2011) ver 3.3 November 2016. Australian Government.

9.0 APPENDIX

Summary table of a report on the sampling and analysis of the treated water from the tailings seepage at the Brukunga mine site by SA Water (South Australian government) is shown below. A copy of the actual report is available on request to Global Aquatica Pty Ltd. The 'raw water' and 'treated water' samples were taken at the same time. Note the sodium and chlorides are higher in the treated water than the raw water. This was due to a 'first flush' rainfall event at the end of summer between the time the water entered the 8 hour process cycle and the time of sampling of the treated water. BioAqua typically does not remove sodium or chloride without additional downstream processes. Therefore it would be expected that the concentration of contaminants in the raw water under treatment were higher than indicated in the results.

Concentrations of solutes in raw water and BioAqua treated water measured by SA WATER.

SOLUTE	UNIT	RAW WATER	TREATED WATER
Aluminium	mg L ⁻¹	47	0.079
Arsenic	mg L ⁻¹	0.0036	0.0009
Barium	mg L ⁻¹	0.0048	0.017
Cadmium	mg L ⁻¹	0.0022	0
Calcium	mg L ⁻¹	384	32.4
Chloride	mg L ⁻¹	215	505
cobalt	mg L ⁻¹	0.0501	0.0001
copper	mg L ⁻¹	0.0069	0.0015
Iron	mg L ⁻¹	2385	0.1249
Magnesium	mg L ⁻¹	325	17.9
Manganese	mg L ⁻¹	100	1.067
nickel	mg L ⁻¹	0.0565	0.0031
potassium	mg L ⁻¹	68.1	9.85
sodium	mg L ⁻¹	201	364
strontium	mg L ⁻¹	0.3982	0.1820
Sulphur (as sulphate)	mg L ⁻¹	6540	176
zinc	mg L ⁻¹	3.03	0.0226

EVALUATING APPLICATIONS OF BED AND FLY ASH FOR CONTROLLING ACID AND METALLIFEROUS DRAINAGE - EXAMPLES FROM TASMANIAN MINE WASTES

A. Parbhakar-Fox^A, R. Clifton^A and N. Fox^B

^AARC Industrial Hub for Transforming the Mining Value Chain (TMVC), University of Tasmania, Private Bag 79, Sandy Bay, TAS 7001, Australia

^BCRC ORE, University of Tasmania, Private Bag 79, Sandy Bay, TAS 7001, Australia

ABSTRACT

The use of alkaline materials (e.g., limestone (CaCO₃), lime (CaO) to neutralise and control acid and metalliferous drainage (AMD) is a well-established global practice. However, these materials are costly, and therefore alternative cost-effective ameliorants for AMD are needed. Alkaline-rich industrial by-products from paper and pulp mills could, in theory, be used. However, the success of such materials is dependent on their physical (e.g., plasticity) and chemical (i.e., chromium, cadmium and copper content) properties.

Hundreds of mine-impacted sites in Tasmania are affected by AMD, and, as many are under the care of the State Government, a cost-effective approach to rehabilitation is needed. This study evaluated the AMD mitigation potential of boiler ash collected from the Boyer Pulp and Paper Mill operated by Norske Skog in Tasmania. These materials were combined in free-draining column leach cells with sulfidic mine waste (tailings and waste rock) from six legacy sites in Tasmania. Two types of ash were used, a fine fly ash (currently landfilled) and a coarser bed ash. Mineralogically, both were Class F ash comprising of mullite, quartz and carbon, minor gypsum and trace CaO.

The column tests were conducted for 24 weeks using a combination of mine waste capped with both types of boiler ash, fly ash blended with lime, and for the tailings, cells using just an organic cover were tested. The use of fly ash as a capping layer was the least effective cover; however its performance was improved when intermingled through waste materials. The use of bed ash as a capping layer was more effective, particularly for tailings. Overall, the best performing cover was blended lime with boiler ash, particularly for low-pyrite, low-As (< 1 wt. %) wastes. These results suggest that boiler ash has a potential application for controlling AMD in bespoke rehabilitation projects.

1.0 INTRODUCTION

Over the past decades, solid and processing mining wastes have been recognized as major sources of acid and metalliferous drainage (AMD), management of which is the single greatest environmental challenge currently facing the mining industry (Younger et al., 2006; Akcil and Koldas, 2006; Mäkitalo, 2015). In 2010 approximately 14 billion tonnes of tailings were produced globally with gigatonnes of solid mine waste also being produced annually (Mudd, 2011; Adiansyah et al., 2015). Once exposed to air and water, acid generation from sulfides can continue for hundreds to thousands of years after mining has ceased (Alakangas et al., 2013). The environmental degradation caused by AMD is profound, representing continual sources of acidity with potential for metal mobilisation, contributing to the acidification of water and soil and posing a threat to the ecological balance and biota (Jia et al., 2014).

Under the current socio-economic climate, management of mine waste is of significant concern for the industry, with 'social licence to operate' (i.e., neglecting mine rehabilitation obligations which are impacting on the sector's image) listed as the seventh biggest risk in 2016-17 for any mining operations (Ernest Young, 2017). However, this was not always the case, with many historical examples of poorly managed mine waste e.g., Iron Mountain, United States (Nordstrom et al., 2000), Rio Tinto mine, Spain (Romero et al., 2006) and Wheal Jane, United Kingdom (Younger et al., 2005). In Australia, there are at least 50,000 sites with historic or legacy mine wastes, the majority of which require rehabilitation (Pepper et al., 2014). To fund rehabilitation work at abandoned mines (i.e., sites that no longer have a mining lease or title and for which the original operator is no longer responsible; Unger et al., 2015), supplementary funding from Government bodies is likely required, a topical issue drawing much media attention in Australia (Roache and Judd, 2016). Ultimately, such funds are sourced from taxes, therefore compromising the allocation of funding towards perceived social priorities, i.e. improved transport infrastructure, upgrading community services. The approach adopted in additive rehabilitation strategies is to use raw materials such as calcium carbonate or calcium hydroxide, both of which are costly (up to \$200 per tonne for water treatment materials). Instead, cost-effective alternative products should be considered for use, particularly if these are waste materials produced by other industries. Such a practice aligns with 'Circular Economy' principles (Lieder and Rashid, 2016), and assists with the adoption of the 2015 United Nations Sustainable Development Goals (UN SDGs; Maurice, 2015). In Tasmania, there are at least 681 metal-related abandoned mines, 215 of which have been identified as a potential environmental threat due to acid producing materials (Gurung, 2001; Pepper et al., 2014). This study focusses on using one waste type (boiler ash) produced by the paper manufacturing industry to ameliorate AMD produced from a range of mine waste materials collected across Tasmania.

2.0 MATERIALS AND METHODS

2.1 Mine Waste Materials

Three tailings and three waste rock sites in Tasmania were selected in this study, representative of different economic mineralisation, host rock geology and local climatic conditions. These sites produce varying quantities of AMD with different environmental impacts. The rationale for choosing these sites was that such heterogeneous mine wastes would allow a comprehensive evaluation of AMD control by boiler ash materials. Of the sites chosen, three (Rossarden, Royal George, Old Spray) are closed and maintained by the State Government. Mount Bischoff is under care and maintenance overseen by Metals X Ltd. The Savage River and Mount Lyell mines continue to operate under 'new' ownership with indemnities in place for historic pollution designated the responsibility of the State Government (Kent and Dineen, 2009). In terms of environmental risk, Mt. Lyell and Savage River historic mine wastes are acid forming with high iron-sulfide contents. Mt. Bischoff is additionally high-risk having been identified as one of the worst AMD sites in northwest Tasmania (Gurung, 2001). Whilst many sites in Tasmania host low sulfide mine-waste, they still have an acid forming potential due to the absence of primary neutralising materials (e.g., Rossarden and Royal George); therefore waste of this nature has also been tested in this study.

2.1.1 Tailings

Tailings were collected from Rossarden and Royal George (east Tasmania) during a site visit in February 2016. These tailings were retrieved using a clean shovel, with a trench (approximately 1 m x 2 m x 0.5 m) dug into fresh tailings to collect these, with the uppermost 10 to 20 cm horizon discarded to alleviate sampling of oxidised material. Up to 20 kg of material was obtained from two separate locations at the Royal George tailings site, and one location at the Rossarden tailings. Grange Resources kindly collected tailings from the Old Tailings

Dam at Savage River (February 2016) from a location known to contain highly acid forming materials (Zone C as designated in Jackson and Parbhakar-Fox, 2016). All tailings were sealed, stored (for < 1 week) in a cool laboratory until their use. Tailings preparation first included oven drying at 40° C (University of Tasmania Laboratories) for at least one-week. Once dry, they were gently disaggregated using a mortar and pestle with larger clumps broken down and foreign matter (e.g., pebbles, organic material) removed. Sizing of tailings confirmed these as fine-grained (< 600 µm), and therefore no further preparation was undertaken. Approximately 1.5 kg of tailings were set aside for each kinetic testing column using riffle-splitter sampling methods.

2.1.2 Waste rock

Waste rock materials were not collected during this study. Instead, these were obtained from the Earth Sciences rock store, University of Tasmania. Previously, these materials (up to 30 kg) had been used in long-term kinetic trials in the CRC ORE Environmental Indicators project (2011-2015). As these were used without a cover, data for these column tests were obtained and used in this research as the 'control' cell. These materials had been stored in air-tight containers; therefore, any recent oxidation was likely to be minimal when compared to that induced under natural surface conditions (as experienced for several decades at each site). These materials were crushed and sieved to the 2-4 mm size fraction as recommended in the AMIRA P387A kinetic testing procedure (Smart et al., 2002), with 6 kg of each material prepared. Representative blends of rock and ameliorant (approximately 500 g) were pulverised in a tungsten-carbide mill (to <125 µm) also for use in column feed characterisation testing.

2.2 Boiler Ash Materials

Class F boiler ash (fly and bed; Stouraiti et al., 2002) materials (approximately 15 kg) were collected in March 2016 from Norske Skog Pulp and Paper Mill, Boyer, located in southern Tasmania. Norske Skog are the largest producer of lightweight coated papers and specialty newsprint in Australia with production capability of 300,000 tonnes per year (Coughanowr et al., 2015). A thermo-mechanical technique of pulping is used, which relies on the steam generated from the boiler. Ash from this boiler and other solid wastes (e.g., wood waste, plant biomass from water and wastewater treatment plants) are reused or recycled when possible, or deposited at the nearby Boyer Mill solid waste landfill facility (Coughanowr et al., 2015). Norske Skog's No. 5 boiler uses 90,000 tonnes per annum of coal to provide steam energy to power machinery on site. Approximately 30 % (25,000-28,000 tonnes) of the coal used is recovered as boiler ash. This accumulates in the base of the boiler (bed ash) or is suspended in flue gases (fly ash; Skousen et al., 2012). The bed ash is moved out of the boiler by a conveyor within the furnace, it is then transferred to silos for storage before being taken off-site. An electrostatic precipitator and particle removal equipment have been installed to meet environmental regulations, which captures fly ash and transfers it to storage silos, where it is temporarily stored. Finally, it is transported to a landfill facility maintained by Norske Skog.

In total, 15 kg of each was collected from Norske Skog Boyer pulp and paper mill in March, 2016, with a further 15 kg obtained in September 2016 for physical testing. The first batches of ash materials were oven dried as required for use in geochemical and mineralogical analyses followed by their use in kinetic column tests. Geochemical data on these materials were provided by Norske Skog (i.e., whole rock analyses, TCLP extractable metals), with these analyses undertaken at the Tasmanian Government Laboratories, New Town, Tasmania using accredited methods. The physical properties (i.e., moisture content, Atterburg limits, particle size) of these ash were tested at ADG Laboratories, Mornington, Tasmania (methods codes: AS1289.6.8.1 and AS1289).

2.3 Kinetic Testing and Leachate Analyses

Free draining column leach tests were established at the University of Tasmania in April 2016 following the AMIRA P387A Handbook (Smart et al., 2002) and ran for 24 weeks. Twenty-seven columns were established using combinations of mine waste, boiler ash, commercial lime and organic materials (mulch) as detailed in Table 1. Measurements of pH and electrical conductivity were made weekly. Every fifth week leachate samples were taken after pH and EC measurements, filtered (through a 0.45 µm PES milipore) and acidified with 1% HNO₃ and stored in a refrigerator until both solution chemistry analyses were undertaken. Leachates from weeks 0, 10 and 20 were measured using a Sector Field Inductively Coupled Plasma Mass Spectrometer at the University of Tasmania (ICP-MS; Thermo Fisher Element 2, Bremen, Germany). Quantification was via the method of external calibration performed using a series of standards prepared from premixed standard solutions (QCD Analysts, Environmental Science Solutions, Spring Lake, USA). Multiple blank solutions and quality control samples were regularly analysed to monitor instrument performance during each analytical sequence. Prior to analysis all supplied samples were diluted 1000x (gravimetrically). Indium (High Purity Standards, Charleston, USA) was added to each sample dilution as an internal standard (present at final concentration 0.1 ppm) with nitric acid added (Seastar Baseline, supplied by Choice Analytical, Sydney, Australia; final concentration 1%).

To determine the bulk mineralogy of the column feed materials ($n= 27$; as well as materials collected intermediately and at the end of the kinetic column test; $n= 88$), a Bruker benchtop D2 Phaser XRD instrument (equipped with a Co tube) was used at the University of Tasmania. Samples were prepared in a ball mill (waste rock) or by mortar and pestle (tailings) to obtain a suitably fine grain size for analysis (i.e., < 10 µm). Each sample was loaded into sample holder, and placed into the machine chamber and analysed for 30 minutes at an operating voltage of 30 kV and 10 mA. Each scan ranged from 5 to 90° with a 0.02° step size and a measurement time of 0.8 seconds per step. The resulting data were processed using DIFFRAC.EVA with the PDF-2 (2012 release) powder diffraction mineral database to identify the mineral phases. The mineral abundances were semi-quantified using TOPAS pattern analysis software. An integration of mineralogical data with leachate chemistry was performed to assist in the identification of the reactions occurring in these experiments.

Table 1. Description of individual columns.

Column number	Site	Type	Treatment	Waste material (kg)	Cover material (kg)
1	Old Spray	Waste rock	Fly ash (cap)	2	0.25
2	Old Spray	Waste rock	Fly ash (intermingled)	2	0.25
3	Old Spray	Waste rock	Bed ash (cap)	2	0.25
4	OTD	Tailings	Bed ash (cap)	1.5	0.25
5	OTD	Tailings	Lime and fly ash cover	1.5	0.125 (fly ash) 0.125 (lime)
6	OTD	Tailings	Fly ash (cap)	1.5	0.25
7	OTD	Tailings	Fly ash (intermingled)	1.5	0.25
8	OTD	Tailings	Control	2	0
9	OTD	Tailings	Fly ash with organic cover	1.5	0.125 (fly ash) 0.125 (organic)
10	Royal George	Tailings	Control	2	0

11	Royal George	Tailings	Fly ash with organic cover	1.5	0.125 (fly ash) 0.125 (organic)
12	Royal George	Tailings	Fly ash (cap)	1.5	0.25
13	Royal George	Tailings	Fly ash (intermingled)	2	0.25
14	Royal George	Tailings	Bed ash (cap)	1.5	0.25
15	Royal George	Tailings	Lime and fly ash cover	1.5	0.125 (fly ash) 0.125 (lime)
16	Mt. Bischoff	Waste rock	Fly ash (cap)	2	0.25
17	BLANK				
18	Mt. Bischoff	Waste rock	Fly ash (intermingled)	2	0.25
19	Mt. Bischoff	Waste rock	Bed ash (cap)	2	0.25
20	Mt. Lyell	Waste rock	Bed ash (cap)	2	0.25
21	Mt. Lyell	Waste rock	Fly ash (intermingled)	2	0.25
22	Mt. Lyell	Waste rock	Fly ash (cap)	2	0.25
23	Rossarden	Tailings	Bed ash (cap)	1.5	0.25
24	Rossarden	Tailings	Lime and fly ash cover	1.5	0.125 (fly ash) 0.125 (lime)
25	Rossarden	Tailings	Fly ash (intermingled)	1.5	0.25
26	Rossarden	Tailings	Fly ash (cap)	1.5	0.25
27	Rossarden	Tailings	Control	1.5	0
28	Rossarden	Tailings	Fly ash with organic cover	1.5	0.125 (fly ash) 0.125 (organic)

3.0 RESULTS

A significant quantity of data was collected in this study; however to keep the presentation of results concise, each cover or application type will be summarised individually in the following section (rather than by site) with reference made to the leachate chemistry and mineralogy. Comparison of leachate data with the 80% ANZECC (2000) Aquatic Protection guideline values only are presented, and, as these are mine-impacted environments, it was considered that a comparison to 95% values may not reflect the natural baseline in these mineralised areas.

3.1 Boiler Ash Characteristics

Both fly ash types are classified as non-plastic materials with average moisture contents of 46 to 47 %. The mineralogy comprises mullite, quartz, organic carbon and also gypsum in the case of fly ash. The bulk chemistry for both materials was dominated by Al and Si with concentrations of Mn, Zn, Pb and Cu measured below ANZECC (2000) ISQG values. However, leach tests reported Al above ANZECC (2000) aquatic protection levels (95 %) trigger but all other measured elements, except Ni, were below the 80% criteria and WHO (2006) drinking water guideline values. Long-term pH tests confirm that both can maintain pH values above 6, with the bed ash a better neutraliser than the fly ash.

3.2 Control Cells

The most acid forming material tested was the OTD tailings, and this also contained the most pyrite (up to 13 wt. %). This was followed by the Mt. Lyell sample (which maintained a column

average of pH 3 over the 24 weeks) closely followed by Mt. Bischoff, the only site to contain pyrrhotite. Whilst they only contained trace quantities of pyrite, both Rossarden and Royal George tailings reported pH values in the PAF field for the first half of the kinetic trial. At week 14, the Royal George tailings pushed into the NAF field, suggesting passivation above pH 6 of pyrite by secondary iron hydroxides may have occurred. In contrast, the Rossarden tailings remained PAF, showing that similar processes did not occur in this cell (despite the similar mineralogy). The least acid forming material tested was the Old Spray waste rock, with a NAF condition reported (column average pH: 6.1) for the majority of the trial (Figure 1).

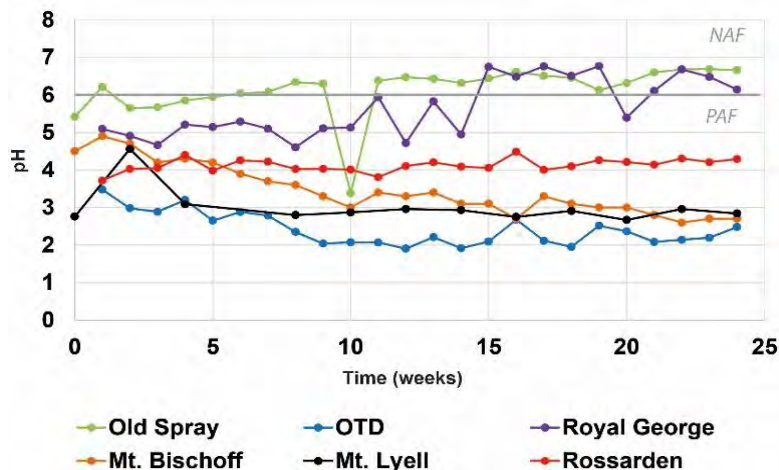


Figure 1. Free draining column leach results for the control cells (n=6).

3.3 Fly Ash Cap

Application of a fly ash cap did not significantly improve leachate quality, with the OTD, Mt. Lyell, Mt. Bischoff and Rossarden columns remaining as PAF (only marginally less so than when untreated). In contrast to the control columns, the Royal George and Old Spray columns now generated a PAF leachate for the majority of the trial (Figure 2). Roy and Berger (2011) suggested that, when open to atmospheric carbon dioxide, leachates from fly ash can decrease in pH. Ponding of water on the surfaces after irrigation was noted in the Royal George and Old Spray cells, and therefore the reactions described by Roy and Berger may have occurred with carbonic acid also forming and contributing to the lower pH in comparison to the control cells (where flow was more rapid). In these experiments the thickness of the cap was approx. 2.5 cm, over approx. 10 cm of waste material. If a greater ratio of ash to waste had been used instead (i.e., Lu et al. (2014) used a 50 cm fly ash cover to protect effectively an equal volume of tailings beneath it), then retardation of oxygen ingress would likely have been observed and leachate pH values higher. For each cell, As in leachate was below the ANZECC (2000) guideline value, but Cu was above these for OTD and Mt. Lyell materials with high Al also measured.

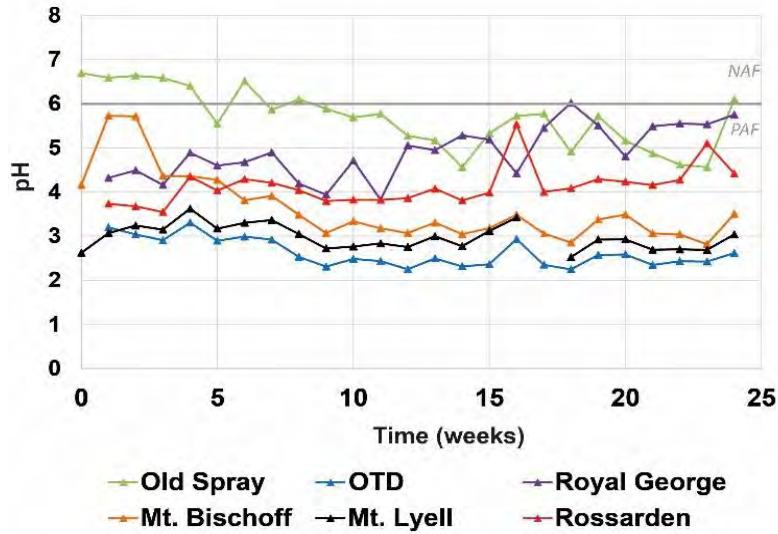


Figure 2. Free draining column leach results for the fly ash capped cells (n=6).

3.4 Intermingled Fly Ash

It was hypothesised that by intermingling fly ash in mine waste, pH sealing layers would form and mechanically armour sulfides (Muraka, 2006). In general, intermingling was more effective at raising pH than applying the ash directly as a capping layer despite using the same ratio of materials, particularly for Old Spray and Royal George, where NAF conditions were maintained (Figure 3). However, for highly acid forming wastes from the OTD and Mt. Lyell, the average column pH did not significantly increase. For the Rossarden material, the pH remained PAF though a net-increase of 0.8 pH units was calculated. This implies that, with an increased experimental time, this may have worked successfully. Arsenic was below the ANZECC (2000) guideline value for all sites, with the greatest As eluted from Mt. Bischoff and Old Spray materials. Aluminium from all sites was once again low with the exception of Mt. Lyell and the OTD cells. Copper decreased over time for the OTD cell (a trend also noted in the fly ash cap cell). All other Cu values were consistently lower than for the fly ash cap. In general, Ni mimicked the trend for Cu, but for the OTD cell it still measured above the ANZECC (2000) 80% guideline value at week 24. Leachate Zn for the Rossarden and Royal George cells were consistently lower than when the fly ash was used as a cap.

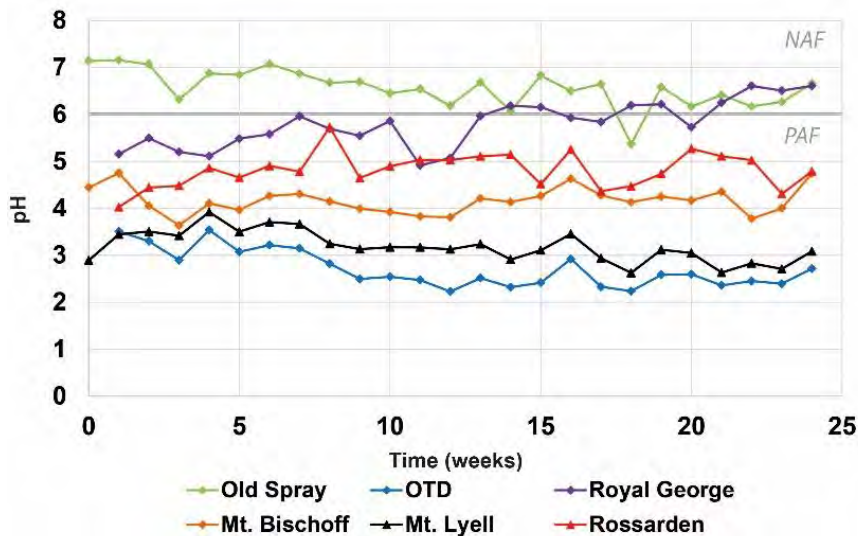


Figure 3. Free draining column leach results for the intermingled fly ash cells (n=6).

3.5 Bed Ash Cap

Fluidised bed ash materials have been recognised as an AMD ameliorant (Taylor et al., 2005); however the availability of this material is limited due to its use as an agricultural soil amendment (Wang et al., 2006). Whilst simple pH testing of the ash materials confirmed bed ash as more alkaline than fly, due to its larger particle size (p_{80} of 67 mm), it was only emplaced as a cap (i.e., not intermingled). Despite this, bed ash appeared ineffective for increasing pH into the NAF field for Mt. Lyell, OTD, Rossarden and Mt. Bischoff materials (Figure 4). Only the Old Spray material was NAF for the majority of weeks (Figure 4). In contrast, for the Royal George cell, a net increase in leachate pH was observed from week 13 onwards; however a similar trend was noted for the control cell, and therefore it may not be attributable to the cover. Arsenic in leachate from Royal George was elevated with respect to the ANZECC (2000) guideline value from week 10 onwards, most likely relating to its geochemical mobility under higher pH conditions (Lottermoser, 2010), whilst all others were below. All sites reported low concentrations of Cu, Pb and Ni with this cover, with the exception of the OTD, for which these did decrease over time. At these proportions, bed ash is not as effective as previously reported (Taylor et al., 2005) and appears best suited to low-sulfide, low As waste.

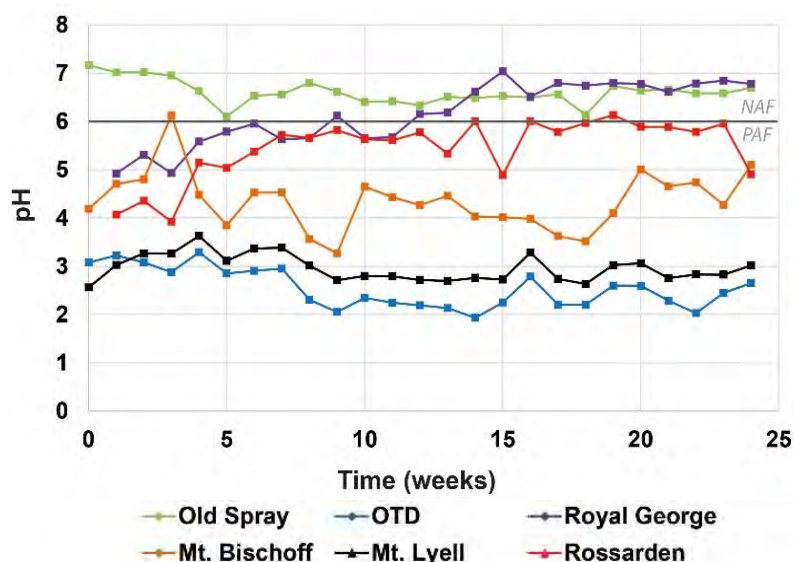


Figure 4. Free draining column leach results for the bed ash capped cells (n=6).

3.6 Blended Fly Ash and Lime

Lime has traditionally been used as an ameliorant for AMD because of its ability to increase alkalinity in the system (Taylor et al., 2005; Zhou et al., 2017). When blended with fly ash, such an effect was observed in Royal George and Rossarden cells with a pH net increase of 3.2 units at Rossarden, the highest recorded in these experiments (Figure 5). Blended lime and fly ash formed a tough cementing layer which has acted as a low permeability hardpan layer. Physical properties of this caliche/hardpan were not determined in this study; however, physical inspections at the time of cell termination showed it had maintained its physical integrity. Alkalinity is provided first by the lime and then ash (Quispe et al. 2013). This cover was much less effective for the OTD material, where the leachate remained PAF over the 24 weeks (Figure 5). Therefore for high pyrite material, an amended fly-ash cover will likely be ineffective. Arsenic at Royal George was above the ANZECC (2000) guideline value suggesting this particular treatment option is unsuitable. Copper decreased over time from the OTD cell (and was very low for Rossarden and Royal George) but remained above the ANZECC (2000) guideline. Nickel was low from both Royal George and Rossarden cells, with a net-decrease observed over time from the OTD material after week 10 also suggesting minor

attenuation (Hale et al., 2012). Zinc showed a net-decrease from both OTD and Rossarden cells and is likely related to alkalinity imparted by the cover (Hale et al., 2012). These results suggest that a blended lime and fly ash capping layer would be effective for low As and sulfide wastes only confirming observations by Muraka (2006) who reported this mixing to be the most effective use for fly ash in this context.

3.7 Organic Cover

The organic cover (applied without ash amendment) did not improve the leachate pH for either the OTD or Rossarden cells (Figure 6) in comparison to the control cell. In contrast, at Royal George, a net increase in pH was recorded pushing leachates into the NAF realm from week 1 onwards showing its efficacy. Such tailings coverage with soils is part of the current integrated management strategy for the site. However, when examining the leachate chemistry, As, the major contaminant at the site, showed a net increase over time. Noble et al. (2016) identified As as scorodite and iron oxide-bound which under reducing acidic conditions can undergo dissolution. Organic acids and a net-reducing condition is established when an organic layer is emplaced, and this is likely what we are observing in the leachate chemistry. The ‘cleanest’ leachate from an OTD cell was reported when using an organic layer, showing that despite not controlling pH effectively, the introduction of organic carbon may be positively influencing these high-sulphide tailings through stimulating heterotrophic microbial growth (Ogbughalu et al., 2017).

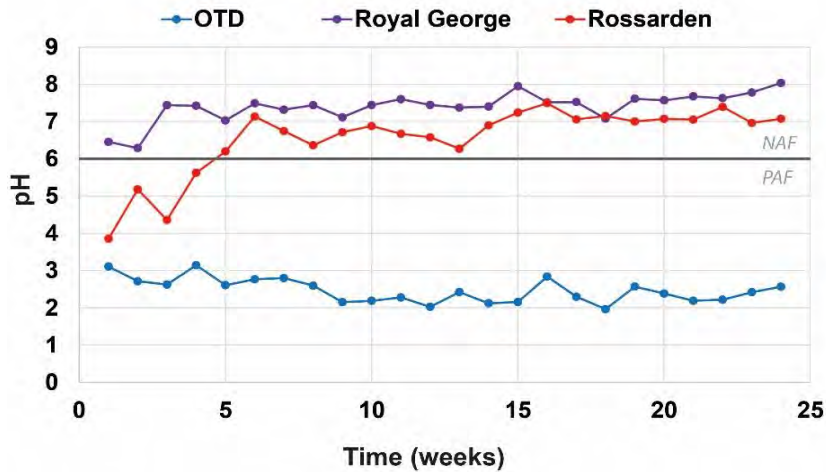


Figure 5. Free draining column leach results for the fly ash + lime capped cells (n=3).

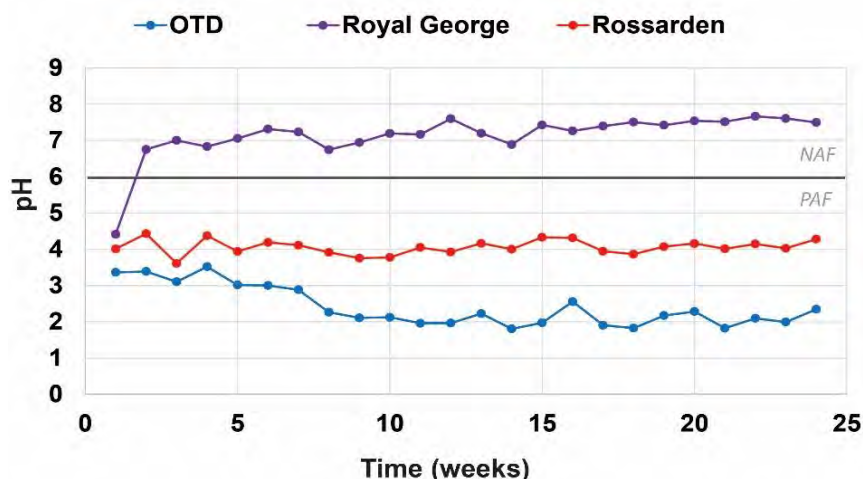


Figure 6. Free draining column leach results for the organic material capped cells (n=3).

4.0 DISCUSSION AND CONCLUSIONS

4.1 Boiler Ash: Applications

Each site has responded differently to each application of boiler ash suggesting that it is not a suitable 'blanket approach' technique. Instead detailed geochemical characterisation of the waste is first required to determine the most appropriate treatment. The physical characteristics of each site (e.g. topography, surrounding land use, access points) also need to be considered. An approximate ratio of waste material to ameliorant of 85:15 was here used as suggested by Sartz et al. (2009) and Lee et al. (2014). However, a higher ratio of boiler ash would have been more effective at raising pH. By using a higher quantity, more ash could be used, and not landfilled, therefore reducing the cost of ash management. Norske Skog has been sending boiler ash to land fill for the past 40 years. Characterisation of aged boiler ash has not been carried out. If it was to have similar mineralogical characteristics as new boiler ash, its use could increase the volume of fly ash available for remediation. Bed ash has more uses within the community, e.g., for agricultural soil amendment, which could make obtaining suitable volumes for remediation work difficult.

Applying a cap provides a cheaper alternative to intermingling the ash at depth; however, this study found that fly ash caps are not as efficient as intermingling. Therefore, intermingling of fly ash to a shallow depth (i.e., 50 cm) could be sufficient to increase the pH of water infiltrating into deeper tailings as discovered by Lu et al. (2014). They used a layer 50 cm thick and found that the influence of the cover was most pronounced in the top 47 cm of tailings. Alternatively, Hallberg et al. (2005) used a 1 m thick layer (of fly ash and biosludge) over 3 m of tailings which induced high pH conditions and the formation of a hardpan layer that impeded oxidation. Lee et al. (2014) found that the hydration of fly ash can generate cementation that can reduce the ingress of water; however in these tests fly ash turned to a thick sludge when wet, and dried into paper thin sheets that disintegrated easily, with ash particles becoming entrained in the extractant fluid during irrigation. Without being confined, this dispersal is likely to remove fly ash from the treatment area, causing fly ash to be less effective over the long term. Due to the pozzolonic nature of fly ash, blending with lime leads to the formation of a caliche style hardpan suitable as a sealing layer, and would be our recommended use of the material.

Quantities of boiler ash to be used as capping layers can be calculated from the surface area of the sampled sites. To achieve a capping layer of 50 cm depth (i.e., as suggested by

Lu et al., 2014) 500 L per m² would be required. At Rossarden, which has a surface area of approximately 20 hectares, this would require 100,000,000 L of ash. Based on one litre of ash weighing 1 kg this would equate to 100,000 tonnes of ash to cover the whole site. As Norske Skog produce only 25,000-28,000 tonnes of boiler ash each year, whole site remediation would have to be carried out over a period of years. Royal George is a smaller site, with a surface area of only 7 hectares, requiring 35,000 L of ash to form a cap 50 cm thick.

4.2 Integrated Rehabilitation Strategy using Boiler Ash

Only a limited number of boiler ash applications were trialed in this study; however, a combination of boiler ash treatments could be used to increase and maintain higher pH (e.g., intermingling bed ash with tailings and applying a fly ash /lime-sealing layer; Figure 7). When used in isolation, boiler ash has not successfully increased pH, but the application of lime (at Rossarden) and organic material (at Royal George) has made a substantial difference. In both cases metal leaching (e.g., As) was notably higher than from other treatment options. Therefore, any rehabilitation scheme using boiler ash should be two phase with pH increased, followed by the removal of metals in leachate using a flow-through reactor /precipitation system. Norske Skog produce other waste types (e.g., wood waste, sewerage sludge) that could be trialed, and there are other agricultural materials available locally that could also be used (e.g., feedlot materials from dairy farms). The financial cost of obtaining boiler ash would be considerably lower than conventional treatments (e.g., lime costs up to \$200 /m²). In the past Norske Skog have offered boiler ash free of charge if collected from site; therefore this could be an attractive opportunity for the management of low-sulphide, low As tailings.

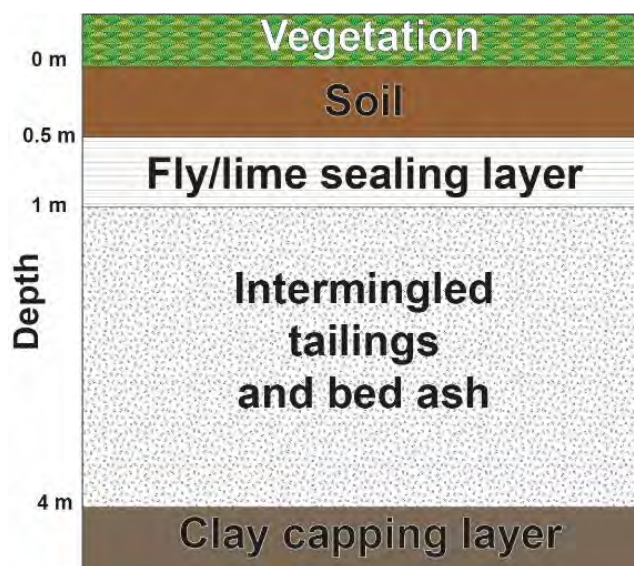


Figure 7. Proposed schematic for the use of boiler ash materials when depositing low-sulphur-low As materials tailings in a well engineered tailings storage facility.

5.0 ACKNOWLEDGEMENTS

This paper is derived from a BSc honours study conducted by the second author as part of the ARC Transforming the Mining Value Chain (TMVC) Industrial Transformation Research Program. Norske Skog are thanked for allowing us to use their boiler ash materials as well as providing geochemical data, with Peter Kearney specifically thanked. Tony Ferguson and Dale Whish-Wilson are thanked for collecting the samples from the OTD. CRC ORE are acknowledged for providing access to waste rock materials and geochemical data.

6.0 REFERENCES

- Adiansyah, J.S., Rosano, M., Vink, S. & Keir, G., 2015. A framework for a sustainable approach to mine tailings management: disposal strategies, *Journal of cleaner production*, vol. 108, no. Part A, pp. 1050-1062.
- Aguilera, A., Manrubia, S.C., Gomez, F., Rodriguez, N. & Amils, R., 2006. Eukaryotic community distribution and its relationship to water physicochemical parameters in an extremely acidic environment, Rio Tinto (Southwestern Spain), *Applied Environmental Microbiology*, vol. 72, pp. 5325-5330.
- Akcil, A. & Koldas, S., 2006. Review article: Acid Mine Drainage (AMD): causes, treatment and case studies, *Journal of Cleaner Production*, vol. 14, pp. 1139-1145.
- Alakangas, L., Andersson, E. & Mueller, S., 2013. Neutralization/prevention of acid rock drainage using mixtures of alkaline by-products and sulfidic mine wastes, *Environmental Science and Pollution Research*, vol. 20, no. 11, pp. 7907-7916.
- ANZECC 2000. Australian and New Zealand guidelines for fresh and marine waters. National Water Quality Management Strategy. Australian and New Zealand Environment and Conservation Council & Agriculture Resource Management Council of Australia and New Zealand, Canberra.
- Coughanowr, C., Whitehead, S., Whitehead, J., Einoder, L., Taylor, U. & Weeding, B., 2015. *State of the Derwent estuary, a review of environmental data from 2009 to 2014*.
- Douglas, G.B., Wendling, L.A., Pleysier, R. & Trefry, M.G., 2010. Hydrotalcite formation for contaminant removal from Ranger Mine process water, *Mine Water and the Environment*, vol. 29, no. 2, pp. 108-115.
- Ernest Young Website. 2017. <http://www.ey.com/gl/en/industries/mining---metals/business-risks-in-mining-and-metals> (accessed 27/10/2017).
- Gurung, S.R., 2001. *1. Acid drainage from abandoned mines in Tasmania*. Supervising Scientist Report.
- Gurung, S.R., Stewart, R.B., Gregg, P.E.H. & Bolan, N.S., 2000. An assessment of requirements of neutralising materials of partially oxidised pyritic mine waste rock, *Australian Journal of Soil Research*, vol. 38, no. 2, pp. 329-344.
- Hallberg, R.O., Granhagen, J.R. & Liljemark, A., 2005. A fly ash/biosludge dry cover for the mitigation of AMD at the Falun mine. *Chemie der Erde- Geochemistry*, vol. 65, pp 43-63.
- Jackson, L.M. & Parbhakar-Fox, A., 2016. Mineralogical and geochemical characterisation of the Old Tailings Dam, Australia: Evaluating the effectiveness of a water cover for long-term AMD control, *Applied Geochemistry*, vol. 68, pp. 64-78.
- Jia, Y., Maurice, C. & Öhlander, B., 2014. Effect of the alkaline industrial residues fly ash, green liquor dregs, and lime mud on mine tailings oxidation when used as covering material, *Environmental Earth Sciences*, vol. 72, no. 2, pp. 319-334.
- Lee, J.K., Shang, J.Q., Wang, H. & Zhao, C., 2014. In-situ study of beneficial utilization of coal fly ash in reactive mine tailings, *Journal of Environmental Management*, vol. 135, pp. 73-80.
- Lieder, M. & Rashid, M., 2016. Towards circular economy implementation: a comprehensive review in context of manufacturing industry, *Journal of cleaner production*, vol. 115, pp. 36-51.

Lockley, J. & Pollington, M., 2006. *Royal George Tin Mine Tailings Rehabilitation Review Report* Mineral Resources Tasmania.

Lottermoser, B., 2010. *Mine wastes : characterization, treatment, environmental impacts*, Berlin ; London: Springer, 3rd Edition; 2010.

Lu, J., Alakangas, L. & Wanhainen, C., 2014. Metal mobilization under alkaline conditions in ash-covered tailings, *Journal of Environmental Management*, vol. 139, pp. 38-49.

Nordstrom, D.K., Alpers, C.N., Ptacek, C.J. & Blowes, D.W., 2000. Negative pH and Extremely Acidic Mine Waters from Iron Mountain, California, *Environmental Science & Technology*, vol. 34, no. 2, pp. 254-258.

Mäkitalo, M., 2015. Green Liquor Dregs in Sealing Layers to Prevent the Formation of Acid Mine drainage: From characterization to implementation, Doctorial thesis thesis, Luleå University of Technology.

Mudd, G.M., Smith, H.D., Kyle, G. & Thompson, A., 2011. In-pit tailings - World's best practice for long-term management of tailings, in *Metallurgical Plant Design and Operating Strategies, METPLANT 2011, August 8- 9, 2011*, Perth, WA, United States, pp. 391-404.

Maurice, J., 2015. UN set to change the world with new development goals, *The Lancet*, vol. 386, pp. 1121-1124.

Murarka, I.P., 2006. *Use of coal combustion product in mine-filling applications: A review of available literature and case studies*, Raleigh, NC.

Noble, T.L., Lottermoser, B.G. & Townsend, A.T., 2016. Mobility of arsenic and environmentally significant elements in mine tailings following liming. *Australian Journal of Earth Sciences*, vol. 63, pp. 781-793.

O'Day, P.A. & Vlassopoulos, D., 2010. Mineral-Based Amendments for Remediation, *Elements (Quebec, Quebec)*, vol. 6, no. 6, pp. 375-381.

Ogbughalu, O.T., Gerson, A.R., Qian, G., Smart, R.C., Schumann, R., Kawashima, N., Fan, R., Li, J and Short, M. 2017. Heterotrophic microbial stimulation through biosolids addition for enhanced acid mine drainage control. *Minerals*, 7, 105; doi:10.3390/min7060105

Pepper, M., Roche, C.P. & Mudd, G.M., 2014. Mining Legacies - Understanding Life-of-Mine Across Time and Space, paper presented to LIFE-OF-MINE 2014 CONFERENCE, Brisbane, QLD, 16-18 July 2014.

Roache, C. & Judd, S., 2016. *Ground Truths: Taking Responsibility for Australia's mining legacies*. <http://www.mpi.org.au/wp-content/uploads/2016/06/Ground-Truths-2016-web.pdf>

Romero, A., Gonzalez, I. & Galan, E., 2006. Estimation of potential pollution of waste mining dumps at Pena del Hierro (Pyrite Belt, SW Spain) as a base for future mitigation actions, *Applied Geochemistry*, vol. 21, pp. 1093-1108.

Roy, W.R. & Berger, P.M., 2011. Geochemical controls of coal fly ash leachate pH, *Coal Combustion and Gasification products*, vol. 3, pp. 63-66.

Sartz, L., Bäckström, M., Karlsson, S. & Allard, B., 2015. Mixing of Acid Rock Drainage with Alkaline Ash Leachates: Formation of Solid Precipitates and pH-Buffering, *Mine Water and the Environment*, 13p.

Schumann, R., Kawashima, N., Li, J., Miller, S., Smart, R. and Stewart, W.S. 2009. Passivating surface layer formation on pyrite in neutral rock drainage. In *Proc. 8th Int. Conf. Acid Rock Drainage*(8 ICARD), Skellefteå, Sweden.

Smart, R., Skinner, W.M., Levay, G., Gerson, A.R., Thomas, J.E., Sobierah, H., Schumann, R., Weisener, C.G., Weber, P.A., Miller, S.D. & Stewart, W.A., 2002. *ARD test handbook: Project P387, A prediction and kinetic control of acid mine drainage*, AMIRA, International Ltd, Melbourne, Australia.

Stouraiti, C., Xenidis, A. & Paspaliaris, I., 2002. Reduction of Pb Zn and Cd availability from tailings and contaminated soils by the applicaiton of lignite fly ash, *Water, Air, and Soil Pollution*, vol. 134, pp. 247 -265.

Taylor, J., Pape, S. & Murphy, N., 2005. A Summary of Passive and Active Tretament Technologies for Acid and Metalliferous Drainage (AMD), in *5th Australian workshop on acid drainage, 29-31 August 2005*, Freemantle, Western Australia.

Thompson and Brett Consulting, 1994. Rossarden/Storys Creek Mine Sites: Rehabilitation Plan. http://www.mrt.tas.gov.au/mrtdoc/dominfo/download/REHAB1994_02/REHAB1994_02.pdf

Unger, C.J., Lechner, A.M., Kenway, J., Glenn, V. & Walton, A., 2015. A jurisdictional maturity model for risk management, accountability and continual improvement of abandoned mine remediation programs, *Resources Policy*, vol. 43, pp. 1-10.

Wang, H., Bolan, N.S., Hedley, M. & Horne, D., 2006. Potential Uses of Fluidised Bed Boiler Ash (FBA) as a liming material, soil conditioner and sulfur fertiliser, in *Coal Combustion Byproducts and Environmental Issues*.

Younger, P.L., Coulton, R.H. & Froggatt, E.C., 2005. The contribution of science to risk-based decision making: lessons from the development of full-scale treatment measures for acidic mine waters at Wheal Jane, UK, *Science of the Total Environment*, vol. 338, no. 1-2, pp. 137-154.

Younger, P.L., Wolkersdorfer, C., Bowell, R.J. & Diels, L., 2006. Partnership for Acid Drainage Remediation in Europe (PADRE): Building a better future founded on research and best practice, in *7th International Conference on Acid Rock Drainage (ICARD)*, Lexington, KY.

Zhou, Y., Short, M.D., Li, J., Schumann, R.C., Smart, R.S., Gerson, A.R and Qian, G. 2017. Control of acid generation from pyrite oxidation in a highly reactive natural waste: a laboratory case study. *Minerals*, 7, 89; doi:10.3390/min7060089.

PORTLAND CEMENT APPLICATION TO CONTROL ACID MINE DRAINAGE GENERATION FROM WASTE ROCKS

M.G. Sephton^A and J.A. Webb^A

^AEnvironmental Geosciences, La Trobe University, Bundoora, VIC, Australia

ABSTRACT

Leaching columns and oxygen consumption tests were used to test the effectiveness of cement application in controlling acid mine drainage generation from waste rocks. Eighteen columns with waste rocks from the Brukunga mine in the Adelaide hills, South Australia, were used to test five different cement slurries in triplicate, with three columns being untreated and used as controls. Leachates collected from the columns over approximately one year after cement application showed that in all cases, cement application greatly decreased acidity release from the waste rocks (by at least 75%). The extent of decrease of acidity was shown to depend on the extensiveness of the cement coverage over the waste rocks within the columns. Low viscosity cement slurries with higher water/cement ratios achieved more extensive coverage over the waste rocks and decreased oxygen consumption, and therefore sulphide oxidation, more than in the columns with more viscous cement slurries, which achieved less extensive coverage but dissolved much more slowly. Cement slurries incorporating fly ash and AMD sludge had similar effects to unblended cements, indicating the viability of using these wastes as cement additives to reduce the cost.

1.0 INTRODUCTION

Although Portland cement has been used in concrete dry covers over waste rock piles in Canada and Sweden (Northwest Geochem, 1996, Karlson et al, 2010), few controlled tests have been undertaken to investigate the effectiveness of cement in controlling sulphide oxidation (Ji et al., 2012). This paper summarises the results of leaching column and oxygen consumption experiments (Sephton and Webb, 2017), to test whether cement slurry applied directly to sulfidic waste rocks is effective in controlling acid mine drainage generation. This paper also summarises results of additional leaching columns used to test the effectiveness of cements blended with fly ash and with acid mine drainage treatment sludge (AMD sludge) compared to unblended cements.

2.0 METHOD AND MATERIALS

The materials used for the experiments were waste rocks from the Brukunga mine in the Adelaide Hills, South Australia, Type GP cement from Cement Australia, Boral Blue Circle Fly Ash, and AMD sludge from the treatment plant at the Brukunga mine (Table 1).

Table 1. Elemental composition of materials used in the experiments, obtained by XRF analysis

	Brukung waste rocks	Type GP cement	Fly ash	AMD sludge
SiO ₂	49.7	19.7	65.3	1.9
Al ₂ O ₃	11.6	5.3	22.9	15.6
Fe ₂ O ₃	7.4	2.7	3.0	14.9
MgO	3.3	1.6	2.6	6.1
CaO	2.4	64.1	1.6	14.4
K ₂ O	2.4	0.7	1.8	0.07
SO ₃	13.5	2.8	<LOD	21.4

Eighteen leach columns, 15.5 cm in diameter and 28-34 cm long, were constructed from PVC pipe. The columns were sealed at the base with a tap outlet to allow for drainage collection, and could be sealed at the top with a screw-on cap, with a 25 mm opening allowing for an oxygen gas sensor to be inserted so that oxygen consumption rate measurements could be obtained. These columns were filled with 4.73 kg samples of Brukung waste rock with grain size ranging from 2-26 mm, and filled to the brim with deionised water, with the volume of water used to estimate the total volume of air in each of the columns, in order to calculate sulphide oxidation rate.

The waste rocks were then leached with 1 litre of deionised water approximately every two weeks for 6 months before cement slurries were applied to the waste rocks. The cement slurries were prepared by weighing the required mass of cement, and where applicable fly ash or AMD sludge, and thoroughly mixing these, before the required mass of water was added and again thoroughly mixed before being poured over the waste rocks (Table 2). After cement application, the columns were leached twenty one times over around one year and the leachates analysed for Fe, S, Al, Ca, Mg, Si, Cu, Mn, Zn using ICP-OES. Prior to cement applications, leachates were collected 24 hours after water application, but after cement application, the permeability of some columns decreased, so one week was allowed for the water to drain through the columns before collection.

In between leaches, oxygen consumption measurements were obtained by sealing the columns with the oxygen sensor in place and recording the rate of decrease of partial pressure of oxygen, which was then used to calculate the sulphide oxidation rate using the ideal gas law; $dn_{O_2}/dt = V/R/T.dP_{O_2}/dt$.

Table 2. Composition of cement slurries applied to leach columns

Columns	Powder composition	Mass of H ₂ O (g)	Water/powder (w/p) ratio
1-3	n.a	n.a	n.a
4-6	250 g cement	200	0.8
7-9	250 g cement	250	1.0
10-12	250 g cement	300	1.2
13-15	187.5 g cement, 62.5 g fly ash	250	1.0
16-18	212.5 g cement, 37.5 g sludge	250	1.0

3.0 RESULTS

3.1 Effect of Cement Composition on Slurry Viscosity

Increasing the water/powder ratio decreased the viscosity of the cement slurry so that it flowed deeper through the waste rocks (Fig. 1c-e). Using 25% fly ash resulted in the cement slurry penetrating slightly less than the unblended cement with the same w/p ratio (Figure 1d), whereas using just 15% AMD sludge greatly increased the slurry viscosity, so that the cement penetration was even less than for slurries with w/p=0.8 (Fig. 1b, f).

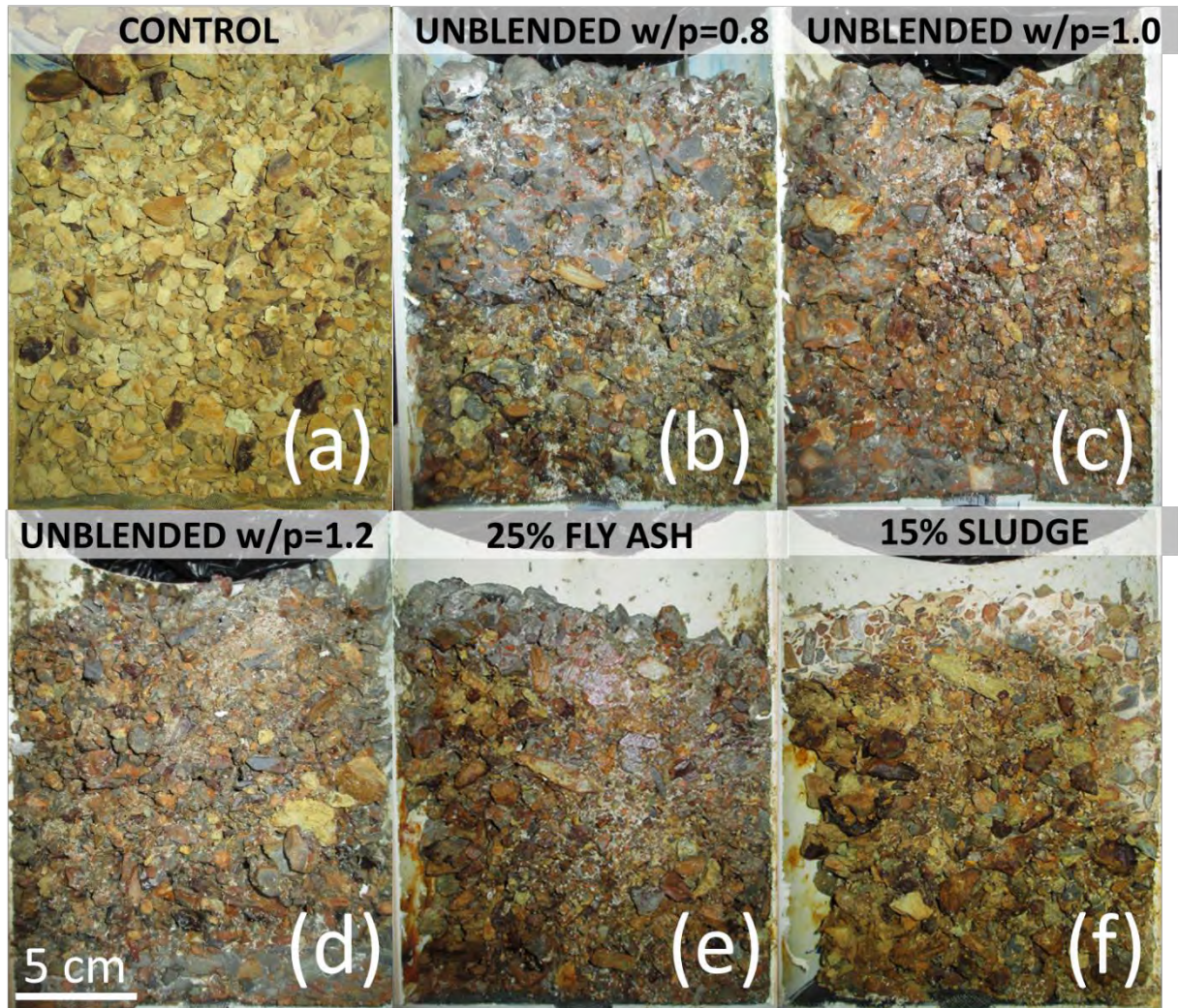


Fig. 1. Cross sections of one representative column from each experimental group

3.2 Effect of Cement Composition on Column Permeability

The differing distributions of cements affected the overall permeability of the columns after cement application. The columns, where the cement was retained at the top, continued to drain freely like the controls, while the columns where the cement had penetrated deeper, drained much more slowly, and over the course of the experiment the rate of drainage decreased over time, reducing the mass of leachate sample (Fig. 2a).

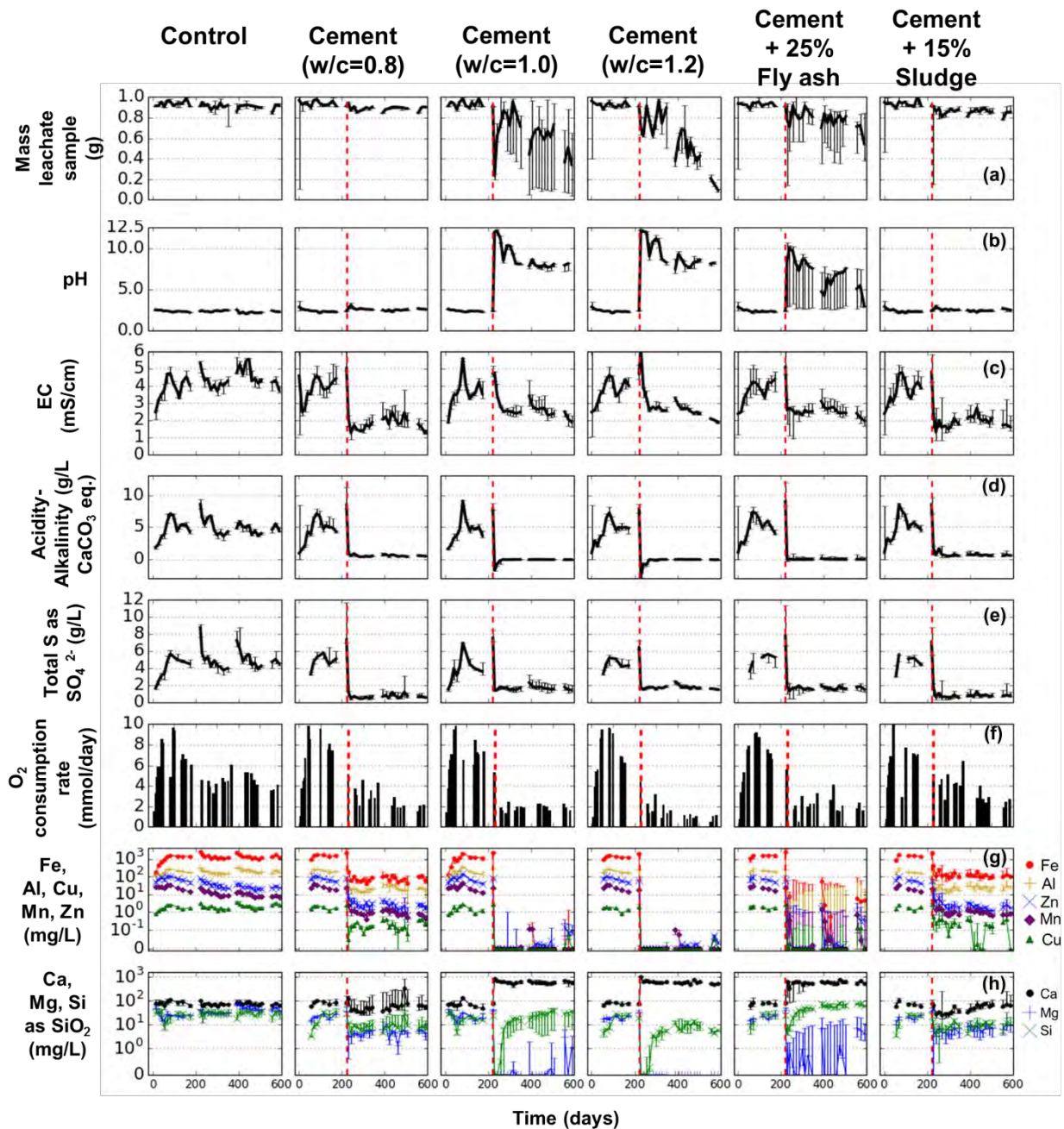


Fig. 2. Time series. a. Mass of leachate sample collected, b. pH, c. Electrical Cond., d. Acidity – Alkalinity, e. Total Sulfur, f. O₂ consumption rates, g. Fe, Al, Cu, Mn and Zn concentrations, h. Ca, Mg and Si concentrations

3.3 Effect of Cement Applications on Sulphide Oxidation Rates

Application of cement caused the oxygen consumption rates to decrease in all columns (Fig. 2f) and decreased most in the columns with less viscous cement slurry applications with cement spread right through the waste rock. The columns with the cement coverage restricted to the top had higher oxygen consumption rates, but still lower than the control columns.

3.4 Effect of Cement Applications on Leachate Compositions

For the columns with cement coverage restricted at the top ($w/p=0.8$ and cement with 15% sludge), after cement application the leachates continued to have a low pH but decreased levels of acidity, Fe, Al, Cu, Mn and Zn (Figures 2b, d and g). This was likely because a significant part of the waste rock at the bottom of these columns had negligible cement coverage and hence contributed acidity to the leachate.

For the columns with deeper cement coverage, leachate pH increased significantly, so that most cases, the leachates were consistently alkaline to neutral and with very low levels of acidity and associated metals (Figures 2b, d and g).

S concentrations in all leachates decreased as a result of cement application (Figure 2e), partly a result of the decrease in sulphide oxidation rates (section 3.3), and partly due to retention of S in secondary minerals such as ettringite, thaumasite and gypsum. A third contributing factor was that some of the waste rock surfaces were no longer being flushed with water after cement application.

3.5 Rates of Cement Deterioration

The Ca content of the leachates can be used to calculate the rate of cement deterioration, since Ca is the main component of the cement. The rate of Ca depletion in the columns treated with cement is much higher for the columns with deeply distributed cement, partly due to the higher contact time between water and the cement because these columns drained slowly, as well as the higher surface area of the cement, which spread out widely over the waste rocks.

If the measured rate of Ca depletion over the first year is maintained into the future, the cements will endure from 10-125 years, depending on how they are distributed within the columns (Table 2).

Table 2. Calculation of rate of depletion of Ca from the cements and simple estimates of the longevity of the cement applications

	Total Ca in 250 g of cement added to column	Total Ca load from leachates (g) after 360 days	% Ca from cement depleted in first year	Projected longevity (yrs)
Control	n.a	1.3	n.a	n.a
Cement ($w/c=0.8$)	114	1.7	1.5%	67
Cement ($w/c=1.0$)	114	9.1	7.9%	13
Cement ($w/c=1.2$)	114	9.5	8.2%	12
Cement + 25% Fly ash ($w/c=1.0$)	86.6	8.8	10.2%	10
Cement + 15% AMD sludge	97.3	0.8	0.8%	125

3.6 Effects of Blending Fly Ash and Sludge with the Cement

The fly-ash blended cement resulted in leachates similar to the unblended cement applications with higher w/c ratios, except with somewhat higher silicon contents (Figure 3g). The sludge-blended cement gave leachates similar to the unblended cement applications with a w/c ratio

of 0.8, which resulted in a similar cement distributions (Figure 1a,e). Overall both fly ash and AMD sludge- blended cements were similar in effectiveness to the unblended cements in decreasing acidity and metal loads (Figure 3).

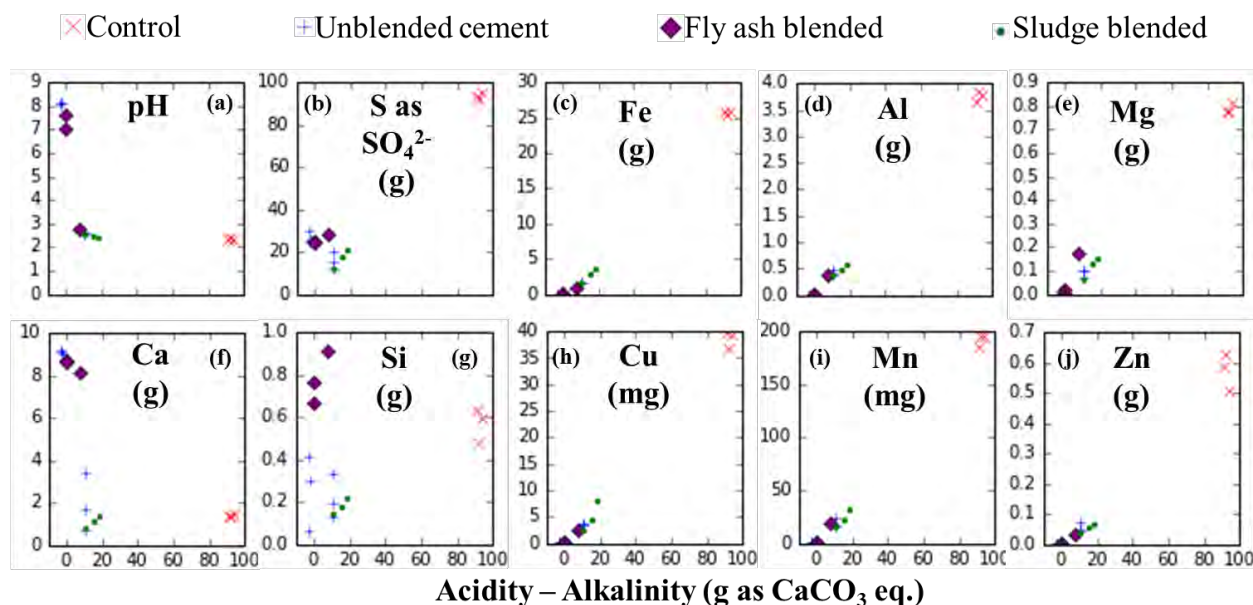


Fig. 3. Median pH and solute loads plotted against acidity loads (g) calculated from leachate analyses from columns after cement application

4.0 CONCLUSIONS

The cement applications had different effects on the permeability of the waste rocks. For columns where the cement penetration was deep, the rate of drainage through the waste rocks was much slower and diminished further over time. Where the cement penetration was not deep, the cement diverted water away from a large proportion of the waste rock in the columns, so that even though the cement coverage was less than 50%, the reductions in acidity release were more than 75%.

Overall, the cement applications decreased release of acidity by 75-100% from the waste rocks for the one year period monitored after cement application. This was partly a result of lower sulphide oxidation rates owing to encapsulation of the sulphide minerals by the cement and partly due to diversion of water away from the acid producing waste rock. There was also a neutralisation effect from the dissolution of the cement in situ.

Fly ash and sludge-blended cements had similar effects on permeability, sulphide oxidation rates and acidity release as unblended cements, indicating that these materials can be used as cement additives to decrease the cost of application.

5.0 REFERENCES

Ji, M., Gee, E., Yun, H., Lee, W., Park, Y., Khan, M., Jeon, B., Choi, J. (2012), Inhibition of sulfide mineral oxidation by surface coating agents: batch and field studies, *Journal of Hazardous Materials* 229-230, pp. 298-306, <http://dx.doi.org/10.1016/j.jhazmat.2012.06.003>

Karlsson, S., Allard, B., Backstrom, M. (2010), Weathering mechanisms and composition of effluents from a sulphide mine waste deposit after covering - Twenty years of field data, Proceedings of IMWA 2010, pp. 359-362

Northwest Geochem (1996) Evaluation of a field scale application of a shotcrete cover on acid generating rock, MEND project 2.34.1

Sephton, M.G., Webb, J.A. (2017), Application of Portland cement to control acid mine drainage generation from waste rocks, Applied Geochemistry 81 (2017) 143-154, <https://doi.org/10.1016/j.apgeochem.2017.03.017>

REHABILITATION PLANNING AT THE FORMER RUM JUNGLE MINE SITE IN NORTHERN AUSTRALIA

Part 1. Geochemical Characteristics of Mine Wastes and Inferred Post Rehabilitation Source Terms

D.R. Jones^A, P. Ferguson^B and T. Laurent^C

^A DR Jones Environmental Excellence, 7 Edith Street, Atherton, QLD 4883, Australia

^B Robertson GeoConsultants Inc, 580 Hornby St, Vancouver, BC V6C 3B6, Canada

^C Northern Territory Department of Primary Industry and Resources, Level 5, Paspalis Centrepoint, Darwin NT, Australia

ABSTRACT

In October 2014, a total of seven large pits were excavated in the three historic waste rock dumps (WRDs) at the former Rum Jungle Mine site to enable vertical profile sampling over 1 m intervals. Numerous small trenches were also excavated across the broader impacted footprint of the site to map out the full extent of contaminated soils and/or waste rock that may also need to be re-located during final rehabilitation.

Waste rock samples were initially characterised/classified using conventional static Acid Base Accounting (ABA) methods. Several customised additional tests were also applied to estimate the components (directly titratable acidity and acidity stored in the secondary mineral jarosite) of total existing acidity content of the waste. This was done to develop a neutralisation strategy appropriate for previously-oxidised waste. Inverse water leach extraction tests at high solid to liquid ratios were done to estimate leachable sulfate (SO₄) and metal concentrations (in presence and absence of added neutralant) under conditions more closely simulating those that will exist in the interior of the relocated waste. The results provided an initial estimate of geochemical source terms to be used for predictive modelling of the outcome of the rehabilitation works.

1.0 INTRODUCTION

Since 2009 the Northern Territory Department of Primary Industry and Resources has been working with the Australian Government and traditional Aboriginal owners to develop a preferred rehabilitation strategy for the former Rum Jungle mine legacy site (Rum Jungle). Successive projects undertaken during this time have enabled ongoing site maintenance, environmental monitoring and stakeholder engagement to underpin rehabilitation planning based on the application of sustainable, leading practice science. The rehabilitation planning has been focused on the development of a fully costed preferred rehabilitation strategy. The key objectives of the geochemical characterisation component of the work program were to:

- Determine the physical and geochemical properties of Potentially Acid Forming (PAF) and Non-Acid Forming (NAF) waste rock in the existing Waste Rock Dumps (WRDs) and other locations on site.
- Identify PAF waste rock types and prioritise for re-location either to the Main Pit or to a new Waste Storage Facility (WSF) near the northern lease boundary as part of the final rehabilitation plan for the site.

- Estimate the amount of neutralant required to neutralise existing acidity in re-located PAF materials.
- Estimate the concentrations of dissolved ions and metals in seepage (geochemical source terms) from PAF and NAF waste rock in the backfilled Main Pit and in the WSF after rehabilitation is complete.

2.0 2014 FIELD PROGRAM

2.1 Sample Collection

In October 2014, seven large 'test pits' (Figure 1) were excavated in the three major WRDs (Main, Intermediate, Dysons). The pits were up to 100 m long and 50 m wide, and usually extended to natural ground (located up to 20 m from the top of the WRD) beneath the WRD. Smaller test pits were excavated in the Main North WRD and in areas where contaminated soils and/or waste rock were thought to be present, including the areas near the Old Ore Stockpile and the former Copper Extraction Pad.

144 samples were collected in 2014. Most of these samples were from test pits in the Main WRD (TP1, TP2, and TP3), in the Intermediate WRD (TP4, TP5 and TP7), and in Dysons WRD (TP6). Samples were described and processed (including sieve siezing, measurement of paste pH and EC) in the field, and then sent to ALS' Brisbane laboratory for further analysis.

2.2 Geochemical Testing Program

Waste rock samples were initially characterised by the standard suite of static tests used for conventional Acid Base Accounting (ABA) to estimate acid and metalliferous drainage (AMD) potential (AMIRA 2002, MEND 2009, Preventing Acid and Metalliferous Drainage 2016). Additional tests were done to quantify the total existing acidity content of waste rock to develop a neutralisation strategy appropriate for previously partially oxidised waste rock. These involved separately estimating the titratable (i.e. immediately available, component of existing acidity) and the portion of acidity stored as jarosite, a poorly soluble secondary mineral found in substantial amounts in the WRDs. Leach extraction tests (and partial acid digestions) were also done to estimate leachable sulfate (SO_4) and metal concentrations in the samples. Powder X-ray diffraction analysis for mineralogy was done at the Queensland University of Technology, Brisbane.

A batch contact procedure was used to assess the effect of adding neutralant to waste rock. A slurry of waste rock in de-ionized water (a mixture with a 0.9 liquid-to-solid (L/S) ratio by mass) was used for this purpose. An inverse cascade batch leach procedure was used to more closely approximate the much lower L/S ratios pertaining in the waste rock dump and the initial condition in the interior of the mass of waste deposited in the pit. This involved (i) rotary inversion mixing water and waste rock over 24h to produce a sample of leachate and (ii) mixing that leachate with a fresh batch of solids to produce another leachate. That leachate, in turn, was then mixed with another fresh batch of solids, and so on until four solutions spanning a L/S ratio of 1:1 to 1:4 were produced.

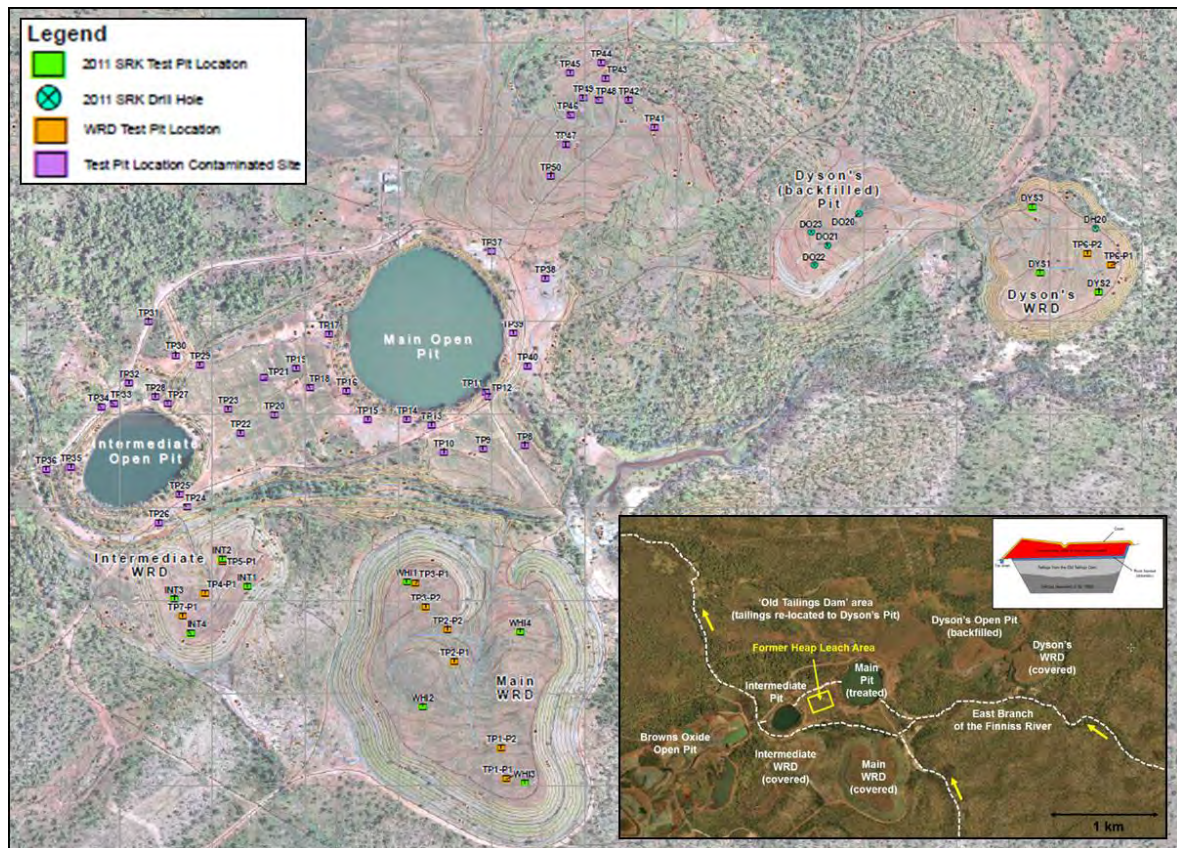


Figure 1. Locations of Test Pits

2.3 Results and Discussion

2.3.1 Waste rock classification

It has been assumed that the distributions of waste rock types determined from the extensive sampling and testing program are broadly representative of the masses of waste rock contained within each of the three WRDs. On this basis about 85% of the total amount of waste rock was determined to be potentially acid forming (PAF) with a substantial excess of acidification potential (AP) over acid neutralising capacity (ANC). AP represents the maximum amount of acidity that could be released by the oxidation of sulfide minerals in a sample. AP is also referred to here as 'incipient acidity', implying that it is acidity that would develop in the future if all of the contained residual sulfides were to oxidise.

Three categories of PAF waste rock were operationally defined (see Table 1). PAF-I waste rock is characterised by the highest sulfide content (highest AP) and the lowest ANC values, with consequently the highest Net Acid Producing Potential (NAPP). NAPP is equal to the difference between AP and ANC. PAF-I waste rock would therefore generate the most AMD in the future if it were to fully oxidise. PAF-II waste rock is characterised by moderate AP and ANC values. PAF-II waste rock would generate substantial AMD in the future, but less than PAF-I waste rock. PAF-III waste rock has a low sulfide content (and relatively high ANC), so it's the least acid-generating PAF type.

Non-acid forming (NAF) waste rock is defined by an Neutralisation Potential Ratio (NPR) value of two or higher (i.e. ANC/AP > 2) and an existing acidity content of less than 0.5 kg H₂SO₄/t. NAF waste rock has a very low sulfide content and has not generated appreciable AMD (based on field measurements of pH and EC) since it was first placed in the 1950s and 1960s. NAF waste rock may not require special containment and could potentially therefore be used in the construction of the WSF. It is recommended, however, that more detailed characterisation of this class of material should be undertaken before consideration is given to using it in more sensitive applications such as for the exterior cladding of the WSF.

Table 1. Average ABA Parameters for PAF and NAF Rock Types

Type	AMD Potential	S _{total} , %	S _{sulfide} , %	AP, kg H ₂ SO ₄ /t	ANC, kg H ₂ SO ₄ /t	NAPP, kg H ₂ SO ₄ /t	NPR
<i>Potentially Acid Forming (PAF) Waste Rock</i>							
PAF-I	High	3.6 (1.4)	3.6 (1.3)	99.5 (38.6)	6.6 (15.4)	92.9 (44.8)	0.1 (0.3)
PAF-II	Medium	1.1 (0.4)	0.9 (0.4)	26.4 (10.9)	7.2 (7.2)	19.2 (12.5)	0.3 (0.3)
PAF-III	Low	0.4 (0.5)	0.3 (0.5)	8.0 (12.2)	11.9 (20.7)	-3.9 (10.3)	1.3 (1.0)
<i>Non-Acid Forming (NAF) Waste Rock</i>							
NAF	SD only	0.08 (0.08)	0.03 (0.03)	1.1 (0.9)	16.5 (8.0)	-15.4 (7.8)	24.3 (25.8)

Notes: All values are averages with one standard deviation in parentheses. SD denotes 'saline drainage'

Samples from 2011(SRK, 2012) and 2014 were used to calculate averages. The calculation of AP assumed essentially all sulfide was present as pyrite (verified by XRD).

2.3.2 Waste inventory and proposed re-location sequence

Estimated distributions of PAF and NAF waste rock types in the historic WRDs are shown in Figure 2. The percentages in this figure are based on the 144 samples collected in 2014 and 110 samples from a previous characterisation program in 2011 (SRK 2012).

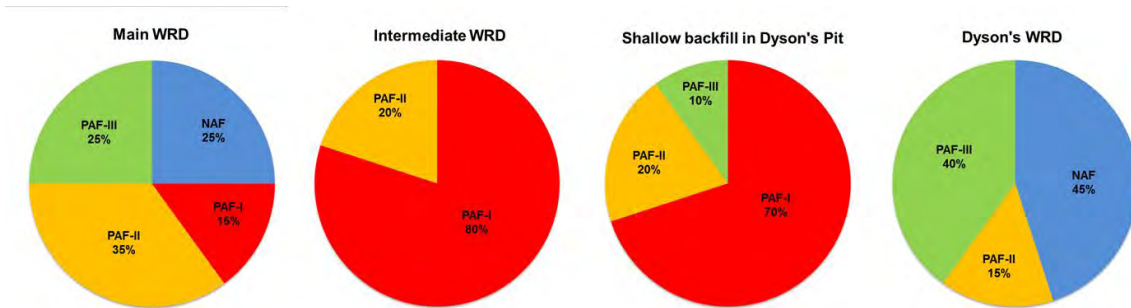


Figure 2. PAF and NAF Types in the WRDs and surface backfill in Dysons Pit

Preventing the future release of incipient acidity from the most acid-generating waste rock by submerging it in the Main Pit is the driver for prioritising the relocation of the three PAF waste rock types. Maintaining permanent saturation by a water cover or equivalent is considered to be the most effective long-term strategy for minimising the future oxidation of sulfide-containing material (Dagenais et al, 2006). All PAF-I and most PAF-II waste rock will be re-located to the Main Pit, whereas the WSF will contain the residual PAF-II, and the PAF-III, and NAF waste rock. About 3 Mm³ of waste rock will be placed in the Main Pit. All of the PAF-I and PAF-II material will be permanently submerged beneath the recovered groundwater table. NAF material (sourced from an offsite non-mineralised borrow area) will be used to fill the 700,000 m³ unsaturated zone of the Main Pit, remaining above the level of the deposited PAF waste rock, to above ground surface.

The remaining waste rock and contaminated materials from elsewhere on the site will be contained in a new lined purpose-built waste storage facility (WSF), with sufficient neutralant added to account for existing acidity. The WSF will be designed to minimise the generation of future AMD by limiting the ingress of oxygen and the egress of solutes by restricting rainfall infiltration. Small amounts of Saline Drainage (SD), neutral pH drainage with high Total Dissolved Solids (TDS) and low concentrations of metals in leachate (see section 2.3.5) collected by the bottom liner of the WSF, may need to be managed after rehabilitation. It is currently proposed to route any seepage to the Intermediate Pit, which will remain water-filled, wherein the seepage will be diluted by mixing and flushed annually by surface water through-flow during the wet season.

2.3.3 Existing acidity content of waste rock

In a historic WRD, a substantial quantity of existing acidity may be present as a result of previous sulfide oxidation. This acidity – which is stored in the waste matrix – is referred to as ‘existing acidity’. It is defined here as the sum of directly titratable acidity and acidity stored in the form of poorly soluble secondary minerals, typically jarosite (Table 3). It should be noted that the use of averages in Table 3 for the amount of each acidity type means that the sum total of the averages for each type does not exactly equal the average calculated for total acidity.

Table 3. Average Acidity Content of PAF and NAF Rock Types

Type	AMD Potential	Rinse Ph	Jarosite Acidity, kg H ₂ SO ₄ /t	Titratable Acidity, kg H ₂ SO ₄ /t	Incipient Acidity, AP kg H ₂ SO ₄ /t	Total Acidity, kg H ₂ SO ₄ /t
<i>Potentially Acid Forming (PAF) Waste Rock</i>						
PAF-I	High	4.4 (0.8)	12.1 (13.8)	2.0 (2.4)	99.5 (38.6)	125.6 (43.7)
PAF-II	Medium	4.4 (1.0)	5.6 (5.5)	1.0 (1.0)	26.4 (10.9)	33.3 (12.9)
PAF-III	Low	5.0 (1.3)	2.9 (3.8)	0.7 (0.8)	8.0 (12.2)	12.0 (16.1)
<i>Non-Acid Forming (NAF) Waste Rock</i>						
NAF	NMD only	6.7 (1.1)	0.9 (1.3)	0.2 (0.6)	1.1 (0.9)	2.0 (2.1)

Notes: All values are means with one standard deviation in parentheses.

Samples from both 2011 and 2014 were used to calculate average incipient acidity.

Existing acidity comprising jarosite and titratable acidity is only available for the 2014 samples.

Titratable acidity consists of free acidity (measured by pH) and soluble metal acidity. Jarosite is a poorly soluble secondary mineral containing a substantial amount of stored acidity that needs to

be measured separately. Jarosite and titratable acidity were not measured as part of the earlier 2011 characterisation program. However, both types of acidity were measured for the 2014 samples, because they are needed to estimate the total neutralant demand of oxidised waste rock. This contrasts with the typical AMD characterisation program that is appropriate for freshly mined sulfidic material, where there has been little, if any, oxidation and production of existing acidity and secondary minerals such as jarosite.

It is proposed to neutralise the existing acidity in the WRDs by amending re-located waste rock with limestone (CaCO_3) or another neutralant, such as magnesite (MgCO_3) or hydrated lime, Ca(OH)_2 .

2.3.4 Estimating neutralant demand for waste rock

PAF waste rock that is placed dry into the Main Pit or the WSF will likely be amended with enough neutralant to neutralise existing acidity. The neutralant demand for each category of PAF waste rock was determined by calculating the 80th percentile of the existing acidity contents of the PAF waste rock samples that have a rinse pH less than 5. These are the most acidic samples within each PAF category, so this is a conservative approach that would lead to over-liming the majority of waste rock and under-liming only a small proportion (less than 20%).

Typically the bulk of leachable salts and acidity in older waste rock dumps is represented by the lower end of the particle size range (Price 2009). An additional degree of conservatism was thus provided by using the existing acidity content of the less than 2 cm particle size range in the WRDs (as opposed to the much coarser particle size distribution of a WRD as a whole), to estimate the acidity content of the whole rock mass. This is because the mg/kg acidity content decreases as a steeply declining function as the particle size increases. A specific investigation of neutralant demand as a function of particle size for the Rum Jungle waste revealed that use of the <2 cm characterisation dataset results in about a 60% overestimate of neutralant demand for the waste rock as a whole.

The target pH for neutralisation was estimated to be around pH 7 based on the concentrations of soluble metals remaining in suspensions of acidic waste titrated to higher pH values by the addition of sodium hydroxide solution. In practice, agricultural lime (calcium carbonate, CaCO_3) will likely be used to amend waste rock that is placed dry in the Main Pit or the WSF. For this neutralant, pH 7 is the about the highest that is practically attainable owing to pH buffering by the carbonic acid/bicarbonate buffer pair in what will effectively be a closed system. Magnesite could also be used, but it reacts much more slowly than limestone and much more leachable Mg and sulfate would be present in the neutralised waste rock after rehabilitation. This could be an issue with future seepage from the WSF. Should a higher pH be needed to remove metals to a greater extent, then hydrated lime could be used as a supplemental neutralant.

The batch leach test results showed that concentrations of most metals were reduced by at least 95% at pH 7. Mn is an exception, as it was only reduced by an average of 87%. Amendment with hydrated lime Ca(OH)_2 removes greater than 99% of all dissolved metals, including Mn, from solution. Hydrated lime also substantially reduces the concentrations of dissolved Mg and SO_4 . However, in practice, the only reason to use Ca(OH)_2 would be if more complete immobilisation of Mn, and substantial removal of Mg and SO_4 were required for primary source control. The modelling carried out in the companion paper (Ferguson et al, 2017) indicates that such additional

reduction should not be required based on the proposed management strategy for produced seepage.

Laboratory test work using mixtures of neutralant and a range of waste rock samples confirmed that the neutralant demand estimates based on directly measured existing acidity were correct, and that limestone performs well for the neutralisation of acidity and removal of leachable metals. Longer term kinetic testwork (using XRD to monitor the content of jarosite) indicates that it could take years for this slowly reacting component of existing acidity to fully react with the neutralant.

In practice finely-crushed limestone would be used to maximise contact of the neutralant with the waste rock. It has been shown elsewhere that coarsely ground limestone is not effective for this type of application owing to the much smaller surface area to volume ratio, resulting in a much greater potential for coating passivation by AMD neutralisation products. These issues and the importance of ensuring good mixing are discussed in Miller et al, 2006. The limestone would be mixed with waste rock during excavation or while it is being placed.

2.3.5 Estimating geochemical source terms

An inverse batch leach method was used to investigate factors controlling the solubility of major ions and metals in waste rock, under conditions likely to be more typical of the very low L/S ratios pertaining in a waste rock dump and the initial condition in the interior of the mass of waste deposited in the pit. Tests were run on both un-amended waste rock and waste rock samples amended with limestone.

Based on the results from the inverse batch least test work, it is inferred that the concentrations of Fe, Al, Co, Cu, Mn, Ni and Zn in seepage from the WSF (assuming neutralisation of existing acidity with limestone) will each be less than 1 mg/L. There is a high degree of confidence that for Fe, Al, Cu and Zn the concentrations will be less than 0.2 mg/L. In the case of U, neutralisation to around pH 7 in the inverse leach work reduced concentrations in solution to less than 10 µg/L. The concentrations of Th are anticipated to be much lower than for U given the very low solubility of Th at this pH. ²²⁶Ra was not measured as part of the testwork since previous studies had shown that ²²⁶Ra activity concentrations in seepage or runoff from the site are very low.

The concentration of Ca will be limited by the solubility of gypsum and could be around 500 to 600 mg/L. This is higher than would be predicted if the system was in equilibrium with the atmosphere and is a consequence of the increased partial pressure of CO₂ caused by the reaction of the CaCO₃ with acid in a closed system.

The behaviour of Mg is more complex (Figure 2). For un-neutralised acidic material, the concentration in solution is a near-linear function of decreasing L/S ratio. Potentially the concentration of Mg under these circumstances could ultimately be limited by the solubility of epsomite (MgSO₄), which is equivalent to 80,000 mg/L Mg (and 320,000 mg/L SO₄). However, the inverse leach work with added neutralant indicates that the solubility of Mg is being controlled by the formation of a secondary (unidentified) mineral phase of much lower solubility than epsomite. Thus, for neutralised material, the seepage could contain much lower concentrations of Mg (e.g. 1,000 to 5,000 mg/L Mg) than would be the case if solubility was controlled by epsomite. This is a very important finding since it indicates that the concentrations of Mg are likely to be much lower in seepage from the WSF than would have occurred in the absence of such a control. SO₄

concentrations in seepage from the WSF will likely be controlled by gypsum solubility (and be on the order to 10,000 to 20,000 mg/L).

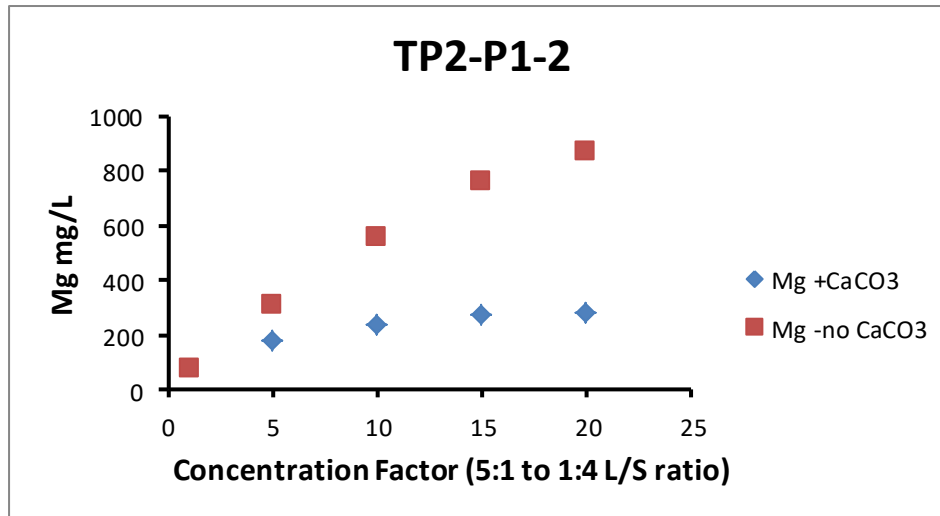


Figure 2. Inverse leach extraction of magnesium in presence and absence of neutralant for sample TP2-P1-2.

3.0 CONCLUSIONS

The geochemical characterisation work conducted on the waste rock dumps at Rum Jungle has enabled a prioritisation sequence to be developed for the placement of the waste in-pit or in the WSF based on its residual (incipient) acid generating potential. Measurements of the directly titratable and jarosite acidity have been used to develop a neutralisation strategy to address this component of the acidity that will be present in waste being placed in both the pit and the newly constructed WSF. Taken together, the results from the program of leaching test work have been used to infer geochemical source terms to be used for predictive modelling of the overall outcome of the preferred rehabilitation strategy on downstream water quality. The results from this modelling will be presented in a companion paper.

4.0 PATH FORWARD

During the next phase of rehabilitation planning, additional neutralisation testwork, field mixing trials of neutralant and waste rock, and a more targeted drilling investigation of the Main waste rock dump are planned. Further neutralisation testwork and inverse leaching will be conducted on the lower end of the range of existing acidity, since this material will comprise the bulk of the WSF. Field mixing trials will be undertaken to develop an effective approach to dry mixing lime and waste rock that can be implemented during rehabilitation, and to provide cost estimates for this component of the rehabilitation project. Targeted drilling will also be undertaken to better define the distribution and location of low PAF material in the Main WRD that would be re-located in years 1 and 2. This is important to optimise the storage available for PAF-I and PAF-II material in the pit.

5.0 REFERENCES

AMIRA (2002), ARD Test Handbook – Prediction & Kinetic Control of Acid Mine Drainage, Project P387A, May 2002.

Dagenais AM, Aubertin M and Bussiere B (2006) *Parametric study on the water content profiles and oxidation rates in nearly saturated tailings above the water table*. In 'Proceedings of the 7th International Conference on Acid Rock Drainage (ICARD)', March 26-30, 2006, St. Louis MO, pp. 405-420. R.I. Barnhisel (ed). Published by the American Society of Mining and Reclamation (ASMR), 3134 Montavesta Road, Lexington, KY 40502.

Ferguson, Jones D and Laurencont T (2017) Rehabilitation Planning at the Former Rum Jungle Mine Site in Northern Australia. Part 2. Environmental Performance Assessment for the Preferred Rehabilitation Strategy, these Proceedings.

Jones DR (2015) Validation of Methods to Determine the Neutralant Demand of Rum Jungle Waste Rock, Report DME001/14, NT Dept of Mines and Energy.

Miller S, Rusdinar Y, Smart R, Andrina J and Richards D (2006) Design and Construction Of Limestone Blended Waste Rock Dumps - Lessons Learned From A 10-Year Study At Grasberg, 7th International Conference on Acid Rock Drainage (ICARD), March 26-30, 2006, St. Louis MO. R.I. Barnhisel (ed.) American Society of Mining and Reclamation (ASMR), Lexington, KY 40502, 1287-1301.

MEND (2009) Prediction Manual for Drainage Chemistry from Sulphidic Geologic Materials. MEND Report 1.20.1.

Preventing Acid and Metalliferous Drainage (2016) Leading Practice Sustainable Development Program for the Mining Industry, Australian Government Department of Industry Innovation and Science, September 2016, 221 pp. www.industry.gov.au/resource/Programs/LPSD/Pages/LPSDhandbooks.aspx#.

Price WA (2009) Prediction Manual for Drainage Chemistry from Sulphidic Geologic Materials. MEND Report 1.20.1. CANMET – Mining and Mineral Sciences Laboratories. Smithers, British Columbia. V0J 2N0.

SRK (2012) Geochemical Characterisation of Waste at the former Rum Jungle, March 2012.

Watson, G.M. (1979), Rum Jungle Environmental Studies – Summary Report, Uranium Advisory Council.

REHABILITATION PLANNING AT THE FORMER RUM JUNGLE MINE SITE IN NORTHERN AUSTRALIA

Part 2. Environmental Performance Assessment for the Preferred Rehabilitation Strategy

P. Ferguson^A, C. Wels^A, D.R. Jones^B, and T. Laurencont^C

^A Robertson GeoConsultants Inc. 580 Hornby St, Vancouver, BC V6C 3B6, Canada

^B DR Jones Environmental Excellence, 7 Edith Street, Atherton, QLD 4883, Australia

^C Northern Territory Department of Primary Industry and Resources, Level 5, Paspalis
Centrepoint, Darwin NT, Australia

ABSTRACT

The Northern Territory Department of Primary Industry and Resources (DPIR) has developed a preferred rehabilitation strategy for the former Rum Jungle mine site. Rehabilitation objectives include meeting Locally Derived Water Quality Objectives (LDWQOs) for the East Branch of the Finnis River (EBFR), the local receiving waterway. This will be achieved by substantially reducing inputs of Acid and Metalliferous Drainage (AMD) to groundwater and surface water.

This paper describes a numerical flow and contaminant transport model that was developed to assess the environmental performance of the preferred rehabilitation strategy and the predicted improvement in the condition of groundwater and the EBFR following rehabilitation. The model was calibrated to observed loads and water quality conditions from 2010 to 2015. Source terms for the model were derived from the results of a separate investigation of the physical and geochemical characteristics of waste rock and contaminated materials at the site (see Part 1 of this paper). Loads were predicted for a period of 30 years after rehabilitation to assess how the situation will improve as a combined result of decreased surface inputs of seepage from the former WRDs and by the flushing through time by rainfall of residual impacted groundwater.

The concentrations of sulfate (a conservative major ion solute) and copper (a key “reactive” metal contaminant) are predicted to decline to well below locally derived water quality criteria within only a short timeframe after completion of the rehabilitation works.

1.0 INTRODUCTION

The Northern Territory Department of Primary Industry and Resources (DPIR) has developed a preferred rehabilitation strategy for the former Rum Jungle mine site (Rum Jungle) (DPIR, 2013). Rehabilitation objectives include achieving Locally Derived Water Quality Objectives (LDWQOs) for the East Branch of the Finnis River (EBFR) by reducing contaminant loads to groundwater.

Rehabilitation objectives will be achieved by:

- Re-locating and consolidating Potential Acid Forming (PAF) waste rock from the Main Waste Rock Dump (WRD) and Intermediate WRD and contaminated soils from Dysons Backfilled Pit to Main Pit.
- Constructing a purpose-built Waste Storage Facility (WSF) to contain the remaining PAF waste rock and Non-Acid Forming (NAF) waste rock.
- Covering the backfilled Main Pit with an earthen cover system designed to shed surface water and include a new low-flow channel around the backfilled Main Pit to replicate the original course of the EBFR (through the flooded Intermediate Pit) to the greatest extent possible.
- Leaving the Intermediate Pit as a water-filled void to provide a passive water management treatment for seepage from the WSF.
- Re-locating waste rock from the Mt Burton WRD to Rum Jungle and backfilling the Mt. Fitch Pit with nearby waste rock from that site.
- Focusing on source control while integrating design elements to meet both environmental and cultural objectives; and
- Supporting economic opportunities for Traditional Owners where appropriate.

The PAF waste rock selected to backfill Main Pit will have the highest sulfide content on site. Leachate from the WSF will be collected using a basal liner and diverted to the Intermediate Pit after rehabilitation is complete. The pH of leachate is predicted to be near-neutral due to the amendment of re-located waste rock with fine-grained limestone, and will therefore contain low concentrations of most metals, such as copper (Cu), and high concentrations of dissolved sulfate (SO₄), and other major ions (e.g. magnesium, calcium) (see Jones et al., 2017).

Residual, AMD-impacted groundwater will persist after rehabilitation until contaminants have been flushed by rainfall infiltration and flows of unimpacted groundwater from upgradient. Also, the backfilled Main Pit and WSF will become small sources of SO₄ and Cu to groundwater and the EBFR. This paper evaluates the degree and timing of predicted future improvements in groundwater and the EBFR after the preferred rehabilitation strategy has been implemented. Specific objectives of the modelling are to:

- Simulate post-rehabilitation groundwater flow and contaminant transport.
- Predict SO₄ and Cu concentrations in the Intermediate Pit and the EBFR.

To achieve these objectives, a transient numerical flow and transport model was developed to simulate post-rehabilitation groundwater conditions for thirty years after rehabilitation (RGC, 2016a)¹. An Excel-based mixing model was also developed to predict post-rehabilitation SO₄ and Cu loads and concentrations in the Intermediate Pit and in the EBFR. An overview of these models is provided in Section 3. Key findings from the modelling and the path forward for the Rum Jungle Rehabilitation Project are described in Section 4 and Section 5, respectively.

¹ Full report is available at: <https://dpir.nt.gov.au/mining-and-energy/mine-rehabilitation-projects>.

2.0 BACKGROUND

2.1 Inferred SO₄ and Cu Plumes in Groundwater

The DPIR routinely monitors more than fifty groundwater bores at Rum Jungle. Groundwater generally flows from east to west across the former Old Tailings Dam area towards the EBFR and towards the flooded pits in the central mining area. In Dyson's Area, groundwater flows south to the upper EBFR. This groundwater flow regime is affected by topography, preferential recharge to the WRDs, and the presence of standing water in the flooded pits.

Groundwater near the Main WRD and the Intermediate WRD (the largest sources of AMD) is characterised by the highest concentrations of SO₄ and most metals, e.g. Cu. Groundwater near Dyson's WRD is less impacted by comparison. Seepage from Dyson's (backfilled) Pit reports to the EBFR directly (not to groundwater), so groundwater near the pit is only moderately-impacted despite the high SO₄ and metal concentrations in seepage.

Figure 1 shows conceptual SO₄ and Cu plumes in groundwater inferred from the water quality observations made across the site in 2014. The SO₄ plume is much larger than the Cu plume at the site, because Cu transport in groundwater is retarded by adsorption and precipitation reactions that slow the rate of transport relative to groundwater.

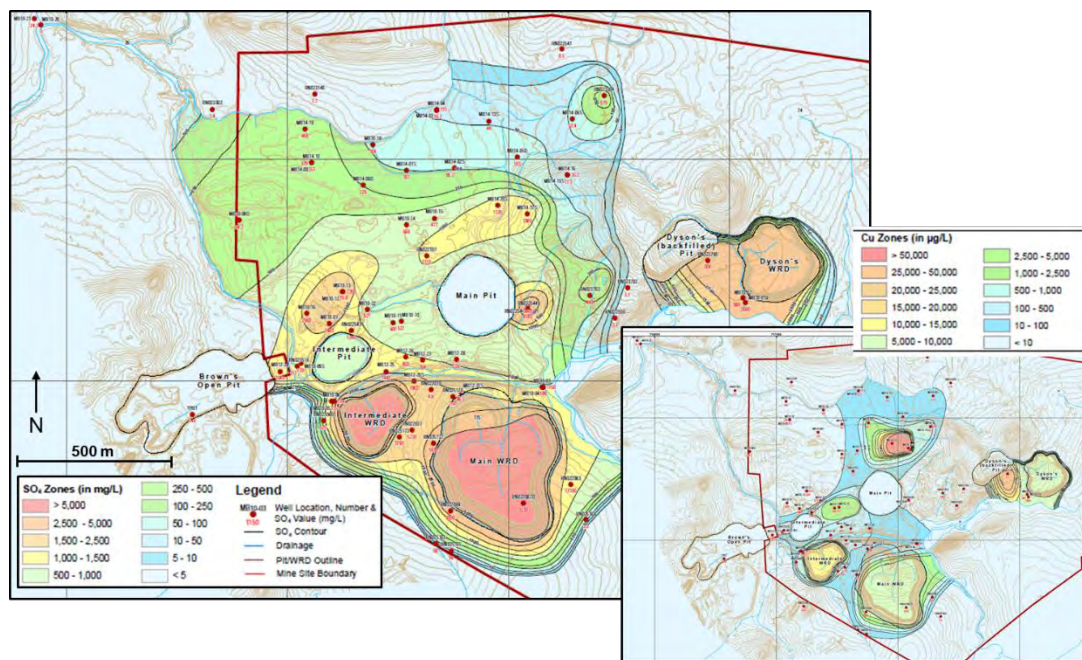


Fig. 1. Inferred SO₄ and Cu Plumes in Groundwater for Current Conditions

2.2 Conceptual Load Balance Model (Current Conditions)

Current contaminant loads from the main sources of AMD to groundwater and to the EBFR are summarised in Table 1. Loads were estimated as the product of recharge and SO₄ and Cu concentrations (see RGC, 2016, for further details). Based on seasonal flow and water quality records, the average SO₄ load in the EBFR is 75% lower than observed in the 1970s and average Cu loads are 95% lower.

Table 1. Conceptual Load Balance for Groundwater and the EBFR, Current Conditions

Source	Area, m ²	SO ₄ , mg/L	Cu, ug/L	Recharge, mm	Recharge (or Flow), ML	SO ₄ Load, t/yr	Cu Load, t/yr
<i>Estimated Contaminant Loads to Groundwater (2010 to 2015), 1438 mm rainfall</i>							
Seepage from the Main WRD	330,000	5,000	5,000	325	107	536	0.5
Seepage from the Intermediate WRD	80,000	15,000	35,000	325	26	390	0.9
Seepage from the Dyson's (backfilled) Pit	61,000	2,500	30,000	196	12	30	0.4
Seepage from Dyson's WRD	90,000	2,500	2,500	650	58	146	0.1
Seepage from former mill area	54,000	1,500	30,000	144	8	12	0.2
Seepage from Copper Extraction Pad area (shallow)	34,000	5,000	7,500	144	5	24	0.0
Sub-total:	649,000	n/a	n/a	n/a	216	1,138	2.2
<i>Estimated Losses from Groundwater</i>							
Geochemical reactions (e.g. precipitation), 30% for Cu	n/a	n/a	n/a	n/a	n/a	0	-0.7
<i>Estimated Contaminant Loads to EBFR from Surface Water</i>							
Diffuse sources (e.g. contaminated soils, liquor, etc.)	n/a	n/a	n/a	n/a	n/a	702	1.1
TOTAL:		n/a	n/a	n/a	n/a	1,840	2.7
<i>Observed Contaminant Loads in the East Branch of the Finniss River</i>						1,840	2.7
<i>Mean Annual Loads, Adjusted for 'Average Year'</i>							

3.0 METHODS AND APPROACH

3.1 Groundwater Numerical Flow and Transport Model

A numerical flow and transport model was developed in MODFLOW to simulate the movement of groundwater and SO₄ and Cu loads to and from the groundwater system (see RGC, 2016b). Boundaries of the numerical model domain are shown in Figure 2. The model domain was defined by local topographic highs and low-lying drainage features which represent no-flow boundaries. This approach implicitly assumes that cross-boundary flows into or out of the groundwater system could be assumed to be negligible. For this reason, net recharge by rainfall and inflows from the flooded Main and Intermediate Pits are the only sources of water to the groundwater system within the model domain, whereas any outflows are accounted for by groundwater discharge and evapotranspiration.

The numerical model domain was spatially discretised into a uniform grid with cell dimensions of 25 m by 25 m. The thickness of the cells varies depending on lithology. The model is composed of 7 layers and extends from a maximum elevation of approximately 100 m AHD to a minimum elevation of -90 m AHD. Surface topography from a recent Lidar survey was used to define the top of Layer 1, including the WRDs and Dysons (backfilled) Pit.

Layer 1 represents shallow overburden at the site, including laterite, fill and waste rock and has a minimum thickness of 2 m. Layer 2 represents saprolite (where present). The top of bedrock (i.e. bottom of layer 2) was based on an interpolation of top of bedrock elevations observed at historical and new bores. In areas with overburden less than approximately 5 m thick, layer 2 is assigned bedrock properties and has a minimum thickness of 3 m. Layers 3 through 5 represent shallow, partially weathered and fractured bedrock and have minimum thicknesses of 5 m, 15 m, and 25 m. Layers 6 and 7 represent deeper, fresh and typically low permeability bedrock and have minimum thicknesses of 60 m.

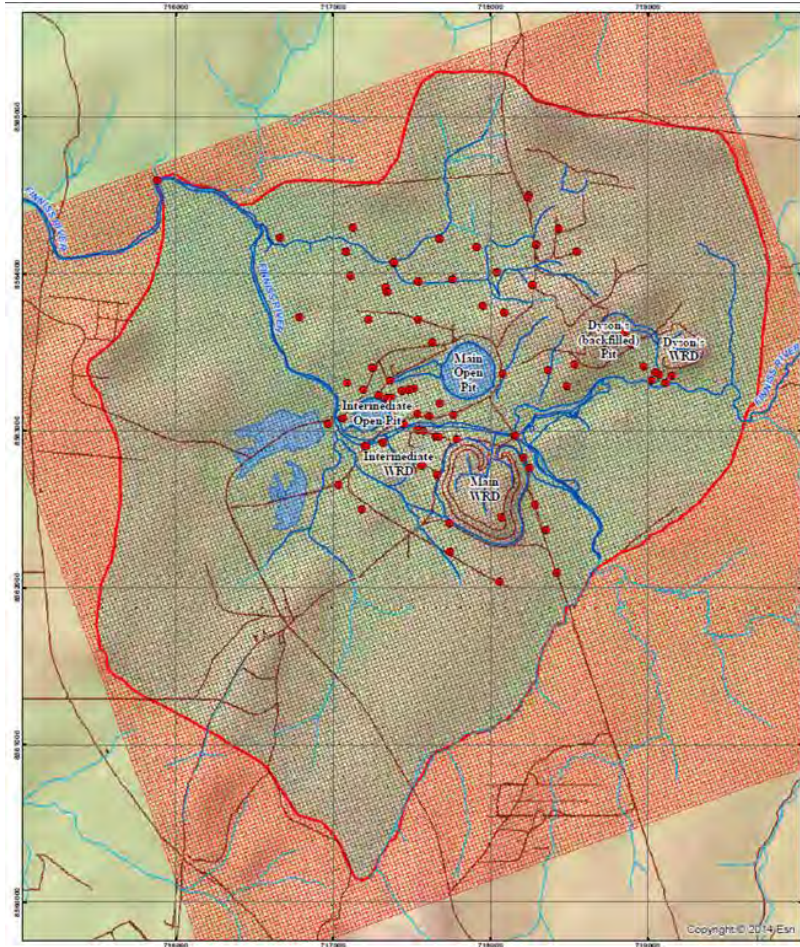


Figure 2. Model Domain and Finite Difference Grid. Black cells represent “active” model domain and red cells are “inactive”.

The model was calibrated to the monthly groundwater level data and contaminant loads that are representative of current conditions and then modified to reflect post-rehabilitation conditions. Simulated head contours for the Wet Season (April) are shown in Figure 3.

After rehabilitation, SO_4 loads to the EBFR from residual, AMD-impacted groundwater in the shallow groundwater system (i.e. overburden and bedrock) are predicted to quickly diminish due to annual wet season flushing by infiltrating rainfall. This groundwater will, however, remain the main source of Cu to the EBFR for some time, as Cu concentrations remain buffered at low levels by the Cu that is currently adsorbed on the rock matrix along the transport pathways. Additional (post-rehabilitation) sources of SO_4 and Cu to groundwater are:

- Cu desorbing from contaminated soils and bedrock in the footprints of the former WRDs and Dysons Backfilled Pit.
- Leachate from limed (PAF) waste rock used to backfill the Main Pit.
- Leakage through the basal liner of the WSF (“basal seepage”).

SO_4 and Cu concentrations in leachate from the backfilled Main Pit and WSF are estimated to be 10,000 to 20,000 mg/L SO_4 and 200 $\mu\text{g/L}$ Cu (see Jones et al, 2017). These concentrations represent Saline Drainage (SD) from neutralised waste rock. 10,000 mg/L SO_4 and 200 $\mu\text{g/L}$ Cu were assumed to simulate post-rehabilitation conditions.

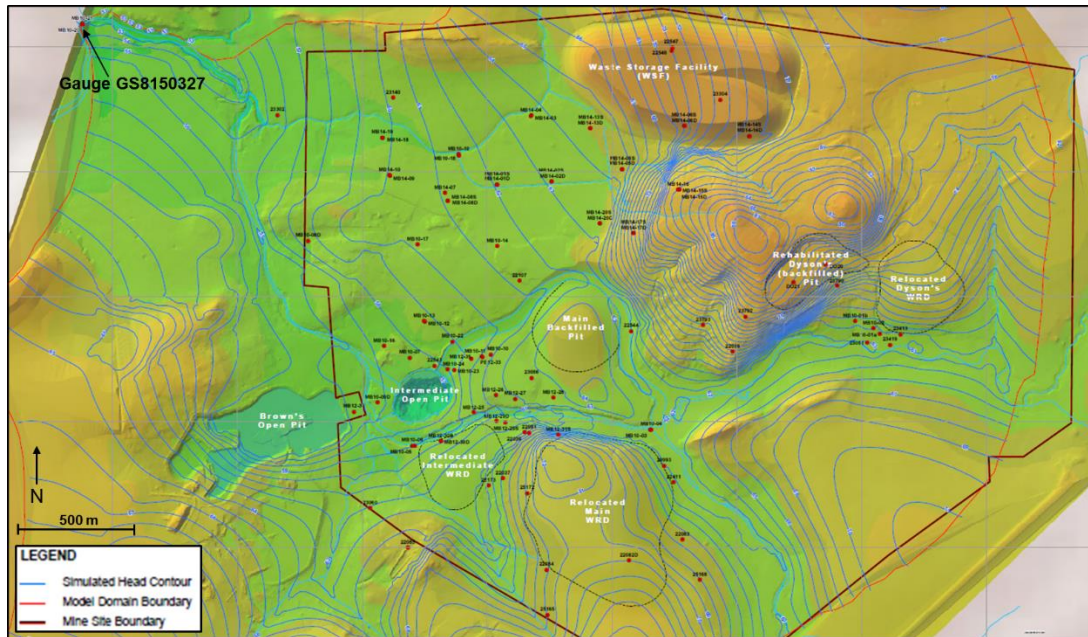


Fig. 3. Simulated Head Contours and Computed Residuals for Wet Season (March 2014)

Seepage from the WSF represents leakage through the occurrence of some presumed defects in the basal liner. A constant rate of “basal” seepage of 19 mm/year was assumed based on seepage modeling completed by O’Kane Consultants Inc. (OKC, 2015). For the backfilled Main Pit, recharge to the domed surface of the post-rehabilitation landform was assumed to be 25% of monthly net precipitation and the source concentrations for Cu and SO₄ above were assigned to PAF waste rock in the pit. Lateral groundwater flow through the backfilled Main Pit represents a secondary (minor) source of contaminant loading from the Main Pit.

3.2 Surface Water EBFR Mixing Model

A mixing model was developed in Excel to predict SO₄ and Cu loads and concentrations in the Intermediate Pit and the EBFR at gauge GS8150327 (see Figure 3 for location) for the first 30 years after rehabilitation. The model includes two separate mixing ‘reactors’, (i) the Intermediate Pit and (ii) the EBFR reach between the Intermediate Pit and gauge GS8150327. Inflows to the Intermediate Pit are assumed to be:

- Seepage collected above the liner from the WSF (i.e. leachate).
- Groundwater inflows from upgradient, i.e. from the central mining area and footprints of the former WRDs.
- Surface water flows from the reinstated EBFR.

SO₄ and Cu loads from groundwater (predicted by the MODFLOW model), in seepage from the WSF, and from the EBFR upstream were “mixed” in the Intermediate Pit, assuming continuous mixing and uniform concentration with depth. A daily time step was used for the 30-year simulation period.

To approximate the effect of pH-controlled geochemical reactions in the pit, an upper limit (or ‘threshold concentration’) of 100 µg/L Cu was applied to total Cu concentrations in the Intermediate Pit. This concentration corresponds to the solubility limit of Cu at pH 7.8. The

veracity of the assumption is supported by the fact that 100 µg/L corresponds to the 80th percentile for observed total Cu in the Intermediate Pit since 2010.

If the predicted total Cu concentration in pit water is less than 100 µg/L Cu, all of the Cu load from the Intermediate Pit is conservatively assumed to report to the EBFR downstream as dissolved Cu. If the total Cu concentration in pit water is predicted to be higher than 100 µg/L Cu, the excess Cu load above that concentration is assumed to remain in the Intermediate Pit as precipitated sludge. This sludge is assumed to remain at the bottom of the pit.

A constant flow of 50 m³/day (or 0.6 L/s) of leachate from the WSF after rehabilitation was assumed (see OKC, 2015). This leachate will be collected by a drain system located above the basal liner and delivered to the Intermediate Pit. Simulated monthly SO₄ and Cu loads from groundwater to the Intermediate Pit for 30 years after rehabilitation were incorporated into the EBFR mixing model. Simulated loads are transient loads that change over time as residual, AMD-impacted groundwater is flushed, and plumes from new sources of SD develop (i.e. basal seepage from WSF) and begin to reach the Intermediate Pit.

For the reinstated EBFR, daily flows were predicted using the SIMHYD hydrological runoff model developed by Water Technology for Rum Jungle using data for the historical 30-year period from 1955 to 1985. This runoff model was incorporated into a GoldSim model that RGC developed to simulate water management during the construction phase of rehabilitation. For background loads in the EBFR, RGC assumed 1 mg/L SO₄ and 1 µg/L Cu in river water from upstream of the site.

4.0 KEY FINDINGS

4.1 Simulated SO₄ Transport in Groundwater

Simulated SO₄ concentrations at 30 years after rehabilitation are shown in Figure 3. The black contour lines represent the predicted (post-rehabilitation) groundwater flow field during Wet Season. Predicted SO₄ transport in groundwater and loading to surface water after rehabilitation are summarised below:

- Residual SO₄ concentrations in shallow overburden soils (model layers 1 and 2) and shallow bedrock (model layer 3) beneath and downgradient of the former WRDs and other impacted areas, e.g. the Old Tailings Dam area, is predicted to decrease within 10 to 15 years due to flushing by local seasonal recharge. Residual SO₄ at greater depths in bedrock is predicted to flush more gradually.
- A new SO₄ plume will develop downgradient of the backfilled Main Pit in less than 5 years and is predicted to migrate in a predominantly northwesterly direction and discharge into the realigned EBFR channel.
- A small amount of leachate, i.e. basal liner seepage, from the WSF is predicted to generate a new SO₄ plume in the Old Tailings Dam area within about 5 years. The SO₄ plume in shallow laterite beneath the WSF is predicted to discharge near the downgradient (western) toe of the WSF.
- The total SO₄ load to surface water is predicted to decrease rapidly from about 1400 t/year (current conditions) to about 610 t/year (a 56% reduction) within 5 years after rehabilitation. The long-term SO₄ load to surface water from groundwater after 30 years is predicted to be 420 t/year representing a 70% reduction from current conditions.
- The SO₄ load from the backfilled Main Pit (309 t/year) is predicted to be the largest future long-term point source after rehabilitation, representing about 74% of the predicted total long-term SO₄ load. In contrast, the future SO₄ load from the WSF represents only about 15% of the predicted total long-term SO₄ load to surface water.

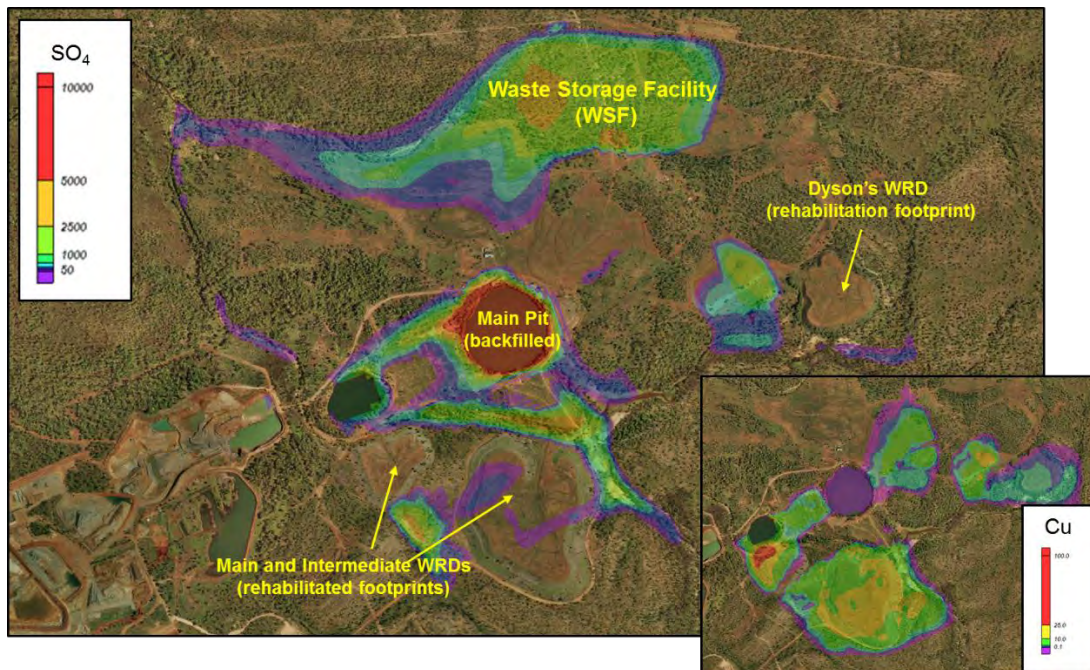


Fig. 3. Simulated SO₄ and Cu concentrations in model Layer 3: 30 years post-rehabilitation.

For Cu transport, three different attenuation scenarios were run:

- 'No Attenuation' scenario, to simulate conservative transport.
- 'Moderate Attenuation' scenario, to simulate sorption in overburden and bedrock and chemical precipitation in dolostone only, plus copper removal in limed footprint areas.
- 'High Attenuation' scenario, to simulate sorption in overburden and shallow bedrock beneath WRDs and chemical precipitation in all bedrock types, plus Cu removal in limed footprint areas.

The 'moderate attenuation' scenario is considered the most likely scenario. Predicted, post-rehabilitation Cu transport for this scenario can be summarised as follows:

- Residual Cu currently present in groundwater and sorbed to aquifer materials will continue to represent the primary source of future Cu loads to surface water. Future Cu loads from the WSF and backfilled Main Pit will be relatively small.
- Removal of waste rock and contaminated WRD footprint area soils and liming of the residual footprints in Dysons Area (Dysons WRD and Dysons Backfilled Pit) and the Main and Intermediate WRDs is predicted to result in very rapid cleanup of the footprint area (layer 1) with more gradual decline in Cu concentrations in the deeper layer 2. However, flushing of residual Cu from the underlying bedrock (layers 3 to 6) is predicted to be very slow (much longer than 30 years).
- Cu concentrations in the deeper bedrock (layers 3 to 6) of the Copper Extraction Pad area are predicted to clean up very slowly (i.e. 30+ years) due to desorption of Cu from bedrock.
- Flows of leachate, and associated Cu load, from the WSF are too small to produce any significant Cu plume or Cu load to Old Tailings Creek and the lower EBFR.
- The total Cu load to surface water is predicted to initially decrease from 2.7 t/year (current conditions) to 1.3 t/year (a 50% reduction) within 5 years after rehabilitation.

This initial reduction is primarily due to removal of above-grade and near-surface Cu sources (waste rock, contaminated soils and foundation material) and liming of the footprint areas.

- Longer-term reduction in Cu loads from groundwater to surface water will be a slow process, because elevated Cu concentrations will be sustained by ongoing desorption from the rock substrate. The total Cu load to surface water after 30 years is predicted to be 1.0 t/year (a 63 % reduction from current conditions).

4.2 EBFR Water Quality

The Intermediate Pit is predicted to receive 535 t/year SO₄ and 0.44 t/year Cu within 5 years of rehabilitation. Simulated, post-rehabilitation loads from groundwater are the largest sources of SO₄ and Cu to the pit (60% of the SO₄ load and 93% of the Cu load). Leachate collected from the WSF accounts for 34% of the SO₄ load to the pit, but only 1% of the Cu load.

About 36% (0.16 t/year Cu) of the Cu load that reports to the Intermediate Pit is predicted to precipitate from pit water if the 100 µg/L Cu solubility limit is applied. Most of this precipitated mass would remain in the pit as sludge, and the residual dissolved Cu load would report to the EBFR via outflows from the Intermediate Pit during the wet season.

Predicted loads to the EBFR for 30 years after rehabilitation are summarised below:

- For SO₄, a load of 749 t/year SO₄ is predicted to report to the EBFR at gauge GS9150327. 72% (535 t/year) of the SO₄ load is delivered to the EBFR via the Intermediate Pit. This load is related to groundwater discharge to the Intermediate Pit and flows of leachate from the WSF (see above). 27% (202 t/year) of the load is related to the discharge of residual, AMD-impacted groundwater directly to the EBFR (mainly from the footprints of the Main WRD and Intermediate WRD). The remaining 1% is from upstream EBFR flows through the East Branch Diversion Channel. 749 t/year SO₄ in the EBFR is about 60% lower than the ~1800 t/year SO₄ load that was observed in the EBFR from 2010 to 2015.
- For Cu, 1.06 t/year Cu is predicted to report to the EBFR at gauge GS8150327. 73% of this Cu load is related to residual, AMD-impacted groundwater that reports directly to the EBFR from the former footprints of the Main and Intermediate WRDs. 26% is delivered to the EBFR via the Intermediate Pit and 1% is from upstream EBFR flows through the EFDC. 50% of the Cu load to the EBFR (0.5 t/year Cu) reports to gauge GS8150327 in the form of dissolved Cu. This dissolved Cu load is about 60% lower than the dissolved Cu load in the EBFR at gauge GS8150327 from 2010 to 2015.

Using the predicted SO₄ and dissolved Cu loads in the EBFR at gauge GS8150327, monthly, flow-weighted concentrations were computed to allow a comparison with LDWQOs. The key findings are summarised below:

- For the first 10 years after rehabilitation, the flow-weighted SO₄ concentration in the EBFR is 32 mg/L SO₄. This is less than 50% of the flow-weighted SO₄ concentration from 2010 to 2015 (and less than 3% of the 997 mg/L SO₄ LDWQO). After ten years, the flow-weighted SO₄ concentration in the river is predicted to be at the most 19 mg/L SO₄.
- With respect to Cu, the annual, flow-weighted mean Cu concentration is predicted to be 18 µg/L for the first 10 years after rehabilitation (assuming the 'moderate attenuation' Cu transport scenario). This concentration is 56% lower than the flow-weighted mean Cu concentration at gauge GS8150327, since the gauge was installed in 2010, and 35% lower than the 27.5 µg/L LDWQO for Cu. From 10 to 30 years after rehabilitation,

the flow-weighted Cu concentration in the EBFR decreases to 13 µg/L Cu, less than 50% of the LDWQO.

- The 'high attenuation' Cu transport scenario predicts a flow-weighted annual Cu concentration of 8 µg/L for the first 10 years after rehabilitation. This concentration is 70% lower than the 27.5 µg/L LDWQO for Cu. From 10 to 30 years after rehabilitation, the mean flow-weighted Cu concentration decreases to less than 3 µg/L Cu. This transport scenario is less likely than the moderate attenuation scenario, but it provides some context for the model predictions.

Table 3. Predicted Post-Rehabilitation Contaminant Loads in the EBFR after 30 years, 'Moderate Attenuation' Cu transport scenario

Source	SO ₄ (30 years)			Cu (30 years)		
	t	t/year	%	t	t/year	t/year
<i>Predicted Contaminant Loads to East Branch of the Finniss River downstream of Intermediate Pit</i>						
Dissolved loads from Intermediate Pit (from GW and WSF leachate)	16,055	535	72%	8.4	0.28	26%
EBFR flows through the EFDC	218	7	1%	0.2	0.01	1%
Loads from residual groundwater to EBFR (Main and Int. WRD)	6,066	202	27%	23.2	0.77	73%
TOTAL (loads to the EBFR at GS8150327):	22,339	745	100%	31.9	1.06	100%
Annual dissolved Cu load in EBFR is 0.5 t/year (annual SO ₄ load is 745 t/year, i.e. conservative transport)						

5.0 CONCLUSIONS

A groundwater flow and transport model was developed in MODFLOW to simulate post-rehabilitation loads to groundwater and downstream water quality for 30 years following the implementation of the preferred rehabilitation strategy for Rum Jungle. These models predict that SO₄ and Cu concentrations decrease rapidly over the first five years after rehabilitation, with a slower rate of decline thereafter.

The most important finding is that the predicted concentrations of both solutes will decline to well below the LDWQOs for the EBFR within a few years of rehabilitation, and that the rehabilitation measures implemented are likely to achieve post-closure land-use aspirations for the site.

6.0 REFERENCES

DPIR (2013), Conceptual Rehabilitation Plan, Rum Jungle Mine Site, May 2013.

Jones, D., P. Ferguson, and T. Laurencont (2017), Rehabilitation Planning at the Former Rum Jungle Mine Site in Northern Australia. Part 1. Geochemical Characteristics of Mine Wastes and Inferred Post Rehabilitation Source Terms, Australian AMD Workshop, November 2017.

RGC (2016a), Environmental Performance Assessment for the Final Rehabilitation Strategy, RGC Report No. 183006/7.

RGC (2016b), Groundwater Flow and Transport Modeling (Current Conditions), Report No. 183006/6, June 2016.

OKC (2015), Rum Jungle – Numerical Modelling for New WSF Construction, 17 December 2015.

A DECADE OF AMD TREATMENT INITIATIVES FOR NEW ZEALAND COAL MINES

P. Weber^A, W. Olds^A, K. Malloch^A and H. Christenson^B

^AO'Kane Consultants (NZ) Ltd., Canterbury, New Zealand

^BCRL Energy Ltd, Christchurch, New Zealand

ABSTRACT

Acid and metalliferous drainage (AMD) from coal mines within the Brunner Coal Measures of New Zealand is well known for the potential to generate poor water quality. Research into treatment options for streams impacted by AMD from these sites commenced in the early part of this century, with trials being undertaken at a number of historic and existing sites. In 2008 a number of investigations, being undertaken at the Stockton Coal Mine (Stockton), were presented at the Australian AMD Workshop in Burnie. This paper provides an update to that work a decade later.

Stockton has utilised active and passive treatment technologies for 10 years, with significant improvements in water quality in the Mangatini Catchment and downstream in the Ngakawau River. A key project for Stockton is the active treatment of the Mangatini Stream, which was identified as the key source of acidity within the greater Ngakawau Catchment, hence the priority catchment for treatment activities. Data indicates that the acidity load in the Mangatini Stream, prior to treatment, is ~8,000 – 10,000 tpa which varies as a function of rainfall with flow being the key driver of contaminant load. For 7 years, treatment of AMD was by ultrafine limestone (UFL). Recently, the site switched to the use of CaO with a subsequent improvement in treatment efficiencies, but with an increase in sludge volumes. Investigations are in progress as to sludge management options and costs, as the Mangatini Sump, designed to collect the AMD sludge and sediment from the mine for 100 years, is now close to being full.

Outside the Mangatini Catchment in remote areas of the site with no mains power, passive treatment systems are one option being considered for treatment of AMD-impacted waterways. A mussel shell bioreactor (MSB) was installed in the Whirlwind Catchment in 2012, which is still performing above design specifications (1 L/s). Based on the success of this system, other systems have been constructed including a MSB at the Escarpment Coal Mine, just south of Stockton. Data indicates the Escarpment MSB is not only treating the acidity load from the Barren Valley Engineered Landform (ELF), but is also neutralising the acidity within the downstream Pit 3 pit lake, with pH >7 due to alkalinity export from the MSB.

Development of passive treatment systems is continuing in New Zealand, with recent trials using low-cost, water-soluble additives, which provides significant improvements in treatment efficiency. Data indicate this could lead to reduced hydraulic residence times or smaller systems, both having economic benefits. Such enhanced passive treatment processes may reset industry accepted standards for what contaminant loads can be treated by passive/active technologies. Such approaches are already gaining international attention.

R&D will continue to be important for optimising treatment processes at mine sites as part of a constant drive to find the least cost approach. However, new technologies can take a number of years to gain industry acceptance and require supporting data and operational-scale trials to show such technologies are robust.

1.0 INTRODUCTION

Acid and metalliferous drainage (AMD) from coal mines within the Brunner Coal Measures (BCM) of New Zealand is well known for the potential to generate poor water quality (e.g. Davies et al., 2011; Pope et al., 2010). Research into treatment options for streams impacted by AMD from such sites commenced in the early part of this century with a variety of trials being undertaken at a number of historic and existing mine sites. In 2008 a number of investigations, being undertaken at the Stockton Coal Mine (Stockton), were presented at the Australian Workshop on AMD in Burnie, Tasmania. This paper provides an update to that work a decade later.

Stockton, formerly owned and operated by Solid Energy New Zealand Ltd, was recently purchased by BT Mining Limited and is operated by Bathurst Resources Ltd. Stockton has utilised active and passive treatment technologies for 10 years, with significant improvements in water quality in the Mangatini Catchment and downstream in the Ngakawau River. Treatment is expected in perpetuity. Technologies developed at Stockton have now been used at other mine sites, including the use of mussel shell bioreactor (MSB) technology.

2.0 BACKGROUND – STOCKTON

Stockton is located on the West Coast of the South Island 35 km north of Westport. The mine is located on the coastal Stockton Plateau, at 700 to 1100 m above sea level, at the top of a steep scarp that rises almost directly from the coast ~4 km away. Orographic rainfall occurs as prevailing westerly winds bring moisture-laden air from the Tasman Sea to the mountains. Annual precipitation at the coast is ~3000 mm/year, increasing to ~6000 mm/year at the mine; frequent rain events, with daily rainfall exceeding 200 mm, can occur at any time throughout the year, and mean annual temperature is ~9°C (Davies et al., 2011).

The mine is located within the Eocene estuarine BCM as thick seams of bituminous coal. Pyrite is abundant (up to 5 wt%) in the upper portions of the coal measures and the lower parts of the overlying marine sediments. Interaction between rainfall, oxygen, and pyritic waste rock results in AMD, which can contain elevated Al and Fe, and trace contaminants of concern, which for the BCM can include As, Cd, Co, Cr, Cu, Mn, Ni, and Zn (see Pope et al., 2010).

Several catchments are affected by AMD (Figure 1). The Mangatini Stream, a significant tributary of the Ngakawau River, was identified as the main source of poor water quality within the Ngakawau Catchment (Figure 2). In 2005, Solid Energy committed to agreed water-quality targets by 2010 for the Ngakawau River at water monitoring location NR of:

- pH \geq 4.7 (99% of the time);
- Al < 1 mg/L (99% of the time);
- NTU \leq 25 NTU based on a 30-day rolling median; and
- Clarity to be >54 cm (NIWA Clarity Tube) > 90% of the time during base flow conditions (base flow is typically observed 70-75% of the time).

To achieve these objectives by the target date of June 2010, significant management systems were developed and infrastructure constructed. Although present, other contaminants of concern were not regulated under the resource consent for the site.

A number of downstream water treatment technologies were installed including the Mangatini AMD treatment plant to increase pH and remove dissolved metals (e.g., Al); and the Mangatini Sump (Figure 3) to capture AMD sludge, unreacted limestone, and sediment.

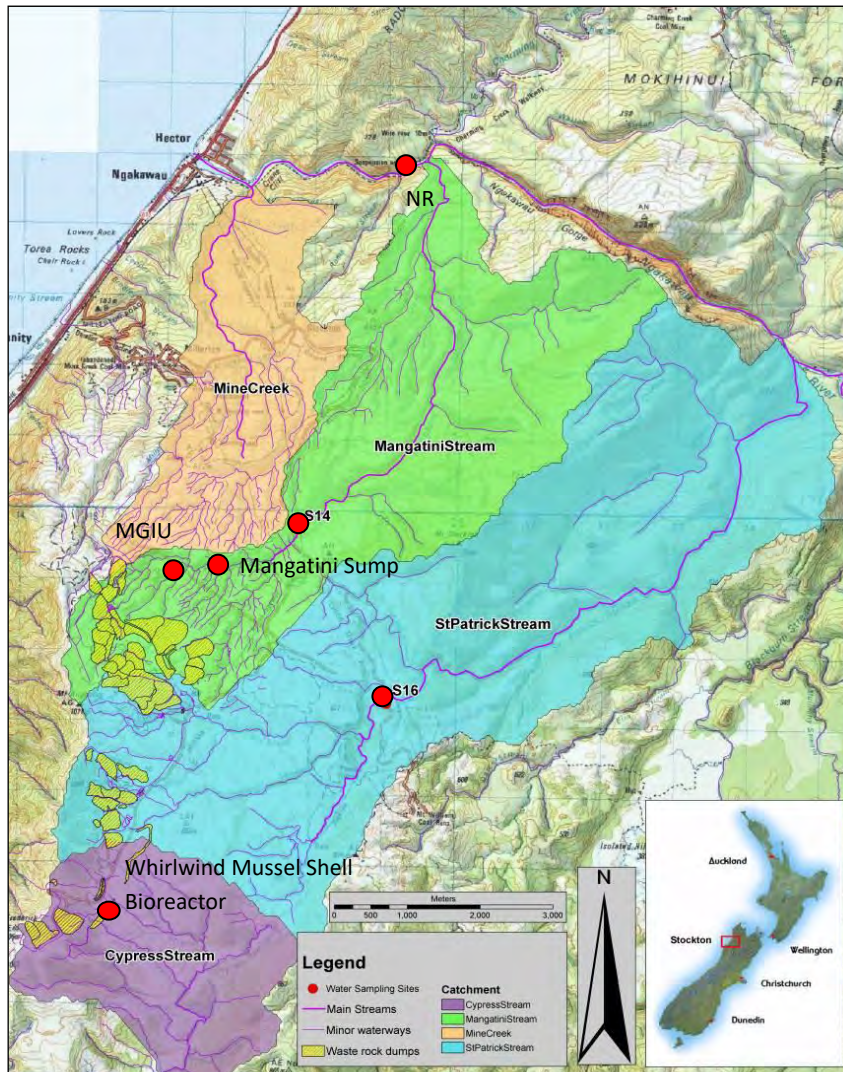


Figure 1. Drainage catchments of the Stockton coal mine. S14, S16, and NR are standard compliance water-monitoring sites. Water monitoring site S4 is 50 m downstream of the Whirlwind Mussel Shell Bioreactor.

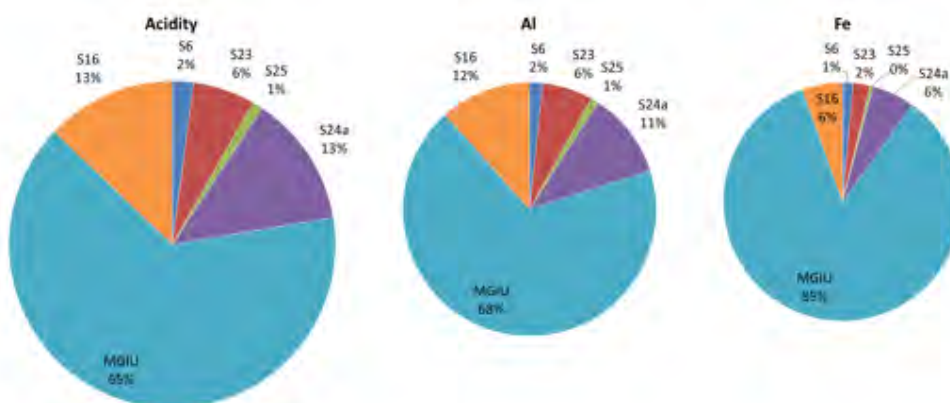


Figure 2. Acidity, Al, Fe loads for key streams draining Stockton. MGIU: Mangatini Stream above the Mangatini Sump; S16: St Patricks Stream; all other streams drain Millerton Mine area and report to either Mine Creek or Granity Stream.



Figure 3. Mangatini Sump (and inset, sludge extracted by coring).

3.0 ACTIVE TREATMENT OF THE MANGATINI STREAM

In 2006 a cost benefit analysis indicated that the cheapest long-term solution for the treatment of AMD was ultrafine limestone (UFL), provided reasonable dissolution efficiencies could be obtained. A pilot-scale plant that could dose UFL into the Mangatini Stream was constructed in 2006, and batch trials were undertaken. It was demonstrated that UFL (90% < 100 μm) was cost effective (at 60% efficiency) when at least 60 minutes tumultuous in-stream mixing was available (~400 m stream length), which could raise the pH to > 5 (Figure 4). In 2007 an operational UFL dosing plant was constructed at S14 and dosed directly to the Mangatini Stream. With ~9 km of mixing time before the compliance water monitoring site NR in the Ngakawau River, the use of UFL enabled the site to achieve water quality compliance for pH and Al (Figure 5, Figure 6).

In 2010 the Mangatini Sump was completed (Figure 3). It was designed to capture and remove sediment by gravity settlement derived from upstream mining areas and also precipitate AMD sludge created by the neutralisation of acidity. The intent was that it would provide AMD sludge and sediment storage capacity from ongoing AMD treatment for up to 100 years. The total water storage capacity for the normal operating level (RL 593.5 m) is about 900,000 m^3 of which approximately 600,000 m^3 is live storage. Flows of up to ~15 m^3/sec are diverted from the Mangatini Stream into the sump via a low diversion structure located on the Mangatini Stream.

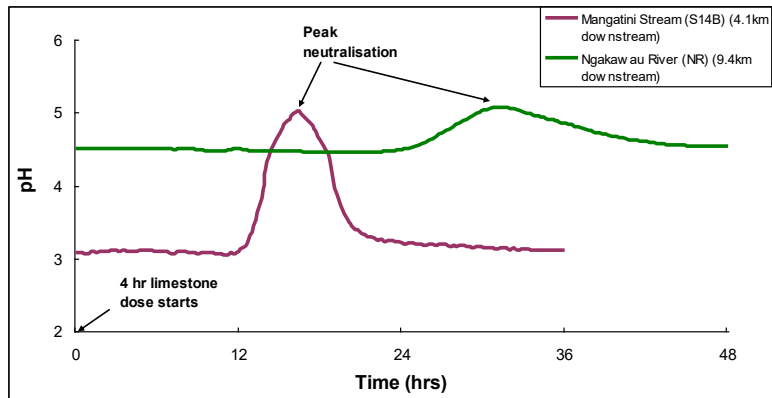


Figure 4. pH in the Mangatini Stream and Ngakawau River after UFL trial dosing.

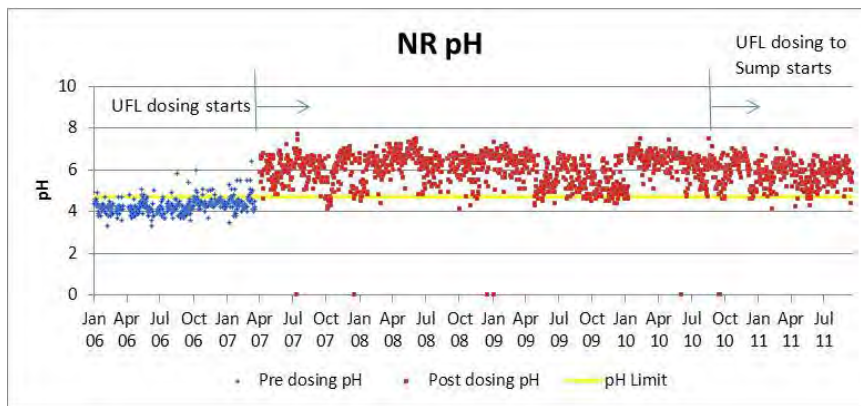


Figure 5. pH profile for Water Quality Monitoring Location NR

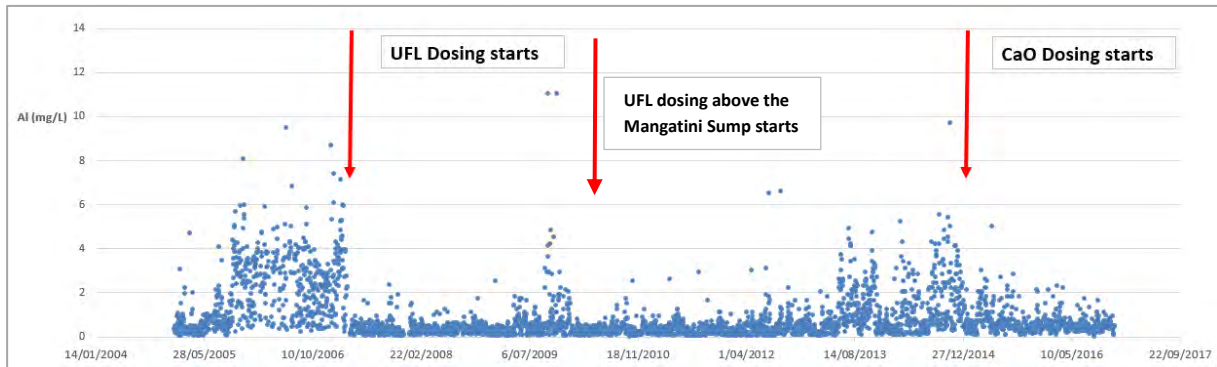


Figure 6. Al profile for Water Quality Monitoring Location NR

UFL treatment continued from 2007 until 2015, although in October 2010 the dosing of UFL commenced upstream of the Mangatini Sump once the sump was commissioned. This meant that the AMD sludge and unreacted UFL was captured before leaving site. However, this reduced UFL mixing/reaction time from 9 km to ~100 - 200 m. With limited space above the sump for a treatment plant (due to requirements to dump waste rock) and a short mixing time, the result was an inability to maintain pH at the target (pH 5 - 6). From ~mid 2013 onwards, there was a gradual deterioration in water quality including increasing dissolved Al (Figure 6).

Cost benefit analysis was a constant tool used by Stockton to determine the most appropriate reagent for neutralisation, which needed to consider reagent cost, reagent efficiency, sludge management costs and the achievement of water quality compliance targets (Table1). In 2014

it was decided that CaO was the preferred treatment options based on reagent cost and efficiency and the ability to meet target pH through better pH control.

Table 1. Factors influencing reagent performance

Factor	UFL	CaO
Reagent cost	Lower	Moderate
Dissolution kinetics (pH < ~4.2)	Moderate	High
Dissolution kinetics (pH ≥ ~4.2)	Low	High
Sludge volume	Lower	Higher
Water Quality Target (long mixing time)	Achievable	Achievable
Water Quality Target (short mixing time)	Poor	Achievable

In January 2015 the new CaO dosing system was installed. Subsequent data indicated significant improvements in water clarity within the sump, an ability to treat to the target pH of ~5 – 6, and reduced reagent costs. Data from 2015 onwards indicated good removal of Fe and Al, with a decreasing removal efficiency for other contaminants of concern. This was related to pH control of metal hydroxide solubilities (Figure 7), where Zn > Ni > Cd > Mn. Sulfate was poorly removed, being ~700 mg/L and below gypsum saturation.

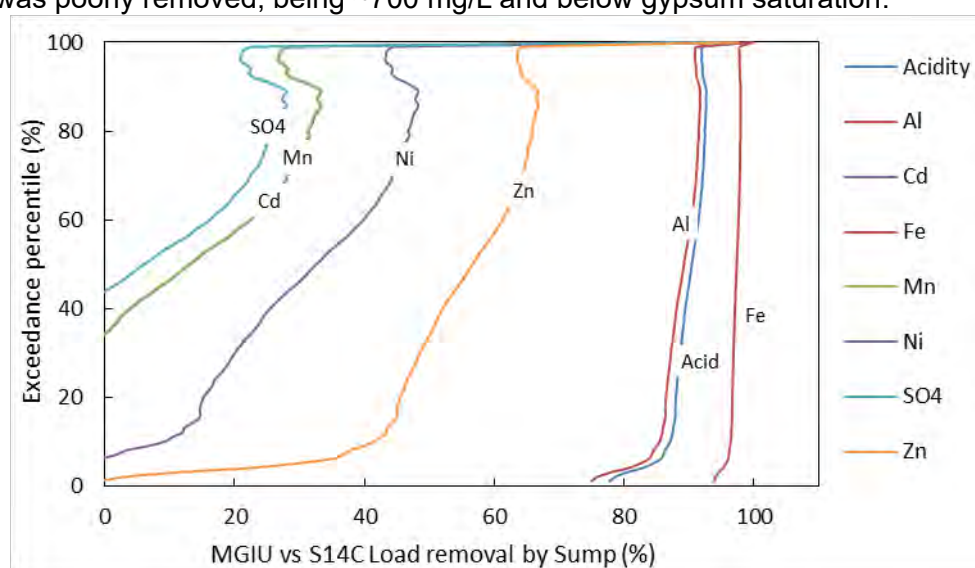


Figure 7. Metal removal by CaO treatment after the Mangatini Sump.

However, in 2016 it was observed that a significant quantity of low density sludge had formed in the Mangatini Sump, reducing the operational life of the structure to < 10 years. Lower density sludge was expected from using CaO compared to UFL, however, and this combined with a high sediment load resulted in a significant shortening of the sump life. Investigations are now underway looking at the use of UFL, CaO, dual reagent treatment, sludge recycling (e.g., high density sludge), and sludge management options to address this issue. Net Present Value (NPV) analysis indicates that, although CaO is the lesser cost product for treatment, the cost of sludge management could have a significant influence on the outcome, given that initial studies suggest UFL sludge is half the volume of CaO sludge.

4.0 MUSSEL SHELLS FOR AMD TREATMENT

Trials were undertaken at Stockton in 2007 to look at the benefits of treating AMD within waste rock dumps (WRDs) by placing layers of mussel shell beneath potentially acid forming (PAF) waste rock. Results indicated the pH increased from ~3 to >7 by such methods with the subsequent removal of significant metals (Weber et al., 2008). Subsequent research led to the development of mussel shell bioreactor (MSB) technology, comprised of 100% shell waste to treat AMD impacted waters. MSB pilot trials constructed in downflow configurations also demonstrated significant improvements in water quality and were presented at the Australian AMD Workshop in Darwin in 2011 (Crombie et al., 2011). Such trials paved the way for industry acceptance of the technology and the subsequent construction of operational reactors.

In 2012 an operational MSB was constructed at Stockton in the Whirlwind Stream. The system was designed for flows of 1L/s with pH = ~3.3, dissolved Al = 7.3 mg/L, dissolved Fe = 1.1 mg/L and total acidity = 71.5 mg CaCO₃/L. Design data for the MSB are provided in Table 2.

Table 2. Whirlwind Mussel Shell Bioreactor design specifications. Calculations are based on a shell density of 990 kg/m³ and a mussel shell ANC of 800 kg/t.

Parameter	Data
Average Plan Dimensions (m) (Shell layer)	14.0 x 21.5
Average Plan Area (m ²) (Shell layer)	302
Average Shell depth (m)	1.2
Ponding depth (m)	0.2 - 0.6
Freeboard (m)	0.8 - 0.4
Volume of shells (m ³)	366
Mass of Shells (t)	362
Pore volume (m ³)	192
Residence time (days) (@ 1 - 6 L/s)	2.2 - 0.44
Total ANC (t CaCO ₃)	290

Treated water from the Whirlwind MSB is typically pH 7, which then enters the Whirlwind tributary at compliance water monitoring point S4 together with additional AMD-impacted drainage that decreases the pH to approximately 5-7 (see Figure 8). A significant increase in pH was observed at the S4 monitoring point within the Whirlwind stream after the MSB was installed (Figure 8), which is due to the export of alkalinity from the MSB (~ 100 mg/L CaCO₃ equiv.). The Whirlwind MSB has been operating continuously since September 2012 (5 years).

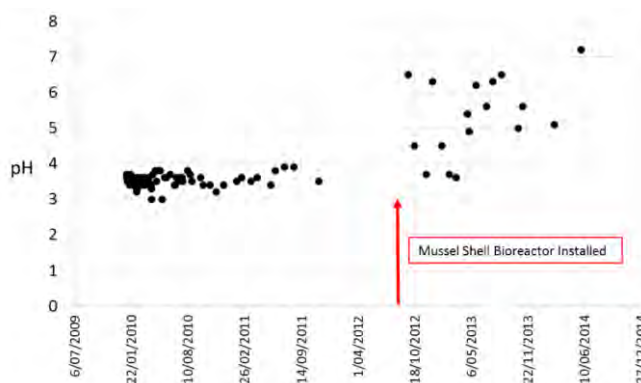


Figure 8. pH versus time for the S4 compliance monitoring point (affected by additional AMD) in the Whirlwind Tributary downstream of the Whirlwind Mussel Shell Bioreactor.

A significant issue for passive treatment systems is longevity and surety that upfront capex costs will be a favourable use of resources for the treatment of AMD-impacted waters in the long term compared to active treatment. The short-term performance of passive treatment systems are often well quantified; however, their long-term effectiveness is still poorly understood. Carbon exhaustion and hydraulic malfunctions are often amongst the most frequent reasons reported for system failure. Confidence in the technology and an understanding of performance issues will increase with time as more MSBs are installed.

Based on the success of the Whirlwind MSB, other systems have been constructed within New Zealand, including a passive treatment system at the Escarpment Coal Mine, just south of Stockton. Escarpment Coal Mine is located with the BCM, having similar geology and environmental conditions to Stockton. Mine development started in 2014. It is currently in care and maintenance and includes a small ~2 Ha engineered landform (ELF). Drainage from the Barren Valley ELF (BV ELF) is captured, treated by a MSB and then discharges to Pit 3, which discharges via Lake Brazil to the receiving environment (Figure 9).

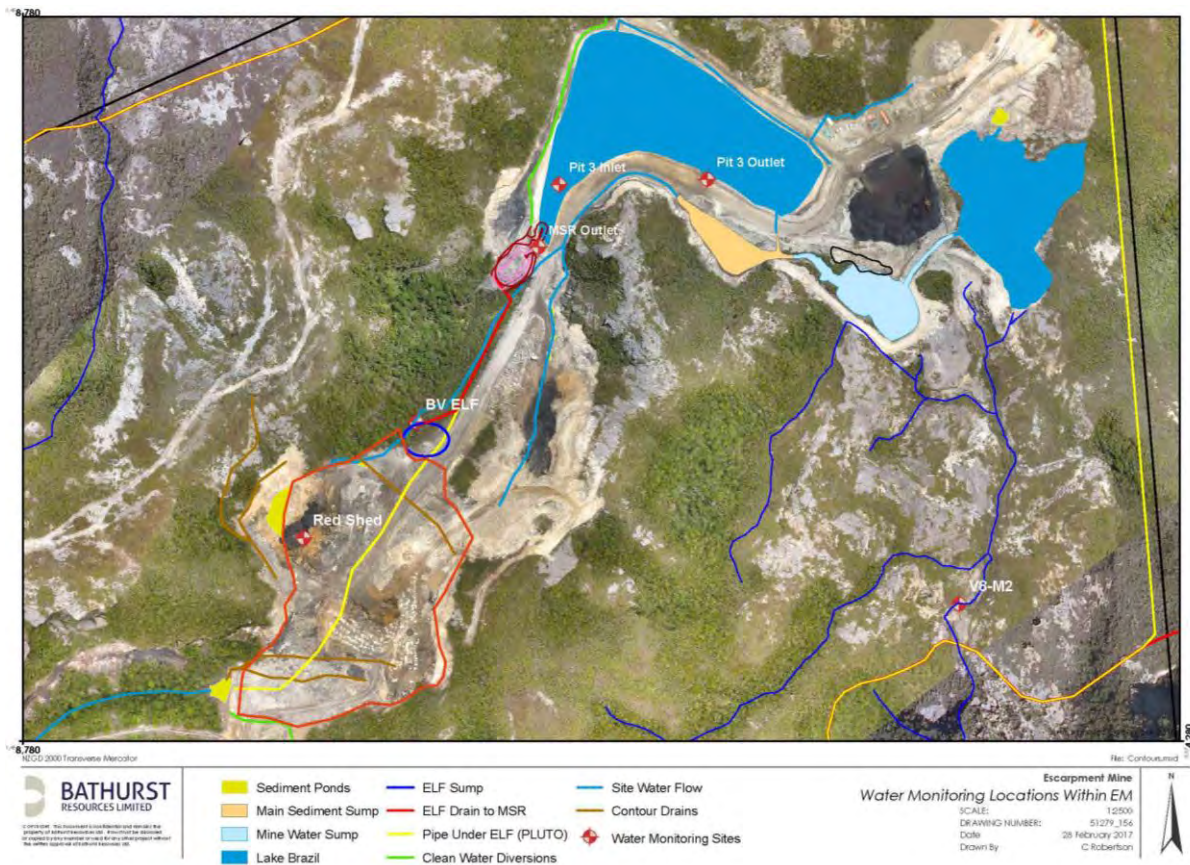


Figure 9. Escarpment Coal Mine. Image and data from Robertson et al. (2017).

Data presented in Figure 10 indicates that the Escarpment MSB is not only treating the acidity load from the BV ELF, but is also neutralising the acidity within the downstream Pit 3 Lake, with pH increasing to circum-neutral conditions.

Longevity of a MSB is estimated based on the influent AMD acid load versus the acid neutralisation capacity and quantity of shells in MSB. The 2016 average acidity from the BV ELF outlet is approximately 140 mg CaCO₃/L. Flow rate is 2.5 L/s, though the previous two

measurements were 3.5 L/s. Thus a conservative estimate of acidity load entering the MSB is 490 mg CaCO₃/s (140 mg CaCO₃/L acidity and 3.5 L/s flow rate) or 15.4 t CaCO₃/yr.

Thus, for an acid load of 15.4 t CaCO₃/yr, the theoretical MSB longevity would be 13 years. Alkalinity contributions from sulfate-reducing bacteria (SRB) have not been considered. In our experience, with such new technology, a longevity of 10 years is advocated for MSB until further data are available.

Maintenance will be required on an annual basis consisting of removal of the upper sludge layer from the MSB to prevent clogging by AMD precipitates. Currently the MSB is a down-flow system, which results in significant Fe-sludge accumulation, although the sludge can simply be scrapped off at minor cost (e.g., Weber et al., 2015). The MSB is configured so that it can be switched to up-flow, which is planned as an operational trial in the next year.

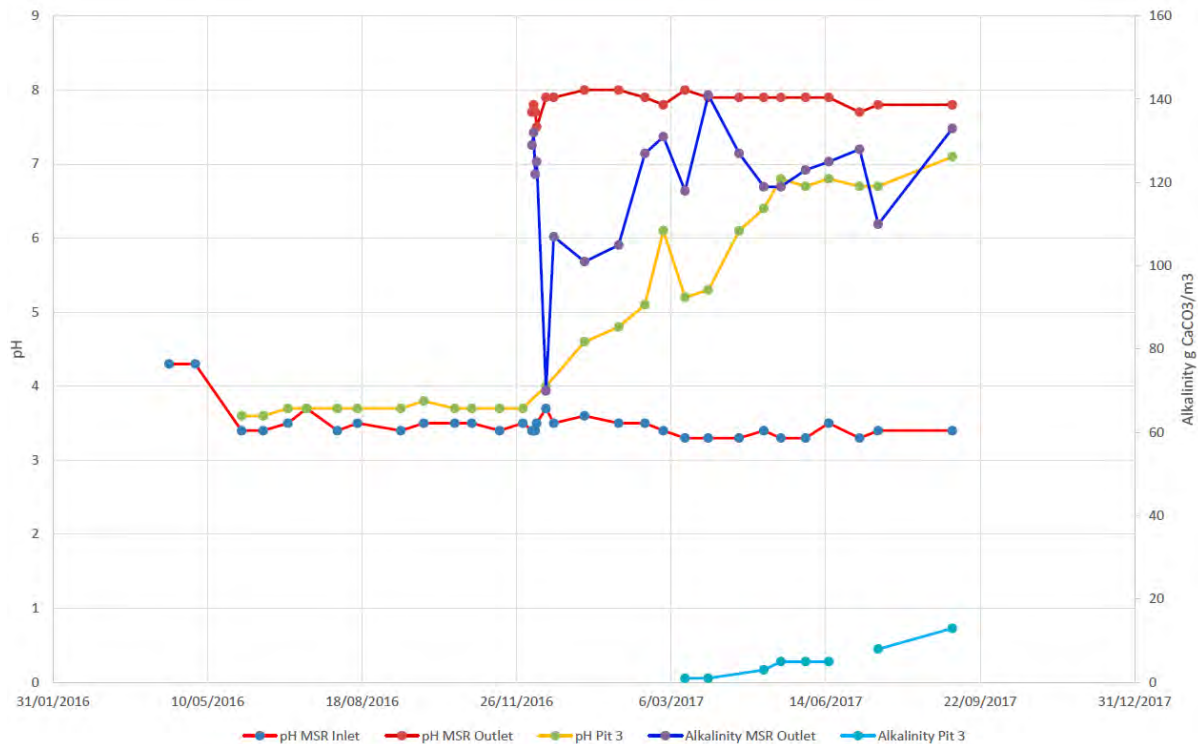


Figure 10. Water quality for the Barren Valley MSB and Pit 3.

5.0 TECHNOLOGY DEVELOPMENT

Development of passive treatment systems is continuing in New Zealand, with recent trials using low-cost, water-soluble additives to passive treatment systems, which provide significant improvements in treatment efficiency. Data suggest this could lead to reduced hydraulic residence times (HRT), or smaller systems, with both having economic benefits for mining operations.

Trials were conducted at CRL Energy's laboratory, where traditional SRB bioreactors using a multimedia substrate (e.g., McCauley et al., 2009) were fed with a low-cost, water-soluble product, and the effect on effluent sulfate concentrations was measured as an indication of SRB activity. Influent AMD was dosed with two nutrient additives (PX1.0 and PX1.5), providing additional nourishment to the SRB. Sulfate was used as an indicator of any improvements to

treatment efficiency during optimisation trials. Trials indicated that a 15-fold improvement to the amount of sulfate removed from AMD, relative to the control systems (Figure 11 and 12).

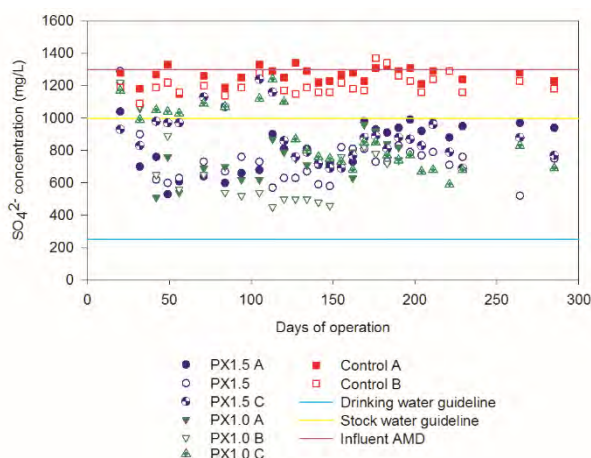


Figure 11. Sulfate concentrations in the reactor effluent. The influent AMD sulfate concentration, and pertinent water quality guidelines are also displayed.

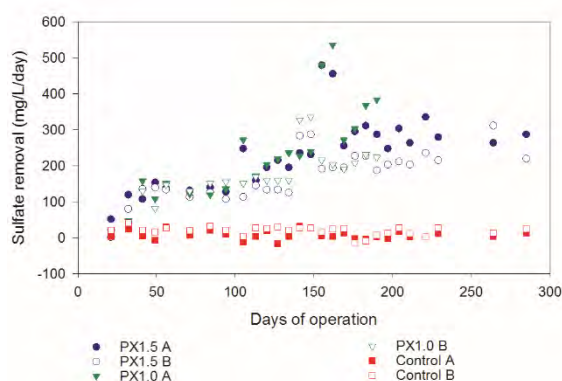


Figure 12. Sulfate removal rate in the control, PX1.5 and PX1.0 dosed reactors.

Dosing AMD with nutrient additives, as shown in the above example, can improve sulfate removal in SRBs. This can reduce the required retention time in reactors, and therefore decrease the capex investment required to install passive SRB reactors at mine sites. Field trials are the next step for this technology.

6.0 SUMMARY

After a decade of investigations into AMD treatment at Stockton, there has been a significant improvement in water quality, although limitations on space and mixing time above the sump (stream length) have required a shift from UFL treatment to CaO treatment. The key driver for change was achieving water quality objectives, where operational constraints prevented the use of UFL. Sludge management is now a priority for the site and investigations are underway.

R&D has been, and will continue to be, important for optimising treatment processes. Work conducted at Stockton on using waste mussel shells for AMD treatment was part of investigations to find least cost processes for treatment. However, new technologies can take a number of years to gain industry acceptance and require supporting data and operational-scale trials to show such technologies are robust and cost effective in the long term.

Enhanced passive treatment processes, which can also be considered active/passive technologies, may reset industry accepted standards for what contaminant loads can be treated by passive systems. This will require further testing and eventually full-scale operations trials to confirm this is the case.

7.0 ACKNOWLEDGEMENTS

The authors would like to acknowledge the staff at Stockton Coal Mine for their support over the years. Funding for parts of this work was provided by the Ministry for Business, Innovation and Employment, Contract CRL1202 as part of research efforts by the Centre for Minerals Environmental Research (CMER). The authors would like to thank Solid Energy New Zealand Limited and Bathurst Resources Limited for the use of data.

8.0 REFERENCES

- Crombie, F.M., Weber, P.A., Lindsay, P., Thomas, D.G., Rutter, G.A., Shi, P., Rossiter, P. and Pizey, M.H. (2011). Passive treatment of acid mine drainage using waste mussel shell, Stockton Coal Mine, New Zealand. In *Proceedings of the Seventh Australian Workshop on Acid and Metalliferous Drainage*, Darwin, Northern Territory. 21-24 June 2011 (Eds L.C. Bell and B. Braddock), pp. 393-405, (JKTech Pty Ltd), Brisbane.
- Davies, H., Weber, P., Lindsay, P., Craw, D., Peake, B. and Pope, J. (2011). Geochemical Changes during Neutralisation of Acid Mine Drainage in a Dynamic Mountain Stream, New Zealand. *Science of the Total Environment* 409: 2971–2980
- McCauley, C. A., O'Sullivan, A. D., Milke, M. W., Weber, P. A., and Trumm, D. A., 2009, Sulfate and Metal Removal in Bioreactors Treating Acid Mine Drainage Dominated with Iron and Aluminum: *Water Research*, v. 43, p. 961-970.
- Pope, J., Weber, P., Mackenzie, A., Newman, N. and Rait, R. (2010). Correlation of acid base accounting characteristics with the geology of commonly mined coal measures, West Coast and Southland, New Zealand. *New Zealand Journal of Geology and Geophysics Special Edition: Mine Drainage* Vol. 53: 153-166.
- Robertson, C., Weber, P., Olds, W., 2017. AMD Passive Treatment System: A Case Study – Escarpment Mine, Denniston Plateau. New Zealand Annual AusIMM Branch Conference, Christchurch, 10 - 13 September.
- Weber, P.A., Lindsay, P., Hughes, J.B., Thomas, D.G., Rutter, G.A., Weisener, C.G. and Pizey, M.H. (2008). ARD minimisation and treatment strategies at Stockton Coal Mine, New Zealand. In *Proceedings of the Sixth Australian Workshop on Acid and Metalliferous Drainage*, Burnie, Tasmania. 15-18 April 2008. (Eds L.C. Bell, B.M.D. Barrie, B. Baddock, and R.W. MacLean) pp. 113-138 (ACMER: Brisbane).
- Weber, P., Weisener, C., Diloreto, Z., Pizey, M.H., 2015. Passive treatment of ARD using waste mussel shells – Part I: System development and geochemical processes. *10th International Conference on Acid Rock Drainage*, April 20-25, 2015, Santiago, Chile, pp 1204 -1213.

BACTERIA-MINERAL INTERACTIONS AT SULPHIDE MINERAL SURFACES

G. Southam^A

^ASchool of Earth & Environmental Sciences,
The University of Queensland, St. Lucia, QLD 4072, Australia

ABSTRACT

*Acidophilic iron and sulphur oxidising bacteria are active in sulphide-bearing mine wastes at circumneutral pH conditions. In these environments, the growth of Acidithiobacillus spp. are characterized by bacterially-colonized crusts of schwertmannite $[\text{Fe}_8\text{O}_8(\text{OH})_{6-4.5}(\text{SO}_4)_{1-1.75}]$, lepidocrocite $[\gamma\text{-FeO}(\text{OH})]$ and jarosite $[\text{KFe}_3(\text{OH})_6(\text{SO}_4)_2]$ at sulphide-mineral surfaces. Exposed sulphide surfaces also exhibit evidence of direct cell attachment sites (pitting). The combined occurrence of schwertmannite, jarosite and pitting suggests that localized acidic microenvironments develop at sulphide surfaces. Growth of a consortium of acidophilic iron and sulphur oxidising bacteria (*A. ferrooxidans*, *L. ferrooxidans* and *A. thiooxidans*) on different sulphides, representing a well characterised system (pyrite), easily leached material (bornite-chalcocite ore) and a difficult bioleaching target (chalcopyrite) demonstrated diverse colonisation strategies. The pyrite samples exhibited preferential attachment of cells to natural surfaces, with almost no attachment to polished surfaces, whereas the ore possessed colonies on all bornite-chalcocite surfaces, and evenly scattered individual cells on the non-sulphidic minerals in the ore. In contrast, the chalcopyrite sample did not result in the growth of microcolonies, though cells were evenly distributed over the entire specimen. All three systems formed precipitates on the mineral surfaces; iron phosphates on pyrite and chalcopyrite, and copper phosphate on the bornite-chalcocite ore. All systems also had viable cell counts that were two orders of magnitude greater than the inoculum by the end of the experiment. The lack of iron both in solution and in the precipitates formed on the bornite-chalcocite ore sample indicates a preferential leaching of chalcocite, with no significant solubilisation of bornite. An increase of copper in solution, coupled with high bacterial counts in the fluid phase showed that colony formation on the surface of chalcopyrite is not essential for bacterial growth, suggesting that copper solubilisation from this mineral is likely due to a biogenically catalysed chemical leach rather than direct biooxidation.*

THE LINK BETWEEN MICROBIAL DIVERSITY AND AT-SOURCE AMD PREVENTION

O.T. Ogbughalu^A, A.R. Gerson^B, G. Qian^{A,C}, R.St.C. Smart^{A,B}, R.C. Schumann^{A,D},
N. Kawashima^C, R. Fan^A, J. Li^A and M.D. Short^{A,C}

^ASchool of Natural and Built Environments, University of South Australia, Mawson Lakes, SA 5095, Australia

^BBlue Minerals Consultancy, Middleton, SA 5213, Australia

^CFuture Industries Institute, University of South Australia, Mawson Lakes, 5095, South Australia, Australia

^DLevay and Co. Environmental Services, Edinburgh, SA 5111, Australia

ABSTRACT

Mining is an important global industry, but is one that generates large volumes of challenging wastes. In particular, acid and metalliferous drainage (AMD) remains a global environmental issue for both operating and legacy sites. Often acidic and frequently associated with high concentrations of heavy metals and metalloids, AMD poses a challenge to the environmental and social acceptance of mining activities due to the deleterious impacts on downstream waterways and adjacent riparian zones.

Here we report on the results of laboratory kinetic leach column experiments designed to mimic a sulfide-containing waste material under typical environmental conditions. We assessed the potential of waste organic carbon sources to successfully mitigate AMD. Results over some 84 weeks of column leaching showed that AMD production was successfully reduced with organic carbon addition, but was not in the unamended control. Mineral phase electron microscopy analysis confirmed the presence of passivation layers across pyrite surfaces. Microbiological analyses revealed enriched heterotrophic microbial populations in the organic carbon-amended columns relative to controls, with metabolic microbial actions thought to play a key role in AMD mitigation. Furthermore, DNA-based microbial community analyses at various intervals revealed the existence of diverse communities and showed strong links between microbial ecology and leachate chemistry.

1.0 INTRODUCTION

Mining is an important global industry, which produces large volumes of wastes, comprising mainly sub-economic waste rocks and tailings. Many of these wastes present unique management challenges for industry, in particular potentially acid-forming materials, which can cause acid metalliferous drainage (AMD). AMD is the biggest environmental issue facing closed and abandoned mines and mine site rehabilitation (Smart et al., 2010). Poor historical waste rock management practices on-site have also meant that waste rock dumps are now recognised as the single largest AMD risk factor at many mine sites (Jones et al., 2016). Silverman and Ehrlich (1964) early research hypothesised that microorganisms found in AMD environments may be substantially responsible for acid generation, with this now well established (Johnson, 2014). While some chemoautotrophic microbes can exacerbate AMD, other groups of microorganisms, such as heterotrophic bacteria, can form protective biofilms on pyrite surfaces reducing the rate of AMD generation by reducing oxidant (O₂, ferric iron) availability at the mineral surface and O₂ availability generally within the waters contained in the wastes (Afzal Ghauri et al., 2007, Johnson, 2014). Accordingly, microbe–mineral

interactions are of considerable potential importance for effective and sustainable AMD management; however, such interactions are yet to be fully understood and exploited for AMD control.

2.0 MATERIALS AND METHODS

2.1 Kinetic Leach Columns (KLCs)

Experimental design consisted of three free-draining kinetic leach columns (KLCs): the control column supplied with Milli-Q water only (Control); a calcite-saturated water-treated column (CSW); and a biosolids-treated calcite-saturated water column (BS+CSW). Each KLC was set up in duplicate and contained 2 kg of natural minerals (GeoDiscoveries Australia) designed to mimic a typical potentially acid-forming waste. Minerals were crushed to particle size of <4 mm. Bulk assay and quantitative XRD analyses were performed on individual minerals to confirm their phase purity.

The KLC watering/flushing protocol is designed to mimic natural wetting–drying cycles, as detailed in Smart et al. (2002). The control and CSW KLCs were primed with Milli-Q water. Subsequent watering and flushing was carried out with Milli-Q water for the Control KLCs and with calcite-saturated water (alkalinity $\approx 30 \text{ mg CaCO}_3 \text{ L}^{-1}$) for the CSW KLCs.

The BS+CSW KLCs flush solution (also used for flush 0) comprised of sterile biosolids nutrient extract using 6-month old biosolids collected from a local wastewater treatment plant in Adelaide, South Australia. Prior to each weekly application, biosolids liquid extract was diluted in calcite-saturated water to a final concentration of $\approx 140 \text{ mg dissolved organic carbon L}^{-1}$. The BS+CSW KLCs were inoculated with an extract of tailings from a legacy pyrite mine located in Brukunga, 40 km east of Adelaide, South Australia ($35^\circ 00' 26'' \text{S } 138^\circ 56' 37'' \text{E}$). Ten grams of Brukunga tailings were vigorously mixed in equal parts of Milli-Q water and applied onto the KLCs as a one-off environmental microbial inoculant.

2.2 Chemistry Analysis

Leachate fractions collected during flushing events were weighed immediately after collection, with weights of the leachate used to normalise inductively coupled plasma mass spectrometry (ICP-MS) concentration data to give total dissolved S and Fe. pH, conductivity, redox potential (E_h , standard hydrogen electrode; SHE) and acidity/alkalinity measurements were conducted at room temperature within 24 h of collection.

2.3 Microbiological Analysis: Heterotrophic Plate Counts and 16S rRNA Community Profiling

Microbiological analyses using the heterotrophic plate count (HPC) method was carried out on the Control and BS+CSW KLCs fortnightly, during the first half of the leaching experiment. Sampling frequency was then reduced to 4-weekly in the second half of the experiments. Ten gram samples from the KLCs were used for each time-point analysis, following a modified HPC protocol from Pepper et al. (2012).

One gram of KLC material was sampled fortnightly, for DNA extraction and community profiling in the first 8 weeks, and then 4-weekly thereafter, over the 80-week period. Bray-Curtis (dis)similarities multivariate analyses were carried out for microbial abundance according to their taxonomical compositions, using PRIMER 7 software (Primer-E, Plymouth, UK).

2.4 Solid Phase Analyses

Mineral morphology analyses were carried out using environmental scanning electron microscopy (E-SEM) (FEI Quanta 450 FEG) with energy dispersive X-ray spectroscopy (EDS) for semi-quantitative surface chemical composition, both operated at 20 keV. Focussed ion beam scanning electron microscopy (FIB-SEM) and scanning transmission electron microscopy (STEM) were used to generate and analyse a cross-section of leached pyrite from both the Control and BS+CSW KLCs. Leached pyrite particles were platinum-coated prior to FIB cross-section generation and electron microscopy analyses.

3.0 RESULTS AND DISCUSSION

3.1 Kinetic Leach Columns

Results from mineralogical and microbial analyses at the beginning of the experiments (week 0) are shown in Table 1. The KLCs comprised quartz (81.3 wt.%), feldspar (10.0 wt.%), chlorite (5.0 wt.%) and pyrite (3.7 wt.%; 2.0 wt.% sulfide). HPC analyses performed at day zero showed the presence of heterotrophic microbes in both the Control (1.0×10^4 CFU g⁻¹) and BS+CSW KLCs (1.4×10^5 CFU g⁻¹) (HPC analysis was not conducted for CSW KLC). The BS+CSW KLCs contained around 10-fold greater microbial population at day zero most likely due to inoculation with the Brukunga mine site tailings (since sterile biosolids were used), which were not added to the Control KLC.

3.2 Leachates Analysis

The pH of the effluent from the Control KLC dropped from pH 4 at the first flush at week 4 to stabilise around pH 2 after around week 8, where it stabilised thereafter (Figure 1a). The pH drop is paralleled by elevated levels of S and Fe in the leachate from the KLC (Figure 1c). An increase in E_h occurred between weeks 4 and 8 from around 600 to 755–851 mV thereafter, a redox level above the pyrite rest potential (660 mV). This increase in E_h is associated with an increase in ferric iron concentration, in conjunction with decreasing pH ($O_2 + 4e^- + 4H^+ \rightarrow 2H_2O$). Each decrease of one pH unit results in an increase in E_h of 58 mV, (in the absence of other redox couples). The conductivity (Figure 1b) was variable averaging 1908 $\mu S\ cm^{-1}$ over the 84-week period. Unsurprisingly, the leachates from the Control KLC showed increased acidity levels from the second flush at week 8 onwards (Figure 1d). The effluent of the CSW KLC was initially near neutral pH with an average of 5.7 over the first 40 weeks of leaching (Figure 1a). However, the pH dropped sharply after around week 44, while E_h (Figure 1b) and acidity levels (Figure 1d) rose after week 48, demonstrating that calcite-saturated water alone was unable to maintain circum neutral pH and prevent acidity generation in our PAF waste material in the long term.

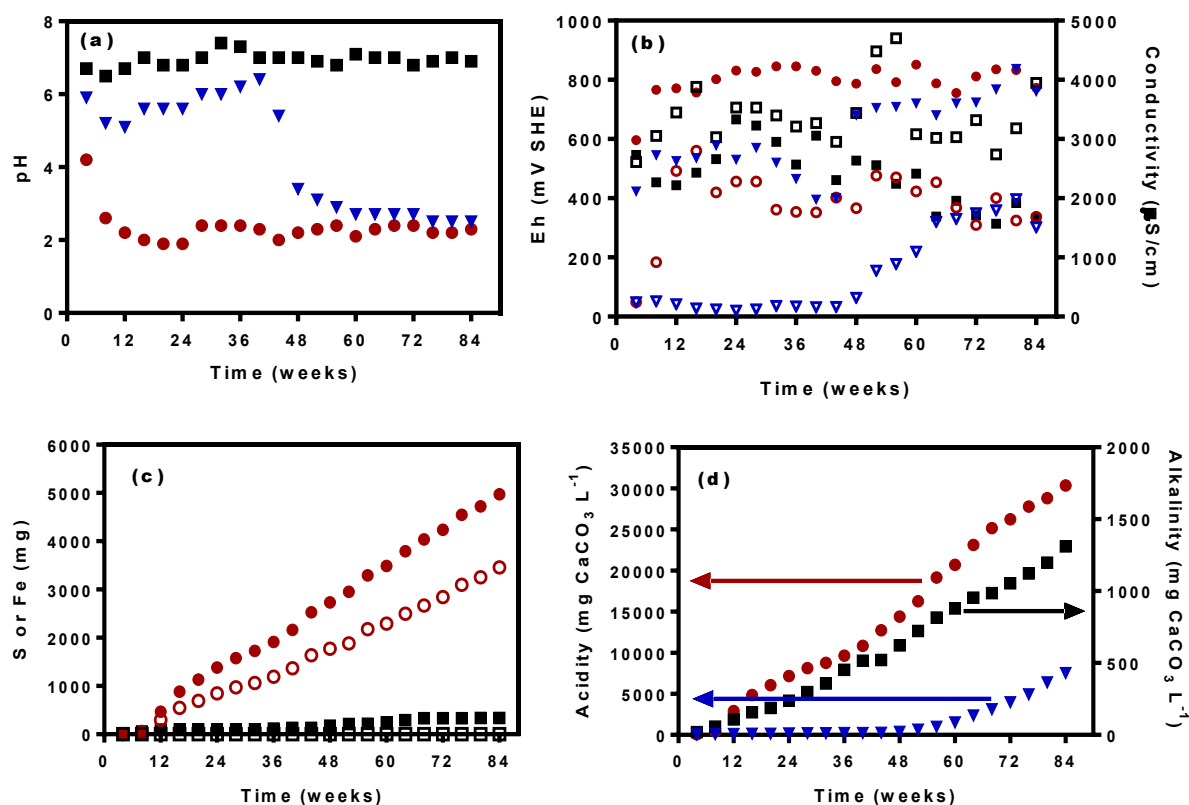


Fig 1. Leachate analyses: (a) pH, (b) E_h , (c) cumulative S and Fe in the effluents and (d) cumulative acidity and alkalinity. Legend for primary y-axes for (a) (b) and (d) and S analysis for (c): ● – Control KLC, ▼ – CSW KLC; ■ – BS+CSW KLC. Legend for secondary y-axes for (b) and Fe analysis for (c): ○ – Control KLC, ▽ – CSW KLC; □ – BS+CSW KLC.

The BS+CSW KLC leachates, on the other hand, maintained circum neutral pH throughout the entire experimental duration (84 weeks). The E_h in the BS+CSW KLCs varied in the first 48 weeks of the leaching experiments, averaging 540 mV, dropping to 393 mV after week 48 (Figure 1b). The redox potential of the BS+CSW KLC over this 84-week period remained below the pyrite rest potential (660 mV, SHE). These results suggest effective inhibition of pyrite oxidation as further evidenced by the very low amounts of S and Fe dissolved over the same period (Figure 1c) (Ogbughalu et al., 2017).

3.3 Microbiological Analysis: Heterotrophic Plate Counts

The Control KLC showed the greatest heterotrophic microbial growth just before week 8, followed by a sudden drop in HPC abundance thereafter (Figure 2). This apparent link to the decline in pH after week 8 (from pH 4.2 to 2.6) suggests that the microbial community grew initially but couldn't successfully maintain a stable population with the onset of adverse physico-chemical conditions (low pH) and conceptually, no nutrients for microbial growth in the Milli-Q water medium.

Unlike the Control KLC, an enhanced microbial population was observed in the BS+CSW KLC (Figure 2). The high microbial population within this KLC can be linked to the consistently near-neutral pH throughout the life of the experiment, in addition to the consistent nutrient supply (from biosolids) for heterotrophic microbial growth.

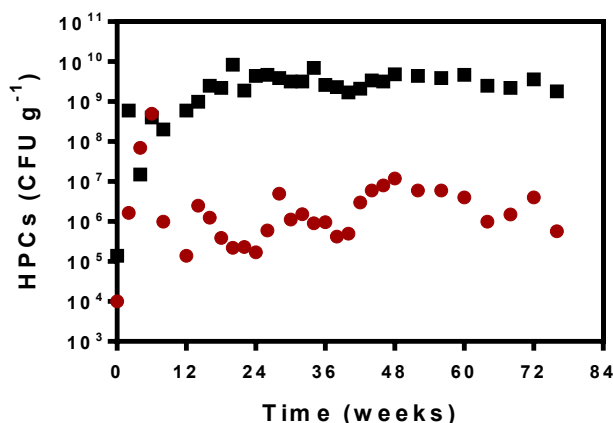


Fig 2. Heterotrophic bacterial counts (\log_{10} scale; CFU g^{-1}) for Control and BS+CSW KLCs showing microbial population over time (Legend: ● – Control KLC; ■ – BS+CSW KLC).

It is likely that microbial respiration played an important role, either via O_2 depletion and/or alkalinity (CO_2) generation, for the effective microbially-mediated AMD control in the BS+CSW KLCs. Microbial respiration rates are dependent on the metabolic state (physiological growth phase) and also vary with taxonomic classification. Application of a microbial O_2 uptake rate (OUR) can provide an indication of likely O_2 consumption patterns in the KLCs. By applying the oxygen consumption rate of a typical bacteria – *Escherichia coli* of 3.6×10^{-13} $\text{gram cell}^{-1} \text{ day}^{-1}$ (Wagner et al., 2011), the daily minimum O_2 consumption rates for our KLCs were calculated to be $7.4 \text{ mg kg}^{-1} \text{ day}^{-1}$ and $1013.5 \text{ mg kg}^{-1} \text{ day}^{-1}$, for the Control and BS+CSW KLCs respectively. This suggests that the microbial respiration rate within the BS+CSW KLC was 1000-fold greater than the O_2 rate within the Control KLC.

3.4 Microbial Diversity and 16S rRNA Profiling

Two dominant microbial classes were identified in the Control KLC using SIMPER analysis – Bacilli and Clostridia. These groups of bacteria are known to thrive in extreme environmental conditions (Nicholson et al., 2000). Taxonomic results showed that the Control KLC contained about 63 participating microbial classes in total. Furthermore, this multivariate analysis also suggests that *Bacillus* and *Clostridium* were the most responsive (impacted) microbial classes to the changing environmental conditions occurring within this leach column. Figure 3 gives a matrix display of the top 50 participating microbial classes.



Fig 3. Matrix display of richness in microbial diversity and abundance using the Bray-Curtis analysis showing top 50 participating microbial taxonomical classes in (a) Control ▲ and (b) Biosolids treated KLCs ▼ over the 80-week period. Relative abundance for each organism at each time point indicated by intensity of shading in the shade plot.

The BS+CSW KLC showed a more diverse microbial population (Figure 3), with a total of 103 participating microbial classes identified. It was observed that no particular group (or taxonomic classes) dominated this column and no one group was found to be present in relative abundance of >6% of the overall microbial community.

3.5 Solid Phase Mineral Analyses

Pyrite surface analyses: SEM imaging of pyrite sampled from the Control and BS+CSW KLCs at 84 weeks shows distinctly different surface morphologies (Figure 4). Pyrite from the Control KLC (pH 2.3) showed strong evidence of oxidation and weathering, with obvious pitting and cracks (Figure 4b) as compared to a fresh pyrite surface (Figure 4a). Conversely, pyrite taken from the BS+CSW KLC (pH 6.9) showed no such oxidation or weathering (Figure 4c), complementing the leachate chemistry and indicating that the pyrite was successfully passivated during this period.

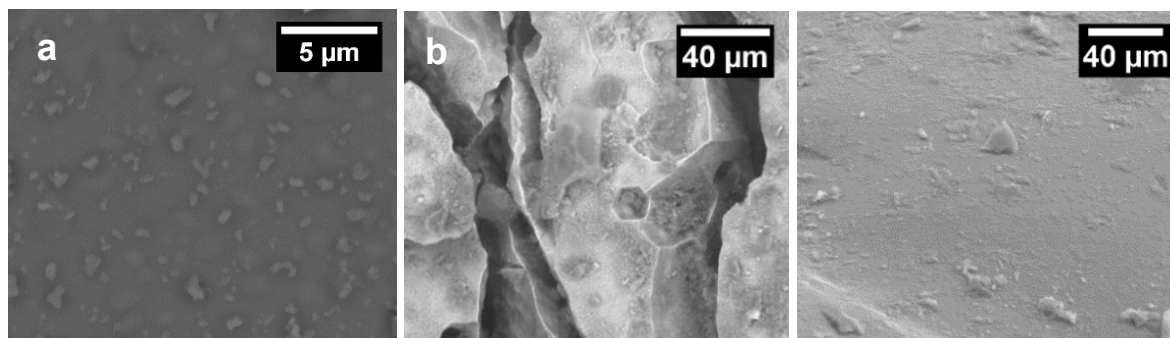


Fig 4. SEM micrographs of (a) pyrite at week 0 (55 wt.% S and 45 wt.% Fe), (b) pyrite from the Control KLC at week 84 (O 17 wt.%, Fe 44 wt.%, Si 6 wt.% and S 34 wt.%) and (c) pyrite from the BS+CSW KLC at week 84 (O 20 wt.%, Fe 19 wt.%, Si 8 wt.% and S 53 wt.%).

Pyrite cross-section mineral analysis and elemental mapping: The FIB TEM cross section analysis revealed the presence of a surface passivation layer across the pyrite surface from the BS+CSW KLC (Figure 5c). Elemental mapping confirmed this layer to be enriched in Si and O (Figure 5d), suggesting the presence of a silicate-stabilised iron oxy-hydroxide passivation layer across the pyrite surface (Miller et al., 2009, Schumann, 2009, Zeng et al., 2013, Fan et al., 2017).

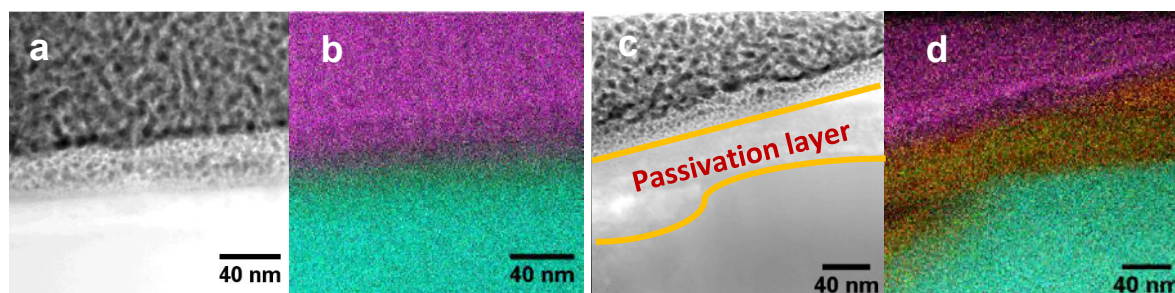


Fig 5. TEM elemental mapping images of (a) and (b) pyrite from the Control KLC; (c) and (d) pyrite from the BS+CSW KLC. (Legend: Fe: Green; S: Blue; O: Red; Si: Yellow and Pt: Purple).

The formation and maintenance of this surface passivation layer can be linked to the consistent circum neutral pH conditions maintained in this column. Furthermore, increased metabolic activities, including reduced oxygen accessibility to pyrite minerals from a greater and more diverse microbial population appeared to play a significant role in providing conditions conducive to the establishment and maintenance of the passivation layer. No such surface layer was found to be present on the pyrite collected from the Control KLC (Figures 5a and 5b), where organic carbon was limiting and microbial populations were much less abundant and diverse. This indicates that pyrite within the Control column maintained direct contact with oxidants, allowing sulfide weathering to occur.

4.0 CONCLUSION

AMD presents an impending liability to current and future mining operations worldwide and also poses a challenge to the environmental and social acceptance of mining activities. This recent work showed that Control and calcite-saturated water KLCs failed to maintain neutral pH beyond weeks 0 and 40, respectively. Without biosolids addition, low-level alkalinity supply alone from calcite-saturated water in the CSW KLC was not able to prevent acid generation beyond week 44. Conversely, nutrient supply from biosolids, supplemented by low-level alkalinity from calcite-saturated water, successfully stimulated heterotrophic microbial

populations and effectively inhibited pyrite oxidation and AMD generation over a period of 84 weeks. While the mechanisms by which this pyrite passivation was achieved remain unclear, it is suggested that increased microbial metabolic activities may play a role via *in situ* O₂ limitation of chemical oxidation processes. The efficacy of natural biosolid-heterotrophic microbial actions in the BS+CSW KLC, combined with low-level alkalinity supply, have the potential to provide a robust system for effective at-source AMD control.

5.0 ACKNOWLEDGEMENTS

The authors thank the Australian Government, Australian Research Council (LP130100568), industry sponsors Teck resources (Canada) and AMIRA International (project P933B).

6.0 REFERENCES

Afzal Ghauri, M., Okibe, N. & Barrie Johnson, D. 2007. Attachment of acidophilic bacteria to solid surfaces: The significance of species and strain variations. *Hydrometallurgy*, 85, 72-80.

Fan, R., Short, M., Zeng, S.-J., Qian, G., Li, J., Schumann, R., Kawashima, N., Smart, R. S. C. & Gerson, A. R. 2017. The formation of silicate-stabilised passivating layers on pyrite for reduced acid rock drainage. *Environmental Science & Technology*, 11317–11325.

Johnson, D. 2014. Recent developments in microbiological approaches for securing mine wastes and for recovering metals from mine waters. *Minerals*, 4, 279-292.

Jones, D. R., Taylor, J., Pape, S., McCullouch, C., Paul, B., Garvie, A., Appleyard, S., Miller, S., Unger, C. J. & Laurencont, T. 2016. Preventing acid and metalliferous drainage-leading practice sustainable development program for the mining industry. *Commonwealth of Australia, Canberra, Australia*.

Miller, S. D., Schumann, R., Smart, R. & Rusdinar, Y. ARD control by limestone induced armouring and passivation of pyrite minerals surfaces. 2009. ICARD.

Nicholson, W. L., Munakata, N., Horneck, G., Melosh, H. J. & Setlow, P. 2000. Resistance of Bacillus Endospores to Extreme Terrestrial and Extraterrestrial Environments. *Microbiology and Molecular Biology Reviews*, 64, 548-572.

Ogbughalu, O. T., Gerson, A. R., Qian, G., Smart, R. S. C., Schumann, R. C., Kawashima, N., Fan, R., Li, J. & Short, M. D. 2017. Heterotrophic microbial stimulation through biosolids addition for enhanced acid mine drainage control. *Minerals*, 7, 105.

Pepper, I. L., Zerzghi, H. G., Bengson, S. A., Iker, B. C., Banerjee, M. J. & Brooks, J. P. 2012. Bacterial populations within copper mine tailings: long-term effects of amendment with Class A biosolids. *J Appl Microbiol*, 113, 569-77.

Schumann, R. Passivating surface layer formation on pyrite in neutral rock drainage. 2009. ICARD.

Silverman, M. P. & Ehrlich, H. L. 1964. Microbial formation and degradation of minerals. In: WAYNE, W. U. (ed.) *Advances in Applied Microbiology*. Academic Press, Cambridge, USA

Smart, R., Skinner, B., Levay, G., Gerson, A., Thomas, J., Sobieraj, H., Schumann, R., Weisener, C., Weber, P. & Miller, S. 2002. AMIRA/EGi ARD Test Handbook. *AMIRA International, Melbourne www.amira.com.au*.

Smart, R. S. C., Miller, S. D., Stewart, W. S., Rrudinar, Y., Schumann, R. E., Kawashima, N. & Li, J. 2010. In situ calcite formation in limestone-saturated water leaching of acid rock waste. *Science of The Total Environment*, 408, 3392-3402.

Wagner, B. A., Venkataraman, S. & Buettner, G. R. 2011. The rate of oxygen utilization by cells. *Free Radical Biology and Medicine*, 51, 700-712.

Zeng, S., Li, J., Schumann, R. & Smart, R. 2013. Effect of pH and dissolved silicate on the formation of surface passivation layers for reducing pyrite oxidation. *Computational Water, Energy, and Environmental Engineering*, 2, 50.

EXTRACTION OF COBALT FROM HISTORIC SULPHIDE TAILINGS USING BIOLEACHING

A. Parbhakar-Fox^A, J. Glen^B and D. Kemp^B

^AARC Industrial Hub for Transforming the Mining Value Chain (TMVC), University of Tasmania, Private Bag 79, Sandy Bay, TAS 7001, Australia

^BALS Metallurgical Laboratories, ALS Global, 43 River Road, Wivenhoe, Burnie, TAS 7320, Australia

ABSTRACT

Mineralogical and geochemical characterisation of sulphide minerals in historic tailings can assist in determining whether there are economic and environmental benefits of reprocessing such materials using modern metallurgical practices. At the Old Tailings Dam (OTD), Savage River, Western Tasmania, 38 million tonnes of pyritic tailings were deposited (1967 to 1982), and have since been generating acid and metalliferous drainage (AMD). Long-term management options considered for this site have included the establishment of either a water, an hard engineered or a vegetation cover. However, due to geotechnical challenges and the lack of success demonstrated by previous pilot studies, these strategies have not been implemented. A detailed mineral chemistry study indicated elevated cobalt in the pyrite (up to 3 wt. %); however, as this is refractory, recovery via biohydrometallurgical processing was tested.

Bulk tailings samples (n = 4) were collected across the OTD from 0.5 to 1.5 m depth specifically targeting three sulphide-bearing facies, across four physical zones (defined by hydrological regime and grain size). A bulk composite of these materials was subjected to bacterial oxidation using BIOX® bacteria to determine if Co could be effectively leached under standard operating conditions. This study focussed on optimising the recommended procedure for undertaking BIOX® experiments, with pH, temperature and iron concentration in the nutrient medium varied. Our findings show that the most efficient conditions for leaching Co were under low pH (1.3-1.6) at 40°C and using a well adapted 4K or 9K nutrient medium. Using these optimal conditions, 100% Co leached from the tailings after 10 to 12 days. Our results suggest that reprocessing these deleterious materials might be a viable option for managing this historic site as part of an integrated tailings management strategy.

1.0 INTRODUCTION

Acid and metalliferous drainage (AMD), as characterised by metal-laden acid-sulphate waters, is the product of sulphide oxidation (e.g., pyrite, pyrrhotite; Jambor et al., 2003). AMD can occur throughout the life of mine (LOM) with numerous case studies published or otherwise reported e.g., Sracek et al. (2004), Parbhakar-Fox et al. (2014), Parvainen et al. (2014) and Buzatu et al. (2016). Current mining practice mandates the adoption of strategic waste planning and management practices in accordance with environmental legislative practices enforced in that particular jurisdiction (e.g., Directive 2006/21/EC; Leading Practice Sustainable Development in Mining, 2011). However, historic mining operations utilised disposal and waste management practices considered inappropriate by today's environmental standards (Salomon and Eagle, 1990; Ramirez-Llonda et al., 2015). Attempting to retrospectively manage historical tailings has proven challenging (e.g., Moncur et al., 2015; Azhari et al., 2016; Harris et al., 2016; Van Veen et al., 2016). Alternatively, if such tailings

were regarded as potential resources and geometallurgically characterised, there could be significant advantages of reprocessing using modern metallurgical techniques resulting in long-term AMD risk reduction. However, conventional mineral processing methods may be inappropriate for complex sulphide ores, thus despite the resource potential, tailings processing may prove uneconomic (Tao and Dongwei, 2014). In such cases, biohydrometallurgical processing could be considered (Johnson, 2015).

Operating since 1999, the Tasmania Au-mine (formerly Beaconsfield) is the best example of a commercial scale Bacox™ Au-bioleaching plant in Tasmania. It was designed to treat 70 tonnes per day of a refractory pyrite-arsenopyrite concentrate, with near complete oxidation of sulphides resulting in > 95% Au extraction (Neale et al., 2000). With at least 215 AMD waste sites identified within Tasmania requiring rehabilitation (Gurung, 2001), there may be an opportunity to employ low-cost biohydrometallurgical processing, adding value to some sites.

In this study we focussed on one such site, the historic Old Tailings Dam (OTD), western Tasmania, which is actively generating AMD. The water quality of the adjacent Savage River has been impacted with elevated Cu loads relative to ANZECC (2000) measured downstream of the OTD (Jackson and Parbhakar-Fox, 2016). To manage this historic mine waste, the Tasmanian Government has evaluated several options. These have included establishing a water cover (Jackson and Parbhakar-Fox, 2016) and investing in a hard engineering solution (e.g., Quispe et al., 2013). However, due to geotechnical complications, neither are feasible. Instead, Parbhakar-Fox et al. (2016) undertook a detailed pyrite laser ablation ICPMS study on OTD materials to determine the metal content, and assess if reprocessing is an option. Significantly high concentrations of cobalt, a critical metal, were measured (up to 3 wt. %); however, as it is refractory, its extraction via well-established mineral processing techniques is complicated. Instead, Co extraction via pyrite bioleaching could be considered with examples from Kasese, Uganda documented in Morin et al. (1993), d'Hughes et al. (1997) and Rawlings (2005). Whilst Watling (2015) described several methods for bioleaching of low grade sulphidic ore, examples of historic waste processing in this manner were not detailed. Considering this, our research focussed on determining if biohydrometallurgical processing of the OTD sediments could liberate economic concentrations of Co. If proven, this would confirm if tailings reprocessing is a viable management option for this contaminated site. This paper builds on our previous research which sought to establish if Co was extractable from pyrite using BIOX®. In this stage, we focussed on varying three experimental parameters (pH, temperature and iron concentration) in batch tests to examine if further optimisation using BIOX® was achievable.

2.0 MATERIALS AND METHODS

2.1 Site Description

The Savage River mine is located on the Savage River 420 km from Hobart on the northwest coast of Tasmania. The operations consist of five open cut workings exploiting a group of magnetite-rich lenses irregularly distributed within a series of highly metamorphosed rocks of marble, schist and metabasic rocks (Jackson and Parbhakar-Fox, 2016). The concentrated magnetite is slurried by pipeline to Port Latta on Tasmania's northwest coast, before shipping to market. The presence of pyrite in the waste materials (i.e., tailings and waste rock) has caused AMD to emanate from the mine operations which is of direct concern to the Savage River Rehabilitation Programme (SRRP; Kent, 2013). Operations during the first 30 years of mine life caused environmental degradation to approximately 30 km of the Savage River. The most severe degradation can be observed downstream of its confluence with Main Creek, with 90% of its invertebrate biodiversity and 99% of its invertebrate abundance lost (Kent, 2013). The OTD, located approximately 3 km from the township and 1.3 km from the processing plant,

contains pyritic tailings from Centre Pit South (CPS) and Centre Pit North (Kent, 2013). During its operation from 1967 to 1982, 38 Mt of pyritic tailings were deposited. Initially they were deposited by end of pipe spilling into the southwest corner of the dam (Kent, 2013). Subsequently, tailings were sprayed as slurry from the dam wall to allow it to be raised in lifts. This deposition method has concentrated coarser, heavier and more permeable material against the dam wall (Kent, 2013). Consequently, the water table in the tailings has decreased proximal to the wall, resulting in extensive oxidation of the tailings in this area and AMD generation. Indeed these tailings remain acid forming and contribute 50% of the AMD emanating from this site (Kent, 2013). Jackson and Parbhakar-Fox (2016) defined four physical zones across the OTD (Zones 1 to 4), based on the tailings characteristics (e.g., mineralogy, grain size) and degree of saturation (Figure 1). Within these materials, at least five tailings facies were defined (A- Hardpan; B- Interbedded oxidised and fresh tailings; C- Clay dominated fresh tailings; D- Sulphide dominated fresh tailings and E- Interbedded sulphide and fresh tailings). Parbhakar-Fox et al. (2016) determined through LA-ICP-MS studies that Co appears concentrated in Facies C to E. Considering this, bioleaching of these materials was prioritised in this study.

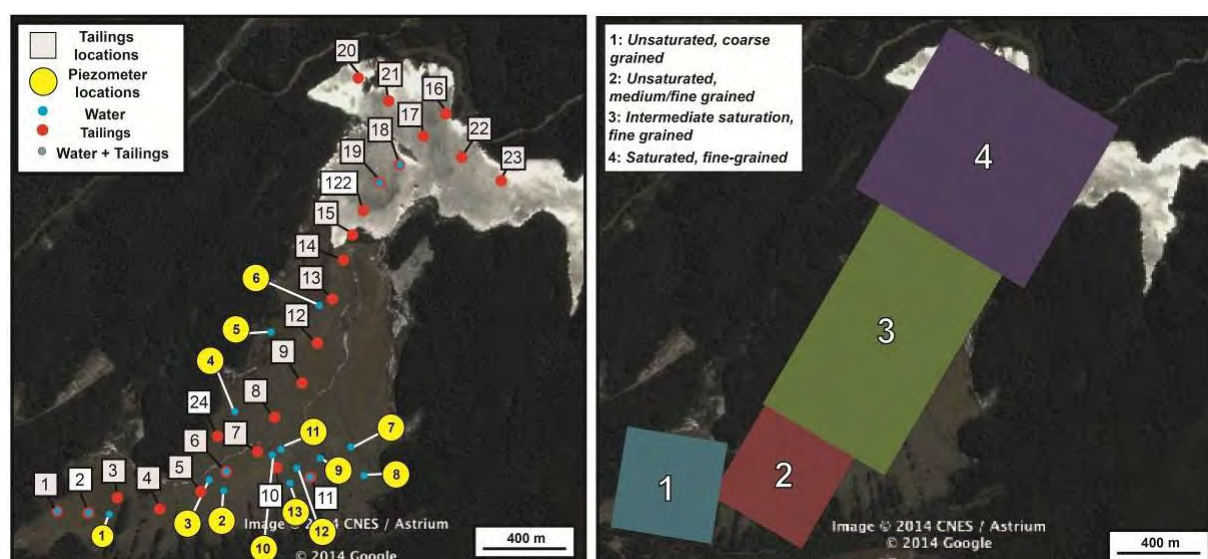


Figure 1. Aerial view of the Old Tailings Dam (OTD), Savage River mine: A) location of tailings and water samples collected in 2014; B) tailings zones delineated by degree of saturation and grain size as defined in Jackson and Parbhakar-Fox (2016). NB. Zone 4 is also referred to as the Northern Pond.

2.1.1 Sample collection and preparation

Tailings materials were collected in February 2016 (by Grange Resources personnel). Specifically, four bulk samples (between 16 and 21 kg) from Zones 1 to 4 were collected. These samples directly targeted materials from Facies C to E (i.e., from 0.5 to 1.5 m depth; Jackson and Parbhakar-Fox, 2016). To extract the materials, trenches were hand-dug with samples collected following visual confirmation of the facies. In Zone D, some challenges were posed due to the degree of tailings saturation, as this sample was collected proximal to the Northern Pond. These materials were transported to ALS-Global metallurgy laboratories in Burnie where they were dried, weighed and prepared to <math><38\ \mu\text{m}</math> (N.B. testing of as received tailings has yet to be undertaken). Material from each individual zone was stored for later experiments, with one composite sample prepared (using approximately 5 kg from of material

from each zone). This material was used in these experiments to determine the bacterial response to a lean feed material.

2.1.2 Mineralogical and geochemical characterisation

The bulk mineralogy of a head sample from each zone and a composite were measured by X-ray (XRD) using a benchtop Bruker D2 Phaser XRD instrument with a Co X-ray tube. Each milled sample was further processed using an agate pestle and mortar to 10 µm. Each sample was analysed for an hour (operating conditions: 30 kV, 10 mA, 0.6 mm (0.3°) fixed divergence slit, 2.5° Soller slit, Fe-filter; scan range: 5 to 120° (2θ), step size: 0.02°). Mineral phases were identified using the Bruker DIFFRAC.EVA software package with the PDF-2 (2012 release) powder diffraction file mineral database. Mineral abundances were semi-quantified by Rietveld analysis using TOPAS (Version 4.2) pattern analysis software. The bulk geochemistry of these materials was determined by assay at ALS Global, Perth (Method Code: MEICP-02) with C (%), Corg (%), S (%), S²⁻ (%), Fe (%), Cu (ppm), As (ppm), Mo (ppm) Ag (ppm), Zn (ppm) Ni (ppm) and Pb (ppm) measured.

2.2 Bioleaching: Experimental Setup

The commercially available BIOX[®] was selected for use in this research. Fundamentally it is a biohydrometallurgical process for the pre-cyanidation treatment of refractory gold ores with demonstrated applications given in Broadhurst (2004), Van Aswegen et al. (2007) and Van Hille et al.(2015). The BIOX[®] process uses a mixture of naturally occurring bacterial population comprising *Acidithiobacillus ferrooxidans*, *Acidithiobacillus thiooxidans* (oxidises sulphur compounds only) and *Leptospirillum ferrooxidans* (oxidises iron substrates only). These chemolithotrophic bacteria can oxidise a range of sulphides (e.g., pyrite, arsenopyrite, pyrrhotite, chalcopyrite, chalcocite, covellite, stibnite, pentlandite and galena) under controlled conditions. Comparative abiotic experiments have yet to be conducted.

Experimental work was conducted at the ALS-Global metallurgy laboratory. In these experiments three parameters, namely pH, temperature and iron concentration, were modified to test the rate of pyrite oxidation response (thereby indicating the amount of Co deporting to the resulting pregnant liquor). Experiments focused on varying: i) pH- with four conditions tested (1.3 to 1.4, 1.5 to 1.6, 1.7 to 1.8 and 2.0 to 2.1); ii) temperature (35°C, 40°C, 45°C); and iii) iron concentration in the nutrient medium (4K, 9K, 12K and 16K). Prior to these experiments, a bacterial adaption experiment was performed, whereby approximately 750 g of the composite tailings sample was weighed out and added to 4000 ml of a 9K nutrient medium (comprising 150 ml of salt A ((NH₄)₂SO₄ + K₂HPO₄ + KCl), 30 ml of salt B (MgSO₄.7H₂O), 150 ml of salt C (CaNO₃) and 150 g FeSO₄.7H₂O). Following its stabilisation, 400 ml of the ALS stock inoculum was added with a pulp density of 16.12%. Both adaption and these optimisation experiments were monitored at least once daily with measurements of pH, redox and dissolved oxygen collected. In addition, the free acid and ferrous iron concentration were measured by titration methods at least every second day. Approximately 60 ml of the slurry was collected from each experiment at least every other day (starting at 0) for up to 19 days. These slurries were pressure filtered with the liquor assayed (ALS Global, Perth, Method Code: MEICP-02 For Co and Fe-AA20a) and the solid dried and analysed again as per the head composite sample (Method Code: MEICP-02, ALS Global, Perth).

3.0 RESULTS

3.1 OTD Composite Characteristics

The composite mineralogy is dominated by magnesiohornblende and chlorite, with only 7 wt. % pyrite indicating that this feed material is relatively lean in comparison to sulphide concentrate materials typically used in bacterial oxidation experiments (e.g., 70 wt. % pyrite; d'Hughes et al., 1997). No additional mineralogical sources of cobalt are present, and reactions between the bacteria and non-sulphide phases were not anticipated. Based on the sample mineralogy, the composite is considered acid forming, as carbonate minerals are absent, with a calculated net acid producing potential of 214 kg H₂SO₄/t. Therefore, if passively managed, this material will continue to pose a geoenvironmental risk. Material collected from all zones were cobalt bearing (Table 1) with a maximum measured in Zone 2 (580 ppm) However, the bulk Co is notably lower (by two orders of magnitude) in the head grade than for individual pyrite grains (Parbhakar-Fox et al., 2016). Nickel was also noted as high (up to 3 wt. %) in individual pyrite grains (Parbhakar-Fox et al., 2016), with concentrations similar to Co in these head samples (Table 1). Arsenic and precious metals (Au, Ag) were below instrument detection limit.

Table 1. Chemical composition Zones 1 to 4 head samples and the composite.

	C	C _{org}	S	S ²⁻	Fe	Cu	Co	As	Mo	Ag	Zn	Ni	Pb
	%	%	%	%	%	ppm	ppm	ppm	ppm	ppm	ppm	ppm	ppm
Zone 1	<0.03	<0.03	0.72	0.56	9.38	98	60	<10	<5	<2	32	75.0	15
Zone 2	0.06	<0.03	15.9	14.2	18.1	2120	580	<10	<5	<2	88	595	25
Zone 3	0.03	<0.03	10.6	9.54	14.1	1480	440	<10	<5	<2	102	375	30
Zone 4	<0.03	<0.03	9.54	8.62	13.6	1640	380	<10	<5	<2	76	305	35
Composite	0.06	<0.03	9.16	8.22	14.0	1400	360	<10	<5	<2	74	325	30

3.2 PH Modification

In these experiments, the temperature was maintained at 40°C with a 9K nutrient medium used. Direct calculations of sulphide oxidation were performed for the modified pH experiments and showed that the feed material contained partially oxidised sulphide material at the start (Figure 2a). Oxidised material has likely originated from Facies C, where oxidation is likely to occur as the ephemeral water table interacts with these sediments (particularly in Zone 3). Bacterial assisted oxidation appeared most effective at lower pH conditions as near total oxidation was calculated, whilst only 88% and 76% was calculated for pH 1.7 to 1.8 and pH 2.0 to 2.1 experiments respectively at Day 19 (Figure 2a). Measurements of Co in the resulting liquor showed pH 1.5 to 1.6 as the most efficient pH condition. However, by Day 10, a similar quantity of Co was measured from the pH 1.3 to 1.4 experiment. These results show the BIOX® consortia do not behave efficiently under higher pH conditions, with the percentage of leached cobalt decreasing with increasing alkalinity (Figure 2b).

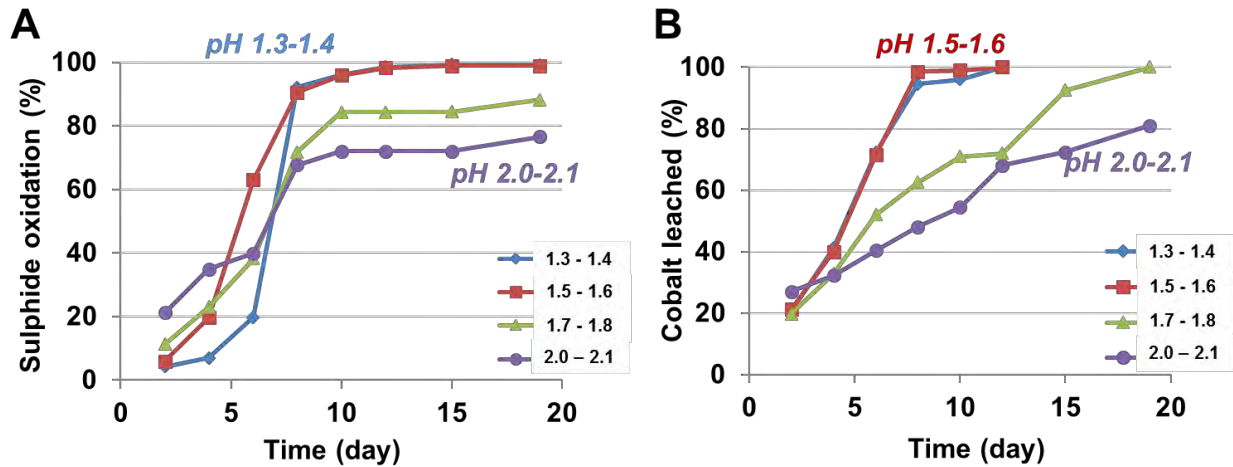


Figure 2. Calculated percentage of a) sulphide oxidation and b) cobalt in leachate for pH-modified experiments.

3.3 Temperature Variation

The BIOX® consortia behave most efficiently at 40°C, but to test if catalysis could be accelerated at a higher temperature, or alternatively a cooler temperature could be used to save on energy costs (associated with heating), two variation experiments were established at 35°C and 45°C. The pH was maintained at 1.5 to 1.6, and a 9K nutrient medium was used. Sulphide oxidation occurred most efficiently at 40°C but up until Day 7 oxidation was broadly similar in the three experiments, with approximately 58% having occurred (Figure 3a). After this time, a slight acceleration in oxidation rate occurred at the higher temperature up to Day 8 after which the rate decreased until Day 15, when it plateaued having achieved 98% oxidation. In contrast, oxidation progress dropped from Day 8 onwards at the cooler temperature with a near-cessation of activity from Day 10 onwards, with only 86% oxidation achieved by Day 19 (Figure 3a). Under the standard temperature, the oxidation rate remained reasonably consistent for the duration of the experiment with 100% oxidation achieved by Day 12 (Figure 3a). The percentage of leached Co was higher under higher temperatures, with > 95% released from pyrite by Day 10 (Figure 3b).

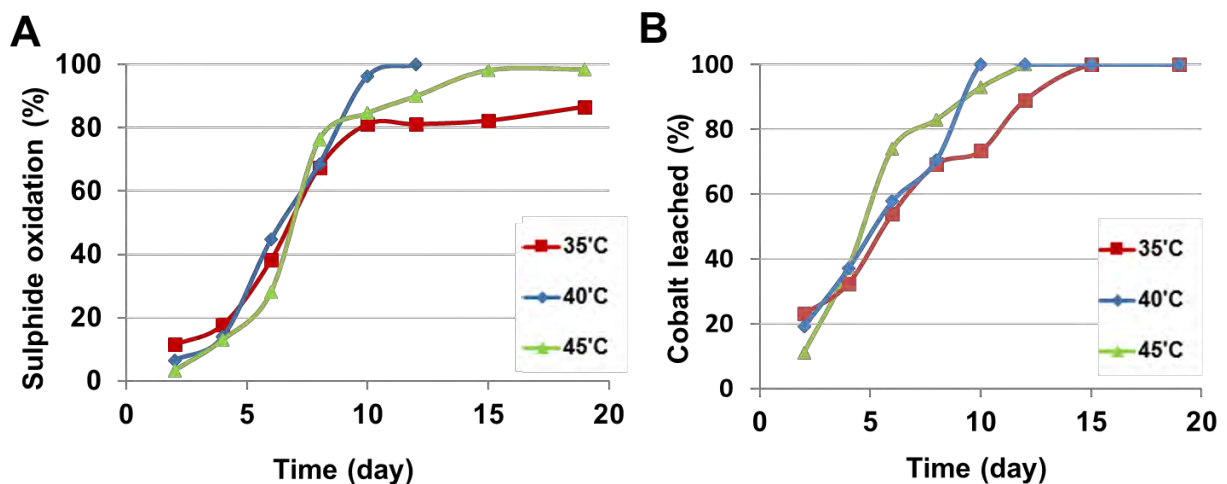


Figure 3. Calculated percentage of a) sulphide oxidation and b) cobalt in leachate for temperature variation experiments.

3.4 Nutrient Medium Amendment

The BIOX consortia[®] require sustenance to maintain activity with the provision of Fe in the nutrient medium vital to generate ferric iron in solution by which pyrite is oxidised and Co leached. To test the sensitivity of these bacteria to changing Fe conditions, three experiments were established using 4K, 12K and 16K media (containing 66.6 g, 200 g and 266.6 g FeSO₄·7H₂O stock solutions respectively; Figure 4a). The least amount of sulphide oxidation variation was observed between these experiments than the previous two batches. Oxidation was most efficient when using a 16K medium with 98% achieved by Day 10. However, the efficiency of the 4K medium was noteworthy, with similar levels achieved by Day 12 and at a greater rate than the 12K medium (Figure 4a). These results show that the Fe concentration used in the nutrient medium itself is less important than ensuring the BIOX[®] consortia are well adapted, as the 9K medium used at the time of adaption (performed 6 weeks prior to these optimisation experiments) shows a much slower rate of oxidation (Figure 4a), impacting the efficiency of leached cobalt. Both 4K and 16K media reported similar cobalt leach rates with >97% in solution by Day 8.

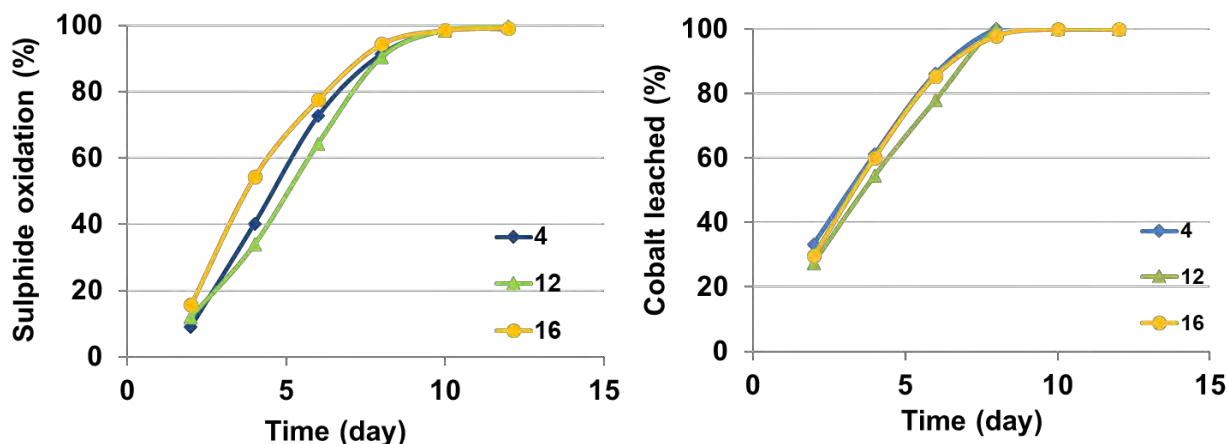
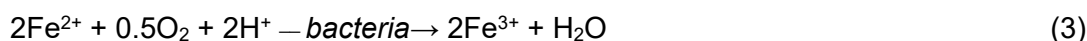
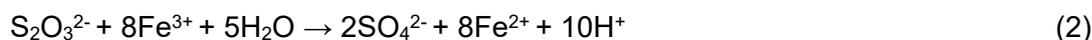
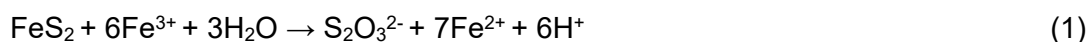
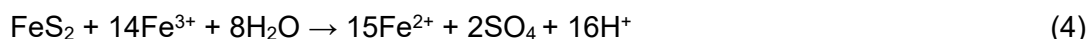


Figure 4. Calculated percentage of a) sulphide oxidation and b) cobalt in leachate for iron amendment in nutrient medium experiments.

4.0 DISCUSSION

The optimisation testwork shows the dissolution rate of cobalt is proportional to the decomposition of pyrite, thus using BIOX[®] under these varied experimental conditions should enable Co recovery even when using a lean tailings feed material such as the OTD composite. Geochemical measurements of ferrous ion content and free acid confirm that mineral dissolution is proceeding via the thiosulphate mechanism (Rawlings, 2005). Essentially, solubilisation is through ferric iron attack on pyrite with thiosulphate produced as an intermediate, and sulphate the main end-product (eqs. 1 and 2). The ferrous iron produced is oxidised to ferric iron by the bacteria (eq. 3), which efficiently oxidises pyrite (eq. 4).





Our results suggest that the optimum conditions for sulphide oxidation and release of refractory Co to the liquor are low pH 1.3-1.6; 40°C; with the Fe-contents in the medium being of lesser importance if the bacteria are well adapted to the feed material (providing these other chemical conditions are maintained). Several of these findings complement those reported by Morin et al. (1993) who examined an ore containing 40.3% Fe and 1.4% Co using bacteria obtained by the Bureau de Recherches Géologiques et Minières (BRGM) comprising *Thiobacillus ferrooxidans*, *Thiobacillus thiooxidans*, with *Leptospirillum*-like bacteria also identified. Specifically, they evaluated the effect of cobalt concentration, pH, temperature, solid content, particle size, and dissolved iron contents. Cobalt concentration (range tested: 3-15 g.L⁻¹) had no reported effect, with pH conditions between pH 1.1 and 2.0 most suitable for biooxidation. Below this pH, bacterial growth is inhibited; however, as pyrite biooxidation progresses, pH conditions below 1 may be occasionally experienced, which can have negative repercussions on Co release. This highlights that regular monitoring (e.g., at least once every 24 hrs) of the geochemical conditions is critical; however, our experiments demonstrated that addition of limestone to bring up the pH can adversely affect sulphide oxidation rate. Morin et al. (1993) reported temperature to have no significant effect upon cobalt solubilisation between 30 and 37°C, with biooxidation inhibited at 40°C. Our findings show this is not the case for the BIOX[®] consortium that demonstrated oxidation activity up to Day 10 at 45°C, after which it slowed, suggesting that their ability to degrade the sulphide substrate may not be sustainable over time. In experiments conducted by Morin et al. (1993), the rate of oxidation increased with solid contents until 10%, with the kinetics of biooxidation decreasing above this regardless of the particle size (with < 20 µm preferred). In our experiments, a 17% solid content was used, therefore, to increase Co-leaching efficiency; a lower quantity could be used in the next experimental stage. Morin et al. (1993) reported that ferric iron concentrations between 9 to 35 g.L⁻¹ slow Co release, and can reduce the final recovery by 10%, with lower concentrations yielding better results. Our results contradict this, as the measured dissolved iron concentrations were within this range for all except for the high pH experiment (2.0 to 2.1) which yielded less Co. This is likely due to *Leptospirillum*, which has the ability to tolerate ferric iron, being a formal part of the BIOX[®] consortium, whereas in the BRGM consortium it is conveyed as a secondary component.

Following on, d'Hughes et al. (1997) examined how additional variables, including agitation rate and nutrient medium, affect Co release and used BGRM inoculum. Stirred tank reactors were constructed with the tested material containing 70% pyrite (with a head grade of 1.25% Co). They established that excessive turbulence and high agitation rates (i.e., tip speed: 2.6 m.s⁻¹ radial flow turbine; 3.8 m.s⁻¹ axial flow impeller) affect bacterial productivity by reducing bacterial contact with the solid substrate. In these experiments, an agitation speed of 800 to 900 rpm was used, and therefore should be reduced in the next stage of testing to accelerate sulphide oxidation. They also reported ammonium as more effective than urea as the nitrogen source in the nutrient medium; ammonium was used in these experiments. Further experimental design optimisation could focus on increasing the amount of dissolved oxygen passing into each reactor, as d'Hughes et al. (1997) suggest that pyrite oxidation requires 0.89 kg of O₂ per kg of pyrite oxidised. In their study, 80% of Co was extracted in 4-5 days showing that further experimental design modifications are required, as in our study, similar quantities were not achieved at Day 4 (Table 2). Indeed, this may be influenced by our use of a lean tailings feed rather than the use of a sulphide concentrate. Despite the use of tailings, these data show that tailings processing can minimise (i.e., flotation can be cut out), and that Co can be leached in about 12 days under all conditions, except at high pH, simply at the expense of time. Based on this study, the optimal experimental conditions to use are pH 1.3 to 1.6, 40°C and a 4K or 9K medium after a long period (6-8 weeks) of bacterial adaption has been allowed.

Table 2. Percentage of Co leached per experiment after 4 days and at the experiment end (*9K Medium; 40°C or pH 1.6 used unless otherwise stated).

Variable	Experiment*	Co (%) leached at 4 days	Final Co (%) leached
pH	1.3-1.4	39	100 (Day 12)
	1.5-1.6	39	100 (Day 12)
	1.7-1.8	32	100 (Day 19)
	2.0-2.1	32	81 (Day 19)
Temperature	35°C	32	100 (Day 15)
	40°C	36	100 (Day 10)
	45°C	36	100 (Day 12)
Nutrient medium	4K	60	100 (Day 9)
	9K	37	100 (Day 12)
	12K	54	100 (Day 9)
	16K	60	100 (Day 10)

This test work has been undertaken to support the business case for extracting Co from these tailings as part of an integrated desulphurisation rehabilitation program. If we assume that 7% pyrite is contained in 38 Mt of tailings, then there exists approximately 2.66 Mt of pyrite, for which we have assumed an average grade of 0.1% Co, amounting to 2,660 t of Co. The price of Co on the London Metals Exchange for a cash seller is US \$60,000 per tonne (<https://www.lme.com/Metals/Minor-metals/Cobalt>). If we assume 90% Co recovery after bioleaching, then the contained value is approximately US \$143 million. Whilst this does not take into CAPEX and OPEX costs, it demonstrates that, in theory, if these materials were reprocessed using the most efficient biooxidation experimental parameters, the opportunity for this venture to self-fund rehabilitation exists, with the new benign tailings to be deposited into a better designed storage facility. Whilst this remains at the conceptual stage, delineation of the Co resource (following JORC codes and practices relevant to tailings projects) should be pursued in parallel to our next stage of experimental work using sulphide concentrates. Additionally, recovery of Ni and Cu should be explored, as their concentrations were also high in the bulk sample head grades.

5.0 CONCLUSIONS

At the Savage River mine, Western Tasmania, The historic OTD contains 38 Mt of reactive pyritic tailings that are actively generating AMD. Due to the geotechnical constraints of the OTD, extending the natural water cover (nor indeed, establishing any cover) across the repository to prevent the ingress of oxygen (i.e., to retard sulphide oxidation rate) is not economically feasible. Using laser ablation ICP-MS, a potential cobalt resource was inferred with up to 3 wt. % contained in pyrite. As this is refractory, biohydrometallurgical mineral processing has been considered to recover Co. Four bulk samples from across the OTD were collected and used to make a tailings composite which containing 7 wt. % pyrite. This was used in adaption experiments to test whether BIOX® could oxidise such a lean tailings material. Our study focussed on determining optimum conditions (pH, temperature and iron concentration in the nutrient medium) for efficient sulphide oxidation and Co leaching. In all experiments, 100% Co was leached, with the best performance at low pH and warm (40°C) temperatures, with the content of Fe in the nutrient medium of lesser importance. We determined that oxidation was impeded at higher pH (2.0 to 2.1) conditions. The study also highlighted the importance of ensuring significant time is allowed for bacterial adaption to occur prior to beginning bioleaching test work. Our next investigations will evaluate whether cobalt recovery can be optimised to achieve similar concentrations in much less time (i.e., < 5 days) using a tailings concentrate (produced via flotation) and optimising agitation speed and the

dissolved oxygen flow rate. Following this, Co precipitation testing will be performed to finally determine how much is recoverable from these tailings. At the OTD, a formal definition of the potential resource (i.e., JORC code) is required. This, along with the metallurgical test work performed in these experiments, will inform the business case for reprocessing tailings at this site. If commissioned, it represents probably the most effective rehabilitation option to reduce AMD from this site, as the source will be retreated, and the new benign tailings can then be managed by today's environmental practices.

6.0 ACKNOWLEDGMENTS

Funding for this research project was provided by the University of Tasmania through the Research Enhancement Grant Scheme. Tony Ferguson and Dale Whish-Wilson are thanked for collecting the samples from the OTD. ALS Burnie staff are thanked for sample preparation and assisting with project organisation. Dr. Nathan Fox is thanked for performing XRD analyses on these materials.

7.0 REFERENCES

Azhari, A.E., Rhouijait, A., Laarabi, E.H.M. 2016. Assessment of heavy metals and arsenic contamination in the sediments of the Moulouya River and the Hassan II Dam downstream of the abandoned mine Zeïda (High Moulouya, Morocco). *Journal of African Sciences*, In Press, doi:10.1016/j.jafrearsci.2016.04.011

Broadhurst, J.L. 2004. Neutralisation of arsenic bearing BIOX[®] liquors. *Minerals Engineering*, 7: 1029-1038.

Buzatu, A., Dill, H.G., Buzgar, N., Damian, G., Maftai, A.E., Apopei, A.I. 2016 Efflorescent sulfates from Baia Sprie mining area (Romania) — Acid mine drainage and climatological approach. *Science of the Total Environment*, 542: 629-641.

d'Hughes, P., Cezac, P., Cabral, T., Battaglia, F., Troung-Meyer, X.M., Morin, D. 1997. Bioleaching of a cobaltiferous pyrite: A continuous laboratory scale study at high solids concentration. *Minerals Engineering*, 10: 507-527.

EU directive <http://ec.europa.eu/environment/waste/mining/legis.htm>

Gurung, S. 2001. *Tasmanian Acid Drainage Reconnaissance – Vol. 1: Acid Drainage From Abandoned Mines in Tasmania (Record 2001/05, Tasmanian Geological Survey, Mineral Resources Tasmania, Dept. of Infrastructure, Energy and Resources and Natural Heritage Trust: Hobart, TAS).*

Harris, T.M., Hottle, T.A., Soratana, K., Klane, J., Landis, A. 2016. Life cycle assessment of sunflower cultivation on abandoned mine land for biodiesel production. *Journal of Cleaner Production*, 112: 182-195.

Jackson, L.M., Parbhakar-Fox, A.K. 2016. Mineralogical and geochemical characterization of the Old Tailings Dam, Australia: Evaluating the effectiveness of a water cover for long-term AMD control. *Applied Geochemistry*, 68: 64-78.

Jambor, J.L. 2003. Mine-waste mineralogy and mineralogical perspectives of acid-base accounting. In: Jambor, J.L., Blowes, D.W., Ritchie, A.I.M. (Eds.), *Environmental Aspects of Mine Wastes*. Mineralogical Association of Canada, Short Course Series, 31, 117-145.

Johnson, B.D. 2015. Biomining goes underground. *Nature Geoscience*, 8: 165-166.

Kent, S., 2013. Development proposal and environmental management plan, South deposit tailings storage facility, Grange Resources (Tasmania) Pty Ltd Savage River Mine. Caloundra Environmental Pty Ltd Report.

Leading Practice Sustainable Development in Mining, 2011. Continuing Opportunities Energy Efficiency Opportunities (EEO) Program – 2010 Report, A look at results for the Energy Efficiency Opportunities Program 2006-2010, Taken from public reports of assessments undertaken during the period July 2006-June 2010. <http://www.industry.gov.au/resource/Documents/LPSPDP/guideLPSPD.pdf>

London Metals Exchange. <https://www.lme.com/Metals/Minor-metals/Cobalt> (accessed: 23/08/2017).

Moncur, M.C, Jambor, J.L, Ptacek, C.J, Blowes, D.W and Jambor, J.L. 2015. Long-term mineralogical and geochemical evolution of sulfide mine tailings under a shallow water cover, *Applied Geochemistry*, 57: 178-193.

Morin, D., Battaglia, F., Ollivier, P. 1993. Study of the bioleaching of a cobaltiferous pyrite concentrate. *Biohydrometallurgical technologies*, Torma, A.E., Wey, J.E., Lakshmanan, V.L (eds.). The Minerals, Metals and Material Society, pp.147-156.

Neale, J.W., Pinches, A., Deeplauk, V. 2000. Mintek-Bactech's bacterial oxidation technology for refractory gold concentrates: Beaconsfield and beyond. *Journal of South African Institute of Mineralogy and Metallurgy*, 100: 415-421.

Parbhakar-Fox, A, Edraki, M., Hardie, K., Kadletz, O., Hall, T., 2014. Identification of acid rock drainage sources through mesotextural classification at abandoned mines of Croydon, Australia: Implications for the rehabilitation of waste rock repositories. *Journal of Geochemical Exploration*, 37: 11-28.

Parbhakar-Fox, A., Fox, N., Jackson, L.J. 2016. Geometallurgical evaluations of mine waste—an example from the Old Tailings Dam, Savage River, Tasmania. The 3rd AusIMM International Geometallurgy Conference, 15th-16th June, Perth, Australia.

Parvainen, A, Mäkilä, M and Loukola-Ruskeeniemi, K. 2014. Premining acid rock drainage in the Talvivaara Ni-Cu-Zn-Co deposit (Finland): Natural peat layers as a natural analog to constructed wetlands, *Journal of Geochemical Exploration*, 143: 84-95.

Quispe, D., Perez-Lopez, R., Acero, P., Ayora, C., Nieto J.M., Tucoulou, R., 2013. Formation of a hardpan in the co-disposal of fly ash and sulfide mine tailings and its influence on the generation of acid mine drainage. *Chemical Geology*, 355: 45-55.

Ramirez-Llonda, E., Trannum, H.C., Evenset, A., Levin, L.A., Andersson, M., Finne, T.E., Hilario, A., Flem, B., Christensen, G., Schanning, M., Vanreusel, A, 2015. Submarine and deepsea mine tailing placements: A review of current practices, environmental issues, natural analogs and knowledge gaps in Norway and internationally, *Marine Pollution Bulletin*, 97: 13-35.

Rawlings, D.E. 2005. Characteristics and adaptability of iron- and sulfur-oxidizing microorganisms used for the recovery of metals from minerals and their concentrates. *Microbial Cell Factories*, 4, doi: 10.1186/1475-2859-4-13.

Salomon, W., Eagle, A.M. 1990. Hydrology, sedimentology and the fate and distribution of copper in mine-related discharges in the Fly River system, Papua New Guinea. *Science of the Total Environment*, 97: 315-334.

Sracek, O., Choquette, M., Gelinac, P., Lefebvre, R., Nicholson, R.V, 2004. Geochemical characterisation of acid mine drainage from a waste rock pile, Mine Doyon, Quebec, Canada. *Journal of Contaminant Hydrology*, 69:45–71.

Tao, H., Dongwei, L. 2014. Presentation on mechanisms and applications of chalcopyrite and pyrite bioleaching in biohydrometallurgy – a presentation. *Biotechnology Reports*, 4: 107-119.

Van Aswegen, P.C., Nierkerk, J.V., Olivier, W. 2007. The BIOX™ process for the treatment of refractory gold concentrates. *Biomining*, pp.33.

Van Hille, R.P, Dawson, E., Edward, C., Harrison, S.T.L. 2015. Effect of thiocyanate on BIOX™ organisms: Inhibition and adaptation. *Minerals Engineering* 75: 110-115.

Van Veen, E., Lottermoser, B.G., Parbhakar-Fox, A., Fox, N., Hunt, J. 2016. A new test for plant bioaccessibility in sulphidic wastes and soils: A case study from the Wheal Maid historic tailings repository in Cornwall, UK. *Science of the Total Environment*, In Press, <http://dx.doi.org/10.1016/j.scitotenv.2016.01.054>

Watling, H.R. 2015. Review of biohydrometallurgical metals extraction from polymetallic mineral resources. *Minerals* 5: 1-60.

INTEGRATED LEACHING/BIOLEACHING AND SULPHATE REDUCING PROCESSES FOR METAL RECOVERY AND TREATMENT OF MINE TAILINGS

D. Villa Gomez^A, H. Hofmann^B, A. Kerr^B, B. Ryan^B, M. Peces^A and G. Southam^B

^ASchool of Civil Engineering, The University of Queensland, QLD 4072, Australia

^BSchool of Earth and Environmental Sciences, The University of Queensland, QLD 4072, Australia

Short title: Leaching/bioleaching and sulphate reducing processes for metal recovery in tailings

ABSTRACT

This study evaluated an integrated process of leaching/bioleaching and biological sulphate reduction for the recovery of metals from mine tailings. The bioleaching process involved shaker flask and column systems to simulate in-situ conditions releasing acid and metals in the tailing. Sulphate reduction occurred in a bioreactor column operated at 30°C with ethanol as substrate. The main released elements were S>Zn>Mn>Ca>Mg, while Al, Ag, Cd, Pb and Fe only occurred with chemical leaching. The solubilisation of Zn was the highest at 14.8, 10.6 and 6.5 mg/g tailing on the three experiments as compared to the other metals. The results showed that having a better control on flow paths and dispersion of leachate would result in higher metal recoveries. The bioreactor could sustain the direct leachate feeding due to the stable sulphide generation (82.1-179 ppm) that allowed up to 99% precipitation of the main metals (Cu, Pb, Fe and Zn) as sulphides (verified by SEM-EDS analysis). The alkalinity generated by SRB increased the effluent pH from 2.5 to 6.8 thus leaving a neutral residue. These results put a step forward on applying bioprocess that can treat and recover metals from tailings in a more efficient and sustainable way.

1.0 INTRODUCTION

Expanding urbanisation and the growth of industrial prosperity have led to a strong increase in demand for commodities provided by the mining sector and metal processing industries (Pokhrel and Dubey 2013). Therefore, lower grade and polymetallic ores are exploited, thus increasing the volume of fine-grained tailings wastes produced (Mudd 2007). The presence of metals from high to low value in mine tailings account for up to 90% of the ore (Nagaraj 2007). This can lead to environmental problems such as acid mine drainage. Thus, treating tailings is of paramount importance in protecting the environment and if metals can be recovered, they can have the potential to return economic value.

Metals in tailings are typically released through a leaching process with acid solutions (Crundwell et al. 2011) or through microbial-assisted process called "bioleaching". Because of the advantages of low cost and environment friendliness, bioleaching has been widely used in the mining industry for metals extraction from low-grade ores solutions (Crundwell et al. 2011). In this process, bacteria from the genus *Acidithiobacillus* is capable of oxidizing the reduced sulfur (elemental sulfur or sulfur compounds) to sulfuric acid, thus creating acidic conditions favourable for metal solubilisation (Cao et al. 2009, Ferroni 2012). The effectiveness of bioleaching is highly dependent on physical, chemical and biological conditions such as the nature of contaminated material, solids concentration, oxygen, pH, bacterial strain and cell concentration (Liu et al. 2007).

Once the metals are released from tailings, several methods (chemical precipitation, membrane separation, solvent extraction and electrodeposition) can be employed for further removal of metals (Fu and Wang 2011); however, the high cost of reagents and the fact that recovery is not always possible constitute major obstacles to their application. Biological sulphate reduction is an established biotechnological process for the treatment of inorganic wastewaters containing oxidized sulphur compounds and metals (Kaksonen and Puhakka 2007). The metal-containing streams and electron donors are fed into a reactor containing sulphate-reducing bacteria (SRB). In this bioreactor, sulphate is reduced and the dissolved metals precipitate with the biologically produced sulphide. This process has been actively used for treatment of surface and groundwater contaminated with acid mine drainage (Paques 2016). Until now, however, only limited information on the use of this technique for metal recovery from tailings leachate is reported. Leachate metal concentrations coming from tailings can be very dynamic, even from a single mine, as it largely depends on the type of ore deposit and technologies used to extract and concentrate the target minerals (Shaw, Petavratzi and Bloodworth 2013). Thus, the sulphate-reducing process should be able to cope with these changes without being prone to failure.

This work shows the results of bioleaching experiments on Pb–Zn–Cu mine tailings. In parallel, it also shows the results of a sulphate-reducing bioreactor treating the leachate produced from the same tailings to assess the feasibility of an integrated process of leaching/bioleaching and biological sulphate reduction for the recovery of metals from mine tailings.

2.0 MATERIALS AND METHODS

2.1 Tailings

Samples of tailings from Century Mine in north-west Queensland were used in this study, one of the largest Australia's open cut zinc mine before its closure in August 2015. The sedimentary exhalative Pb-Zn-Ag deposit possessed average grades of approximately 10.2% Zn, 1.5% Pb and 36 g/t Ag. Mineralization comprises fine-grained sphalerite with minor galena and pyrite (Broadbent, Myers and Wright 1998). Scanning Electron Microscopy-Energy Dispersive Spectroscopy (SEM-EDS) showed abundant fine-grained and sub- μm -scale material, with silica and quartz phases, pyrite, jarosite, and sphalerite (data not shown).

2.2 Leaching/Bioleaching experiments

2.2.1 Inoculum and media

Iron-oxidising bacteria (*Acidithiobacillus ferrooxidans*) and sulphur-oxidising bacteria (*Acidithiobacillus thiooxidans*) at populations measured by most probable number (5×10^7 per mL) were used in the bioleaching experiments. Bacterial growth was supported using medium containing: 0.1 g KCl, 0.5 g K_2HPO_4 , 0.5 g $\text{MgSO}_4 \cdot 7\text{H}_2\text{O}$, 3.0 g $(\text{NH}_4)_2\text{SO}_4$ in 1 L of distilled water. The pH of the culture medium was adjusted to pH 2.3 with H_2SO_4 , filtered (0.45 μm) and transferred into a 1 L glass bottle for storage until use in the column and shaker flask bioleaching experiments.

2.2.2 Bioleaching process

The bioleaching process involved shaker flask and column systems to simulate in-situ conditions releasing acid and metals in the tailing. The shaker flasks were set up in triplicate by adding 10 g tailings into three 250 mL Erlenmeyer flasks. These flasks contained 96 mL of medium and 2 ml of sulphur-oxidising bacteria and 2 mL of iron-oxidising bacteria. The flasks

were shaken at 150 rpm and incubated for 3 months. Samples of the liquid phase were taken once a week for analysis. The column system was set using 60 cc syringes positioned upright and filled with 10 cc of glass wool at the base, followed by 50 g of tailings. Each contained 20 mL of medium as well as 2 g of iron-oxidising bacteria and 2 g of sulphur-oxidising bacteria. The resulting leachate was recirculated twice the first week and then collected every week, for a total of 12 weeks.

2.2.3 Chemical leaching

Chemical leaching was done by adding 2.5 g of the Century Mine tailings to 250mL of 15% hydrogen peroxide (H_2O_2). After one hour, the whole solution was boiled for two minutes to remove any excess of peroxide that would be toxic to the sulphate reduction process. The solution was then centrifuged for five minutes at 4500 rpm and then decanted.

2.3 Bioreactor Set-up and Operation

An up-flow anaerobic sludge blanket (UASB) bioreactor (1.4 L) with internal recirculation (up-flow velocity of 1.3 m/h) was operated at 30°C with ethanol as substrate. The bioreactor was inoculated with 10 g of volatile solids (VS)/L of anaerobic granular sludge treating brewery wastewater (XXXX Brewery in Milton, Queensland). A stock feed solution for the bioreactor consisted of ethanol, sodium sulphate ($NaSO_4$), and a basal medium consisting of micro- and macro-nutrients (Angelidaki, Ellegaard and Ahring 1999). The bioreactor operation was divided in three periods: enrichment (days 1-80), metals addition (days 81-108), and leachate addition (days 109-172). The hydraulic retention time (HRT) from day 0 to day 9 was 8 days and from day 10 onwards was maintained at 4 days. The organic loading rate (OLR) was 0.5 g chemical oxygen demand (COD)/L·d and a COD/ SO_4^{2-} ratio of 0.67 gCOD/g SO_4^{2-} . The reactor was fed twice a day and operated at a flow rate of 87.5mL/min (175 mL/feeding event). Stock feed and effluent were pumped and drained simultaneously.

A concentrated metal stock solution was prepared using $ZnSO_4 \cdot 7H_2O$, $FeSO_4 \cdot 7H_2O$, $CuSO_4 \cdot 5H_2O$ and $PbSO_4$ in distilled water at the following concentrations: 152 mg Zn/L, 56 mg Fe/L, 3 mg Cu/L, 2 mg Pb/L. Ascorbic acid (2mM) was added to avoid metal oxidation. For the leachate addition period, chemical leachate was prepared as explained in Section 2.2.3. During metals addition and leachate addition periods, the stock feed consisted on two separate reservoirs to avoid metal precipitation or oxidation prior being added to the bioreactor.

2.4 Analysis

COD was measured using Merck COD Spectroquant® test kits. Sulphide was measured using the colorimetric method set by Cord-Ruwisch (Cord-Ruwisch 1985). Sulphate was measured using a Thermo Fisher Dionex ICS-1100 Ion Chromatograph (IC). Metals were measured with an Inductively Coupled Plasma Optical Emission Spectrophotometer (ICP-OES) Perkin Elmer Optima 7300DV after filtering and digesting the samples with nitric acid. Volatile fatty acids (VFA) (acetate, propionate, butyrate, valerate, and caproate) and alcohols (methanol, ethanol, and butanol) were analysed with an Agilent 7890A gas chromatograph equipped with an Agilent DB-FFAP column. SEM-EDS was used to generate images of the biomass used in the bioreactor as well as of the metals precipitated. Samples were processed at the Centre for Microscopy and Microanalysis at the University of Queensland on a Hitachi TM3030 SEM.

3.0 RESULTS AND DISCUSSION

3.1 Metal Solubilisation during Bioleaching

Figure 1 shows the metals released from the tailings through bioleaching and chemical leaching. Column leaching results are shown after 12 weeks of bioleaching, although the release of metals have not yet stopped the experiment did due to liquid depletion that could interfere on the reliability of the results. Shaker flask results are shown after 16 weeks of bioleaching, which was the time when the release of metals ceased. On the three experiments the main released elements were S>Zn>Mn>Ca>Mg, while Al, Ag, Cd, Pb and Fe release was not evident, except for Fe (5.6 mg/g tailing) during the chemical leachate experiment. It can be observed that chemical leachate was the most effective method for the release of metals. The solubilisation of Zn was the highest at 14.8, 10.6 and 6.5 mg/g tailing on the three experiments as compared to the other metals. The solubilisation of Fe and Pb was only observable in the chemical leaching experiment probably due to the pH-dependent solubility of the metal forms (Lewis 2010).

Sulphur concentration was similar in both bioleaching experiments, which is in accordance to the pH values and thus sulphuric acid generation due to bacterial activity (Cao et al. 2009, Ferroni 2012). Although barely noticeable, the pH was slightly higher in the column experiments probably due to a higher amount of solids concentration in the experiment, that provide alkalinity and thus buffering capacity (Liu et al. 2007).

By comparison between the two bioleaching experiments, it is observed a higher efficiency in the shaker flask experiments, which could be related to a better mass transfer (Liu et al. 2007). In agreement, it was also observed, that in the column experiments, there were preferential flow paths that led unreacted tail material in the experiments. This suggest that having a better control on flow paths and dispersion of leachate would result in higher metal recoveries.

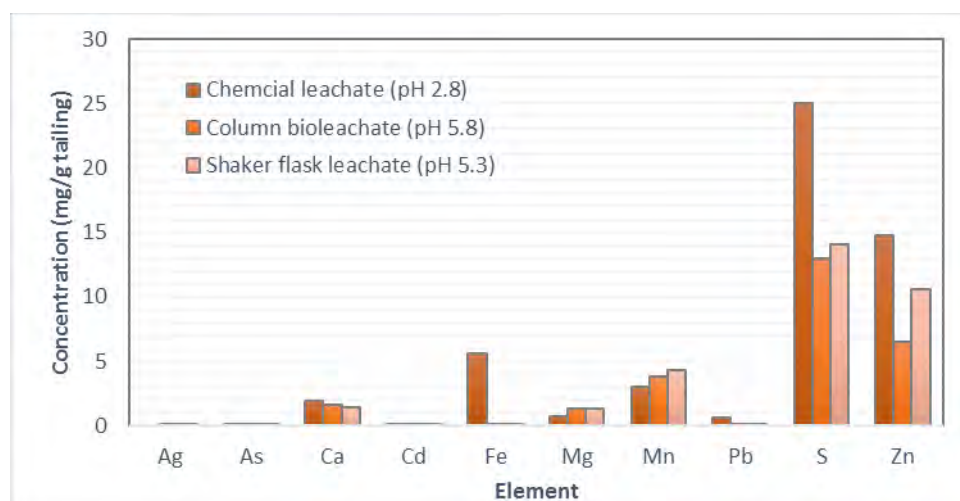


Fig. 1. Metals and sulphur concentrations released at the end of the chemical leaching, column bioleaching and shaker flask leaching experiments.

3.2 Sulphate Reduction Process

Table 1 summarizes the overall bioreactor performance during 172 days of operation. Enrichment period was characterised by low COD and sulphate removal efficiencies (32.6 and 59.5%, respectively) and high acetate concentration (1168.9 mg/L) as compared to the following periods. After reaching a constant effluent concentration, metals were added, giving rise to an increase in COD removal (54.7%) that resulted also in a decrease in acetate (674.2

mg/L). Such trend continued after leachate addition along with an increase in sulphate removal of up to 88%.

Table 1. Treatment efficiency during operation of the bioreactor for sulphate reduction and metal precipitation (mean \pm 1 standard deviation).

Experimental periods	Enrichment period	Metals addition	Leachate addition
Days	1-80	81-108	109-172
COD removal efficiency (%)	32.6 \pm 6.3	54.7 \pm 4.0	90.7 \pm 3.5
SO ₄ ²⁻ removal efficiency (%)	59.5 \pm 2.7	53.1 \pm 1.8	88.0 \pm 8.2
Acetate concentration (g COD/L)	1168.9 \pm 79.4	674.2 \pm 44.1	269.9 \pm 99.9
Sulphide concentration (mg/L)	179.0 \pm 19.4	94.7 \pm 26.9	82.1 \pm 18.0
Influent/Effluent pH	7.0/6.2 \pm 0.0	4.2/6.7 \pm 0.2	2.5/6.6 \pm 0.2
Influent/Effluent Zn (mg/L)	NA	152/91.22	196.89/99.48
Influent/Effluent Fe (mg/L)	NA	56/91.74	122.21/99.68
Influent/Effluent Cu (mg/L)	NA	3/65.94	0.80/99.29
Influent/Effluent Pb (mg/L)	NA	2/93.4	5.07/99.55

NA: Not applicable

The pH was increased from 4.2 and 2.5 in the metals addition and leachate addition periods, respectively, to 6.7. This increase was likely caused by the CO₂ produced by the SRB (Costa and Duarte 2005) as well as the consumption of acetate (Table 1). The increase in sulphate reduction efficiencies observed after metals and leachate addition was attributed to a decrease in sulphide concentration due to its precipitation with metals, hampering sulphide inhibition (Villa-Gomez et al. 2011).

Metal removal rates averaged 91.2% for Zn, 91.7% for Fe, 65.9% for Cu, and 93.4% for Pb. These values are comparable to the high removal rates of metals in other studies treating synthetic effluents (Dvorak et al. 1992) as well as acid mine drainage (Villa-Gomez and Lens 2017). SEM-EDS images in the solids (biomass and metal precipitates) within the bioreactor revealed the presence of rod-shaped bacteria, consistent with the cellular morphology of members of the genera *Bacillus* and *Vibrio*. It also showed the presence of agglomerates odd to the SRB biomass. EDS analysis allowed to confirm that these agglomerates were precipitates that contained Fe, Cu, Zn and S. This imply that metal sulphides might be the major precipitation form. Contrary to other studies (Utgikar et al. 2002), metal precipitates within the bioreactor did not appeared to affect SRB activity, by observing the parameters monitored (Table 1).

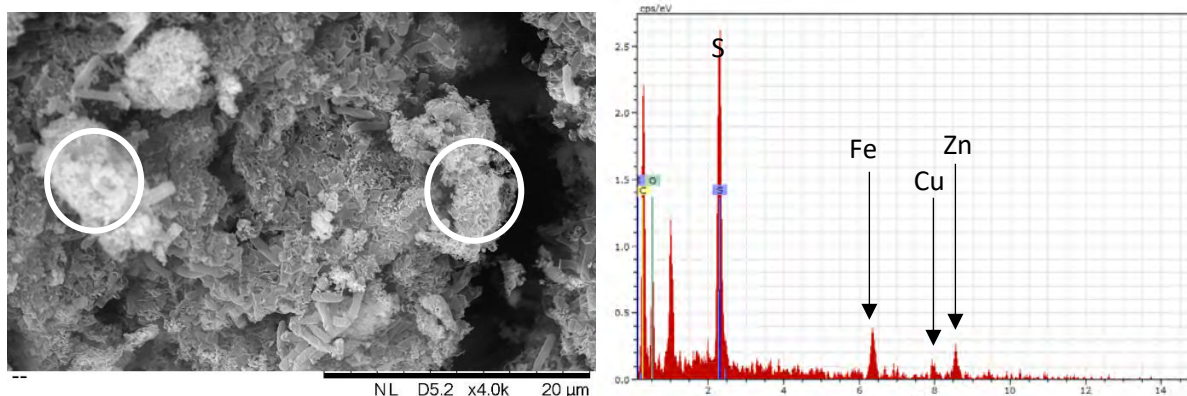


Figure 3. SEM-EDS image X4000 zoom of sludge after metals addition. White circles indicate possible metal sulphide precipitates.

4.0 CONCLUSIONS

This work shows that bioleaching can be used to treat and recover metals from Pb-Zn-Cu mine tailings, thus avoiding their release under uncontrolled conditions as acid mine drainage. The main released elements were S>Zn>Mn>Ca>Mg, while Al, Ag, Cd, Pb and Fe only occurred with chemical leaching. This work also assessed the feasibility of an integrated process of leaching/bioleaching and biological sulphate reduction for the recovery of metals from mine tailings. The operational conditions in the sulphate reducing bioreactor allowed precipitating the metals from the chemical leachate and increasing the pH of the leachate from 2.5 to 6.8 thus leaving a neutral residue.

5.0 REFERENCES

- Angelidaki, I, L Ellegaard and BK Ahring (1999) A comprehensive model of anaerobic bioconversion of complex substrates to biogas. *Biotechnology and Bioengineering*, 63, 363-372.
- Broadbent, GC, RE Myers and JV Wright (1998) Geology and origin of shale-hosted Zn-Pb-Ag mineralization at the Century Deposit, Northwest Queensland, Australia. *Economic Geology*, 93, 1264-1294.
- Cao, J, G Zhang, Z Mao, Z Fang and C Yang (2009) Precipitation of valuable metals from bioleaching solution by biogenic sulfides. *Minerals Engineering*, 22, 289-295.
- Cord-Ruwisch, R (1985) A quick method for the determination of dissolved and precipitated sulfides in cultures of sulfate-reducing bacteria. *Journal of Microbiological Methods*, 4, 33-36.
- Costa, M and J Duarte (2005) Bioremediation of acid mine drainage using acidic soil and organic wastes for promoting sulphate-reducing bacteria activity on a column reactor. *Water, air, and soil pollution*, 165, 325-345.
- Crundwell, F, M Moats, V Ramachandran, T Robinson and WG Davenport. 2011. *Extractive Metallurgy of Nickel, Cobalt and Platinum Group Metals*. Burlington: Burlington : Elsevier Science.
- Dvorak, DH, RS Hedin, HM Edenborn and PE McIntire (1992) Treatment of metal-contaminated water using bacterial sulfate reduction: Results from pilot-scale reactors. *Biotechnology and bioengineering*, 40, 609-616.

Ferroni, LGLaGD. 2012. *Bioleaching*. Hoboken, NJ, USA: Hoboken, NJ, USA: John Wiley & Sons, Inc.

Fu, FandQ Wang (2011) Removal of heavy metal ions from wastewaters: A review. *Journal of Environmental Management*, 92, 407-418.

Kaksonen, AHandJA Puhakka (2007) Sulfate Reduction Based Bioprocesses for the Treatment of Acid Mine Drainage and the Recovery of Metals. *Engineering in Life Sciences*, 7, 541-564.

Lewis, AE (2010) Review of metal sulphide precipitation. *Hydrometallurgy*, 104, 222-234.

Liu, Y-G, M Zhou, G-M Zeng, X Li, W-H XuandT Fan (2007) Effect of solids concentration on removal of heavy metals from mine tailings via bioleaching. *Journal of Hazardous Materials*, 141, 202-208.

Mudd, GM (2007) Global trends in gold mining: Towards quantifying environmental and resource sustainability. *Resources Policy*, 32, 42-56.

Nagaraj, DR. 2007. Minerals Recovery and Processing. 595-595. Kirk-Othmer Encyclopedia of Chemical Technology, Wiley-VCH

Paques, bv. 2016. Paques, Leading in biological wastewater and gas treatment.

Pokhrel, LRandB Dubey (2013) Global Scenarios of Metal Mining, Environmental Repercussions, Public Policies, and Sustainability: A Review. *Critical Reviews in Environmental Science and Technology*, 43, 2352-2388.

Shaw, RA, E PetavratziandAJ Bloodworth (2013) Resource Recovery from Mine Waste. 44-65.

Utgikar, VP, SM Harmon, N Chaudhary, HH Tabak, R GovindandJR Haines (2002) Inhibition of sulfate-reducing bacteria by metal sulfide formation in bioremediation of acid mine drainage. *Environmental Toxicology*, 17, 40-48.

Villa-Gomez, D, H Ababneh, S Papirio, DPL RousseauandPNL Lens (2011) Effect of sulfide concentration on the location of the metal precipitates in inversed fluidized bed reactors. *Journal of Hazardous Materials*, 192, 200-207.

Villa-Gomez, DKandPNL Lens. 2017. Metal recovery from industrial and mining wastewaters using sulphate-reducing bioreactors. . In *Sustainable Heavy Metal Remediation: Volume 2: Case studies*, eds. E. R. Rene, E. Sahinkaya, A. Lewis & P. Lens. Cham, Switzerland: Springer International Publishing.

GAS FLUX RATES AND THE LINKAGE WITH PREDICTING AMD LOADS IN WASTE ROCK DUMPS, AND DESIGNING PRACTICAL ENGINEERED SOLUTIONS – FIELD BASED CASE STUDIES

S. Pearce^A, M. Barteaux^B and J. Pearce^A

^AO’Kane Consultants, 3A Vale Street Denbigh Wales LL163AD, UK

^BO’Kane Consultants, Fredericton NB, Canada

^BO’Kane Consultants, Unit 1, 11 Collingwood Street Perth, WA 6017, Australia

ABSTRACT

Oxygen flux into waste rock dumps (WRDs) and the various strategies to reduce the processes are conceptually well understood as processes, as well as the ubiquitous roll oxygen plays in the development of acid and metalliferous drainage (AMD). As such, industry best practice is generally considered to include the construction of engineered landforms with an aim to reduce oxygen flux rates (and thus AMD risk). However as volumes of research data indicate, the ability to practically manage gas flux (if at all) is a highly site specific factor, for which reliable performance-based engineering design and validation methods are yet to be proven.

O’Kane Consultants (OKC) has had the opportunity to complete detailed assessments of gas flux rates as part of large scale WRD investigations and AMD management engineering design projects at sites in two distinct climates that includes a semi-arid environment Western Australia, and at a Tropical Rainforest Environment in Indonesia. Within these sites, detailed instrumentation has been installed in waste rock storage facilities including oxygen probes, temperature sensors, matric potential sensors, volumetric water content sensors, and vibrating wire piezometers.

The extensive data set that OKC has collected as part of the numerous field programs has allowed the improvement of oxygen flux conceptual models by utilising multiple lines of evidence to calculate oxygen ingress rates, which has allowed for the progress of numerical simulations of landform performance, and also the improvement of scaling up lab-based studies to the field. The following paper presents data from the two distinct climates that demonstrate the approaches to oxygen flux controls at each site.

1.0 INTRODUCTION - GAS FLUX IN WRD

In the field, AMD risks are known to be complex and interrelated and are strongly related to the structure of the waste and how this influences oxygen ingress and water flow into the waste pile, where subsequent oxidation reactions can occur. The influence of airflow, water infiltration and flow, and the site-specific diurnal or seasonal variations in these are likely to be key risk drivers. Geochemistry forms only one of these risk factors; however it is interesting to note that typical industry approach to AMD assessments is for the study to be based for the most part on laboratory testing related to geochemical properties only. While these geochemistry-based assessments are robust, they are essentially just methods to classify and categorize materials based on the results of tests carried out in laboratory conditions. The use of laboratory kinetic leach column data for example, although considered to be the gold standard to estimate field estimates of sulfide

oxidation rates and seepage quality, requires careful consideration when extrapolating to field conditions. This is because scaling factors will considerably impact the validity of the results (Pearce et al 2015).

A simple summary of these observations is to state that, although the characterisation of materials is important, the method and timing of placement, and the site environment in which they are placed, are perhaps more important variables, and are often disregarded. In this regard it is therefore important to recognise that independent of any geochemical assessment that may be carried out (in particular those based on wet chemistry methods), that site-specific factors that directly influence the dynamic process of gas/water flux are given due consideration. These factors include material characteristics (physical, geochemical and geotechnical), waste rock dump geometry and climate.

Material is generally placed in WRDs in an unsaturated state and will over time move to an equilibrium state that is semi or fully saturated condition. During this process, the flux of water and gas through the pore spaces will occur at rates that vary on a relative basis over time depending for the most part on climate and material properties. It is this relative nature of the flux rates that is the key concept that requires to be understood to explain the significant differences in seepage quality outcomes that can result from placement of the same material in a different manner or in a different climate.

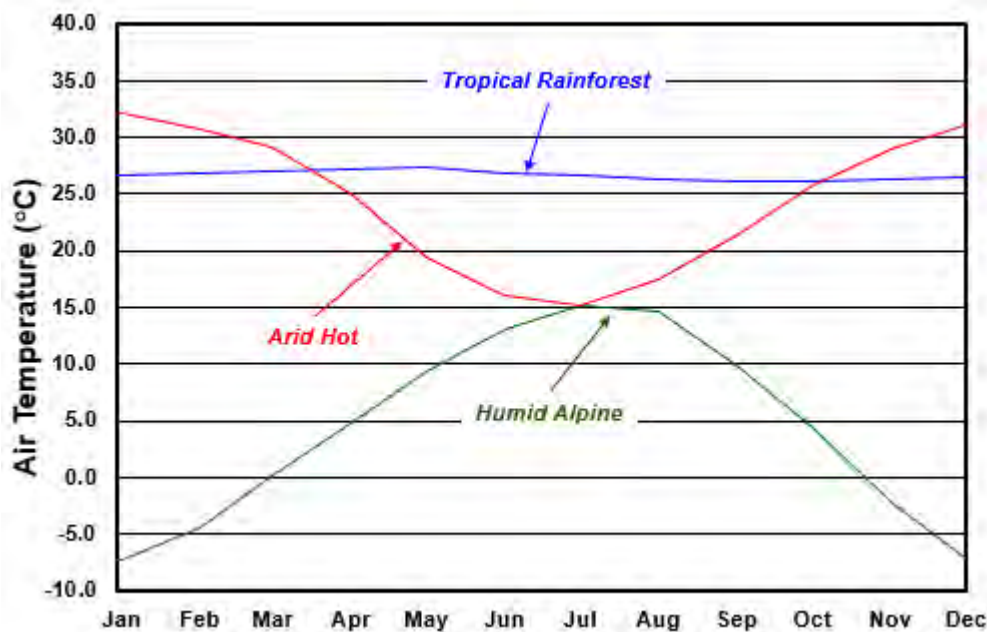


Fig. 1. Average daily temperature in different climate zones

Convective transport of oxygen into waste rock is the dominant mechanism supplying oxygen to oxidation sites, and air convection driven by temperature gradients and partial pressure differentials are much more effective at transporting oxygen than diffusion processes in WRDs (Brown et al., 2014). Figure 1 shows average daily temperatures for three distinct climate zones. Given temperature gradients are known to be a key factor driving convective gas flux, it should be clear that climate has a direct link to oxygen flux rate into WRDs. Because WRDs have a high

thermal mass, internal temperatures are generally constant around the annual average daily air temperature. The magnitude of the temperature gradient driving air convection therefore depends on the differential temperature with the surrounding air mass. For a given mass of waste with the same physical properties, gas flux rates can therefore be expected to be lower in tropical environments than semi-arid or humid alpine environments by virtue of the fact the temperature differential is lower.

Work by Wilson (2011) and Pearce (2014) shows that, for end-tipped waste, oxygen ingress will primarily occur at the bottom of the pile, with gas flux being into the toe and basal rubble zone of the waste pile moving upwards through the free draining course material layers by the process of thermal advection. Vapour flux also occurs along with gas flux and is an important aspect of the overall redistribution of water within the waste, and moisture loss from waste masses. This process is termed advective drying and is described by Pearce (2014). Air flow rates calculated by OKC based on site data indicate that, where coarse basal zones are present, air flux rates through waste mass of around $1-2 \times 10^{-4} \text{ m}^3/\text{m}^2\text{s}$ can be expected. Based on typical sulfide oxidation rates, the oxygen flux that derived from gas flux of this magnitude is sufficient to allow oxidation to occur at unconstrained rates (Pearce et al 2015). Advective airflow rates through the waste are the primary control on oxidation rates for sulfides.

The following paper reviews two case studies located in two different climate zones, and provides monitoring data to support the conceptual model of oxygen flux in those regions, and how this relates as a key modifier to AMD risk. Specifically, the climate zones include (Peel 2007):

- tropical rainforest– Northern Sumatra, Indonesia;
- arid hot desert – Pilbara, Australia.

2.0 TROPICAL RAINFOREST CLIMATE CASE STUDY

The Tropical Rainforest site reviewed in this paper is characterized by high rainfall with an annual average of approximately 4,426 mm based on a 35 year climate database. Daily rain events are common, usually occurring in the afternoon, and temperatures are hot and humid. As part of AMD mitigation, the site mining teams have employed a progressive waste rock management strategy which aims to mitigate the AMD risks of a WRD by selectively placing finer-grained material at the outer edge of the waste facility as construction progresses. The encapsulation method is a viable option for AMD risk management at this site due to the presence of sufficient volumes of low risk (respect to AMD) material that has suitable texture (i.e. finer grain size fractions), and high rainfall. These contributing factors mean that there is greater probability for the material to remain tension-saturated, thereby reducing the airflow capacity into the waste mass. In addition, because of the high rainfall volumes, it was understood that net percolation was going to be challenging to manage in the long term, therefore an approach to manage oxygen ingress was determined to be the optimal strategy in AMD management (Pearce and Barteaux 2017).

Specialised instrumentation has been installed by OKC through 2014 - 2017 to monitor the performance of the WRD. Specifically, the performance of the fine-grained encapsulation layers has been assessed against engineering design objectives such as: decrease of oxygen ingress to acceptable levels and limiting AMD. Instrumentation utilised to date includes oxygen sensors, volumetric water content / electrical conductivity sensors, matric potential and pore-water pressure (Pearce 2014).

Figure 2 presents suction data from monitoring of the outer 2m of the waste profile. At shallow depths, wetting and drying cycles are observed; however below a depth of 1m, suction levels remain very low indicating high levels of saturation are maintained. Figure 3 presents temperature data through the waste profile reflected as a temperature differential (internal waste temperature minus ambient air temperature). The internal temperature profile results in a very low relative differential temperature values between internal and ambient conditions of up to approximately 2°C difference). These conditions result in very low temperature gradients to prevent advective airflow.

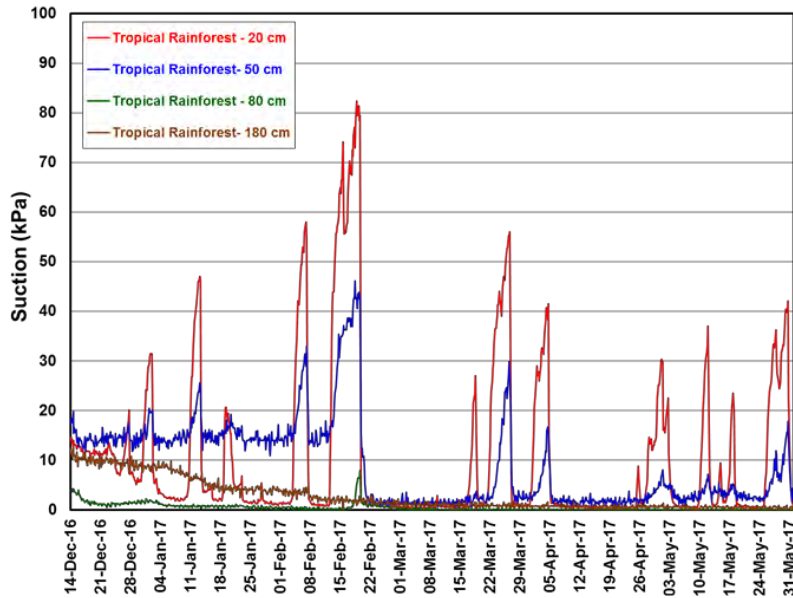


Fig. 2. Saturation condition at the tropical rainforest case study

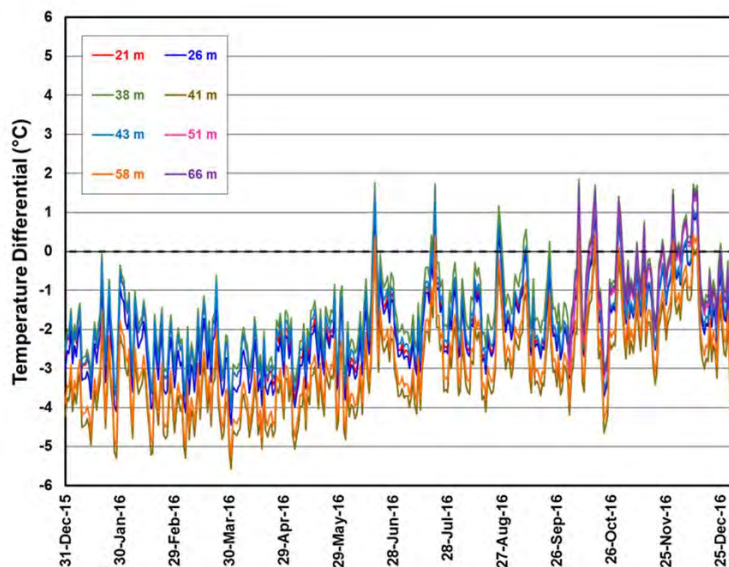


Fig. 3. Temperature differential at the tropical rainforest case study

Data from Figure 2 and Figure 3 indicate that the material placement method and climatic setting effectively reduces the risk of advective gas flux being a significant contributor to oxygen ingress. Based on the temperature data, there is little to no evidence of exothermic activity within the waste which would be present if significant sulfide oxidation were occurring. This provides strong evidence that limited advective or convective air flow forcing air into or out of the landform. The low levels of gas flux can be attributed to the high moisture retention characteristics of the encapsulation material which results in low air permeability functions for the waste material. The volumetric water content and suction state data collected from the site show that the encapsulation layer has a high degree of saturation and very low suction, supporting this interpretation.

3.0 ARID HOT DESERT CLIMATE

Based on the Köppen-Geiger system (Peel 2007), this study site is classified as an arid hot desert (BWh), and is located in the Pilbara, Western Australia (WA). Almost 75% of the rainfall occurs during summer (October to March, inclusive), and the site experiences hot to very hot summers (with atmospheric temperatures up to 50°C) and warm to cool winters (near zero degrees). The long-term annual average rainfall for the area as quoted by the Australian Bureau of Meteorology is 320 mm. The WRD's studied at the site are constructed with high tip heads (40 m), which has resulted in significant material segregation as a result of gravity sorting. As a result of the material sorting, the development of coarse rubble zones at the base of the tip heads has resulted, acting as potential pathways for air entry into the landform (Pearce 2014). OKC had the opportunity to complete the installation of over 150 instruments in various waste rock dump landforms in this area during 2013-2015. Instruments were installed using the sonic drilling technique and include galvanic oxygen probes, soil matric potential sensors, temperature sensors, and vibrating wire piezometers (Pearce and Barteaux 2017).

Figure 4 presents suction data from instrumentation installed at shallow depths within the WRD profile. When compared to the suction data from the tropical site (Figure 2), it is clear that the material has significantly lower levels of moisture retention over time, as suction values are generally greater than 1,000 kPa. After a large rainfall event in July, suction levels fall to within the range of those noted at the tropical site (Figure 2) of <50 kPa; however these low suction levels are maintained for a matter of weeks.

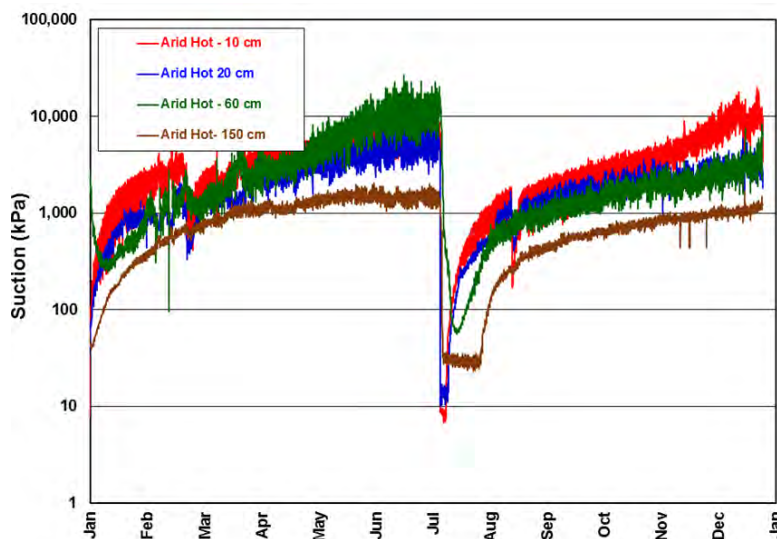


Fig. 4. Saturation condition at the arid hot desert case study

Figure 5 shows temperature data from instrumentation placed within the WRD waste profile, and also calculated gas flux rates based on the temperature differential data, material properties and saturation data. The middle of the waste profile is noted to have elevated temperatures up to 60 degrees centigrade that cannot be accounted for by climate alone and relates to exothermic production of heat from sulfide oxidation. The calculated gas flux rates are significant as a result of this heating and are positive all year round. Because temperature differentials are lower in the summer as a result of high ambient temperatures, gas flux rates are lower during this period indicating that winter periods result in higher gas flux and likely AMD production rates. A seasonal component to AMD production is inferred from this data.

An important observation made from the monitoring data from other locations in the hot arid environment sites was even WRD's, that are constructed from inert materials, experience significant seasonal temperature gradients, meaning that high levels of gas flux will occur irrespective of the presence of internal heating caused by exothermic reactions. This is a key difference from the tropical environment, where seasonal temperature gradients are lower, and internal heating is required to generate significant temperature gradients.

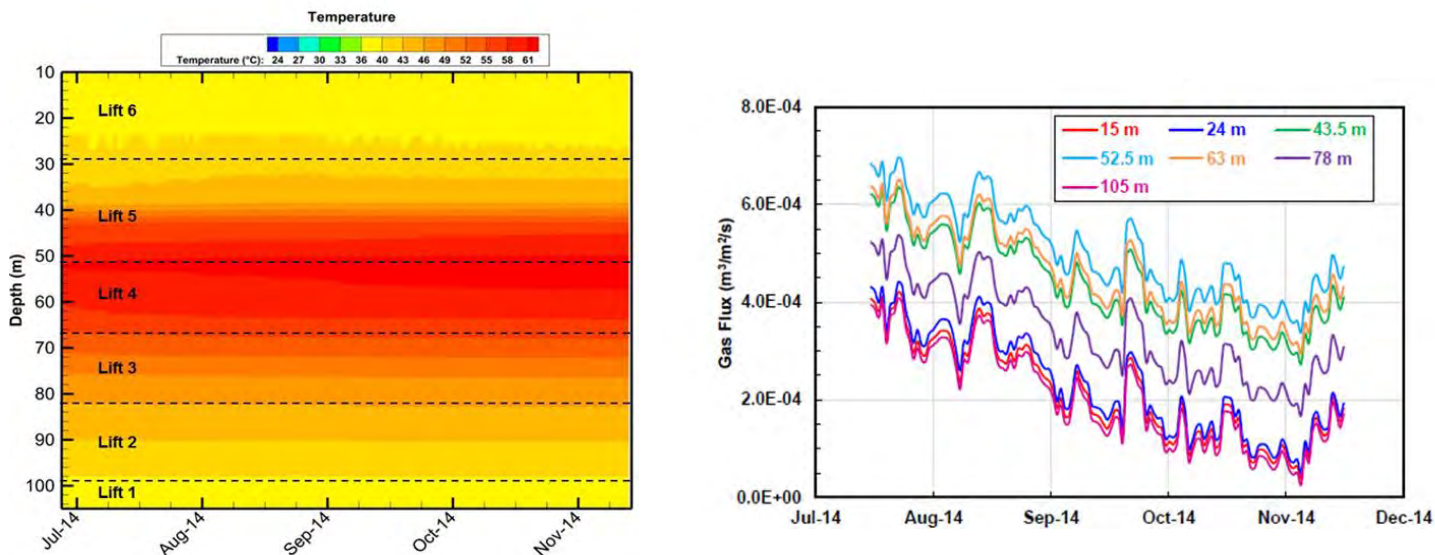


Fig. 5. Temperature profile and gas flux rates at the arid hot desert case study

4.0 DISCUSSION

Based on the data presented, it is clear that, because of the direct link to gas flux rates, climate itself is a significant driver of AMD risk and therefore requires consideration when making assessments regarding AMD load predictions and management techniques. In general:

- Tropical climates have lower and less variable seasonal temperature differentials meaning temperature-driven advection is less prominent than other climates, and so AMD production rates are likely to be lower for a given material type;
- Arid hot environments have a high maximum temperature gradient potential with respect to ambient. A very strong seasonal component with respect to temperature differential is

noted, and even daily differentials are significant. AMD production rates are likely to be significant in these environments as a result;

- Tropical environments have high rainfall levels which makes creation of simple tension saturated “advection barriers” feasible using even using non-engineered run of mine material that has been subject to minimal treatment;
- Semi-arid environments have low rainfall levels which makes creation of tension saturated advective barriers more challenging and would require the use of significantly more engineered materials (and may preclude the use of run of mine materials);
- AMD risk is to a large extent independent of geochemical properties, when gas flux is taken as primary risk driver;
- AMD management measures need to be based on climate and materials as much as, if not more than, geochemistry; and
- What works in one climate may not work in another.

With respect to engineering controls, it has been demonstrated that strategies implemented in tropical climates, which utilize engineering controls that employ finer textured material within outer embankment cover layers to promote tension saturated conditions, can be extremely successful in limiting oxygen flux rates and thus AMD generation. In addition the low temperature gradients in tropical environments imply that, even if high saturation levels cannot be maintained, gas flux rates may be significantly lower than for the same material placed in a hot arid environment. For climates such as a hot arid desert which lacks the sufficient rainfall to allow development of tension saturated layers, and high inherent gas flux rates due to temperature gradients, this would not be a viable option. For areas such as this, it is clear that the key focus should be on waste placement technique, such as limiting the amount of segregation during placement, compaction of waste in low lifts, or the use of advective barriers (such as toe bunds and compacted internal covers), which cut off the inflow of air through coarse rubble zones. These techniques can provide additional risk reduction by reducing the potential flux of air when high temperature gradients exist.

AMD load models, built on a conceptual model formed from the field data gathered, indicate that, in hot arid environments, stored acidity loads are likely be generated at relatively high rates based on elevated oxygen flux rates. Over the short term timeframe (<20 years), significant pore water flushing and vertical drainage through the waste (and production of seepages) are not likely to occur, and so AMD will be stored as semi-volatile acid salts within pore spaces. Once “wetting up” conditions are reached and seepages begin, AMD loads are likely to be significant as the dissolution of the stored products will be at low liquid: solid ratios, and concentrations will be close to solubility constraints for key metals and sulfate. It is notable that it is common for the lack of AMD seepages from waste dumps in semi-arid environments to be used as proof that AMD risks are limited. However the implications of the work presented in this study extend to a significant reappraisal of the potential AMD risks of reactive waste rock stored in semi-arid environments, and further to the effectiveness of engineered controls that rely on maintaining saturation in the outer layers of the waste mass like cover systems as a “panacea” to manage AMD risks in these environments.

5.0 REFERENCES

Australian Bureau of Meteorology (2017) www.bom.gov.au

Ayres BK, Lanteigne L, O’Kane MA, Meiers G (2012) Whistle mine backfill pit dry cover case study – performance based on six years of field monitoring data. In ‘Proceedings of the 9th International Conference of Acid Rock Drainage (ICARD)’, Ottawa Ontario, Canada 2012. May20-26.

Harries J (1997) Acid mine drainage in Australia: Its extent and potential future liability, Supervising Scientist Report 125, Supervising Scientist, Canberra, 94 p.

Lu N (2001) An analytical assessment on the impact of covers on the onset of air convection in mine wastes. Numerical and Analytical Methods in Geomechanics. August 1999, pp 347–364.

Morin KA, Hutt NM, Aziz ML (2010). Twenty-three years of monitoring minesite-drainage chemistry, during mining and after closure: The Equity Silver minesite, British Columbia, Canada. http://www.mdag.com/case_studies/cs35.html

Patterson RJ (1987) Environmental and reclamation measures at Equity Silver Mines Ltd. In Acid mine drainage seminar-workshop, Halifax NS, pp457-477.

Pearce SR, Barteaux M (2014) Instrumentation of waste rock dumps as part of integrated closure monitoring and assessment. In ‘Mine Closure 2014 Proceedings of the Ninth International Conference on Mine Closure’. Johannesburg, South Africa 2014. (Eds A.B. Fourie and M. Tibbett).

Pearce SR (2014) Beyond The PAF Cell. In ‘Proceedings of the Eighth Australian Workshop on Acid and Metalliferous Drainage’. Adelaide, South Australia 2014. (Eds H Miller and L Preuss), pp 97-110.

Pearce SR, Barteaux M (2017) Gas Flux Rates and the Linkage with Predicting AMD Loads in Waste Rock Dumps, and Designing Practical Engineering Solutions – Field Based Case Studies in Three Distinct Climates. In Proceedings of the 13th IMWA Annual Conference. June 2017, Lappeenranta, Finland.

Peel MC, Finlayson BL, McMahon TA (2007) Updated world map of the Koppen-Geiger climate classification. Hydrology and Earth System Sciences, **11**, 1633-1644.

O’Kane MA, Ayres B (2012) Cover systems that utilise the moisture store-and-release concept – do they work and how can we improve their design and performance?. In ‘Proceedings of Mine Closure 2012’, Brisbane, Queensland 2012. (Eds A.B. Fourie and M. Tibbett) pp 401-417. (Australian Centre for Geomatics: Brisbane).

O’Kane MA, Wilson GW, Barbour SL (1998) Instrumentation and monitoring of an engineered soil cover system for mine waste rock. Canadian Geotechnical Journal **35**, 828-846.

Wilson GW (2011), Rock dump hydrology: an overview of full-scale excavations and scale-up experiments conducted during the last two decades. In ‘Proceedings of the Seventh Australian Workshop on Acid and Metalliferous Drainage’. Darwin, Northern Territory. 2011. (Eds L.C. Bell and B. Braddock) pp307-322.

WATER QUALITY PREDICTIONS UNDER HIGHLY VARIABLE MOISTURE AND TEMPERATURE: A CASE STUDY ON THE IMPORTANCE OF THERMODYNAMICS

Y. Tian^A, R. Strand^A, G. Wang^A, J. Tuff^A and B. Usher^A

^AKlohn Crippen Berger, Level 5 – 43 Peel Street, South Brisbane, QLD 4101, Australia

ABSTRACT

In dry climates such as the Australian interior, mine waste storage facilities are beset by extreme weather conditions, resulting in low water to rock ratios. Waste reactivity can be aggravated by seasonality, producing high loads, and sufficient mobility in the wet season to significantly influence downstream receptors.

Mine planning has, in recent years, used water quality modelling to assess the risk and impact of waste management plans, however, these models were built to assess chemistry under more dilute conditions ($I < 0.5 \text{ mol/L}$) for which the Davies Debye-Hückel equation is generally appropriate.

However, for cases of low water content and/or elevated temperatures, which often arise from sulphide oxidation, correction for high ionic strengths and higher temperatures is required to produce valid predictions.

In this study, we consider a system with temperatures in the range of $60 \text{ }^\circ\text{C}$ – $100 \text{ }^\circ\text{C}$ and seasonally variable water content. A GoldSim-based water quality prediction model was built that adopts 1) temperature-dependent K_{sp} values for key minerals, 2) an extended WATEQ Debye-Hückel equation (suitable for ionic strength up to 3 mol/L), and 3) metal complexations which affect sulphate solubility. The importance of accounting for these non-ideal conditions can be shown through comparative predictions.

1.0 INTRODUCTION

In the past decade, integrated water balance and water quality prediction models have been successfully applied in the mining industry, both in Australia and internationally, to assist with life-of-mine planning and/or decision-making for mine closure to meet requirements from local government regulations (e.g. Strand et al. 2010, Strand and Usher 2014, Tuff et al. 2015, Usher et al. 2010). One of the core components of the water quality prediction model is the thermodynamic dataset. Thermodynamic properties for simulating fluid-rock interactions include (but are not limited to): solubility products (K_{sp}) of the key minerals that define solubility controls, the ionic activity model used to calculate activity coefficients of the cations/anions in aqueous solutions, and the dynamic equilibrium between free ions and complexed species in response to changing conditions (e.g., temperature, redox, fluid chemistry and flow rate).

Solubility controls using thermodynamic properties at room temperature (25°C , 298K) are only applicable within a small temperature range around 25°C . In addition, the Davies Debye-Hückel equation is generally appropriate for solutions with relatively low ionic strength ($I < 0.5 \text{ mol/L}$);

physical-chemical environments that fall outside these ranges make water quality prediction challenging. As an example, this study focuses on a relatively dry (but seasonally wetted) waste storage facility in northern Australia, where water quality prediction is hampered by seasonally variable water content and low water: rock ratios in dry seasons, and high temperatures of 60 °C – 100 °C or higher due to sulphide oxidation. These have resulted in high ionic strength and high salinity sulphate-rich solutions (e.g., $I > 2$ mol/L and sulphate $> 20,000$ mg/L). A predictive model must account for these conditions and correct activity coefficients for the high ionic strength solutions. Furthermore, in contrast to dilute systems, high salinity, sulphate-rich solutions favour formation of divalent metal sulphate complexes over speciation of metals and sulphate. A model, therefore, is required to not only predict precipitation of sulphate and metal cations but also the formation and deformation of metal complexes to simulate dynamic metal speciation.

To address the challenges of water quality prediction in such environments, this paper outlines hydrogeochemical approaches to calculate precipitation, dissolution and complexation, incorporating temperature-dependent solubility controls and activity corrections appropriate for high ionic strength condition.

2.0 MODELLING APPROACH

2.1 Conceptual Model and Framework

Typically, a waste rock storage facility can be conceptually divided into different zones. Such zones are differentiated based on the waste management plan, and serve specific functions such as housing reactive waste, shedding water, or insulation of the reactive waste. The water balance framework is an overlay on the conceptual model, and the interactions between zones are constrained by outputs from saturated/unsaturated flow models of the waste. Infiltration is the primary means of transporting dissolved mass from reactive source material into the zones of the dump that may hold water. The volume of this water fluctuates according to seasonal variations in infiltration (inflows) and seepage (outflows).

2.2 Geochemistry Overview

Following previous studies (Strand et al. 2010, Strand and Usher 2014, Tuff et al. 2015, Usher et al. 2010), the model uses the kinetic rates of reaction from laboratory and field testing of waste rock types and considers pyrite oxidation (based on conservative estimates where there is sufficient oxygen and water available) as the primary driver of acidity generation and the model utilizes thermodynamic solubility control that is likely to be the primary control on seepage water quality. Carbonate minerals provide neutralisation of acidity. The model includes theoretical fundamental reactions and responses to pH changes. The detailed structure and mechanism of a similar approach in GoldSim is provided in Strand et al 2017 as part of these proceedings.

2.3 Addressing Temperature Variation

Mineral saturation and potential geochemical interactions within the modelled temperature range have been determined based on the interpretation of site water quality data using hydrogeochemical software such as PHREEQC (Parkhurst and Appelo 2013). The key minerals from this interpretation include a series of carbonate, sulphate and oxide/hydroxide minerals, which are included in this model (Table 1). Solubility product constants (K_{sp}) as a function of temperature up to 100 °C are partially sourced from the new Pitzer database (Appelo 2015) with a few updated thermodynamic properties derived from previous experimental studies based on a modified method of molar volume calculations to better account for temperature-pressure

dependence (Appelo et al. 2014). The MINTEQA and WATEQA4F databases (Allison et al. 1991, Ball and Nordstrom 1991) provided the other sources of data for minerals which are not included in the Pitzer database.

Table 1. Solubility product constants ($\log K_{sp}$) of the key minerals used in the model over the temperature range of 25 to 100 °C.

Mineral	Formula	25 °C	40 °C	55 °C	70 °C	85 °C	100 °C
Calcite	CaCO ₃	-8.50	-8.65	-8.81	-8.98	-9.17	-9.38
Dolomite	CaMg(CO ₃) ₂	-17.00	-17.29	-17.56	-17.80	-18.02	-18.22
Rhodochrosite	MnCO ₃	-10.41	-10.48	-10.55	-10.61	-10.67	-10.72
Cerussite	PbCO ₃	-13.20	-12.99	-12.80	-12.63	-12.47	-12.33
Otavite	CdCO ₃	-13.74	-13.76	-13.78	-13.80	-13.81	-13.83
Smithsonite	ZnCO ₃	-10.00	-10.15	-10.29	-10.42	-10.54	-10.64
Siderite	FeCO ₃	-10.55	-10.74	-10.91	-11.06	-11.20	-11.33
CoCO ₃	CoCO ₃	-11.20	-11.31	-11.40	-11.49	-11.57	-11.65
Malachite	Cu ₂ (OH) ₂ CO ₃	-33.17	-32.79	-32.44	-32.11	-31.82	-31.54
Gypsum	CaSO ₄ .2H ₂ O	-4.60	-4.63	-4.68	-4.76	-4.85	-4.96
Epsomite	MgSO ₄ .7H ₂ O	-1.85	-1.75	-1.67	-1.61	-1.56	-1.52
Alunite	KAl ₃ (SO ₄) ₂ (OH) ₆	-85.33	-82.38	-79.70	-77.26	-75.01	-72.96
Anglesite	PbSO ₄	-7.79	-7.71	-7.65	-7.58	-7.53	-7.47
Barite	BaSO ₄	-9.84	-9.71	-9.61	-9.54	-9.49	-9.48
Chalcanthite	CuSO ₄ .5H ₂ O	-2.64	-2.59	-2.54	-2.50	-2.46	-2.43
Melanterite	FeSO ₄ .7H ₂ O	-2.47	-2.37	-2.28	-2.79	-2.86	-2.05
Celestite	SrSO ₄	-6.66	-6.74	-6.83	-6.93	-7.04	-7.15
Goslarite	ZnSO ₄ .7H ₂ O	-1.96	-1.84	-1.74	-1.64	-1.55	-1.47
Na_Jarosite	NaFe ₃ (SO ₄) ₂ (OH) ₆	-95.18	-93.64	-92.24	-90.97	-89.79	-88.72
K_Jarosite	KFe ₃ (SO ₄) ₂ (OH) ₆	-98.78	-97.07	-95.52	-94.10	-92.79	-91.60
Gibbsite	Al(OH) ₃	-33.22	-32.62	-32.07	-31.56	-31.11	-30.69
Brucite	Mg(OH) ₂	-10.88	-10.71	-10.55	-10.41	-10.28	-10.17
Goethite	FeO(OH)	-41.49	-40.60	-39.78	-39.03	-38.36	-37.73
Ferrihydrite	Fe(OH) ₃	-38.79	-38.23	-37.72	-37.25	-36.82	-35.76
Hematite	Fe ₂ O ₃	-87.99	-86.26	-84.69	-83.26	-81.95	-80.74
Manganite	MnO(OH)	-42.23	-40.83	-39.55	-38.38	-37.32	-36.34
Cr ₂ O ₃ (s)	Cr ₂ O ₃	-31.38	-30.88	-30.42	-29.99	-29.60	-29.24
Nantokite	CuCl	-6.76	-6.41	-6.09	-5.80	-5.53	-5.29
Fluorite	CaF ₂	-10.60	-10.45	-10.33	-10.25	-10.20	-10.16

2.4 Ionic Strength

A number of activity models have been developed to extend the applicability of activity coefficients in high ionic strength solutions (Table 2) based on ion-association theory. The WATEQ Debye-Hückel equation has been selected for this study because it is applicable at ionic strength up to 1 mol/L (Truesdell and Jones, 1974). Figure 1 compares the activity coefficients of Ca²⁺, Mg²⁺ and SO₄²⁻ calculated using the WATEQ Debye-Hückel equation with those calculated by the Davies

equation (identical for all divalent ions). This example shows that the calculated activity coefficients are in good agreement for the two equations at low ionic strength ($I < 0.3$ mol/L), but the Davies equation overestimates the activity coefficients at higher ionic strength ($I > 0.5$ mol/L). This results in the overestimation of ion activities, which has an impact on predicting dissolution, precipitation and complexation in high ionic strength solutions.

Activity coefficients calculated by the WATEQ Debye-Hückel equation are typically valid for ionic strength up to 1 mol/L (Truesdell and Jones, 1974). The Pitzer equation, based on ion-interaction theory (Pitzer 1973), could be used to estimate activity coefficients for higher ionic strengths (e.g., $I > 3$ mol/L). According to Merkel and Planer-Friedrich (2008), the activity coefficients of divalent ions (e.g., Ca^{2+} , Mg^{2+} and SO_4^{2-}) and chloride ion calculated by WATEQ Debye-Hückel equation are still in good agreement with those calculated using the Pitzer approach up to ionic strength of 3 mol/L. Since the divalent ions are the major components in the aqueous solutions in this case, the use of WATEQ Debye-Hückel equation is valid for this study.

Table 2. Summary of activity models and their applicable range of ionic strength

Activity model	Equation	Applicable range of ionic strength	Reference
Debye-Hückel equation	$\log(\gamma_i) = -A * z_i^2 * \sqrt{I}$	$I < 0.005$ mol/L	Debye and Hückel (1923)
Extended Debye-Hückel equation	$\log(\gamma_i) = \frac{-A * z_i^2 * \sqrt{I}}{1 + B * a_i * \sqrt{I}}$	$I < 0.1$ mol/L	Debye and Hückel (1923)
Davies equation	$\log(\gamma_i) = -A * z_i^2 \left(\frac{\sqrt{I}}{1 + \sqrt{I}} - 0.3 * I \right)$	$I < 0.5$ mol/L	Davies (1938)
WATEQ Debye-Hückel equation	$\log(\gamma_i) = \frac{-A * z_i^2 * \sqrt{I}}{1 + B * a_i * \sqrt{I}} + b_i * I$	$I < 1$ mol/L	Truesdell and Jones (1974)

Note: z_i is the valence of the i^{th} ion; I is stoichiometric ionic strength (pre-equilibrium); a_i & b_i are ion-specific parameters (dependent on the ion radius) from MINTEQA2 and WATEQ4F databases (Allison et al. 1991, Ball and Nordstrom 1991); and A & B are temperature-dependent parameters calculated from empirical equations (see details in Merkel and Planer-Friedrich 2008).

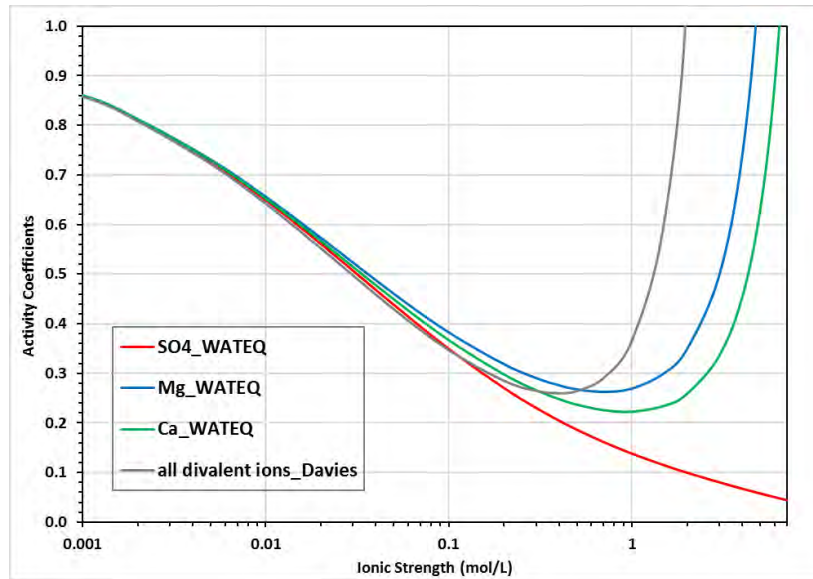


Figure 1. Comparison of activity coefficients for Ca^{2+} , Mg^{2+} and SO_4^{2-} by Davies and WATEQ Debye-Hückel equations as a function of ionic strength.

2.5 Dissolved Mass Differentiation

As a development of previous models (Strand et al. 2010 and related investigations), dissolved aqueous ions are considered to exist in two major groups: free ions and complexes. The sum of the molar mass of the two groups combined is the total concentration of the element of interest (Eqn. 1). Using the $\text{MgSO}_{4(aq)}$ complex (Eqn. 2) as an example, the mass balance (Eqn. 3) is solved for the condition of over-equilibrium (Eqn. 4) and under-equilibrium (Eqn. 5). Solving these formulas for the change (δ) in the cation, anion and complex, the molar change in the activity and concentration can be determined dynamically and non-iteratively to return the solution to (near) equilibrium. The metal complexation function works concurrently with dissolution, precipitation and sorption to maintain a dynamic (near) equilibrium between dissolved free ions, dissolved complexes, sorbed ions and precipitated minerals in every time step for each zone.

$$WQ_{tot} = WQ_{free\ ions} + WQ_{complexes} \quad [1]$$



$$K_{eq(MgSO_4)} = \frac{[\text{MgSO}_{4(aq)}]}{[\text{Mg}^{2+}][\text{SO}_4^{2-}]} \quad [3]$$

$$([\text{Mg}^{2+}] - \delta[\text{Mg}^{2+}])([\text{SO}_4^{2-}] - \delta[\text{SO}_4^{2-}])K_{eq(MgSO_4)} = ([\text{MgSO}_{4(aq)}] + \delta[\text{MgSO}_{4(aq)}]) \quad [4]$$

$$([\text{Mg}^{2+}] + \delta[\text{Mg}^{2+}])([\text{SO}_4^{2-}] + \delta[\text{SO}_4^{2-}])K_{eq(MgSO_4)} = ([\text{MgSO}_{4(aq)}] - \delta[\text{MgSO}_{4(aq)}]) \quad [5]$$

Table 3 shows the metal complexes and their equilibrium constants (K_{eq}) up to 100 °C used in the model. These species were chosen based on PHREEQC-calculated speciation and identification of the most abundant species. As the system is dominated by sulphate ions with chloride, carbonate and fluoride ions being minor or trace amount, only major complexes such as metal sulphate complexes and a few chloride complexes are considered in this paper, and minor

complexes (e.g. hydroxide and carbonate complexes < 10%) are not included for the sake of computational efficiency.

Table 3. Equilibrium constants ($\log K_{eq}$) of the key complexes used in the model over the temperature range of 25 to 100 °C.

Aqueous complex	25 °C	40 °C	55 °C	70 °C	85 °C	100 °C
AlSO ₄ ⁺	3.81	3.84	3.86	3.95	4.16	4.54
MgSO _{4(aq)}	2.26	2.31	2.35	2.39	2.43	2.46
CaSO _{4(aq)}	2.36	2.42	2.47	2.52	2.57	2.61
ZnSO _{4(aq)}	2.34	2.39	2.44	2.48	2.52	2.56
* Zn(SO ₄) ₂ ²⁻	3.28	3.28	3.28	3.28	3.28	3.28
PbSO _{4(aq)}	2.69	2.69	2.69	2.69	2.69	2.69
* Pb(SO ₄) ₂ ²⁻	3.47	3.47	3.47	3.47	3.47	3.47
CdSO _{4(aq)}	2.37	2.44	2.51	2.57	2.63	2.68
* Cd(SO ₄) ₂ ²⁻	3.50	3.50	3.50	3.50	3.50	3.50
MnSO _{4(aq)}	2.25	2.32	2.39	2.45	2.51	2.56
SrSO _{4(aq)}	2.30	2.37	2.43	2.48	2.53	2.58
NiSO _{4(aq)}	2.30	2.35	2.39	2.43	2.47	2.50
FeSO _{4(aq)}	2.39	2.46	2.52	2.57	2.62	2.67
CuSO _{4(aq)}	2.36	2.43	2.50	2.56	2.62	2.67
CoSO _{4(aq)}	2.30	2.35	2.40	2.44	2.48	2.52
NaSO ₄ ⁻	0.74	0.75	0.76	0.76	0.77	0.78
KSO ₄ ⁻	0.85	0.96	1.05	1.14	1.23	1.30
MgCl ⁺	0.60	0.63	0.66	0.69	0.72	0.74
CaCl ⁺	0.40	0.43	0.46	0.49	0.52	0.54
CuCl _(aq)	3.10	3.10	3.10	3.10	3.10	3.10
NaCl _(aq)	-0.30	-0.37	-0.43	-0.48	-0.53	-0.58
KCl _(aq)	-0.30	-0.33	-0.36	-0.39	-0.42	-0.44

Note: * indicate the complex has only room temperature equilibrium constant and there is no available deltaH value to calculate equilibrium constant at higher temperature; K_{eq} values are sourced from the new Pitzer database (Appelo 2015) as well as MINTEQA2 and WATEQ4F databases (Allison et al. 1991, Ball and Nordstrom 1991).

3.0 RESULTS AND DISCUSSION

3.1 Calibration

Monitored seepage at the toe of the waste rock dump (WRD) was used to calibrate the water quality predicted in the model (e.g. Figure 2, 3 and 4). Calibrated concentrations of Ca, Mg and sulphate are reasonably consistent with the field data over a 12-month simulation. There is also good agreement in predicted and measured seasonal variation, which is mainly caused by seasonal runoff diluting the load bearing seepage flows.

3.2 Solution Parameters and External Checks

The charge balance, effective ionic strength (post-equilibrium) and the molar percentage of complexed species to the total elemental concentration are calculated for each zone in every time step. Charge balance (the balance of cations and anions in solution) is used to assess the validity of the simulated solutions. For example, the basal seepage charge balance does not exceed 8% over a 600-month simulation, indicating that the solution remains electrically neutral during the simulation (Figure 5). PHREEQC is used to calculate the effective ionic strength and proportions

of molar complexed species as an additional check. The effective ionic strength (post-equilibrium) is generally lower than the stoichiometric ionic strength (pre-equilibrium) due to the neutral and/or low-charge species that are mostly present as complexes. The highest stoichiometric ionic strength in this model is no more than 3 mol/L, which is within the applicable range of the WATEQ Debye-Hückel equation. The effective ionic strength calculated in GoldSim, approximately 50% of the stoichiometric ionic strength, is in excellent agreement with PHREEQC calculated values (Figure 6). GoldSim calculated proportions of complexed species for major components (e.g., SO_4 , Cl, Mg, Ca, K, and Na) are in reasonably good agreement with those calculated in PHREEQC (Figure 7), as are minor components (e.g. Cd, Zn and Mn) compared at selected time intervals (Table 4). Table 4 shows some discrepancies between GoldSim and PHREEQC calculated values for Cu, Fe and Pb during the first few years of simulation. The discrepancies are largely caused by: 1) species such as carbonate and/or hydroxide complexes, that are not included in GoldSim, may become important in carbonate-rich and/or alkaline solutions; 2) PHREEQC iteratively solves the geochemical solution by minimizing numerical errors until convergence is reached, in contrast to the GoldSim model, which performs several hundred calculations in every time step to approximate WQ prediction in order to keep the solution under a dynamic equilibrium.

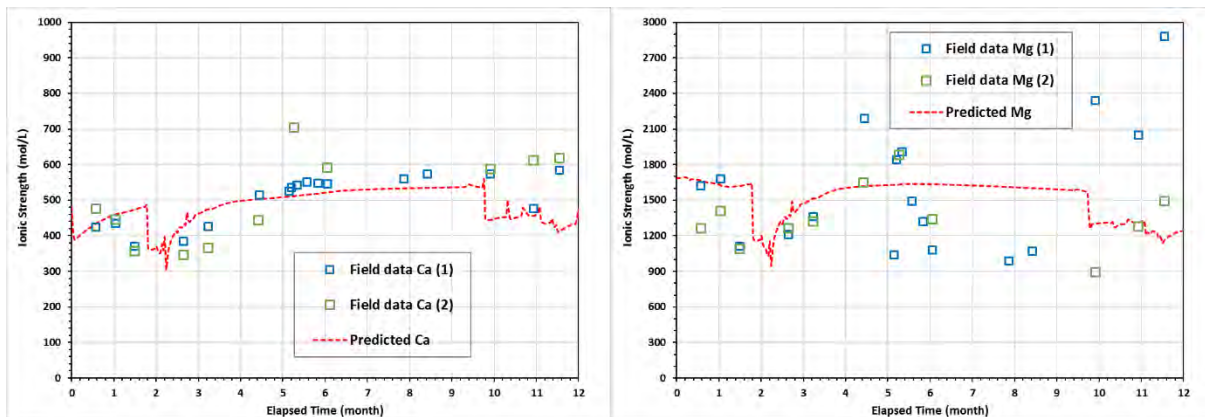
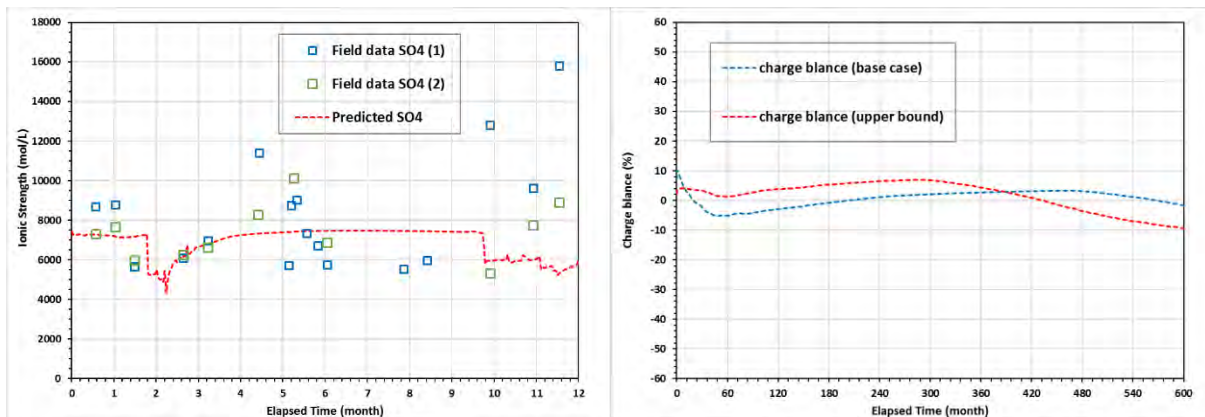


Figure 2 (left). Calcium calibration and Figure 3 (right). Magnesium calibration to two monitoring points at the toe of WRD



**Figure 4 (left). Sulphate calibration to two monitoring points at the toe of WRD
Figure 5 (right). Charge balance of modelled basal seepage WQ**

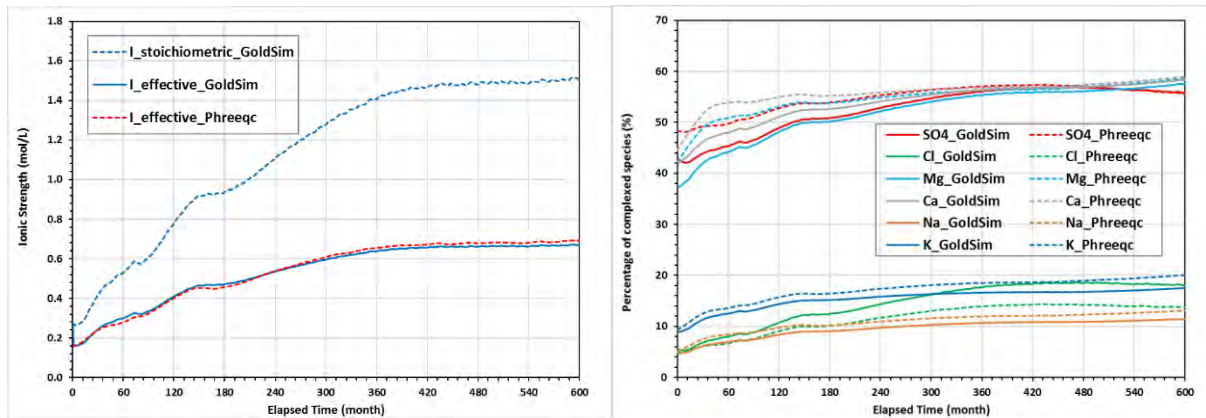


Figure 6 (left). Simulated stoichiometric and effective ionic strength of basal seepage and PHREEQC calculated effective ionic strength

Figure 7 (right). Proportions of complexed species by GoldSim and PHREEQC over time (for major components)

Table 4. Comparison of complexed species by GoldSim and PHREEQC for 60-month increments

Component	Source	24 (month)	84 (month)	144 (month)	204 (month)	264 (month)	324 (month)	384 (month)	444 (month)	504 (month)
Cd complexes (%)	GoldSim	58.8	65.2	69.0	69.8	71.1	71.7	72.1	72.1	72.4
	Phreeqc	72.7	80.9	79.1	76.6	77.4	78.1	78.7	78.6	79.2
Zn complexes (%)	GoldSim	51.0	57.6	63.2	64.3	66.7	68.5	69.6	69.9	70.3
	Phreeqc	77.0	89.4	81.1	72.7	70.1	68.7	68.0	67.5	67.9
Cu complexes (%)	GoldSim	55.9	53.6	58.3	65.7	72.8	76.7	78.7	79.6	79.6
	Phreeqc	96.6	98.3	96.8	93.7	91.0	88.6	86.8	85.1	83.5
Fe complexes (%)	GoldSim	48.3	52.6	55.5	56.1	57.4	58.3	58.9	59.0	59.3
	Phreeqc	82.6	93.0	88.1	78.5	74.0	70.9	69.1	67.5	66.7
Pb complexes (%)	GoldSim	57.5	60.7	61.8	61.8	62.2	62.0	61.9	61.8	62.0
	Phreeqc	98.6	99.5	98.9	97.5	96.2	95.1	94.2	93.3	92.7
Mn complexes (%)	GoldSim	48.6	54.6	59.9	61.2	63.6	65.4	66.6	66.9	67.3
	Phreeqc	48.5	50.9	51.5	51.2	51.2	51.1	51.1	51.1	51.7

3.3 Non-ideality Function Comparison

Mineral solubility in aqueous solutions generally increases with rising salinity, as formation of aqueous metal complexes becomes favorable (Appelo and Postma 2005). WATEQ calculated activity coefficients are generally smaller than Davies calculated values especially at higher ionic strength (> 0.5 mol/L; Figure 1). WATEQ Debye-Hückel equation, with metal complexation functionality, is expected to calculate higher concentration than the Davies equation, without metal complexation functionality, under the same conditions. Figure 8 compares predicted seepage water quality using the WATEQ and the Davies Debye-Hückel approach to account for non-ideality. The results indicate that the sulphate concentration calculated using the Davies equation without complexation is generally 10% – 15% lower than that calculated using WATEQ equation

with complexation. This is expected since the effect of complexation is to add dissolved mass in the final concentration, but effectively ‘hides’ that dissolved mass for other solution reaction processes (i.e. precipitation/dissolution). Heavy metals of environmental significance (e.g. Pb and Cd) are around 40% – 60% lower. A longer-term prediction (Figure 9) suggests that the same conditions may persist over time (sulphate and Mg concentrations calculated using the Davies equation without complexation are about 15% – 40% lower than those calculated using the WATEQ equation with complexation). Similarly, heavy metals of environmental significance (e.g. Pb and Cd) are around 60% – 90% lower. However, the difference of pH prediction caused by the two activity models is negligible, as pH is predominately dependent on the MPA/ANC ratio and remaining ANC in the system.

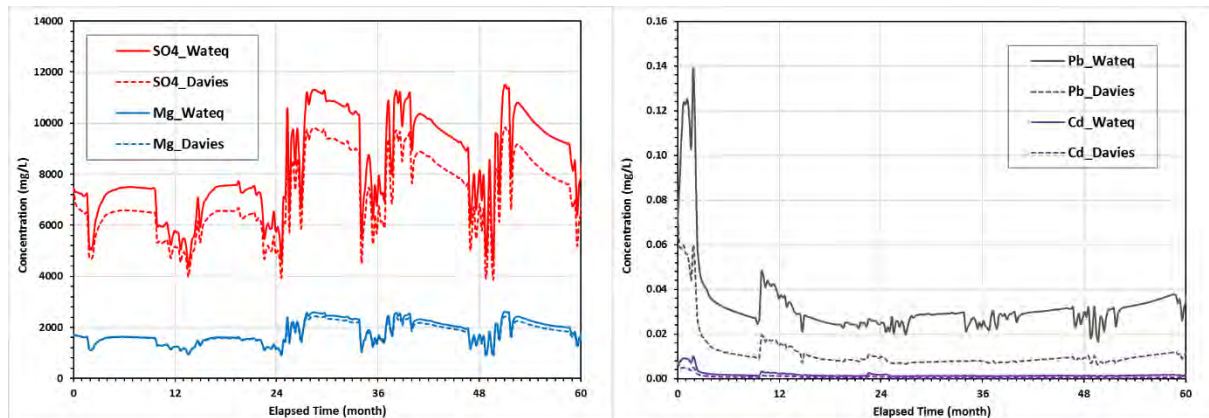


Figure 8. Comparison of simulated Mg and SO₄ concentrations (left) and Pb and Cd concentrations (right) of toe seepage as a function of different activity correction models

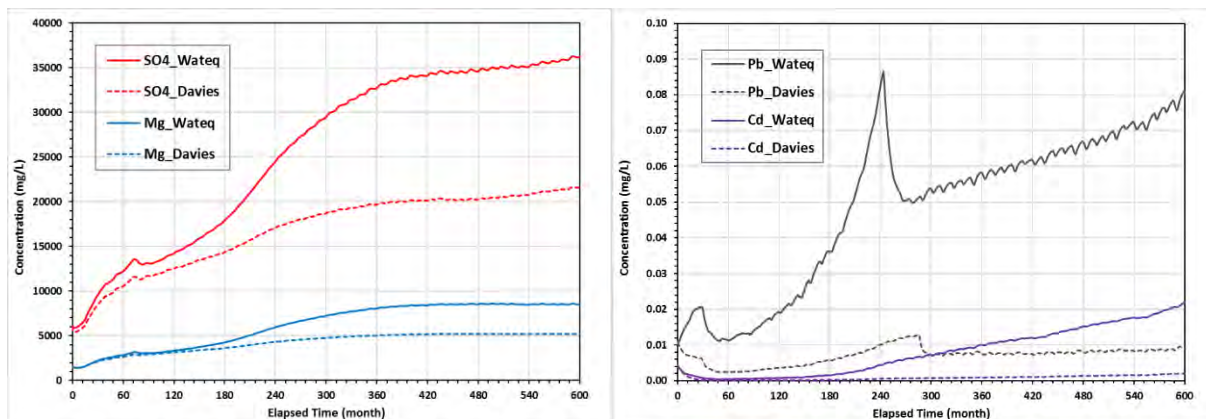


Figure 9. Comparison of simulated Mg and SO₄ concentrations (left) and Pb and Cd concentrations (right) of basal seepage as a function of different activity correction models

4.0 CONCLUSIONS

This paper shows the importance of accounting for non-ideality especially when environmental conditions favor buildup of weathering products and low water flow, or a combination of low flow, elevated temperatures and reactive waste. This study utilizes a higher ionic strength

thermodynamic approach using a non-iterative solution set of algorithms within a GoldSim framework. The results suggest that the approach provides greater geochemical representation and a higher level of robustness for water quality predictions in mining- influenced waters where concentrations may become elevated.

Predicted water quality calculated using the WATEQ Debye-Hückel equation, with metal complexation functionality, are generally higher than that those calculated using the Davies equation, without metal complexation functionality. The Pitzer equation, based on a more sophisticated ion-interaction theory, could be used for higher salinity and ionic strength conditions (e.g. hypersaline with $I > 5$ mol/L), although additional parameters are required for calculations of activity coefficients, making it difficult to directly implement this in GoldSim without adding significant numerical complexity.

The external validation of the approach, via calibration to field data and comparison to more complete PHREEQC assessments of various snapshots of the water quality, suggests that this model provides a means of considering the multitude of geochemical variables that arise when simulating mine waste reactions under conditions typically encountered on Australian mine sites. This study has successfully implemented metal complexation functions and higher ionic strength corrections into GoldSim and provided a strong basis for water quality prediction for higher reactivity waste rock facilities.

5.0 REFERENCES

Allison JD, Brown DS, Novo-Gradac KJ (1991) MINTEQA2, A geochemical assessment database and test cases for environmental systems: Vers.3.0 user's manual. Report EPA/600/3-91/-21. Athens, GA: U S EPA

Appelo C.A.J. and Postma D. (2005) Geochemistry, groundwater and pollution. 2nd ed. A.A. Balkema Publishers, Leiden, The Netherlands. Taylor & Francis Group plc.

Appelo C.A.J, Parkhurst D.L., Post V.E.A. (2014) Equations for calculating hydrogeochemical reactions of minerals and gases such as CO₂ at high pressures and temperatures. *Geochimica et Cosmochimica Acta* (125) 49–67.

Appelo C.A.J (2015) Principles, caveats and improvements in databases for calculating hydrogeochemical reactions in saline waters from 0 to 200 C and 1 to 1000 atm. *Applied Geochemistry* (55) 62-71.

Ball J.W. and D.K. Nordstrom (1991) WATEQ4F – User's manual with revised thermodynamic data base and test cases for calculating speciation of major, trace and redox elements in natural waters, USGS Open-File Report 90-129, 185 p.

Davies CW (1938) The extent of dissociation of salts in water. VIII. An equation for the mean ionic activity coefficient of an electrolyte in water, and a revision of the dissociation constant of some sulfates.- *Jour.Chem.Soc.*: pp 2093-2098.

Debye P and Hückel E (1923) Zur Theorie der Elektrolyte.- *Phys.Z.*; 24: pp 185-206.

GoldSim Technology Group (2010) User's Guide - GoldSim, Probabilistic Simulation Environment. Washington, USA.

Merkel Broder J., Planer-Friedrich Britta (2008) *Groundwater Geochemistry: A Practical Guide to Modeling of Natural and Contaminated Aquatic Systems*. 2nd ed. Springer Science & Business Media.

Parkhurst, David L., and C. A. J. Appelo. (2013) *Description of Input and Examples for PHREEQC Version 3: A Computer Program for Speciation, Batch-Reaction, One-Dimensional Transport, and Inverse Geochemical Calculations*. US Geological Survey Techniques and Methods, Book 6, Modeling Techniques.

Pitzer KS (ed) (1991) *Activity coefficients in electrolyte solutions*. 2nd edition, CRC Press, Boca Raton, pp 542.

Strand Ro, Usher Brent, Strachotta Chris and Jackson Jim (2010) *Integrated water balance and water quality modelling for mine closure planning at Antamina*. In *Proceedings of the 5th International Conference on Mine Closure*, Nov 23-26, 2010, Viña del Mar, Chile.

Strand Ro and Usher Brent (2014) *Integrated Site Water Balances and Water Quality Models for Decision Making over Life-of-Mine*. 2nd Life of Mine Conference, 2014, Brisbane QLD, Australia.

Strand Ro, Tuff James and Usher Brent (2017) *Non-iterative modelling of mine site hydrogeochemistry*, 9th Australian AMD workshop, Tasmania.

Truesdell AH, Jones BF (1974) *WATEQ, a computer program for calculating chemical equilibria of natural waters*. *Journal of Research, U.S.G.S.* v.2, p.233-274.

Tuff James, Harrison Bevin, Choy Sergio Yi, Strand Roald and Usher Brent (2015) *Assessing the Robustness of Antamina's Site Wide Water Balance/Water Quality Model over 5 Years of Implementation*. 10th ICARD | IMWA 2015 Conference – Agreeing on solutions for more sustainable mine water management” Santiago, Chile ISBN 978-956-9393-27-3.

Usher Brent, Strand Ro, Strachotta Chris, Jackson Jim (2010) *Linking fundamental geochemistry and empirical observations for water quality predictions using GoldSim*. IMWA 2010 Sydney.

NON-ITERATIVE MODELLING OF MINE SITE HYDROGEOCHEMISTRY

R. Strand^A, J. Tuff^A and B. Usher^A

^AKlohn Crippen Berger, Level 5 43 Peel Street South Brisbane 4101, Australia

ABSTRACT

Using GoldSim as platform to integrate a variety of simultaneous processes, the authors have taken the core components of the MINTEQ database (aqueous chemistry thermodynamic controls), and recompiled them in a modular system to allow predictive geochemistry for mining facilities. The authors have successfully applied this modular system to provide rapid, thermodynamically relevant, predictive geochemical modelling at over 50 mine sites across Australia, the Pacific and internationally.

With appropriate data (static, kinetic, climate, spatial, volumetric) to populate the model, using the concepts and components outlined in this paper, an integrated model simulates the evolution of mine waste using a multipronged approach that includes processes such as oxidation of sulphides, metal release, consumption of neutralisation, source term depletion, dissolution and or precipitation of secondary minerals, carbonate equilibria, pH prediction, acidification and/or stagnation, degassing, dilution, ionic strength, ion activity, and electrical balance.

The components of the integrated geochemical systems interact in each time step to equilibrate solution chemistry. The required components of the integrated geochemical subsystem are: pH-ranked loading rates; source term depletion of sulphides and carbonates; calculation of solution parameters (ionic strength, activities); alkalinity balancing; complexation; and mineralogical controls. These components support the simulation of geochemical processes, introduce redundancies in the system to correct minor errors, and provide time-variant equilibrated water qualities across the modelling infrastructure.

1.0 INTRODUCTION

Aqueous geochemical modelling techniques have traditionally centred on attempting to find chemical properties of a solution (Garrels and Thompson, 1962). Later, Helgeson (1968) introduced the first computer program to perform equilibration and reaction path models. As computers gained in processing power, numerical geochemical models have been built and used by more geochemists to assess geochemical processes. Modern geochemical models offer depth of analysis and significant breadth to investigate a solution for processes such as precipitation of minerals, dissolution, gas exsolution and a number of other phenomena. The geochemical systems as discussed in this document provide a robust approach to simulating complex solution geochemistry as a non-iterative process, making these systems a valuable inclusion in a larger water balance (WB)/mass balance (MB) *integrated* model.

This paper discusses six key components required to enable an existing WB/MB and water quality model (WQM) to operate with *integrated geochemical equilibration mechanics*. The value of integrated geochemical equilibration mechanics that do not require iterations to converge, is time saving. Furthermore, there is significant utility in being able to not only simulate water flows, but to simulate geochemical mechanics and solution chemistry of waste seepage concurrently.

2.0 DEVELOPMENT OF INTEGRATED MODELLING APPROACH

Initial versions of *integrated* water balance and water quality models contained several of the components that define an integrated model, those being a water balance intended to simulate several water flows and storage related processes, a conservative mass balance, and several methods of constraining the dissolved mass in solution. These offered some geochemical control on simulations of the solutions. As an example, the original model employed empirical solubility limits, with some dynamic mineral controls such as gypsum to limit dissolved mass based on pH and salinity; as well as source term depletion (Usher et al. 2010). It was an early attempt to bring together water balance modelling and water quality modelling in substantially more detail than simple dilution modelling.

While initial attempts provided a significant improvement on mass-balance models, the limitations of the simplifications necessitated a more detailed approach. The basis of the integrated approach includes several dynamic mineralogical controls of stoichiometry of form 1:1, (e.g. CaSO_4), ionic strength and activity calculations (Strand et al. 2010), simplified acid-base accounting and rudimentary approaches to solve alkalinity and the inclusion of the effect of dissolved inorganic carbon on water quality processes (Usher et al. 2010).

As these models proved their value in simulating mine water quality at site-wide scale, further refinements of the geochemical equilibration process were added to improve robustness. Further, the WB/WQM aspect of the model was significantly improved to provide a range of planning options, including options to assess water treatment design, and tackling compliance evaluations in a variety of environments (Strand et al. 2010).

To handle more complex chemistry, algebraic formulas were needed to solve more complex stoichiometric equations of composition 1:2 (e.g. $\text{Zn}(\text{OH})_2$), 1:3 (e.g. $\text{Al}(\text{OH})_3$), 1:1:2 (e.g. $(\text{Ca Mg})(\text{CO}_3)_2$), 2:3 (e.g. Fe_2O_3), and adjusting the assumptions used to govern mass flux. Further advances were made in adaptations to the method of data processing; and a process was developed to account for including the evolution of kinetic loading rates as a function of pH.

At a separate mine site, the requirement for inclusion of minerals such as Jarosite and Alunite simulation arose. The highly complex stoichiometry of form 1:3:2:6 (e.g. Jarosite - $\text{NaFe}_3(\text{SO}_4)_2(\text{OH})_6$) required a range of mechanics running in series to solve precipitation and/or dissolution in a single iteration; at the same time, mineral acidity, proton flux, Kw competition and a more complex inorganic carbonate system were added to the models to provide a more consistent .

Note: in all stages of advancement, comparisons to external geochemical solution solvers such as PHREEQC (Parkhurst and Appelo 2013) and/or Geochemists Workbench (Bethke 2007) were used to provide the details of the geochemical mechanisms, validate and verify that the models are functioning properly.

3.0 METHODOLOGY

3.1 Components

Aside from the broader model architecture required for the conventional water and mass balance model (not discussed), there are six components necessary to build an integrated model:

- Calculation and utilisation of pH-ranked loading rates (external to the model)
- Dynamic acid/base balance including source term depletion of sulphides, neutralization potential
- Calculation of solution parameters such as ionic strength and activity coefficients

- Aqueous phase alkalinity/acidity including inorganic carbon balance
- Complexation
- Mineralogical control

3.2 Purpose

Broadly, the purpose of the integrated model is to provide rapid simulation of a complex geochemical system. Secondary, or peripheral purposes stem from what can be accomplished in the time savings: compare different options for waste management, or compare different water handling plans, or assess environmental impact of one plan versus another. These options and scenarios are included as part of the WB/WQM, but the value is that it is time consuming to utilise separate software to refine the WQ predictions based on external geochemical equilibration.

In order for a non-iterative geochemical sub-model to calculate the equilibrium of an un-equilibrated solution, there are following steps that expedite the process:

1. Start with near equilibrium water quality
2. Add geochemical load which is already near electrically balanced (and relevant for that pH range) but stresses the system
3. Calculate the solution parameters for the stressed system
4. Employ the dynamic numerical solution algorithm to *return* to (near) equilibrium within one timestep

The difference between the integrated, non-iterative model, and a dedicated geochemical software, is, of course, the differentiation at the point where iteration is necessitated by less complex application of the solution solving algorithms. Whereas dedicated geochemical software must converge based on a number of inputs, which may require many multiple iterations of solution solving, the benefit of using the dynamic algorithms, produce a similar (not exact) result within one timestep, significantly reducing computing power and simulation runtime.

Each of these components offers benefits for supporting the model mechanics for equilibration of the mine water in each time step.

The purpose of these components (respectively, Section 3.1) is to:

- Account for the kinetic rate reaction of stored mine waste in terms of dissolved load entering the mass balance ;
- Account for the source term depletion of sulphides and neutralisation potential which may provide insight as to how the system will evolve geochemically;
- Account for ionic strength, which informs calculations for activity, which subsequently informs several more calculations – this step is very important because it is through the activity coefficient that the efficacy of mineralogical controls are constrained;
- Account for the dissolved alkalinity and acidic stresses on the aqueous system (replenished by minerals such as calcite and/or dolomite as well as the partial pressures of carbon dioxide);
- Complexation is less important in dilute systems, but plays an important role in more saline and concentrated water. Complexation calculations account for dissolved mass partitioned or sequestered in a complex form, which adds cumulatively to dissolved mass, but is not involved in mineralogical controls; and,
- Finally, mineralogical controls are fundamentally the most important component in an integrated model that provides robust geochemical predictions for seepage water quality. The conservative mineralogical constraint is a core component for simulating

alkaline, neutral and transitioning systems, and is necessary for making accurate metal and salt predictions in acidic environments. Simply put, all the other components support the equilibration mechanisms, without which, a water balance/mass balance model is simply a mixing and dilution model.

The following sections will expand on each of these components and discuss the process of inclusion in a WB/WQM.

3.3 PH-Ranked Loading Rates

In order to process kinetic data (as leachate concentration) to pH-ranked loading rates follows a similar pattern for most kinetic data, provided the data is acquired in a generally standard way, for example:

- a measured volume of leachate is collected; measured for pH; concentrations for a suite of parameters are analysed by ICP-MS, or alternative methods
- Leachate volumetric collections are timestamped

The initial processing of kinetic data follows the processes provided in the Price guide (Price and Errington 1998) or GARD (Verburg et al. 2009). The subsequent steps are what differentiate the process in calculating pH-ranked loading rates:

- The dataset can now be distributed or sorted by the pH in the leachate to calculate the pH-ranked loading rate (median of all loading rates within a range are taken to be representative of the loading rate of that parameter in that pH range)
- Median loading rates for each parameter within a specific pH range (e.g. 6.3 - 8.3, or 4.5 - 6.3) are employed in the model as a function of the predicted pH for each time step in the model (feedback loop)

The pH-ranked loading rate is an important part of the calculations, because it supplies the load for the system, and the first step to getting a *relatively* ionic-charge balanced solution prior to subsequent equilibration calculations.

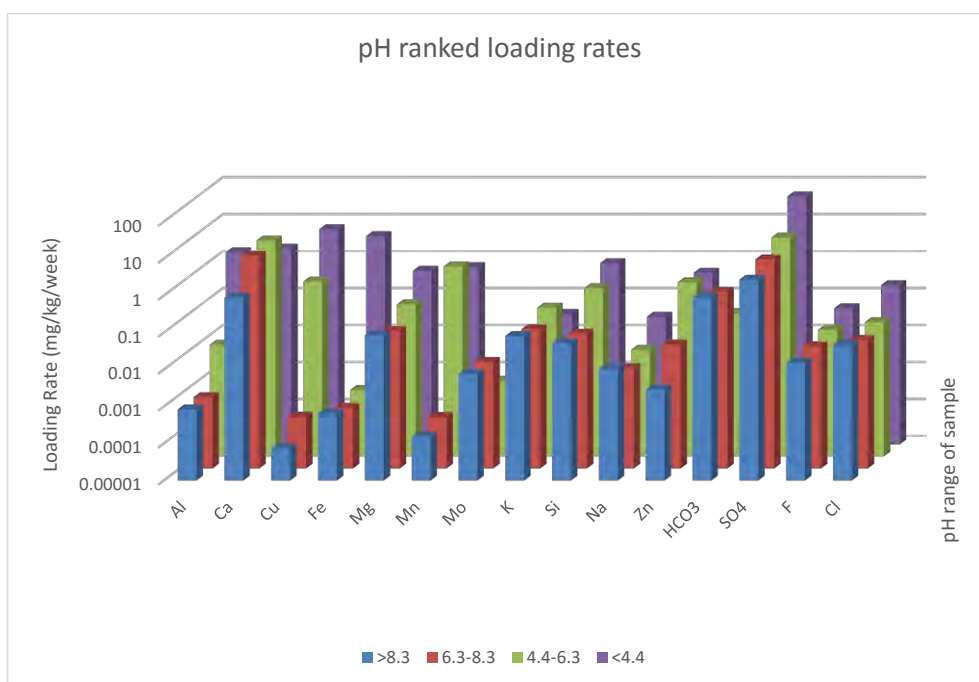


Figure 3.3-1 Example of Median pH ranked loading rates (n= 2951 samples)

When using pH-ranked loading rates in a model, loadings are generated by multiplying the loading rate by the tonnage of material (ideally distributed into the same classifications as used in the kinetic tests).

The pH used to determine the appropriate loading rate is generated from the negative log of molar H^+ concentration in the resulting solution (note that the H^+ concentration is affected by alkalinity, water formation and dissociation).

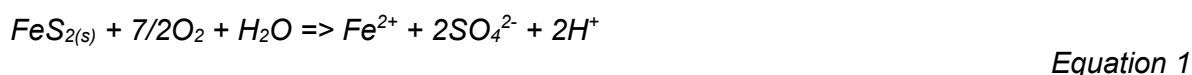
3.4 Acid Base Accounting

To complement the loading rates, the next component of the integrated model is calculation of the acid/base balance. While the loading rate governs the *intensity* of the reactions, source term consumption (with starting values based on static geochemical testing data) allows calculation of timing before a significant change occurs.

In order for a system that is currently in an alkaline state to transition to an acidic state, generated acidity must consume or isolate the *effective* neutralisation agents that are actively neutralising the generated acidity (Price and Errington 1998).

Where possible, thorough analysis of static data sets (pre and post kinetic trials) compared to actual progression of the kinetic testing results should be completed such that a conceptual understanding of the efficacy of the NP is known prior to populating the model with static data, such that the lag time (time before system turns acidic) can be accurately predicted (Li and Bernier 1999). Kinetic data (loading rates) and static data (source term) are both needed to predict the lag time.

In order to include source term depletion systems in a WB/WQM, the neutralisation potential (or Acid Neutralisation Capacity) per waste class (in terms of kg $CaCO_3$ /tonne) is used to define the quantity of NP present at waste placement. NP is consumed when acidity is generated by sulphides oxidising in proximity or upstream of the NP; assumptions about the proximity of the NP and sulphidic content may need to be made in the conceptual model. Primary pyrite (Iron sulphide) weathering is shown in Equation 1 (Seal and Hammarstrom 2003):



Iron oxidation is relatively rapid when oxygen is present Equation 2,

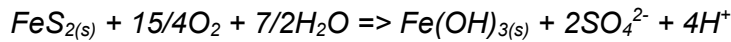


However, due to the insolubility of Fe^{+3} , Equation 3

Equation 3 is a better representation of iron oxidation inclusive of precipitation of ferrihydrite:



Therefore, the combined reaction as seen in Equation 4 (Nicholson, Gillham, and Reardon 1988) is a more complete process in neutral conditions:

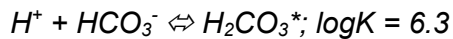


Equation 4

From Equation 4, every mole of pyrite will likely generate four moles of acid. Neutralisation of the acid occurs when dissolved carbonates are protonated successively from carbonate -> bicarbonate -> carbonic acid, or as shown in Equation 5 and Equation 6 (Appelo and Postma 2005):

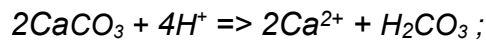


Equation 5



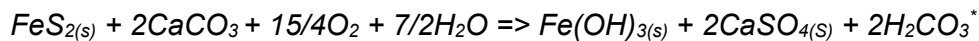
Equation 6

Which can be summed up by the dissolution of calcite and subsequent neutralization of one mole of sulphur in pyrite, in Equation 7 (Jambor 2003):



Equation 7

Based on stoichiometry in Equation 7, we can infer the bulk conservative neutralisation process, as seen in Equation 8:



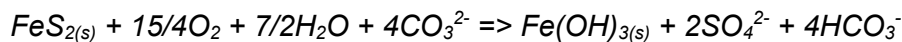
Equation 8

H_2CO_3^* is not, however, the endpoint of inorganic carbon. Build-up of H_2CO_3 may occur under acidic conditions, but it is more likely that carbonic acid will dissociate into aqueous carbon dioxide and water, and degas in an open system (Stumm and Morgan 1981):



Equation 9

Depending on the reactivity of the waste and the ventilation of the system, degassing of carbon dioxide may not occur, resulting in a higher concentration of alkalinity in the system where the mass gain of alkalinity from dissolution of solid phase carbonates balances the mass loss of alkalinity via flushing (as dissolved mass). If reaction rates are slower, with sufficient solid phase alkalinity present to maintain a steady supply of dissolved carbonate, partial protonation of carbonates in alkaline conditions can be seen in Equation 10 (Nicholson, Gillham, and Reardon 1988).



Equation 10

The carbonate and alkalinity system calculations in Section 3.6 provide a robust method to account for the protonation and deprotonation of inorganic carbon in context of ambient pH, atmospheric interactions, and peripheral processes, in a non-iterative manner.

If calcite is considered the primary NP source, this is first consumed at a rate accorded by the relative stoichiometry of Equation 8, that being two moles of CaCO_3 per mole of pyrite; and secondly as the source of alkalinity (and replacement of CO_3^{2-} and subsequently HCO_3^-) in Equation 10. Carbonates, therefore, are not only consumed in the neutralisation of the acidity produced by the sulphide oxidation, but also in maintaining the alkalinity in the

aqueous phase, which is further discussed in Section 3.6. On occasion, it may be calculated that in less reactive systems with high flowthrough, source term consumption of carbonates is secondary to dissolution to maintain alkalinity levels. In these types of systems, it may be shown that dissolved alkalinity is sufficient to neutralise all acidity produced by sulphide oxidation.

In order to account for these processes in an integrated model, consumption of carbonates is similarly divided into two separate processes, the first process being source term consumption as governed by the rate of pyrite oxidation and the consumption of carbonates through losses through maintaining alkalinity in the water.

3.5 Calculation of Solution Parameters

The ionic strength, can be calculated using the condensed algorithm (Appelo and Postma 2005):

$$I = \frac{1}{2} \sum (m_i / m_i^0 \cdot z_i^2) \equiv \frac{1}{2} \sum (m_i \cdot z_i^2)$$

Equation 11

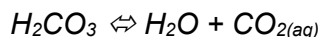
Activity coefficients can be calculated in a number of different ways. An applicable method, based on the expected ionic strength is used in the models:

- For $I < 0.1$ mol/L, Debye-Hückel is sufficient (Debye and Hückel 1923),
- The Davies equation is sufficient for $I < 0.5$ mol/L (C. W. Davies 1938), (C. Davies 1962).
- For up to $I < 1$ mol/L, the Truesdell–Jones WATEQ adaptation to Debye-Hückel (Truesdell, Jones, and Plummer 1976), can be used.
- For greater than 1 mol/L ionic strength, ion interaction theory (Pitzer 1973) becomes relevant.

3.6 Dissolved Alkalinity Balance

Continuing from Section 3.4, the alkalinity balance follows closely in concept to the consumption of source term carbonates. Whereas the source term consumption is largely a function of pyrite oxidation in most mining wastes, further consumption of carbonates occurs when carbonates are exposed to water and dissolve according to the solubility product of the mineral in question. Acidity from other sources can also consume alkalinity and carbonates.

As mentioned in Section 3.4, degassing may occur when there is a build-up of $H_2CO_3^*$ and the concentration of $CO_{2(aq)}$ exceeds the equilibrium partial pressure of atmospheric gas in contact with the system and occurs via the dissociation of carbonic acid via Equation 12:



Equation 12

Inorganic carbon (carbonate, bicarbonate and carbonic acid) interact with other ions in solution to form precipitates when saturation index for that mineral exceeds the solubility product (discussed in more detail in Section 3.8). Dissolution of inorganic carbon (as carbonate), protonation of carbonate to bicarbonate, and the formation of mineral precipitates is governed by the applicable solubility product, or equilibrium constant; however, it is the mode of employment that is important in an integrated model. The following mechanics are built into the geochemistry system to provide a practical means to estimate the effect of thermodynamic control, without engaging in the iterative solutions. This process requires some subtle changes in how method is employed for solving equilibria.

As an example, the alkalinity system utilises the basic premise of mass transfer using Equation 13. Instead of solving the equation multiple times in an attempt to converge, the change required to reach equilibrium is solved for *directly*. In the following equation, the equilibrium constant (K_a) is a known. Similarly, the concentrations $[H^+]$ and $[HCO_3^-]$ are also known, since this is the un-equilibrated starting position. Delta change ($\partial[H^+]$ and $\partial[HCO_3^-]$) are the unknowns are solved in each time step:

$$([H^+] + \partial[H^+])([HCO_3^-] + \partial[HCO_3^-]) = K_a$$

Equation 13

Since $\partial[H^+] = \partial[HCO_3^-]$ due to known stoichiometry, the equation can be simplified to isolate only one unknown.

Change in concentration is achieved by multiplying the desired change in concentration $\partial[H^+]$ by the volume of water in the system and dividing by the time over which the change occurs (one timestep), then subtracting or adding to the total solute mass (of H^+ and HCO_3^-) in the system. This algorithm is present in other parts of the alkalinity system and is representative of the systematic approach used to govern changes in solution chemistry. This method is used in a similar method for all the equilibria solved in the model.

3.7 Complexation

Complexation of ions is an important aspect of the geochemical equilibration because, in absence of complexation, mineralogical controls can, under some conditions, over-precipitate some minerals, causing predictions to be too low. The effect of complexation, is to segregate ions into a form which contributes to overall dissolved concentration, but does not contribute to the ionic form of a specific ion which is used in the mineralogical control calculations. For example, Al may exist in solution in a variety of hydroxylated states (e.g. $Al(OH)_2^+$), which has the net effect of increasing dissolved aluminium (after equilibration), but reduces the concentration of the non-hydroxylated Al^{3+} which can be removed via precipitation of gibbsite or diaspore.

Complexation mechanics utilise similar algorithms as those used in the previous section; however, there are fundamental differences that merit discussion (See Tian et. al 2017 as part of these proceedings).

3.8 Mineralogical Controls

Weathering processes and oxidation of metal sulphides may liberate metal ions (Fe, Zn, Pb, Cu) from source mineralogy (Ptacek and Blowes 2003). These metal ions may form precipitates with anions (e.g. hydroxide, carbonate and sulphate) such as malachite, goethite, smithsonite, cerrusite (Peterson 2014), if the saturation index for a mineral exceeds the solubility product. In certain conditions, such as a significant rainfall event, or even seasonal flushing, excess water may cause a reversal in the process, lowering the saturation index enough that re-dissolution may occur. It is imperative, therefore, that conservation of mass is employed in an integrated model to capture such phenomena.

The process of removing mass from solution and storing it in a reservoir for potential future re-dissolution, is accomplished by employing an algorithm similar to Equation 13; however, in this case the elements used in the equation may pertain to those found in a salt, for example, $CaSO_4$ (gypsum).

Equation 14 is the un-solved version of the basic dynamic algorithm. One of the most commonly formed secondary minerals is gypsum, which forms when sulphide oxidation products (SO_4^{2-}) react with calcium containing carbonates which consumes CO_3^{2-} (via Equation 8) and liberates Ca^{2+} , this process maintains dynamic control on many 1:1 stoichiometrically balanced minerals by the general form Equation 14 (shown for gypsum, CaSO_4):

$$([\text{Ca}^{2+}] + \partial[\text{Ca}^{2+}])([\text{SO}_4^{2-}] + \partial[\text{SO}_4^{2-}]) = K_{sp_{\text{gypsum}}} \quad \text{Equation 14}$$

Similar to the previous process (in Section 3.6), $\partial[\text{Ca}^{2+}]$ is equated with the delta change in anion concentration based on stoichiometry (e.g. $\partial[\text{Ca}^{2+}] = \partial[\text{SO}_4^{2-}]$). A quadratic equation is used to solve for the delta term, so the difference between the loss of mass (precipitation), and gain of mass (dissolution) can be calculated. Note: preliminary solution assessment in a dedicated geochemical modelling software such as PHREEQC is recommended to compile the likely mineralogical controls on the solution.

Once the concentration controls have been built, the mass transfer into (and out of) the solid state is governed by the change occurring over the timestep (concentration change multiplied by the volume over which the change is occurring and dividing by the timestep length).

By following these steps, the final concentration for the system is found after the dynamic mineralogical controls are applied as a rate loss in mass/time from the system, and conservation of mass is consistent and conservative via storage in dedicated reservoirs for precipitated mass.

This fundamental approach can be adopted for a range of other stoichiometry relationships, making some assumptions based on high order polynomials to remove excess complexity for high order exponents on the delta terms (which provide negligible accuracy improvement).

4.0 SUMMARY

The controls on mine water chemistry that can range from neutral and dilute to highly concentrated and acidic are more complex than described in this paper, but the understanding of the geochemical reactions and supporting algebraic formulations are fundamental in moving from a conservative, dilution/mixing mass balance model, to the beginnings of a dynamically controlled geochemical *integrated* model. The process outlined in this document has been used on over 50 water quality models for mine sites in a range of commodities and climates throughout Australia and internationally. The method has been thoroughly checked by a multitude of calibrations and compared against dedicated thermodynamic software (e.g. PHREEQC). Methods to determine whether the dynamic single step solution was working as intended involve obvious checks such as allowing the PHREEQC and the solution check to solve the equilibrium condition for a un-equilibrated solution, results have been consistent for simple salts of stoichiometry 1:1, as well as metal carbonates, hydroxides and some oxides. The system is less robust when complexation is not included for high salinity systems. Some minerals that have inconsistent or variable kinetic formation rates can be problematic (e.g. molybdates), and highly complex stoichiometry minerals (alunite, jarosite, K-jarosite) may pose some problems in solutions with either significant flux, or elevated hydroxide (high pH).

The single step dynamic geochemical submodels for use in integrated water balances and water quality models is still developing, but significant improvements have been made in the last decade, significantly bolstering robustness and applicability in a wide variety of

environments, and has become the mainstay of many site wide WB/WQM's for mines sites, where water management is core component of their closure or operating plan.

As with all modelling, there is a strong pre-requisite in data gathering, which may be a significant limitation in developing a robust integrated model, and a good understanding of the mechanisms at play in different mine waste facilities is required to develop adequate conceptual models to allow integrated models to be used as reliable tools to assist mine sites with compliance, management and mitigation of mine water.

5.0 REFERENCES

- Appelo, Tony, and Dieke Postma. 2005. *Geochemistry, Groundwater and Pollution*. 2nd ed. Amsterdam, the Netherlands: A.A. Balkema Publishers.
- Bethke, Craig M. 2007. *Geochemical and Biogeochemical Reaction Modeling*. Leiden: Cambridge University Press. <http://public.eblib.com/choice/publicfullrecord.aspx?p=328930>.
- Davies, Cecil. 1962. *Ion Association*. Butterworths.
- Davies, Cecil W. 1938. "397. The Extent of Dissociation of Salts in Water. Part VIII. An Equation for the Mean Ionic Activity Coefficient of an Electrolyte in Water, and a Revision of the Dissociation Constants of Some Sulphates." *Journal of the Chemical Society (Resumed)*, 2093. doi:10.1039/jr9380002093.
- Debye, Peter, and Erich Hückel. 1923. "Zur Theorie der Elektrolyte." *Physikalische Zeitschrift*, no. 24: 185–206.
- Jambor, John L. 2003. "Mine-Waste Mineralogy and Mineralogical Perspectives of Acid-Base Accounting." In *Environmental Aspects of Mine Wastes*, 31:117–45. Mineralogical Association of Canada.
- Li, Michael, G., and Louis R. Bernier. 1999. "Contributions of Carbonates and Silicates to Neutralization Observed in Laboratory Tests and Their Field Implications." In , 69–78. <http://pdf.library.laurentian.ca/medb/conf/Sudbury99/AcidicDrainage/AD8.PDF>.
- Nicholson, Ronald V., Robert W. Gillham, and Eric J. Reardon. 1988. "Pyrite Oxidation in Carbonate-Buffered Solution: 1. Experimental Kinetics." *Geochimica et Cosmochimica Acta* 52 (5): 1077–1085.
- Parkhurst, David, L., and C.A.J. Appelo. 2013. *PHREEQC (version 3)*. A Computer Program for Speciation, Batch- Reaction, One-Dimensional Transport, and Inverse Geochemical Calculations: U.S. Geological Survey.
- Peterson, Holly E. 2014. "Unsaturated Hydrology, Evaporation, And Geochemistry of Neutral and Acid Rock Drainage in Highly Heterogenous Mine Waste Rock at the Antamina Mine, Peru." Doctor of Philosophy, Vancouver, British Columbia: University of British Columbia.
- Pitzer, Kenneth S. 1973. "Thermodynamics of Electrolytes. I. Theoretical Basis and General Equations." *The Journal of Physical Chemistry* 77 (2): 268–277.
- Price, William Andrew, and John C. Errington. 1998. *Guidelines for Metal Leaching and Acid Rock Drainage at Minesites in British Columbia*. Ministry of Energy and Mines British Columbia, Canada. http://www2.gov.bc.ca/assets/gov/farming-natural-resources-and-industry/mineral-exploration-mining/documents/permitting/ml-ard_guidelines.pdf.
- Ptacek, Carol J., and David W. Blowes. 2003. "Environmental Aspects of Mine Wastes." In *Environmental Aspects of Mine Wastes*, 31:239–60. Mineralogical Association of Canada. <http://geea.geoscienceworld.org/content/4/2/181>.

Seal, Robert R., and Jane M. Hammarstrom. 2003. "Geoenvironmental Models of Mineral Deposits: Examples from Massive Sulfide and Gold Deposits." In *Environmental Aspects of Mine Wastes*, 31:11–50. Mineralogical Association of Canada.

Strand, R., B. Usher, C. Strachotta, and J. Jackson. 2010. "Integrated Water Balance and Water Quality Modelling for Mine Closure Planning at Antamina." In *Proceedings on the First International Seminar on the Reduction of Risk in the Management of Tailings and Mine Waste, Mine Closure*, 63–74.

http://sponsored.uwa.edu.au/geomechanics/___data/page/7095/MC10_Sample_paper4.pdf.

Stumm, Werner, and James J. Morgan. 1981. *Aquatic Chemistry: An Introduction Emphasizing Chemical Equilibria in Natural Waters*. 2d ed. New York: Wiley.

Truesdell, Alfred, Blaire Jones, and Niel Plummer. 1976. "WATEQF - A Fortran IV Version of WATEQ, a Computer Program for Calculating Chemical Equilibrium of Natural Waters." *U.S. Geological Survey*, no. Water-Resources Investigations 76-13 (September): 73.

Usher, B. H., C. Strachotta, R. Strand, and J. Jackson. 2010. "Linking Fundamental Geochemistry and Empirical Observations for Water Quality Predictions Using Goldsim." In *Wolkersdorfer Ch, Freund A, Proc, Mine Water and Innovative Thinking—International Mine Water Assoc Symp, Cape Breton Univ Press, Sydney, NS, Canada*, 313–317.

http://imwa.de/docs/imwa_2010/IMWA2010_Usher_486.pdf.

Verburg, Rens, Nico Bezuidenhout, Terrence Chatwin, and Keith Ferguson. 2009. "The Global Acid Rock Drainage Guide." Springer-Verlag. <https://doi.org/10.1007/s10230-009-0078-4>.

THE ROLE OF AMD IN PILBARA IRON ORE: MOBILISATION AND FATE OF TRACE ELEMENTS DURING SURFACE AND GROUNDWATER FLOW

P. Ware^A and R.T. Watkins^{AB}

^A The University of Western Australia, Crawley, Australia

^B Environmental Geochemistry Services, Bibra Lake, Australia

ABSTRACT

Disturbance of sulphide-bearing shales during mining of sedimentary iron ore, such as that found in abundance in the Pilbara region of Western Australia, poses the risk of generating acid and metalliferous drainage (AMD) with associated mobilisation and migration of contaminant metals and metalloids. The precise chemical character of the AMD, and thus the potential pollution risk to the environment, is distinctly different to that generated by other types of mining. Whilst sulphide oxidation is capable of generating highly acidic, low pH, sulphate- and iron-rich solutions, characteristic of AMD, the content of dissolved metals typically is not as elevated as in drainage formed during base metal and gold mining. AMD associated with Pilbara iron ore mining has traits akin to those of coal deposits, where biophile elements, such as the metalloids arsenic and selenium, and the metals mercury and cadmium, are notable environmental pollutants.

The impact of geochemical contamination from mining and eventual mine closure upon sensitive environmental receptors is determined by the chemical stability of dissolved metal/metalloid chemical species within the AMD and the degree of their attenuation during surface and groundwater movement. In most aqueous systems, the largest part of the contaminant load is adsorbed to sediment particles and/or mineral surfaces in aquifer rocks. Although monitoring of the dissolved metal/metalloid content of mine drainage is useful and necessary, it is insufficient for comprehensive understanding of contaminant transport and environmental impact. It is important to consider the water/sediment/rock interactions as a dynamic chemical system, and gain an understanding of how changes in prevailing conditions (pH, salinity, etc.) will affect contaminant mobilisation and bioavailability.

This paper reviews current literature, summarises previous projects and describes current research to progress our understanding of the behaviour of prevailing contaminants in AMD at Pilbara iron ore mines and the extent of risk they pose for the environment.

1.0 INTRODUCTION

Soils and water located in historic mining areas are frequently enriched in trace elements to potentially toxic concentrations. Such enrichments can arise naturally from geochemical weathering of mineralised outcrops, or be a result of anthropogenic influences including mining and smelting of metallic ores (Gauszka, 2015).

Numerous trace elements may be of concern to the health of humans, plants and animals due to their potentially high toxicity, cumulative characteristics and inability to decompose by natural processes in the environment (Chuncaí et al. 2014). Although many trace elements are essential for both human and animal health, if released to the environment in an uncontrolled manner, they may become either a contaminant (present where it would not normally occur, or above background concentrations) or a pollutant (may cause adverse biological effects) (Prasad, 2008).

The Pilbara terrain is host to the largest iron ore deposits in the world, accounting for some 22% of known reserves. Iron ore is the predominant economic product of the region, with annual production of ~430 mt. With regard to the target hematite and silica banded ironstones and reworked channel iron deposits (CID), the mining may be considered an essentially benign activity, not least because the ironstones are mined at shallow depth and form natural exposures over large parts of the ancient weathered Precambrian terrain. However, it poses the risk of generating acid and metalliferous drainage (AMD) with associated mobilisation and migration of contaminant metals and metalloids, on account of disturbance of rocks interbedded and overlying the iron ore. The AMD arises predominantly from oxidation of pyrite, FeS₂, present within carbonaceous shale units interbedded with the sedimentary ironstone, and as localised secondary mineralisation. Disseminated pyrite and secondary pyritic veining may also be abundant in lignite occurring locally in the overburden. The precise chemical character of the AMD, and thus the potential pollution risk to the environment, differs from that generated by other types of mining. While pyrite oxidation is capable of generating highly acidic, low pH, sulphate- and iron-rich solutions, characteristic of AMD, the content of dissolved metals generally is neither as elevated, nor as varied, as in drainage formed during base metal and gold mining. AMD associated with Pilbara iron ore mining is found to have traits similar to those of coal deposits, where biophile elements, such as the metalloids arsenic and selenium, and the metals mercury and cadmium, are notable environmental pollutants.

In order to evaluate the propensity of these trace elements to become pollutants, and predict long-term environmental impacts, a clear understanding is required of the **source** of key elements of concern and the mechanisms by which they may be mobilised; the **pathways** along which they may migrate from the mine site; and the **receptors** that may be impacted upon within the arid and sparsely populated Pilbara terrain.

2.0 TRACE ELEMENT CONTAMINANT SOURCES

Precise delineation of the source rock geology is clearly key to understanding element associations with major rock types (Nordstrom, 2011). In the Pilbara region, iron ore is mined from three major stratigraphic entities; the Turee Creek Group, the Hammersley Group and the Fortescue Group. The local geology of each deposit varies; however, the most problematic formations with potentially acid-forming rocks are considered to be the black shale units such as those found in the Mount McRae Shale, Brockman Iron and Marra Mamba Iron Formations (Buller, 2014; Porterfield et al., 1993). These formations are present to some extent at most mine sites in the region (Buller, 2014).

Lignite is also known to be present in the overburden at a number of iron ore operations in the Pilbara. Owing to the discreet occurrence of lignite in the region, little is presently known about its geochemical properties and environmental significance during storage within overburden stockpiles (Fajrin, 2013). However, both lignite and shale lithologies are known to host sulfide mineralisation (Green and Borden, 2011).

There have been countless static and kinetic studies conducted by Pilbara iron ore operators investigating the geochemical properties of black shale and other key waste lithologies; however, few data have been published to date.

Fajrin (2013) analysed pyritic black shale samples from the Nammuldi Member (MU) of the Marra Mamba Iron Formation and the Undifferentiated Jeerinah Formation (N). Also included in the study were samples from a significant deposit of Tertiary Lignite found in the Cenozoic Detrital (CZD) 2 stratigraphic unit at the South Jumblebar prospect in the Pilbara. Focus of the study was on 21 elements considered to have environmental significance based on known toxicity to lifeforms.

Table 1 shows the average concentration of the 21 potentially toxic elements compared to the median soil abundance reported by Bowen (1979) and the degree of enrichment shown as the Geochemical Abundance Index (GAI) reported in Fajrin (2013). Trace element analysis for Jeerinah shale samples (N) indicated significant enrichment (12 to 24x) compared to the median soil content (GAI ≥ 3) for Cd and Se, with noticeable enrichments also in Ag, Hg and Zn. Samples from the Nammuldi (MU) member were found to be significantly enriched in Ag, with other noticeable enrichments in Cu and Hg. Considerable range was observed in total sulfur content, averaging 1.02 wt% in samples from the Nammuldi Member, and a significantly higher average of 3.04 wt% from the Jeerinha Formation (which had a maximum concentration of 19.9 %).

Trace element analysis of lignite indicated relatively high enrichment (24 to 48x) compared to the median soil abundance (GAI ≤ 4) for As, Be, and Tl, with noticeable enrichment of Co, Hg, and Se. The lignite samples were found to contain an average of 2.33 wt % total sulfur and a maximum of 35.1 wt %.

The various enrichment of toxic elements in lignite and shale can be explained by the high sulfur content. Sulfide minerals are known to constitute significant minor and trace elements as substitutions in the crystal structure based on favourable size and charge characteristics. For example, S can be substituted by As, Sb and Se in the pyrite crystal, whereas Fe can be substituted by Co, Cu, Mo, Ni, Tl and Zn because of similar chemical properties (Kolker, 2012).

Table 1. Average elemental composition and GAI enrichment of shale and lignite samples (ppm). Elements with GAI values >2 are shown in bold type.

Element	Be	Ag	As	Cd	Co	Cr	Cu	Hg	Mn	Mo	Ni	Pb	Sb	Sc	Se	Th	Ti	Ti	U	V	Zn	
Median Soil Abundance	0.3	0.05	6	0.35	8	70	30	0.06	1000	1.2	50	35	1	7	0.4	9	5000	0.2	2	90	90	
MU Shale²	0.57	0.68	4.12	0.06	16.7	42.4	134	0.31	295	0.09	34.4	11	0.02	4.8	0.41	5.21	60.8	0.15	0.69	17.5	190	
GAI	0	3	0	0	0	0	2	2	0	0	0	0	0	0	0	0	0	0	0	0	0	
N Shale³	0.53	0.22	14.5	4.67	20.2	69.3	102	0.32	44.2	0.57	40.2	29.7	0.03	3.05	5.2	2.31	76.1	0.76	1.47	27.2	581	
GAI	0	2	1	3	1	0	1	2	0	0	0	0	0	0	3	0	0	0	1	0	2	
Lignite⁴	5.86	0.03	127	0.1	35.7	89.3	45.4	0.47	102	3.56	137	35	3.82	11.3	2.3	6.51	204	6.11	6.8	77.8	73.2	
GAI	4	0	4	0	2	0	0	2	0	1	1	0	1	0	2	0	0	0	4	1	0	0

¹Bowen, 1979; ²n=10; ³n=8; ⁴n=6

Samples analysed by Fajrin (2013) were taken from exploration cores in which pyrite was present locally in secondary mineral veins. As recognised by Fajrin, this inevitably makes some absolute values of the trace elements unrepresentative of the bulk lithologies that will report to waste rock storage. Nevertheless, the study was useful in indicating prospective contaminant trace elements that may characterise these waste rock lithologies. Of particular importance is the likely enrichment in (i) metalloid elements, As, Se and possibly Sb; and (ii) the heavy metals of known high toxicity Cd, Hg and Tl. Other apparent degrees of enrichment, whilst to be noted, are likely be of lesser environmental significance given the nature of the trace elements, namely Cu and Zn (necessary micro-nutrients) and Ag, which have a potentially lower degree of bioavailability and toxicity.

Selenium has been a contaminant of interest to regulatory authorities in Western Australia. The metalloid is notable in exhibiting siderophile, chalcophile and biophile affinities. In a preliminary investigation of selenium in waste rock types associated with Pilbara iron ore mining, Tabesh (2014) found a significant correlation between Se and both C and S content of the rocks. While small, but significant, amounts of Se were recorded from some samples of Banded Iron Formation, the metalloid was most concentrated in carbonaceous lithologies and lignite. A maximum concentration of 17 ppm was reported from a lignite sample. The precise distribution of Se between sulphide and carbonaceous matter in pyritic shales and mudstones was uncertain from the pilot study of Tabesh (2014) and is the subject of a soon-to-be commenced comprehensive study of Se distribution and speciation.

Occasionally elevated concentrations of Cd and Hg have been recorded during studies of Pilbara iron ore mine wastes (e.g. Gardiner 2003) and in routine programs of waste rock characterisation. The elements' characteristic affinity for both sulphide and carbonaceous matter indicate a likely predominant association with pyritic shales.

Though some similarities in trace element enrichment may be extrapolated between shale and lignite formations there is likely to be a high degree of variability in enrichment on both a local and regional scale as a result of their occurrence as mineral impurities. Waste rock materials must therefore continue to be investigated on a site-specific basis to understand the extent of mineral enrichments that occur and the propensity for those elements to be mobilised through the oxidation of the sulphide minerals and transported via acid and metalliferous drainage. It should be noted here that during this process, other elements may be dissolved from associated secondary minerals which are not discussed here, such as felsic meta-volcanic rocks and doleritic waste units that may also contribute to the total elemental load.

A vast amount of geochemical data is now generated from the Pilbara iron ore mining industry as a result of waste rock management programs. Such data may be of value in revealing particular examples of the concentration of the trace element contaminants discussed above. However, it should be noted that the concentrations of the predominant trace metals and metalloids believed to characterise the Pilbara iron ore AMD risk, namely As, Se, Cd and Hg, each may be difficult to determine precisely at low concentrations in waste rocks using methods of routine geochemical characterisation, specifically ICP-OES and ICP-MS.

3.0 TRACE ELEMENT FATE AND TRANSPORT

The propensity of a trace metal to behave toxically in the environment is dependent upon both the mobility and bioavailability of the element, and is an inherent function of its chemical speciation and partitioning within water, soil, sediment or dust matrices (Prasad, 2008). Nordstrom (2011) generalised that, for a trace element to be mobilised, at least four key characteristics must be met: (1) Occurrence: it must be present in the source rocks; (2)

Abundance: it must be present in sufficient quantities; (3) Reactivity: it must be soluble; and (4) Hydrology: it must be in the water flow path.

It has been discussed in Section 2.0 how a particular limited suite of metals and metalloid elements of environmental importance *occur* in the source rocks of Pilbara Iron Ore waste units with *abundance* significantly greater than the crustal and soil averages. The following two sections discuss the characteristics of *reactivity* in the context of the Pilbara region.

3.1 Trace Element Reactivity

The fate and transport of a metal in the environment is governed by various physical, chemical and biological processes. Adriano (2001) defined the major biogeochemical processes that regulate metal behaviour as ion exchange (adsorption-desorption), solubilisation (precipitation-dissolution) and absorption (assimilation or immobilisation). The reactivity and mobility of metals is influenced by the oxidation state and chemical species of the element in the environment. Of the contaminant elements that typify the Pilbara AMD, the metalloids can each exist in multiple oxidation states As(-III, 0, III, V), Se(-II, II, IV, VI), Sb (III, V), while Hg (0,II), Fe (II, III) and Mn (0, II, IV, VII) also form varied inorganic oxides. In addition, each of these elements may readily be present in metal-organic complexes. Such chemical speciation of the contaminants of concern is critical in the understanding of their mobility in the environment, as well as their bioavailability and potential toxicity to receptors. For example, the most bioavailable and toxic form of Hg is mono-methyl Hg (CH_3Hg^+), which bioaccumulates in fish muscle and is directly absorbed by the gastrointestinal tract when consumed by animals (Adriano, 2001).

The principal drivers for the major biogeochemical processes mentioned above are pH, Cation Exchange Capacity (CEC) and redox potential. It is generally considered that trace metal retention in soil increases with rising pH to around circum-neutral. However, there are exceptions. Under alkaline conditions the elements As, Se, Cd (and Zn, Cr, Mo, Ni, and V) are commonly more mobile (Green and Borden, 2011; Adriano, 2001). The pH has a major effect on the surface charge of clays, organic matter and colloidal Fe and Al oxides, and also plays a critical role in precipitation-dissolution reactions and redox reactions. The amount of metals a soil can attenuate is driven by the CEC, which is largely dependent on the amount of clay, organic matter and Fe, Al and Mn oxides. Furthermore, a soil with strongly reducing conditions can decrease the solubility of metals, as compared to a strongly oxidised soil (Adriano, 2001) by favouring the formation of insoluble metal sulphides.

4.0 TRACE ELEMENT RECEPTORS

There is much evidence to suggest that the total aqueous concentration of a metal is not a suitable indication with which to assess its relative degree of bioavailability. As discussed in Section 1.2, the bioavailability and potential toxicity of a trace element to an organism is constrained by the chemical speciation of the element. Table 2 presents important chemical species of trace metals in soil and water with respect to their bioavailability and potential toxicity to organisms.

Table 2. Important environmental chemical species of trace metals with regard to their bioavailability and potential toxicity to organisms. Source Logan and Trainer (1993) modified in Adriano (2001)

Metal	Dominant chemical species ^a		
	Soil	Water	Most toxic species ^b
Ag	Ag ⁺	Ag ⁺	Ag ⁺
As	AsO ₄ ³⁻	AsO ₄ ³⁻ ; AsO ₃ ³⁻	AsO ₄ ³⁻
B	B(OH) ₃	B(OH) ₃	B(OH) ₃
Ba	Ba ²⁺	Ba ²⁺	Ba ²⁺
Be	Be ²⁺ ; Be _x O _y ^{2x-2y}	Be ²⁺	Be ²⁺
Bi	Bi ³⁺ ?	Bi ³⁺ ?	?
Cd	Cd ²⁺	Cd ²⁺	Cd ²⁺
Co	Co ²⁺	Co ²⁺	Co ²⁺
Cr	Cr ³⁺	Cr ³⁺ ; Cr ⁶⁺	Cr ⁶⁺
Cu	Cu ²⁺	Cu ²⁺ -fulvate	Cu ²⁺
Hg	Hg ²⁺ ; Hg ²⁺ -fulvate	Hg(OH) ₂ ⁰ ; HgCl ₂ ⁰ ; CH ₃ Hg	CH ₃ Hg
Mn	Mn ⁴⁺ ; Mn ²⁺	Mn ²⁺	Mn ²⁺
Mo	MoO ₄ ²⁻	MoO ₄ ²⁻	MoO ₄ ²⁻
Ni	Ni ²⁺	Ni ²⁺	Ni ²⁺
Pb	Pb ²⁺	Pb(OH) ⁺	Pb ²⁺
Sb	Sb ^{III} O _x ?	Sb(OH) ₆ ⁻ ?	?
Se	HSeO ₃ ⁻ ; SeO ₄ ²⁻	SeO ₄ ²⁻	SeO ₄ ²⁻
Sn	Sn(OH) ₆ ²⁻ ?	Sn(OH) ₆ ²⁻ ?	?
V	V ^{IV} O _x ?	?	?
W	WO ₄ ²⁻ ?	WO ₄ ²⁻ ?	?
Zn	Zn ²⁺	Zn ²⁺	Zn ²⁺

^a Does not account for ion-pairs or complex-ion species.

^b Considers degree of bioavailability.

? = Most likely species.

4.1 Environmental Receptors in the Pilbara Region

There are numerous priority ecological communities (PECs) and threatened ecological communities (TECs) located throughout the Pilbara which have been identified as being important receptors of value by the Minister for Environment and the Environmental Protection Agency (EPA). Much emphasis is placed on protecting the groundwater dependent ecology which includes riparian vegetation communities (such as the *Melaleuca argenta*, *E. camaldulensis* and *Acacia aneura*), and subterranean fauna (including stygofauna and troglofauna). Also of great concern is the protection of priority drinking water sources including dams (e.g. Ophthalmia Dam which supplies the town of Newman) and regional borefields, and the numerous pit lakes and other smaller water bodies created by mining that may be used by birds, including long-distance migratory species.

4.1.1 Stygofauna

Metal contamination of groundwater is of global importance, not only effecting drinking water supplies, but the unique diversity of subterranean ecosystems (Hose et al., 2016). Little ecotoxicological data exist with which to assess the risks of trace metal mobility and uptake by subterranean fauna in the Pilbara. Reeves et. al. (2007) undertook a broad study of the distribution and diversity of subterranean ostracods in the Pilbara region and suggested that stygofauna are likely to be present in all aquifers of the Pilbara. In addition, the occurrence of

taxa within an aquifer was found to be primarily governed by alkalinity, salinity and pH, with many taxa being restricted to single aquifers. Such findings raise significant implications for conservation and management of stygofauna communities in the Pilbara influenced by mining activities, particularly given that new species are continually being discovered and such little information is known on their physiochemical adaptation to stress.

There are currently no groundwater ecosystem-specific water quality criteria available to identify metal toxicity risks to stygofauna. In the absence of these, Australian fresh water quality criteria (ANZECC and ARMCANZ 2000) are conventionally applied. Hose et al. (2016) tested the sensitivity of two species of copepods sourced from aquifers in NSW, Australia to As (III), Cr(VI) and Zn. The study assessed toxicity over increasing exposure periods and found that the copepods were variably sensitive to As, Cr and Zn, with Cr being the most toxic. The study suggested that currently applied water quality targets in Australia may not be entirely protective of groundwater ecosystems, given that copepod mortality occurred at similar levels to, or just above, the freshwater quality criteria for both As (III) (0.024 mg/L) and Cr(VI) (0.01 mg/L).

Such findings present a concerning risk to populations adjacent to, or downstream of AMD affected areas in the Pilbara considering that metal contaminants such as arsenic are known to be significantly enriched in some mined waste rocks.

4.1.2 Riparian vegetation and grazing animals

Plant species vary widely in their ability to tolerate excess trace metals in contaminated soils. Whereas some species might thrive (*hyperaccumulators*), others are sensitive and may perish. The riparian tree species *Eucalyptus camaldulensis* (River Red Gum) is broadly distributed in the Pilbara in proximity to watercourses. The species generally has a high tolerance for trace element contamination in soils, is known to accumulate metals into above-ground biomass and is considered advantageous for phytostabilization in countries such as Spain and Italy where there is a lack of adapted herbivores to feed on the biomass (Mughini et al 2013; Madejon, 2017). Whereas some plants may be tolerant to a certain excess of metals in soils, more elevated concentrations may cause toxicity. In Australia there is potentially a risk that trace elements may be transferred to the food chain, for example, by grazing animals such as sheep and cattle which may feed on the young seedlings growing in metal contaminated areas.

5.0 DISCUSSION AND CONCLUSIONS

While there may be a divergence in values of trace elements depending upon local geological and environmental factors, it is possible to recognise a relatively limited suite of potentially toxic trace elements that characterise the geochemical risk of iron ore mining in the Pilbara. These are sourced predominantly from widespread pyrite-bearing units of carbonaceous shale interbedded with the banded ironstones shales and localised occurrences of younger Cenozoic lignite. The various enrichment of toxic elements can be explained by the high sulfur content and the propensity for sulfide minerals, almost exclusively pyrite, to exhibit trace element substitution in the crystal structure. For a trace metal to behave toxically in the environment, it must be both mobile and bioavailable, which is an inherent function of the chemical speciation and partitioning within water, soil, sediment or dust matrices.

The Pilbara region of Western Australia, whilst arid and relatively isolated, hosts a diversity of ecosystems that may be susceptible to trace element toxicity. The relative paucity of both permanent surface freshwater sources and groundwater of useable quality, makes the ecological systems based on these water resources especially sensitive to contamination resulting from mining and waste rock storage. A further consideration when assessing the geochemical risks from mining activities in the Pilbara is climate change. Factors such as increased rates of salinisation and effects of more abundant large-scale cyclonic rainfall

episodes may significantly alter the rates of release and transport of trace element contaminants.

Focussed geochemical research is being conducted to understand better the speciation of trace metals found in AMD affected waters of the Pilbara and the characteristics of fate and transport in order to gain a more complete understanding of the long-term risk posed to important environmental receptors.

6.0 REFERENCES

Adriano, C. 2001. Trace elements in terrestrial environments. Biogeochemistry, bioavailability and risk of metals. Second edition. Springer.

BHP, 2016. Central Pilbara Water Resource Management Plan. Draft for consultation. Version 2.0. IDN: 0102609.

Bowen, H. 1979. Environmental chemistry of the elements. London; New York: Academic Press.

Buller, E. (2014). Net solute load response to the installation of infiltration limiting dry cover systems over acid forming waste piles. Thesis (Masters) University of Western Australia.

Chunca, Z., Gujian, L., Dun, W., Ting, F., Ruwei, W., & Xiang, F. 2014. Mobility behaviour and environmental implications of trace elements associated with coal gangue: A case study at the Huainan Coalfield in China. *Chemosphere*, 95.

Fajrin, A. (2013). Environmental impact of storage of lignite and black shale waste rocks at South Jimblebar Iron Ore Mine, Western Australia. Curtin University, Department of Applied Geology.

Finkelman, R.B., Orem, W., Castranova, V., Tatu, C.A. Belin, H.E. and Zheng, B. 2002. Health impacts of coal and coal use: possible solutions *Int. J. Coal Geol.*, 50, pp. 425–443.

Gardiner, S.J. 2003. Impacts of mining and mine closure on water quality and the nature of the shallow aquifer, Yandi Iron Ore Mine. MSc thesis (unpubl.), Curtin University.

Gauszka, A., Migaszewski, Z. M., Dogowska, S., Michalik, A., & Duczmal-czernikiewicz, A. 2015. Geochemical background of potentially toxic trace elements in soils of the historic copper mining area: A case study from miedzianka mt., holy cross mountains, south-central poland. *Environmental Earth Sciences*, 74(6), 4589-4605.

Green, R., and Borden, K. 2011. Geochemical Risk Assessment Process for Rio Tinto's Pilbara Iron Ore Mines, Integrated Waste Management - Volume I, Mr. Sunil Kumar (Ed.), InTech, DOI: 10.5772/20473.

Hose, G., Symington, K., Lott, M., & Lategan, M. 2016. The toxicity of arsenic(III), chromium(VI) and zinc to groundwater copepods. *Environmental Science and Pollution Research*, 23(18)

Kolker, A. 2012. Minor element distribution in iron disulfides in coal: A geochemical review. *International Journal of Coal Geology*, 94.

Madejon, P., Maranon, T., Navarro-Fernandez, C., Dominguez, M., Alegre, J., Robinson, B., & Murillo, J. 2017. Potential of *Eucalyptus camaldulensis* for phytostabilization and biomonitoring of trace-element contaminated soils.(Research Article)(Report). *PLoS ONE*, 12(6).

Mughini, G., Alianiello, F., Benedetti, A., Mughini Gras, L., Gras, M., & Salvati, L. (2013). Clonal variation in growth, arsenic and heavy metal uptakes of hybrid *Eucalyptus* clones in a Mediterranean environment. *Agroforestry Systems*, 87(4).

Nordstrom, D. 2011. Hydrogeochemical processes governing the origin, transport and fate of major and trace elements from mine wastes and mineralized rock to surface waters. *Applied Geochemistry*, 26(11).

Porterfield, D.C., Miller, S. and Waters, P. 2003. A strategy for managing acid rock drainage in arid climates – The Mt Whaleback Story. Sixth International Conference on Acid Rock Drainage. 6th ICARD, 14-17 July, 2003. Cairns, Queensland.

Prasad, M. 2008. Trace Elements as Contaminants and Nutrients Consequences in Ecosystems and Human Health (1st ed.). Hoboken.

Rajabian Tabesh, D. 2014. Determination of the selenium contents of waste rocks of iron ore mining in the Pilbara, Western Australia using ICP-MS. Curtin University, Western Australian School of Mines.

Reeves, J., Deckker, P., and Halse, S. 2007. Groundwater Ostracods from the arid Pilbara region of northwestern Australia: distribution and water chemistry. *Hydrobiologia*, 585(1).

GEOCHEMICAL AND MINERALOGICAL CHARACTERISATION OF A TAILINGS-RICH SEDIMENT BANK, KING RIVER, WESTERN TASMANIA

S. Gilmour^A, A. Parbhakar-Fox^A, L. Jackson^A and D.R. Cooke^B

^AARC Industrial Hub for Transforming the Mining Value Chain (TMVC), University of Tasmania, Private Bag 79, Sandy Bay, TAS 7001, Australia

^B ARC Centre of Excellence in Ore Deposits (CODES), University of Tasmania, Private Bag 79, Sandy Bay, TAS 7001, Australia

ABSTRACT

The Queen-King River system, Western Tasmania, has been severely impacted by historical mining operations (1890s onwards) at the Mt. Lyell Copper mine, Queenstown. For several decades until 1995, riverine processing waste disposal was practiced with approximately 100 Mt of mine tailings and slag materials discharged directly into the Queen River, a tributary of the larger King River. The movement of these wastes has contributed to the genetics of the 2.5 km² King River delta at Macquarie Harbour, which contains approximately 10 Mt of mine tailings, with a further 10 Mt of fine tailings deposited at the delta front. In this study, we characterised one sediment bank in the King River system (termed Bank D) located approximately 2.5 km from Macquarie Harbour. The objectives were to examine the mine tailings (quantity, degree of oxidation) in the upper 15 cm of the bank and; ii) determine the mobility of elements contained in these surface sediments. In addition basic water quality parameters (pH, EC, dissolved oxygen and redox potential) were analysed in-field using waters collected from an existing nest of piezometers, and a trench dug to 1 m to examine the tailings profile. After drying, sediments (n = 29) were subjected to a range of traditional acid-base accounting tests and mineralogical analyses by X-ray diffractometry and field-emission scanning electron microscopy, and three leach tests. Results showed that the majority of sediments are acid forming with primary pyrite observed and secondary framboidal pyrite actively precipitating. Acidic pH values were measured in pore waters and the King River itself. These sulphides are enriched in Cu and Zn. The sediments also contain iron-oxides enriched in Mn, Zn and Ni which are relatively immobile under these surficial conditions. Our results highlight the need for further characterisation and remediation of these sediments, which, after 98 years since their deposition, continue to pose a geoenvironmental risk to Macquarie Harbour.

1.0 INTRODUCTION

At Mt Lyell, Queenstown, Western Tasmania, more than 20 sulphide-rich volcanic-hosted massive sulphide ore bodies have been worked for copper since 1883 (KoeHNken, 1997). The Cambrian Mount Read Volcanics host this mineralisation, and it is associated with an extensive zone of hydrothermal alteration. Further, the area has also experienced greenschist-grade metamorphism. The early open pit mining at the Iron Blow produced approximately 5.6 Mt of ore at 1.8% Cu, 1% Zn, 0.2% Pb, 15 g/t Ag and 2 g/t Au, with approximately 4.5 Mt of sulphide-bearing waste rock dumped on surrounding hillsides (Locher, 1997). Later mining activities at

North Lyell, Crown Lyell, Cape Horn, Royal Tharsis, Lyell Comstock and Lyell Tharsis were almost exclusively underground, with grades ranged from 1.4% to 4.3% Cu, 0.4 g/t to 0.7 g/t Au and 2.8 g/t to 33 g/t Ag. The mining of these ore bodies produced an additional 1.5 Mt of ore and a similar amount of waste rock to that from Iron Blow. However, the largest open cut operation occurred at West Lyell (1934 to 1978) and produced 58 Mt of ore with 47 Mt of pyritic waste rock dumped in the area (Koehnken, 1997). The most recent mining operations, beneath the floor of the West Lyell open pit, were underground. A total of 87.6 Mt has been produced from mining the Prince Lyell orebody at average grades of 0.9% Cu, 0.3 g/t Au and 2 g/t Ag.

The environmental impact of the mine is extensive and is a globally renowned example of acid and metalliferous drainage (AMD). Haulage Creek drains the mine, transporting AMD from historic adits and waste rock pile seepage, and is a tributary of the Queen River which is in turn a tributary to the King River. The King River drains into Macquarie Harbour on the west coast of Tasmania. However, both the Queen and King Rivers are severely impacted in addition to aquatic life in Macquarie Harbour (e.g., fish kills in trout farms in the harbour). Aside from AMD resulting from the waste rock piles, there is a huge impact from slag (1.4 Mt) and mine tailings (97 Mt) which were deposited into the Queen and King River systems since mineral processing began in Queenstown in 1918 (Locher, 1997). The sediments are rich in pyrite, which resides in overbank, river bottom and delta deposits associated with the King River. The sediments and their pore waters contain potentially dangerous concentrations of metals and acid that are toxic to aquatic life in the King River and Macquarie Harbour (Locher, 1997). In order to quantify the current impact of the mine-impacted sediments on water quality (i.e., 98 years after mineral processing began), an integrated program of field and analytical work was conducted in this study. Specifically, surface sediment samples and pore waters from piezometers were collected at Haulage Creek and at a location termed 'Bank D' (approximately 2.5 km inland from Macquarie Harbour; Figure 1) on the King River.

2.0 MATERIALS AND METHODS

2.1 Study Location and Sampling

At Bank D, 29 sediment samples (i.e., adjacent to piezometer locations and from a trench as shown in Figure 1) were hand-collected from the upper 5 to 15 cm of the sediment bank using a clean trowel in September 2016. A trench was hand-dug to 1 m and sediments were also collected at the surface and at 50 cm depth. These were placed into labelled paper bags and transported to UTas. In addition, piezometers were sampled with basic water quality parameters (pH, electrical conductivity, redox potential, dissolved oxygen, temperature) assessed in-field, and a geophysical survey conducted. To provide a geochemical and mineralogical contrast, a sediment sample from the iron-terraces on the banks of Haulage Creek was collected prior to its confluence with the Queen River.

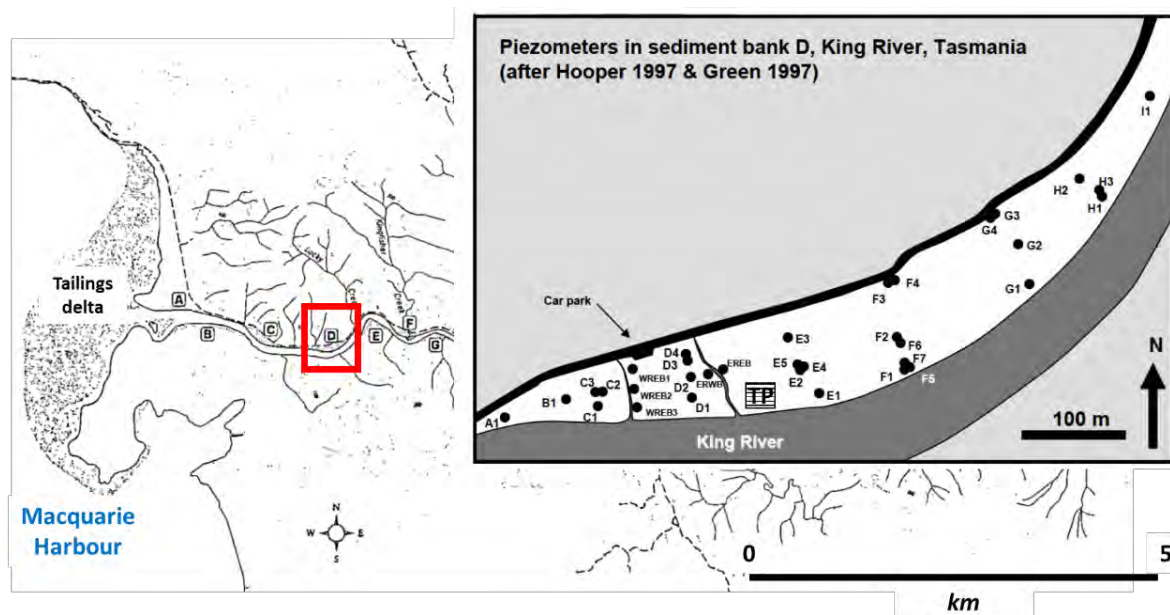


Fig. 1. Location and designation of the King River sediment banks and inset the piezometers established in sediment Bank D, King River Tasmania where surface sediments were collected in addition to the trench (given the designation TP; modified from Locher, 1997).

2.2 Mineralogical Characterisation

The bulk mineralogy of each sample was measured by X-ray (XRD) using a benchtop Bruker D2 Phaser XRD instrument with a Co X-ray tube. Each milled sample was further processed using an agate pestle and mortar to 10 μm . Each sample was analysed for an hour (operating conditions: 30 kV, 10 mA, 0.6 mm (0.3°) fixed divergence slit, 2.5° soller slit, Fe-filter; scan range: 5 to 120° (2θ), step size: 0.02°). Mineral phases were identified using the Bruker DIFFRAC.EVA software package with the PDF-2 (2012 release) powder diffraction file mineral database. Mineral abundances were semi-quantified by Rietveld analysis using TOPAS pattern analysis software). Minerals were identified using the Bruker DIFFRAC.EVA software package with the PDF-2 (2012 release) powder diffraction file mineral database. Mineral abundances were semi-quantified by Rietveld analysis using TOPAS (Version 4.2) pattern analysis software.

To observe the presence and morphology of pyrite in these sediments, several ($n=4$) were analysed using a Hitachi SU-70 field emission scanning electron microscope (FE-SEM) at UTas. This instrument allows for high-resolution imaging and permits X-ray element mapping. Polished resin mounts containing oven-dried powdered sediments were prepared and carbon coated prior to analyses. Samples were then loaded into the instrument and analysed in both back scattered electron and scanning electron imaging modes. Oxford AZTEC software was used to assist in mineralogical identification.

2.3 Geochemical Analyses

To measure the bulk chemistry, powdered samples ($n=29$) were loaded into plastic XRF cups covered with 4 μm polypropylene microanalytical film and portable XRF (pXRF) analyses were performed at UTas using an Innov-X Delta DP-6000 Premium instrument equipped with a rhodium (Rd) X-ray tube anode. Analyses were performed in two modes; three beam soil mode (40 keV, 40 keV and 15 keV) with 40 seconds of analysis time for each beam, and 2 beam (40

keV and 15 keV) environment mode with 60 seconds of analysis time for each beam. Each sample was measured twice on each setting, and physically moved between measurements. Reference standards (MT13NF059, GSS7, GXR4 (542), Tas Bas, Tas Dol and Tas Gran and an SiO₂ blank) were used throughout the analysis. Data processing was performed in MS Excel, with correction factors for each element calculated from the references standards, and applied to the data. In addition, total sulphur (wt. %) and carbon (wt. %) were measured separately using a Thermo Finnigan EA 1112 Series Flash Elemental Analyser.

A series of leach experiments were performed on select samples (n=15; i.e., where there was enough sample material). This included using a paste pH testing following the procedure outlined in Smart et al. (2002) to replicate a water soluble fraction. The pH measurements were recorded in triplicate, with the standard deviation calculated as <0.03. Following measurements, a portion of each leachate (20 mL) was extracted and filtered (0.45 µm PES milipore) and preserved by acidification with 1% HNO₃ for elemental analyses by ICPMS. Next, the single-addition NAG test was performed to determine the oxidisable or sulphide-bound fraction. The procedure of Smart et al. (2002) was followed with measurements of pH and EC performed as per the paste pH measurement protocols (standard deviation: <0.05). The resulting leachates were also filtered and acidified for elemental analyses. Finally, to determine the elements associated with the iron oxide fraction, the sequential extraction leach procedure given in Dold (2003) was performed. Solution ICPMS was performed on the leachates using an Element 2 HR-ICP-MS instrument. Calibration standards were made up using single and multi-element analytical solutions. The major element standard (K, Fe, Al, Na, Ca, Mn and Pb) were made up to 10, 50, 100 and 10,000 ppb. Trace element standards were made up to 10, 100, 200 and 1000 ppb. Internal standards In115 and Re185 were used and added inline. Finally, these data were processed using MassHunter software from Agilent.

3.0 RESULTS

3.1 Bulk Characteristics

The surficial sediments comprised of a brown, medium-grained sand with silt. Hardpan had formed in areas distal to the creeks observed on the sediment bank surface. This horizon was underlain by an organic-matter bearing medium-grained sand (note- *juncus pallidus* had extensively recolonised across the bank, causing some difficulty during sampling). Ferricrete/hardpan horizons were observed at the base of each layer depicting paleosurfaces. Examination of deeper trench sediments showed the presence of an organic matter layer (30 cm depth) that comprised of woody organics and an organic-rich clay. Diagenetic pyrite had precipitated on the woody organics. The XRD patterns were sharp, suggesting minimal content of amorphous material. The bulk mineralogy was dominated by quartz (46 to 74 wt. %), muscovite (15 to 28 wt. %) and chlorite (up to 5 wt. %) for the majority of samples. Up to 5 wt. % pyrite, 1 wt. % chalcopyrite and 1 wt. % jarosite were measured, with goethite present in all Bank D samples at concentrations ranging from 2 to 10 wt. % in addition to hematite, identified in all up to 2 wt. %. In contrast, a grab sample taken from Haulage Creek contained 20% amorphous material, with 30 % quartz, 26 % goethite and up to 1 % pyrite. Measurements of bulk chemistry reported maximum contents of potentially deleterious elements across all samples including Cu (up to 0.2 wt. %), Zn (320 ppm), Pb (100 ppm), As (90 ppm) and Ni (45 ppm). Other elements including Al, Cd and Co were below the instruments detection limit.

Calculation of maximum potential acidity (MPA) based on total sulphur values gave a range of 2 to 148 kg H₂SO₄/t with the highest value reported at location A1 (note, this is a conservative estimate as the presence of jarosite has not been discounted). As no carbonate minerals (e.g., calcite, dolomite) were identified during bulk-XRD analyses, it is assumed negligible acid neutralising capacity. Measurements of pH distribution show higher pH conditions where creeks are observed to the east and west of the site, with a pH of 4.9 measured in the King River (Figure 2).



Fig. 2. Measurements of pH across sediment bank D of the King River.

A geochemical plot of paste pH against NAG pH values confirms this showing there are no NAF samples in this cohort (Figure 3). The highest risk sample was from Haulage Creek (HC1) with the other high-risk samples from the trial pit trench (TP1) and E1B, located to the south of the site, where low groundwater pH values were also measured (Figure 2). Ten samples fell into the uncertain field; however these samples contained high quantities of iron-oxides which have released protons readily during paste pH testing causing this (Noble et al., 2016). The remainder are distinctly acid forming.

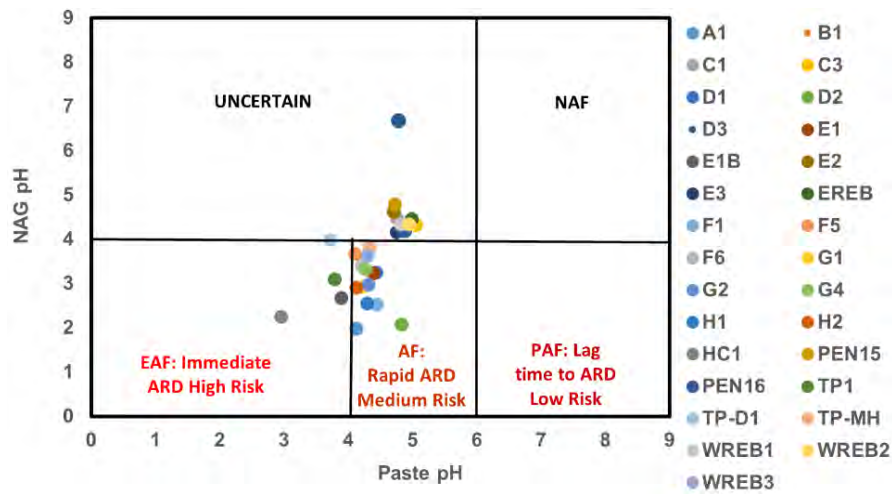


Fig. 3. Geochemical plot showing NAG pH vs. paste pH classifications for Bank D and Haulage Creek sediments.

3.2 Pyrite and Iron-oxide Characteristics

Pyrite in Haulage Creek sediments was predominantly encapsulated in quartz as anhedral blebs up to 75 μm diameter (Figure 4a). In addition, massive iron oxide phases with variable major element compositions (i.e., both goethite and hematite) were observed with quartz veining occasionally observed to cross cut these (Figure 4b). However, iron oxide phases were also observed to rim smaller (50 μm diameter) liberated grains of pyrite (Figure 4c) with autigenic framboidal pyrite (20 μm diameter) also recognised (Figure 4d). As these materials move downstream towards Bank D, they have undergone attrition with iron oxide phases intensely fractured (Figure 4e) and both pyrite and chalcopyrite phases liberated (i.e., bright phases shown in Figures 4e and 4f). Framboidal pyrite similar to that in Figure 4d were also observed in these sediments. The increased degree of fracturing, and liberation of these minerals, suggests that there is high potential for their release, under the right geochemical conditions, at Bank D. Element mapping of these phases recognised major elements only, therefore, relating differences in texture to trace element chemistry was not possible, with the exception of Bank D pyrite, which was depicted as Cu-bearing.

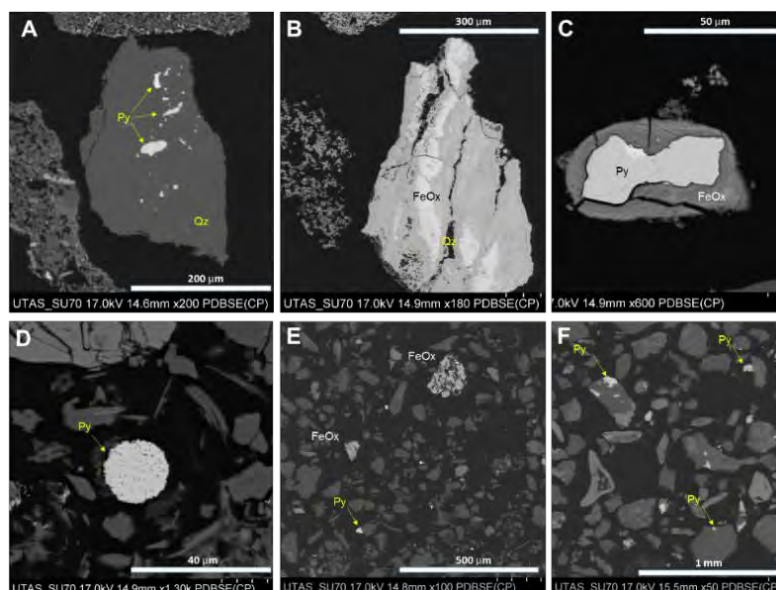


Fig. 4. Back scattered electron images of pyrite and iron oxide phases observed in Haulage Creek and Bank D sediments (abbreviations: FeOx, iron oxide; Py, pyrite; Qz, quartz).

3.3 Leach Characteristics

Relative to ANZECC aquatic protection guideline values (2000) at the 95% level, no exceedances were recorded for Cd, Ni or As from Bank D sediments when deionised water was used as the extractant. However, for Cu and Zn, exceedances were reported at 10 (0.01 to 0.2 mg/l) and 13 (0.01 to 0.29 mg/l) of the 14 studied locations respectively. For Cu, no spatial relationship was recognised, but, in the case of Zn, highest values were measured in proximity to the King River, with the concentration decreasing away from the tideline. Similarly, at Haulage Creek, exceedances for Cu (3.91 mg/l) and Zn (24.9 mg/l) were also reported, albeit 1 to 2 orders of magnitude greater, with Al also considerably high (75.5 mg/l). When hydrogen peroxide was used as the extractant, 12 exceedances were reported for Cu (0.01 to 7.12 mg/l) and 7 for Zn (0.01 to 0.65 mg/l). In addition, 4 exceedances for Ni were also recorded (0.01 to 0.18 mg/l), but not for As or Pb. A large range of values were reported for Al (0.06 to 13.37 mg/l) with the highest reported at location A1. Cobalt (up to 1 mg/l, with maximum also at A1) was also notably higher compared to when using water as the extractant. Leachate derived from the Haulage Creek sample reported 11.23 mg/l Cu, 3.79 mg/l Zn, 0.07 mg/l Ni and 0.04 mg/l Pb, all of which are above guideline values, suggesting that, on oxidation, these contaminants will leach. Finally, the iron oxide targeted leachates reported 13 exceedances of Cu (0.01 to 0.19 mg/l), 7 for Zn (0.01 to 0.27 mg/l) and all were Ni (0.05 to 0.31 mg/l) and Co (0.03-0.1 mg/l) bearing, suggesting under reductive conditions (e.g., vegetation cover) there remain contaminant risks. The Haulage Creek sample reported lower concentrations of Zn (7.42 mg/l) and Cu (0.79 mg/l) but slightly higher Ni (0.17 mg/l) and Pb (0.06 mg/l).

A relative comparison of leachates concentrations from the three leach tests are shown in Figures 5 and 6 with a focus on select potential deleterious elements (Cd, Pb, Co, Ni, Cu, Zn and As). For the Haulage Creek sediments (Figure 5), Cd, Co, Ni, Zn and As are predominately water-soluble, whilst the Cu (70%) is associated with oxidisable phases (e.g., sulphides) in addition to Cd, Pb and Co, though these are present at much lower quantities. A significant proportion of Pb departs to iron oxides, with a roughly equal quantity of Cd, Co, Ni, Zn

(approximately 20%) and Cu (5%) also associated with these oxides. In contrast, at Bank D, a greater proportion of these elements are associated with the iron-oxide fraction, particularly Pb, Ni and As (Figure 6). Copper is now almost exclusively associated with the oxidisable fraction (i.e., pyrite and chalcopyrite), and the proportion of Cd and Co associated with this fraction has also increased with their concentration in the water-soluble fraction notably decreasing.

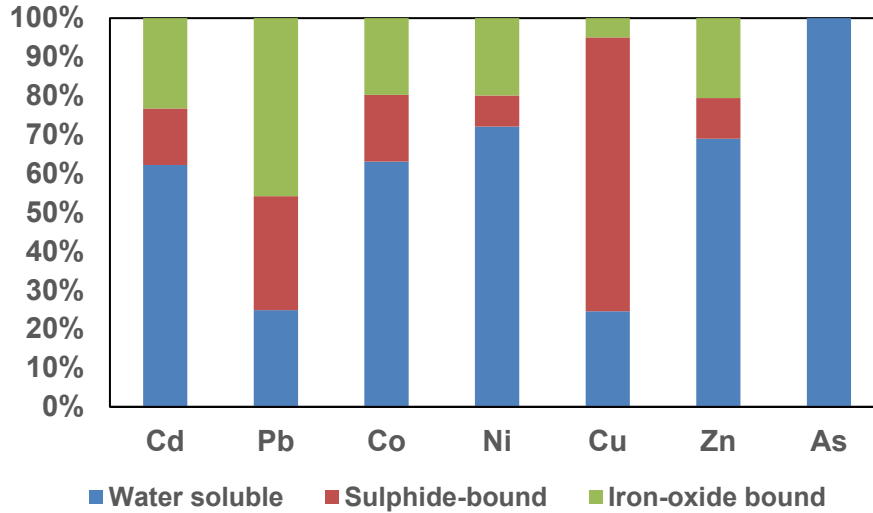


Fig. 5. Comparison of leached metal concentrations in the Haulage Creek sediment sample.

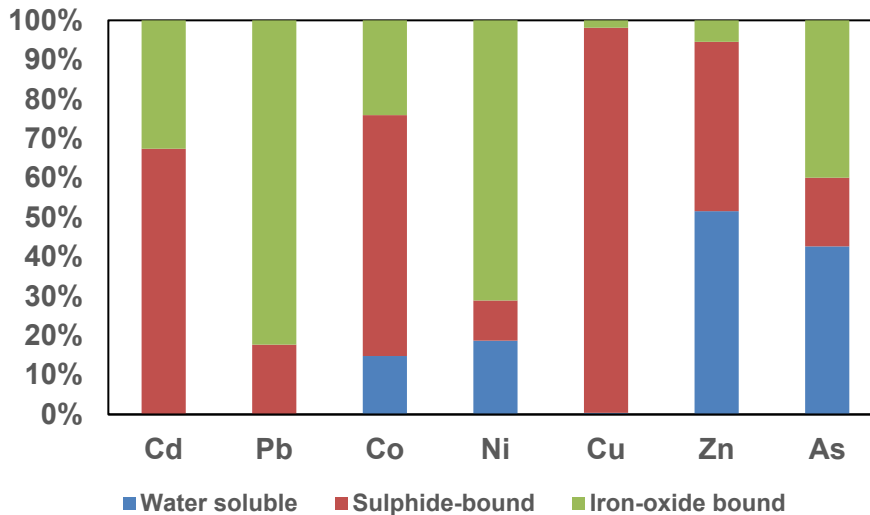


Fig. 6. Comparison of leached metal concentrations in the Bank D sediment samples (n =14).

4.0 DISCUSSION AND CONCLUSIONS

The majority of mine waste deposited in the Queen/King river system has been carried in suspension and deposited in the delta at the mouth of the King River and has also prograded out to form a delta front on the harbour floor. This study corroborates observations made by Locher (1997), whereby it was noted that sediments (i.e, > 100 µm) of the tailings (up to 30

Mt) have not yet made it out of the river system and continue to infill the King River to just below sea level. The sediment collected at Haulage Creek showed several pyrite types exist in these materials, those that are encapsulated in silicate (i.e., quartz) phases and much younger, liberated, diagenetic framboidal pyrite. This framboidal pyrite is likely Cu-bearing, whilst older, euhedral, encapsulated pyrite is Co and Ni bearing (Lehner and Savage, 2008). These sediments remain reactive with elevated concentrations of Cu, Zn, Ni and Pb leaching naturally, from amorphous phases contained in these sediments (i.e., loosely adsorbed cations at their surface allowing them to be readily water-soluble; Dold, 2003), and through the oxidation of liberated framboidal pyrite, with a high surface area for reaction (Weisner and Weber, 2010). At Bank D, reactive mine waste sediments remain at shallow depth; however they are notably more oxidised than at Haulage Creek, with extensive formation of iron-oxides and jarosite. Hardpan layers have developed, reducing the geoenvironmental impact of these sediments through retarding oxidation. Movement of groundwater through Bank D is slow, with at least two aquifers likely present, one of which is confined between the clay horizons observed in the trench profile. Measurements of pH show that the most acidic areas are at the tideline, this area is the most affected by flow and tidal erosion and exposure of fresh sediments to oxidation processes, with the least well developed hardpan observed here. More alkaline waters were measured in the middle of Bank D, and towards the train line, indicating fresh water recharge. Significant quantities of Cu were measured in the sulphide fraction. Based on our hydrological testing, we calculate that approximately 0.24 to 1.42 kg/day Cu enters the King River from Bank D. Whilst 1.5 Mt of slag materials were reported to have entered the Queen-King river system, they were not observed in our trench, or SEM studies, suggesting they are located at depth, or have migrated further towards Macquarie Harbour.

Collectively these data suggest that, if left passively managed, this sediment bank still presents a geoenvironmental risk to Macquarie Harbour, an area that is used actively for fish-farming (e.g., <https://www.huonaqua.com.au/about/truth/macquarie-harbour/>). A management plan to remediate this site is necessary to protect the future of this industry; however, it is likely that all sediment banks upstream of this location (Figure 1) possess similar, if not more severe, characteristics, as our sediment sample from Haulage Creek indicates. A study conducted by Taylor et al. (1996) calculated that based on hydrogeological parameters and groundwater chemistry, the metal mass loadings recorded from groundwater discharge and surface water runoff are predicted to continue for thousands to tens of thousands of years. Forstner (2005) stated that remediation techniques for contaminated sediments are much more limited than for other solid waste materials as the diverse contamination sources produce a mixture of pollutants, which can be more difficult to treat than an industrial waste. Taylor et al. (1996) recognised that disturbance of the sediments (i.e., exposure of fresh tailings to oxidation processes) would promote low pH conditions and further negatively impact on water quality. Instead, they recommended the installation of low permeability, reactive substrates (clay + calcium/magnesium carbonate + organic matter) on the sediment banks prior to revegetation. This was intended to assist with decreasing groundwater discharges, decreasing surface water / tailings interaction, and developing sustainable revegetation programmes. Further, they stated that enhancing and extending naturally occurring bioremediation processes in the delta would be the most cost-effective method for improving the quality of groundwater discharges from the delta. However, this could only be achieved by inundating dry sediment with water and providing organic matter to promote the growth of sulphate reducing bacteria.

Alternatively, a reactive phased approach could be adopted whereby the river water could be neutralised with lime; however, iron coatings can form and inhibit further reaction and can also fix metals unless an anoxic limestone drain is used. However, the CAPEX and OPEX costs associated with such a scheme will likely exceed that available to spend on remediation by the State Government. A remediation scheme that focusses on the management of the contaminant source is likely to be the most robust long-term approach, whereby the vertical and lateral extent of tailings/slag is mapped spatially (using geophysical techniques). Next, the mineral chemistry properties of these materials should be determined, for example, pyrite emanating from Mt Lyell tailings is enriched in cobalt (Raymond, 1996); therefore a characterisation program should be undertaken to determine if it can be metallurgically recovered. Further, these mineral chemistry investigations should extend to characterising if the slag materials still contain economic quantities of base-metals which have potential to be efficiently recovered. These sediments should be removed through a well-designed dredging program (e.g., van Maren et al., 2016; Alvarez et al., 2017). Whilst this is also a costly approach to remediation and rehabilitation of this river system, funds could be recovered if these processed mine wastes contain value. Research into the geometallurgy of Macquarie Harbour sediments will commence in 2017 with these results assisting in planning for the future of this mine-impacted catchment.

5.0 ACKNOWLEDGEMENTS

The UTas Dean of Science, Engineering and Technology Summer Research Scholarship program provided financial assistance to the first author. The ARC Transforming the Mining Value Chain are thanked for providing research funds. Dr Ashley Townsend (UTas) is thanked for assisting with ICP-MS analyses and Dr Nathan Fox (UTas) for assisting with XRD analyses. Finally, the UTas KEA 348 Class of 2016 are thanked for their assistance with sample collection and transportation.

6.0 REFERENCES

- Alvarez, M., Carballo, R., Ramos, V. and Iglesias, G. 2017. An integrated approach for the planning of dredging operations in estuaries. *Ocean Engineering*, 140: 73-83.
- ANZECC 2000. Australian and New Zealand guidelines for fresh and marine waters. National Water Quality Management Strategy. Australian and New Zealand Environment and Conservation Council & Agriculture Resource Management Council of Australia and New Zealand, Canberra.
- Dold, B. 2003. Speciation of the most soluble phases in a sequential extraction procedure adapted for geochemical studies of copper sulphide mine waste. *Journal of Geochemical Exploration*, 80:55-68.
- Förstner, U. 2005. NEAR Curriculum in Natural Environmental Science, *Terre et Environnement*, Vol. 50, 93-108, ISBN 2-940153-49-3 <http://www.unige.ch/sciences/near/pdf/Forstner%202005.pdf>
- Koehnken, L. 1997. Final report: Mount Lyell Remediation Research and Demonstration Program. Supervising Scientist Report 126. ISSN 1325-1554/ISBN 0 642 24326 3. <http://www.environment.gov.au/science/supervising-scientist/publications/ssr/final-report-mount-lyell-remediation-research-and-demonstration-program>

Lehner, S. and Savage, K. 2008. The effect of As, Co and Ni impurities on pyrite oxidation kinetics: Batch and flow-through reactor experiments with synthetic pyrite. *Applied Geochemistry*, 72: 1788-1800.

Locher, H. 1997. Sediment Transport in the King River. Supervising Scientist Report 120. ISSN 1325-1554/ ISBN 0 642 24320 4.
<https://www.environment.gov.au/system/files/resources/15e6c76e-ade4-4cc2-ae9-17700543d558/files/ssr120part1.pdf>

Noble, T.L., Lottermoser, B.G. and Parbhakar-Fox, A. 2016. Evaluation of pH testing methods for sulfidic mine waste. *Mine Water and the Environment*, 35: 318-331.

Raymond, O.L. 1996. Pyrite composition and ore genesis in the Prince Lyell copper deposit, Mt Lyell mineral field, western Tasmania, Australia. *Ore Geology Reviews*, 10: 231-250.

Smart, R., Skinner, W.M., Levay, G., Gerson, A.R., Thomas, J.E., Sobieraj, H., Schumann, R., Weisener, C.G., Weber, P.A., Miller, S.D. and Stewart, W.A. 2002. ARD test handbook: Project P387, A prediction and kinetic control of acid mine drainage, Melbourne, Australia: AMIRA, International Ltd, Ian Wark Research Institute.

Taylor, J., Weaver, T.R., McPhail, D.C. and Murphy, N.C. 1996. Characterisation and impact of mine tailings in the King River system and delta, Western Tasmania. Project No.5 of the Mount Lyell Remediation Research and Demonstration Program.
http://www.earthsystems.com.au/wp-content/uploads/2012/03/Mt_Lyell.pdf

Van Maren, D.S., Oost, A.P., Wang, Z.B. Vos, P.C. 2016. The effect of land reclamations and sediment extraction on the suspended concentration in the Ems Estuary. *Marine Geology*, 276: 147-157.

Weisener, C.G. and Weber, P.A., 2010. Preferential oxidation of pyrite as a function of morphology and relict texture, *New Zealand Journal of Geology and Geophysics*, 53: 22-33.

INTRINSIC NEUTRALISATION POTENTIAL FROM AUTOMATED DRILLCORE LOGGING FOR IMPROVED GEOENVIRONMENTAL DOMAINING

L. Jackson^A, A. Parbhakar-Fox^A, N. Fox^B, D.R. Cooke^A,
A.C. Harris^C and E. Savinova^D

^ATransforming the Mining Value Chain, ARC Industrial Transformation Research Hub,
University of Tasmania, Private Bag 79, Hobart TAS 7001, Australia

^BCRC ORE II, University of Tasmania, Private Bag 79, Hobart TAS 7001, Australia.

^CNewcrest Mining Limited Level 8, 600 St Kilda Road, Melbourne, VIC 3004, Australia

^DCorescan PTY, LTD, 1/127, Grandstand Road Ascot, WA 6104, Australia

ABSTRACT

Hyperspectral analysis integrating near-infrared (NIR), shortwave infrared (SWIR) and longwave infrared (LWIR) spectrometry can accurately identify carbonate, silicate and serpentine-group minerals. Significantly these mineral-groups offer short and long term neutralising capacity respectively in a range of mine waste environments. Routine hyperspectral mineral analysis is increasingly used for geometallurgical and geological domaining of ore deposits; however the mineralogical information obtained is rarely used for deposit-scale geoenvironmental characterisation. Evaluating the location, volume, and chemistry of neutralising gangue materials early in the mine planning process will permit prudent economic forecasting with regards to mine closure and beyond. By accurately identifying short- and long-term neutralising minerals in low (or below) grade material, their use within rock and tailings storage facilities can help to alleviate the need to acquire costly neutralising materials particularly at the time of mine closure.

This study focusses on using data generated by hyperspectral mineralogy platforms to develop geoenvironmental domaining algorithms. Seven drill holes from a porphyry Au-Cu deposit were analysed, with hyperspectral results validated against established geoenvironmental characterisation tests (including acid base accounting and X-ray diffractometry). These data show that neutralising characteristics of differing alteration types can be predicted accurately from hyperspectral data. Furthermore, when used in conjunction with NAG pH, these data could be used to precisely identify neutralizing and acid forming zones.

1.0 INTRODUCTION

Mining impacts on the environment can occur at any point during the life-of-mine (LOM) with many examples published in the scientific literature (e.g., Hyndman, 2001, Harris et al., 2003, Edraki et al., 2005, Parbhakar-Fox et al., 2014, Candeias et al., 2014, Staebe, 2015 and Myers, 2016). While sulfide oxidation and acid and metalliferous drainage (AMD) is significant, other environmental impacts of mining include: vegetation clearance for the construction of access roads, infrastructure (e.g., processing, milling, survey lines, drill sites, and exploration tracks); hydrological disturbance; creation of waste repositories and landforms (e.g., tailings dams and waste piles); surface subsidence, excessive water use, dust generation, and release of solid, liquid, or gaseous contaminants into surrounding ecosystems (e.g., Castilla 1993; Harries

1997; Davis et al., 2000; Harris et al., 2003; Edraki et al., 2005; Candeias et al., 2014; Schoenberger, 2016 and Venkateswarlu et al., 2016). Failure to predict and manage mine waste appropriately from the beginning of operation, such as at the Mt Lyell mine, (Waggitt and Jones, 1996) and Rio Tinto (Hudson-Edwards et al., 1999), highlights the extensive timeline of continual metal leaching and AMD resulting in long-term ecosystem degradation.

Australia alone has more than 60,000 abandoned mines (ABC, 2017), some of which represent a significant threat from contamination; others may pose safety risks; and still others may be losing their value as cultural heritage (Unger et al., 2011). Estimated rehabilitation costs for mining legacy sites are over AUD \$1 billion in liabilities (Pepper et al., 2014), which is considered much greater than the cost of managing potentially acid forming wastes during mine operation. Mudd (2008) stated that lower grade ore deposits are being exploited for a large-range of commodities (e.g., Ag, Au, Cu, Sn); consequently the mining industry is producing significant volumes of mineral waste, approximately 4 gigatonnes/year (Haas et al., 2015). Globally, mineralized waste is one of the largest industrial waste streams (Lèbre et al., 2017).

The mining industry needs protocols in place to effectively minimise environmental footprints and work towards benign mine closure. An understanding of the long-term release of contaminants requires a solid knowledge of the factors that control discharge. However, the most significant factor influencing contaminant release is the mineralogy (and textural arrangement of these minerals) of the resource host rocks and therefore is critical to define for adequate geoenvironmental prediction. Robust upfront mineralogical characterisation could not only prove advantageous in the long-term for environmental management but also could result in identification of useful secondary remediation materials which would otherwise end up in the waste rock piles or tailings dams. Therefore, the challenge is to develop predictive AMD protocols that can be implemented in early LOM stages, (i.e., pre-feasibility/feasibility) to effectively characterise waste material in order to minimise potential AMD liabilities. This would allow for a detailed understanding of the AMD and metal leaching characteristics of a deposit to be established prior to mine operation. In this study, drill core from an operating porphyry Au-Cu mine was used to develop and test this new methodology.

2.0 MATERIALS AND METHODS

2.1 Mineralogical Characterisation

2.1.1 Hyperspectral analysis

Split drillcore were scanned using the Corescan[®] HCI- 3 system. The scanning measurements operate across the VNIR and SWIR bands from 450 nm – 2500 nm at a spectral resolution of ~4 nm (Figure 1). The Corescan[®] system produces full, continuous images along-core, with operating ranges as follows: photography, 50 µm; spectral imagery, 500 µm; and profiler image, 200 µm. High quality optics focus the spectral measurement to a 0.5 mm point on the core, maximising signal (average 2000:1 across the measured spectrum) and minimising spectral mixing therefore providing a near-pure spectral signature at each point on the core. This results in ~ 150,000 spectra per meter of scanned core. In addition, a spectrally calibrated RGB camera provides a high-resolution visual record of the core at 60 µm-pixel size. Measurement of core surface features, texture and shape is captured using a 3D laser profiler with a surface profile resolution of 20 µm.

The Corescan® hyperspectral imaging data were processed in-house. Reflectance spectral signatures were compared to an amalgamated reference spectral library. Identification and classification of mineral signatures were performed with proprietary Corescan® software based on a linear regression technique that isolates the position and overall architecture of spectral absorption minima and maxima that uniquely identify specific minerals (Martini et al., 2014). Classified mineral maps for the core are used to compute relative downhole mineralogy counts (exported as .csv files). The final 'product' identified 17 minerals and 3 additional mineral mixtures, and these were used to create mineral distribution, composition and classification maps. Aspectral is reported for minerals that do not reflect in the VNIR and SWIR spectrum.



Figure 1. Portable Corescan® container and instrument.

2.1.1.1 Hyperspectral sample selection

Corescan® offers visual classified mineral maps of continuous drillcore through an interactive viewing platform called Coreshed. Classified mineral maps of complete drillholes ($n=5$) were used to domain and guide sample selection (Figure 2). Figure 2 demonstrates how drillholes were broken up into mineralogical domains, drill tray numbers were selected from these domains, and a sample was chosen at random from the selected tray to best represent that domain.

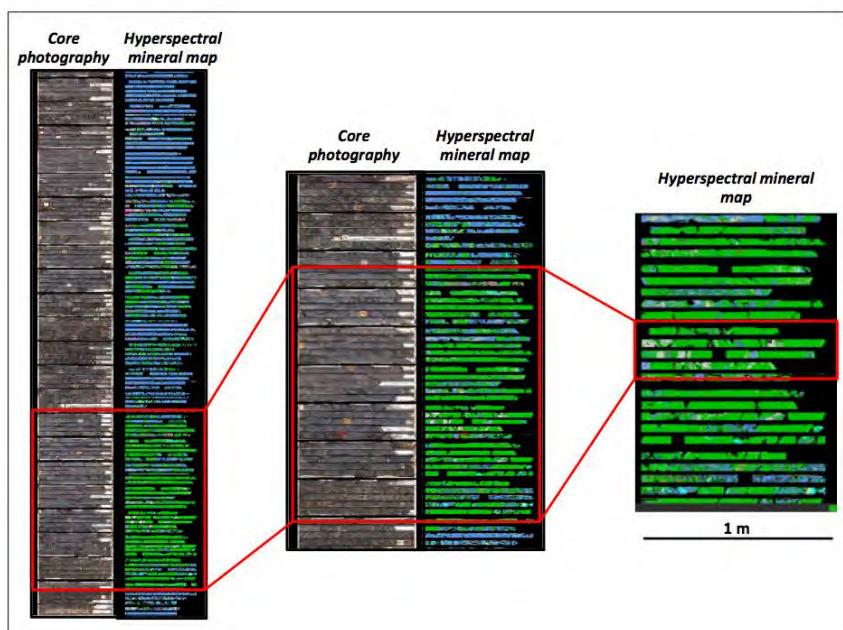


Figure 2. Example of Coreshed viewing platform used for mineralogical domain driven sampling. Red boxes indicate sampling guides and propagation to sample selection.

2.1.1.2 Hyperspectral geoenvironmental domaining

Corescan[®] offers visual qualitative mineralogical assessments through Coreshed. However, to gain semi-quantitative mineralogy, mineral counts were extracted and relative downhole mineralogy was used to calculate relative abundance. Individual mineral relative abundance was converted to percentage (*Equation 1*).

$$(min\ 1\ counts / (min\ 1\ counts + min\ 2\ counts + min\ 3\ counts) \dots) \quad (Eq.\ 1)$$

This can then be used to compare mineralogy on a sample by sample basis. This mineral percentage was multiplied by recognised mineral standard values obtained under experimental conditions. Jambor et al. (2007) and Parbhakar-Fox and Lottermoser (2014) measured neutralising potential (NP) for pure mineral specimens, and Sverdrup (1990) measured relative reactivity (RR) of pure mineral specimens (Table 1). These standards were used in the algorithm to allow forecasting of acid neutralising behavior (*Equation 2*), which we have termed Geoenvironmental Domaining Index (GDI).

$$(Min1\% * ((NP\ or\ AP) * RR) * 1000) + (Min2\% * ((NP\ or\ AP) * RR) * 1000) + (Min3\% * ((NP\ or\ AP) * RR) * 1000) \dots \quad (Eq.\ 2)$$

To simplify this algorithm, we used a scaled standard number for each mineral which accounts for both NP and RR and have termed it the Geoenvironmental Domaining Index Standard (GDIS). Equation 2 can be shortened (*Equation 3* and Table 1). Table 2 shows mock examples of how the GDI can change based on mineralogy.

$$(Min1\% * (GDIS)) + (Min2\% * (GDIS)) + (Min3\% * (GDIS)) \dots \quad (Eq.\ 3)$$

Table 1. Mineral neutralising potential values, relative reactivity values and corresponding GDIS values used for this study. * Indicates mineral mixtures where two separate spectra are unable to be separated due to small grain size and intergrowths.

Mineral	Neutralising Potential (kg CaCO ₃ /t) <i>Jambor et al. (2007); Parbhakar-Fox and Lottermoser (2014)</i>	Relative Reactivity <i>Sverdrup (1990)</i>	Geoenvironmental Domaining Index Standard (GDIS)
Amphibole	0.003	0.02	0.06
Aspectral	0	0	0
Biotite		0.02	0
Carbonate	1	1	1
Chlorite	0.006	0.02	0.12
Epidote	0.001	0.02	0.02
Gypsum	0.008	1	8
Laumontite	0.002	0.004	0.008
Magnetite	0	0.02	0
Montmorillonite	0.001	0.02	0.02
Phlogopite	0.008	0.02	0.16
Prehnite	0.006	0.02	0.12
Saponite	0.001	0.02	0.02
Sericite	0.001	0.01	0.01
Silica/quartz*	0	0.004	0
Tourmaline	0	0.02	0

Table 2. Mock examples of differing mineral combinations and corresponding GDI values.

Example	Mineral 1	%	Mineral 2	%	Mineral 3	%	GDI value
A	Carbonate	80	Quartz	20	-	-	80
B	Carbonate	50	Chlorite	30	Quartz	20	53.6
C	Carbonate	20	Chlorite	60	Quartz	20	27.2
D	Chlorite	80	Quartz	20	-	-	9.6

Table 3. First pass GDI risk classification

GDI value	GDI risk grade	Description of AMD risk classes
0 to 100	Low/potential risk	Dominated by silica/quartz, sericite, chlorite. Few sulfides present, primary neutralisers < 10%.
100 to 400	Low risk	Carbonate present as first mineral: 40 to 10%.
400 to 1,000	Very low risk/ ANC potential	Carbonate dominate as first mineral > 40%. Long term net-neutralising capacity likely.

2.1.2 XRD

To determine the bulk mineralogy, samples were analysed using a benchtop Bruker D2 Phaser XRD instrument at the University of Tasmania (with a Co X-ray tube). All drillcore samples were crushed, milled and micronised. Analysis was performed for 1 hour at an operating voltage of 30 kV and 10mA. Minerals were identified using the Bruker DIFFRAC.EVA software package with the PDF-2 (2012 release) powder diffraction file mineral database. Mineral abundances were semi-quantified by Rietveld refinement using TOPAS (Version 4.2) pattern analysis software.

2.2 Static Testing

The current acidity was assessed using the ASTM D4972-13 (2013) paste pH method following recommendations given in Noble et al. (2015). In addition, measurement of total sulfur (wt. %) for the calculation of maximum potential acidity (MPA) was performed using an Eltra C-S 2000 ($n=30$) with AR4015 and AR007 standards and a Thermo Finnigan EA 1112 Series Flash Elemental Analyser ($n=70$). Sample duplicates and blanks were incorporated to enable data processing, when both instruments were used. Multi-addition net acid generation (NAG) pH testing was conducted following the method outlined in Smart et al. (2002). Acid neutralising capacity testing (ANC) was conducted following the AMIRA P387A AMD Test Handbook method (Smart et al., 2002).

3.0 RESULTS

One example from the skarn alteration type of the porphyry deposit was chosen to compare results (Sample Z). Sample Z was visually logged to have abundant carbonate 60%, quartz 30% and minor chlorite 10%.

3.1 Hyperspectral Evaluation

Hyperspectral qualitative mineralogy for Sample Z is displayed in Figure 3. Figure 3a shows

the core sample as an RGB image. Figure 3b shows the carbonate spectral match. Warm colours (red, orange, yellow) indicate a high confidence between carbonate spectra recorded from analysis and carbonate spectra in the mineral library. Cool colours (green, blue) indicate a lower confidence between spectra recorded from analysis and carbonate spectra in the mineral library. Black shows no similarity between measured spectra and a match between carbonate. Figure 3c shows a Corescan[®] mineral class map. This represents identified mineralogy on a colour scheme. Sample Z shows a high abundance of carbonate throughout the sample. Corescan[®] calculated relative mineral abundance are displayed (Figure 3d). Aspectral, carbonate, quartz and sericite dominate (36.9%, 34.4%, 16.6% and 6.1% respectively). Semi-quantitative bulk mineralogy data from XRD are displayed for Sample Z (Figure 3e). Carbonate, quartz and chlorite dominate (56.3%, 28.7%, 4.7% and 4.4% respectively). The calculated GDI for Sample Z is 343.68, which is categorised as low risk (Table 3).

3.2 Geochemical Characteristics

Geochemical data were compiled into an interactive dashboard. Through this tool, all geochemical data can be displayed and easily compared. Each graph is then automatically scored and labeled according to the predetermined category (i.e., NAF = non acid forming). Figure 4 is an example of the interactive display page of the dashboard. Data displayed corresponds to sample Z. Figure 4a – 4e (S Total vs acid rock drainage (ARD) index, Paste pH vs S Total, Paste pH vs ARD Index and NAG pH vs paste pH) show that geochemically Sample Z is non-acid forming (NAF) and the sample is below economic grade (Figure 4f).

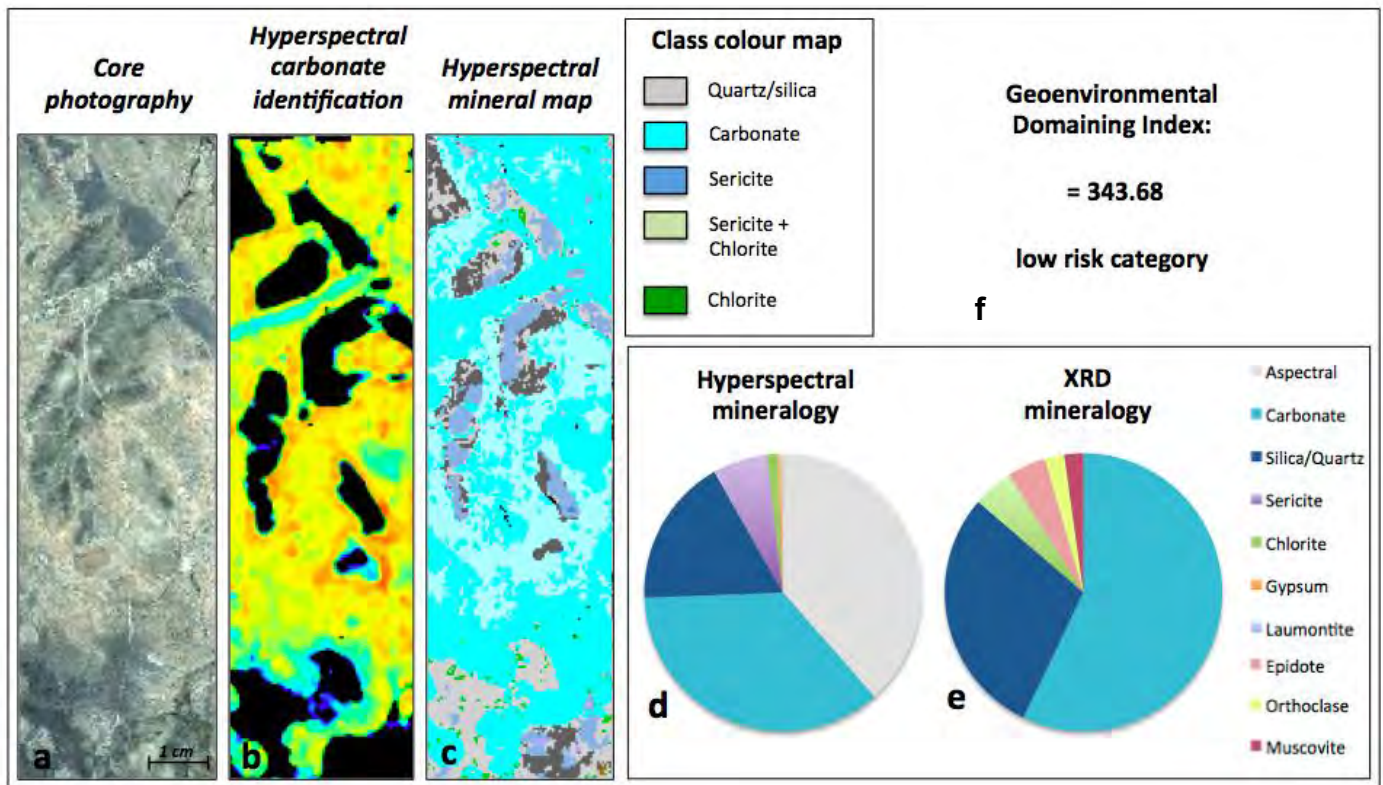


Figure 3. Mineralogy results for sample Z. a, b and c show qualitative hyperspectral mineral outputs: RGB core photography, hyperspectral carbonate identification and hyperspectral mineral map respectively; d displays relative hyperspectral mineral abundance; e shows XRD semi-quantified mineralogy and f shows the overall GDI classification.

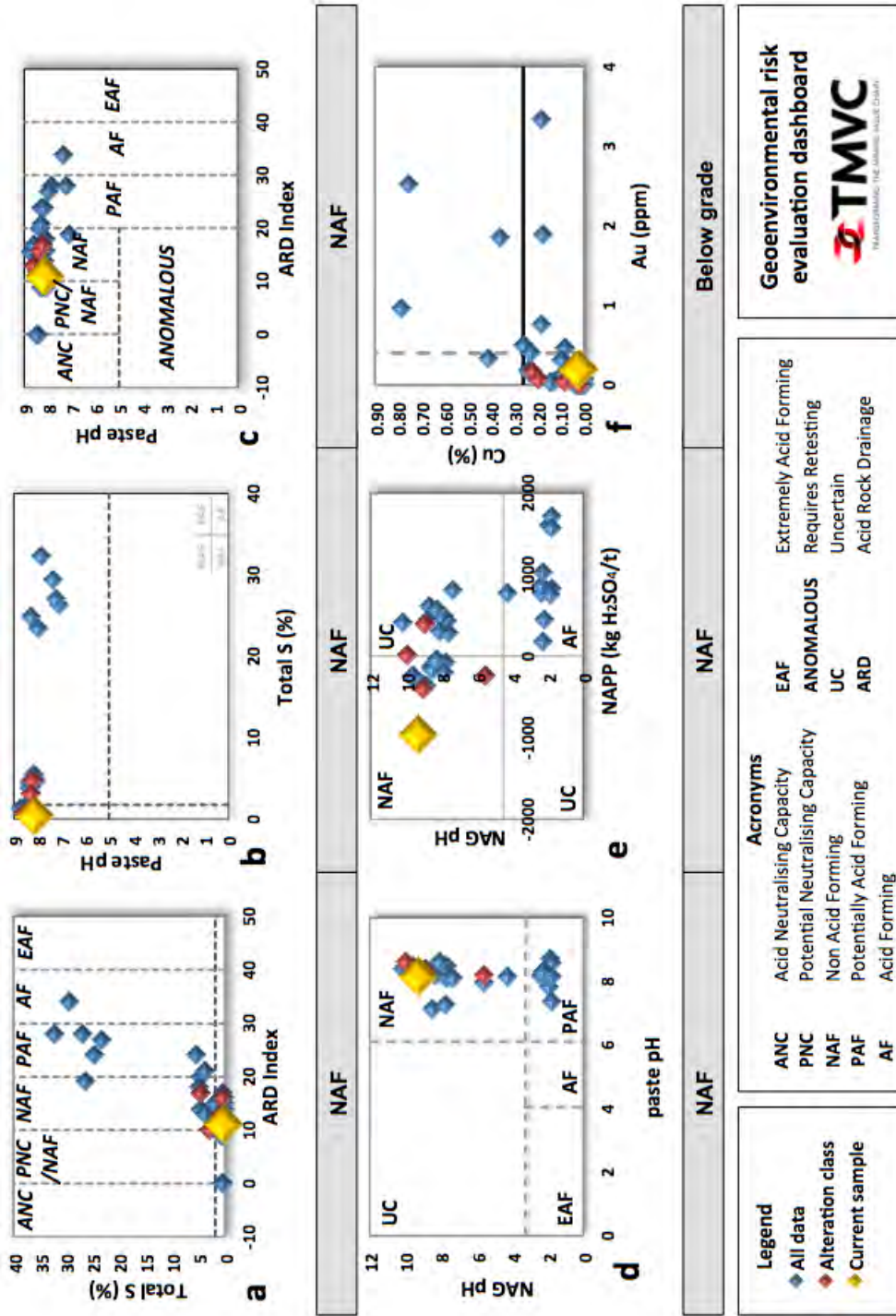


Figure 4. Geochemical dashboard display of two drill holes ($n = 30$ samples). The yellow diamond represents example Z, the red diamonds represent samples from the same alteration type and the blue diamonds represent all data. Specific values for sample Z: total S, 0.3%; ARDI value, 11; Paste pH, 8.1; NAG pH, 9.3; NAPP, 963 Kg H₂SO₄/t; Cu 0.02% and Au 0.2

3.3 Comparison of GDI and Geochemical Characteristics.

NAG pH vs Paste pH classification show that a large proportion of samples analysed is NAF (Figure 5). NAG pH values range from 1.8 to 10.2 with a distinct NAF population pH 8. This graph demonstrates that it is difficult to use geochemistry alone to distinguish between NAF and ANC material. However, comparisons between the GDI and NAG pH show that discrimination could be possible (Figure 6). It also shows that NAG pH values compared to mineralogy could help identify high and moderate ANC material, especially when combined with classifications from Table 3.

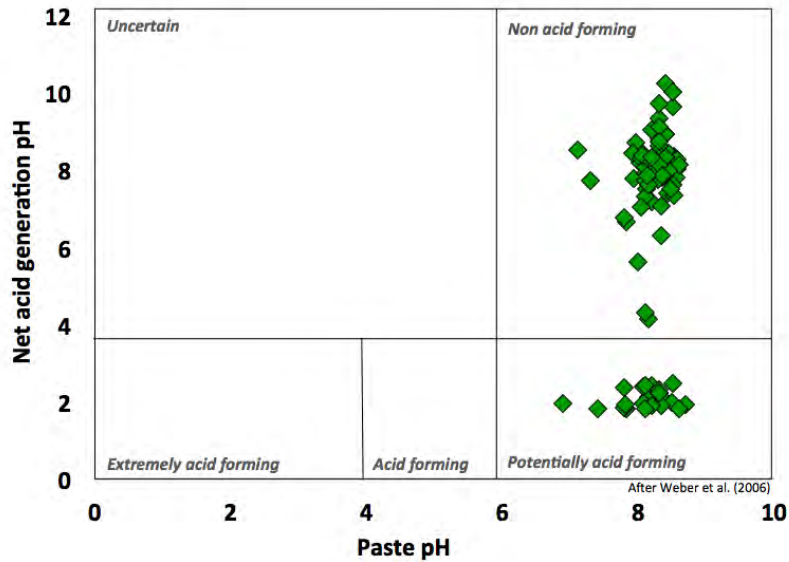


Figure 5. NAG pH vs Paste pH plot ($n= 100$), after Weber et al. (2006).

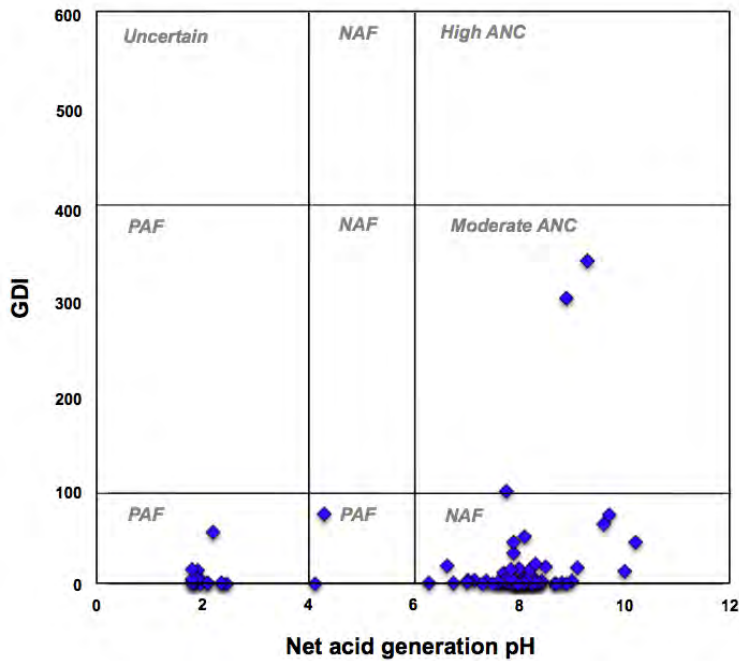


Figure 6. GDI vs NAG pH plot ($n=100$).

4.0 DISCUSSION AND CONCLUSIONS

When used correctly, industry geochemical tests are able to accurately predict acid and metalliferous waste material (e.g., Windy Craggy; Morin and Hutt, 2001; Macraes gold mine; Schroeder et al., 2005; Pebble porphyry deposit; Harraden et al., 2013). While these geochemical, geological and mineralogical tools can discriminate between acid forming and neutralising capacity of mine waste, they have limitations and can easily be misused. Limitations of these tests are well documented in literature (e.g., Parbhakar-Fox and Lottermoser, 2015 and Dold, 2016) and can include compounding laboratory errors, as well as being consuming of both time and cost. Inadequate geological and mineralogical understanding of waste material including inappropriate testing and misinterpretation of available data can compromise effective mine waste planning, storage design and management (Wei et al., 2013). Recently, Parbhakar-Fox et al. (2017) demonstrated how new techniques of blended static testing holds opportunities to improve first pass waste-rock handling practices and waste pile design. Thorough up front waste characterisation like this is vital, as neutralising minerals are not always available when required or accessible in mined waste or in the waste storage facility, and can be costly to import. The imperative importance of neutralising material is being recognized, as an increasing number of studies are looking outside of the mining industry for solutions. Monte et al. (2009), Mäkelä et al. (2010) Mäkitalo et al. (2015) and Mäkitalo et al. (2016) all investigate the integration of solid residues from steel, pulp and paper industries with mine waste as alternate management methods. However, by identifying inherent neutralising materials on site, one could maximise resource value by making use of all materials (not just ore) and minimising waste. Incorporation of tools that can rapidly and correctly discriminate NAF from ANC material during early LOM is a critical missing step.

Differentiation of waste material using only ABA does not always lead to AMD prevention or allow for detailed mineralogical interpretation or classifications. Examples of failures to predict and prevent acid formation can be found throughout the literature (e.g., Morin and Hutt, 2001; Akcil and Koldas, 2006; Nieto et al., 2007; Rao et al., 2017). Furthermore, lack of mineralogical understanding can result in inappropriate test choices when deciding which geochemical procedure to follow. For example, Parbhakar-Fox and Fox (2017) noticed differences in reported NAG pH values when using 30% H₂O₂ as opposed to 15% H₂O₂ on samples with high wt. % sulfide (i.e., >2 wt.%). When the post NAG powders were analysed under Scanning Electron Microscopy (SEM), it was noticed that sulfides were not completely oxidised. Similarly, Noble and Lottermoser (2017) found significant inconsistencies in pH values of standards through a range of geochemical tests (e.g., paste pH and NAG pH). These examples highlight the need for caution when selecting and undertaking geochemical testing and when interpreting results. In addition, Villanova et al. (2017) states that, in order to correctly define representative samples and proper analytical techniques, you must fully understand the mineralisation. Therefore using mineralogy to guide testing, such as NAG tests, can only improve reliability, reproducibility and confidence in undertaking testing and in reporting. This study has shown that mineralogy collected through hyperspectral core logging can quickly and reliably provide semi-quantified data useful to inform geoenvironmental testing. In addition, using Coreshed, while undertaking traditional core logging, can help maximise logging effectiveness, remove subjectivity, produce more accurate and detailed logging data bases and aid with sampling (e.g., Figure 1, 2 and 3).

Statistically, sampling campaigns often fall short of adequately assessing best practice sample numbers as recommended in Price (2009). As a consequence, the accuracy of waste management planning is likely to be reduced, increasing the potential for environmental risk later in the LOM. Parbhakar-Fox and Dominy (2017) argue that the

importance of sample selection cannot be underestimated. They suggest sample selection is the single most critical aspect of any geoenvironmental investigation. Inadequate comprehensive sampling before commencement of mining could therefore contribute to excessive variance, difficulties in interpretation and incorrect assessment of results. Observations from Dominy (2017) in gold grade variability were enhanced by poorly designed sampling and testwork protocols. He argues that testwork throughout the mine value chain must be supported by high-quality representative samples. These comments not only apply to gold mining but also to environmental sampling. Optimisation processes must consider geological/mineralogical nature of ore type(s) and likely domains (Dominy, 2017).

Rapid mineralogical mapping tools can provide qualitative and semi-quantitative mineralogical data, improving speed and accuracy and removal of the subjective nature of traditional core logging. There is also a large potential for this type of technology to be used to classify mineable waste domains reliably, be able to direct sampling campaigns at deposit scale and therefore improve waste storage design and minimise AMD. This study used Coreshed for mineralogical domain-driven sampling on five drill holes (Figure 2). Sampling using this method dramatically increased confidence, reproducibility and modeling of geochemical data, as opposed to random sample selection used on two the other drill holes. Utilising drillcore mapping tools to domain waste, focus sampling and determine mineralogy before geochemical testing can ensure certainty in testing results, confidence in propagating those results across a larger domain, allow construction of a larger comprehensive deposit scale waste characterisation datasets and hence a fully-inclusive planning tool.

Development of the GDI utilising hyperspectral data has proven to be a valid domaining tool for characterising potentially neutralising material. It is able to rapidly incorporate all mineralogy and give a quantified number relevant to a risk category (Table 2 and 3). Fast hyperspectral data collection speeds (2 km drill core/day) can allow for rapid geoenvironmental domaining of large areas. This can allow for targeted sampling campaigns (Figure 2) and lead to better overall waste forecasting. Initial results show that mineralogy-driven domaining of this sort corresponds well with standard geochemical testing (Figure 3 and 4). The advantage of utilising hyperspectral data gives complete downhole assessments as opposed to point sampling. It also incorporates ANC from all minerals (e.g., Table 2). It allows for a robust estimate by including all carbonate and silicate mineralogy. Additional incorporation of relative reactivity values provides an indication of potential neutralising capacity when exposed to acidity generated by oxidation of sulfides. Integration of the GDI with other techniques to give mineral chemistry (such as, LA-ICPMS) can lead to best practice waste rock assessment and waste planning.

The GDI, as it stands, does not include mineralogical influences endemic to acid forming minerals. Improved sulfide recognition on hyperspectral platforms would allow for improved domaining. Deposit scale assessment of all materials, categorising ANC, as well as AF and PAF, material could have a large impact in the way sampling campaigns are undertaken, deposits are mined, scheduling of material and waste rock pile design. Further work includes improving sulfide identification to allow for acid producing potential inclusions into the GDI. Kinetic testing (current run time = 23 weeks; scheduled run time = 60 weeks to fit with project timeline) has been established to investigate robustness of waste domaining using the GDI.

The lack of long-term consideration for the whole LOM and the inherent instability of mining projects contribute significantly to irreversible mineral losses and resource sterilization (Lèbre et al., 2017). Lèbre et al. (2017) suggest further research should address the identification of practices and strategies that (1) anticipate for future use

of material beyond the closure of a mining project or (2) contribute to making mining projects economically viable in the longer term. The movement towards more sustainable practices in mining is exponentially increasing. Utilisation of technologies such as hyperspectral mineral identification can assist in improvements for rapid mineral identification and subsequently geoenvironmental sampling and domaining.

5.0 REFERENCES

Akcil, A and Koldas, S, 2006. Acid Mine Drainage (AMD): causes, treatment and case studies. *Journal of Cleaner Production*, 14(12), pp.1139-1145.

Candeias, C, Melo, R, Ávila, PF, da Silva, EF, Salgueiro, AR and Teixeira, JP, 2014. Heavy metal pollution in mine–soil–plant system in S. Francisco de Assis–Panasqueira mine (Portugal). *Applied Geochemistry*, 44, pp 12-26.

Castilla, N, 1993, April. Greenhouses in the Mediterranean area: technological level and strategic management. In *International Symposium on New Cultivation Systems in Greenhouse* 361, pp 44-56.

Davis Jr, RA, Welty, AT, Borrego, J, Morales, JA, Pendon, JG and Ryan, JG, 2000. Rio Tinto estuary (Spain): 5000 years of pollution. *Environmental Geology*, 39(10), pp 1107-1116.

Dold, B. 2016. The biogeometallurgical approach – the information we need to increase the sustainability of mining. Proceedings of the Third International AUSIMM Geometallurgy Conference, 15-16 June 2016, Perth, WA, pp 169-171.

Dominy, SC, 2017. Optimised sampling protocols for the grade and metallurgical evaluation of selected vein gold deposits, Proceedings of the 8th World AUSIMM Conference on Sampling and Blending, 09-11 May 2017, Perth, WA.

Edraki, M, Golding, SD, Baublys, KA and Lawrence, MG, 2005. Hydrochemistry, mineralogy and sulfur isotope geochemistry of acid mine drainage at the Mt. Morgan mine environment, Queensland, Australia. *Applied Geochemistry*, 20(4), pp 789-805.

Harraden, C.L., McNulty, B.A., Gregory, M.J. and Lang, J.R., 2013. Shortwave infrared spectral analysis of hydrothermal alteration associated with the pebble porphyry Copper-Gold-Molybdenum Deposit, Iliamna, Alaska. *Economic Geology*, 108(3), pp.483-494.

Harries, JR, 1997. Acid mine drainage in Australia: Its extent and potential future liability. Canberra: Supervising Scientist, pp 1-5.

Harris, DL, Lottermoser, BG, Duchesne, J, 2003. Ephemeral acid mine drainage at the Montalbion silver mine, north Queensland. *Australian Journal of Earth Sciences*, 50, pp 797–809.

Haas, W., Krausmann, F., Wiedenhofer, D. and Heinz, M., 2015. How circular is the global economy?: An assessment of material flows, waste production, and recycling in the European Union and the world in 2005. *Journal of Industrial Ecology*, 19(5), pp.765-777.

Hudson-Edwards, KA, Schell, C and Macklin, MG, 1999. Mineralogy and geochemistry of alluvium contaminated by metal mining in the Rio Tinto area, southwest Spain. *Applied Geochemistry*, 14(8), pp 1015-1030.

Hyndman, D, 2001. Academic responsibilities and representation of the Ok Tedi crisis in postcolonial Papua New Guinea. *The Contemporary Pacific*, 13(1), pp.33-54.

Jambor, JL, Dutrizac, JE and Raudsepp, M, 2007. Measured and computed neutralization potentials from static tests of diverse rock types. *Environmental geology*, 52(6), pp.1019-1031.

Lèbre, É, Corder, G and Golev, A, 2017. The role of the mining industry in a circular economy: A framework for resource management at the mine site level. *Journal of Industrial Ecology*, 21(3), pp.662-672.

Lottermoser, BG, 2010. Mine Wastes (3rd Edition): Characterization, Treatment and Environmental Impacts. Characterization, Treatment and Environmental Impacts, pp 1-400.

Mäkelä, M, Watkins, G, Dahl, O, Nurmesniemi, H and Pöykiö, R, 2010. Integration of Solid Residues from the Steel and Pulp and Paper Industries for Forest Soil Amendment. *Journal of Residuals Science & Technology*, 7(4).

Mäkitalo, M, Mácsik, J, Maurice, C and Öhlander, B, 2015. Improving properties of sealing layers made of till by adding green liquor dregs to reduce oxidation of sulfidic mine waste. *Geotechnical and Geological Engineering*, 33(4), pp.1047-1054.

Mäkitalo, M, Stenman, D, Ikumapayi, F, Maurice, C and Öhlander, B, 2016. An Evaluation of Using Various Admixtures of Green Liquor Dregs, a Residual Product, as a Sealing Layer on Reactive Mine Tailings. *Mine Water and the Environment*, 35(3), pp.283-293.

Martini, BA, Conroy, K, Carey, R, 2014. Tracking mica chemistry in copper porphyry using core imaging spectroscopy. *In Proceedings International Applied Geochemistry Symposium*, April 20-24, Tucson, AZ, USA.

Monte, MC, Fuente, E, Blanco, A and Negro, C, 2009. Waste management from pulp and paper production in the European Union. *Waste Management*, 29(1), pp.293-308.

Morin, KA and Hutt, NM, 2001. *Environmental geochemistry of minesite drainage: Practical theory and case studies, Digital Edition*. MDAG Publishing (www.mdag.com), Surrey, British Columbia. ISBN: 0-9682039-1-4.

Mudd, GM, 2008. Sustainability reporting and water resources: a preliminary assessment of embodied water and sustainable mining. *Mine Water and the Environment*, 27(3), pp 136-144.

Myers, T, 2016. Acid mine drainage riskseA modeling approach to siting mine facilities in Northern Minnesota USA. *J. Hydrol.* 533, 277e290.

Nieto, JM, Sarmiento, AM, Olías, M, Canovas, CR, Riba, I, Kalman, J and Delvalls, TA, 2007. Acid mine drainage pollution in the Tinto and Odiel rivers (Iberian Pyrite Belt, SW Spain) and bioavailability of the transported metals to the Huelva Estuary. *Environment International*, 33(4), pp.445-455.

Noble, TL and Lottermoser, B, 2017. Modified Abrasion pH and NAG pH Testing of Minerals. *Environmental indicators in metal mining*, Springer, pp. 220-229.

Noble, TL, Lottermoser, BG, Parbhakar-Fox, A, 2015. Evaluation of pH testing methods for sulfidic mine waste. *Mine Water Environment*.

Parbhakar-Fox, A and Dominy, SC, 2017. Sampling and blending in geoenvironmental campaigns – current practice and future opportunities, Proceedings of the AUSIMM 8th World Conference on Sampling and Blending, 09-11 May 2017, Perth, WA, pp. 45-54.

Parbhakar-Fox, A and Fox, N, 2017. Evaluation of NAG pH testing: Tracking reaction pathways and products. Preliminary Report prepared for ARC Research Hub for Transforming the Mining Value Chain, University of Tasmania, 28p.

Parbhakar-Fox, A and Lottermoser, BG, 2015. A critical review of acid rock drainage prediction methods and practices. *Minerals Engineering*, 82:107-124.

Parbhakar-Fox, AK and Lottermoser, BG, 2014. Predictive waste classification at the Rosebery Mine using field and advanced laboratory techniques. CRC ORE Technical Report.

Parbhakar-Fox A, Edraki M, Hardie K, Kadletz O, Hall T, 2014. Identification of acid rock drainage sources through mesotextural classification at abandoned mines of Croydon, Australia: Implications for the rehabilitation of waste rock repositories, *Journal of Geochemical Exploration*, 137, pp 11-28.

Parbhakar-Fox, A, Fox, N, Hill, R, Ferguson, T and Maynard, B, 2017. Improved mine waste characterisation through static blended test work. *Minerals Engineering*, (In Press).

Pasternack, GB, Gilbert, AT, Wheaton, JM and Buckland, EM, 2006. Error propagation for velocity and shear stress prediction using 2D models for environmental management. *Journal of Hydrology*, 328, pp.227-241.

Price, WA, 2009. Prediction manual for drainage chemistry from sulphidic geologic materials. *MEND report*, 1(1), p.579.

Rao, Y, Gu, R, Guo, R and Zhang, X, 2017. Measures to restore metallurgical mine wasteland using ecological restoration technologies: A case study at Longnan Rare Earth Mine. In *IOP Conference Series: Earth and Environmental Science* (Vol. 52, No. 1, p. 012080). IOP Publishing.

Schoenberger, E, 2016. Environmentally sustainable mining: The case of tailings storage facilities. *Resources Policy*, 49, pp 119-128.

Schroeder, K., Rufaut, C.G., Smith, C., Mains, D. and Craw, D., 2005. Rapid plant-cover establishment on gold mine tailings in southern New Zealand: glasshouse screening trials. *International journal of phytoremediation*, 7(4), pp.307-322.

Smart, R, Skinner, WM, Levay, G, Gerson, AR, Thomas, JE, Sobieraj, H, Schumann, R, Weisener, CG, Weber, PA, Miller, SD, Stewart, WA, 2002. ARD test handbook: Project P387, A prediction and kinetic control of acid mine drainage, Melbourne, Australia, AMIRA, International Ltd, 10 p.

Staebe, K, 2015. Determination of the Bacterial Diversity of a Natural Freshwater Wetland Impacted by Acid Mine Drainage. Ph.D. thesis. Stellenbosch University.

Sverdrup, HU, 1990. The Kinetics of Base Cation Release Due to Chemical Weathering. Lund, Sweden: Lund University Press. 246 pp.

Unger, CJ and Van Krieken, A, 2011. A discussion paper on Abandoned Mine Mangement in Australia on behalf of AusIMM Sustainability Committee. (The Australasian Institute of Mining and Metallurgy: Melbourne).

Venkateswarlu, K, Nirola, R, Kuppusamy, S, Thavamani, P, Naidu, R and Megharaj, M, 2016. Abandoned metalliferous mines: ecological impacts and potential approaches for reclamation. *Reviews in Environmental Science and Bio/Technology*, 15, pp 327-354.

Villanova, FLSP, Heberle, A and Chierigati, AC, 2017. Heterogeneity tests and core logging – a final reconciliation, Proceedings of the 8th AUSIMM World Conference on Sampling and Blending, 09-11 May 2017, Perth, WA.

Waggitt, P, and Jones, W, 1996. The Mount Lyell Remediation Research and Demonstration Program-the Half Time Picture. In *1996 National Engineering Conference: Engineering Tomorrow Today; the Darwin Summit; Preprints of Papers* (p. 387). Institution of Engineers, Australia.

Wei, Z, Yin, G, Wang, JG, Wan, L and Li, G, 2013. Design, construction and management of tailings storage facilities for surface disposal in China: case studies of failures. *Waste Management & Research*, 31, pp.106-112.

Whitehead, PG, Cosby, BJ and Prior, H, 2005. The Wheal Jane wetlands model for bioremediation of acid mine drainage. *Science of the total environment*, 338(1), pp.125-135.

CHARACTERISATION OF ARSENIC GEOCHEMISTRY IN MINE TAILINGS FROM A MESOTHERMAL AU DEPOSIT

H. Christenson^A, J. Pope^A, D. Craw^B, J. Johns^C and N. Newman^A

^ACRL Energy Ltd, 97 Nazareth Ave, Christchurch, New Zealand

^BGeology Department, University of Otago, 360 Leith Street, Dunedin, New Zealand

^COceana Gold Ltd, Macraes, Otago 9483, New Zealand

ABSTRACT

Macraes mine was opened in 1989, and extracts mesothermal gold from a shearing zone in the Otago schist. The gold occurs in pyrite and arsenopyrite, which comprise 1 % of the ore. In September 2015 an 80 m core was drilled through the northern end of the Mixed Tailings Facility (MTF) that receives flotation and sulfide concentrate tailings. The core encompasses tailings deposited over much of the lifetime of Macraes mine including the changes that have occurred in gold extraction and tailings management, such as the introduction of pressure oxidation of sulfide concentrate in 1999.

Preliminary study of the core has involved characterisation of a section at 44 m depth, and a section at 77 m depth. The shallower sample has brown tailings, indicative of iron oxide minerals produced during pressure oxidation. The deep sample is grey, consistent with the persistence of sulfide minerals. The tailings pore water at both depths contains 2 ppm As. Arsenic in the tailings is associated predominantly with iron oxide minerals at 44 m depth, and with sulfide minerals at 77 m depth. The sequential extraction showed promise as a way to investigate mineral associations in the MTF, and preliminary geochemical modelling suggests that sorption equilibria are more important than solubility equilibria in determining As concentrations in pore water of the tailings facility.

1.0 INTRODUCTION

The Macraes mine extracts mesothermal gold from a mineralised shear zone in the Otago Schist (Figure 1). The ore typically has 1 % pyrite and arsenopyrite which contain encapsulated gold, in the order of 1.6 grams of gold per tonne (Milham and Craw 2009). The mine was opened in 1989, and has undergone several changes to the ore processing regimes over its lifetime (Figure 2). This has led to variations in the chemistry and composition of the mine wastes over this time.

The ore processing regimes use a combination of physical and chemical processes to extract the gold. The ore is crushed and ground to sand and the sulfide rich fraction is concentrated using froth flotation. The gangue is deposited into the Mixed Tailings Facility (MTF), while the concentrate is further milled to $15 \pm 10 \mu\text{m}$ prior to oxidation and gold extraction. The gold is extracted from the sulfide fraction by carbon-in-pulp cyanidation (Craw et al. 1999). When the mine opened in 1989 this extraction was performed directly on the sulfide concentrate, without the oxidation step. Between 1989 and 1993, the arsenopyrite-bearing concentrate tailings were stored in a separate facility to the flotation tailings (Craw et al. 1999), however from 1993 onwards the concentrate tailings were also sent to the MTF.

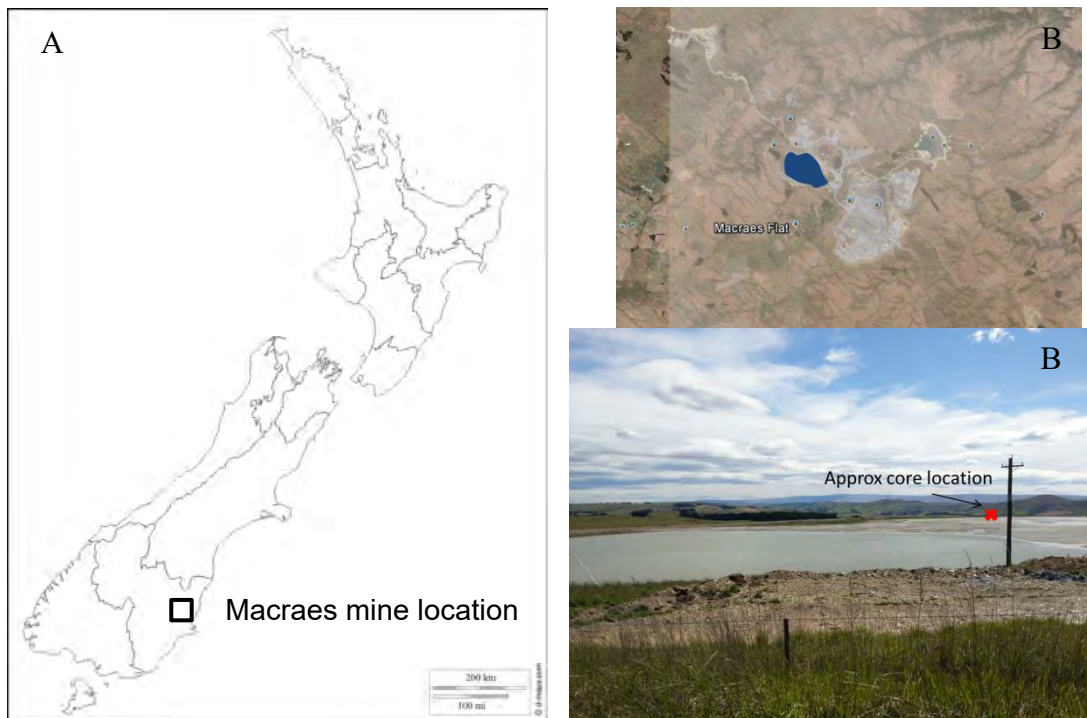


Fig. 1. The location of the macraes mine (A), tailings dam (B, blue shading) and core site (C) in Otago. Images A and B adapted from d-maps and Google Earth respectively.

In order to maximise gold extraction, a pressure oxidation plant was commissioned in 1999 which treated the sulfide concentrate prior to cyanidation (Craw 2003). The concentrate is roasted in an oxygen rich autoclave (225 °C, 3800 kPa O₂) for 1 hour which causes nearly complete oxidation of the sulfides (Craw 2006). The oxidation process generates sulfuric acid, which is managed via limestone addition to maintain a solution pH between 1 and 2. The principal wastes formed in the pressure oxidation plant are calcium sulfate (as anhydrite and/or gypsum), jarosite, iron (oxyhydr)oxide (as hematite or ferrihydrite), and amorphous iron arsenate. The discharge from the pressure oxidation plant is treated by carbon-in-pulp cyanidation and then deposited in the MTF with the flotation tailings. Between 1999 and 2000, the concentrate tailings collected between 1989-1993 were reprocessed through the oxidation plant and sent to the MTF. In 2007, the plant also started processing concentrate from the Globe mine near Reefton, which has 4% stibnite in addition to pyrite and arsenopyrite (Milham and Craw, 2009).

Arsenic is an environmentally relevant element that is present in the MTF at Macraes mine. Consent conditions for Macraes set As limits and monitoring requirements for the mine and associated facilities. Seepage from the tailings is captured in a dedicated drainage system and returned to the processing plant as part of the process water circuit. Release of As from the MTF is an environmental risk, the magnitude of which is dependent on the geochemistry of the tailings and the in situ processes occurring in the impoundment. The changes in ore processing over the lifetime of Macraes mine has altered the geochemistry of the As bearing phases in the tailings. Characterisation of the tailings and processes controlling As mobility will help to inform management practices required into the future. In 2015, a core was taken through 80 m of the MTF. This paper tests a sequential extraction to investigate the association of As with

minerals in tailings from two sections of the core that have undergone different gold extraction processes.

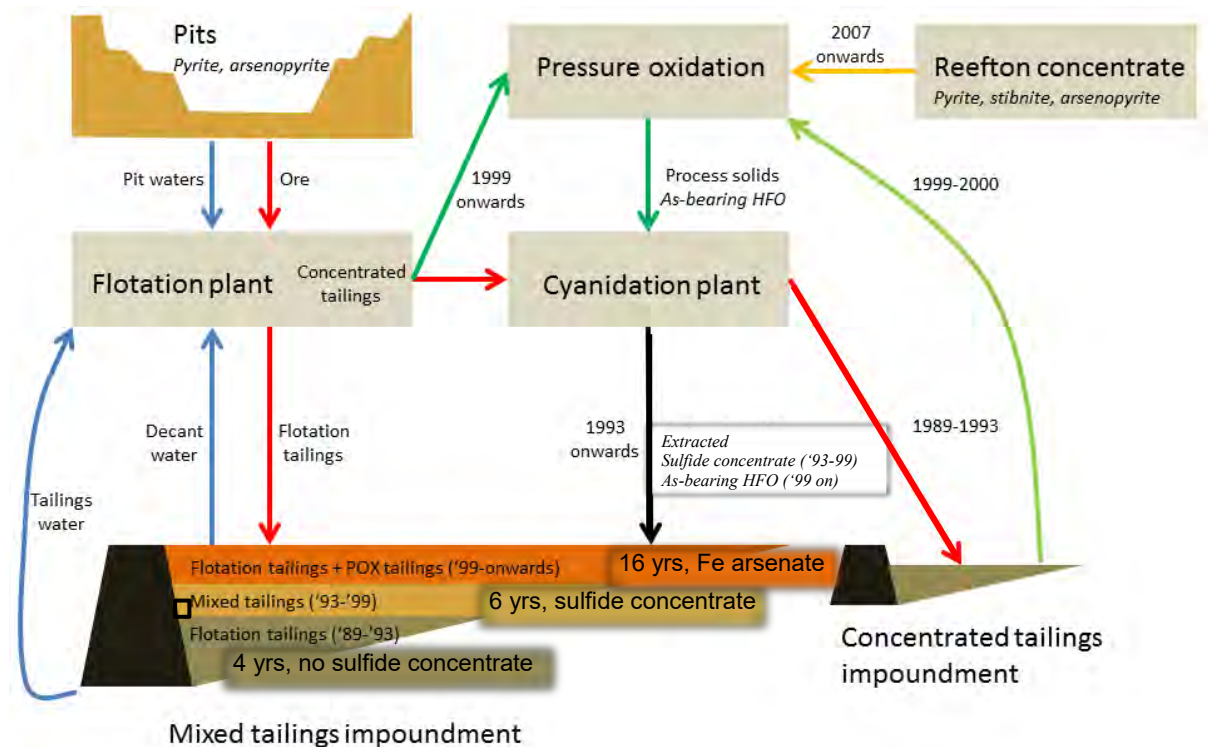


Fig. 2. Processing systems at Macraes mine, modified from Milham and Craw (2009).

2.0 METHODS

The core was extracted from the MTF in September 2015, and was cut into sections, wrapped in cling film, and frozen. The frozen sections were stored at -18°C prior to analysis. Two core depths were selected for provisional study; one at 77 m depth near the base of the core, and one at 44 m depth. Ten centimetre subsamples were cut from the frozen sections with a saw, and thawed in a nitrogen atmosphere in a glove box. A plastic knife was used to remove sample that had been in contact with the metal saw. The 10 cm sub-sample was homogenised by mixing, and then placed into 50 mL centrifuge tubes. The tubes were centrifuged for 16 hours and pore water that pooled on top was collected. The pH of the pore water was measured with a calibrated pH meter. Subsamples of the pore water were then diluted with degassed distilled water prior to analysis.

Arsenic speciation in the pore waters was measured using the spectrophotometric method of Johnson and Pilon (1972). This method takes advantage of the reactivity of arsenate and phosphate with molybdenum blue complexes, and manipulates arsenic oxidation state to determine the arsenate and arsenite concentrations by difference.

The phase associations of arsenic in the tailings were investigated using sequential extraction techniques. These techniques use increasingly aggressive chemical reagents to target dissolution of mineral groups in un-dried solid samples depending on their reactivity. This results in operationally defined fractions that are intended to represent elemental relationships with particular mineral constituents of the tailings. In this study an extraction scheme used by

Nieva et al. (2016) was adapted to target arsenic associated with soluble, exchangeable, amorphous and crystalline oxides, and sulfide phases (Fig. 3.). After each extraction step the sample was centrifuged for 15 minutes and the supernatant filtered and collected for analyses. The next reagent was added to the remaining solid in the centrifuge tube. In addition, an extraction was performed in aqua regia to determine the total concentration of arsenic present in the tailings. A certified reference material (CRM-RTS 3a from Canmet Mining) comprised of sulfide ore mill tailings, was extracted alongside the tailings extracts. The pore water, sequential extraction and aqua regia extracts were analysed for Al, As, Fe, Mn, P, S and Sb by ICP-MS and for chloride and sulfate by ion chromatography methods at an accredited laboratory.

Geochemical modelling was performed using Visual MINTEQ (Gustafsson, 2009), with the default comp_2008.vdb, thermos.vdb and type6.vdb databases for component, aqueous species and solubility thermodynamic data. Bicarbonate was not analysed due to insufficient sample volume, and so a calculated concentration to balance ions in solution was used for modelling. Sorption to iron oxides was modelled using the diffuse layer model (DLM) with the "HFO (Dzombak and Morel)" and "Goethite (Weng et al)" models in Visual MINTEQ.

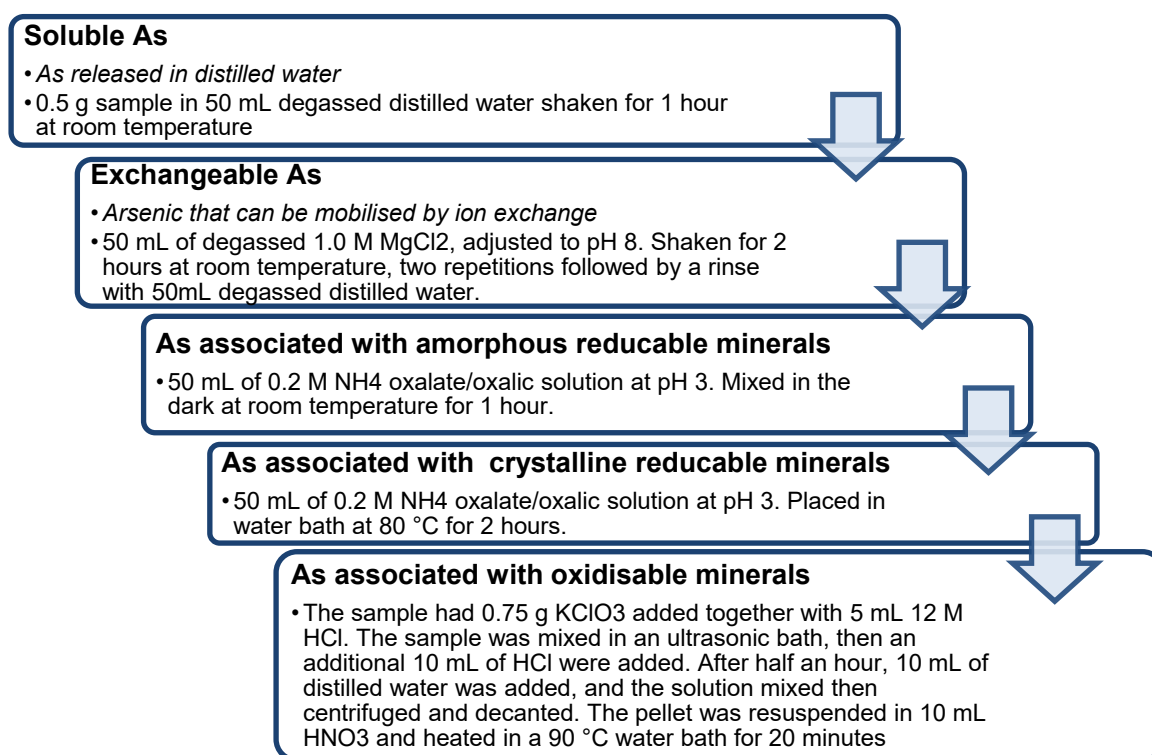


Fig. 3. A summary of the sequential extraction from Nieva et al. (2016).

3.0 RESULTS

The tailings from 77 m depth in the MTF were grey, with a clay-like texture (Fig. 4). The grey colouring is similar to that of the schist that is visible around the Macraes area. A few millilitres of pore water were able to be extracted from the tailings, and the pore water pH was 8.58. Unfortunately, the volume was too small to allow for speciation analyses to be performed, however ICP-MS revealed 2 ppm of arsenic is present in the pore water. The tailings from 44 m depth were brown in colour (Fig. 4.), and had some coarser material mixed in with the clay-

like textured material. A greater volume of pore water was able to be extracted from the 44 m tailings. Pore water pH was 8.14, and the 2 mg/L of arsenic present was speciated entirely as As V. Provisional modelling indicated that at both depths the tailings were saturated with respect to aluminium hydroxide phases, and that the tailings at 44 m depth were close to saturation with respect to gypsum and anhydrite.

The sequential extraction results show markedly different As chemistry in the tailings at the two depths (Fig. 5.). At 77 m depth, arsenic was predominantly associated with sulfide minerals, and at 44 m depth, arsenic was predominantly associated with reducible metal oxide minerals. There were higher concentrations of soluble and exchangeable As in the tailings from 77 m depth. In the CRM and the 44 m depth tailings sample, the sum of the sequential extraction concentrations was very similar to the concentration from the aqua regia digest. The 77 m sample had significantly lower concentrations extracted with aqua regia than in the sequential extraction. The CRM sample had 99% recovery of As, indicating good extraction by both the sequential extraction and aqua regia methods.



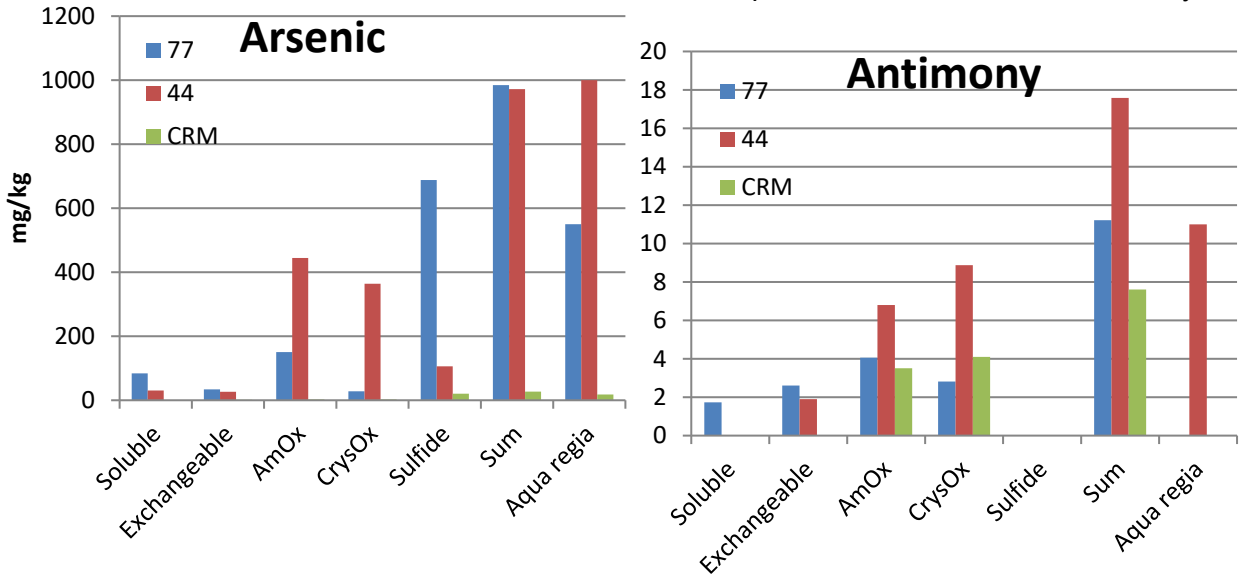
Figure 4. Subsamples of tailings from 77 m depth (grey, above) and 44 m depth (brown, below) showing the colour difference between the samples.

Antimony was predominantly associated with reducible metal oxide minerals in both of the tailings samples, and no sulfide associated Sb was detected (Fig. 5.). The deep tailings sample had greater concentrations of soluble and exchangeable Sb than the shallower tailings that have undergone pressure oxidation. For the aqua regia digestion, the detection limit of the method was 10 mg/kg of tailings. The 44 m depth tailings had a lower aqua regia extractable Sb concentration than the sum of the sequential extracts. The sum of sequential extraction extracts was close to or less than the aqua regia 10 mg/kg detection limit in the 77 m sample and the CRM, and no detectable Sb was found using the aqua regia method.

Iron in the tailings was predominantly in an oxidised form. The mineral forms were not identified, but in the deep tailings a greater proportion of Fe was mobilised in the extraction phase targeting amorphous metal oxides. In the shallow tailings more than twice as much iron was present in a crystalline rather than amorphous iron oxide form. There was more sulfide associated iron in the deep tailings from 77 m than the shallow tailings at 44 m, however some sulfide associated iron persisted in the shallow sample. Iron in the CRM was 88 % recoverable in aqua regia.

There was considerable soluble sulfur present in the tailings, 145 and 318 mg/kg in the 77 m and 44 m depth samples respectively. No detectable (> 100 mg/kg) sulfur was released during the reducing steps indicating that little, if any, sulfur is present in oxy or hydroxyl sulfate minerals. In the 77 m depth sample, an additional 1376 mg/kg of S was released during the extraction step targeting sulfide minerals, indicating persistence of sulfide minerals in the deep tailings. The CRM had high sulfur concentrations, mostly in the form of sulfide minerals, and 80% recovery of S was achieved through the extractions.

The DLM was used to predict As sorption onto iron oxides present in the tailings. Where all of the iron in oxide phases was entered into the model as hydrous ferric oxide (HFO), the model predicted lower pore water arsenic concentrations than was observed at 44 m depth (Table 1). When the amorphous Fe was entered as HFO and the crystalline Fe was entered as goethite, the model predicted far higher pore water concentrations of As at 44 m depth. The model predicted As should be entirely



sorbed to iron oxides in the tailings at 77 m depth, for both scenarios.

Fig. 5. Concentrations of elements dissolved in each step of the sequential extraction, together with the sum of concentrations, and the concentration dissolved in aqua regia. The CRM had more than an order of magnitude more sulfur present than the tailings samples, and so this graph is displayed with a logarithmic scale on the y axis. Results that were below detection are not shown on the graphs.

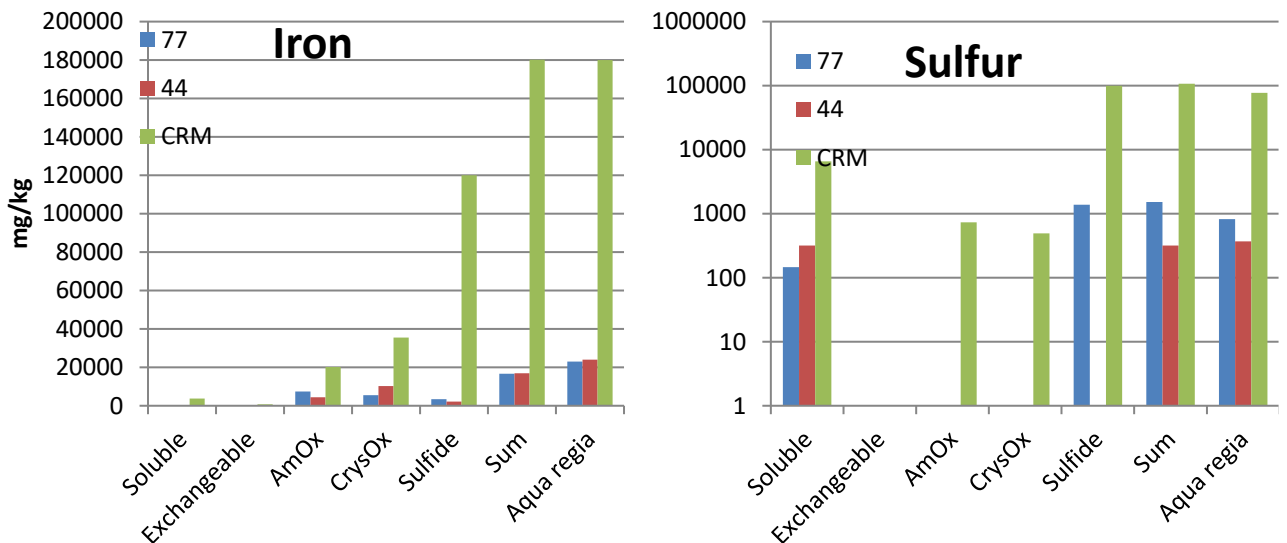


Table 1 The predicted concentration of As in porewater when the porewater chemistry was modelled together with the concentrations of As and Fe that were associated with amorphous and crystalline metal oxides in the tailings. The Fe that was released from the tailings in these extraction steps was assumed to be HFO or goethite by the model.

Tailings depth	44 m		77 m	
Scenario modeled	HFO	HFO + Goethite	HFO	HFO + Goethite
Porewater As (mg/L)	1.6	168	0	0

4.0 DISCUSSION

The concentration of arsenic in both the pore water of the tailings, and the tailings themselves was similar at the 44 m and 77 m sample depths. However, the phase associations of arsenic in the tailings were distinct. Arsenic in the ore occurs predominantly in pyrite and as arsenopyrite, and it is apparent the changes in gold extraction practises used at the mine have altered the distribution of arsenic between the operationally defined mineral fractions in the tailings.

Preliminary modelling of pore waters showed no arsenic minerals close to saturation at either depth, and so it seems likely sorption equilibria may be more important for determining pore water As concentrations than solubility equilibria. It was interesting however that despite identical As concentrations in the pore water, the soluble and exchangeable As fractions in the tailings was substantially larger in the 77 m depth tailings. This is likely a result of greater solubility of the As containing minerals at depth. For instance arsenopyrite is more soluble than iron arsenate. Other possible reasons may include pH and arsenic speciation. The 77 m depth pore water sample was not analysed for As III/V speciation, however if there was a proportion of As present as As III, it may be more easily mobilised by the extractions than As V due to its typically lower affinity for iron oxide surfaces at pH ~8. The pore water pH was 8.58 at 77 m depth, compared to 8.14 at 44 m.

If adsorption equilibria are a primary control on As mobility, comprehensive modelling of the pore water solutions and the adsorbing phases may improve understanding on the processes controlling pore water As concentrations in the system. This will be performed as this project progresses. As part of this further assessment methods such as those employed by Keon et al. (2001), using a phosphate solution to competitively desorb As from iron oxides may be employed. This will allow some distinction to be made between adsorbed versus co-precipitated As species, which may have different mobilities.

At 44 m depth 83% of the arsenic present was associated with iron oxides, with 45 % associated with amorphous iron oxides and 38 % associated with crystalline iron oxides. At the Giant mine in Canada, milled concentrate showed a similar distribution of As association to those observed in the tailings at Macraes mine. Prior to roasting, As was principally associated with sulfide minerals in the mill product, while the roasted product had As predominantly associated with amorphous metal oxides (Walker et al. 2015). The arsenic distribution is contrasting to that of the iron itself, which had a greater proportion present in crystalline forms in the pressure-oxidation tailings at Macraes mine. These results are consistent with papers interpreting mineralogy of pressure oxidation tailings from Macraes, which contain amorphous iron arsenate, jarosite, amorphous iron oxy-hydroxide and hematite

(Craw 2003; Craw 2006). At 77 m depth, 70 % of the arsenic present was associated with sulfide minerals. It seems little alteration of the As containing minerals in the ore occurred during processing. A small proportion of sulfide bound As persists in the pressure oxidation tailings from 44 m as well, which may be due to incomplete oxidation of the sulfide concentrate, and/or incomplete removal of the sulfide fraction during flotation.

The sequential extraction technique showed some interesting and coherent results, however other results indicate some further method development will be required. The aqua regia extraction targets most non-silicate phases, however concentrations of Sb, As and S were at times lower in the aqua regia extract than the sum of extracts from the sequential extraction. For As, this only occurred in the 77 m depth tailings sample, which had a sum of 984 mg/kg As as opposed to 550 mg/kg As by aqua regia extraction. The values extracted by sequential extraction and aqua regia were within a few percent of each other for the 44 m and CRM samples, and equated to 99% recovery of As in the CRM (Table 1.). Unfortunately the liquid:solid ratios used for the aqua regia extraction meant that a detection limit equivalent to 10 mg/kg Sb was achieved. The CRM Sb concentration was below this, and although the sum of extracts for the 44 m depth sample was nearly 18 mg/kg, no Sb was detected in the aqua regia extract. The results for sulfur were within 15% of each other for the 44 m and CRM samples, however the 77 m sample had nearly double S by sum of extracts than was measured in the aqua regia extraction. This is the same sample that showed low As in the aqua regia extraction. This may point to incomplete sulfide oxidation, except that the CRM had far greater sulfide concentrations, so we propose subsample heterogeneity may be responsible for these results. Going forward there will be greater repetition of samples to ensure we understand the capabilities of the method.

The adsorption modelling performed to date is preliminary, however indicates that sorption processes are a key control on porewater As concentrations in the MTF. The observed porewater As concentrations were between the two 'extreme' points considered for the model at 77 m depth – one where all Fe dissolved by the ammonium oxalate extraction steps was present as HFO, and one where the crystalline Fe oxide phases were entirely goethite. There was an order of magnitude difference in As concentrations between these extremes. This indicates that sorption processes have a strong control on porewater As in the pressure oxidised tailings. A major constraint of this modelling is that the crystalline iron oxide phase used for modelling was goethite, whereas hematite and scorodite seem to be the dominant crystalline phases of oxidised Fe in the pressure oxidation tailings (Craw 2003). At 77 m depth, modelling predicts that Fe oxide minerals have the capacity to entirely adsorb porewater As. This was not observed in the system, and ongoing work will focus on identification of minerals in the tailings and enhancing the model to better reflect the minerals and processes occurring within the MTF.

5.0 CONCLUSIONS

The As chemistry in the MTF at Macraes mine is influenced by gold extraction techniques. Tailings that were directly extracted have As predominantly associated with sulfide minerals, whereas tailings that have undergone pressure oxidation have As associated largely with metal oxides. The solid tailings contain close to 1000 mg/kg of As, though pore water concentrations are 2 mg/L at both tailings depths. It is likely that sorption equilibria are more important regulating As concentrations than solubility equilibria, at both depths studied.

Continuing study of the core will characterise pore water and tailings chemistry throughout the length of the core, and geochemical modelling will be applied to assess the processes controlling pore water arsenic concentrations.

6.0 ACKNOWLEDGEMENTS

This research is funded by the New Zealand Ministry of Business, Innovation and Employment under contract FRST CRLE1403 – Mine Environment Life Cycle Guide. We acknowledge OceanaGold and staff for provision of the core samples.

7.0 REFERENCES

Craw, D. (2003). "Geochemical changes in mine tailings during a transition to pressure-oxidation process discharge, Macraes Mine, New Zealand." *Journal of Geochemical Exploration* **80**(1): 81-94.

Craw, D. (2006). "Pressure-oxidation autoclave as an analogue for acid-sulphate alteration in epithermal systems." *Miner Deposita* **41**: 357-368.

Craw, D., D. Chappell, M. Nelson and M. Walrond (1999). "Consolidation and incipient oxidation of alkaline arsenopyrite-bearing mine tailings, Macraes Mine, New Zealand." *Applied geochemistry* **14**(4): 485-498.

Johnson, D. L. and M. E. Q. Pilson (1972). "Spectrophotometric Determination of Arsenite, Arsenate, and Phosphate in Natural Waters." *Analytica Chimica Acta* **58**(1972): 288 - 299.

Keon, N., C. Swartz, D. Brabander, C. Harvey and H. Hemond (2001). "Validation of an arsenic sequential extraction method for evaluating mobility in sediments." *Environmental Science & Technology* **35**(13): 2778-2784.

Milham, L. A. and D. Craw (2009). "Antimony mobilization through two contrasting gold ore processing systems, New Zealand." *Mine Water and the Environment* **28**: 136-145.

Nieva, N., L. Borgnino, F. Locati and M. García (2016). "Mineralogical control on arsenic release during sediment-water interaction in abandoned mine wastes from the Argentina Puna." *Science of the Total Environment* **550**: 1141-1151.

Walker, S., H. Jamieson, A. Lanzirotti, G. Hall and R. Peterson (2015). "The effect of ore roasting on arsenic oxidation state and solid phase speciation in gold mine tailings." *Geochemistry: Exploration, Environment, Analysis* **15**(4): 273-291.

Posters

INVESTIGATING THE GEOCHEMISTRY OF SELENIUM IN THE RESIDUAL FROM BIOLOGICAL WASTEWATER TREATMENT AT A COAL MINE

L. Desauvoy^A and D. Kirste^A

^ASimon Fraser University – Department of Earth Science,
Burnaby, British Columbia, Canada

ABSTRACT

Selenium has the potential to be extremely toxic in high concentrations and is of particular concern due to its propensity to bioaccumulate within food chains. Coal mining in eastern British Columbia has resulted in elevated levels of selenium in the wastewater and ultimately in the nearby surface water bodies. Bacterially-mediated redox based methods are used to treat the wastewater. The by-product of this treatment is a solid state residual which contains selenium at concentrations of up to 4480 mg/kg. This research aims to understand how selenium occurs within the residual, and under what conditions it may remobilize. The speciation of selenium within the residual is of particular importance, as redox state impacts the toxicity and mobility. The mobility controls on selenium in the residual were determined through a series of aqueous batch experiments that simulated a variety of redox and pH conditions using O₂, Fe³⁺ and NO₃⁻ as oxidants. While selenium was mobilized under all simulated conditions, the highest concentrations were detected under mildly oxidizing conditions. Adsorption effects were also observed, as the concentration of selenium in aqueous phase increased initially, followed by a steady decrease. pH had little effect on the adsorption extent suggesting iron oxyhydroxides were not involved. The selenium speciation of the residual will be characterized in both pre- and post-experiment samples using X-ray Absorption Near Edge Structure (XANES) techniques. Changes in the relative proportion of selenium species will be used to indicate the vulnerability to mobilization under the varying redox and pH conditions. Once the speciation and mobilization mechanisms are known, proper disposal methods can be developed for the residual to minimize the risk to the local ecosystem and human health.

VALIDATION OF SEQUENTIAL LEACHING TESTS TO PREDICT POTENTIAL IMPACTS OF LOW SULFUR IRON ORE WASTE ON SURFACE AND GROUNDWATER QUALITY

S. Black^A, B. Price^A, N. Rothnie^A, R. Sharma^A, R. Marton^B and D. Allen^C

^AChemCentre, Resources and Chemistry Precinct, Bentley, WA, Australia

^BBHP Billiton Minerals Australia, Perth, WA, Australia

^CMBS Environment, 4 Cook Street, West Perth, WA, Australia

ABSTRACT

Accelerated sequential leaching methodologies, which typically involve the leaching of waste rocks with a sequence of increasingly aggressive solvents, have been used to characterise municipal wastes, soil, sediments and mineral processing wastes and more recently waste rocks associated with the mining of base metals. These can be used to predict the likely order of species mobilisation and extent of dissolution of metal ions and metalloids (metal oxyanions) and the potential impact on ground and surface water quality.

The key advantage of these methodologies is that they are rapid, taking only weeks to complete, compared with longer term kinetic studies which can last for several years, and can be used to identify both the likely order of metal extraction through time and the potential metal /rock type associations that may impact on ground and surface water quality.

ChemCentre has developed a sequential leaching procedure that has been customised for variably weathered, low sulfur iron ore waste rock from BHP Billiton's operations in the Pilbara Region of Western Australia.

Seven waste rock samples considered representative of Western Australian iron ore deposits were initially analysed using four published selective extraction methods. An optimal method for these mine waste types has subsequently been developed. The predictive value (metal/rock type risk identification) of this test, complemented by results from static waste rock characterisation tests and mineralogy by XRD, is being compared against longer term (up to two years) kinetic column testing.

This work is part of a project funded by BHP Billiton and the Minerals Research Institute of Western Australia, MRIWA.

DETERMINING BIOACCESSIBILITY RISKS AT THE HISTORIC ABERFOYLE TAILINGS SITE, NORTHEAST TASMANIA: OPPORTUNITIES FOR EFFECTIVE REHABILITATION

R. McLaine^A, A. Parbhakar-Fox^A, N. Fox^B and M. Reid^C

^AARC Industrial Hub for Transforming the Mining Value Chain (TMVC), University of Tasmania, Private Bag 79, Sandy Bay, TAS 7001, Australia

^B Co-operative Research Centre for Optimising Resource Extraction (CRC ORE), University of Tasmania, Private Bag 79, Sandy Bay, TAS 7001, Australia

^C Mineral Resources Tasmania, Department of State Growth, 30 Gordons Hill Road, Rosny Park, TAS 7018, Australia

ABSTRACT

The historic Aberfoyle Mine at Rossarden, north eastern Tasmania operated from 1931 to 1982 producing 11,000 tonnes of tin and 3,500 tonnes of wolfram. Ore from the Aberfoyle Mine and the nearby Story's Creek Mine was processed on site and pyritic tailings were pumped into nine tailings dams also on site. Metal sulphides within the tailings dams are a known contaminant and a source of acid mine drainage (AMD), with metal levels including cadmium measured above ANZECC (2000) guideline values. Major rehabilitation works previously undertaken have included the emplacement of an earth capping over the tailings dams and vegetation trials. The vegetation trials have however shown limited success, with only grass species growing with a patchy coverage to approximately 20 cm high.

In this study, tailings samples ($n = 75$) to a depth of 2 m were collected from the site. These tailings were logged and then subjected to a rigorous mineralogical and geochemical characterisation programme. This included analysis by field-portable XRF and routine static geochemical tests (i.e., acid-base accounting, paste pH, NAG pH). Mineralogical analyses involved X-ray diffractometry, reflected light and scanning electron microscopy. A new bioaccessibility test method developed by van Veen et al. (2016) was also performed on these materials and enabled us to determine the quantity of potentially harmful elements readily available for uptake by plants. The findings from our study will enable us to develop a preliminary rehabilitation programme for this tailings site that includes i) strategic further earthworks; and ii) new vegetation trials, with an emphasis on monitoring the response of plants specifically selected to tolerate the site-specific levels of potentially deleterious elements.

PHYSICOCHEMICAL PROPERTIES OF IRON OXIDES OPPORTUNITIES FOR USEFUL AMD PRODUCTS?

B. Mooney^A, B. Paull^A, T. Lewis^B and A. Parbhakar-Fox^C

^AAustralian Centre for Research on Separation Science (ACROSS),
University of Tasmania, Private Bag 75, Sandy Bay, TAS 7001, Australia

^B School of Physical Sciences (Chemistry), University of Tasmania,
Locked Bag 1371, Launceston, TAS 7250, Australia

^C Industrial Hub for Transforming the Mining Value Chain (TMVC), University of Tasmania,
Private Bag 79, Sandy Bay, TAS 7001, Australia

ABSTRACT

Acid mine drainage (AMD) is formed by biotic and abiotic processes, characterised by high sulphate and heavy metal concentrations, and is difficult to treat due to the complex iron/ferric oxidation chemistry. Advances in detecting iron oxides (including oxyhydroxides) at the nanoscale indicate that the size and shape of an iron oxide phase influences the stability and metals in environment. Precipitation, dissolution and reprecipitation of various iron oxides phases with exchanged or adsorbed metals, depend on factors such as pH/redox, temperature and biological activity. For this reason, the presence of iron oxides and associated biofilms may serve as water quality indicators of the type of environment in which found. Understanding the pigmentation, adsorption and catalytic properties of the various iron oxides in situ will contribute to the gaps in knowledge of iron cycling, but also serve to as improve AMD management by better control/valorisation of AMD products. This project aims to develop a suite of lower cost techniques that may identify and characterise ferruginous material for improved management or valorisation strategies.

The selected site for study is the Mount Lyell region which has produced over 1.3 million tonnes of copper, 750 tonnes of silver and 45 tonnes of gold since mining commenced in the early 1890's. Environmental controls were non-existent for the majority of the period of mining and processing operations and consequently there is a legacy of environmental degradation. Eluting from the site are various types of iron oxide phases, including precipitates from active treatment and legacy (untreated) material. It is anticipated that the materials will have different physicochemical properties depending on the various metals or organic material associated with the iron oxide structure, and results will be related to the water quality parameters. Chromatographic techniques that address both inorganic and organic components will be used. The findings will identify conditions that produce either a more reactive or a stable iron oxide product with useful pigment or catalytic properties. Ultimately understanding the natural iron oxide chemistry may lead to better management or recovery/valorisation resources to off set AMD treatment costs.

GEOENVIRONMENTAL CHARACTERISATION OF THE ABANDONED SCOTIA MINE, NORTH EAST TASMANIA: IMPLICATIONS FOR MANAGEMENT PRACTICES

**A. Parbhakar-Fox^A, T. Lewis^B, P. Hamill^B, A. Wakefield^C,
R. Botrill^C and J. Parnell^C**

^AARC Industrial Hub for Transforming the Mining Value Chain (TMVC), University of Tasmania, Private Bag 79, Sandy Bay, TAS 7001, Australia

^B Discipline of Chemistry, School of Physical Sciences, University of Tasmania, Private Bag 1371, Launceston, TAS 7250, Australia

^C Mineral Resources Tasmania, Department of State Growth, 30 Gordons Hill Road, Rosny Park, TAS 7018, Australia

ABSTRACT

The Scotia mine site, northeast Tasmania was operated by Van Diemen Mines (VDM) Pty Ltd (2007 to 2009) and predominantly targeted tin and sapphire. Whilst production of these commodities was never formally reported, the footprint of the mine included the processing area, main pit, three tailings dams and a freshwater dam. Since 2010, the mine has been in the care of the Tasmanian Government with no rehabilitation works having been undertaken by VDM.

This study examining the mineralogy and geochemical properties of tailings (n = 85; depth of 1.5 m) and sediments from around the site (n = 68; depth of 1 m) to identify potential geoenvironmental risks. In addition a detailed pit-lake chemistry study was conducted, and kinetic cells (n = 12) were established to evaluate the benefits of introducing a lime-cover if dewatering of the tailings dams was to occur as part of a larger rehabilitation programme. The tailings mineralogy is dominated by silicates with only trace- content of sulphides and no primary neutralisers. Despite this, the sampled materials were geochemically classified as potentially acid forming. As these materials are under water covers sulphide oxidation is retarded, but mildly acidic pH values still prevailed in each dam, with the chemistry of the main-extraction pit lake indicating metal concentrations in excess of ANZECC (2000) guidelines. The use of commercial lime sufficiently raised leachate pH to an alkaline range in kinetic trials and largely prevented continuous elution of metals (including As, Cu, Cd, Pb and Zn) above ANZECC (2000) aquatic protection values (80 % trigger-level) with the exception of Al. Trials to attenuate metals in solution using red mud were effective for the majority of metals, however, caution was exercised to maintain the pH conditions at 6-8 to prevent Al from dissolving. These results have assisted in developing a rehabilitation plan for this site.

WASTE NOT, WANT NOT – USING WASTE HAY TO IMPROVE PIT LAKE WATER QUALITY

R. Green^A, C. Mather^A, C. Kleiber^A, S. Lee^A, M. Lund^B and M. Blanchette^B

^ARio Tinto Iron Ore, 152-156 St Georges Terrace, Perth, WA 6000, Australia

^BMine Water and Environment Research Centre (MiWER), Edith Cowan University, 270 Joondalup Drive, Joondalup, WA 6027, Australia

ABSTRACT

Pit lakes can present a significant financial, environmental and reputation risk to the company responsible for their management and all stakeholders. If the pit lake is acidic, the stakes are higher. A novel field scale trial, involved the placement of spoilt hay bales into an acidic pit lake, located in the Pilbara region of Western Australia. The aim of the trial was to test whether waste hay would improve lake water quality by promoting the growth of sulfate-reducing bacteria.

Two pit lakes (West and East; pH 3.6 and 5.8, respectively; >1000 mg/L SO₄, depth <10 m, area <1.5 ha, age 5 years) were used for the trial, which ran from August 2015 to March 2016 in both the treated (West) and untreated (East) lakes. Approximately 19 t of waste hay was added to West Lake to create a layer approximately 0.3 m thick across the sediment. Water quality parameters (nutrients, select metals, pH, ORP, conductivity, SO₄ and Cl) were monitored at surface and bottom of the water column, throughout the trial using a combination of grab samples and continuous in-situ monitoring. Data were described over time.

Both lakes were thermally stratified with differences of 3-4 °C over 5 m however, salinity stratification was less obvious. The sulfate to chloride ratio remained constant in the surface water of the East Lake, but there was an indicative decrease in sulfate concentrations (from approximately 10,000 to 8,000 mg/L) and the sulfate to chloride ratio in the West Lake bottom water. Results suggest the deposition of hay had some impact on the quality of deeper (benthic) lake waters, in particular for promoting reducing conditions. The dissolved oxygen concentration in bottom waters decreased from >4 mg/L prior to hay deposition to <3 mg/L.

Waste hay could provide a local source of material for pit lake remediation. However, future trials should focus on assessing the long-term effects of the remediation beyond the 7-month trial, and adding multiple treatment and control lakes.

1.0 INTRODUCTION

Pit lakes can form in open cut mining pits, which extend below the pre-mine water table. Once dewatering ceases, groundwater, surface water and direct rainfall contribute to the formation of a pit lake. As a result of current open cut mining practices extended well below the water table, the quantity and size of potential pit lakes have increased over the last decade.

Pit lakes can present a significant financial, environmental and reputation risk to the company responsible for their management and all stakeholders. This is particularly relevant for pit lakes that are expected to generate Acid and Metalliferous Drainage (AMD). Backfill plans exist for many of these potential pit lakes, however, backfill may need to be done post-closure which may involve rehandling. In some cases pit backfill costs can be over \$300

million, therefore, there may be significant advantages to mining companies by not backfilling pits deemed to have a low risk to the environment (McCullough et al. 2013).

2.0 BIOREMEDIATION

Sulfur Reducing Bacteria (SRB) have the potential to remediate AMD as sulfate is converted to sulfide under reducing conditions, using labile organic carbon substrates as electron donors. This process under low redox conditions forms amorphous FeS and FeS₂, removing the elevated acidity, sulfate and associated metals from pit lake water and therefore breaking the acid generating cycle (Castro and Moore 2000). SRB activity can be initiated by the addition of organic materials. However, the success of SRB-based bioremediation is largely determined by the suitability of the material (Neculita et al. 2007). Effective SRB-based bioremediation requires highly labile organic material for sufficient reactivity and must have efficient longevity to sustain the bacterial reduction over a long time frame. Additionally, the organic materials produce anaerobic conditions and facilitate growth of facultative anaerobic bacteria which helps break down recalcitrant organic materials into more labile forms (Wendt-Potthoff and Neu 1998).

Following promising theoretical and laboratory research (Lund et al. 2017), the availability of hay waste from local agricultural projects provided an opportunity to test bioremediation using green waste at the field scale. The water quality results from this trial are presented in this paper. This paper is a descriptive study of water quality trends and forms part of a larger study investigating water quality statistics and the variability of microbial assemblages over time in lakes and microcosms

3.0 LOCATION

Two temporary pit lakes (referred to as East and West Lakes) that began forming in 2010 after active mining and dewatering ceased, were the focus for the trial. These lakes were located in an iron ore mine in the Pilbara region of Western Australia. The climate at the mine site is semi-arid to arid with hot summers and mild winters. Mean maximum temperatures range from 35.9-38.3 °C in summer (Dec-Feb) and 23-25.5 °C in winter (Jun-Aug). Rainfall is highly variable and characterised by periodic high intensity rainfall events occurring predominantly in summer months, followed by extended periods of drought. Mean annual rainfall is 399 mm and evaporation is generally >3000 mm annually, exceeding rainfall by an order of magnitude.

In September 2015, approximately 19 t (27 hay bales) of waste hay was added to West Lake to create a layer approximately 0.3 m thick across the sediment. East Lake was monitored however no amendments were added. The pit contained approximately 252,300 m² of reactive black shale surface exposures on the pit wall, and most exposures were estimated to have >0.1% sulfur. The pits were groundwater sinks and acidic lake water was most likely constrained to the base of the pit, where it was underlain by relatively impermeable Mount McRae Shale (MCS). West Lake was primarily surface water fed however, East Lake had groundwater input.

Low pH values (3.6-5.8) and elevated sulfate concentrations (>1,000 mg/L) have been recorded for the pit lake waters suggesting that the black shale pit wall exposure may have resulted in some oxidation of sulfides and formation of acidic waters within the pit lakes.

4.0 METHODS

4.1 Pit Lake Bathymetry

A remote controlled boat with a logging GPS and depth sounder was utilised to record the bathymetry of West Lake. West Lake, which was found to have a maximum depth of approximately 9.5 m in the north western pod, with depth decreasing toward the east. A bathymetric survey could not be completed for the East Lake due to presence of abandoned dewatering pipework.

4.2 Water Quality Analysis

The pH, Electrical Conductivity (EC), redox, Dissolved Oxygen (DO) and temperature of both lakes was measured in situ using a combination of Hanna Instruments, Odyssey and Hobo loggers (on thermistor strings). Samples were collected from the pit lake surface and analysed for pH, EC, Total Dissolved Solids (TDS), metals/metalloids, sulfate, chloride, acidity, dissolved organic C and nutrients once every 3 months. Two samples were collected from near the bottom of West Lake, using a low flow bladder pump (QED MP50) 0.5 m from the bottom of the thermistor string.

The dissolved oxygen sensor on the Hanna probe used the Clark cell methodology. This methodology requires a frequent calibration schedule for accurate data collection that was not adhered to for this trial. Scaling and to a lesser extent biofouling were an issue on probes, particularly in shallow waters. Cleaning was completed when the instruments were removed for calibration (as noted in Figures 1-10).

5.0 RESULTS

5.1 Logistics and Field Technology

There are a number of difficulties associated with discerning the effects of hay deposition and potential activity of SRB. Most significantly is the fact that the trial was held on an operational mine site, which created a variety of issues, such as limited access and the project being cut short due to early backfill of the pits. Six months between the deposition of hay and the completion of the trial may not be enough time to see the full *in situ* effects.

The thermistor strings were useful for collecting continuous data. However, issues with biofouling and scaling on the probes meant some probes may have been reporting incorrect data for periods of time and cleaning and calibration needed to be performed quite regularly (as indicated in Figures 1-6).

The untreated East Lake was also monitored to provide a comparison for conditions in the hay treated West Lake. However, there were differences in water chemistry and chemical responses between the West and East Lakes. The East Lake is groundwater connected and therefore far less influenced by rainfall and evaporation processes than West Lake (which has little groundwater input). This meant that East Lake data was less useful as a control for the hay trial.

5.2 Water Levels

Water level monitoring of the West Lake revealed a drop during the dry period indicating the lake level is strongly influenced by evaporation and precipitation. In contrast, the East Lake level stays more constant as groundwater inflow is roughly equal to the water lost by

evaporation. This result is consistent with the variation of ~2 m in the calculated water depth above the pressure logger for the West Lake compared to <1 m for the East Lake.

5.3 Thermal Stratification

Both lakes were thermally stratified with differences of 3-4 °C over 5 m (Figures 1 and 2). However, temperature stratification disappeared in the upper 1-2 m in both lakes following rainfall events of >20 mm. No clear complete turnover of bottom and surface waters was observed.

5.4 Continuous In-Situ Water Quality

Prior to the deposition of hay, the pH at the surface of West Lake ranged from 3.3 to 3.5. There was a noticeable drop of ~0.5 pH units following the deposition of the hay in September 2015, which was followed by a gradual increase in pH (Figure 3). Following the Hanna Probe being moved to deeper waters in November 2015 in West Lake, the bottom water pH varied over of 0.7 pH unit range, in an apparent cyclic manner. This cyclical change may have been associated with recharge although it does not correlate well with rainfall data. Additionally, this cyclical pattern is only visible in the deep water which suggests that it is associated with unique processes possibly caused by the hay. From late January 2016 there was a rapid increase in bottom water pH, starting from a low of ~3.1 reaching pH 4.5 just prior to the end of the trial. The beginning of this sharp change coincided with a high rainfall event. However, the observed subsequent exponential increase in pH would not be consistent with a change due to higher rainfall. The change in pH was mirrored by a lowering of redox potential (Figure 4) and indicates that reducing conditions developed within the deeper lake waters and that these changes may have been associated with microbial (SRB) activity in the deeper waters of the lake. Similarly, DO concentrations at 4-5 m depth were close to zero for the same period (Figure 5). Slight periodic increases in bottom water DO appeared to have coincided with rainfall events and may represent the percolation of oxygenated meteoric waters into the water column. In comparison, the DO measured at 7 m in East Lake indicated fairly oxygenated waters at depth (Figure 6).

5.3 Grabbed and Pumped Water Quality

The pH measurements of surface waters from both lakes were variable and there was a considerable change in pH for both lakes between February 2015 and May 2015 (Figure 7). However, the pH of the West Lake surface water fell from around 4.8 to 3.4 and the pH of East Lake surface water rose from ~3.8 to 4.7. This difference between lakes was likely due to the higher groundwater inflow into the East Lake. The lower pH in West Lake may have been exacerbated by surface water runoff over PAF exposures in the pit wall. The salinity (EC and TDS) of water was generally higher in the West Lake and higher for bottom water compared to surface water (Figure 8). This is consistent with the higher influence of evaporative concentration in West Lake compared to East Lake. The EC does appear to fall following large rainfall events and then rise during dry periods. However, there are no obvious changes in salinity relating to hay deposition.

Major ion concentrations are mostly correlated and follow the same trend of EC suggesting they are mostly influenced by evaporative concentration during dry months and dilution following rainfall events. Decreased sulfate concentrations in West Lake deep waters (4-5 m depth) may indicate that SRB activity has occurred (Figure 9). Sulfate reduced by 2,200 mg/L despite increased chloride and salinity between November 2015 and March 2016. This suggests the changes in sulfate are not associated with normal evaporation and dilution processes because sulfate would have increased linearly with chloride (Figure 10).

Furthermore, an increase in West Lake bottom water pH from 3.5 to 4.5 was recorded. Unfortunately there is no data for bottom water prior to hay deposition and only two points overall so it is not possible to compare or observe the full extent of variation in bottom water chemistry. These changes were not observed in the surface water chemistry. Metal concentrations did not follow the same trend for sulfate in bottom waters, with a number of metals (e.g. Fe and Mn) increasing and only Cu decreasing between the two collected time points.

6.0 CONCLUSIONS

Temperature, water pH, dissolved oxygen and sulfate concentrations highlight changes in water chemistry and thermal stratification of the West Lake between anoxic deeper waters and more acidic and oxic shallow waters. Deep waters in West Lake increased in pH levels and decreased in dissolved oxygen and sulfate, most notably from late January 2016, which could be attributed to SRB activity following hay deposition. The water quality changes seen in West Lake after hay treatment were not seen in East Lake.

The results from this trial are promising and suggest addition of hay may be capable of improving pit lake water quality. However, it is difficult to produce firm conclusions and determine the potential long term success of the remediation. Further work is required and any opportunity to implement a longer term remediation trial in existing pit lakes would be invaluable for investigating and providing techniques for remediation of acidic pit lakes.

7.0 ACKNOWLEDGEMENT

The Hamersley Agriculture Project and RTIO mine site operations were instrumental in implementing this project safely.

8.0 REFERENCES

Castro JM and Moore JN (2000). Pit lakes: their characteristics and the potential for their remediation. *Environ. Geol.* **39**, 1254-1260.

Lund MA, Blanchette ML, Gonzalez Pinto J, Green R, Mather C, Kleiber C and Lee S (2017). Are Microcosms Tiny Pit Lakes?. In '*Mine Water & Circular Economy*' (Eds C Wolkersdorfer, L Sartz, M Sillanpää and A Häkkinen). Vol II. pp 1204 – 1206 (Lappeenranta University of Technology, Lappeenranta, Finland).

McCullough CD, Marchand G and Unseld J (2013) Mine Closure of pit lakes as terminal sinks: best available practise when options are limited? *Mine water Environ.* **32**, 302-313.

Neculita CM, Zagury GJ and Bussiere B (2007). Passive Treatment of Acid Mine Drainage in Bioreactors using Sulfate-Reducing Bacteria: Critical Review and Research Needs. *J Environ Qual.* **36**, 1-16.

Wendt-Potthoff K and Neu TR (1998). Microbial processes for potential in situ remediation of acidic lakes. In '*Acidic Mining Lakes*' (Eds W Geller, H Klapper and W Salomons) pp. 269-284 (Springer, Berlin, Germany).

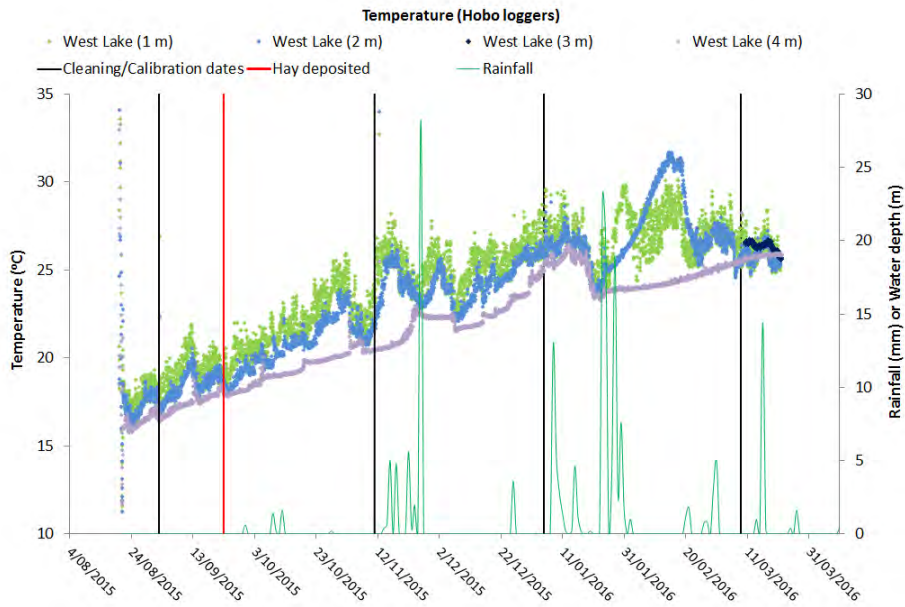


Fig. 11. Temperature within West Lake at various depths.

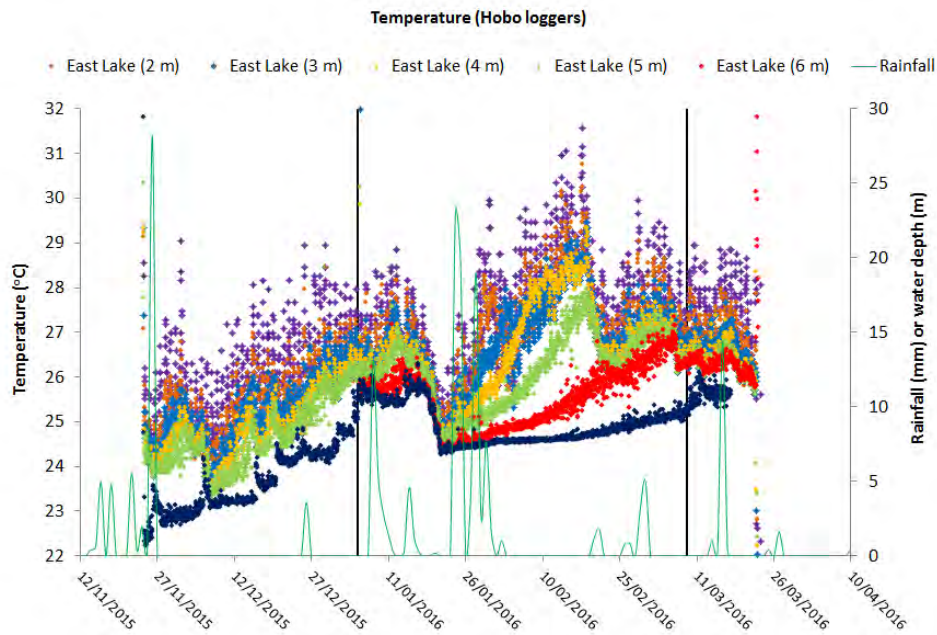


Fig. 2. Temperature within East Lake at various depths.

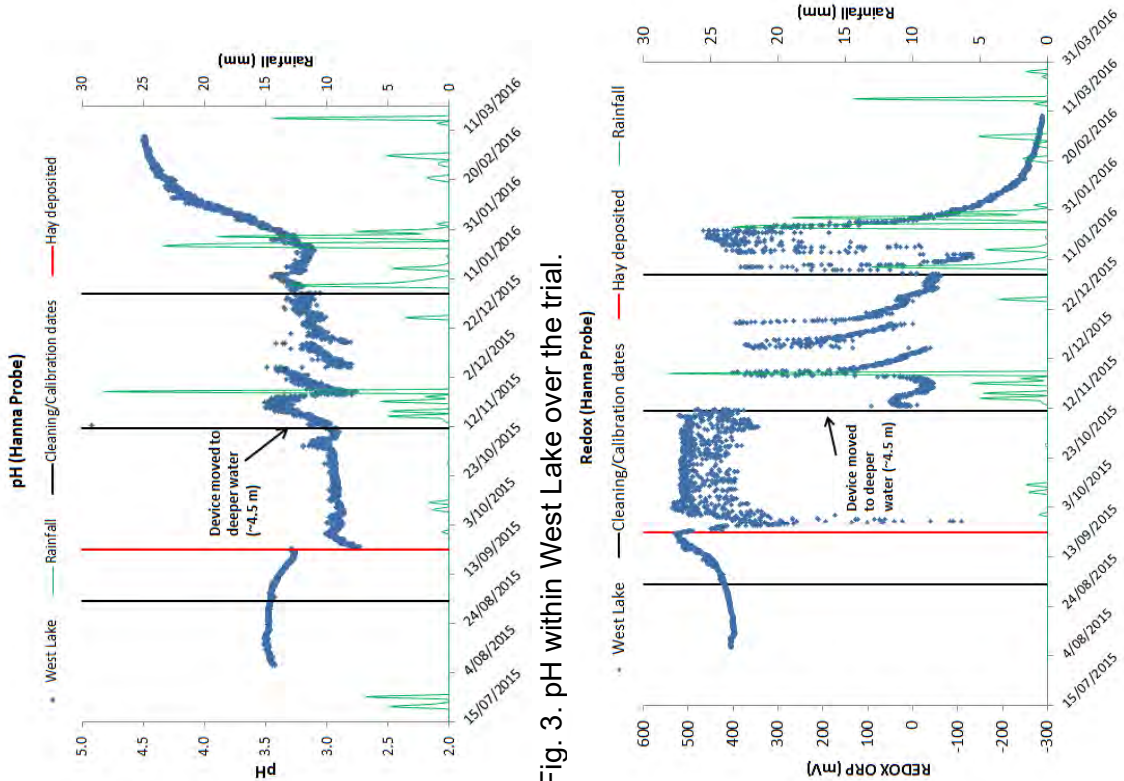


Fig. 3. pH within West Lake over the trial.

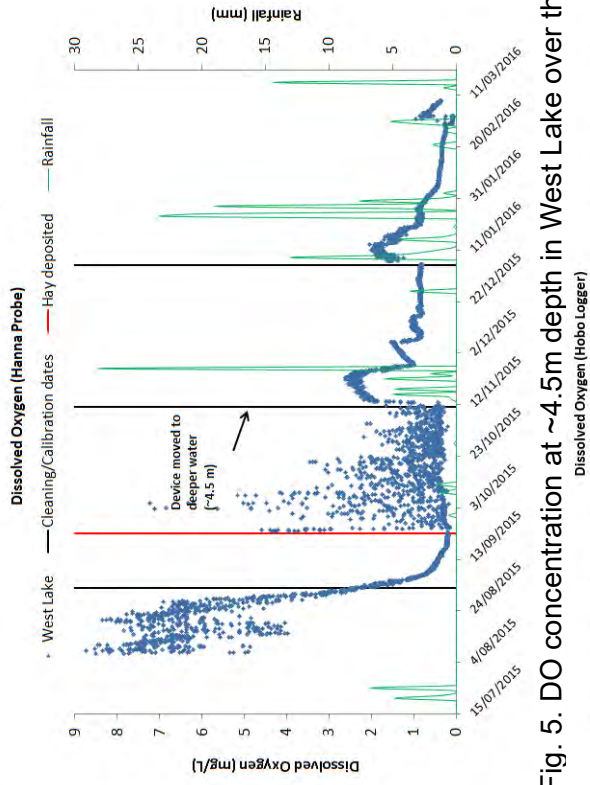


Fig. 5. DO concentration at ~4.5m depth in West Lake over the trial.

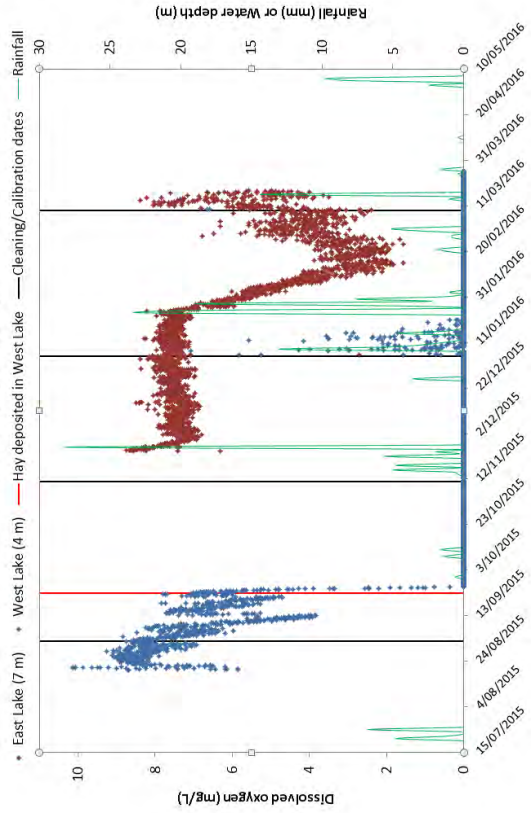


Fig. 6. DO concentrations measured at ~4m in West Lake and ~7m in East Lake over the trial.

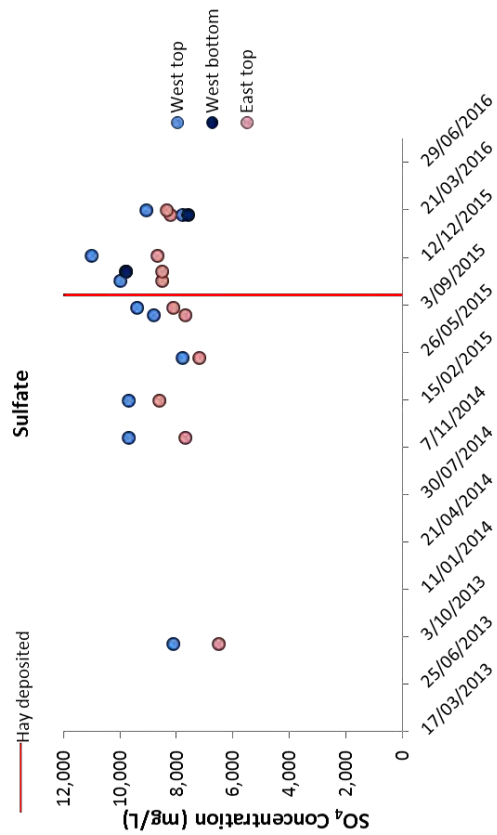


Fig. 9. Sulfate concentration of surface water measured at the West and East Lakes.

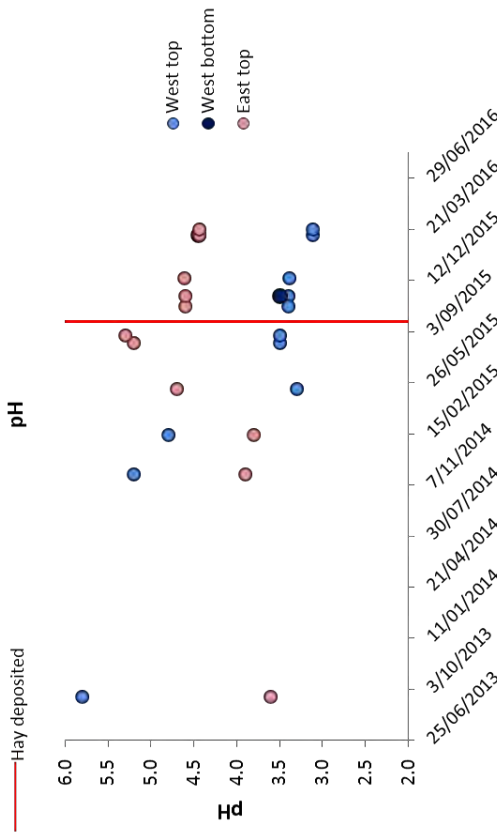


Fig. 7. The pH of surface water measured in the East and West Lakes.

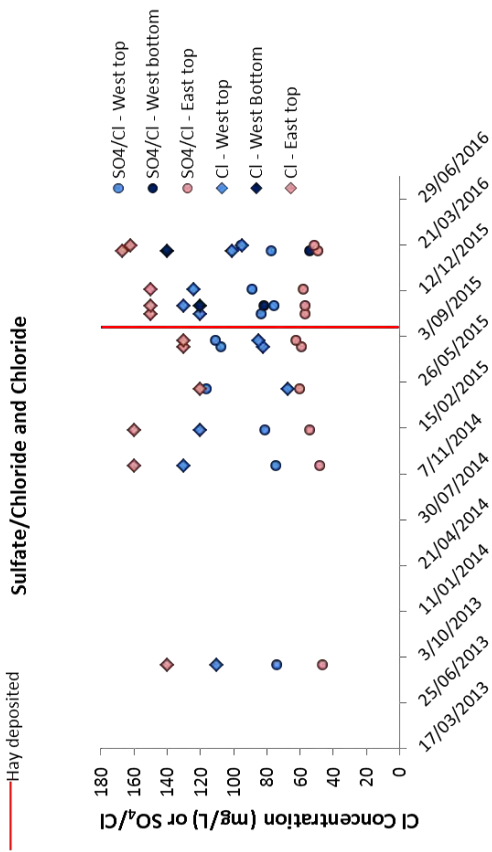


Fig. 10. Sulfate to chloride ratio and chloride concentration of surface water measured at the West and East Lakes.

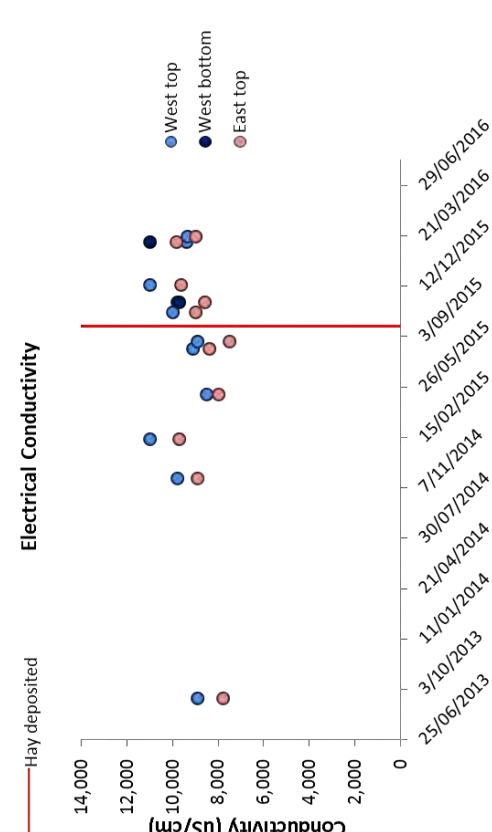


Fig. 8. The electrical conductivity of surface water measured in the East and West Lakes.